University of Nottingham
UK | CHINA | MALAYSIA

Improving the Maturation of Human Pluripotent Stem Cell - Derived Hepatocyte-Like Cells Using an Automated-Design of Experiments Approach

Submitted by

Lazaros Fotopoulos BSc, MSc

School of Medicine

Division of Cancer and Stem Cells

University of Nottingham

September 2017

Thesis submitted to The University of Nottingham for the

Degree of Doctor of Philosophy

ACKNOWLEDGEMENTS

I would firstly like to say a big thank you to my supervisor Prof Lorraine Young for providing support, guidance, patience and help to get through the PhD and to Prof Chris Denning for always being there to help, guide and advise. Also, I want to thank Prof Andrew Bennett for his helpful comments through my PhD and for providing samples of human adult primary hepatocytes for the purposes of this thesis.

I would like to thank all those who have provided technical support and training in the different phases of my PhD. Mr. Ralph Hyde, who helped me with the TECAN Freedom Evo providing a 24/7 support. Mr. Jayson Bispham who has kindly helped with the Flow Cytometry experiments and analysis. Mrs Katarzyna Lis-Slimak for the Operetta related queries. Dr Qian Liu for training me when I started my PhD. Dr Gary Duncan for kindly providing me with the human induced Pluripotent Stem Cell (hiPSC) lines. Mrs Monika Owen for her help with the isolation and preparation of the human adult primary hepatocytes. And all the present and past STEM group members that I had the pleasure to work with and learn from. My appreciation also goes to James S, James C, Jamie P, Gary D, Luke F, Alex P, Jamie B and Diogo M for their friendship and company during this time.

Most importantly, I want to thank my parents, my brother and family members for their endless love, understanding and support. Thank you to my very close friends who provided psychological support when I needed it and without them, I would have never made it. Finally, I want to thank all those I have neglected to mention.

DECLARATION

I hereby declare that this thesis has been composed by myself and has not been submitted for any other degree previously. Acknowledgements of specific procedures not performed by myself are stated; otherwise, the work described is my own.

Lazaros Fotopoulos: _____

Date: _____

ABSTRACT

Human primary hepatocytes (pHEPs) are used as the gold standard model for drug screening and toxicity testing in the drug development pipeline. However, the rapid post isolation changes in cell structure, morphology, gene expression and metabolic activity, together with donor availability and heterogeneity, limit their utility. Directed differentiation of human embryonic stem cells (hESCs) or human induced pluripotent stem cells (hiPSCs) into hepatocyte-like cells (HLCs) can be achieved within a short time and in unlimited quantities; however their metabolic activity closely represents foetal hepatocytes but not an adult hepatocyte metabolic profile. Studies have identified compounds that can increase expression of some adult enzymes, but a systematic evaluation of multiple compounds in a range of concentrations has never been reported in human cells. Studying the maturation of HLCs requires identification of distinct markers that are only expressed in the adult liver cells to clearly evaluate maturation characteristics as the current literature predominantly investigates the expression of the characteristics observed during the foetal stages.

In this thesis, the current status of the field is reviewed in Chapter 1. The existing hepatocyte differentiation protocol has been re-designed in Chapter 3 taking into consideration up-to-date methods, cell line differences and culture medium, availability of human Pluripotent Stem Cells (hPSCs) and differentiation into HLCs on a TECAN Freedom Evo 200 automated cell culture robot. Based on a published proteomic study, a quantifiable high-throughput assay was developed to identify distinct adult enzyme markers Cytochrome 450 1A2 (CYP450 1A2), Cytochrome 450 2C9 (CYP450 2C9) and Cytochrome 450 2A6 (CYP450 2A6) in Chapter 4. Finally, Design of Experiment (DoE) approaches were utilised in Chapter 5 to screen 46 identified candidate compounds at a range of concentrations. The results predicted that SR12813 at 1.5uM, taurocholate acid at 155uM, CHIR 99021 at 8.5uM, all-trans retinoic acid at 3uM and ascorbic acid at 1.5mM can enhance the expression of

CYP2C9. Chapter 6 discusses the advances of this thesis and their relevance to the current literature and the HLCs field.

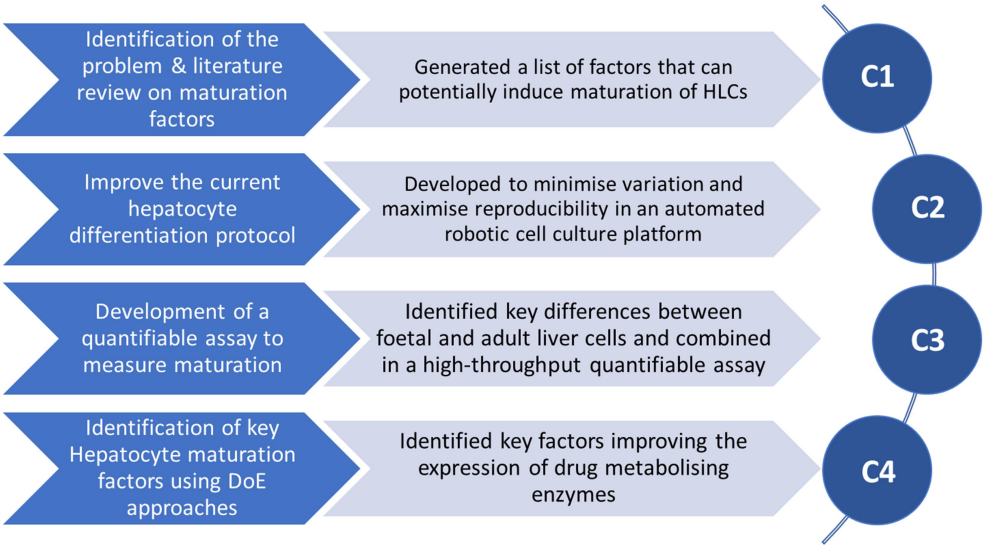

Figure 1 Overview of the thesis plan and aims.

Table of Contents

ABBREVIATIONS

Abbreviation	Description	Abbreviation	Description
%	Per Cent	hPSC	Human Pluripotent Stem Cells
9CRA	9-cis Retinoic Acid	ICG	IndoCyanine Green
ANOVA	Analysis of Variance	ITE	2-(1H-Indol-3-ylcarbonyl)-4-thiazolecarboxylic acid methyl ester
ATP	Adenosine Triphosphate	ITS	Insulin Transferrin Selenium
ATRA	All Trans Retinoic Acid	KSR	Knock out Serum Replacement
BME	Beta-Mercaptoethanol	LCA	Lithocholic Acid
BSA	Bovine Serum Albumin	LDL	Low Density Lipoprotein
cAMP	Cyclic Adenosine MonoPhosphate	LiHa	Liquid Handler
CCD	Central Composite Design	LT	LifeTechnologies
CDM	Chemically Defined Medium	MC	Medium C
CYP450	Cytochrome P450	MCA96	Multichannel 96 Head
DAPI	4',6-DiAmidino-2-PhenylIndole	MCAH	Medium C All High
DE	Definitive Endoderm	MCDM	Medium C + DMSO
DIHEXA	N-hexanoic-Tyr-Ile-(6) aminohexanoic amide	MEF	Mouse Embryonic Fibroblasts
DMEM	Dulbecco's Modified Eagle's medium	MEF-CM	MEF - Conditioned Medium
DMSO	Dimethyl Sulfoxide	mRNA	Messenger RiboNucleic Acid
DNA	Deoxyribonucleic Acid	MS	Media Supplement
DNC	Double Nuclei Cells	NaB	Sodium Butyrate
DOE	Design of Experiments	NIH	National Institute of Health
E	Embryonic Development Day	NR	Nuclear Receptor
ECM	Extracellular Matrix	OFAT	One Factor At a Time
EMT	Epithelial Mesenchymal Transition	PAS	Periodic Acid Staining
FBS	Foetal Bovine Serum	PBS	Phosphate-Buffered Saline
FDA	Food and Drug Administration	PCR	Polymerase Chain Reaction
FH1	Functional Hit 1	PFA	Paraformaldehyde
FI/MI	Mean Fluorescent Intensity	pHEP	Primary Hepatocytes
FPH1	Functional and Proliferation Hit 1	RA	Retinoic Acid
GF	Growth Factor	RNA	RiboNucleic Acid
GR	G protein coupled Receptors	RoMa	Robotic Manipulator
GSK	Glycogen Synthase Kinase	ROS	Reactive Oxygen Species
GST	Glutathione S Transferase	RPMI	Roswell Park Memorial Institute Medium
h	Human	RSM	Response Surface Methodology
HCM	Hepatocyte Culture Medium	STM	Septum Traversum Mesenchyme
hESC	Human Embryonic Stem Cells	T3	Triiodothyronine
hIPSC	Human Induced Pluripotent Stem Cells	T4	Thyroxine
HLC	Hepatocyte Like Cells	TCA	Taurocholate Acid
HM	Homemade	TSA	Trichostatin A

GENE SYMBOLS AND NOMENCLATURE

Abbreviation	Full Name	Abbreviation	Full Name
AAT	alpha-1-Antitripsin	MIXl	Mix-like homeobox gene
AFP	alpha-Fetoprotein	NODAL	Nodal Growth Differentiation Factor
AhR	Aryl Hydrocarbon Receptor	OC	Onecut
AKT	Protein Kinase B	OCT3/4	Octamer-Binding Protein 3/4
ARNT	Aryl Hydrocarbon Nuclear Translocator	OSM	Oncostatin M
BMP	Bone Morphogenetic Proteins	PGC1α	Peroxisome proliferator-activated receptor Gamma Coactivator 1-alpha
C/EBP	CCAAT/Enhancer-Binding Protein	PI3K	Phosphatidylinositol 3-Kinase
CAR	Constitutive Androstane Receptor NR1I3	PPARα	Peroxisome Proliferator Activated Receptor alpha
CK	Cytokeratin	PROX	Prospero-Related Homeobox
c-MYC	MYC proto-oncogene, bHLH transcription factor	PXR	Pregnane X Receptor NR1I2
E-CAD	E-Cadherin	RAR	Retinoid Acid Receptor NR1B1
EGF	Epithelial Growth Factor	ROR	Retinoic Acid Receptor related Orphan Receptors
EPCAM	Epithelial Adhesion Molecule	RXR	Retinoid X Receptor NR2B1
FGF	Fibroblast Growth Factor	SOX	Sry-related HMG box
FOXA2	Forkhead Box A2	SSEA	Stage-Specific Embryonic Antigen
FXR	Farnesoid X Receptor	TAT	tyrosine aminotransferase
G6P	Glutathione 6 Phosphatase	TCF/LEF	T-Cell Factor/Lymphoid Enhancer Factor
GPCR	G Protein–Coupled Receptors	TGFb	Transforming Growth Factor b
GSK	Glycogen Synthase Kinase	TRA-1-81	Podocalyxin Like Gene
HGF	Hepatocyte Growth Factor	VDR	Vitamin D Receptor
HHEX	Hematopoietically Expressed Homeobox	VDRE	Vitamin D Response Element
HIF	Hypoxia Inducible Factor	WNT	Wingless-Type MMTV Integration Site Family
HNF	Hepatocyte Nuclear Factor	YAP1	Yes Associated Protein 1
KLF4	Kruppel Like Factor 4		

According to current guidelines from the Human Genome Nomenclature Committee (http://www.gene.ucl.ac.uk/nomenclature/), abbreviations for human genes are capitalised and italicised, while their respective proteins are capitalised but not italicised.

CHAPTER ONE

IMPROVING THE MATURATION OF HUMAN PLURIPOTENT STEM CELL (HPSC)-DERIVED HEPATOCYTE-LIKE CELLS USING AN AUTOMATED-DESIGN OF EXPERIMENTS (DOE) APPROACH

1.1. Introduction - Liver's central role in Biology

The liver is the largest organ in the body and is important for xenobiotic detoxification, decomposition of red blood cells and removal of the toxic by-product of urea cycle ammonia (Starzl and Lakkis, 2006, Corless and Middleton, 1983). Amongst its key characteristics, it is a metabolic and a storage site for nutrients such as glycogen, iron, copper and vitamins and regulates the balance of amino-acids and fats known as homeostasis. It responds to hormones such as insulin, glucagon and glucocorticoids, resulting in the maintenance of normal glucose levels. It also aids digestion of lipids upon bile production, thus controlling the cholesterol levels. The liver produces essential proteins such as albumin and alpha-1-antithrypsin (AAT), enzymes responsible for the metabolism and detoxification such as Cytochrome 450 enzymes (CYP450) and clotting factors such as fibrinogen, thrombopoietin and antithrombin. Thus, the liver has key roles in processes that range from food digestion, drug metabolism, detoxification, nutrient storage, protein production to hormone homeostasis and immunity (Zorn, 2008, Ramadori et al., 2008, Si-Tayeb et al., 2010a, Starzl and Lakkis, 2006, Corless and Middleton, 1983).

The importance of the liver in human health and disease, as well as its remarkable regenerative capacity, has been well known since the ancient times highlighted in the story of Prometheus (Power and Rasko, 2008, Chen and Chen, 1994). In Greek mythology, Prometheus was punished for giving fire to humans and chained with unbreakable chains against a solid rock where a giant eagle would tear his liver daily, causing it to regenerate during the night for the eagle to return again repeating the process. (Chen and Chen, 1994).

1.2. Drug Metabolism

Among the many functions that the liver undertakes, one of the most critical is the drug metabolism. Has been described as the body's inherent ability to metabolise and remove foreign and/or hazardous compounds, xenobiotics, that either intentionally or unintentionally have made their way to systemic circulation (Sinz, 2012). These xenobiotics can be naturally occurring substances or synthetic drugs. Metabolism works as the main line of defence inducing chemical changes in their structure so-called biotransformation, in an attempt to transform them into more polar, easily extracted from the human body, but most importantly pharmacologically inactive (Doogue and Polasek, 2013, Benedetti et al., 2009). Energy for the processes is secured by the membrane-bound CYP450 oxidoreductase that donates electrons to the enzymes involved in the metabolism (Pandey et al., 2013).

In the presence of a xenobiotic, the liver responds by activating key enzymes such as oxidases, reductases and hydrolases and enzymatically converting lipid-soluble substrate into a water-soluble and easily exportable metabolite (Kirchmair et al., 2015). An overview of the above stages is shown in Figure 2. Often the by-products of metabolism are less soluble, pharmacologically active or toxic compounds that once overcome absorption and bioavailability converting into an active drug, potentially damaging to the system (Obach, 2013). In the development of drugs, investment costs are not recouped off at a later stage ie human clinical trials that flag up as toxic (Sinz, 2012). For this reason, a deeper understanding of the metabolism of candidate drugs in the early stages of drug development is of paramount interest for the pharmaceutical industry to avoid unnecessary complications, drug failures and cost.

A plethora of metabolic enzymes are responsible for the xenobiotic metabolism of substances across the body with tissue-specific activity differences (Krishna and Klotz, 1994). However, the liver is the main site (Almazroo et al., 2017, Sahi et al., 2010). There are three

main categories of enzymes that metabolise xenobiotics.

Phase I enzymes comprise the CYP450 superfamily composed of 57 genes (Preissner et al., 2010) (Figure 3). Their role is to chemically modify drugs by adding a functional group and

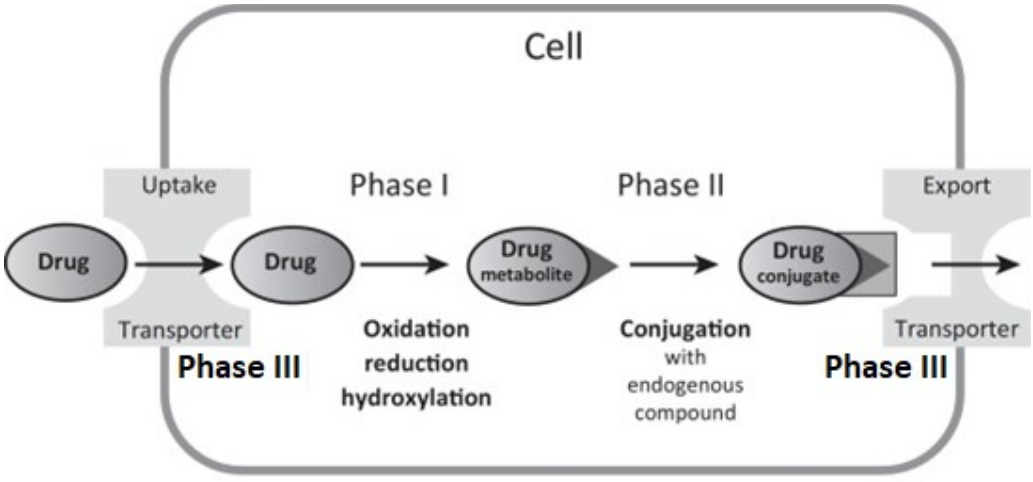

Figure 2 Overview describing the metabolism of xenobiotics. Following uptake of a drug and transportation into the cell, it is metabolized using the Phase I enzymes via oxidation, reduction, or hydroxylation, leading to insertion or uncovering of a reactive hydrophilic moiety. At the Phase II, the drug is conjugated with endogenous compounds such as glutathione or saccharides and finally the resulting conjugate is excreted by export transporters. Adapted from (Matoušková et al., 2016) and modified.

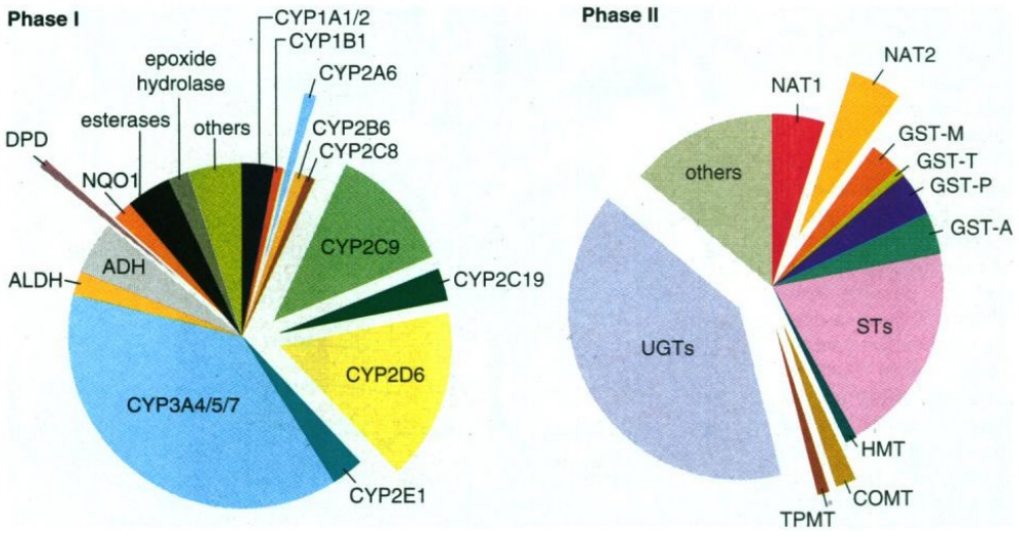

Figure 3 Overview of the enzymes involved in Phase I and Phase II metabolism. Pie charts demonstrate the percentage of phase I and phase II metabolism of drugs that each enzyme contributes to. ADH, alcohol dehydrogenase; ALDH, aldehyde dehydrogenase; CYP, cytochrome P450; DPD, dihydropyrimidine dehydrogenase; NQ01, NADPH:quinone oxidoreductase or DT diaphorase; COMT, catechol O-methyltransferase; GST, glutathione S-transferase; HMT, histamine methyl- transferase; NAT, N-acetyltransferase; STs, sulfotransferases; TPMT, thiopurine methyltransferase; UGTs, uridine 5'-triphosphate glucuronosyltransferases. Adapted by (Evans and Relling, 1999) and modified.

diverting them into more water-soluble products to aid their excretion (Figure 2). Major substrates for Phase I are steroids, fatty acids, eicosanoids, vitamins, xenobiotics and also still unknown substrates (Almazroo et al., 2017, Iyanagi, 2007). Trace elements such as iron are important for binding of substrates to the catalytic centre of the enzymes. CYP450 enzymes are predominantly localised in the membrane of the endoplasmic reticulum however, they can also be found in other cellular compartments such as the cell surface or mitochondria (Neve and Ingelman-Sundberg, 2010).

Phase II drug metabolism consists of different families of enzymes (Figure 3), mainly transferases that further convert Phase I products that cannot be excreted from the body, into highly-polar and readily-extractable molecules by conjugating hydrophilic endogenous elements (Crettol et al., 2010). The most common Phase II enzymes are the UDP-glucuronosyltransferases (UGTs), N-acetyltransferases (NATs), sulfotransferases (SULTs), glutathione S-transferases (GSTs), thiopurine S-methyltransferases (TPMTs) and catechol O-methyl-transferases (COMTs) (Almazroo et al., 2017, Jancova et al., 2010). This process occurs mainly in the cytoplasm, however it has been described in both the mitochondria and peroxisomes (Jancova et al., 2010). The by-products of Phase II metabolism require assistance from Phase III metabolism to facilitate transportation in/out of the cells.

Phase III metabolism consists of drug transporters in the form of transmembrane proteins that assist transportation of conjugated metabolites into the hepatocytes and then into the bile canaliculi to successfully excrete the highly hydrophilic by-products from the body (Xu et al., 2005). Overall, the most common enzymes responsible for the biotransformation (70-80% of all drugs and foreign substances) are Phase I and in particular enzymes that belong to the CYP450 families 1, 2 and 3. The most important of those are CYP450 enzymes 1A2, 2A6, 2B6, 2C8, 2C9, 2C19, 2D6, 2E1, 3A4 and 3A5 (Zanger and Schwab, 2013).

1.3. Drug Development & Key Stages

The drug discovery process is a lengthy route that may take between 11-16 years and with costs ranging from millions to billions of pounds (Hughes et al., 2011, Avorn, 2015, Ware and Khetani, 2016). Figure 4 shows an overview of the drug discovery and development progress summarising the key elements in each stage.

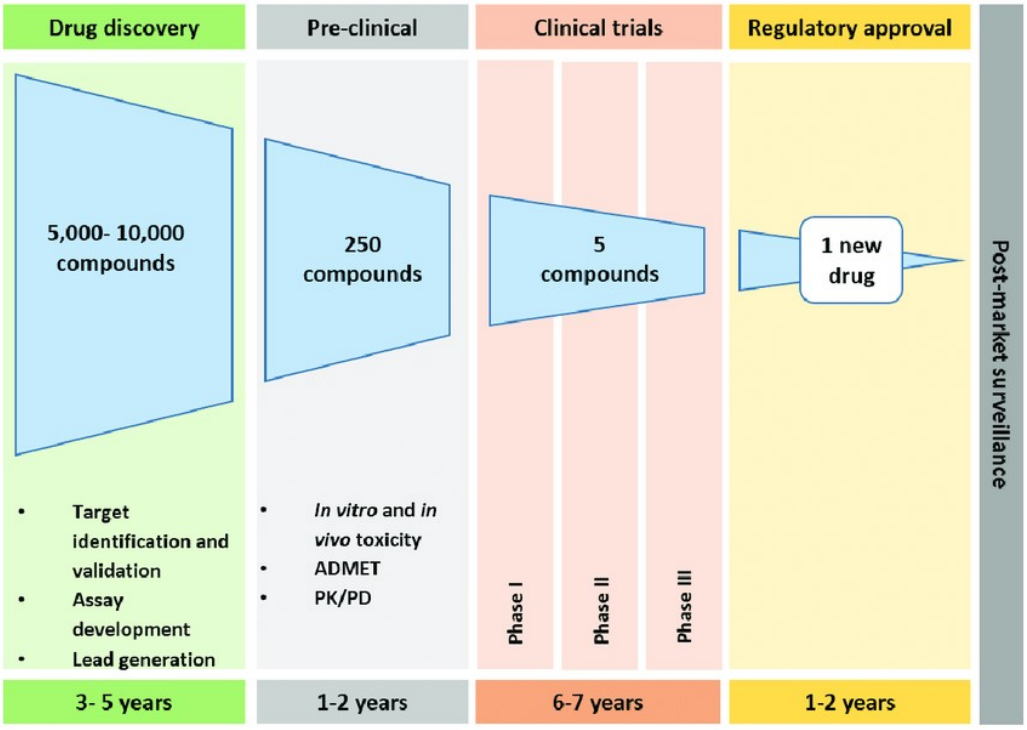

Figure 4 Overview of the Drug Discovery and development process divided in 4 key stages. The first stage starts with target identification and validation, assay development and lead generation screening up to 10.000 compounds and lasts from 3 to 5 years. The second stage is the pre-clinical that evaluates in vitro and in vivo toxicity, studies the absorption, distribution, metabolism, and excretion (ADME) of the candidate drugs with additional pharmacokinetics and pharmacodynamics. The third stage is divided into the 3 clinical trial phases that usually last between 6 to 7 years and the regulatory approval at the fourth stage requires 1 to 2 years. Adapted by (Matthews, H. 2016)

Commonly, drugs at the final clinical stages fail to succeed because of concerns in safety and efficacy that were not predicted in the previous phases of development (Hwang et al., 2016) or due to adverse effects that lead to induced cardiotoxicity (Liang et al., 2013). Lack of predictive power of animal models for humans often causes drug failure at the clinical stages (Shanks et al., 2009, Mak et al., 2014). To reduce the failure of drugs and subsequently cost of the drug development, pharmaceutical companies now follow the "failing fast and cheap" model (Owens et al., 2015). This is usually accomplished by improved toxi-

cology screens, establishing predictive translational models through a more thorough understanding of the disease and by identifying predictive biomarkers combined with well-designed animal model trials (Hughes et al., 2011). Another reason for drug failure is the extensive genetic polymorphism among the population that leads to distinct pharmacogenetic phenotypes and the enzymes that metabolise drugs at different rates or show a different substrate selectivity that might lead to different responses (Zanger and Schwab, 2013). Translation of this knowledge into drug development is slow and difficult but important for the development of effective drugs.

1.4. Requirement for *in vivo* Models of Liver

The need for drug testing in animals became a necessity after incidences that led to human tragedies. Examples include the use of Diethyl Glycol as a solvent for a drug while its toxicity to humans was not known and 105 fatalities occurred in the USA in 1937 (Wax, 1995). This and similar incidents in the USA resulted in establishing laws that require the safety testing of drugs on animals before they go to the market. In Europe, the major incident was due to the drug thalidomide. This was used as an effective painkiller for coughs, insomnia, headaches, cold and to treat morning sickness in pregnant women. Soon after the drug went to market, more than 10,000 children in 42 countries were born with body malformations including missing limbs (Botting, 2002). Even though animal testing was performed, it had not been tested not done in pregnant animals to identify foetal toxicity (Botting, 2002, Rehman et al., 2011).

Apart from incidences similar to the above, drugs may lead to idiosyncratic “Drug Induced Liver Injury” (DILI) (Stine and Chalasani, 2015). Idiosyncratic DILI is caused by induced hepatotoxicity without obvious aetiology (Teschke and Danan, 2016). Individual variability, genetic and environmental factors may affect the CYP450 enzymes and result in incompetent metabolism of a drug that leads to liver toxicity and result in acute liver injury (Chalasani

and Björnsson, 2010). Information about potential adverse drug reactions are provided along with the drug, however data on hepatoxicity investigations is not always easily accessible (Björnsson, 2016). Drug and toxicity testing models that represent a wide spectrum of the population are required so that idiosyncratic DILI cases can be potentially prevented.

Overall, regulatory authorities concerned on public health, still require animal experimentation to establish the safety of drug at the pre-clinical stages. However, concerns about the humane treatment of animals are widely recognised (Akhtar, 2013). *In vitro* models can help understand aspects of the underlying biology and toxicity of drugs; however they are not entirely predictive of the whole-body situation (Akhtar, 2015, Shanks et al., 2009).

1.5. Animal Models in Research, Species Differences & Limitations

A range of animal models are currently available ranging from models to identify the function of a single enzyme/transporter or mouse models where the liver has been repopulated with human hepatocytes (Denayer, 2014). However, species differences must be considered when selecting a model as this will potentially affect the translation of the results into clinical trials. Table 1summarises the key advantages and disadvantages of each model.

Table 1 Advantages and disadvantages of animal models in the drug development and testing

Model	Advantages	Disadvantages
Knock-out models of the selected enzymes or transporter.	-Address questions related to a single enzyme or transporter. -Understanding the function of particular genes in drug metabolism by genetic inactivation of the gene of interest (Jiang et al., 2011)	-Data generated from pre-clinical animal models is frequently different in humans. -Species differences caused by a lack of specific enzyme in humans/ animals, presence of a similar enzyme (orthologue) that produces a different form of metabolite in different species or reduced enzyme activity in animals when the same enzyme is highly active in humans (Baillie and Rettie, 2011)
Humanised mouse models	-Generated by deletion of the mouse orthologue gene and insertion of the human genes (Brehm et al., 2013) such as mutant superoxide dismutase	-Expression of the gene cannot be controlled and adjusted at human levels thus the expression can be lower or in a different scenario, expression at the wrong tissue due to

	1 which is the cause of Amyotrophic lateral sclerosis (Gajowiak et al., 2015)	lack of regulatory sites and promoter in the mouse genome relevant to the human (Sinz, 2012, Jiang et al., 2011) -Species differences are significant and data collected in any single species cannot translate to induction in other species and particularly in humans (Sinz et al., 2008, Martignoni et al., 2006, Graham and Lake, 2008)
Chimeric mouse model	-Recapitulate key areas of drug metabolism based on human liver cells (Katoh and Yokoi, 2007). -Capable to demonstrate metabolic profile specific to humans and separate from the wildtype mice as well as prediction of human metabolites derived from multiple metabolic reactions (Kamimura et al., 2010, Strom et al., 2010, Denayer, 2014)	-As the mice are immunocompromised, cannot be used to analyse immune-mediated drug toxicity -Cannot be used to identify extrahepatic human-specific factors affecting drug metabolism or clearance -As the degree of biliary tract humanization varies, cannot be used to predict the clearance of drugs in humans as it is dependent on human-specific transporters (Nishimura et al., 2013)

1.6. Animal Welfare & Reduction, Replacement and Refinement (3Rs)

Animal research has contributed a vast amount of information during the last decades however, its usefulness and suitability is currently debated. In the years before regulation of animal research, major discrepancies had been made and the lack of consistencies was evident in experimental planning which provided misleading conclusions that later did not translate in the clinical domain (Pound et al., 2004, Denayer, 2014). Examples of these discrepancies are lack of set guidelines for reporting animal data, methodological biases towards healthier animals and exclusion of negative results, the use of young animals that have no diseases, flaws in experimental design, initiation of the clinical trial before completion of the pre-clinical trial, but more importantly lack or randomisation and blinded trials (Hackam, 2007, Pound et al., 2004, Denayer, 2014). As a result, translation into the clinic was difficult and required more stringent criteria and methodologies to justify the use of animals in research.

In the United Kingdom (UK), efforts to minimise the number of animals in research and use of *in vitro* models was highlighted in 1959 with a seminal book "The Principles of Humane Experimental Technique" setting the cornerstone that later formed the framework for the "National Centre for the Replacement, Refinement & Reduction of Animals in Research – 3R's". The three proposals were to reduce the number of animals to the minimum necessary per study, replacement of animal model with non-sentient models or *in vitro* experiments and if animals have to be used, then refinement of an experimental procedure to cause the minimum pain and distress (Flecknell, 2002). The 3R's framework is used as an area of common ground for research workers who use animals influencing the way animal research is done (Flecknell, 2002, Festing and Wilkinson, 2007). Considering the disadvantages of animal research as well as animal welfare and alternatives currently available, *in vitro* drug testing and toxicity studies is becoming the best option.

1.7. *In vitro* Models of Liver Toxicity Testing

Advantages of *in vitro* models have been acknowledged since the early 90s and include a reduced number of animals used in research, reduced cost to animal maintenance and care, shortening of the time needed, use of smaller quantities of the drugs, high throughput experiments for multiple candidate drugs and metabolites (DelRaso, 1993, Soldatow et al., 2013). In addition, due to the considerable variability in metabolism among different species, it is essential that the *in vitro* system can be used to more accurately predict metabolism (Kirchmair et al., 2015). Table 2 summarises the key advantages and disadvantages of each model.

Table 2 Advantages and disadvantages of *in vitro* models in the drug development and testing

System	Advantages	Disadvantages
Recombinant single enzymes in a controlled environment	-Simple and easy to use -Controlled environment	-Rarely used nowadays -Not high throughput
S9 fraction	-Contains Phase I and Phase II	-Some metabolic pathways require

	Enzymes and is isolated by a series of centrifugation steps (Richardson et al., 2016).	complete cellular models that contain all 3 Phases of metabolising enzymes and can simulate complicated biotransformation processes (Sinz, 2012).
Microsomal fraction	-Specifically contains the CYP450 enzymes responsible for Phase I.	
Organ slices	-Level of intercellular connections between multiple cell types such as endothelial cells and fibroblasts (Liu et al., 2014). - prepared and used predominantly for liver but also for kidney, intestine, heart, brain and lungs (De Kanter et al., 1999).	-Declining enzyme activity, within 24 to 96 hours upon culture conditions -The slices have to be used fresh and cannot cryopreserved (Sinz, 2012, Westra et al., 2016). - The thickness of the slice often acts as a diffusion barrier for access of drug and oxygen. Necrosis occurs within 48-72 hours in culture and the rate of metabolic activity is significantly reduced after 6-72 hours (Vickers and Fisher, 2004).
Organ perfusion	-Adjustment of concentration of the drug, rate of drug delivery in a way that is not possible in whole animal experiments (Curtis et al., 2002).	- An organ is required for each individual experiment, which translates as an equal number of animals to an animal study.

1.8. Immortalised Cell Lines

Early drug discovery and high-throughput studies usually employ immortalised cell lines whereas, in later stages and drug characterisation, primary cells constitute a favourable option (Soldatow et al., 2013). Immortalised cell lines can grow and divide indefinitely in culture hence providing a readily available, inexpensive supply of cells for drug screening. Commonly used immortalised liver-derived cell lines in use are Fa2N4, Hep3B, HBG and predominantly HepG2 and HepaRG (Guillouzo et al., 2007, Ramboer et al., 2015b, Soldatow et al., 2013). The HepG2 cell line was generated in the 1970 and shows expression of liver-specific genes, however the expression is variable between different laboratories or between passages of HepG2 cells leading to difficulties comparing results and making conclusions. HepaRG cell line was isolated from a hepatic-differentiated grade 1 Edmonson hepatocholangiocarcinoma (Gripon et al., 2002). It shows high proliferation capacity, expression of liver-specific genes, Phase I, II and III enzymes, nuclear receptors and membrane transporters. Unfortunately, expression of liver-specific enzymes in HepaRG, HepG2 and in im-

mortalised cell lines is considerably lower than the expression in primary hepatocytes and is highly variable (Guo et al., 2011, Gerets et al., 2012). HepaRG cell line's expression is closer to the primary human cells; however the sensitivity to identify hepatotoxic compounds within a screen is considerably lower compared to primary hepatocytes (Gerets et al., 2012). Lastly, because of the large variation in expression of drug metabolising enzymes and transporters within the population, immortalised cell lines derived from a single donor have a very low predictive value for the whole human population and the results generated cannot be representative (Sison-Young et al., 2015).

1.9. Primary Hepatocytes

Because of the disadvantages of all the above systems, primary animal and human primary hepatocytes (pHEPs) have been the gold standard for *in vitro* toxicity testing producing a comprehensive picture of hepatic metabolism for candidate drugs (Zeilinger et al., 2016). They can be used fresh but also cryopreserved for long periods of time, enabling routine and high-throughput assays. Isolation is based on a two-step perfusion method and dissociation with collagenase (Lee et al., 2013). The disadvantage of cryopreserved hepatocytes is that the quality is not always consistent (Stéphenne et al., 2010) as well as the scarcity of human liver tissue as a key issue (Lecluyse and Alexandre, 2010).

When in two-dimensional culture conditions, pHEPs can maintain functional activities for approximately 24-48 hours (Elaut et al., 2006, Zeilinger et al., 2016). This window of opportunity is enough for enzyme induction studies, inhibition studies and allows medium-throughput screening of compounds however, it doesn't allow for long-term studies. After a few days in culture, primary cells will start to undergo changes in cellular morphology, structure, polarity, significantly reduced gene expression and liver-specific functions that are all described under the term "dedifferentiation" (Treyer and Müsch, 2013). Dedifferentiation occurs due to loss of the liver microenvironment that translates as loss of cell to cell

interactions, loss of polarity within the liver and membrane-bound structures or even due to different oxygen tension (Guo et al., 2017). Therefore, a major bottleneck to the two-dimensional studies is the longevity of the cell culture and the significant deterioration of the metabolic functions.

To maintain liver-specific functions in primary cell cultures for longer periods, recapitulation of the three-dimensional environment within the liver has shown significant advances, improved stability and function of drug metabolising enzymes. Use of the "sandwich" configuration where primary cells are placed between two layers of matrix that can be Matrigel or Collagen and leads to increased liver-related functions, restored morphology of the cells, induced the formation of cell to cell interactions, prolonged the expression of drug metabolising enzymes and mimic *in vivo* biliary excretion (Keemink et al., 2015).

Suspension culture of primary hepatocytes represents a functional unit of drug metabolism containing enzymes and co-factors that are required to demonstrate complex multistep metabolic reactions (Soldatow et al., 2013). However, drug testing in different vessels requires single cells the use of digestive enzymes to dissociate cell clumps. This leads to damage in surface receptors, cell junctions, antigens and cell membranes of the dissociated cells, leading to the loss of their metabolic activity within 4-8 hours after isolation (Weeks et al., 2013).

Co-cultures of primary hepatocytes with liver sinusoidal endothelial cells within a collagen gel have improved functions of the hepatocytes such as albumin production and CYP450 activity essentially highlighting improved stability and long-term culture (Bale et al., 2015). Use of spheroids as a model system to investigate DILI have been developed with primary human hepatocytes and whole proteome analysis identified that the cells retained their phenotype, morphology and hepatocyte-specific functions for a minimum of 5 weeks (Bell et al., 2016). Development of bioreactor systems has offered advantages in mass culture

and maintenance of primary hepatocytes (Ebrahimkhani et al., 2014). Different designs have been employed and tested over time. Sophisticated devices such as hollow fibre bio-reactors deliver media to the cells through a network of capillaries, in a similar manner to the delivery of blood *in vivo*, proved advantageous in aspects such as albumin production compared to monolayer cultures (Storm et al., 2016). Another model is the microfluidic devices that can combine chambers of different living cells, interconnected with porous membranes where the flow of media simulates in-vivo conditions reporting increased survival of primary hepatocytes (Prodanov et al., 2016). Recently the combination of the 4 main types of murine hepatic cells were included in a microfluidics device and was reported that key structures, hepatic functions and primary immune responses were maintained in the physiological microenvironment (Du et al., 2017).

1.10. Human-Pluripotent Stem Cell-Derived Hepatocyte Liver Cells (HLC)

Current models of drug testing and toxicity screening do have advantages and translational power into the clinic, however as discussed above, each has its own limitations and disadvantages hence their potential and usefulness are limited. Since the new era in the drug industry requires screening of libraries containing thousands of compounds, efficient methods that use scalable hepatocyte populations in high-throughput studies are required and need to be developed. For this reason, models that are representative of the human population as well as readily available sources of functional hepatocytes and not limited by numbers of donors, are required.

hPSC could be used to generate a scalable population of HLC as an alternative to primary hepatocytes and immortalised cell lines (Szkolnicka and Hay, 2016). The key attributes that hPSCs show are self-renewing and the ability to differentiate into virtually any cell type in the human body. hPSCs are separated into two categories, human embryonic stem cells (hESC) and human induced pluripotent stem cells (hiPSC) that share common characteris-

tics but also have differences too. The key point is that the hPSC-derived HLCs could potentially become the next model for drug testing as they can be produced in unlimited numbers, within a short period of time and most importantly, hiPSC can be derived from different individuals that represent for the diversity within the population (Kilpinen et al., 2017).

1.11. Human Embryonic Stem Cells

Human ESCs were first derived from human blastocysts that were unsuitable for human implantation in 1998 (Thomson et al., 1998). Their characteristics were described that maintained a normal karyotype, producing cells with a high nucleus to cytoplasmic ratio, prominent nucleoli, express cell surface markers that characterise primate embryonic stem cells and express high levels of telomerase activity while they show the absence of markers and characteristics of early lineages (Thomson et al., 1998). After 4-5 month long-term *in vitro* culture, the hESC maintained the potential to differentiate to all three embryonic germ layers and terminal cell types such as neurons for ectoderm (Schulz et al., 2003), cardiac cells for mesoderm (Zweigerdt et al., 2003) and hepatocytes for endoderm (Shirahashi et al., 2004) as well as extraembryonic tissue (Thomson et al., 1998). Since then, a plethora of research laboratories have isolated and generated hESC lines, which have been used to generate cell types and enabled in-depth study of basic biology, disease modelling and further applications (Watt and Driskell, 2010).

Along with the major achievement and potential that has been given to science by the isolation of hESC, destruction of blastocysts, even though unsuitable for implantation, was a centre of controversy leading to the prohibition of work in some countries (Dhar and Hsi-En Ho, 2009). Therefore, efforts were made to establish hESC lines without destroying the blastocyst and subsequently human embryos. Derivation of hESC lines from a single blastomere of cleavage stage embryos was an alternative as mimics the procedure of preimplantation genetic diagnosis, a routine procedure in the assisted reproduction field for

selection of healthy embryos (Sills et al., 2005). Formal description of the type of research and potential impact on donor's privacy and future health was suggested to help couples undertaking *In vitro* fertilisation to decide whether the surplus of blastocysts is cryo-preserved, discarded or donated to science (Scully et al., 2012). Donation for human development research was already possible but now donation for stem cell research was an additional option (Kalista et al., 2011).

Generation of hESC lines that carry specific monogenic inherited diseases was possible and would help to model the diseases in a dish and potentially developing therapies (Ilic and Ogilvie, 2017). As a consequence, a small number of hESC lines have been derived from a small spectrum of diseases, due to the limited number of couples requesting for a Preimplantation Genetic Diagnosis. Even though the potential of these cell lines in finding treatments for those diseases was high, the cell lines haven't been widely used because of the limited spectrum of diseases represented, but mainly due to ethical issues associated with the destruction of the human blastocysts (Ilic and Ogilvie, 2017, Zheng, 2016)

1.12. Human Induced Pluripotent Stem Cells

Human iPSCs have been initially derived after re-programming of differentiated somatic cell types into stem cells by inducing expression of a set of 4 transcription factors *Oct 3/4, Sox2, c-Myc* and *Klf4* (Takahashi and Yamanaka, 2006). Delivery of the transcription factors occur using retroviral vectors that assist insertion of the transcription factor genes into the genome of the host cell leading to gene expression (Takahashi et al., 2007). However, due to the viral vectors not specifically targeting sites for integration, multiple genomic insertions could occur and the potential for spontaneous re-activation of transgenes could potentially lead to increased oncogenesis in the cell line (Seki and Fukuda, 2015, Shi et al., 2017, Okita et al., 2007).

Since then, developments in the delivery methods devoid of genomic insertions was achieved using a range of methods such as episomal DNA (Yu et al., 2009), adenovirus (Stadtfeld et al., 2008), PiggyBac transposons (Woltjen et al., 2009), non-viral minicircle vector (Jia et al., 2010), direct delivery of recombinant proteins (Kim et al., 2009), synthetically modified mRNAs (Warren et al., 2010), microRNAs (Miyoshi et al., 2011), small molecules (Biswas and Jiang, 2016) and non-integrated Sendai Virus technology (Fusaki et al., 2009) as the most competent system for hiPSC generation (Lieu et al., 2013, Shi et al., 2017). As a result, a plethora of hiPSC lines has been generated across the laboratories at different efficiencies and with different genetic and epigenetic variations (Liang and Zhang, 2013).

The differentiation potential of hiPSC is similar to the hESC and cell types from all the three lineages have been generated from hiPSC such as neuronal differentiation for ectoderm (Denham and Dottori, 2011), cardiac cells for mesoderm (Lim et al., 2016) and hepatocyte cells for endoderm (Song et al., 2009b). Compared to hESC, hiPSC demonstrate major advantages upon their use, enabling further applications. The major advantage of hiPSC compared to hESC is that since these cells are not derived from the destruction of a human blastocyst that later could form an embryo, their use is not ethically controversial (Zheng, 2016). As a result, hiPSC could now replace hESC in applications that previously ethical restrictions were applied.

Secondly, since the generation of hiPSC can be achieved from theoretically any individual, a collection of hiPSC lines that represent a range of genetic background could be generated (Holmqvist et al., 2016, Park et al., 2017). Finally, hiPSC have been derived from diseased patients and *in vitro* disease models have been generated enabling study of diseases in a dish that in combination with more recent genome editing CRISPR/CAS9 technologies (Kato and Takada, 2017) could potentially correct the disease leading to personalised cell therapies (Chamberlain, 2016, Molinari et al., 2017, Avior et al., 2016).

1.13. Differentiation of hPSC into Hepatocyte-Like Cells

Differentiation of the hPSC into cell types of all three germ layers opened the doors and enabled the study of a wide range of cell types including the highly important HLCs. Differentiation of hPSC into HLC could potentially generate a model that fulfils the criteria required for an expandable cell population that can mimic the complex biology of the human liver. One of the very first generations of HLC population from hESC, was achieved in 2003 and were characterised by expression of liver-associated proteins, accumulation of glycogen, inducible CYP450 activity and lack of AFP expression (Rambhatla et al., 2003).

That major milestone would have not been possible without previous knowledge and studies in model organisms predominantly mouse and rat (Hamazaki et al., 2001). Directing the differentiation of the hPSC into HLC is a procedure that closely mimics in-vivo liver developmental signalling pathways and mechanisms, artificially in a dish, using growth factors that are present *in vivo*. Therefore, understanding how liver development occurs *in vivo*, is essential to re-assure that the appropriate signals are present at the right time and concentration to drive the differentiation to a population that is phenotypically and functionally as close to primary human hepatocytes.

1.14. Liver Development

The development of the liver is a multistep process that occurs under defined signalling cascades, precisely regulated in a time and concentration dependent manner (Si-Tayeb et al., 2010a, Zaret, 2002). Development can be subdivided into 3 distinct stages each of which, cells acquire lineage specific characteristics and ultimately, specify into functional hepatocytes. Developmentally, hepatocyte specification follows three distinct stages. At the first stage the inner cell mass generates the three embryonic layers which are the endoderm, mesoderm and ectoderm. At the second stage, the endoderm generates a bipotential population of hepatoblasts that then, at the third stage, specifically mature into

hepatocytes (Zaret, 2002).

In vitro, evaluation and optimization of the required signalling molecules for each stage of the hepatocyte differentiation is the subject of a numerous reports however, lack of generally established criteria (Schwartz et al., 2014) as well as cell line differences (Allegrucci and Young, 2007) lead to variations on the protocols and duration for each treatment (Hay et al., 2008a, Magner et al., 2013, McLean et al., 2007, Teo et al., 2012, Sui et al., 2013). *In vitro* differentiation follows *in vivo* developmental rules; hence it is subdivided into the same three stages.

1.14.1. Stage I - Definitive Endoderm

According to mouse embryonic studies, upon zygote formation the stages that development follows are strictly regulated and lead to an increased cell number and implantation that then allows gastrulation mechanisms to the embryonic body plan as described (Tam and Loebel, 2007, Tang et al., 2016). Developmental cues that follow the blastocyst stage are relevant to mimic the liver development *in vivo*. Initially, gastrulation is evident in the mouse on day 6.5 by the appearance of the primitive streak in the posterior epiblast (Murry and Keller, 2008). Cells in the epithelial layer of epiblast, ingress through, migrate away and specify into mesoderm and endoderm whereas the remaining cells specify into ectoderm (Zorn and Wells, 2009, Murry and Keller, 2008). This process is called the Epithelial Mesenchymal Transition (EMT) and starts at embryonic day 7 (E7) in mouse (Zhao and Duncan, 2005, Murry and Keller, 2008). EMT is triggered upon the presence of appropriate stimuli and functions through changes in transmembrane adhesive proteins of polarized epithelial cells, enabling cell movement (Le Bras et al., 2012).

The signalling cues predominantly required for specification into Definitive Endoderm (DE) upon *Activin A/Nodal* and through the *TGFβ* receptor activation (Zorn and Wells, 2007, Arnold and Robertson, 2009) and *WNT/Frizzled* receptor pathway (Zhang et al., 2013,

Clevers, 2006).

Activin A/Nodal ligands seem to play a double role in cell development regulating both maintenance of pluripotency and differentiation to certain lineages (Brown et al., 2011). However, in differentiation studies to germ layers, studies have demonstrated that Nodal acts as morphogen, organizing the axial structures and giving a lineage identity to the epiblast cells (Shen, 2007, Lee et al., 2011). The importance of *Activin A* was proved upon inhibition of *TGFβ* receptors and commitment of cells to neuroectodermal lineage (Smith et al., 2008) together with the absence of DE marker expression (Kopper and Benvenisty, 2012). The developmental decision between mesoderm and endoderm is dependent upon Activin/Nodal concentration where low doses induce mesoderm and high doses induce endoderm formation (Shen, 2007, Vincent et al., 2003, Zorn and Wells, 2007).

Binding of Activin/Nodal to its receptor Alk4/7 activates phosphorylation of the cytosolic proteins Smad2/Smad3 (Singh et al., 2012, Costello et al., 2011). The phosphorylated Smad2/3 proteins, bind to Smad4 and the complex translocates to the nucleus where it associates with DNA-binding transcription factors such as Mix-like homeodomain proteins (Mixl1), Forkhead box H1 (FoxH1), Gata-zinc finger factors (GATA) and Sox domain factors (SOX) that are essential for stimulation of a gene cascade committing cells to the Definitive Endoderm lineage (Zorn and Wells, 2007, Vincent et al., 2003, Le Lay and Kaestner, 2010, Singh et al., 2012).

Mixl1 is an important regulator of this stage playing a role in lineage restriction and maintenance of high *Nodal* expression levels by an autoregulatory loop (Lim et al., 2009). Mixl1 is induced by *Nodal* and has an additional role to repress *Brachyury* expression, a master gene-regulator that upon Fibroblastic Growth Factor (FGF) presence, leads the differentiation into mesoderm (Pereira et al., 2011). Therefore, maintenance of a high *Activin/Nodal* expression during EMT is of utmost importance. *In vitro*, *Nodal* activity is replaced

by *Activin A* which binds to the same receptors, triggering similar cascades as *Nodal* (Wu and Hill, 2009, D'Amour et al., 2005, Sulzbacher et al., 2009).

In addition to the Activin/Nodal signalling, a successful EMT is also dependent upon activation of the WNT/Frizzled pathway. During EMT, changes in cellular adhesion molecules are essential to achieve cell migration (Tam and Loebel, 2007). Regulation of cellular adhesion is accommodated by the co-operation of a cell surface protein *E-cadherin* (van Roy and Berx, 2008) and the intermediate molecule *β-catenin*, that binds to the cytoskeleton and induces morphological changes (Choi et al., 2006). In the absence of *WNT* ligands, the cytoplasmic free β-*catenin* is flagged for degradation by the Glycogen Synthase Kinase 3 (GSK-3) impairing changes in cellular adhesion (Li et al., 2012, Larsen et al., 2003).

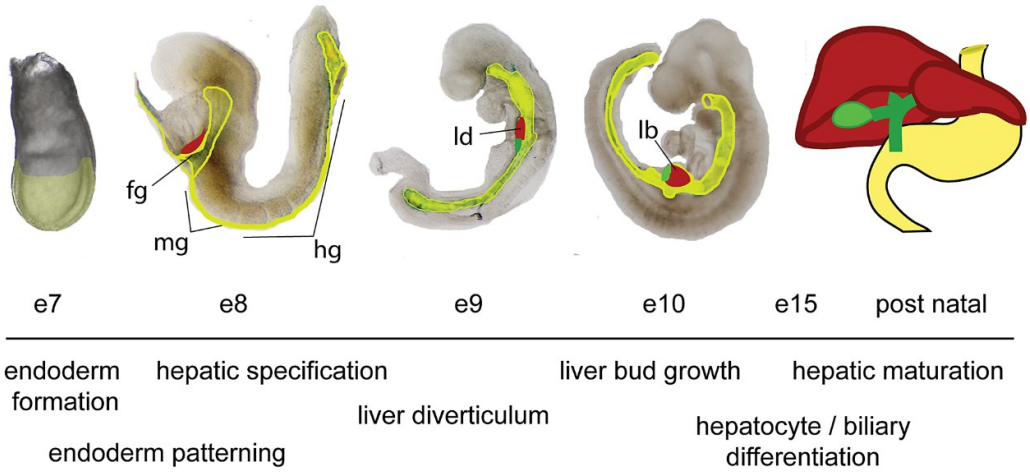

Figure 5 Early Mouse Liver Developmental stages from day 7 (e7) to postnatal. Gastrulation starts with signalling cues and the Primitive Streak gives rise to the Definitive Endoderm. The Definitive Endoderm is then formed as a tube from the anterior to the posterior, folds and generates the primitive gut tube with distinct regions of Foregut (fg) Midgut (mg) and Hindgut (hg). The liver develops from the Foregut region into the Liver Diverticulum (ld) and then the Liver Bud (lb) that eventually develops into the postnatal liver. Adapted from (Tang et al., 2016, Zorn and Wells, 2009, Murry and Keller, 2008).

In the presence of WNT ligands, inhibition of *GSK-3* is achieved and results in increased availability of *β-catenin* (Clevers, 2006). The cytoplasmic free *β-catenin* then plays a role as a transcription factor, binding to the DNA in a multiplex with the Transcription factor/Lymphoid enhancer-binding factor (TCF/LEF) and co-factors activating genes responsible for the proliferation and proteases such as *ADAM10* and *Presenilin-1*. Proteases, when

free in the cytoplasm, cleave the *E-Cadherins* to release the *β-catenin* to feed an autoregulatory loop. As a result, the *E-Cadherins* are not connected to the cytoskeleton (Huber et al., 2001), the cell is not adherent anymore enabling migratory capacity and invasiveness to assist EMT and DE specification (Kalluri and Weinberg, 2009, Heuberger and Birchmeier, 2010). Ultimately, DE emerges as a flat sheet of cells arising from the anterior end of the primitive streak, displacing the visceral extra embryonic endoderm of the yolk sack and surrounding the external surface of the mouse embryo (Zorn and Wells, 2009, Zhao and Duncan, 2005).

1.14.2. Stage II - Hepatoblast Cells

The flat sheet of DE cells folds in order to create the primitive gut tube structure (Si-Tayeb et al., 2010a). Formation of the primitive gut starts at E7.5 in mouse, simultaneously at both the anterior and posterior ends, where the epithelial sheet folds over towards the ventral midline, forming the foregut and hindgut pockets (Zorn and Wells, 2009). These two events expand towards each other, leading to the formation of a primitive gut tube by day 8 (Figure 5). The primitive gut is patterned in 3 major domains where each gives rise to different parts of the gastrointestinal track (Moore-Scott et al., 2007), the liver arises from the foregut endoderm along with gall bladder, pancreas and lungs (Figure 6) (Tremblay and Zaret, 2005). The midgut forms the small intestine and the hindgut generates the colon (Tremblay and Zaret, 2005).

Once the primitive gut is formed, the second wave of signalling cascade and transcription factors initiate. Position of the early liver cells named “Liver Diverticulum” occurs adjacent to the developing heart called the “Cardiogenic Mesoderm” and Septum Transversum Mesenchyme (STM). Both are key to drive the differentiation towards the hepatic specification of the Liver Diverticulum (Serls et al., 2005, Rossi et al., 2001, Si-Tayeb et al., 2010a). The Cardiogenic Mesoderm and STM are sources of Fibroblastic Growth Factors (FGFs) and

Bone Morphogenetic Proteins (BMPs) respectively, that induce initiation of hepatoblast specification resulting in the Liver Diverticulum formation by day 9 (Figure 5). FGFs act in a concentration dependent manner, highlighting the importance of DE position in relation to the heart (Serls et al., 2005). The DE cells distal to FGF signalling are exposed to low FGF levels, hence proceed to a pancreatic fate, whereas DE cells next to the Cardiogenic Mesoderm initiate a lung gene expression program (Tremblay and Zaret, 2005, Zaret, 2002). DE cells in between of these two regions, receive intermediate levels of FGF and this initiates a liver related differentiation program, into hepatoblasts that initially show expression of albumin (ALB) protein (Zorn and Wells, 2009, Calmont et al., 2006). In addition to the FGFs, BMPs secreted from the Septum Transversum, play an essential role in facilitating a hepatic gene expression program while restricting the pancreatic fate (Zaret, 2008). BMPs induce expression of the nuclear transcription factor Gata4 and together with the master hepatocyte transcriptional regulator FoxA2, initiate expression of ALB securing an early hepatic gene expression program (Zorn and Wells, 2009, Si-Tayeb et al., 2010a). FoxA2 has been identified as a master transcriptional regulator because not only does it bind DNA and activates transcription, but due to the conserved wing-helix motif in its structure, it can facilitate de-condensation of tightly compacted nucleosomes. Compaction of DNA at the early developmental stages is a mechanism to assist and help with maintenance of a pluripotent profile. However, during liver development, restriction to the liver faith is achieved by FoxA2 binding to a conserved region at the enhancer site of ALB, de-compacting the DNA and enabling transcriptionally activation, restricting the potential of the cells to the liver lineage (Shin and Monga, 2013, Le Lay and Kaestner, 2010).

Expression of Haematopoietically expressed *Homeobox hex* (*Hhex*) genes are also required to enhance the liver-specific gene expression program in the developing liver diverticulum (Watanabe et al., 2014, Hunter et al., 2007, Bort et al., 2006). However, in the presence of WNT ligands, the WNT pathway represses *Hhex* gene expression and instead initiates an

intestinal gene expression programme by activation of Caudal-related homeobox genes (Hunter et al., 2007). Therefore, the presence of WNT inhibitors is ensuring the expression of genes related to the liver specification (McLin et al., 2007, Si-Tayeb et al., 2010a). In summary, generation of the liver diverticulum is primarily achieved upon successful expression of *Hhex* and *Albumin* (Zorn and Wells, 2009, Zhao and Duncan, 2005).

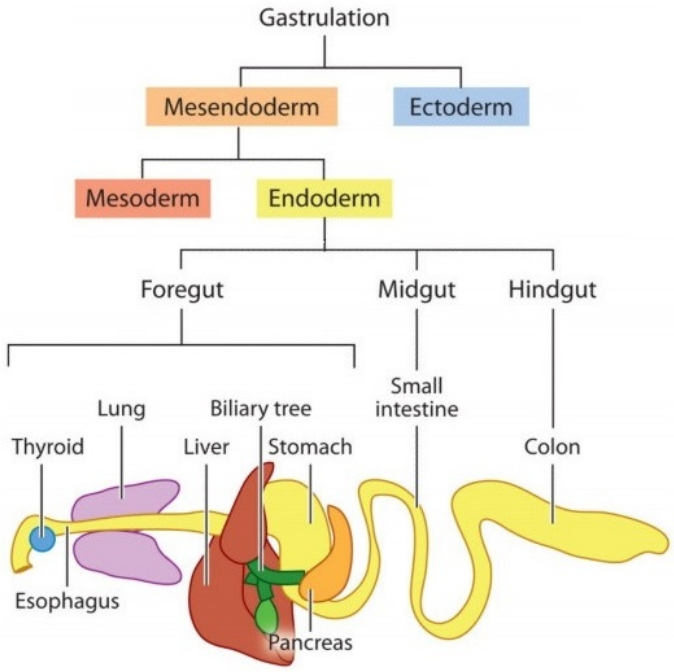

Figure 6 Specification of the gut tube and generation of the gastrointestinal organs from foregut, midgut and hindgut. Adapted from (Zorn and Wells, 2009).

Proliferation and expansion of the hepatoblast population within the liver diverticulum, is accompanied by a transition of the cells from a simple cuboidal morphology, into a pseudo-stratified epithelium (Bort et al., 2006). The hepatoblast cells now have proliferated to a number that cannot be restricted into the liver diverticulum resulting in breakage of the surrounding basement membrane and migration into the STM forming the Liver Bud by day 10 (Figure 5) (Zorn, 2008, Zorn and Wells, 2009, Si-Tayeb et al., 2010a). The process of cell migration into the STM is under the control of defined inductive signals (Si-Tayeb et al., 2010a).

The transcription factor *Prospero-Related Homeobox 1 (Prox1)* is essential for migration and formation of the Liver Bud (Burke and Oliver, 2002). Expression of *Prox1* initiates on day 8.5 and induces downregulation of *E-Cadherin*, enabling cells to transition from mesenchymal to epithelial, and form the liver bud (Bort et al., 2006). In addition, the transcription factors *Onecut-1 (HNF6 or OC-1)* and *Onecut-2 (OC-2)* have an inductive role into the degradation of the basal lamina and promoting of hepatoblast migration (Margagliotti et al., 2007).

In vitro differentiation of DE cells to hepatoblasts is achieved by recapitulating *in vivo* conditions with the use of *BMP4* and *FGF2* growth factors (Yanagida et al., 2013, Si-Tayeb et al., 2010a, Song et al., 2009b). Another approach commonly used for hepatoblast specification is the use of Dimethyl Sulfoxide (DMSO) (Hay et al., 2007). The exact mechanism of action is not known, however it is known that the DMSO is able to maintain liver metabolic functions and morphology features in primary hepatocyte monolayer cultures (Discussed in (Su and Waxman, 2004)) as well as acts as a stabiliser for cell membranes leading to improved hepatocyte morphology (Duan et al., 2010). Additionally, since cost is a factor of consideration, the use of DMSO is a viable alternative for *in vitro* differentiation.

1.14.3. Stage III - Liver Cells

The liver bud can morphologically be identified as an anatomical outgrowth that rises from the ventral wall of the foregut (Zorn, 2008). Invasion of hepatoblasts into STM and the formation of the liver bud is accommodated by the development of hepatic vasculature (Shin and Monga, 2013). Endothelial cells and developing stellate cells from STM, contribute in the liver bud development secreting expression of proteins and growth factors (Shin and Monga, 2013, Freedman et al., 2007) as well as chemotactic factors assisting proliferation and differentiation of the bipotential hepatoblast population into hepatocytes or biliary cells (Zorn, 2008, Tatsumi et al., 2007). Expansion of the hepatoblast population occurs upon activation of multiple signalling pathways with a significant cross-talk and cell-cell inter-

actions. The inducing factors are produced from the endothelial cell, Hepatic Stellate Cells and Haematopoietic Stem Cells present in the surrounding tissues (Shin and Monga, 2013).

Hepatocyte Growth Factor (HGF), the most potent growth factor for the liver lineage, is produced by mesothelial cells from the STM and stimulates proliferation, motility and angiogenesis in developing liver (Nakamura and Mizuno, 2010, Onitsuka et al., 2010, Ishikawa et al., 2012). It mediates its action by binding to its only high-affinity receptor, c-Met (Ishikawa et al., 2012). Receptor c-Met is widely expressed in hepatoblasts and upon HGF binding, it translocates b-catenin in the nucleus leading to activation of genes responsible for hepatocyte maturation and proliferation (Nejak-Bowen and Monga, 2008). Additionally, HGF regulates expression of integrins that are required for attachment to the ECM, hepatocyte proliferation and successful liver structure (Pinkse et al., 2004). A knockout mice model for c-Met fails to complete and dies *in utero* with multiple abnormalities and an underdeveloped liver (Bladt et al., 1995). HGF is used by a plethora of research groups at the final differentiation stage (Hannan et al., 2013, Hay et al., 2008b, Touboul et al., 2010).

In the developing embryo, haematopoiesis occurs in the liver and hematopoietic cells produce Oncostatin M (OSM), which induces a paracrine effect and is essential for the last phase of the differentiation (Kamiya et al., 2001, Richards, 2013). OSM induces characteristics of mature hepatocytes such as the morphological characteristics, induction of differentiation markers for the postnatal liver and functional maturation (Kamiya et al., 1999). The effect of OSM is mediated by the signal transducer gp130. Mice deficient for the glucocorticoid receptor show impaired expression of hepatic differentiation markers suggesting that gp130 is implicated in the process of hepatic maturation *in vivo* (Kamiya et al., 1999). At birth, the locus of haematopoiesis is changed from the liver to the bone marrow and subsequently, the levels of OSM are reduced. Decreasing the concentration of OSM at the last stages of hepatocyte differentiation could potentially mimic the embryonic development

closer (Jagannathan-Bogdan and Zon, 2013, Ding and Morrison, 2013). OSM is an essential factor in the *in vitro* differentiation protocols (Magner et al., 2013, Duan et al., 2010, Hannan et al., 2013, Toivonen et al., 2013).

The canonical WNT pathway is involved in the differentiation process from the embryonic stages to the later stages. Activation of WNT signalling during the early stages is required for a successful DE specification, discussed previously. Additionally, studies have shown that activation of WNT after the hepatic specification stage, allowed successful generation of proliferative bipotent hepatoblasts, which then were efficiently differentiated into hepatocytes (Touboul et al., 2016). Additionally, through complex signalling cascades induces hepatocyte specific signalling pathways. Activation of the β-catenin by secreted WNT ligands from the STM leads to initiation of glycogen storage, a characteristic hepatocyte function for regulation of glucose levels (Matsumoto et al., 2008). Finally, the importance of WNT3a and b-catenin expression for the later stages of liver development such as an outgrowth, expansion and differentiation, maturation, zonation and metabolic activity are highlighted by pioneering studies (Nejak-Bowen and Monga, 2008). The small molecule CHIR 99021 can bind on the GSK3β kinase and initiates the same responses as the WNT3a ligand, but with a reduced cost and increased stability (Leach et al., 2015).

Activation of the hepatocyte differentiation programme leads to activation of key transcription factors CCAAT/enhancer-binding protein beta (C/EBP) and Hepatocyte Nuclear Factor 4a (HNF4a) both essential for enhancing a hepatocyte gene expression program (Si-Tayeb et al., 2010a). The transcription factor C/EBP binds to the ALB enhancer region in the nucleus driving hepatocyte differentiation while inhibiting cholangiocyte lineage (Benet et al., 2010). The HNF4A's role is equally important as its binding to enhancer regions is crucial for expression of liver-related genes (Odom et al., 2004, Fang et al., 2012a). Additionally, HNF4a regulates cell adhesion proteins such as E-cadherin, an important regulator of

hepatocyte polarity and cell junction assembly for proper liver structure (Battle et al., 2006, Satohisa et al., 2005).

Glucocorticoids such as Dexamethasone and Hydrocortisone have shown to induce expression of both HNF4a and C/EBP, described as a powerful signal to assist hepatocyte differentiation (Michalopoulos et al., 2003). Differentiation and maturation of the hepatocytes are assisted by the activation of the Glucocorticoid Receptor and by regulation of the glucose metabolism affecting the maturation of the hepatocytes (Zhang et al., 2011b).

Differentiation of hepatoblasts into biliary cells is accommodated predominantly by activation of the transcription factors HNF1b and HNF6 (Si-Tayeb et al., 2010a). When C/EBP is suppressed, biliary differentiation takes place through the expression of HNF6 and HNF1β (Yamasaki et al., 2006). For differentiation into the biliary lineage, gradients of Activin on the TGFβ receptor regulate the differentiation of hepatoblasts into bile duct cells. High gradients of Activin are produced from the portal mesenchyme and can lead to the differentiation of hepatoblasts into biliary cell fate. Equally, lower gradients of Activin acting on the parenchyma cells are inhibited by the transcription factors OC-1 and OC-2 allowing only hepatocyte fate gene expression (Clotman et al., 2005).

The Notch pathway is also involved, inducing differentiation of hepatoblasts into biliary cells. Localisation of hepatoblasts next to the portal vein mesenchyme is affected by a secreted Notch activator, Jagged 1, that triggers downregulation of hepatocyte transcription factors such as c/EBP, ALB, HNF4A (Tchorz et al., 2009) while upregulates HNF1β and HNF6 resulting in differentiation into biliary epithelial cells (Tanimizu and Miyajima, 2004).

Morphology of HLCs in culture resembles the morphology of isolated primary hepatocytes in-vitro (Figure 7). The cells are characterised as a) polygonal shaped cells b) they have distinct round nuclei, c) may be multi-nucleated cells, d) formation of vacuoles is indicative of mature hepatocyte functions such as glycogen storage, e) distinct cell membrane and e)

representative size approximately >30-50uM (Schmelzer et al., 2006, Hannan et al., 2013, Behbahan et al., 2011, Hay et al., 2008b).

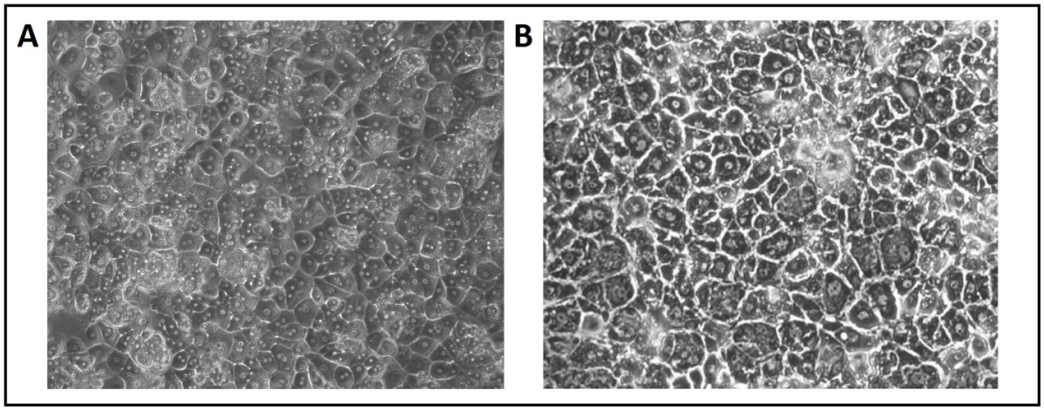

Figure 7: Images demonstrating hepatocyte morphology A) Human primary hepatocytes **B)** hESC-derived hepatocytes. Cells exhibit polygonal morphology, distinct round nuclei often multi-nuclei, presence of vacuoles and distinct cell membrane with thick regions. A) adopted by www.vitacell.com and B) adopted by (Hay et al., 2008b) Original images do not provide scale bars.

Overall, liver development is a strictly regulated process, accommodated by several signalling pathways, activated by secreted factors produced by hepatoblasts/hepatocytes as well as from the surrounding environment. Time precise activation of signalling cascades is equally essential for the appropriate flow of the events. All these factors will eventually lead to successful liver formation and function within the developing embryo. *In vitro*, hepatocyte maturation stands as the final and most variable part of the differentiation among different research labs. Strategies have been designed to replicate the role of growth factors in embryonic development and signalling pathways induced by factors discussed above (Si-Tayeb et al., 2010a). However, the key recipe to generate HLC morphologically and functionally like the adult human liver has not been described yet.

1.15. Advantages and Disadvantages of Hepatocyte-Like Cells

Differentiation of hPSC to hepatocytes cultured in two-dimensions is the current standard method for HLC production across different laboratories (Hannan et al., 2013, Sullivan et al., 2010, Hay et al., 2008b, Touboul et al., 2010). Advantages and disadvantages associated with HLCs are presented in Table 3. In addition to, a great advantage is that can be used as

models to study biological systems such as viral infection and replication (Si-Tayeb et al., 2012) especially when it comes to modelling hepatitis B (Sakurai et al., 2017) and hepatitis E (Helsen et al., 2016) virus replication and host interaction, modelling of liver metabolic disorders (Rashid et al., 2010, Yusa et al., 2011) such as fatty liver disease (Graffmann et al., 2016) or basic biology and regulation of gene expression (Schadt et al., 2008) as well as many more examples (Guguen-Guillouzo and Guillouzo, 2010). Finally, can also be used for drug screening of new compounds (Csöbönyeiová et al., 2016, Davidson et al., 2015).

Table 3 Key advantages and disadvantages of the Hepatocyte Like Cells.

Advantages	Disadvantages
Quick generation of HLCs within 17-23 days (Hay et al., 2007)	Long term maintenance of metabolic enzyme functionality (Tayeb et al., 2010)
Expression of key metabolising enzymes and secretion of key soluble proteins (Si-Tayeb et al., 2010b)	Limited by the cell culture conditions and low activity of drug metabolizing enzymes (DMEs) (Kim et al., 2016)
Morphology characteristics similar to the human primary Hepatocytes (Hay et al., 2008)	Low level of Phase I and Phase II metabolizing activities (Jensen et al., 2009, Kia et al., 2013)
Model system to study liver-related diseases (Schwartz et al., 2016)	Cells are not connected to the circulation or other organ systems and lead to lack of suitable absorption, distribution, metabolism, and excretion (ADME) properties (LeCluyse, 2001)

This difference in the maturity levels and expression of mature enzymes and functions in stem-cell derived populations is not surprising. An in-depth study comparing HLCs with human foetal and human adult hepatocytes evaluated aspects such as hepatocyte marker expression via immunocytochemistry, proteomic analysis, gene expression analysis by RNA-sequencing and phenotypic analysis. The results have indicated that indeed the differentiation stages mimic the human liver development, but the HLCs produced to show a higher degree of similarities to the human foetal than human adult hepatocytes (Baxter et al., 2015).

Stem-cell derived cardiomyocytes face the same limitations exhibiting a functionally immature, disorganized, foetal-like phenotype; therefore ways to close the big functionality gap

is currently an area of interest (Scuderi and Butcher, 2017, Kolanowski et al., 2017). Not only cardiomyocytes but also Stem-Cell derived neurons (Lam et al., 2017), insulin-producing beta cells (van der Meulen and Huising, 2014) and lung organoid models (Dye et al., 2016) face similar limitations.

The advantage of generating cell populations from stem cells within a few days is already a huge progress in the field. However, since the adult cells have had a longer life span in the human body, are expected to show a higher degree of adaptation and maturation. To achieve a full mature profile that recapitulates characteristics of adult liver cells in the generated HLC population, manipulation of cell intrinsic and extrinsic signalling pathways is required. Understanding the importance of fine adjustments in transcriptional activation and expression of drug metabolising enzymes and transporters (Rashid et al., 2015). The metabolic functions of the liver are divided further into foetal, neonatal and adult stages, which reflect and are also influenced by differences in the source of nutrition. Therefore, there are critical maturation steps toward adulthood during which hepatocytes prepare for a new phase of life (Kamiya et al., 1999). This is the basis that this thesis has been built on and is investigating factors that could achieve progress towards this direction and go a step further towards adult hepatocytes.

1.16. Maturation of HLCs

Maturation of HLC has been the topic of multiple publications in the field. Strategies to increase expression of Phase I and II enzymes have achieved a considerable progress however, a set of factors that can be used during the differentiation to assist the generation of HLCs to as close as possible to the human primary hepatocytes has not been found. In this literature review, identification of compounds that have achieved to induce a positive change in HLC and generate more mature, adult-like HLCs was completed. The list contains a plethora of different factors such as nutrients, hormones, cytokines, vitamins, growth fac-

tors, small molecules, epigenetic agents, bile acids, environmental factors, signalling pathway modulators, lipids and trace elements. Out of the total number, 40 factors have been selected as the most potent and/or physiologically relevant to be included in this study (Table 23 Appendix).

1.17. Efficient Evaluation of Multiple Parameters Simultaneously & Design of Experiments

There are limited methods for characterising the impact (effect) of a certain parameter (factor) or a number of parameters in a system and evaluate the outcome (response). The most common method, extensively used in the literature, is the traditional One Factor At a Time (OFAT) designs. OFAT are based on a trial and error method, characterising the effect of a single factor measuring the response generated (Collins et al., 2009, N Politis et al., 2017).

OFAT design is simple and straightforward in application and analysis yet suboptimal. This is because the factors vary in concentration separately, exploring a very small fraction of the experimental space, hence generating graphs with the responses separately (Figure 8A) (Anderson, 2010). As a result, evaluation of multiple factors, one at a time, leads to multiple experiments increasing the experiment time, the labour and the expense. Most importantly, since in biology interdependencies among the factors (factor interactions) are vital, an OFAT approach will ignore these interactions and will remain concealed. Therefore, alternative methods are required to improve understanding of the experimental space, generate more informative results, reduce the labour and decrease the expense.

Design of Experiments (DoE) is a methodology developed to accommodate experiments dealing with multiple factors yet yielding the maximum amount of information possible. Inspired by Sir Ronald Fisher, a statistician working in the agricultural field in the 1920's, factorial and reduced-factorial designs were developed to study many factors in parallel,

matrix-based test plans (Hand, 2015). DoE offers tremendous efficiencies over the serial OFAT designs. Experimental runs combine a low or a high concentration for each factor, can simultaneously evaluate the effect of the factors and identify the best region of optimum within the experimental space (Figure 8B). In summary, the DoE offers the following advantages over OFAT a) fewer runs leads to fewer resources, hence less expensive, b) less time consuming, c) more precise estimates of the effects of each factor, d) information obtained covers a wider experimental space than an OFAT design and e) interdependencies among factors are revealed (Collins et al., 2009, Buyel and Fischer, 2014).

The majority of studies to date attempting to improve the maturation of hepatocytes *in vitro* have used the traditional OFAT approach testing single factors. Therefore, the main focus of this thesis was to apply a DoE approach to investigate multiple factors in the current hepatocyte differentiation model established in the laboratory and evaluate the effect of factors that may induce maturation of HLCs.

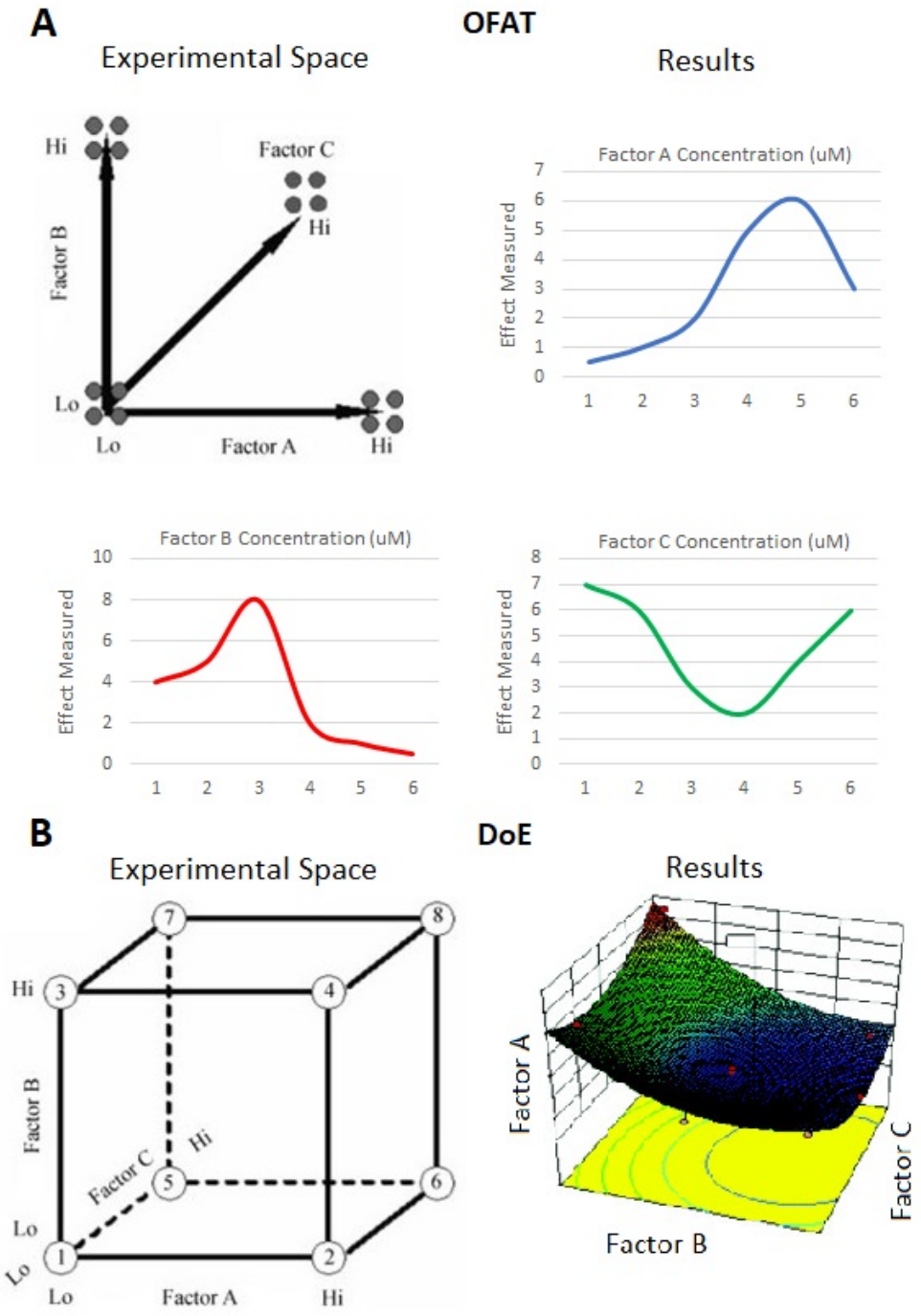

Figure 8 Description of OFAT and DoE Designs. A) OFAT Design and the experimental space that the low and high of each factor can investigate. Example graphs of data generated for each individual factor at different concentrations **B)** DoE and the cubic example of the experimental space, combining low or high concentration for the factor simultaneously and the results generated highlighting the experimental space optimum (Anderson, 2010).

CHAPTER TWO

MATERIALS & METHODS

2. Materials & Methods

2.1. Media Composition

hPSC Un-Conditioned Medium: DMEM/ F12 (LifeTech 11320), KSR 15% (LifeTech 10828), GlutaMAX 1% (LifeTech 35050), NEAA 1x (LifeTech 11140), bFGF 8ng/ml (Peprotech 100-18B), BME 100nM (Sigma M7522).

hPSC Essential 8 Commercial (LT-E8): Thermo-Fisher (Cat #A1517001).

hESC Essential 8 Homemade (HM-E8): The HM-E8 was made following the recipe provided by (Burridge et al., 2014) and containing the following: DMEM/F12 with L-glutamine and HEPES (Corning 10-092-CM), 64 µg/mL L-ascorbic acid 2-phosphate (Sigma 49752), 20 µg/mL insulin (LifeTech A11382), 5 µg/mL transferrin (Sigma T3705), 14 ng/mL sodium selenite (Sigma S5261), 100 ng/mL FGF2 (Peprotech 100-18B), 2 ng/mL TGFβ1 (Peprotech 100-21), 100 ng/mL heparin sodium salt (Sigma H3149).

Hepatocyte Differentiation Media:

Medium A: RPMI 1640 (LifeTech 21875), B27 1x (LifeTech 17504), Activin A 100ng/ml (Peprotech 120-14), WNT3A 50ng/ml (R&D 5036-WN-010)

Medium B: DMEM/F12 (LifeTech 11320), KSR 15% (LifeTech 10828), GlutaMAX 1% (LifeTech 35050), NEAA 1x (LifeTech 11140), bFGF 4ng/ml (Peprotech 100-18B), BME 100nM (Sigma M7522), DMSO 1% (Sigma D2650).

Medium C: L15 Medium (Sigma L5520), Tryptose Phosphate Broth 8.3% (Sigma T8159), FBS 8.3% (Sigma F-4135), Insulin 1uM (Sigma I9278), Hydrocortisone– Hemi succinate 10uM (Sigma H4881), L-glutamine 0.83% (Invitrogen cat # 25030-024), Ascorbic Acid 0.245uM (Sigma A7631), HGF 10ng/ml (Peprotech 100-39), OSM 20ng/ml (R&D 295-OM-010).

HepG2 Maintenance Medium: DMEM (Invitrogen cat # 2121969035), 10% FBS (EU Approved, Invitrogen cat # 10270-106), 1% of L-Glutamine (Invitrogen cat # 25030-024) and 1% of Non-Essential Amino Acids (Invitrogen cat # 11140035).

Primary Human Liver Cell Supplements Media Supplement 1 (MS1) and Media Supplement 2 (MS2)

MS1: In 24ml water, dissolve 9.15g nicotinamide (Sigma N3376, Niacinamide) add:

i. 3ml of 3.75mg/ml zinc sulphate (Z4750) (= 13mM) final 1.3mM
ii. 3ml of 1.0mg/ml copper (II) sulphate (= 6mM) final 0.6mM
iii. 37.4µl of 4mg/1ml dexamethasone/Ethanol (SIGMA **D4902 or D1756) (=**10mM) final 12 µM
iv. 0.3ml of 0.25mg/ml sodium selenite (CARE! very toxic. Consult COSSH data for handling.) (Sigma S9133 1mg, to be dissolved in 4ml water, stored at 4°C) (= 1.5mM) final 15µM
v. filter sterilise

MS2: 2.5mg/ml transferrin (Sigma T1428) (approx. 3.1mM) in water (prepare 75mg/30ml); filter sterilise.

Small Molecules & Maturation Factors:
Manufacturing guidelines and specification sheet details are followed to prepare the stock concentrations in each case. Safety cabinet level 2 is used for stock preparation and filter sterilisation of the final product before aliquoting and storage. Stocks are kept at -20^{o}C unless specified to store at -80^{o}C.

2.2. Cell Culture

Type II biological safety cabinet was used for all manual cell culture. A type II biological safety cabinet enclosed the TECAN Freedom Evo 200 where the automated cell culture was conducted. Cells were maintained at 37^{o}C in a 5% CO_2 and humid atmosphere. Brightfield images were captured using a Nikon ECLIPSE TE2000-S inverted microscope or Cellavista Imaging Platform, SynenTec.

2.3. Cell lines

Human pluripotent stem cell lines were used to generate the data presented in this thesis, two being hESC lines (HUES7 and H9) and five being hiPSC lines (CP1, RBL, PhiCr, BT2, RBL_PAT). The hiPSC lines were generated using lentiviral vectors for OCT4, SOX2, LIN28 and NANOG or using the Sendai-virus based Cyto-Tune 2.0 system. Validation of the hiPSC

lines is currently written into a publication, data is kept confidential until publication date. Mouse embryonic fibroblasts were also used for the purpose of conditioning medium.

2.4. Coating culture surfaces with Growth Factor Reduced Matrigel™

hPSCs were routinely cultured on Matrigel™ basement membrane matrix (Matrigel) (BD Biosciences, 354234) coated flasks. Matrigel (BD Biosciences 354234) coating was achieved by diluting stock Matrigel at the ratio 1:100 into ice-cold 4°C DMEM (Invitrogen cat # 2121969035) and coating at 200ul/cm^2 of surface area. Coated surfaces (flasks and 96well plates) were left at RT for 45 minutes, or at 4°C overnight for the Matrigel to fully polymerise. Surfaces were stored at 4oC for up to a week. Prior to seeding cells, required a PBS (Invitrogen 14190169) wash and were left at 37°C to warm up.

2.5. Preparation of Mouse Embryonic Fibroblasts

Mouse embryonic fibroblasts (MEFs) were isolated from 13.5-day old mouse embryos. These were collected by sacrificing the pregnant female by cervical dislocation, removing the uterine horns and collecting the mouse embryos which were sacrificed by decapitation. Embryos were kept in Dulbecco's phosphate buffered saline (DPBS) (ThermoFisher Scientific, 14190-169), homogenised mechanically and by enzymatic dissociation using 0.25 % Trypsin EDTA (ThermoFisher Scientific, 10780384) and plated for expansion on 175 cm^2 T175 flasks (Nuclon Δ treated surface, ThermoFisher Scientific, 178883) with MEF culture medium. MEF culture medium was made using Dulbecco's Modified Eagle's Medium (DMEM, ThermoFisher Scientific, 10749764), 10 % (v/v) foetal bovine serum (FBS, ThermoFisher Scientific, 10664083), 1 % (v/v) L-Glutamine (ThermoFisher Scientific, 10104042) and 1 % (v/v) non-essential amino acids (NEAA, ThermoFisher Scientific, 10358342). Cultures were incubated at 37°C and 5% CO2 in a humidified incubator (Heracell 150). Passaging MEFs for expansion and for cryopreservation was carried by washing with DPBS, harvesting with 0.05 % trypsin EDTA (ThermoFisher Scientific, 10462502) for 1 min, neutralis-

ing with MEF culture medium, centrifugation at 200 g for 5 min (3-16 Sigma centrifuge) and re-plating in the fresh MEF medium. Cryopreserved stocks of MEFs were made at passage 1 by harvesting and then re-suspending cells after centrifugation in 10 % (v/v) DMSO (Sigma, D2650), 40 % (v/v) FBS and 50 % (v/v) MEF medium. The cell suspension was transferred to 1.8 ml cryotube™ vials (cryovials) (ThermoFisher, 377267) and stored at -80 °C for 24 hours in a Mr. Frosty™ Freezing container ((Mr. Frosty) Fisher Scientific, 5100-0001) containing isopropanol before transfer to liquid nitrogen.

2.6. Conditioning of Medium for hPSC culture (MEF-CM)

For generating MEF conditioned medium (MEF-CM), MEFs were thawed from liquid nitrogen, cultured to passage 3 where they were seeded on 0.1 % Gelatin- (Sigma, G9391) coated flasks and treated with Mitomycin C (ThermoFisher Scientific, 10286710) at a concentration of 10 µg/ml in MEF medium and seeded at a density of $4.8x10^6$ cells per 75 cm^2 flask (T75, Nuclon Δ treated surface, ThermoFisher Scientific, 156472). MEF-CM was generated by incubating MEFS in 25ml of hESC medium containing DMEM Ham's F12 (DMEM-F12) (Fisher Scientific, 11320-074), 15 % (v/v) KnockOut™ Serum Replacement (Fisher Scientific, 10236902) 1 % (v/v) NEAA, 1 % (v/v) Glutamax (Fisher Scientific, 10388582) 0.01 % (v/v) β-mercaptoethanol (Sigma, M7522) and 4 ng/ml human basic fibroblast growth factor (FGF, Peprotech, EC100-18) for 24 hr, after which this medium was harvested. The procedure was repeated daily for 7 collections and the collected MEF - Conditioned Medium (MEF-CM) was used after 0.2um filtration and addition of 8ng/ml FGF2 within 3 days of being stored at 4^oC or 3 months when stored at -20^oC. Multiple MEF batches were used during this work. Each batch of MEFs corresponded to a different mouse from which embryos were taken.

2.7. Growth and passage of hESCs with MEF-CM

Human embryonic stem cell line HUES7 were kindly gifted by Harvard University (Cowan et al., 2004). Successful continued culture was maintained by Accutase (Sigma, A6964) passag-

ing every 3 days on Reduced-Growth factor Matrigel pre-treated T25-flasks (T25, Nunclon Δ treated surface, Thermo-Fisher Scientific, TKT-130-150L) with CM for 24 hours. Medium was changed daily for cell culture. Human embryonic stem cell line H9 continued culture was maintained by Trypsin 0.05% (Invitrogen, cat #25300062) passaging every 3 days on Matrigel pre-coated T25-flasks with CM for 24 hours. Medium was changed daily for cell culture.

Briefly, on the 3rd day the cells were washed first with PBS and then 0.5ml of Accutase or Trypsin was added for 3 minutes at 37^{o}C. The cells were then detached and the enzyme neutralised using unconditioned medium and collected in a 30ml universal tube. A sample was collected for manual cell count and the cells were centrifuged at 160g for 4 minutes. The supernatant was aspirated and MEF-CM medium was added to a final concentration of 1x10^{6} cells per ml. Then, 1.5 ml containing 1.5x 10^{6} cells were seeded into a fresh Matrigel-coated T25 flask in a final volume of 5ml MEF-CM.

2.8. Growth and passage of hPSCs with LT-E8 or HM-E8

Culture of hPSCs (hESCs and hiPSCs) with LT-E8 or HM-E8 was maintained by TrypLE Select (Invitrogen cat# 12563011) enzymatic passage every 3 days on Matrigel pre-coated T25-flasks or Robot-Flasks. Medium was changed daily for cell culture. Briefly, on the 3rd day the cells were washed first with 5ml of PBS and then 2ml of TrypLE Select was added for 4 minutes at RT. The TrypLE was aspirated and the flask tapped until the cells detach. Then 5ml of medium was added with a final 10uM Y27632 (Tocris #129830-38-2) to collect the cells. Manual or Cedex counts were performed and 1x 10^{6} cells were seeded into a fresh T25 flask, 3x 10^{6} cells into a Robot-Flask in a final of 5ml or 20ml medium in the presence of 10uM Y27632.

2.9. Growth and passage of HepG2 with HepG2 Maintenance Medium

Culture of HepG2 cells was maintained by Trypsin 0.05% (Invitrogen, cat #25300062) enzymatic passage every 7 days in T75-flasks. Medium was changed every 3 days for cell culture maintenance. Briefly, on the 7^{th} day the cells were washed with 10ml of PBS and then 2ml of Trypsin was added for 4 minutes at 37^{o}C. The cells were then detached and collected in a 30ml tube using HepG2 medium. A sample was collected for manual cell count and the cells were centrifuged for 4 minutes at 160g. The supernatant was aspirated and HepG2 medium was added to a final concentration of $1x10^6$ cells per ml. Then, 1ml of Medium containing $1x\ 10^6$ cells were seeded into a fresh T75 flask in a final volume of 15ml.

2.10. hPSC (hiPSCs and hESCs) Differentiation to Hepatocytes

Differentiation of hESCs to Hepatocyte initially followed the published protocol from (Medine et al., 2011) and modified. In brief HUES7 cells (passage number between 25 and 32) were dissociated from a confluent flask and counted manually or using the Cedex (Hi-Res Cell Counter, Roche) and then seeded on a Matrigel pre-coated 96-well plate at the density of 17.000cells per well of 96 well plate or 52.000 cells/cm^2. 24 hours later confluency measurements were taken using the Cellavista (Automated Multi-Parameter cell analysis equipment Cellavista®, Synen-Tec). When the confluency was between 40-60%, treatment with 67ul of Medium A for 3 days was started (d0-d2). On d3, the medium was replaced by 134ul of Medium B. Cells were fed on d5 and d7 with 134ul of Medium B. On d8 the medium was replaced by 134ul of Medium C. Cells were fed with 134ul of Medium C on d10 and d12 and with 34ul of Medium C on d14, on d15 and on d16. Key difference in the technical step at the final version of the protocol developed in this thesis was the wash step with plain RPMI medium before initiation of the differentiation. For the days 0-2, use 100ul of Medium A instead of 67ul. For days 8-17, 200ul of Medium C were added and 100ul were replaced every other day until day 17.

2.11. Liver Perfusion and isolation of Hepatocytes

Perfusion of liver isolations was performed within the FRAME laboratories (Prof Andrew Bennett, University of Nottingham) following established protocols and methods for the isolation and culture of the human liver cells. The cells were collected upon perfusion and were seeded in 96 well plate formats, at the density of 126,300 cells per cm^2. Plates were fed for the desired number of days and fixed with 4% PFA at the FRAME laboratories and then were collected for further immunocytochemistry experiments.

2.12. Cell Analysis

2.12.1. Cell growth Curves

Determination of cell growth characteristics or population doubling times has been achieved by culturing in parallel at least 2 flasks of the same cell type for more than 5 passages (unless otherwise stated). Cell counts were taken at each passage and population doublings calculated based on the following equations:

- Cumulative population doubling = Sum (Log_{10}(fold increase in cell number per passage)/Log_{10}(2))
- Population doubling time (hours) = Cumulative time in culture/Cumulative population doubling.

2.12.2. Karyotype Analysis

Cell samples for karyotype analysis were collected at an exponential phase of growth, usually 48 hours post seeding. The cells were treated with 100ng/ml of KaryoMAX® Colcemid (Invitrogen 1512012) diluted in the culture medium for 1 hour at 37°C. All the contents, culture medium and cells, were collected and centrifuged. The pellet was resuspended in 0.6% sodium citrate (Fisher Scientific S/3320) and incubated for 20 minutes at RT. Then the sample was centrifuged and supernatant aspirated. The cells were resuspended in the fixing solution containing 16.7% glacial acetic acid in methanol, centrifuged and resuspended 3

times in total and then stored in -20^{o}C. G-band analysis of 30 metaphase spreads were completed by Mr Nigel Smith, Clinical Cytogenetics, Nottingham City Hospital in accordance with the International System for Human Cytogenetic Nomenclature International Guidelines (ISCN, 2005) and results were collected.

2.12.3. Immunocytochemistry

In brief, cell samples washed in PBS, fixed with 4% PFA for 15-20 minutes and permeabilised for 10 minutes using 0.1% Triton-X in PBS. Cells were washed 2x with PBS and then incubated with 10% Bovine Serum ALB Fraction V made in 0.1% Tween in PBS for 1 hour at RT. Cells were then washed 3x with 200ul of 0.1% Tween in PBS and incubated with 50ul per well of the primary antibody diluted in 1% Bovine Serum Albumin Fraction V made in PBS and incubated overnight at 4^{o}C. Cells were then washed 3x with 200ul of 0.1% Tween in PBS and incubated with 50ul per well of the secondary antibody diluted in 1% Bovine Serum Albumin Fraction V made in PBS for 1 hour at room temperature. Samples were washed 3x with 200ul of 0.1% Tween in PBS and incubated with DAPI (1ug/ul) for 30 minutes at RT and then washed and 200ul of PBS was added. Images were taken using either the Leica DMIRB inverted Fluorescence microscope or the Cellavista Automated Multi-Parameter cell analysis equipment Cellavista®, Synen-Tec or the High Content Imaging System Operetta ®, Perkin Elmer. Operetta wavelength details. Dapi: Excitation 360-400nm Emission 410-480nm, 488/EGFP: Excitation 460-490nm Emission 500-550nm, 568/DsRED: Excitation 520-550nm Emission 560-630nm, 647/DRAQ5: Excitation 620-640nm Emission 650-760nm. Negative controls containing the secondary only antibodies were included in the experiments showing specificity of the primary antibody. However, these results are not presented unless necessary.

2.12.4. Flow Cytometry

Cell samples were prepared to run through Flow Cytometry for identification of pluripotency marker expression. Briefly, a minimum of $0.5x10^6$ cells for each condition were dissociated using the specified enzyme and then centrifuged. The excess of enzyme was aspirated and the cells were washed with 20ml of PBS and centrifuged at 160g for 4 minutes. Then, the cells were fixed with 5% PFA for 15 minutes, centrifuged at 160g for 4 minutes and upon aspiration of the supernatant, the cells were resuspended with 20ml of PBS and were stored at 4^oC for up to 7 days until they were stained and analysed. Flow cytometry staining protocol and equipment provided by Mr. Jayson Bispham, University of Nottingham. Results and statistical analysis were performed with the help of Mr Jayson Bispham, University of Nottingham using the Beckman Coulter Moflo XDP equipment, Flow Cytometry Suite, Queens Medical Centre, Nottingham. The protocol used for staining and analysis parameters are kept confidential due to a pending publication.

2.12.5. Statistical Analysis

T-test analysis and two-way ANOVA performed where appropriate using the software GraphPad-Prism version 7. Significance represented by *$p<0.05$ and **$p<0.001$.

Table 4 Antibodies used for Immunocytochemistry

	Antibody	Company	Cat.Number	Fluorophore	Dilution	Specie
Primaries	FOXA2 / HNF3B	R&D	AF2400	-	1:100	Goat
	SOX17	R&D	AF1924	-	1:150	Goat
	AFP	ABCAM	ab3980	-	1:500	Mouse
	EpCAM	ABCAM	ab20160	-	1:500	Mouse
	CK19	ABCAM	ab7754	-	1:500	Mouse
	CK18	Invitrogen	18-0158Z	-	1:100	Mouse
	HNF4A	Santa Cruz	sc-8987	-	1:50	Rabbit
	ALB	Sigma	A6684	-	1:500	Mouse
	CYP450 3A4	Santa Cruz	sc-53850	-	1:100	Mouse
	A1AT	Thermo	PA1-37072	-	1:100	Mouse
	CYP450 1A2	Santa Cruz	sc-53241	-	1:100	Mouse
	CYP450 2C9	ABCAM	ab150364	-	1:600	Rabbit
	CYP450 2A6	Origene	TA503832	-	1:100	Mouse
	VIMENTIN	Dako	#M0725	-	1:400	Mouse
Secondaries	Goat anti Mouse	Invitrogen	A11001	AF488	1:400	Goat
	Goat anti Rabbit	Invitrogen	A11008	AF488	1:400	Goat
	Goat anti Rabbit	Invitrogen	A11011	AF568	1:400	Goat
	Rabbit anti Goat	Sigma	F7367	FITC	1:300	Rabbit
	Goat anti Mouse IgG2a	Invitrogen	A-21241	AF647	1:400	Goat

Table 5 Factors evaluated in the Chapter 5, DoE in hepatocyte maturation

Factor	Ventor	Product code	Factor	Ventor	Product code
Cyclic AMP	Biolog	B 007	5-Aza-2'-deoxycytidine	Sigma	A3656
Lithocholic Acid	Sigma	L6250	GW7647	R&D	1677
Taurocholate Acid	Merck	580217	Progesterone	Sigma	P7556
Vitamin K2	Sigma	V9378	Testosterone	Sigma	86500
FH1	Tocris	5254	17β Estradiol	Sigma	E2758
T3	Sigma	T6397	Dihexa	Washington State University	
Verteporfin	Tocris	5305	Epinephrine	Sigma	E4642
CITCO	Sigma	C6240	Glucagon	Sigma	G2044
Hydrocortisone– hemi succinate	Sigma	H4881	Cobalt(II) chloride hexahydrate	Sigma	C8661
Flavone	Sigma	F2003	Sodium butyrate	Sigma	B5887
SR12813	Sigma	S4194	Lipid Mixture 1	Sigma	L0288
Melatonin	Fisher	10255030	FGF19	R&D	969-FG-025
All-trans Retinoic Acid	Sigma	R2625	K-SR	LifetTech	10828
SR11237	Sigma	S8951	Ascorbic Acid	Sigma	A7631
Bexarotene	Sigma	SML0282	Insulin	Sigma	I9278
Calcitriol	R&D	2551	D-Glucose	Sigma	G7021
Chenodeoxycholic acid	Fisher	10266950	GlutaMAX	LifeTech	35050
ITE	R&D	1803	BSA Solution 7.5%	Sigma	A8412
Dexamethasone	Sigma	D4902	MS-1	Prof.Andrew Bennett Lab	
Y27632	Tocris	129830-38-2	MS-2 Transferrin	Sigma	T1428
CHIR99021	Tocris	4423	HGF	Peprotech	100-39
Trichostatin A	R&D	1406	OSM	R&D	295-OM-010
LY 294002	Tocris	1130			

CHAPTER THREE

OPTIMISATION AND GENERATION OF A MODEL CELL SYSTEM FOR THE INVESTIGATION OF MATURATION OF HUMAN EMBRYONIC STEM CELL-DERIVED HEPATOCYTES

3. Chapter 3

Chapter three aims to:

- Evaluate the current hepatocyte differentiation protocol in terms of hESC line, seeding density, timing and technical issues to increase expression of HLC markers
- Improve maintenance culture by the use of a chemically defined culture medium
- Evaluate the use of the robotic platform for automated maintenance and hepatocyte differentiation of hPSC
- Finally, screen hiPSC lines, generated in lab, to identify a line that is automation compatible and can generate HLC following the established protocol.

Factors affecting the maintenance of hPSCs such as culture medium and culture substrate are discussed. Following, there is a summary of current approaches for *in vitro* hepatocyte differentiation and stage specific factors to drive the differentiation. Finally, a review of automated cell culture systems is presented, and the Tecan Freedom Evo 200 culture robot is introduced.

3.1. Introduction

3.1.1. Culture methods for hPSC

For many years, the majority of hPSC cultures relied on undefined and/or xenogeneic containing culture systems. Initially, hESCs were derived and cultured on a layer of mouse-embryonic fibroblasts (MEF) with serum supplemented medium (Thomson et al., 1998). The foetal bovine Serum supplement is an extremely complex, highly variable mixture with un-

defined components that may contain factors that induce differentiation of the cells (Skottman and Hovatta, 2006). As a result, high variability was introduced into the system and batch to batch variation led to low reproducibility of the experiments (Khodabukus and Baar, 2014). In addition, animal-derived material carries a risk of transmitting animal pathogens to cultures of human cells and therefore studies aiming to transplant cells in a human would carry a contamination risk (Koivisto et al., 2004). The induced variability led to limited applications of hPSC, therefore defined culture systems had to be developed to support maintenance of the pluripotent nature of the hPSC and self-renewal of the population (Chen et al., 2014b).

Initial attempts were made to replace the animal-derived serum with chemically defined Serum Replacement and suggested that a 20% serum replacement, the addition of 8ng basic FGF and Insulin, Transferrin and Selenium worked as the best combination to support culture and maintenance of hPSC (Koivisto et al., 2004). However, serum replacement contained animal derived albumin, thus it was still not completely defined in nature (Amit et al., 2004). Since then, several attempts have been made for the production of expensive chemically defined media that support cultures of hPSC lines, achieving various efficiencies (Yao and Tatsuma, 2017).

Recently a defined medium has been developed that contains only essential compounds that can support proliferation, maintenance and survival of hPSC cultures as well as derivation of hiPSC lines (Chen et al., 2011). “Essential 8” or E8 has been developed as a simplified medium that is based in DMEM/F12 medium supplemented with human recombinant proteins Insulin, Selenium, Transferrin, L-ascorbic Acid, FGF2, TGFβ and $NaHCO_3$ to regulate the pH (Chen et al., 2011). E8 has already been applied in the field supporting passaging and scalable xeno-free expansion of both hESC and hiPSC (Badenes et al., 2016, Beers et al., 2012, Wang et al., 2013), also demonstrated to support highly efficient differentiation to

populations of variable lineages (Lippmann et al., 2014) among them into HLC (Siller et al., 2015).

Apart from the progress in the culture medium and transition into defined recipes, use of undefined substrate such as MEF feeder cells could hinder the differentiation of cells, add increased batch to batch variation and potentially introduce xenogeneic factors (Skottman and Hovatta, 2006). The advantage of MEF feeder layer is the secretion of growth factors and extracellular proteins that induce cell survival and block differentiation of hPSC (Sarkar et al., 2012). Development towards xeno-free feeder cells included isolation and mitotic inactivation of human placental fibroblasts (Genbacev et al., 2005) or other derivatives of human origin supporting maintenance of the karyotype, pluripotency and self-renewal (Lee et al., 2005, Amit et al., 2003). Except from the known batch to batch variation, upon γ-irradiation to mitotically inactivate the cells, over time expression of apoptotic genes was found to initiate and that influence self-renewal and proliferation of hPSC (Villa-Diaz et al., 2009).

Because the MEF feeder layer limited the reproducibility of the cultures and introduced a batch to batch variation, transition into the use of a soluble basement membrane extracted from the Matrigel (Engelbreth-Holm-Swarm mouse sarcoma) (Xu et al., 2001) was proposed. Matrigel contains several types of extracellular matrix proteins as well as unknown animal derived factors posing a risk to clinical and therapeutic applications (Lei et al., 2007). Matrigel has been used widely in the stem cell community reporting optimal growth, long term maintenance of pluripotency, self-renewal and karyotype stability. However, issues in the culture might be induced due to batch to batch variation (Hughes et al., 2010). More recently, completely defined approaches have been developed with single extracellular proteins such as recombinant human laminin 511 alone (Rodin et al., 2010) or mixed with E-cadherin (Rodin et al., 2014) and human recombinant Vitronectin (Braam et al., 2008) re-

porting support and long term maintenance of hPSCs.

Key advances for the expansion of stem cell population was the transition from mechanical methods of dissociation to enzymatic methods that were less labour intensive, less costly and could generate single cell populations (Ellerström et al., 2007). However, enzymatic methods of dissociation and passaging of the cells have been described to induce significant cell disruption of the cell surface proteins (Ohnuma et al., 2014). Additionally, genomic alterations in the long term culture of hESC are known (Maitra et al., 2005) however, recurrent gain of chromosomes and genomic instability was associated with the length of culture conditions and mainly due to the harsh enzymatic treatment (Tosca et al., 2015, Rebuzzini et al., 2015).

Comparison of mechanical dissection method to the enzymatic method of collagenase-IV showed that the occurrence of genomic instability is similar in those two methods to the advantage of less time consuming when the latter is used (Tosca et al., 2015). Enzymatic passage using Accutase had also been reported in the past, suggesting that maintenance of karyotype/genomic stability can be achieved for several months, although issues may arise upon freeze-thaw of cells (Kim et al., 2012). The key advantage of enzymatic methods was the production of single cell suspension, important for accurate cell measurement experiments.

In chemically defined cultures of hPSC lines, an EDTA-based passaging method served the purpose of long term passaging clumps of cells (Beers et al., 2012). It was reported as achieving maximum cell survival without a requirement for centrifugation and removal of the enzyme after the incubation, reducing material requirement and limiting the risk of contamination (Beers et al., 2012). In a similar manner to EDTA, TrypLE which is a recombinant cell-dissociation enzyme replacing porcine trypsin reported for its ability to generate single cell populations in hESC and hiPSC lines plus the advantage of being chemically de-

fined reducing variation previously described (Chen et al., 2011).

Progress towards a defined culture medium, defined substrates and dissociation methods for culture of hPSC lines, enabled increased reproducibility and reduced batch to batch variation in experiments. With all the development in the cell culture and maintenance of hPSC populations, generation of HLC that closely recapitulate human primary hepatocytes could be possible. Ideally, considering the advantages and ethical constraints, hiPSC derived HLC would be a valuable tool for drug development, toxicity screening and shedding light to the genetic variability within the population.

3.1.2. Hepatocyte Differentiation *in vitro*

Differentiation of hPSCs into HLC *in vitro* is currently a well-established stepwise approach that follows distinct liver developmental phases as discussed above (Zaret, 2002, Zhao and Duncan, 2005). In the early 2000s, work using mouse embryonic stem cells (Hamazaki et al., 2001, Yamada et al., 2002) as a model for HLC differentiation, helped to establish a stepwise approach and evaluate differentiation growth factors and their effect in signalling pathways. The first reports for differentiation of hESCs into HLCs were published after 2003 and reported generation of a 10-15% homogenous HLC population that expressed liver-associated proteins and liver-related functions such as CYP450 activity (Rambhatla et al., 2003, Shirahashi et al., 2004). The first higher efficiency differentiation studies were published in 2007-8 (Cai et al., 2007, Hay et al., 2008a) and after that multiple reports established differentiation protocols reporting a high expression of liver-related proteins and functions that represent human liver cells (Table 6).

The key differentiation steps are as explained in the liver-development process, starting with the differentiation into definitive endoderm (DE), then specification into the hepatoblast lineage and finally direction into the hepatocyte stage (Shin and Monga, 2013). In all

Table 6 Review of the hepatocyte differentiation protocols for hESC and hiPSC lines used in the literature.

Reference	Cell Line	DE Stage	Days	Hepatoblast Stage	Days	Hepatocyte Stage	Days	Total Days
(Toivonen et al., 2013)	FES29 (hESC), FiPS5-7 (hiPSC)	RPMI, Activin A 100ng/ml, B27 2%, WNT3A 75ng/ml, NaB 1mM D1/ 0.5mM D2-7	7	KO-DMEM, KOSR 20%, DMSO 1%	7	L-15, FBS 8.3%, Tryptose Phosphate Broth 8.3%, Hydrocortisone 10uM, Insulin 1uM, HGF 10ng/ml, OSM 20ng/ml	7	21
(Medine et al., 2011)	H1, H9, RCM-1	RPMI, Activin A 100ng/ml, WNT3A 50ng/ml, B27 1x	3	KO-DMEM, KOSR 20%, DMSO 1%	5	L-15, FBS 10%, HGF 10ng/ml, OSM 20ng/ml	9	17
(Cai et al., 2007)	H1, H9	Activin A 100ng/ml, ITS 0% D1/0.1% D2, 1% D3	3	Hepatocyte Culture Medium (Camdex), FGF4 30ng/ml, BMP2 20ng/ml	5	HCM, HGF 20ng/ml D1-5 / HCM, HFG 20ng/ml, OSM 10ng/ml, 0.1uM Dex	15	23
(Hay et al., 2008a)	H1, H9	RPMI, Activin A 100ng/ml, WNT3A 50ng/ml	3	DMEM, KOSR 20%, DMSO 1%	7	L-15, FBS 8.3%, Tryptose Phosphate Broth 8.3%, Hydrocortisone 10uM, Insulin 1uM, HGF10ng/ml, OSM 20ng/ml	7	17
(Si-Tayeb et al., 2010b)	H9	RPMI, B27, Activin A 100ng/ml, O2 20%	5	RPMI, B27, FGF2 10ng/ml, BMP4 20ng/ml, O2 4%	5	HCM-Lonza (-EGF/ +SingleQuotes), OSM 20ng/ml, O2 20%	5	20
				RPMI, B27, HFG 20ng/ml, O2 4%	5			

Reference	Cell Line	DE Stage	Days	Hepatoblast Stage	Days	Hepatocyte Stage	Days	Total Days
(Song et al., 2009b)	H1 (hESCs) / 3U1 and 3U2 (hiPSCs)	RPMI, Activin A 100ng/ml, 0.5mg/ml Albumin fraction A, ITS 0% D1/ 0.1% D2/ 1% D3	3	Hepatocyte Culture Medium (Camdex), FGF4 30ng/ml, BMP2 20ng/ml	4	HCM, OSM 10ng/ml, Dex 0.1uM	6	22
				HCM, HGF 30ng/ml, KGF 20ng/ml	6	DMEM, N2, B27	3	
(Hay et al., 2008b)	H1, H7	RPMI, Activin A 100ng/ml, 1x B27, Sodium Butyrate 1mM D1 / 0.5mM D2-3	3	DMEM, KOSR 20%, DMSO 1%	7	L-15, FBS 8.3%, Tryptose Phosphate Broth 8.3%, Hydrocortisone 10uM, Insulin 1uM, HGF10ng/ml, OSM 20ng/ml	7	17
(Agarwal et al., 2008)	H9/H1-GFP	RPMI, Actinin A 100ng/ml, FBS 0.5% D1-2/ KOSR 2% D3-5	5	RPMI, KOSR 2%, FGF4 10ng/ml, HGF 10ng/ml	3	HCM+SingleQuotes, FGF4 10ng/ml, HGF 10ng/ml, OSM 10 ng/ml, Dex 0.1uM	9	20
				MDBK-MM, BSA 0.5mg/ml, FGF4 10ng/ml, HGF 10ng/ml	3			
(Asgari et al., 2013)	Royan hiPSC1 / Royan H5	RPMI, Actinin A 100ng/ml, ITS 0% D1/ 0.5% D2/ 1.5% D3	3	RPMI 90% D1-6 / RPMI 50% - HCM 50% D7-8, 10% KOSR, FGF4 10ng/ml, HGF 10ng/ml	8	HCM, 10% KOSR, 10ng/ml OSM, 0.1uM Dex	10	21
(Chen et al., 2012b)	H9/ CFB46 (hiPSC line)	RPMI, Activin 100ng/ml, Wnt3A 50ng/ml, HGF 10ng/ml	3	DMEM, 20% KOSR, DMSO 1%	4	IMDM, OSM 20ng/ml, Dex 0.5uM, ITS (premix) 50mg/ml	5	12

Reference	Cell Line	DE Stage	Days	Hepatoblast Stage	Days	Hepatocyte Stage	Days	Total Days
(Touboul et al., 2010)	H9	CDM, Activin A 100ng/ml, BMP4 10ng/ml, FGF2 20ng/ml, LY294002 10uM	3	CDM/PVA, FGF10 50ng/ml	3	CDM/PVA, FGF4 30ng/ml HGF 50ng/ml, EGF 50ng/ml	10	18
				CDM/PVA, FGF10 50ng/ml, Retinoic Acid 0.1uM, SB431542 10uM	2			
(Hannan et al., 2013)	H9, Val9, FES22/29, hSF-6 and hiPSC lines	CDM-PVA, Activin A 100ng/ml, FGF2 100ng/ml, BMP4 10ng/ml, LY294002 10uM, CHIR99 3uM	2	RPMI, Activin A 50ng/ml	3	HBM, HGF 50ng/ml, OSM 30ng/ml	1-19	11-29
		RPMI, Activin A 100ng/ml, FGF2 100ng/ml	1	RPMI, BMP4 10ng/ml, FGF10 10ng/ml	4			
(Duan et al., 2010)	H9	RPMI, Activin A 100ng/ml D1-2 / RPMI, Activin A 100ng/ml, B27 1x, NaB 0.5mM D3-8	8	RPMI, FGF4 20ng/ml, HGF 20ng/ml, BMP2 10ng/ml, BMP4 10ng/ml D9 / + DMSO 0.5% D10-22	13	HCM+SingleQuotes, FBS 5%, DMSO 0.5%, Dex 100nM, FGF4 20ng/ml, HGF 20ng/ml, OSM 50ng/ml	10	31
(Magner et al., 2013)	H9	RPMI, Activin A 100ng/ml BSA 0.5% D1-2 / B27 D3-8	8	IMDM, FBS-Hyclone 20%, 1-thioglycerol 0.3mM, Dex 100nM, h-Insulin 0.126 U/ml	8	HBM+HCM+SingleQuotes, DMSO 0.5%, Dex 100nM, FGF4 20ng/ml, HGF10ng/ml, OSM 50ng/ml	8	24
(Siller et al., 2015)	H1, Detroit 551 (ATCCCCL-110), hESC207	RPMI1640, B27 1x, CHIR 99021 3/4uM	1	KO-DMEM, Serum Replacement 20%, DMSO 1%	5	L-15, FBS 8.3%, Tryptose Phosphate Broth 8.3%, Hydrocortisone 10uM, Insulin 1uM, Sodium ascorbate 50ug/ml, Dihexa 100nM, Dexamethasone 100nM	10	17
		RPMI1640, B27 1x, +/- Insulin	1					

Reference	Cell Line	DE Stage	Days	Hepatoblast Stage	Days	Hepatocyte Stage	Days	Total Days
(Baxter et al., 2015)	HUES7, H9	RPMI1640, Activin A 100ng/ml, WNT3a 25ng/ml, FBS 0.5%	2	Hepatocyte Culture Medium (HCM), BMP2 20ng/ml, FGF4 30ng/ml	6	Hepatocyte Culture Medium (HCM), HGF 20ng/ml	5	30
		RPMI1640, Activin A 100ng/ml, FBS 0.5%	2			Hepatocyte Culture Medium (HCM), OSM 10ug/ml, Dexamethasone 100nM	15	
(Takayama et al., 2014)	H1, H9, KhES1-4,	L-Wnt3A-expressing cell (ATCC, CRL2647)-conditioned RPMI1640 medium, Activin 100ng/ml, FBS 0.2%, B27 1x	4	RPMI1640, BMP 30ng/ml, FGF4 20ng/ml, B27 1x,	5	RPMI1640, HGF 20ng/ml, B27 1x	5	25
						Hepatocyte Culture Medium Lonza, Oncostatin 20ng/ml	11	
(Asplund et al., 2016)	SA121, SA167, SA181, SA461, Val9, ChiPSC4, ChiPSC6b, ChiPSC20	Cellartis DE Differentiation Kit (Takara Bio Europe AB; Y30030)	6	Re-plating into Fibronectin-coated wells, Hepatocyte Thawing and Seeding Medium (Cellartis Hepatocyte Differentiation)	3	Hepatocyte Progenitor Medium (Cellartis Hepatocyte Differentiation Kit)	5	29
						Williams Medium E, HCM Single Quots, OSM 10ng/ml, HGF 40ng/ml, Dex 100nM, BIO 1.4uM	15	

the above approaches (Table 6), the key similarities for each stage and the growth factors commonly used, are presented. For the DE stage, use of Activin A is essential for activation of the TGFβ receptor (Zorn and Wells, 2007) and in most reports WNT3a is used for the activation of the WNT/Frizzled receptor (Zhang et al., 2013). Some reports include factors like Foetal Bovine Serum or Albumin, Insulin-Transferrin-Selenium, Sodium Butyrate, B27, HGF, LY294002 and CHIR99021 that have identified to induce differentiation and generate a more robust population of DE cells.

For the Hepatoblast specification, the field is divided into using the defined developmental signals of BMP/FGF or use of the chemical inducer DMSO (Baxter et al., 2015, Takayama et al., 2014) however, cost implications and batch to batch variation in growth factors led to the use of DMSO. Additionally, Serum replacement or serum albumin, B27, HGF, KGF, Retinoic Acid, SB431542 and insulin are used by various groups (Table 6). The hepatocyte specification stage is the most variable of all including a variety of growth factors and small molecules. Mainly the differentiation is accommodated by the use of two key growth factors, described in liver development, HGF and OSM (Zaret, 2002). Additionally, protocols have used Insulin, Hydrocortisone or Dexamethasone, Serum, Tryptose Phosphate Broth, B27, N2, FGF4, FGF10 and EGF. Commercially available proprietary medium formulations for this stage are also available however, require the addition of growth factors (Takayama et al., 2014, Baxter et al., 2015, Magner et al., 2013). Although not necessary, in some differentiation protocol steps were divided into two phases, using different factors in each so that specification into a more relevant type is assisted (Song et al., 2009b, Agarwal et al., 2008, Hannan et al., 2013).

Key differences in all the reports presented in Table 6 are a) cell lines that have been used, b) time of treatment for each stage, c) the concentration of each factor used in the protocol and d) criteria to judge the final population. The cell lines used, cover a wide range of hESC

and hiPSC that are either commonly available or derived in the same laboratory. Predominantly, the field uses the H1, H7 and H9 hESC lines derived from Thomson in 1998 at the University of Wisconsin-Madison (Thomson et al., 1998) however, hiPSC lines are used in a range of protocols (Toivonen et al., 2013, Song et al., 2009b). The time to achieve formation of the desired population, in each differentiation step, is highly variable and is ranging between 17 and 31 days (Duan et al., 2010, Hay et al., 2008b). More specifically, the DE stage ranges between 2-8 days, the hepatoblast between 4-10 days and the hepatocyte specification between 5-20 days. The concentration of each factor used in each study, varies according to the laboratory's optimisation procedures, adding another element of variability among the current protocols. Finally, the criteria to characterise the HLC population generated are variable across the field and between labs. Common guidelines have not been established and this is causing difficulties cross-comparing studies, results and efficiencies (Discussed in Chapter 4).

Recombinant growth factors are commonly used in the hepatocyte differentiation increasing the cost of HLC production. Exception in the above differentiation protocol table is the Siller et al study, which presented a protocol using chemically synthesised small molecules to generate HLCs, at a similar efficiency as the growth factor approaches (Siller et al., 2015). This approach opened new opportunities for minimising the cost of the differentiation protocol enabling large scale HLC production. Recently, a combination of commercially available step-directing differentiation kits replaced parts of the step-wise protocols and demonstrated efficient generation of HLC from multiple cell lines (Asplund et al., 2016).

3.1.1. Automation in the field of Stem Cells

Exploiting the full potential of stem cells is dependent on the consistency in the production of genetically stable cell populations, maintenance, expansion and differentiation of them in an operator dependent manner (Liu et al., 2010, Daniszewski et al., 2017). hPSCs are

highly sensitive to culture conditions (Veraitch et al., 2008). Maintenance and expansion of hPSCs in the undifferentiated state is labour intensive and requires considerable manual input, skilled operators and a long time for generating large population numbers (Kami et al., 2013).

Variation in manual culture is introduced by the use of undefined components such as serum and substrates as discussed in the section above (Skottman and Hovatta, 2006). However, factors such as exposure to laboratory conditions, fluid flow, dissociation enzymes, centrifugation forces and shear forces are all dependent on the judgment of the operator to achieve the desired phenotype (Veraitch et al., 2008). Environmental induced differences that the cells have been exposed in the establishment and culture can introduce additive inherited variation in the genetic and epigenetic status of cells (Allegrucci and Young, 2007).

To avoid process variability, automated methods that tightly control physical forces could lead to minimised variation in environmental conditions and achieve maintenance of phenotype and high yield of cells (Veraitch et al., 2008). Additionally, to meet the demand required by industry or clinicians, automating bioprocess could enable high-throughput applications (Thomas et al., 2009, Daniszewski et al., 2017). Especially in pharmaceuticals where screening of drugs and testing conditions in stem cell derived populations requires that the final cells have been prepared in an identical way. Automation provides reproducibility, scalability and reduces the cost for expansion of the cells (Archer and Williams, 2005) and removes the operator dependent variation (Thomas et al., 2009).

The risk of a contamination of the manual culture of cells may arise from poor operator aseptic technique or laboratory environment (Stacey, 2011). Maintaining cultures within a closed system and transferring culture plates directly between the incubator and the worktable can minimise the risk of contamination during automated handling, avoiding exposure to airborne contaminants in the laboratory and improving operator safety (Note, 2010,

Kato et al., 2010).

For those reasons, automated systems have been developed that incorporate liquid and labware handling in enclosed cabinet systems to ensure sterile conditions combining incubator, centrifuges or other equipment in a modular set up (Daniszewski et al., 2017). Therefore, attempts to automate stages or complete processes have been described by several groups discussed below (Joannides et al., 2006, Thomas et al., 2009).

Enzymatic methods of dissociation and passaging of the cells had been described to induce significant cell damage and disruption of cell surface proteins (Ohnuma et al., 2014). To avoid cell damage, initial attempts in the field of stem cells targeted to automate the passaging of hESC populations and move from manual, time-consuming enzymatic passaging, that requires a skilled operator to judge the minimum incubation time, to automated mechanical passaging using an automated mechanical dissection of the colonies (Joannides et al., 2006). In this method, use of the McIIwain tissue chopper (Mickle Engineering, Gomshall, Surrey, UK) was used to produce colony fragments of approximately 200um wide, achieving a reproducible and automated passaging method and reporting maintenance for more than 100 days in culture (Joannides et al., 2006).

Automation of hESC lines and their cultures on the CompacT SelecT (The Automation Partnership, Cambridge) achieved to maintain 90xT175 flasks simultaneously, generating proof of principle data and confirming automated production of approximately 3 billion hESC for further applications (Thomas et al., 2009). Maintenance of pluripotency, consistency of the expansion rate, expression of hESC markers, karyotype stability, differentiation into the 3 germ layers and successful production of pharmacologically responsive cardiomyocytes were reported (Thomas et al., 2009). The same platform was also used to expand hiPSC lines growing as aggregates, maintaining their pluripotent capabilities and differentiating into the three germ layers that was reported as better than manual methods (Soares et al.,

2014).

The need for visual assessment and consistent density identification to determine the appropriate time for stem cell passaging was required upon inconsistent outcomes from manual operator decisions (Ker et al., 2011). In 2013 the robotic system AutoCulture® was developed to assist with large-scale reproducible cultivation of stem cells for clinical trial applications (Kami et al., 2013). That was an automated real-time computer vision-based system consisted of a phase-contrast time-lapse microscope and a server, the next step towards automation of automated passaging of the cells and density measurements. This system replaced the operator need and could handle the maintenance and expansion of cells based on a morphological assessment by capturing images and assessing confluency of cells. The system was reported to maintain growth rate, expansion and characteristics of the cells from multiple cell lines (Kami et al., 2013).

Development of automated platforms led to the establishment of a modular robotic platform that is capable of iPSC reprogramming, maintenance and differentiation with minimal manual intervention. When an automated platform was used to produce iPSC lines, it was demonstrated that can generate a high number of iPSC lines at better efficiencies than those manually produced (Paull et al., 2015).

An important parameter of the automation is the liquid handling function to reassure homogenous cell suspensions. Pipetting cell suspensions must be carefully controlled to maximise accuracy and precision while reducing exposure to fluid flow (Veraitch et al., 2008). Currently, liquid-handling robots are widely used in the pharmaceutical industry for high-throughput screening of large compound libraries. Advantages of their use highlight the increased accuracy and reproducible dispensing, low variation and elimination of a potential manual error (Gaisford, 2012). Additionally, reduced usage of experimental reagents has also been reported (Gaisford, 2012) along with time efficiency and practicality com-

pared to manual liquid handling (Kong et al., 2012). Applications of low-volume liquid handling robots refer mainly to quantitative-PCR studies and the epigenetic field (Gaisford, 2012) but also gene sequencing, protein crystallisation, antibody testing and drug screening (Kong et al., 2012). Biological sample dilution preparation is a process that when is completed manually, is prone to human error, especially when a large number of factors are needed. Therefore a way to automate the process is by use of the TECAN Freedom EVO150 (Tecan, Zurich, Switzerland) liquid handling unit that is able to generate accurate and precise bioanalytical data (Jiang et al., 2012).

Since the development of maintenance and expansion of hPSC in automated platforms was achieved the next step included automated differentiation of those cells into lineages of the three germ layers. Generation of ectoderm derivate dopaminergic neurons and endoderm derivative pancreatic islet cells was described from an automated culture of hiPSC (Konagaya et al., 2015). The key characteristic of these reports is that manual and automated approaches generated comparable populations; however noticeable inter-sample variation was identified upon manual differentiations (Paull et al., 2015, Konagaya et al., 2015, Daniszewski et al., 2017).

3.1.2. Tecan Freedom Evo 200 Culture Robot

To facilitate the maintenance of hPSC lines and differentiation into HLC using automation, the robotic platform TECAN Freedom Evo 200 culture robot was utilised (Figure 9A). This platform is a modular robotic system that incorporates warm (37^{o}C) and cold (4^{o}C) incubator (StoreX) and integrated cell counter facility (Cedex Hi-Res). The incubators are linked to the robotic platform with a trolley system (Figure 9B-C). The robotic platform is enclosed in a sterile level 2 safety cabinet (Big Neat Class II safety cabinet) (Figure 9H).

The platform is equipped with three robotic arms to facilitate liquid and labware handling. Liquid handling is facilitated by the LiHa arm with 4 high volume fixed tips and 4 low volume

disposable tips. Pipetting volumes in 96 well plate formats is facilitated by a 96-tip multi-channel head (MCA96) while movement of culture vessels, by the Robotic Manipulator (RoMa) arm (Figure 9G).

On the automated platform, there are additional hardware systems in place, to enable the maintenance of hPSC lines and facilitate a variety of experimental protocols. The hardware contains a) station for MCA96 tips, b) warm carrier for 300ml medium troughs to warm up medium to 37^{o}C, c) various sizes holding vessels, d) liquid waste collection vessels, e) lab-ware waste collection, f) cell culture plate holders, g) flask flipper that can hold Roboflasks and h) connection to the cell counter (Figure 9).

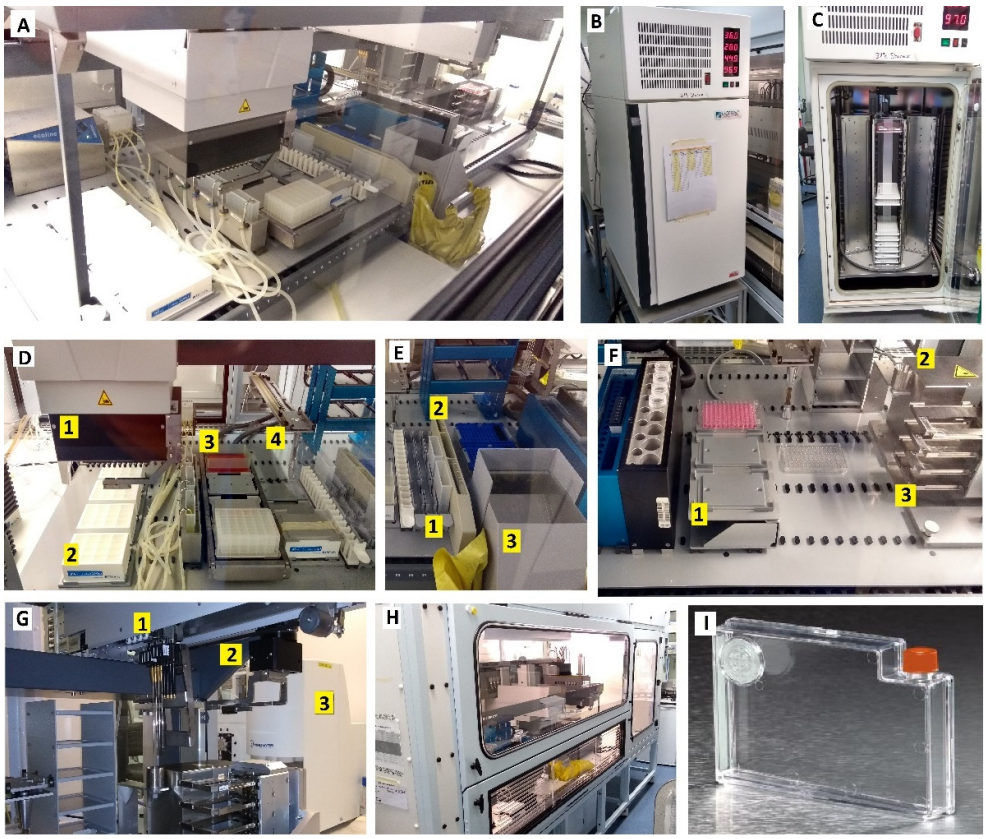

Figure 9 Images of Tecan Freedom Evo 200 Culture robot. A) Overview of the robotic platform, B) StoreX warm incubator, C) StoreX warm incubator towers and roboflasks/plates capacity, D) Overview of the platform 1=MCA96, 2=position for MCA96 tips, 3=warm carrier, 4=trolley connecting warm incubator, E) Overview of the platform 1=various size holding vessels, 2=liquid waste station, 3=labware waste station, F) Overview of the platform 1=plate holder, 2=connection with Cedex, 3=flask flipper, G) 1=LiHa robotic arm, 2=RoMa robotic arm, 3=Cedex cell counter, H) Overview of the platform enclosed in the Big Neat cabinet and I) Roboflask.

3.2. Results

3.2.1. Culture and Phenotype Assessment of HUES7 hESCs Demonstrated Maintenance of the Pluripotent Characteristics and Growth Rate

HUES7 hESCs (Cowan et al., 2004) were adapted in lab to feeder-free Matrigel culture in MEF conditioned medium (Denning et al., 2006). Cells were typically maintained in culture at low passages between 20 and 32 to minimise karyotype instability upon long-term culture (Lund et al., 2012, Rajamani et al., 2014). HUES7 cells showed characteristics such as low cell death and densely packed cells with angular cell walls when ready for passage (Figure 10).

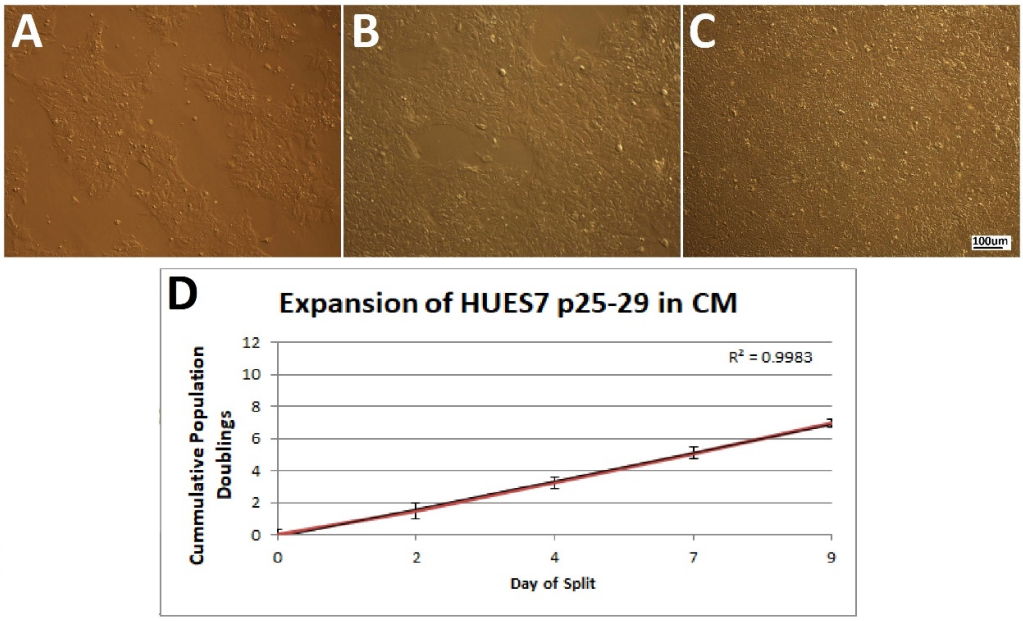

Figure 10 Culture of HUES7 hESCs A-C) Brightfield images from representative stages of the HUES7 culture in MEF-conditioned medium **A)** on day 1 when cells seeded at 1.5 million per T25, **B)** on day 2 and **C)** on day 3 before passage **D)** Growth Curve of HUES7 expansion starting from passage 25 to passage 29. Duplication time calculated as 2.5 days based on parallel cultures. N=3 flasks Scale bar **(A-C)** represents 100um

Cells were passaged by accutase enzymatic dissociation for 3 minutes at 37^{o}C and seeded at the density of 1,500,000 cells in a T25 flasks, every 72 hours. Expansion of the cells is characterised as linear with a doubling time of 2.5 days. Typically, the karyotype of HUES7 hESCs was normal at low and high passages, (Passage 20, Spreads 30, Karyotype 46,XY[27], 45,XY,-5[1], 45,XY,-11[1] and 45,XY,-20[1] and Passage 32, Spreads 30, Karyotype 46,XY[27],

45,XY,-11[1], 47,XY,+12[1], 47,XY,+22[1]). Karyotypes were performed by Mr Nigel Smith, Clinical Cytogenetics, Nottingham City Hospital.

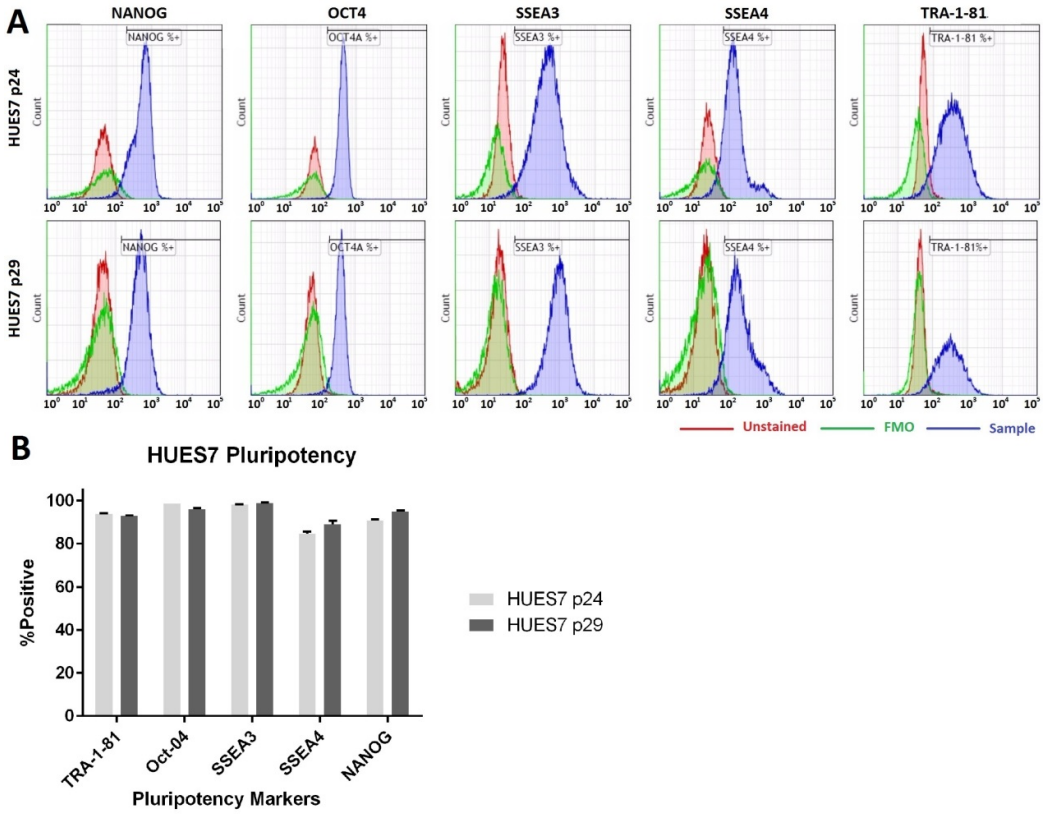

Figure 11 Maintenance of pluripotency in HUES7 hESCs. A) Flow cytometry of HUES7 p24 and p29 samples and screening for expression of TRA-1-81, OCT4, SSEA3, SSEA4 and NANOG **B)** Percentage of positive HUES7 hESCs for each of the pluripotency markers as defined by unstained control and Fluorescence Minus One (FMO) control. Error bars represent standard deviation of the mean. Replicates =3, N=1

To assess the pluripotency markers expressed in the HUES7 MEF-CM cells, samples from a low (p24) and late (p29) passage were collected and screened using a Multicolour Flow Cytometry panel developed by Mr Jayson Bispham, University of Nottingham. Figure 11A shows 85%-97% of cells positive for TRA-1-81, Oct4, SSEA-3, SSEA-4 and NANOG. Not significant differences were identified between p24 and p29 HUES7 MEF-CM (Figure 11B). Overall, these results demonstrate that HUES7 MEF-CM hESCs maintain cell morphology, expansion rate and markers of pluripotency between the passages that the cells were used for subsequent experiments.

3.2.2. HUES7 cells cultured in Conditioned Medium Demonstrate Differentiation into Hepatocyte-like cells and Expression of Hepatocyte Markers

Initially, HUES7 were differentiated into HLCs in a 96 well plate at the density of 17.000 cells/well following the protocol established in the laboratory by Dr Yan Sun. As shown in Figure 12A, this was a modification of the protocol developed in Dr David Hay Laboratory (Medine et al., 2011) with the addition of FGF2 from days 3-8.

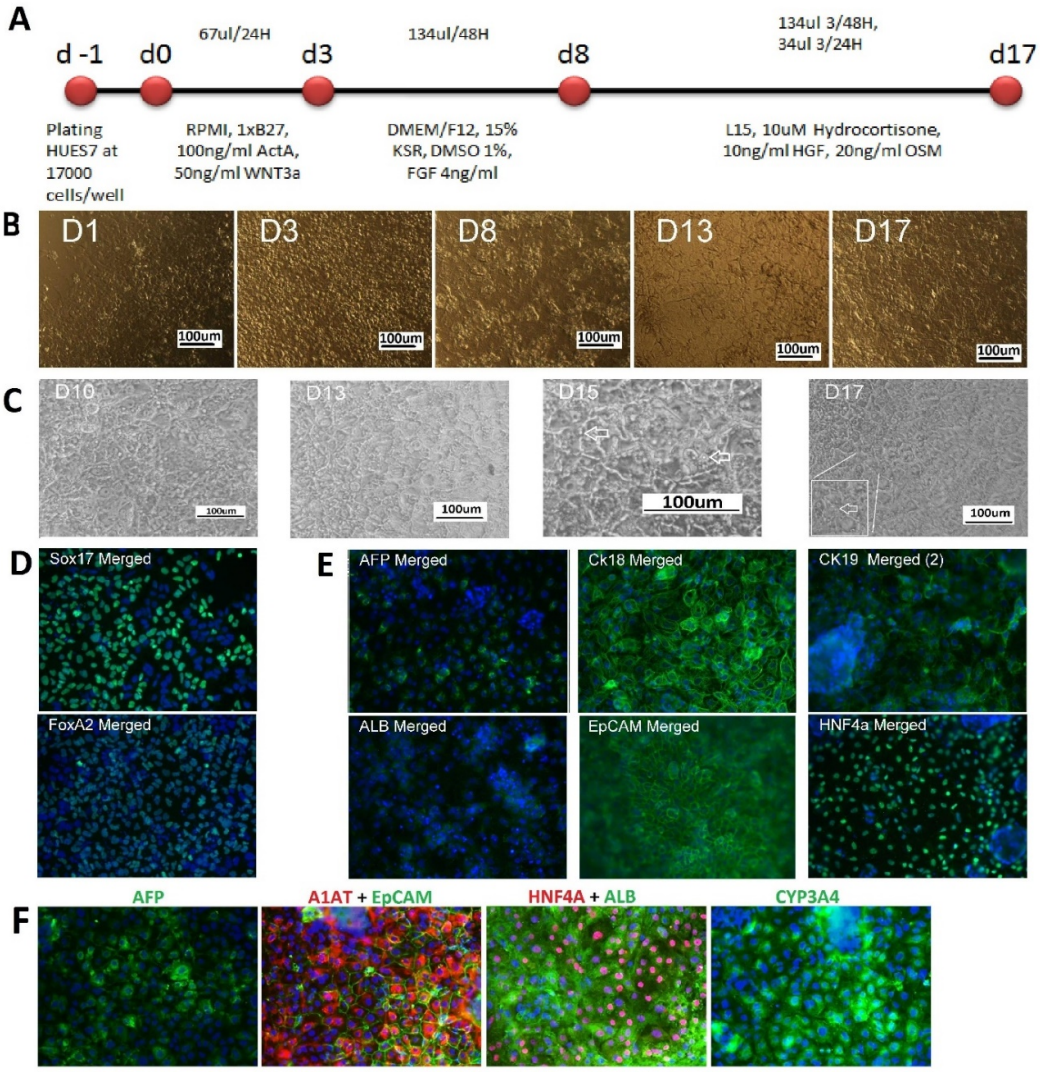

Figure 12 Demonstration of differentiation HUES7 hESCs into HLCs. A) Schematic of the differentiation protocol showing stages, day plan, medium used and concentration of each component **B)** Brightfield images of the differentiation phases, **C)** Phase contrast images during the last stage of the differentiation, white arrows indicate distinct cell borders **D)** Immunofluorescence staining for SOX17 and FOXA2 expression on Day3, **E)** Immunofluorescence staining for AFP, CK18/19, ALB, EpCAM and HNF4a expression on D8 and **F)** Immunofluorescence staining for AFP, A1AT, EpCAM, HNF4a, ALB and CYP3A4 expression on Day 17 **(D-F)** 20x magnification lenses.

On day 0 the differentiation initiated and on day 1 the cells started to expand and form Definitive Endoderm (DE). By day 3, the cells had formed DE-like cells with morphology of cobblestoned, tightly packed and small round-shaped cells as indicated in Figure 12B. To assess the expression of DE markers on day 3, immunofluorescence staining was performed for SOX17 and FOXA2. The results showed positive expression for both SOX17 and FOXA2 confirming a successful production of DE (Figure 12D).

By day 8, the cells became flatter and larger than the day 3 cells, starting to resemble hepatoblasts (Figure 12B) (Medine et al., 2011). Immunostaining showed that the cells stained positive for hepatoblast markers AFP, CK18/19, ALB, EpCAM and HNF4A (Figure 12E). During the last phase of the differentiation, hepatoblasts further increased in size-diameter to approximately 40-60um, showing a monolayer of cells with distinct cell borders (Figure 12B/C). Immunostaining for AFP, A1AT, EpCAM, HNF4a, ALB and CYP450 3A4 indicate hepatocyte characteristics of the day 17 cells (Figure 12F), (Medine et al., 2011).

3.2.3. Potentially improved conditions were identified from (Szkolnicka et al., 2013)

More recent alterations to the Hay protocol were reported to increase expression of the drug-metabolising enzymes CYP450 3A4 and CYP450 1A2 (Szkolnicka et al., 2013). A collaborative visit was made to the laboratory in 2014 to further learn their latest culture developments. In Edinburgh, H9 cells were cultured in mTeSR and differentiated to HLC as shown in Figure 13A.

As found, morphology on day 3 indicated formation of DE cells with the presence of cobblestoned, tightly packed and small round-shaped cells (Figure 13B). Day 3 cells expressed SOX17, GATA4 and GATA6 (Figure 13C). On day 8, the expected hepatoblast morphology was observed. Expression of GATA4/6 was maintained from day 3. HNF4a, ALB, AFP and CK19 were expressed similar to HUES7 MEF-CM in section 2.3.2 (Figure 14A). Notably, re-

gions of cells that generate compact 3-dimensional structures were observed and remained throughout the differentiation. On day 17, the cells generated a characteristic hepatocyte morphology (Figure 14B) and cells expressed ALB, AFP, CK18/19, CYP450 3A4 and HNF4 similar to HUES7 MEF-CM. CYP450 2D6, E-CAD and MRP1 (Figure 14B) were also shown to be expressed although these were not evaluated in HUES7 MEF-CM.

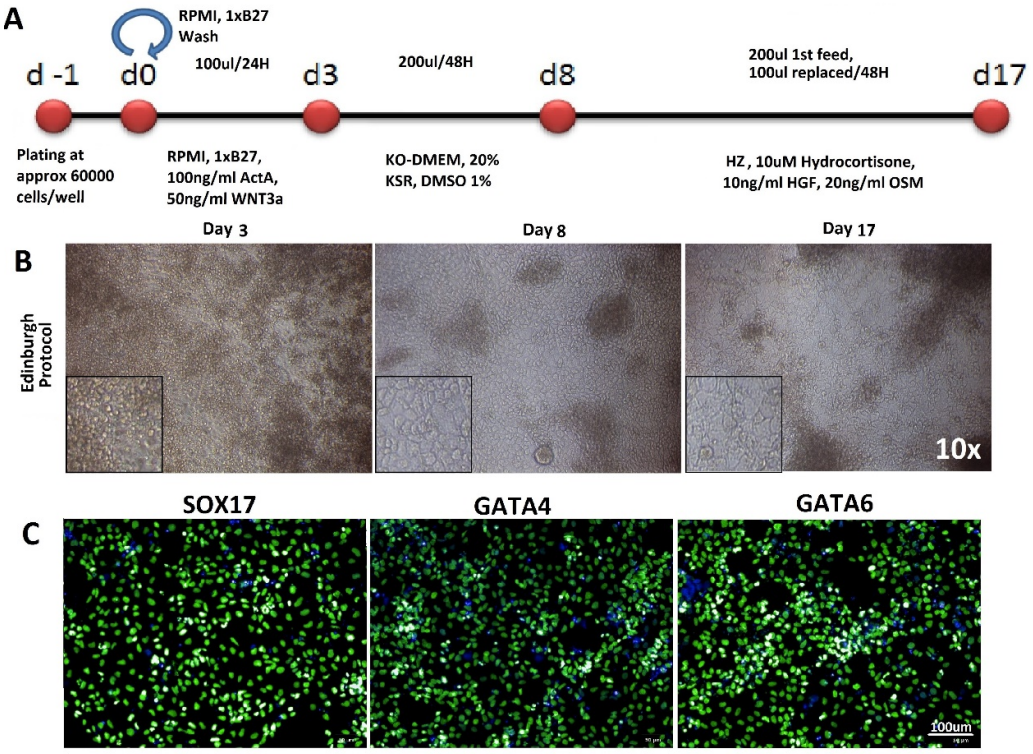

Figure 13 Differentiating h9 into HLCs with 2013 Edinburgh differentiation protocol. A) Timeline and conditions for Edinburgh differentiation protocol, **B)** Phase contrast images for morphology of the cells on days 3, 8 and 17 taken with 10x lenses, **C)** Immunofluorescence staining for SOX17, GATA4/6 on the day 3 cells. Scale bar **(D)** represents 100um.

Multiple differences were identified between the protocols as shown in Table 7. The differences were split into 4 categories: 1) hESC line, 2) culture medium and substrate, 3) seeding density for experimental set up and 4) technical aspects on the differentiation protocol. After comparing the full set of differences, a shortlist of factors perceived as most critical was highlighted for further investigation and shown in the right column in Table 7. Undesirable for this thesis were: (2) use of mTeSR medium and passaging with collagenase as collagenase passaging generates clumps (Heng et al., 2007) and counting accurate number of

cells with the Cedex cell counter would cause issues, (3) Matrigel increased cost for use of 1-36 compared to 1-100 when a high-throughput experiment is designed and (8) Hepato-ZYME is a proprietary medium produced by Thermo-Fisher and the contents are not available, thus not compatible with a study that investigates maturation factors. Additionally, it includes EGF (Garcia et al., 2001) which predominantly induces proliferation of hepatocytes.

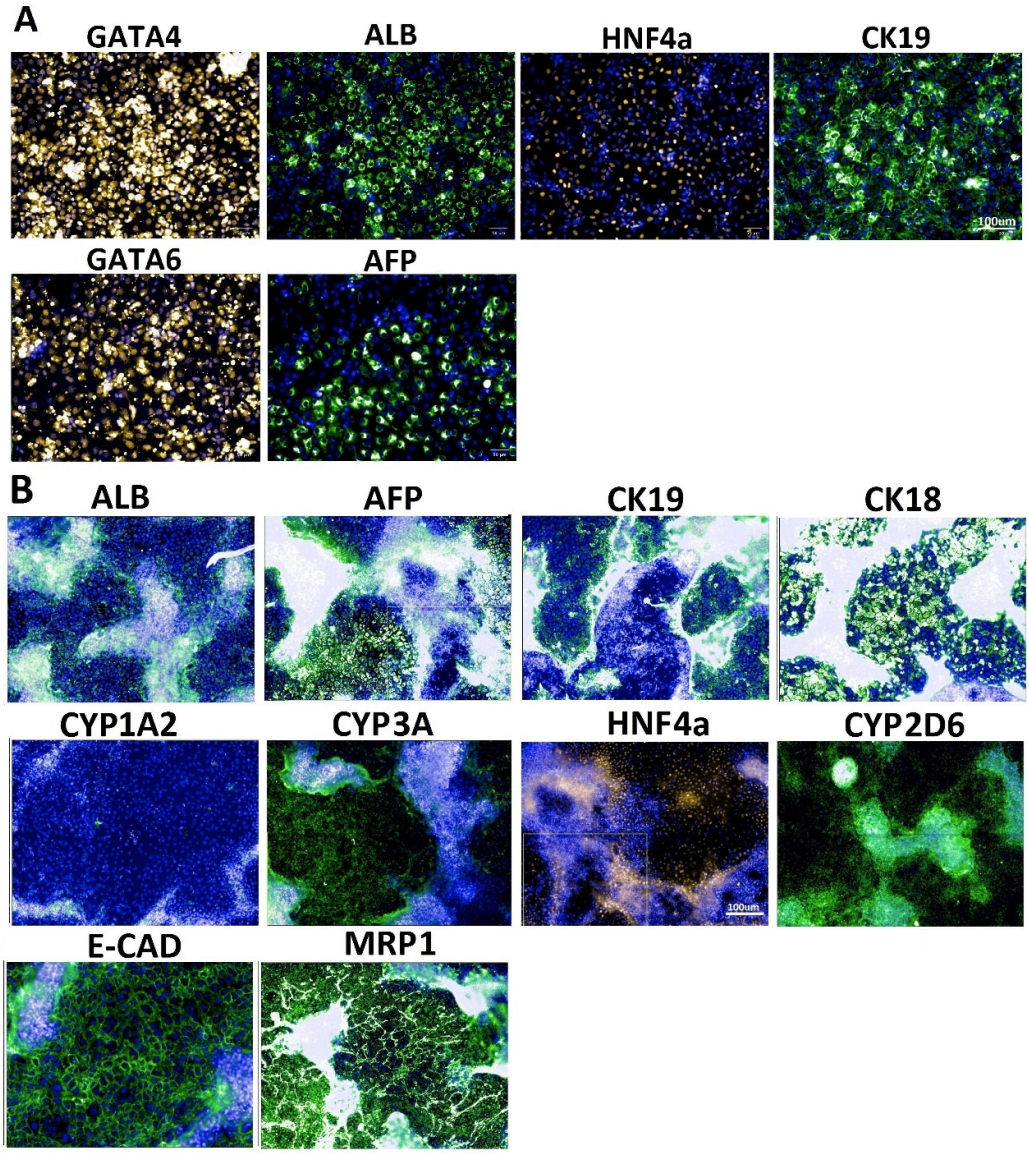

Figure 14 Day 8 and Day 17 Immunostaining of H9 differentiated with the Edinburgh protocol A) Day 8 cells evaluating the profile of the hepatoblast cells GATA4/6, HNF4a, ALB, AFP and CK19 **B)** Day 17 cells evaluating the HLC profile of cells ALB, AFP, CK18/19, CYP450 1A2, CYP450 2D6, E-CAD, CYP450 3A, MRP1 and HNF4a **(A,C)** Scale Bar represents 100um.

Table 7 Differences identified between Nottingham Protocol and Edinburgh Protocol.

	Differences	Nottingham Protocol	Edinburgh Protocol	TEST
1	Cell Line	HUES7	H9	√
2	hESC Medium/ Dissociation Enzyme	MEF-CM /Accutase	mTeSR/Collagenase	X
3	Matrigel	1-100	1-36	X
4	Medium A	RPMI+B27+Activin A+WNT3a	RPMI+B27+Activin A+WNT3a	NA
5	Medium A Feeds	67ul every 24H	100ul every 24H	√
6	Medium B	DMEM/F12, 15% KSR, DMSO 1%, bFGF 4ng/ml	KO/DMEM, 20% KSR, DMSO 1%	X
7	Medium B feeds	134ul every 48H	200ul every 48H	√
8	Medium C	L15, 10uM Hydrocortisone, 10ng/ml HGF, 20ng/ml OSM	HepatoZYME, 10uM Hydrocortisone, 10ng/ml HGF, 20ng/ml OSM	X
9	Medium C Feeds	134ul 3x every 48H, 34ul 3x every 24H	200ul 1st feed, 100ul replaced every 48H	√
10	Seeding Density	52.000cells/cm2 (17000cells/well)	200.000cells/cm2 (60000cells/well)	√
11	Growth Factors	Pre-added In the Medium	Added fresh	√
12	Pre-Medium A Wash	NO	YES	√

3.2.4. Evaluating the effect of Technical Differences between the Edinburgh (2013) and Nottingham protocols on HLC differentiation

The key technical variations identified for further evaluation were a) pre-wash with RPMI+B27 to remove the growth factors from the MEF-CM that cells were set up with, b) feeding with different volumes of medium and c) fresh or frozen medium A and C (Figure 15).

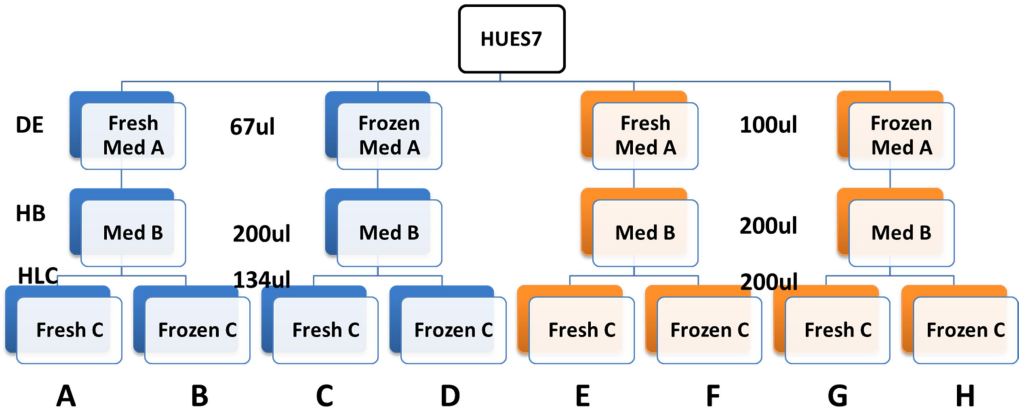

Figure 15 Experimental set up to evaluate the technical differences between the Nottingham hepatocyte protocol and the Edinburgh hepatocyte protocol. HUES7 cells were used for the experiment that split into appro-

priate number of wells to accommodate the different conditions. Blue-shaded conditions follow the feeding volumes from Nottingham protocol (Medium Volumes) and orange-shaded conditions the feeding volumes described at the DH protocol (High Volumes). Freshly made medium A and Frozen (ready-made) Medium A and Medium C was evaluated.

To evaluate the effect of the above changes, HUES7 cells were set up in a 96 well plate format at 17.000 cells per well and allowed to grow overnight. On day 0, differentiation initiated taking into consideration the different volumes described at the previous section and in Figure 15. The differentiation process was assessed on day 3 and day 17, immunofluorescence staining for DE/hepatocyte markers and on day 17 by brightfield microscopy.

Quantification analysis for nuclear localisation and co-localisation with nuclear stain (Dapi), demonstrated that on average there was an 80% of positive expression for both FOXA2 and SOX17. Two-way ANOVA identified that there are no significant differences in the expression of FOXA2 or SOX17 (Figure 16).

On day 17, brightfield microscopy showed formation of cobblestoned cells, densely packed with distinct cell borders and polygonal appearance in all conditions. High Volume, Fresh medium A generated a homogenous monolayer of HLCs, whereas Frozen Medium A, generated regions with sparse HLCs as indicated by the white arrows (Figure 17A). In Medium-volume cases, there was formation of HLCs similarly across the board (Figure 17A).

There was also a higher expression of HLC specific markers on the cells treated with High volumes and Fresh Medium A and C compared to the other conditions (Figure 17B). Expression of ALB was similar across the samples but very low in conditions C and D, HNF4a expression was lower in conditions B, G and H (Figure 17B). CYP450 3A4 was expressed higher in conditions A and B, lower in conditions C and D and very low for E, F, G and H. CYP450 2D6 expression was higher in conditions A and B and lower in the rest. The HLC markers CYP450 1A2, A1AT, CK19 and Vimentin showed stable expression were across the conditions (Figure 17B). Examples are shown in Figure 17C.

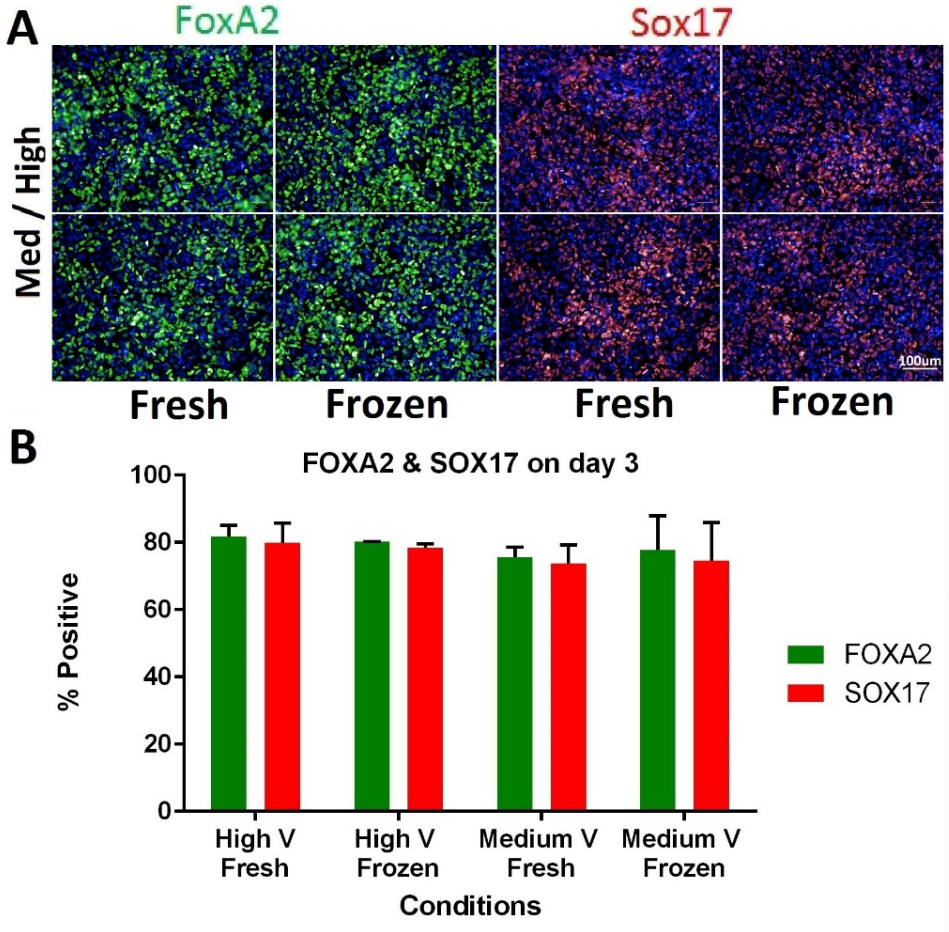

Figure 16 Effect of Medium Volume + Fresh or Frozen on SOX17/FOXA2 in d3 A) Expression of FOXA2 and SOX17 at the different samples as labelled for the 1st row fed with High Volume and Fresh or Frozen Medium A and the 2nd row fed with Medium Volume and Fresh or Frozen Medium A **B)** Quantification for the nuclear expression of FOXA2 and SOX17 for the different conditions. No statistical significance between the treatments. Error bars represent standard deviation of the mean. Scale Bars A) 100um

In summary, there was not a significant effect observed on the day 3 DE cells, however, it was demonstrated that generations of cobblestoned HLCs, densely packed with distinct cell borders, polygonal appearance and a higher expression of ALB, HNF4a, CYP450 3A4 and CYP450 2D6 was observed with High volumes and fresh Medium. Therefore, these alterations were incorporated into the Hepatocyte Differentiation protocol.

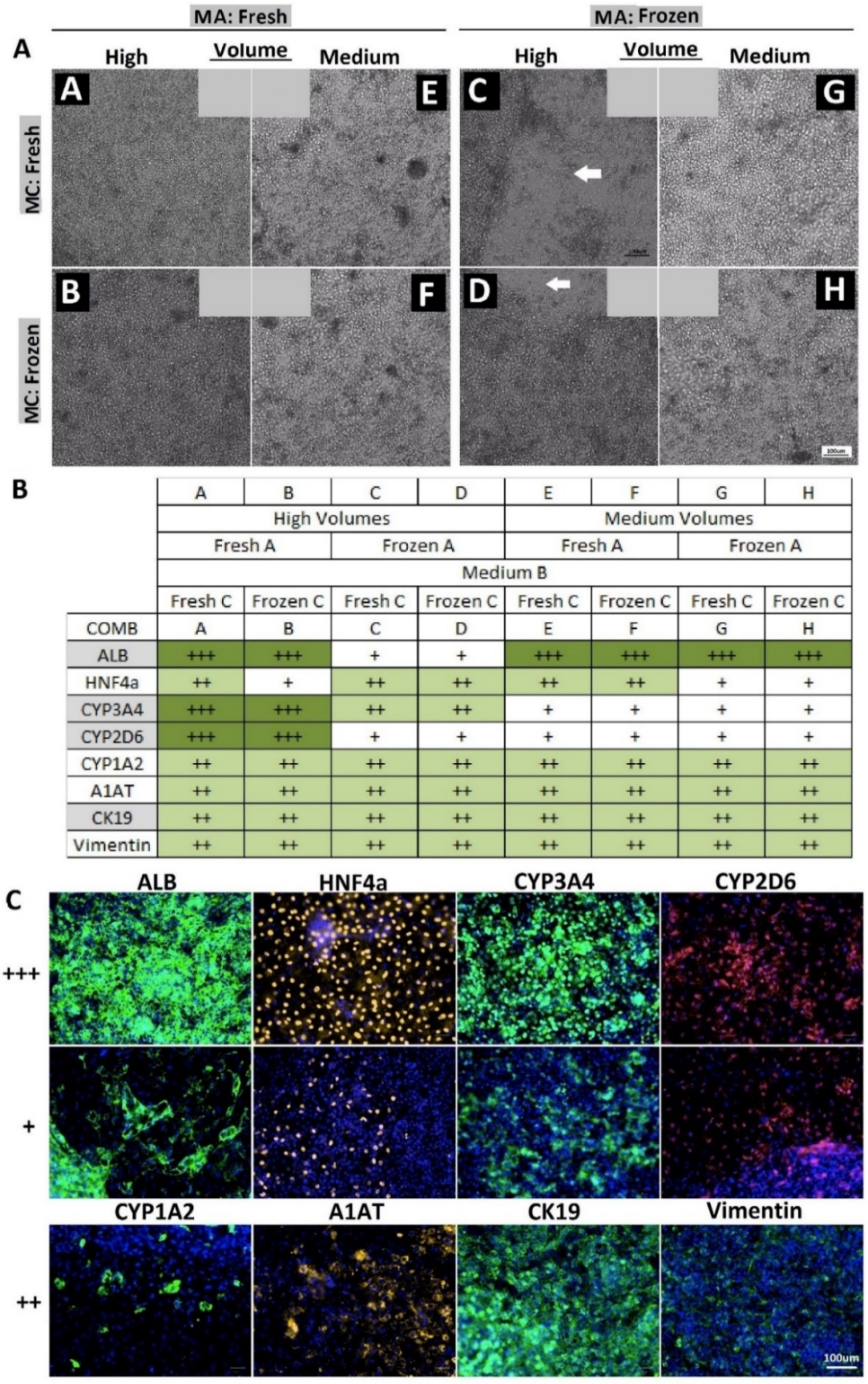

	A	B	C	D	E	F	G	H
	High Volumes				Medium Volumes			
	Fresh A		Frozen A		Fresh A		Frozen A	
	Medium B							
	Fresh C	Frozen C	Fresh C	Frozen C	Fresh C	Frozen C	Fresh C	Frozen C
COMB	A	B	C	D	E	F	G	H
ALB	+++	+++	+	+	+++	+++	+++	+++
HNF4a	++	+	++	++	++	++	+	+
CYP3A4	+++	+++	++	++	+	+	+	+
CYP2D6	+++	+++	+	+	+	+	+	+
CYP1A2	++	++	++	++	++	++	++	++
A1AT	++	++	++	++	++	++	++	++
CK19	++	++	++	++	++	++	++	++
Vimentin	++	++	++	++	++	++	++	++

Figure 17 Evaluating the effect of different technical parameters on the differentiation of HUES7 cells into HLCs on day 17. A) Brightfield images of day 17 cells at the different conditions. White arrows indicate areas with sparse hepatocyte morphology, **B)** Summary table presenting a qualitative assessment comparing expression of HLC markers across the different conditions and **C)** Representative examples of staining from HLC markers on the day 17 cells at different conditions. Scale bar **(A &C)** 100um.

3.2.5. H9 hESC line Differentiated to Hepatocytes, Showed a Significantly Higher percentage of positive Hepatocyte Marker Expression on Day 17 Compared to the HUES7 cells

To evaluate the differences between H9 and HUES7 hESC lines, as well as the seeding density effects, H9 cultures were established. H9 hESCs (Thomson et al., 1998) were previously used in the lab by Dr. Elena Matsa and were adapted to a Matrigel culture in MEF-CM medium. Cells appeared healthy with low cell death, densely packed cells when ready for passage with angular cell walls (Figure 18A-C).

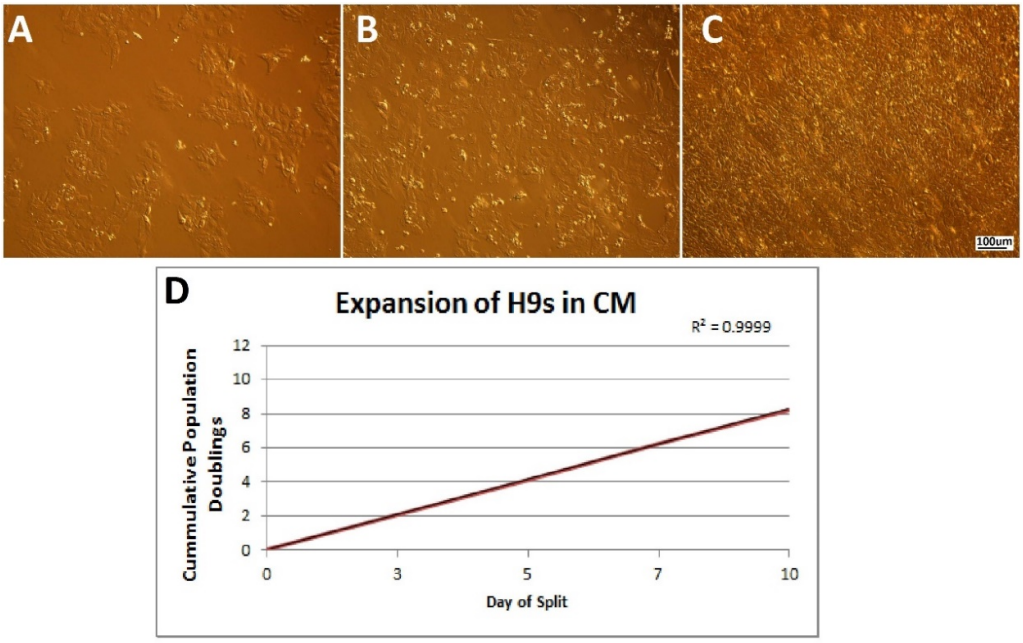

Figure 18 Culture of H9 hESCs A-C) Brightfield images from representative stages of the H9 culture in MEF-conditioned medium A) on day 1 when cells seeded at 1.500.000 cells per T25, **B)** on day 2 and **C)** on day 3 before passage **D)** Growth Curve of H9 expansion starting from passage 40 to passage 45. Duplication time calculated as 2.8 days**.** Scale bar **(A-C)** represents 100um

Cells were passaged by trypsin enzymatic dissociation for 3 minutes at 37^{o}C and seeded at the density of 1,500,000 cells in T25 flasks every 3 days. Expansion of the cells was characterised as linear with a duplication time of 2.8 days. Typically, the karyotype of H9 hESCs was normal at low and high passages (Passage 40, Spreads 30, Karyotype 46,XX[28], 45,XX,-13[1] and 45,XX,-15[1] and Passage 50, Spreads 30, Karyotype 46,XX[29], 45,XX,-17[1]). Kar-

yotypes were performed by Mr Nigel Smith, Clinical Cytogenetics, Nottingham City Hospital. Flow cytometry for pluripotency markers was identified positive for 95%-100% of cells stained for NANOG, OCT4, SSEA4 and SSEA3 (Figure 19). To compare HUES7 to the H9 cell line, hepatocyte differentiations were set up. H9 cells were set up in a 96 well plate at 17,000, 30,000 and 60,000 cells-per-well and the HUES7 at 17,000 and 30,000 cells per well and allowed to grow overnight. The 60,000 cells-per-well for HUES7 was not possible since lab users were reporting high cell death and low viability in past experiments.

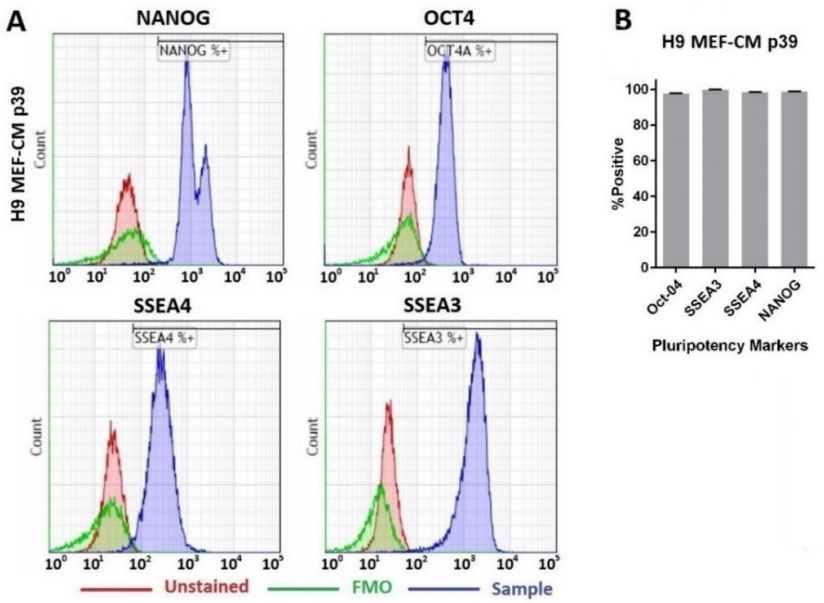

Figure 19 Expression of pluripotency markers in H9 hESCs. A) Flow cytometry of H9 CM p39 samples screened for expression of NANOG, OCT4, SSEA4 and SSEA3 **B)** Percentage of positive HUES7 hESCs for each of the pluripotency markers as defined by unstained control and Fluorescence Minus One (FMO) control. Error bars represent standard deviation of the mean. Replicates =3, N=1

On day 0, approximately 50-60% of the surface was covered at the density of 17.000 cells per well for both H9 and HUES7 cells (Figure 20B - white arrows indicate empty area), whereas at the densities of 30.000 and 60.000, a 100% coverage was identified (Figure 20B). By day 3, DE was generated as indicated by the characteristic morphology of cobblestoned, tightly packed and small round-shaped cells, (highlighted with the black arrows in Figure 19B) with no significant differences between SOX17 or FOXA2 (Figure 20C). On both days 8 and 17, both cell lines acquired the expected HLC characteristic morphology

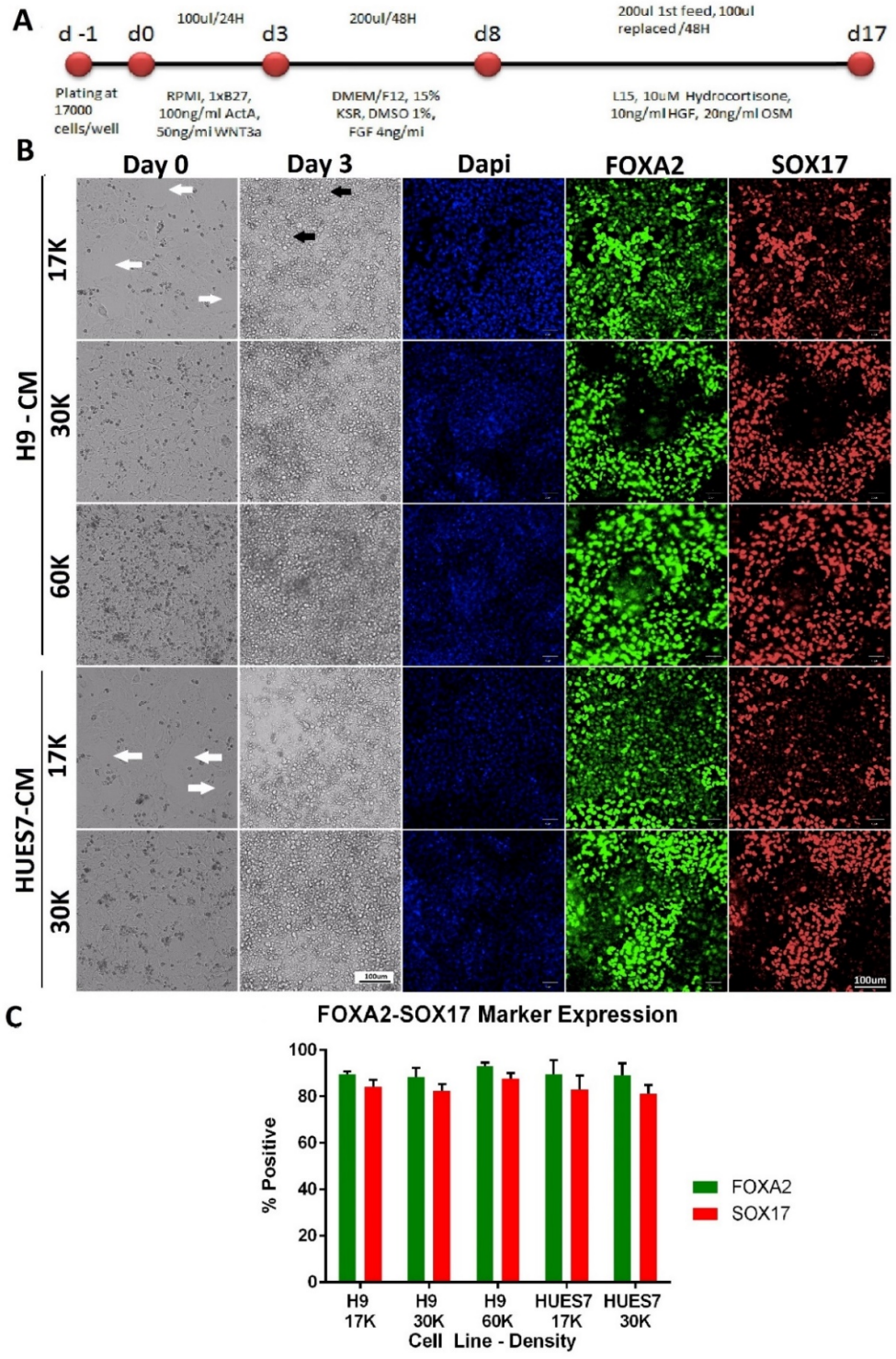

Figure 20 Differentiation of HUES7 and H9 hESCs at different densities. A) Hepatocyte differentiation protocol followed, **B)** Brightfield images of the different conditions on day 0 and day 3. White arrows indicate empty area. Immunofluorescence staining representative images from the day 3 samples for FOXA2 and SOX17 **C)** Quantification analysis for nuclear expression of FOXA2 and SOX17 on day 3 cells at different conditions. Error bars represent standard deviation of the mean. Scale bars 100um.

(Figure 21). At the 30.000 cell per well densities, regions lacking HLC morphology and show-

ing characteristics of dedifferentiation (lack of cell wall definition) were identified (highlighted with black arrows) in both cell lines (Figure 21B). The 60,000 density generated 3D structures in H9 and was not evaluated further (Figure 21B - white arrows).

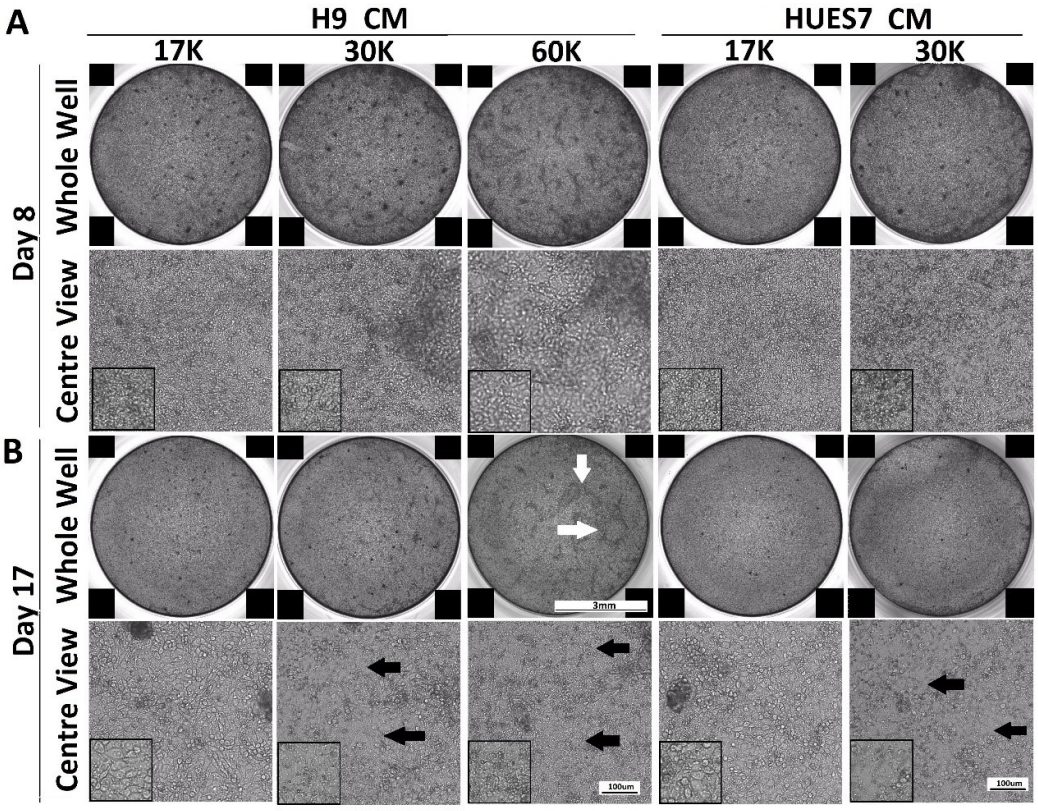

Figure 21 Assessment of HUES7 and H9 cells on day 8 and 17 by brightfield microscopy A) Images taken from representative wells to demonstrate morphology of the cells on day 8. Whole well image, followed by an image of the centre of the well, **B)** Similar as **(A)** for day 17 HLCs. White arrows indicate 3D structures and black arrows indicate flat cells with no HLC characteristic morphology, Scale bar **(A-B)** Whole well 3mm and well centre 100um.

The 17.000 density expressed ALB with a 40% of cells; this was significantly higher compared to the other conditions (Figure 22B). Expression of AFP was significantly lower at HUES7 cells at 17.000 density (Figure 22B). Expression of HNF4a, A1AT and CYP450 3A4 was on average under 20% of cells and no significant differences identified (Figure 22B). In conclusion, differentiation of the H9 hESC line seeded at 17.000 density was more efficient on the basis of HLC specific marker expression (Figure 22).

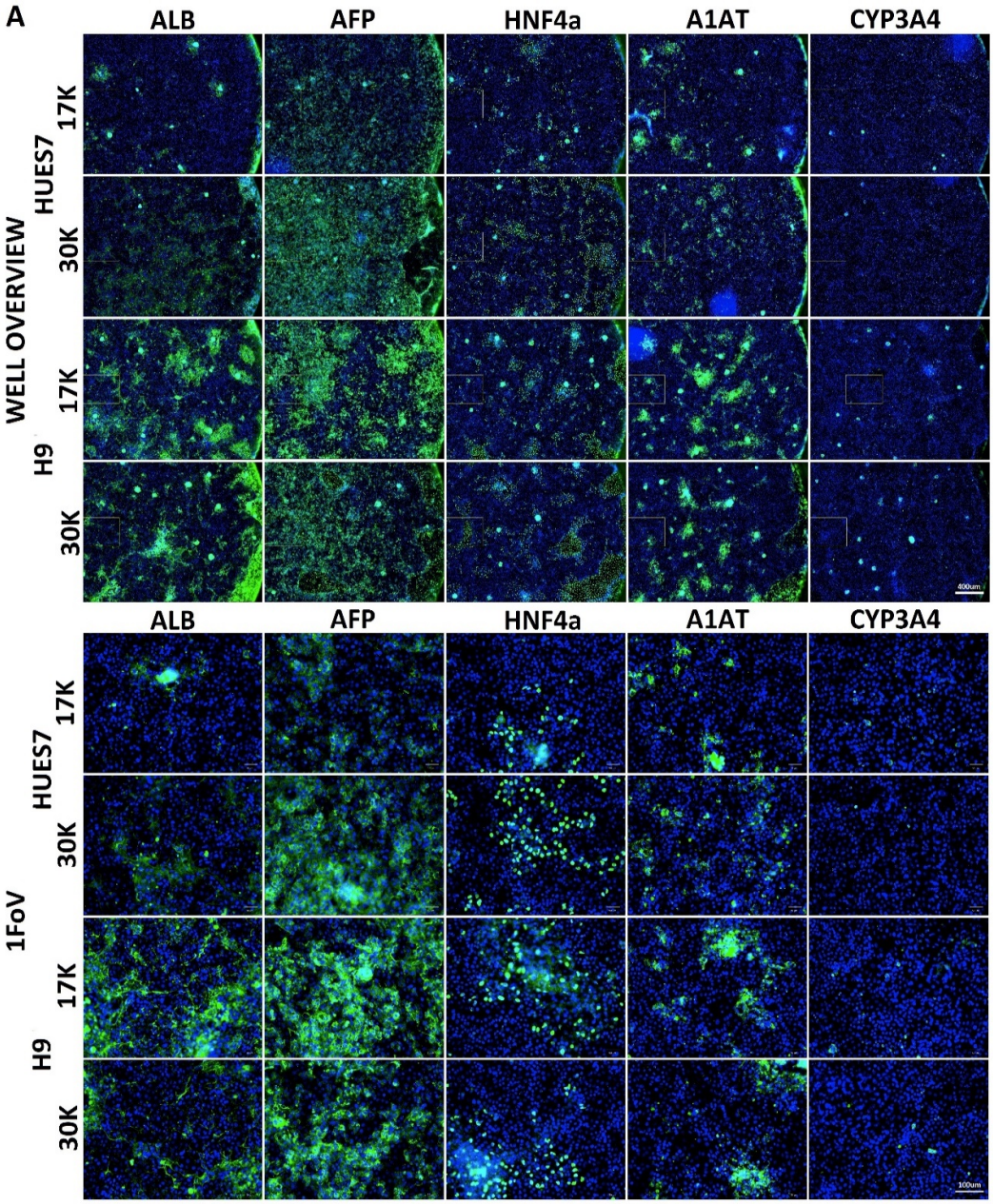
A
ALB
AFP
HNF4a
A1AT
CYP3A4
WELL OVERVIEW
HUES7
17K
30K
H9
17K
30K
400um
ALB
AFP
HNF4a
A1AT
CYP3A4
1FoV
HUES7
17K
30K
H9
17K
30K
100um

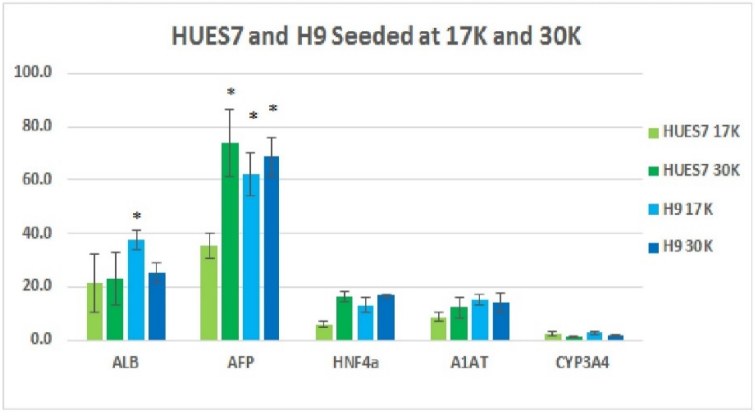
B
HUES7 and H9 Seeded at 17K and 30K
100.0
80.0
60.0
40.0
20.0
0.0
ALB
AFP
HNF4a
A1AT
CYP3A4
HUES7 17K
HUES7 30K
H9 17K
H9 30K

Figure 22 Assessment of HUES7 and H9 cells on day 17 by immunofluorescence staining A) Representative images for expression of ALB, AFP, HNF4a, A1AT and CYP450 3A4. Top panel presents the well overview and lower panel presents 1 Field of View (FoV). **B)** Quantification analysis and ANOVA for positive HLC marker expression on day 17 cells upon immunofluorescence staining. Significance represented as * $p<0.05$. Error bars represent standard deviation of the mean. Scale bar **(A)** Well overview 400um, 1FoV 100um. Replicates =3, N=1

3.2.6. Transition of H9 hESCs Into Chemically Defined, Essential 8 Medium to Achieve a More Controlled Environment for Pluripotent Stem Cell Culture

In our lab experience, MEF batches showed considerable variation, growth rates, cell death, morphology and differentiation efficiencies. To maintain a fully defined hESC /hPSC culture expansion, a fully defined media was evaluated. Life-Technologies Essential 8 Medium (LT-E8) is a xeno-free and feeder-free medium formulated for the growth and expansion of human pluripotent stem cells while it has been extensively tested and proved to maintain pluripotency in multiple iPSC lines, maintaining stable karyotype overtime (Chen et al., 2011).

Transition from MEF-CM to LT-E8 occurred on the day before the cells were passaged directly into LT-E8 (Figure 23A-a). Cells maintained the typical confluent characteristic morphology of MEF-CM cells as monolayer before the first passage (Figure 23A-b). On day 2 after the passage, the cells started organising into colonies (Figure 23A-c) that proliferated by day 3 and required a second passage (Figure 23A-d). By day 4, cells were organised into colonies (Figure 23A-e), the day after the colonies were greater in size (Figure 23A-f) and by day 6 another passage was required (Figure 23A-g). The cells were considered LT-E8 cultured upon 3 passages maintaining the characteristic colony morphology (Figure 23A-h/i).

Growth curve of LT-E8 H9 hESCs showed a duplication time of 1.6 days which enabled use of low seeding densities (500.000 cells per T25 flask) requiring a passage every 3rd day (Figure 23B). Overall, transition of H9 hESCs from MEF-CM into LT-E8 was successful, showing a stable proliferation rate and colony morphology of the cells.

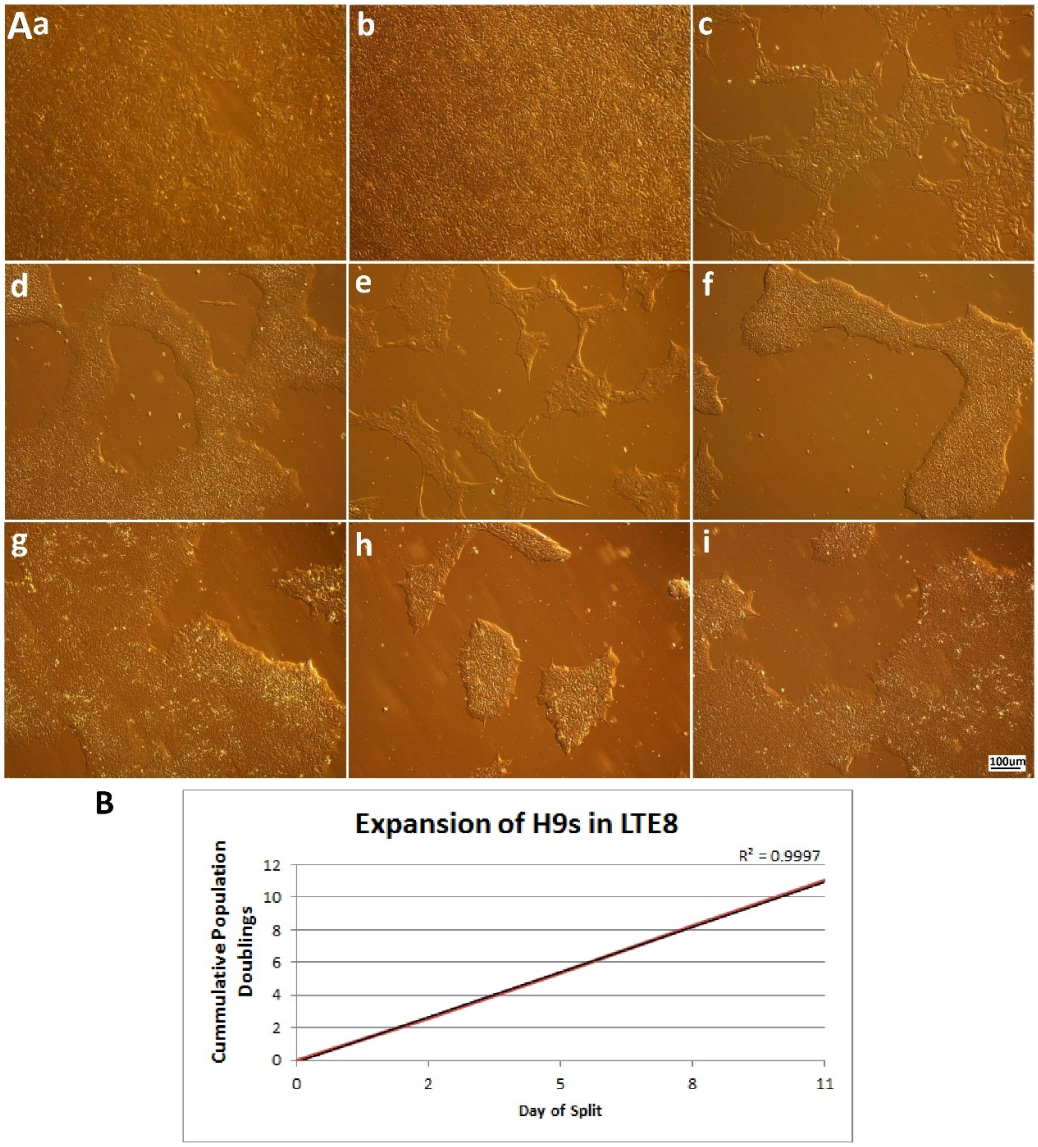

Figure 23 Transition of H9 cells cultured in MEF-CM into LT-E8 defined medium. A) Series of images for morphological changes the cells undertaking during transition. a)pre-transition cells fed with LT-E8, b)maintenance of the typical confluent layer pre-passage, c) morphology upon the first passage with LT-E8, d) increased confluency of LT-E8 cells and requirement for a passage, e) morphology upon the second passage with LT-E8 f) expansion upon the second passage, g) morphology before the third passage, h) morphology upon the third passage and i) morphology the day after. **B)** Growth Curve of H9 cells cultured in LT-E8 starting from passage 49 to passage 54. Duplication time calculated as 1.6 days**.** Scale bar **(A)** represents 100um.

3.2.7. Effect of Differentiation initiation time on Hepatocyte Differentiation

Since differentiation efficiency is known to be influenced by starting cell state, H9 LT-E8 cells were plated at 17,000 cells per well in a 96 well plate for 24 or 48 hours prior to initiating the latest protocol shown in Figure 24. All conditions generated cells with the expected HLC morphology of cobblestoned cells, although the 48H pre-differentiation time point formed 3-dimentional structures (Figure 25-black arrow).

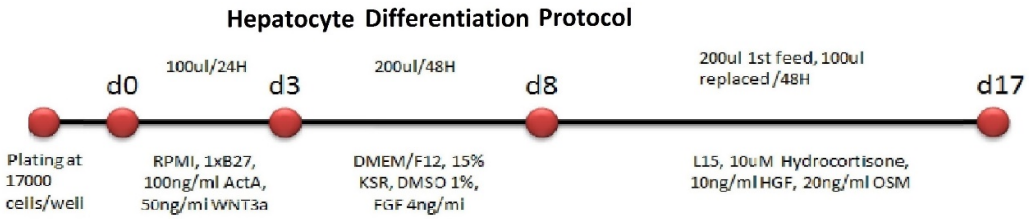

Figure 24 Hepatocyte Differentiation protocol and stages of differentiation with required supplements.

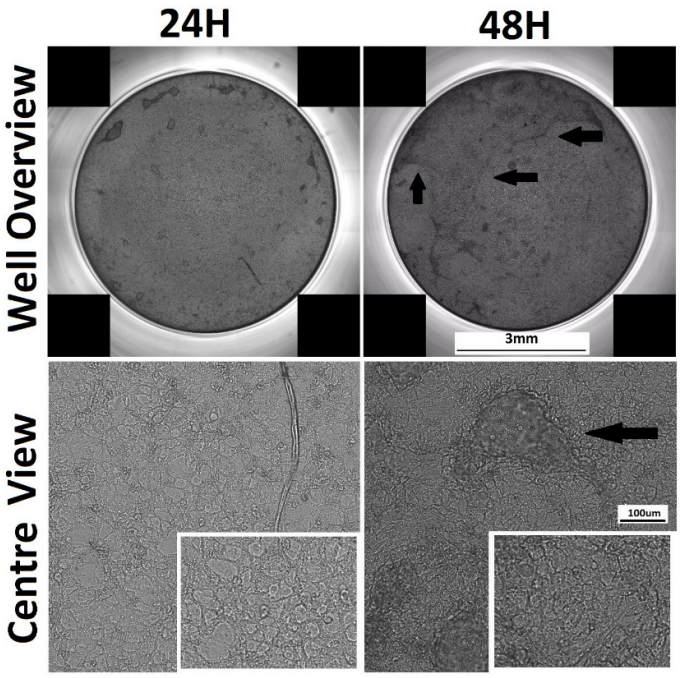

Figure 25 Importance of the pre-differentiation time on LT-E8 H9 cells for the generation of a flat monolayer of HLCs. Morphology of H9 cells on day 17, presence of 3d structures indicated with black arrows in the centre of the well or in whole well view. Scale Bars Well overview 3mm, Centre View 100um.

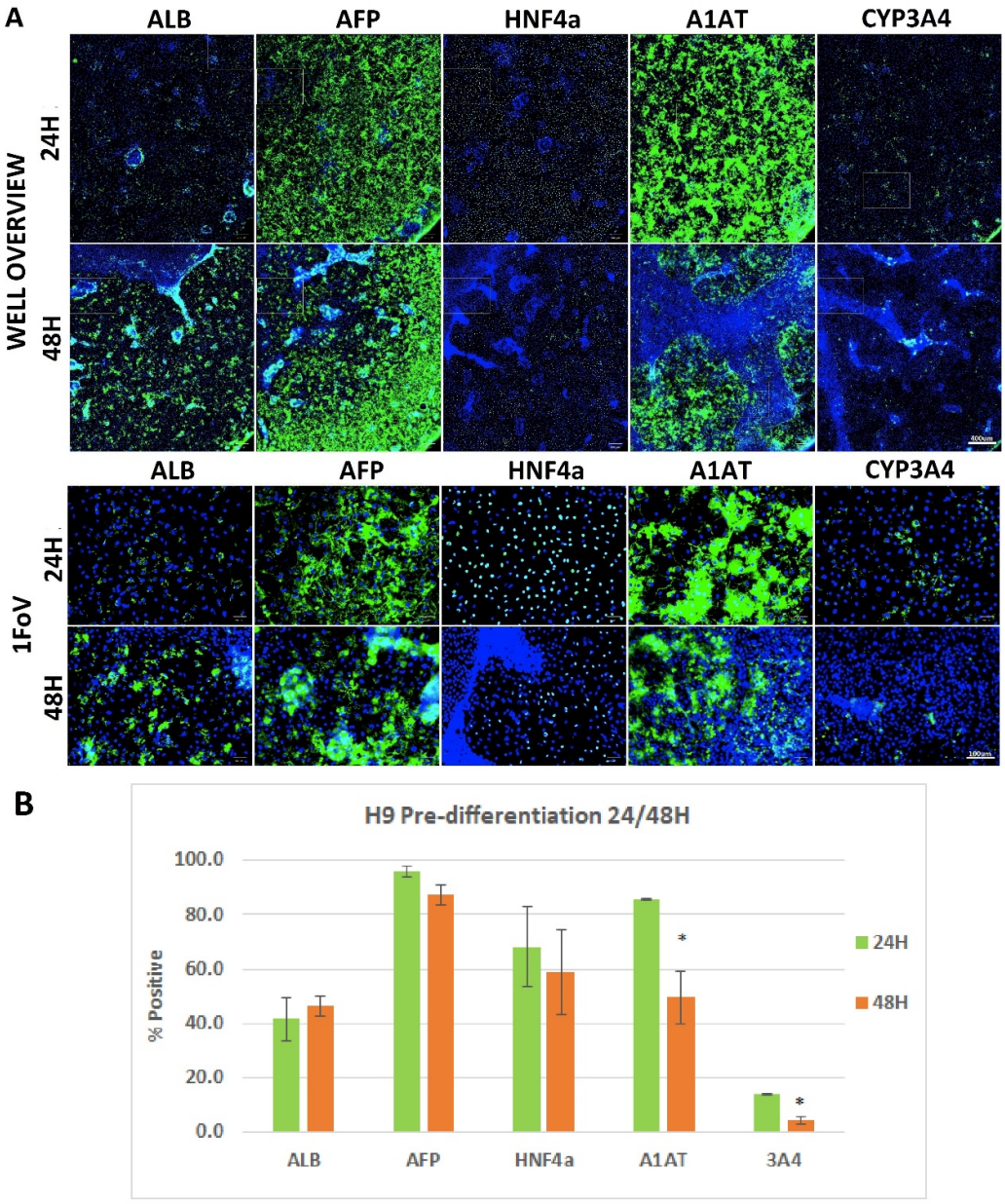

Figure 26 Assessment of H9 cells differentiated to HLCs upon 24H or 48H pre-differentiation time. Assessed on the expression of HLC markers on day 17 by immunofluorescence staining. A) Well overview of a representative well for the markers ALB, AFP, HNF4a, A1AT and CYP450 3A4. Lower panel shows 1 representative Field of View (FoV) for each condition described above. FoV taken from the central region. **B)** Quantification analysis and two-way ANOVA for the expression of the hepatocyte markers ALB, AFP, CYP450 3A4, HNF4a and A1AT in H9 HLCs upon the pre-differentiation times. Significance represented as * $p<0.05$. Error bars represent standard deviation of the mean. Scale Bars **(A)** Well overview 400um/ 1FoV 100um

ALB, AFP and HNF4a were expressed at similar levels in 24H and 48H pre-treatments, although expression of A1AT and CYP450 3A4 were significantly lower in the 48H (Figure 26B). Since 3-dimensional structures were not formed in the 24H pre-differentiation time point, the 24H time point was selected for future experiments.

3.2.8. Automated HLC Differentiation of H9 LT-E8 cells

To minimise user variability, hPSC maintenance was evaluated using the automated, liquid handling platform "TECAN Freedom Evo 200". At the start of this project, protocols for automation of routine maintenance of hPSCs had been developed in the laboratory. Key for consistency of the established harvesting and seeding methods, was the ability of the automated platform to produce single cell suspensions using functions of the Flask Flipper, that enabled accurate cell counting using the automated cell counter Cedex High Resolution (Cedex Hi-Res).

Manual processes performed for passaging the cells, were translated into a series of robotic actions, with scripts developed to control accurate movements of the robotic arms and precise liquid handling operations. The robotic protocols used for culture of hESCs refer to the main requirements for the maintenance of pluripotent cells which are a) feeding and b) passaging of cells subdivided into harvesting and seeding protocols. The robotic protocols used for (a) and (b) are described in tables 8-9.

Table 8 The flow diagram depicting the automated feeding process for hPSCs using the "TECAN Freedom Evo 200". Green highlighted boxes describe positioning and transfer of flask into the desired location, Orange highlighted box describes removal of spent medium and Blue highlighted box for the addition of fresh medium.

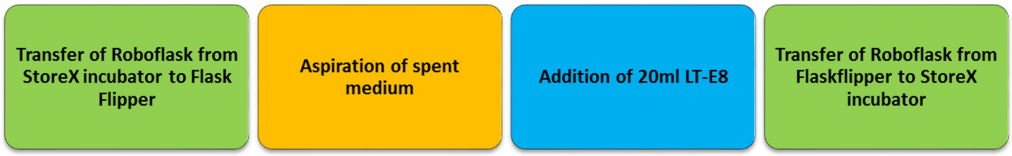

Table 9 The flow diagram depicting the automated passaging process of hPSCs using the "TECAN Freedom Evo 200". Green highlighted boxes describe positioning and transfer of flask into the desired location, Orange highlighted boxes describe harvesting processes and Blue highlighted box describes seeding processes.

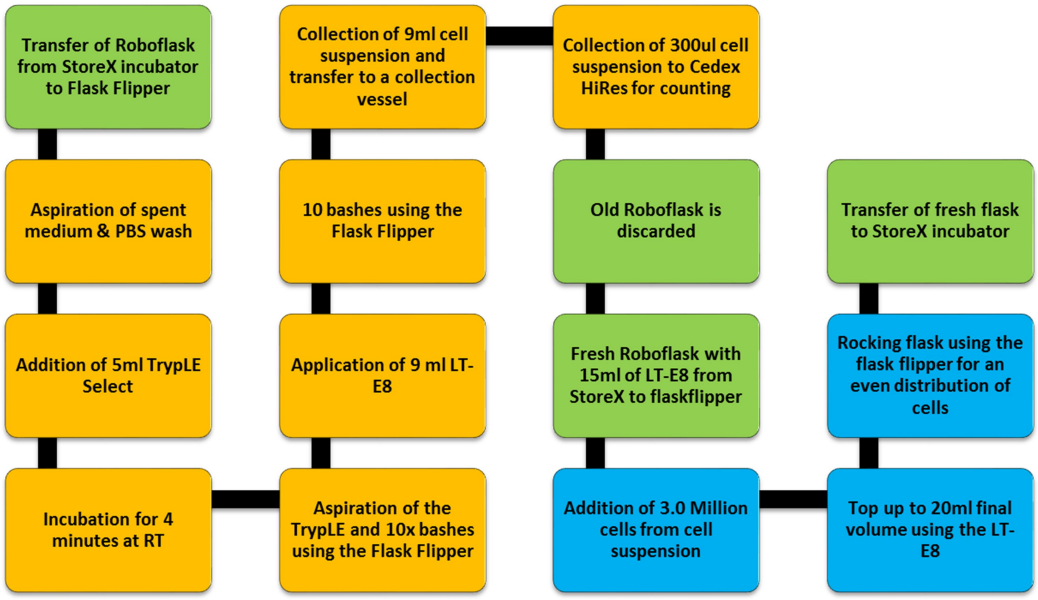

Prior to each robotic protocol, a manual action was required to supply the required consumables for each process to the allocated positions. For the feeding protocol, the only supply required was (a) a 100ml trough containing the appropriate volume of fresh medium that was placed on the warm carrier (Figure 27A).

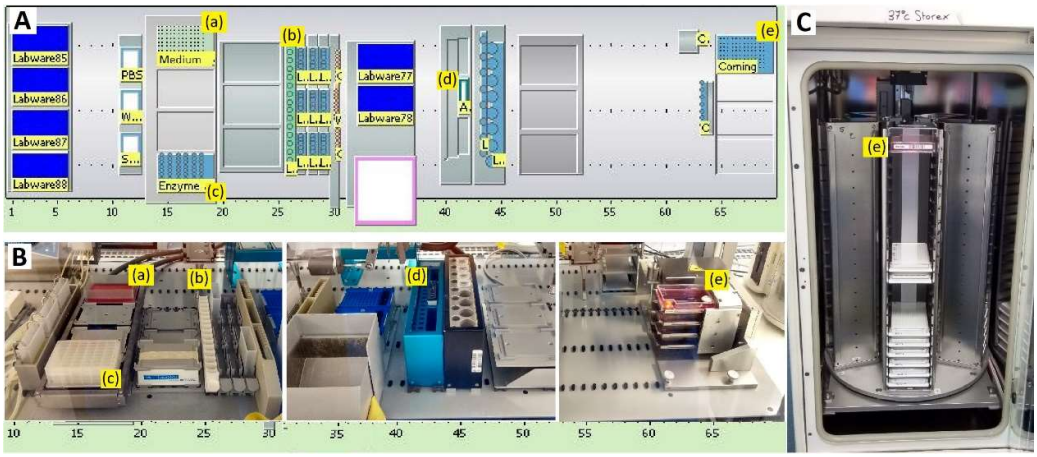

Figure 27 Overview of the Tecan Freedom Evo deck prior to an automated passaging protocol and positions for allocated labware and consumables. A) Screenshot of the deck shown in the Freedom Evo software, (a) 100ml trough, (b) position for collection vessel, (c) enzyme block, (d) cold carrier for TrypLE and (e) Roboflask on the Flask Flipper **B)** Actual Tecan Freedom Evo deck and **C)** Incubator StoreX.

For the passaging protocol (a) a 100ml trough containing the appropriate volume of fresh medium was placed on the warm carrier, (b) a collection vessel was required to collect the cell suspension upon dissociation of cells, at collection vessels position 1, (c) enzyme block to warm up the enzyme on the warm carrier, (d) 10ml of TrypLE enzyme loaded in the enzyme trough on the cold carrier and (e) the required Roboflask for passaging, in StoreX incubator position 1 tower 1, that when was moved on the deck (e), a fresh Roboflask containing 15ml of medium was placed in the same position (Figure 27).

To evaluate the maintenance of hPSCs in the robotic platform, H9 cells routinely cultured in MEF-CM, transitioned as described before (Section 2.4.7) into LT-E8 cultured and after 3 passages in LT-E8 the cells were transferred to the robotic platform where they were maintained for 8 passages, from p46 to p54.

To assess the pluripotency markers expressed after 8 passages in LT-E8, cultures at p54 were compared to manual cultures of H9 in MEF-CM isolated at a previous time (Figure 28A). Expression of OCT4, SSEA3 and NANOG was similar between the conditions (Figure 28A). The growth curve of the automated cultures was monitored for 5 consecutive passages and demonstrated a stable expansion rate with a duplication time of 2.3 days (Figure 28C). The karyotype of H9 LT-E8 cells was normal at low and high passages when maintained in the robotic platform (Passage 54, Spreads 30, Karyotype 46,XX[28], 45,XX,-18[1] and 45,XX,-20[1] and Passage 63, Spreads 30, Karyotype 46,XX[28], 45,XX,-11[1] and 45,XX,-9[1]). Karyotypes were performed by Mr Nigel Smith, Clinical Cytogenetics, Nottingham City Hospital. Overall, the results demonstrated that the conditions in robotic platform can maintain a stable population of pluripotent cells.

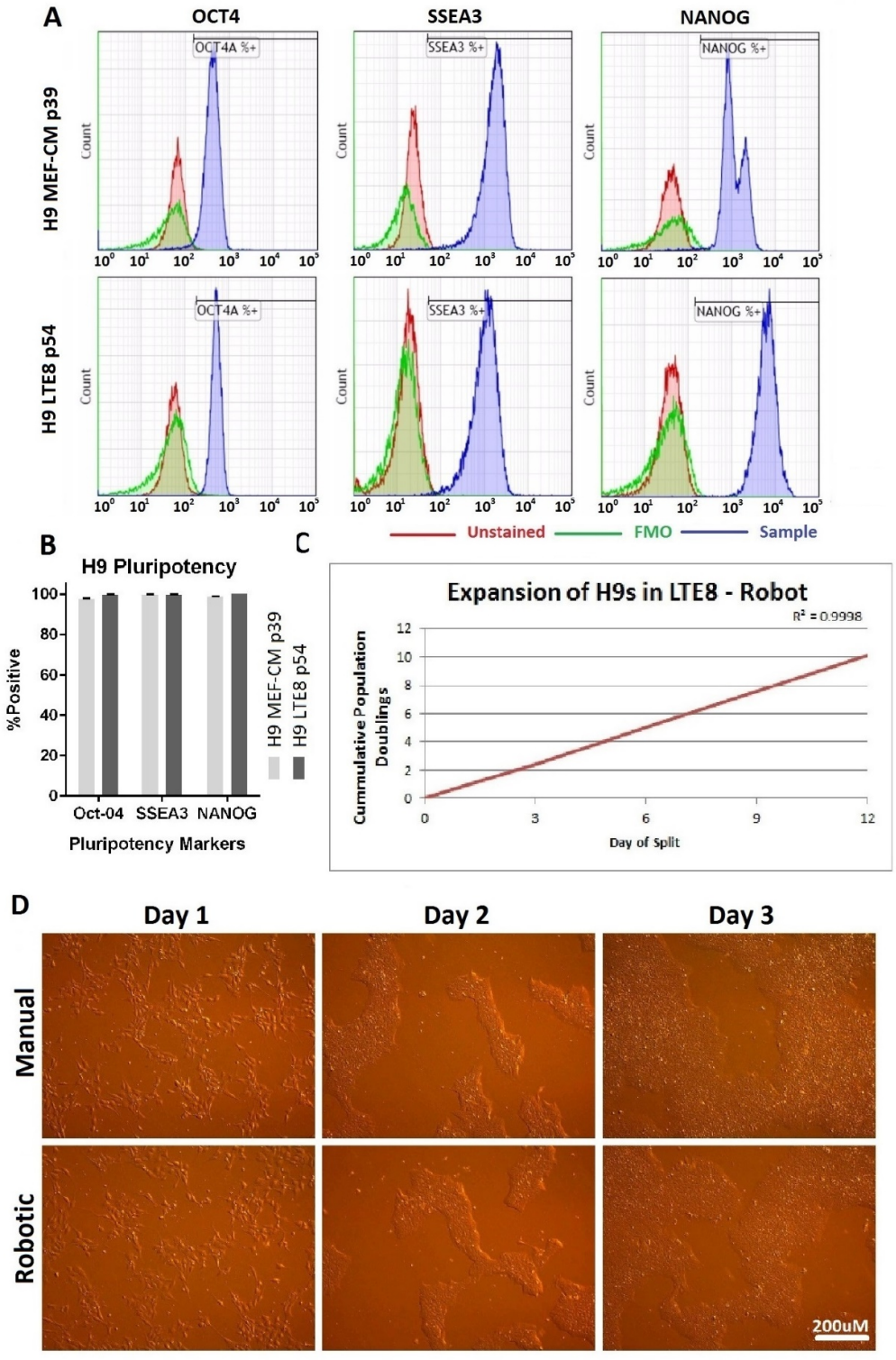

Figure 28 Assessment of pluripotency for H9 LTE8 automated platform culture. A) Multicolour Flow Cytometry for pluripotency markers in cultures of H9 in CM p39 and after transition and transfer to the automated platform H9 LTE8 p54. **B)** Quantification of the pluripotent marker expression and student t-test. Significance represented as * $p<0.05$. **C)** Growth curve of H9 cells cultured on the robotic platform and **D)** Brightfield images showing daily expansion and colony morphology of H9 cells. Error bars represent standard deviation of the mean. Scale Bar **(D)** 200um.

3.2.9. Robotic Cell Culture Can Successfully Differentiate the H9 Cell Line into HLCs in 96 well plates.

The automated Hepatocyte Differentiation protocol described in section 2.8 was divided into two distinct processes, (a) cell seeding in 96 well plates and (b) stage-specific medium-change. Upon harvesting of a Roboflask as described above, an appropriate volume of the remaining cell suspension containing 17.000.000 cells was diluted into 50ml of LT-E8 medium in a trough (making a final concentration of 17.000 cells per 50ul). The trough was placed on the warm carrier and seeding of the cells in the 96w/p was achieved using the "PlatingMCA96 well_1" automated protocol described in Table 10. Labware required for the process was a set of 96 well-tips for the MCA96 head placed on the Labware position as indicated in Figure 29A.

Table 10 Flow Diagram for automated seeding protocol of hPSCs in 96 well plates using the "TECAN Freedom Evo 200". Green highlighted boxes describe positioning and transfer of 96 well-plate into the desired location, Orange highlighted box describes removal of spent medium and feeding with fresh medium.

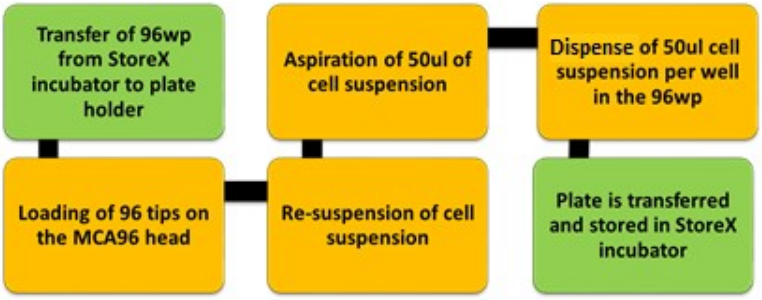

The second phase responsible for stage specific-medium change (PlateFeed96wellHepDiff), required positioning of the prepared volume of medium in a 100ml trough and position on the warm carrier as shown in Figure 29. In addition, prior to the robotic protocol, manual positioning of labware was required at the appropriate locations; an empty 100ml waste trough was required and 2 sets of 96 well-tips were needed for the MCA96 head (Table 11 & Figure 29).

Table 11 Flow Diagram for automated feeding process of Hepatocyte Differentiation 96 well plates using the "TECAN Freedom Evo 200". Green highlighted boxes describe positioning and transfer of 96 well-plates into the desired location and Orange highlighted boxes describe removal of spent medium and feeding with fresh.

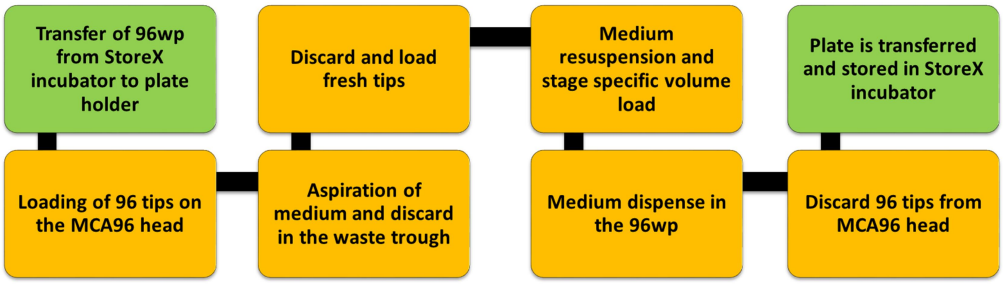

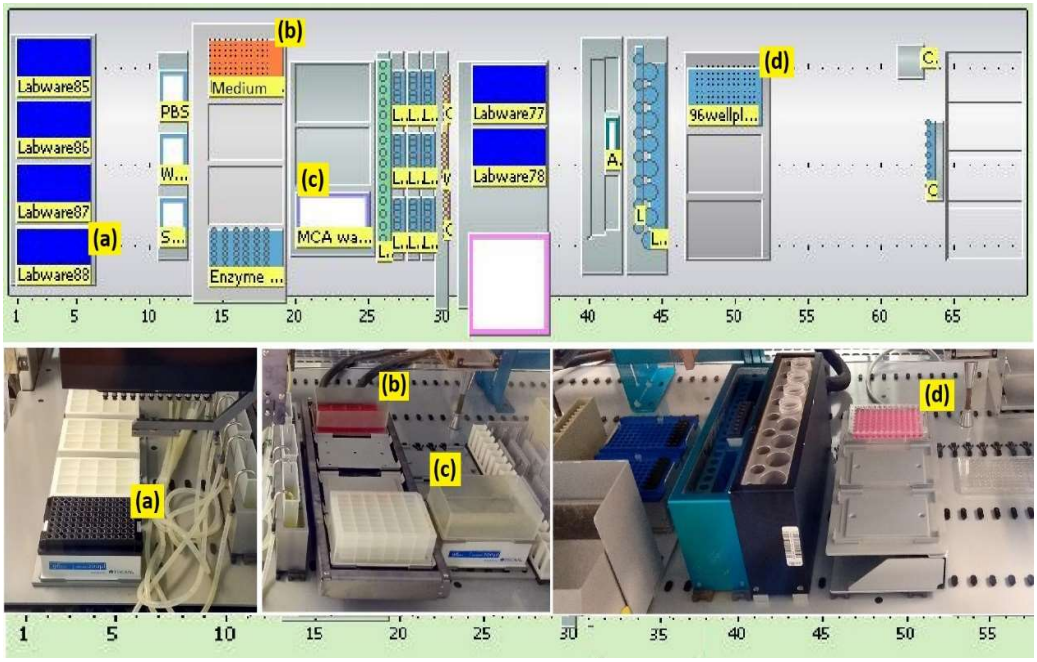

Figure 29 Overview of the Tecan Freedom Evo deck prior to an automated passaging protocol and positions for allocated labware and consumables. A) Screenshot of the deck shown in the Freedom Evo software, **B)** Actual Tecan Freedom Evo deck and **C)** Incubator StoreX.

Typical confluency measurements across wells of the H9 LT-E8 96 well plates were determined using a CellaVista plate reader (SYNENTEC, Germany) shown to be between 40-60% (Figure 27). It is worth mentioning that due to sheer forces and resuspension of the medium containing cells for seeding, the outside wells of the 96 well plate were showing an increased Standard Deviation in the cell confluency and that would lead to variable results on day 17. Therefore, it was decided that the outside wells of the 96 well plates will not be taken into account for experiments (Figure 27). The differentiation was initiated following

Figure 30 Cellavista measurement for confluency of 96 well plate in format of heatmap before initiation of the Hepatocyte Differentiation. Increased Standard Deviation when taken into account all 96 wells but it is lower when the inside wells (green box) are used. Blue represents a low confluency, Red represents high confluency and colours in between average confluencies.

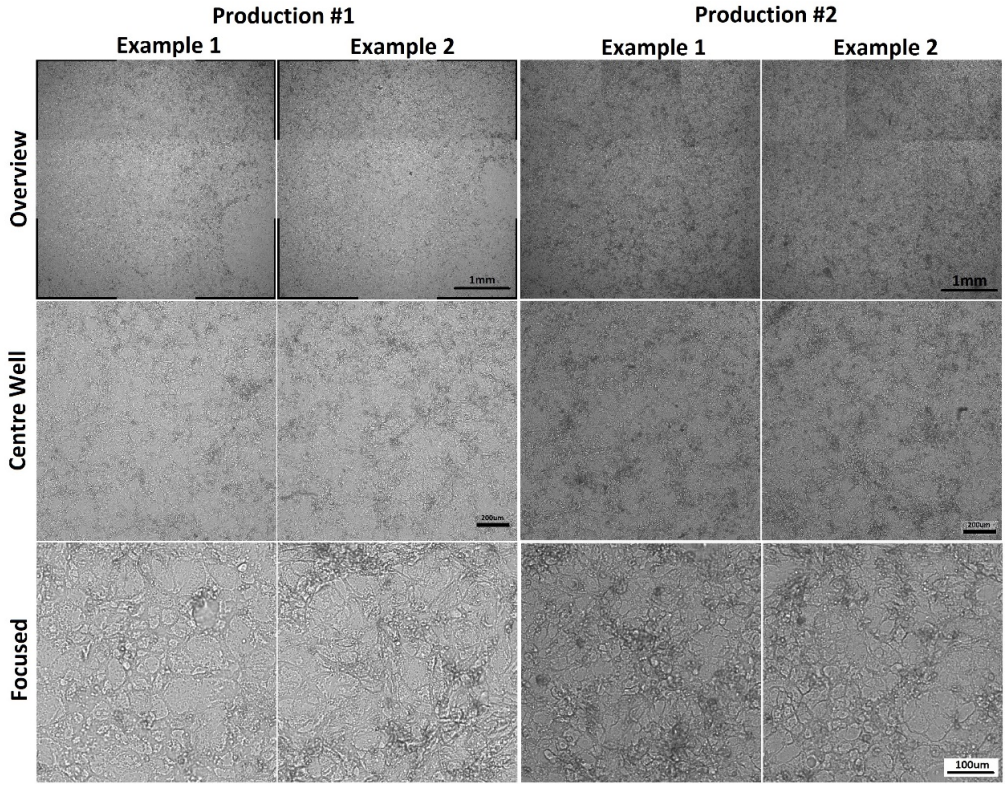

Figure 31 Brightfield microscopy for two separate production runs for day 17 HLCs generated using the automated platform. Overview of two example wells for each production highlight the absence of 3-dimentional structures, centre well images demonstrates HLC formation and focused images show the characteristic HLC morphology that was identified on day 17. Scale bars Overview 1mm, Centre well/Focused 100um.

the stage-specific “PlateFeed96 wellHepDiff” automated protocol.

Typically, the morphology obtained on day 17 followed the characteristics of HLC described before. Two separate production runs are shown in Figure 31 with examples of two representative wells. ALB, AFP, HNF4a, A1AT and CYP450 3A4 were expressed similarly in both productions, confirming the reproducibility of the hepatocyte differentiation using the automated platform (Figure 32). Quantification detected ALB 39.4%±9.7, AFP at 80.7%±12.8, HNF4a at 64.2%±7.9, a1-antithrypsin at 71.6%±1.5 and CYP450 3A4 at 8.3%±2.2. Two-way ANOVA analysis, identified no significant differences between the two separate productions (n=3), confirming reproducibility of the experiment (Figure 32B).

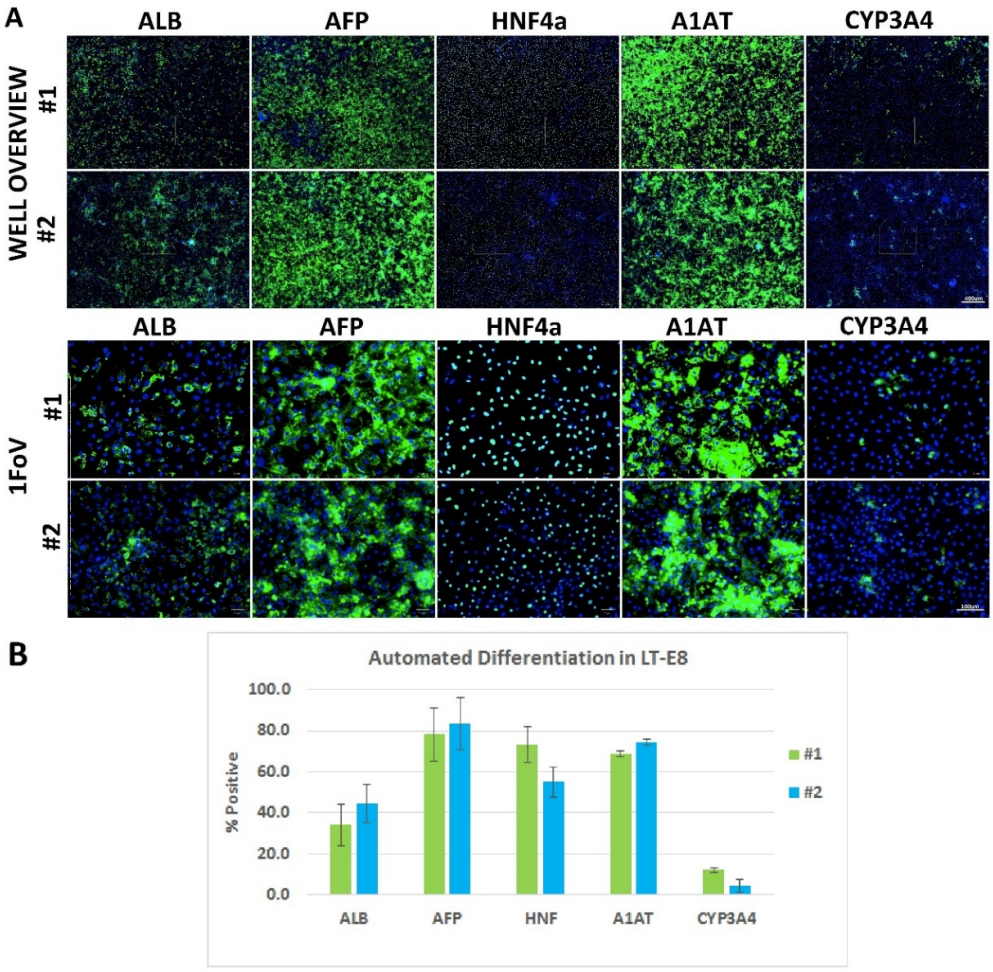

Figure 32 Assessment of HLC differentiation by immunocytochemistry staining for HLC markers on the day 17 HLCs generated using H9 LT-E8 cultured cells p50 and p52 in the automated platform. A) Well overview of representative wells for the markers ALB, AFP, HNF4a, A1AT and CYP450 3A4. Lower panel shows 1 representative Field of View (FoV) for each condition described above. **B)** Quantification analysis and two-way ANOVA for

the expression of the hepatocyte markers ALB, AFP, HNF4a, A1AT and CYP450 3A4. Significance represented as * p<0.05. Error bars represent standard deviation of the mean. Scale Bars **(A)** Well overview 400um/ 1FoV 100um. N=3, Runs=2**.**

3.2.10. Transition from commercially-produced LT-E8 into Home-Made E8 can Maintain Characteristics of H9 hPSCs Long Term and generate HLCs

Experimental cost for the commercial LT-Essential 8 culture medium was a burden to the scientific research and the experimental design for the project. Home-Made Essential 8 (HM-E8) culture medium was estimated that can be produced significantly cheaper (16,7% of the price) by buying the 8 components in bulk and preparing it in-house (Table 12). The recipe for the HM-E8 was followed from the published protocol (Burridge et al., 2015).

Table 12 Cost differences between Commercial Life-Tech Essential 8 and Home-Made Essential 8.

Ingredients as per protocol (Burridge et al., 2015)	Size	Price £	250L	Total
DMEM/F12 (Corning, cat. no. 10-092-CM)	0.5L	£11.65	500x 0.5L	£2,912.50
L-ascorbic acid 2-phosphate tri sodium salt (Sigma 49752-10G)	10g	£26.10	16g	£26.10
Recombinant human insulin (Life Technologies, cat. no. A11382ij)	5g	£469.36	5g	£1,540.00
Recombinant human transferrin (Sigma-Aldrich, cat. no. T3705-1G)	1g	£340.50	1250mg	£340.50
Heparin sodium salt (Sigma-Aldrich H3149-250KU)	250KU	£186.00	10 mg/mL stock	£186.00
Sodium selenite (Sigma-Aldrich, cat no. S5261-10G)	10g	£20.00	70 mg/50 mL	£0.00
Recombinant human FGF2 (Peprotech, cat. no. 100-18B)	10x1mg	£3,000.00	25mg	£7,500.00
Recombinant human TGFB1 (Peprotech, cat. no. 100-21)	500ug	£1,700.00	500ug	£1,700.00
			LT E8	**HB8**
		per 500ml	£169.30	£28.41
		per 250L	£84,650.00	£14,205.10

Adaptation of H9 cells into the HM-E8 started the day before cells become confluent. The cells were passaged, fed and allowed to grow with HM-E8, until confluent. The process re-peated for 3 passages (Figure 33A). Morphology and colony formation of the cells was maintained before and after the transition, similarly for the characteristic morphology of the colonies, as seen in Figure 33A. The level of cell death was noted as higher compared to the LT-E8 cultures. Another difference noted was the extended growth of colony edge cells as shown in the examples in Figure 33B. The extended colony edge cell morphology was maintained through the culture using HM-E8 culture medium.

Transitioned cells had a duplication time of 2.4 days and their expansion rate was stable over the 12 days (Figure 34). Normal karyotype was retained (Passage 54, Spreads 30, kary-

otype 46,XX[28], 45,XX,-19[1], 45,XX,-20[1]). Duplicate flasks of H9 cells cultured in LT-E8 and in HB-E8 were maintained for additional 14 passages (from p48 to p62).

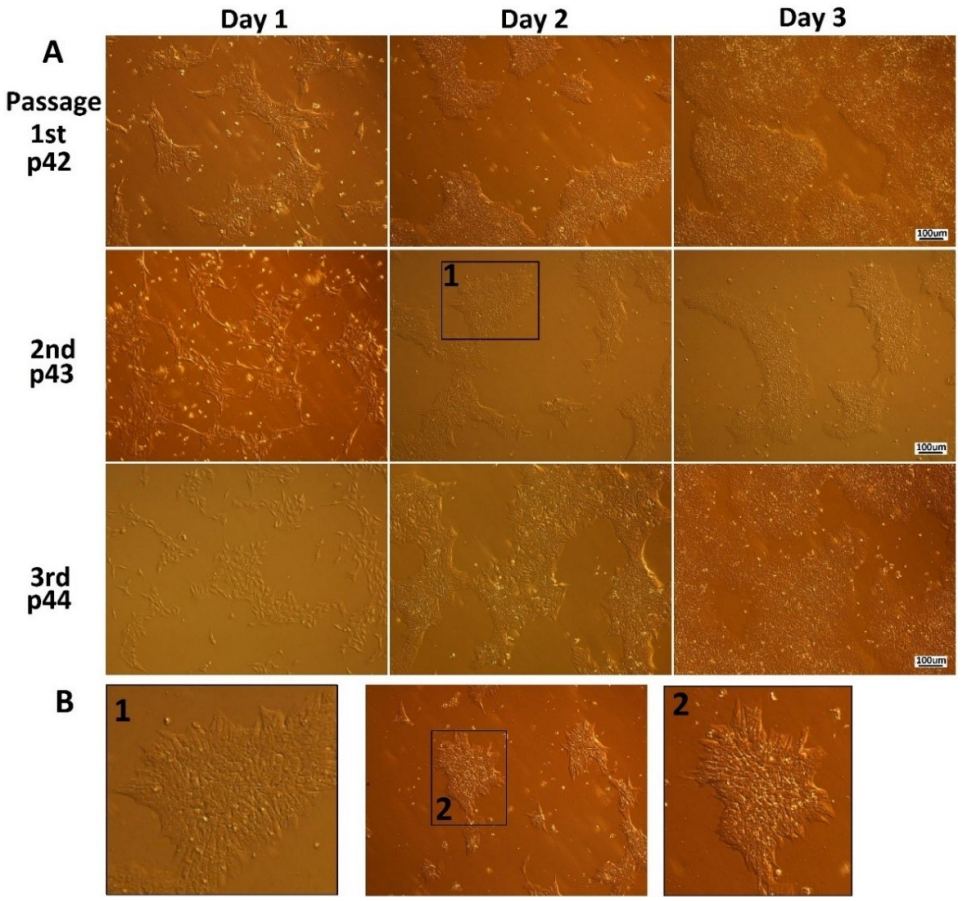

Figure 33 Transitioning of LT-E8 H9 cells into HM-E8 culture Medium. A) Morphology of the cells during each day of the first 3 transitioning passages. **B)** Examples of extended colony edges. Scale bars (A) 100um.

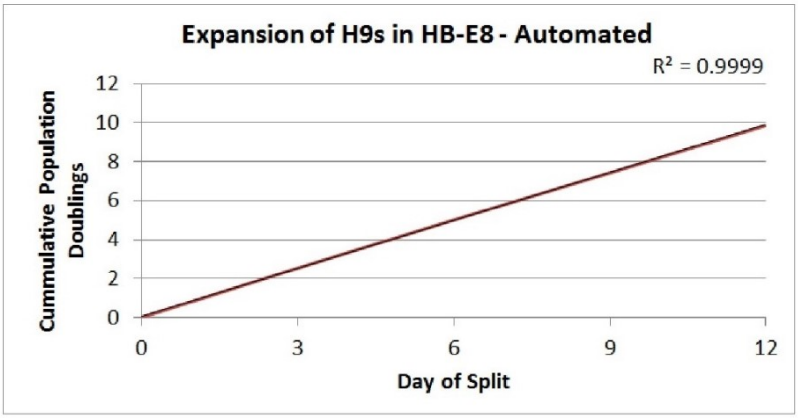

Figure 34 Growth curve of H9 cells cultured in HB-E8 (Post-transitioning) Duplication time was calculated as 2.4 days. Stable expansion rate was maintained.

CellaVista confluence measurements were similar for LT-E8 and HB-E8 cultures (Figure 35C). Note that, because measurements of the whole surface required in average 40 minutes per Roboflask, a representative area of the Roboflask was scanned instead (Figure 35A). A confluence between 30-40% was identified for day 1, 40-60% for day 2 and on day 3 the confluency was ranging between 80-100% (Figure 35B). Therefore, the growth rate of H9 cells in both media was confirmed as stable over long-term cultures.

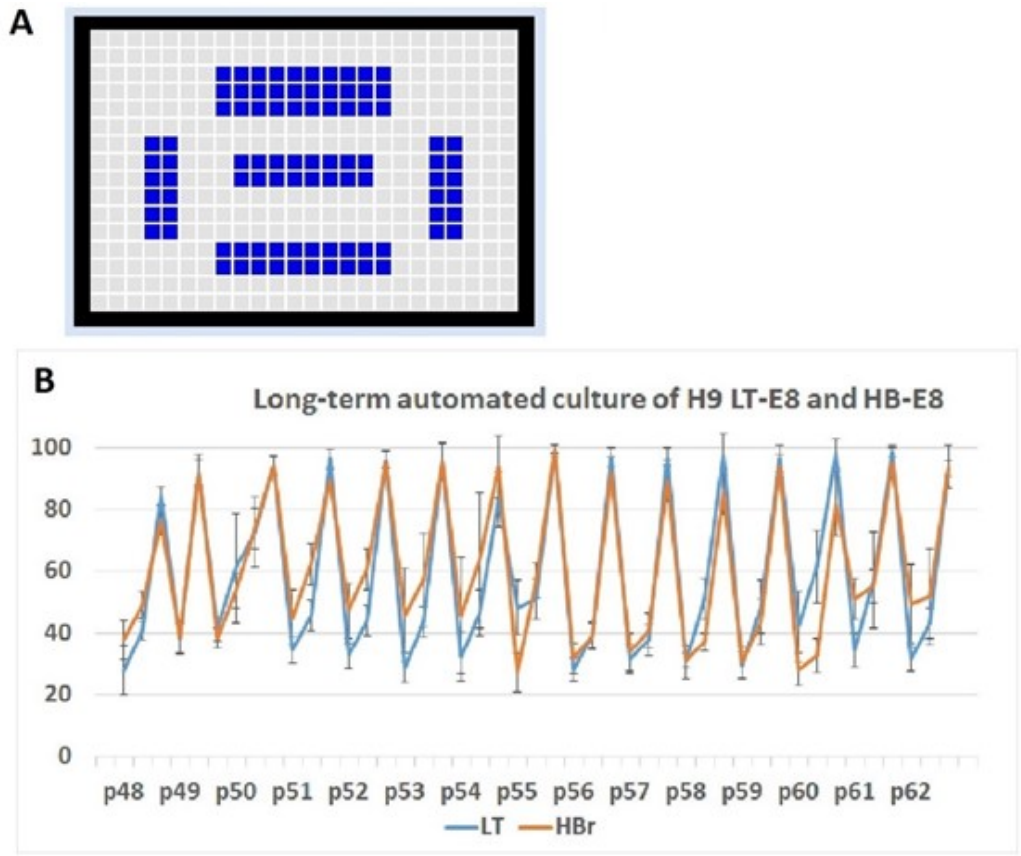

Figure 35 Long term culture of H9 cells in LT-E8 and HB-E8. A) Representative area of a Roboflask evaluated for confluency measurements **B)** Image of the Daily confluency measurements for H9 cells cultured in LT-E8 and HB-E8 between passages 48 and 62. Error bars represent standard deviation of the mean.

As seen in Figure 36, morphology of cells in day 1 was highlighted by small clumps of cells, on day 2, colonies were formed, expanded in size and separated from other colonies and on day 3 the colonies had merged and expanded more in size ready for the next passage (Figure 36). The only difference between the LT-E8 and HM-E8 was the morphology of the colonies, as described during the transition into HM-E8, with cells on the edges appearing to

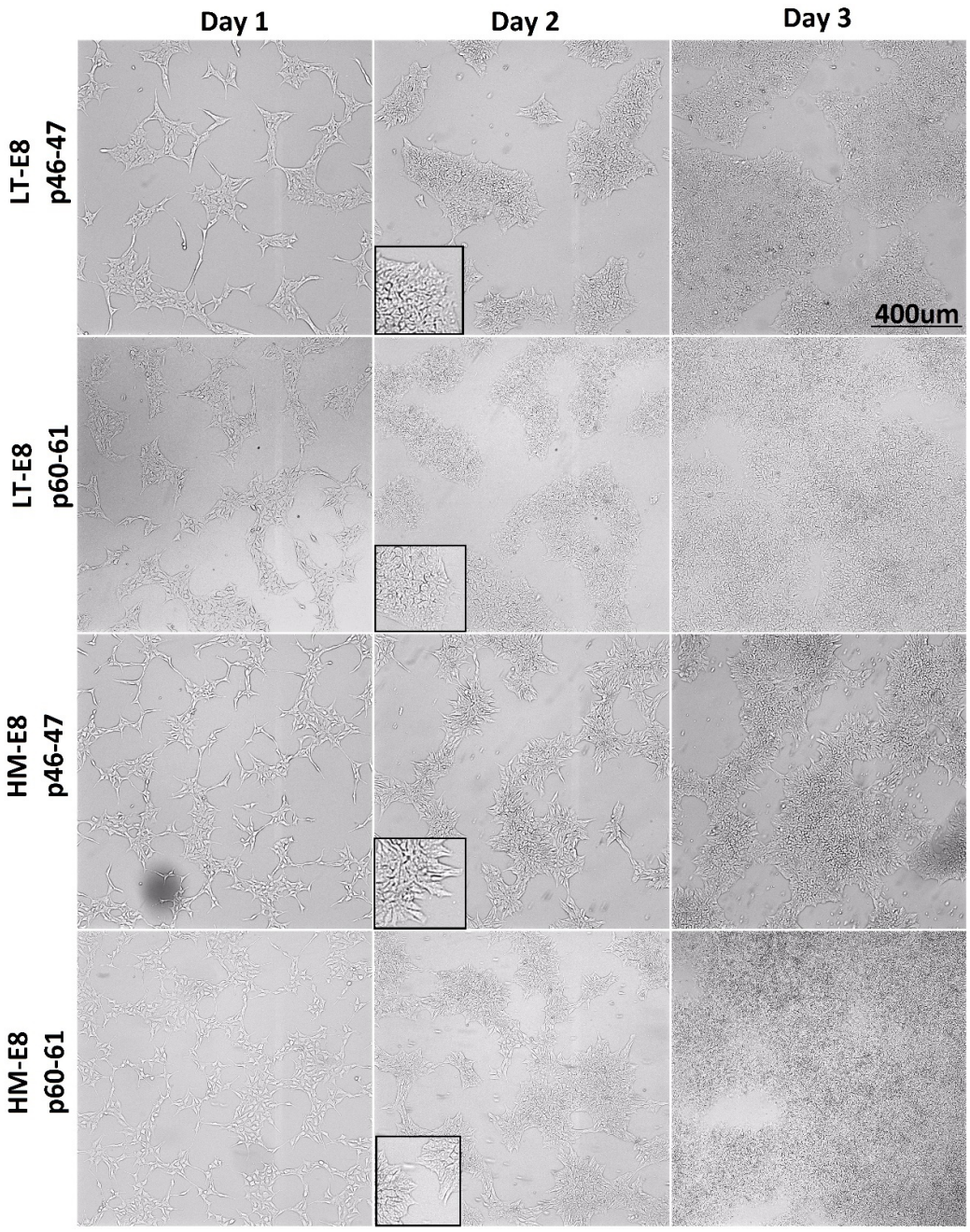

Figure 36 Long term culture of LT-E8 and HM-E8 H9 cells demonstrated similar characteristics over time. Images were taken from both cultures, daily, from passage 46 to 47, as an early stage and from passage 60 to 61 as a late stage. Days 1 to 3 are shown. Characteristic morphology of expanded edge cells for HM-E8 compared to absence of this morphology for LT-E8. Scale bar 400um.

reach other colonies (Figure 36/Figure 33B). Karyotype at passage 63, Spreads 30, was 46,XX[30]. Overall, the above data demonstrated that the H9 cells can be cultured in either LT-E8 or HM-E8 for long term, using the automation platform and automated scripts developed.

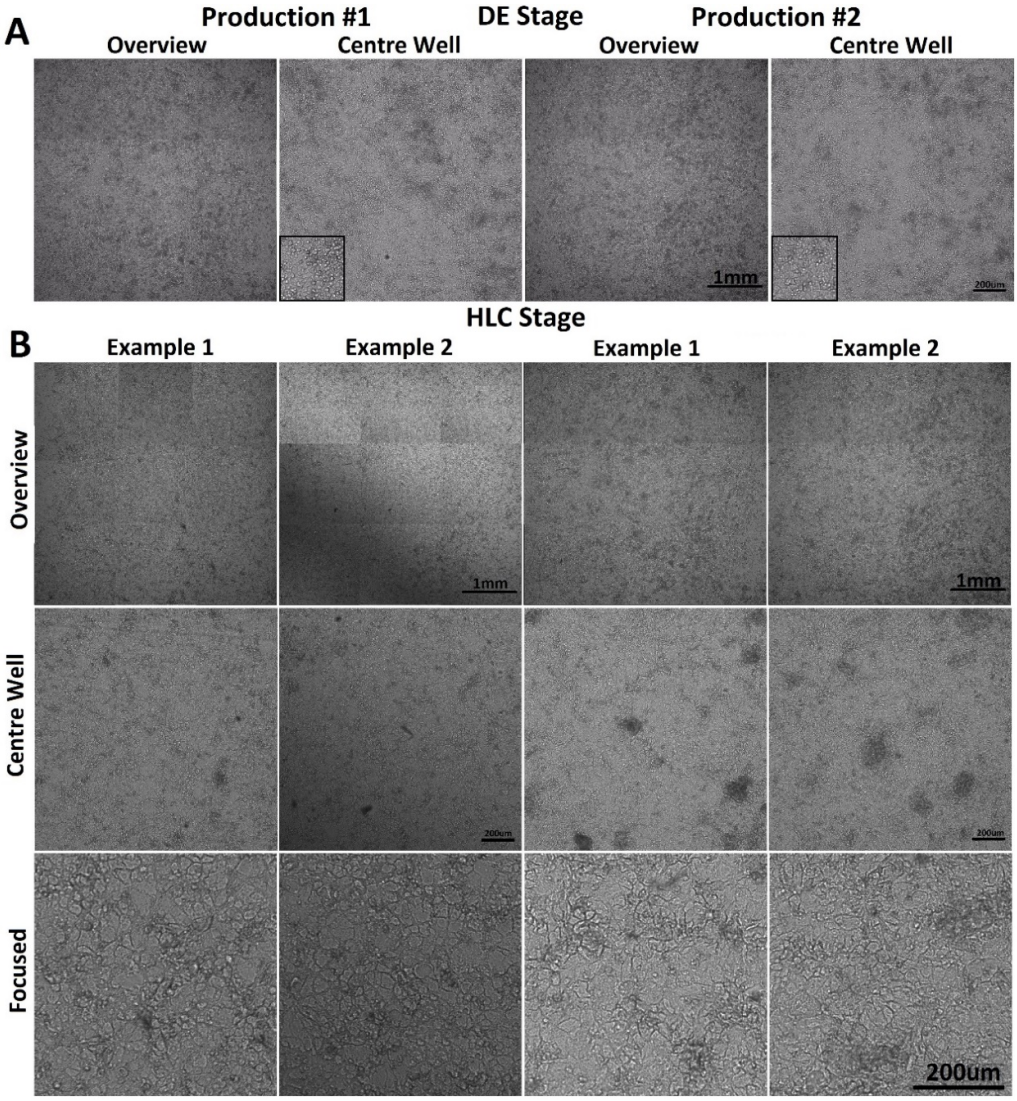

Figure 37 Brightfield microscopy for the day 3 and 17 DE and HLCs generated using H9 HM-E8 cultured cells in the automated platform. Two separate productions of HLC were generated. **A)** Overview of DE cells **B)** Overview of HLC stage. Representative wells and absence of 3-dimentional structures, Centre well images demonstrated HLC formation and Focused images indicate the characteristic HLC morphology. Scale bars Overview 1mm, Centre well/Focused 100um. N=3 Runs=2.

Hepatocyte differentiation was initiated with transitioned H9 HM-E8 cells in the robotic platform as described before in Section 2.3.9. Two separate productions were prepared and the cells generated on day 3 and day 17 indicated characteristics of the distinct phases of DE and HLCs (Figure 37). Quantification analysis detected ALB expressed 40.4%±11.5, AFP 69.8%±2.4, HNF4a 17.2±2.0, A1AT 80.9%±8.2 and CYP450 3A4 12.7%±1.4 of cells (Figure 38). Two-way ANOVA analysis, identified no significant differences between the two runs confirming reproducibility of the experiment.

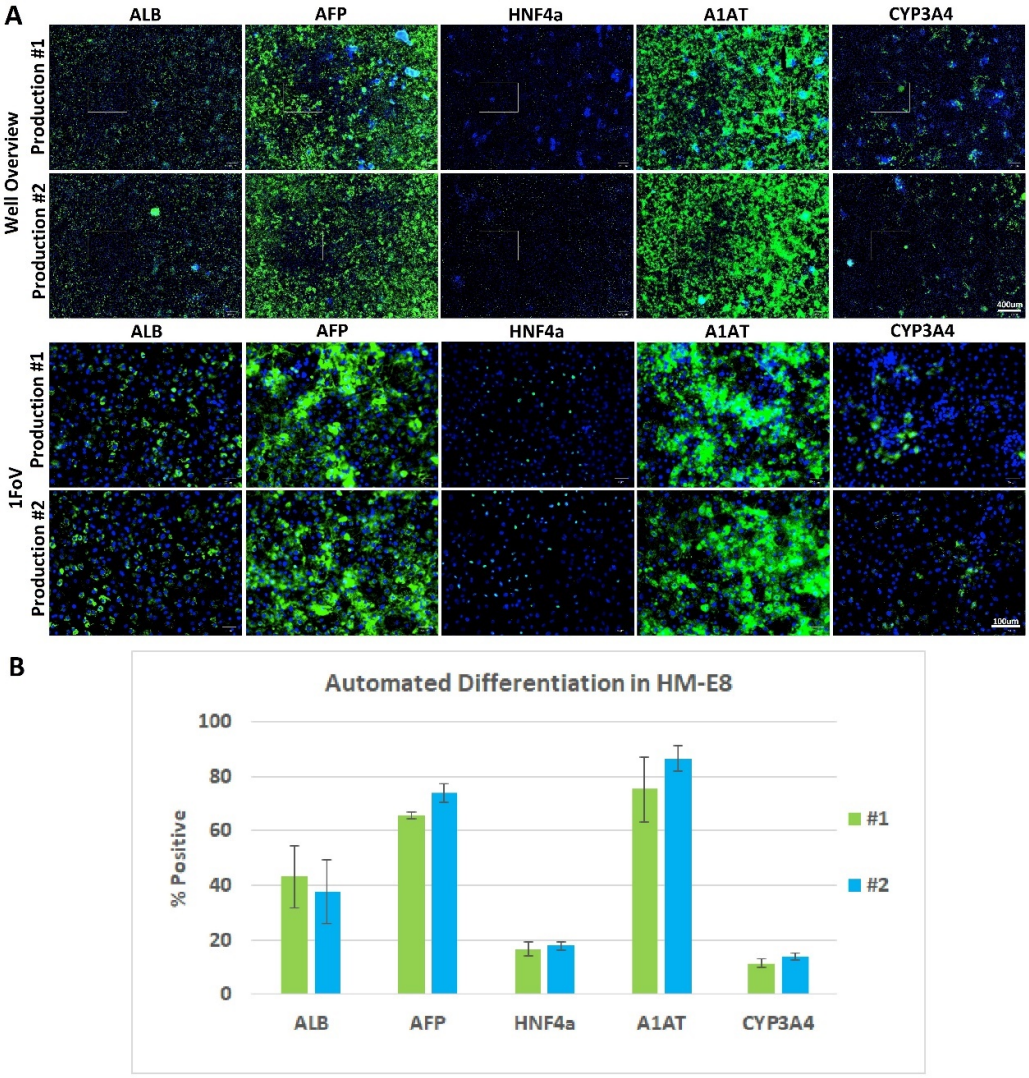

Figure 38 Assessment of HLC differentiation by immunocytochemistry staining for HLC markers on the day 17 HLCs generated using H9 HM-E8 cultured cells p54 in the automated platform. A) Well overview of representative wells for the markers ALB, AFP, HNF4a, A1AT and CYP450 3A4. Lower panel shows a representative Field of View (FoV) for each condition described above. **B)** Quantification analysis and two-way ANOVA for the expression of the hepatocyte markers ALB, AFP, HNF4a, A1AT and CYP450 3A4. Significance represented as * $p<0.05$. Error bars represent standard deviation of the mean. Scale Bars **(A)** Well overview 400um/ 1FoV 100um. N=3, Runs=2**.**

3.2.11. CP1 Induced Pluripotent Stem Cell Line (iPSCs) Can Differentiate to HLC at a Significantly Greater Efficiency Among the Commonly Used iPSC Lines Generated in the Lab.

To enable clinical translation of research and future applications for hPSCs-derived HLCs, use of iPSCs was required to evaluate the protocol and identify a cell line that can produce HLCs. For this reason, 5 different iPSC lines generated in the lab, were screened for their

potential to form HLCs. Cell culture was achieved by using LT-E8 culture medium and enzymatic passage using TrypLE for 3-4 minutes at room temperature and cells seeded at 1 million per T25 flask. The cell lines used for this experiment were the RBL_PAT, BT2, PhiCr, RBL and CP1. Hepatocyte differentiation was initiated following the protocol described before the DH/Edinburgh additions.

On day 3, cells had formed DE cells however, BT2 showed a slower expansion rate and formation of 3-dimentional structures (Figure 39). On day 8, cells had adopted a hepatoblast-like morphology, exception were the BT2 that generated clusters of 3D structures (Figure 39) and on day 17 cells had generated HLCs as seen in Figure 39. Limited Images are presented due to computer hard drive failure and loss of data.

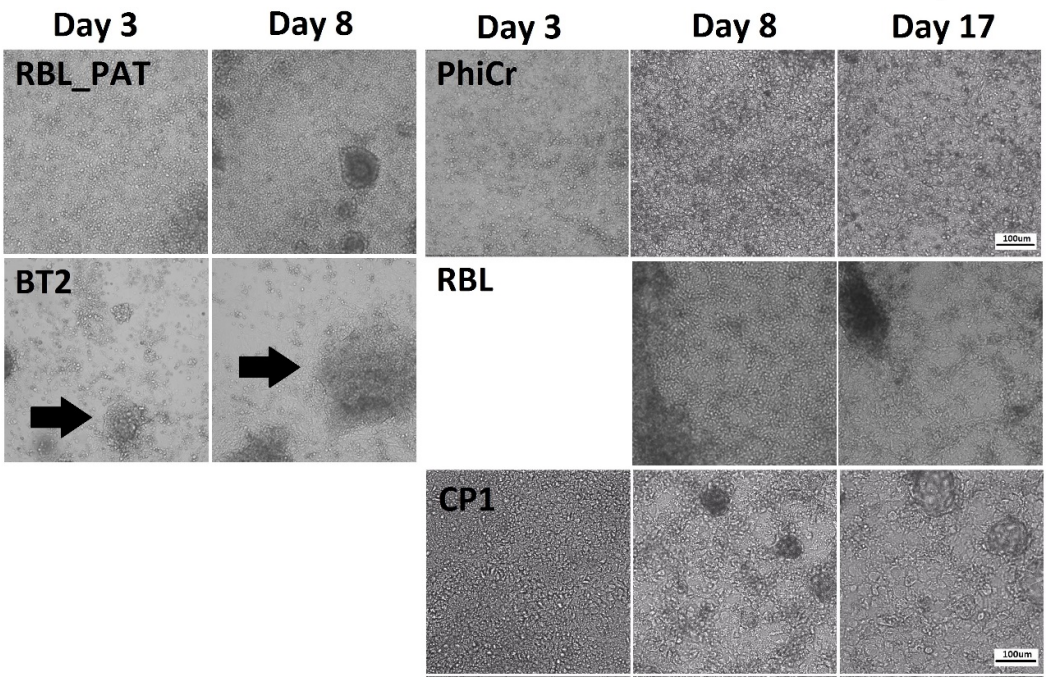

Figure 39 Morphological assessment of the iPSC lines RBL_PAT, BT2, PhiCr, RBL and CP1 on days 3, 8 and 17 following the hepatocyte Differentiation protocol. Images missing due to computer hard drive failure and loss of raw data. Black arrows indicate 3-dimentionsl structures noticed at the BT2 cell line. Scale bar 100um.

Day 17 staining demonstrated variable levels of protein expression and patterns of 3D structures generated on day 17 (Figures 40-41). Quantification of protein expression, showed that RBL and CP1 cells have an overall significantly higher expression than

RBL_PAT, BT2 and PhiCr (Figure 41B). Overall, cell morphology and protein expression data indicated that the CP1 iPSC line has achieved to generate HLCs that express proteins of hepatocyte lineage. RBL_PAT, BT2 and PhiCr had a significantly lower expression of markers and morphology characteristics that could not fit to the HLC definition. RBL cell line achieved equally well to the CP1 however, it had significantly lower expression of ALB and CYP450 3A4 compared to CP1. Therefore, CP1 was selected as the hiPSC for future experiments.

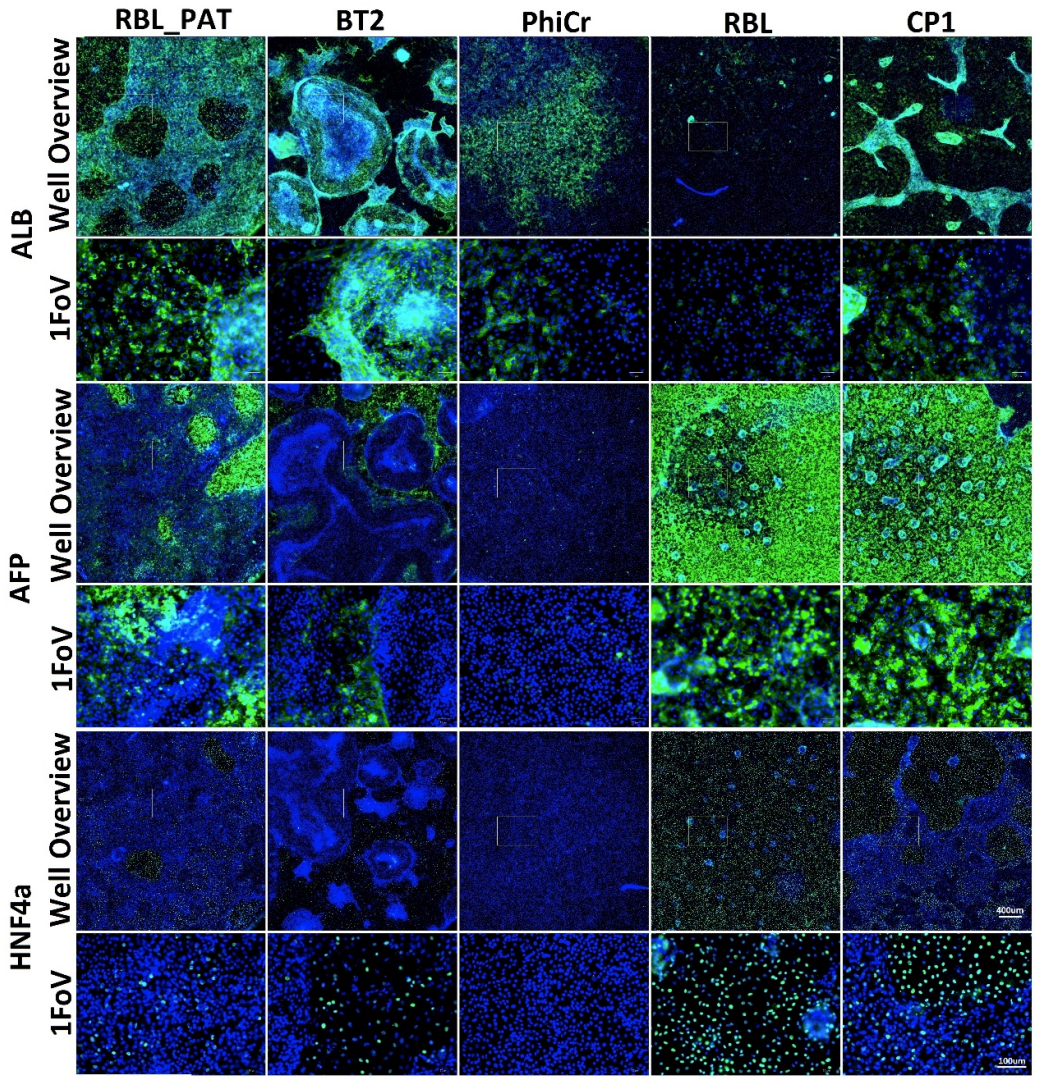

Figure 40 Immunocytochemistry for ALB, AFP, HNF4a, A1AT and CYP450 3A4 on day 17 on iPSC Lines differentiated to HLC. Well overview of representative wells for the markers ALB, AFP, and HNF4a. Lower panel shows a representative Field of View (FoV) for each condition described above. Scale Bars Well overview 400um/ 1FoV 100um. R=3, N=1

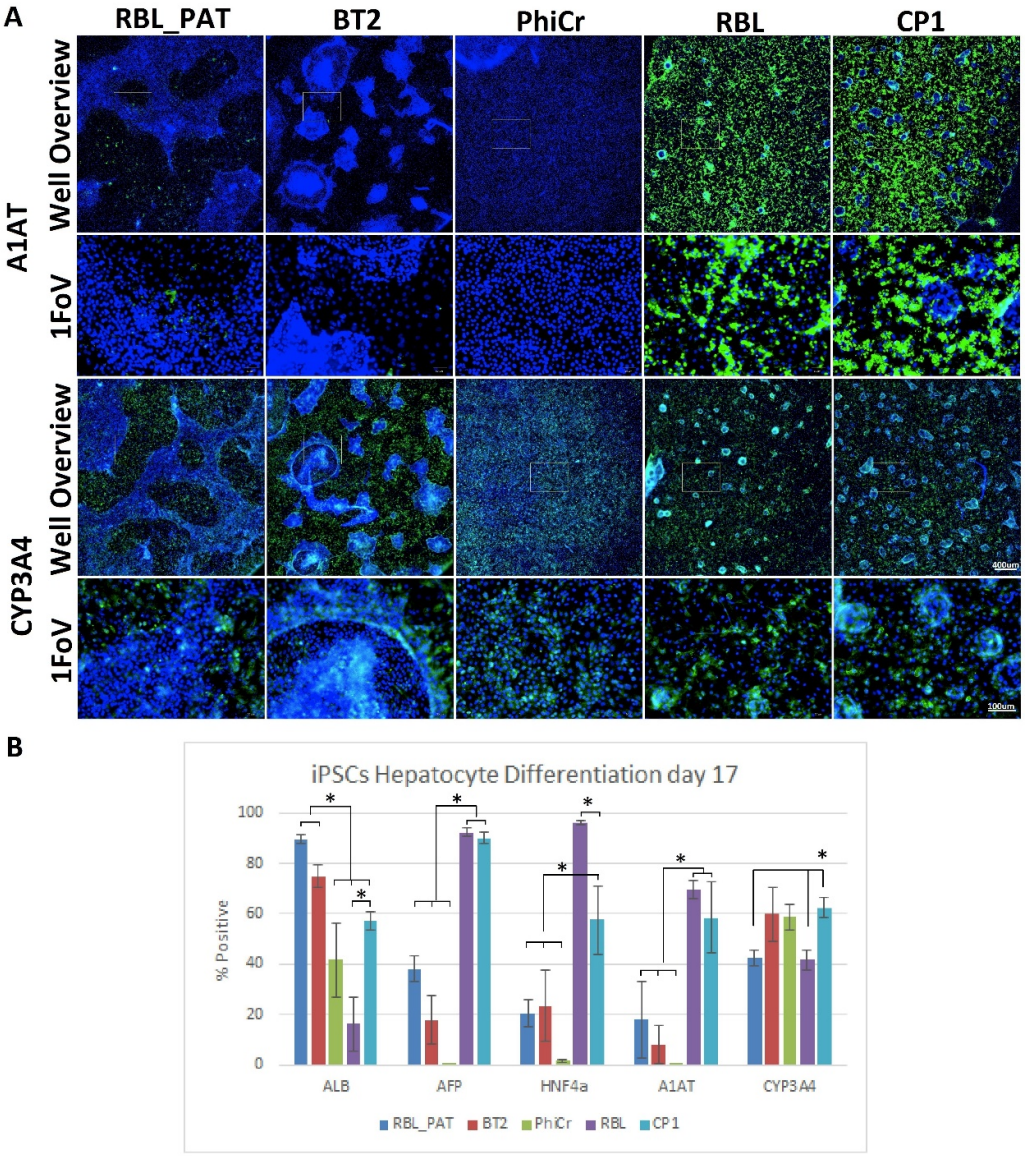

Figure 41 Immunocytochemistry for ALB, AFP, HNF4a, AAT and CYP450 3A4 on day 17 on iPSC Lines differentiated to HLC and Quantification of the results. A) Well overview of representative wells for the markers a1-antithrypsin and CYP450 3A4. Lower panel shows a representative Field of View (FoV) for each condition described above **B)** Quantification analysis and two-way ANOVA for the expression of the hepatocyte markers ALB, AFP, A1AT, HNF4a and CYP450 3A4. Significance represented as * $p<0.05$. Error bars represent standard deviation of the mean. Scale Bars **(A)** Well overview 400um/ 1FoV 100um. R=3, N=1

3.2.12. Reproducible Hepatocyte Differentiation of CP1 Cells into HLCs Cultured with HM-E8 Provides a System for Hepatocyte Maturation Screening Study

To accommodate for the hepatocyte maturation screening study in Chapter 4, a system that combines use of the CP1 hiPSC line which can differentiate into HLCs in the robotic

platform was investigated. Initially, it was investigated whether the use of the latest hepatocyte differentiation protocol, with 24H pre-differentiation time, could eliminate the formation of 3-dimentional structures (LT-E8 Manual). The second step evaluated the use of HM-E8 culture medium (HM-E8 Manual) and the third step evaluated the automated platform to generate HLCs (HM-E8 Robotic). The results are presented together.

Initially, cell culture of CP1 cells was achieved using LT-E8 culture medium and passaged using TrypLE enzyme every 3rd day and seeding at 1,000,000 cells per T25 flask. CP1 cells were transitioned into HM-E8 as described previously (Section 2.3.10) and maintained in manual cultures as well as in the automated platform.

CP1 cells from each cell culture condition set up at 17.000 cells per well. On day 3, all conditions had formed DE with the characteristic morphology of cobblestoned, tightly packed and small round-shaped cells (Figure 42). On day 17, all conditions formed HLC as it was evident by the presence of densely packed cobblestoned cells, distinct cell borders and polygonal appearance (Figure 42). Absence of 3-dimentional structures was evident indicating the generation of a monolayer structure (Figure 42).

Staining on day 17 (Figure 43A) indicated that LT-E8 cells generated a significantly higher population for HNF4a, a1-antithrypsin and CYP450 3A (Figure 43B). Expression of markers between the manual culture and the robotic culture of HM-E8, did not show significant differences, maintaining expression at a similar rate that was ALB 29.5%±4.7, AFP 81.5%±4.0, HNF4a 79.2%±4.9, A1AT 50.5%±6.6 and CYP450 3A4 6.1%±3.2 (Figure 43B).

Overall, this experiment demonstrated that the hepatocyte differentiation protocol using the CP1 iPSC line was reproducible when the cells were cultured using the HM-E8 culture medium. In conclusion, CP1 cells achieved to efficiently produce HLCs in the automated platform confirming reproducibility which was essential for use of the cell line in future experiments.

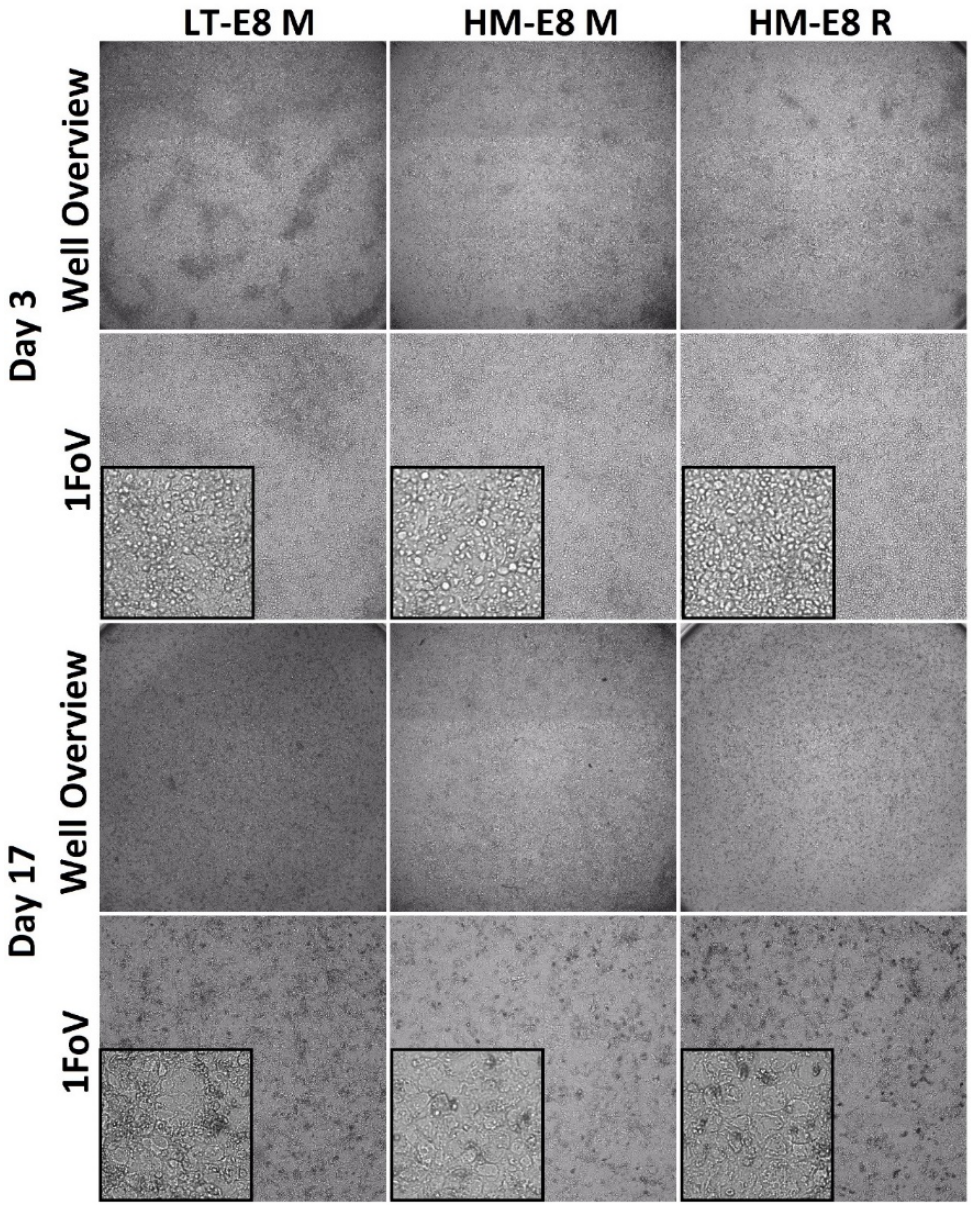

Figure 42 Brightfield assessment for the CP1 cells cultured in LT-E8 M, HM-E8 M and HM-E8 R on day 3 and on day 17. Day 3 cells demonstrate generation of Definitive Endoderm cells with the characteristic morphology and day 17 cells demonstrate generation of HLC cells excibiting HLC characteristics. Top panel shows the well overview and lower panel shows the central field of view (1FoV). Scale bars Overview 1mm, Centre well/Focused 100um. N=3, 2 productions per condition.

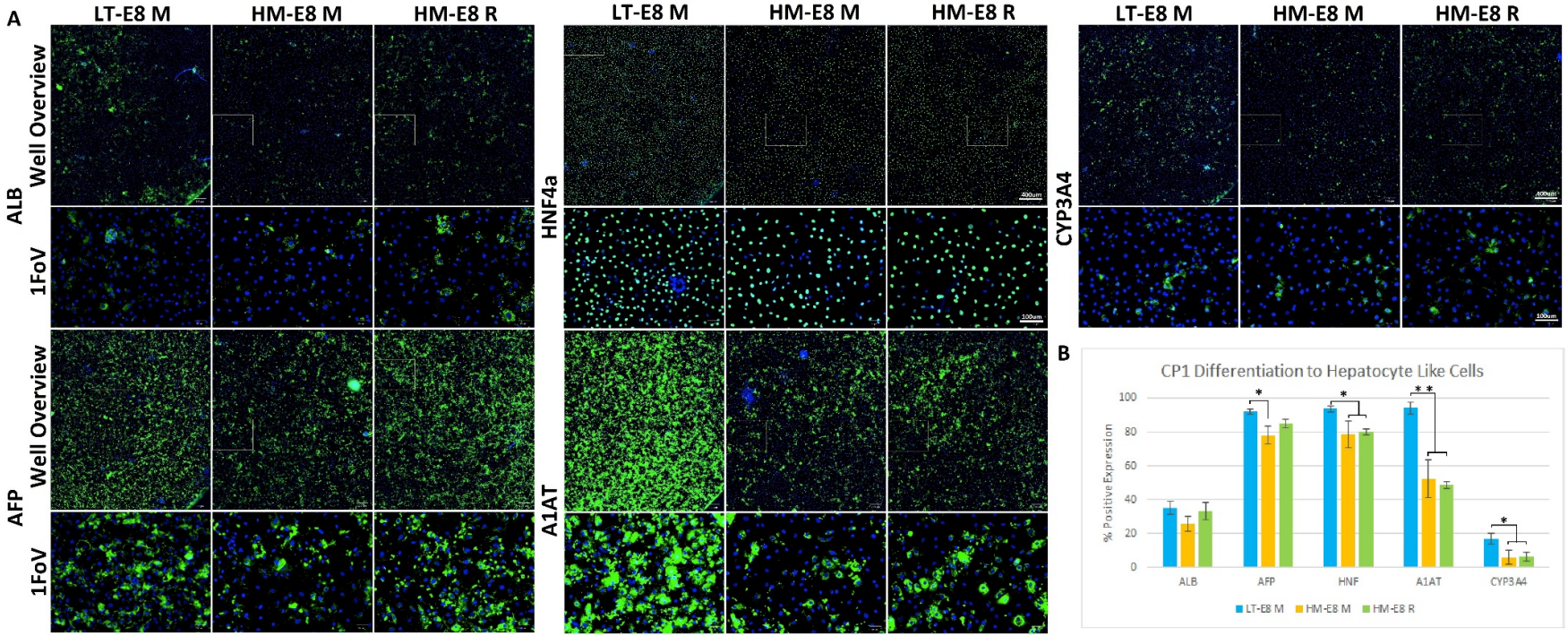

Figure 43 Immunocytochemistry for ALB, AFP, HNF4a, AAT and CYP450 3A4 on day 17 upon differentiation of CP1 cells to HLCs and Quantification of the results. A) Well overview of representative wells for the markers above. Lower panel shows a representative Field of View (FoV) for each condition described above **B)** Quantification analysis and two-way ANOVA for the expression of the hepatocyte markers ALB, AFP, A1AT, HNF4a and CYP450 3A4. Significance represented as * $p<0.05$, **$p<0.001$. Error bars represent standard deviation of the mean. Scale Bars **(A)** Well overview 400um/ 1FoV 100um. N=3, 2 productions per condition.

3.3. Discussion

Summary

In this chapter, HLCs generated from the hepatocyte differentiation protocol were shown to express markers of hepatocyte cells ALB, AFP, A1AT, HNF4a and CYP450 3A4. The hepatocyte differentiation protocol from the University of Edinburg was tested and differences with the currently used were compared. Incorporation of technical features, also comparing HUES7 and H9 cell lines and starting density, generation of a significantly higher expression of HLCs was achieved. Increased reproducibility of experiments was attempted by testing a chemically defined culture medium LT-E8 that also generated HLCs. Use of the robotic platform to facilitate maintenance, expansion and differentiation was tested successfully with commercial LT-E8 or in-lab prepared HomeMade-E8, generating HLCs reproducibly, at similar efficiencies. Lastly, in-lab developed hiPSC lines were evaluated for their efficiency to generate HLCs and the CP1 cell line was selected and tested in the automated platform with HM-E8.

Generation of Hepatocyte-Like Cells

Hepatocyte differentiation of hPSCs into HLCs demonstrated expression of markers commonly used in the literature (Touboul et al., 2010, Hannan et al., 2013, Medine et al., 2011). Immunostaining and images acquired in this study for ALB demonstrated intensity of expression higher than in (Touboul et al., 2010) similar to (Toivonen et al., 2013, Asplund et al., 2016), similar to the day 15 immature hepatocytes generated in (Si-Tayeb et al., 2010b, Agarwal et al., 2008) but not as high as the HLCs produced at (Hay et al., 2008b). AFP was highly expressed, similarly to (Baxter et al., 2015, Asgari et al., 2013, Agarwal et al., 2008, Toivonen et al., 2013) or similar to the small molecule approach in (Siller et al., 2015). Variation in the expression of HNF4a was detected, low expression in the hESC-derived HLCs but high in the hiPSCs-derived HLCs while it was expressed higher in (Si-Tayeb et al., 2010b, Toivonen et al., 2013, Agarwal et al., 2008, Asplund et al., 2016). A1AT was expressed high-

er than in (Asplund et al., 2016, Baxter et al., 2015, Touboul et al., 2010) and similar to (Siller et al., 2015, Asgari et al., 2013). Lastly, CYP450 3A4 was lower than in (Hay et al., 2008b).

Overall, similarities and differences with the current literature are present. However, direct comparison of hepatocyte marker expression may lead to incorrect conclusions due to technical differences in immunostaining and imaging acquisition protocols (Lamvik et al., 2001). Additionally, current literature only presents images of a specified area of expressing cells, omitting the overview that might include areas of lower expression. In this study, the aim was to generate HLCs reproducibly that could later be used to evaluate factors identified and their effect on HLC generation. Therefore, comparison to the current literature was not required as long as the results from staining indicate that the day 17 cells have acquired hepatocyte characteristics.

A few studies show sequential morphology figures of the differentiation process to compare with and similarities can be identified at the DE and hepatoblast stages (Hay et al., 2008b, Song et al., 2009b, Hannan et al., 2013, Wu et al., 2012). Regarding the expected hepatocyte morphology, it is described as polygonal, distinct nucleus and multinuclear morphology with distinct regions along the cell membrane that indicate presence of bile canaliculi at the end stage of differentiation (Krueger et al., 2013, Asgari et al., 2013, Takayama et al., 2013, Cai et al., 2007) which are similar to the HLCs generated in this thesis. The increased similarity to primary hepatocytes confirms the phenotypic characteristics, thus increasing the confidence for the generated HLC population (LeCluyse et al., 2005, Sunman et al., 2004). Finally, hepatocyte size generated in this study was approximately between 40-60um while in the literature, it is reported between 30-50um (Turner et al., 2011).

Variability of hPSCs and HLC generation

In this thesis, the hESC lines H9 and HUES7 were evaluated in the HLC differentiation and identified that H9-derived HLCs could express hepatocyte related markers with a greater efficiency. Current literature for HLC generation primarily uses the hESC line H9 (Hay et al., 2008b, Si-Tayeb et al., 2010b, Cai et al., 2007, Agarwal et al., 2008, Chen et al., 2012b, Touboul et al., 2010, Hannan et al., 2013, Duan et al., 2010, Magner et al., 2013, Baxter et al., 2015, Takayama et al., 2014) while few studies have generated HUES7-derived HLCs (Baxter et al., 2015). As discussed above, differences in the differentiation protocols in between laboratories lead to different HLC generation efficiencies. Additionally, in this thesis, 5 hiPSC lines were differentiated with the same protocol at the same time and variability was identified in the expression of hepatocyte related markers. This variability is explained by genetic and epigenetic variations in hESCs and hiPSCs that contribute to the functional variability between cell lines leading to lineage bias (Cahan and Daley, 2013) and complication when the development of universal protocols is attempted (Ortmann and Vallier, 2017).

Comparison of cell lines and assessment of differentiation potential into pancreatic and cardiac lineages reported that the HUES 8 hESC line produced the highest expressing pancreatic cells and the HUES3 the highest expressing cardiomyocytes (Osafune et al., 2008). In a similar manner, differentiation of 17 cell lines into motor neurons highlighted that significant differences in 2 of them differentiating at either significantly low or significantly high efficiency (Di Giorgio et al., 2008). Recently a differentiation protocol was developed that allowed differentiation of 5 hESC and 20 hiPSC lines to HLCs however, functional assays and expression of proteins varied in each line (Asplund et al., 2016). In conclusion, the inherent cell line variability affects the generation of differentiated cell populations, therefore attempts for quick cell line screens to identify capability for further differentiation (Siller et al., 2016) are required to reduce the cost and time associated.

Seeding Density & Initiation Time for HLC Generation

Seeding density, culture medium and initiation time for hepatocyte differentiation in this thesis, demonstrated to have an impact in both the expression of metabolising enzymes and generation of a monolayer sheet of HLCs on day 17. The best performing seeding density for hepatocyte differentiation was identified at $5.2x10^4$ cells/cm^2 (or 17.000 cells per well) while the 9.1 $x10^4$ cells/cm^2 (30.000 cells per well) or 18.3 $x10^4$ cells/cm^2 (60.000 cells per well) led to significant loss of metabolising enzyme expression and led to significant formation of three-dimensional structures.

In the hPSC field, seeding density was reported to affect the generation of insulin secreting pancreatic beta-cells (Gage et al., 2013). High seeding densities ($5.3x10^4$ cells/cm^2) showed increased expression of PDX1 and pancreatic related markers compared to the medium/low seeding densities ($3.3x10^4$ cells/cm^2) concluding that seeding densities should be optimised for differentiation protocols. Additionally, the high seeding densities ($5.3x10^4$ cells/cm^2) also improved definitive endoderm differentiation judged by SOX17/CXCR4 positive cells (Gage et al., 2013). Densities of $3.0x10^4$ to $4.0x10^4$ cells/cm^2 were used in other studies reporting high CYP450 1A, 2C9, 2D6 and 3A activities (Asplund et al., 2016).

Initiation of differentiation occurs when the confluence is between 50% and 70% (Hay et al., 2008b) while others reported higher confluencies of 70% (Cai et al., 2007) or 80% (Agarwal et al., 2008). Similarly, Siller et al reported that each cell line requires optimised cell density while the differentiation initiated 24 hours post seeding (Siller et al., 2015). Overall, details for seeding densities and time before initiation of the differentiation are omitted, making difficult to replicate experimental procedures (Agarwal et al., 2008, Cai et al., 2007, Touboul et al., 2010, Toivonen et al., 2013, Song et al., 2009b). In conclusion, even though these parameters should be optimised for each cell line, the optimised seeding density, the time before initiation of differentiation and confluency for the cell lines used in this

thesis was in accordance with published studies.

Maintenance of Cell Cultures in Chemically Defined Medium

Maintenance of the hESCs in MEF-CM and transition to the commercial LT-E8 and then HM-E8 was accompanied by noticeable changes in the cells. Initially, colony formation of the hESCs was identified, similar to reports in the literature upon the use of the LT-E8 (Chen et al., 2011). Differentiation into HLCs in this study led to the formation of HLC morphology as discussed above and as achieved in (Siller et al., 2015) where LT-E8 was the maintenance medium.

Interestingly, in this study, transitioning from LT-E8 to the HM-E8 was accompanied by two noticeable alterations. Initially, the cell morphology in HM-E8 was changed with the cells at the edge of the colonies appearing to reach nearing cells and secondly the expression of HNF4a in the day 17 HM-E8 derived HLCs was significantly lower compared to the day 17 LT-E8 derived HLCs. In the original publication where HM-E8 was developed, morphology alterations were not mentioned (Burridge et al., 2015). Additionally, another report presenting a HM-E8 recipe did not report morphology alterations (Beers et al., 2012). However, expression of pluripotency markers by flow, cell growth and expansion rates were presented comparable to the LT-E8.

A significant difference was identified by the expression of hepatocyte markers in LT-E8 and HM-E8. In HM-E8 expression of HNF4a for hESCs and HNF4a, A1AT and CYP450 3A4 in hiPSC was significantly lower than LT-E8. Although similar results are not reported in literature, it has been discussed that the differentiation protocols require optimisation. In this case, the differentiation protocol from LT-E8 was transferred to HM-E8 cultures. Potentially, an addition of 1-2 extra days at the final stage of hepatocyte maturation could increase the expression of the markers above. Future work should include stage optimisation towards this target.

Maintenance & Differentiation on the Robotic Platform

Since manual cultures were reported as labour intensive, operator dependent and highly sensitive to culture conditions (Kami et al., 2013) use of robotics and automation could increase reproducibility of cell cultures by minimising variables (Veraitch et al., 2008). In this thesis maintenance of hPSCs was succeed for at least 14 passages on the TECAN Freedom Evo system and the cells reported to maintain expansion rate and stable karyotype over time. Automated cultures in the literature are reporting maintenance of hiPSCs for >5 passages on a similar customised TECAN Freedom Evo (Crombie et al., 2017), 20 passages on a custom made automated culture system (Konagaya et al., 2015), or 8-10 passages using the CompacT SelecT system (Thomas et al., 2009) maintaining expression of pluripotency markers and expansion rate. Even though there are advantages using the robotic platform, a disadvantage noticed was the uneven seeding of cells into the 96well plates and not use of the outer wells leading to a reduced number of wells per plate. Using automation can achieve better seeding confluencies but a reduced number of wells that can be used. Overall, successful maintenance of hPSC line culture for 14 passages in this thesis can be compared with current literature and highlighted the advantages of using the automated platform.

Differentiation of hPSCs to HLCs in an automated culture system has not been reported before using an automated platform. However, only recently, the same robotic platform was reported for maintenance of hiPSC lines and differentiation towards retinal cells (Crombie et al., 2017).

Future Work

Re-plating of DE cells is presented as an alternative way to produce an increased quality of the hepatocyte cell population. Duan et al (Duan et al., 2010) demonstrated highly increased drug metabolic activity of the generated HLCs, while (Hay et al., 2008a) and (Agarwal et al., 2008) presented that re-plating of cells improved expression of markers

that recapitulate liver development (Duan et al., 2010, Hay et al., 2008a, Agarwal et al., 2008). Additionally, a uniform morphology was reported, indicative of a homogeneous population (Agarwal et al., 2008). Recently, re-plating of DE cells was reported as a key in differentiation for 25 hiPSC lines into HLCs (Asplund et al., 2016). Time constraints in this thesis did not allow evaluation of a re-plating step, upon DE generation and additionally, automating the step in the robotic platform would require time consuming trial and error methods, therefore the differentiation was completed without passaging of the cells.

Matrices for hepatocyte differentiation influence the success of HLC generation due to the presence of growth factors, proteins and components within (Suzuki et al., 2003). In this study use of Matrigel was the common practice during maintenance of hPSCs and hepatocyte differentiation achieving the results reported above. Initial studies for HLC generation were conducted on MEFs (Song et al., 2009b, Brolén et al., 2010) and as a consequence not useful for clinical use due to the danger of viruses and exogenous antigens (Skottman and Hovatta, 2006). Those studies reported efficient differentiation into HLCs not highlighting issues with the nature of MEFs. However, the requirement for a MEF seeding density was reported as a key parameter affecting the culture and survival of hESCs (Heng et al., 2004) Therefore, considerations regarding the use of uncontrolled and undefined MEF feeder layers were discussed (Chen et al., 2014b). Pioneering studies used Matrigel instead (Hay et al., 2008a) reporting efficient differentiation into HLCs and expression of a range of markers such as ALB, AFP, HNF4a and A1AT as well as morphology that resembles primary hepatocytes. Evaluation of fibronectin-coated surfaces reported generation of HLCs that could facilitate the development of clinical grade hepatocytes for transplantation (Touboul et al., 2010). More recently, fibronectin used as the supporting matrix to study differentiation of 25 hPSC lines demonstrating functional activities following a differentiation protocol partially based on commercially available kits (Asplund et al., 2016). Lastly, Cameron et al, used recombinant laminin substrates and reported significant improvements in cell function and

phenotype (Cameron et al., 2015). A future step in the differentiation protocol presented in this thesis could evaluate the use of recombinant laminins or fibronectin as substrates replacing the need for Matrigel in an attempt to minimise variability between Matrigel batches and undefined factors.

CHAPTER FOUR

ESTABLISHING A QUANTIFIABLE IMMUNOFLUORESCENCE ASSAY FOR THE IDENTIFICATION OF MATURE MARKER CYP450 EXPRESSION IN DAY 17 GENERATED HEPATOCYTE-LIKE CELLS

4. Chapter 4

Chapter four aims to:

- Investigate the current set of outputs available in literature to evaluate efficiency of hepatocyte differentiation protocols
- Identify the requirement for markers that characterise a mature phenotype of HLCs
- Identify and select proteins based on a complete human proteome study
- Evaluate the selected proteins and their expression in HLCs and pHEPs
- Identify quantifiable differences between HLCs and pHEPs
- Built a quantification assay that can detect expression of the selected proteins at comparable intensities to pHEPs.

Therefore, the current outputs and functional assays to identify hepatocyte characteristics in HLCs are presented. Following, the need for markers that can identify the maturity level of HLCs is presented. Then, a step wise approach to identify mature markers is followed, the markers are evaluated in both HLCs and pHEPs and a finally a quantification script is built step by step to accurately measure characteristics of mature CYP450 expression.

4.1. Introduction

4.1.1. Hepatocyte Differentiation Outputs

As discussed in the previous chapter, hepatocyte differentiation protocols are variable among laboratories. Similarly, outputs measured to confirm the generation of HLC are highly variable (Table 24 Appendices). Morphology of the HLCs using brightfield or phase con-

trast microscope is presented in the majority of the studies and the HLCs have been characterised as polygonal cells with distinct cell walls and prominent nuclei (Duan et al., 2010, Hannan et al., 2013). Immunostaining is commonly used to identify the presence of cells expressing specific proteins such as ALB, AFP, A1AT, CYP450 3A4 and HNF4a, that characterise both HLCs and pHEPs (Si-Tayeb et al., 2010b, Hay et al., 2008b). Polymerase Chain Reaction (PCR), developed in the 1990s (Mullis, 1990) is used in the HLC field investigating mRNA/gene expression of key hepatocyte genes in key studies (Hay et al., 2008a, Baxter et al., 2015). Additional methods used are Flow cytometry (Touboul et al., 2010, Hannan et al., 2013) and Western blot (Si-Tayeb et al., 2010b, Baxter et al., 2015) however, these are only used in rare occasions (Table 24 Appendices).

Primary hepatocytes and HLCs produce and secrete proteins that can be detected in the cell culture medium using techniques such as Enzyme-Linked Immunosorbent Assay (ELISA) (Table 24 Appendices). The most common are ALB which is essential for the regulation of osmotic pressure and as a carrier for compounds (Buyl et al., 2015, Levitt and Levitt, 2016), AFP as a foetal marker produced during pregnancy and perinatal development (Kuhlmann and Peschke, 2006, Mizejewski, 2004), A1AT that protects primarily the lungs by neutrophil elastase (O'Reilly et al., 2014, de Serres and Blanco, 2014), urea as a by-product produced upon ammonia detoxification (Bolleyn et al., 2015) and fibrinogen as a scaffolding molecule used in tissue repair processes (Zuliani-Alvarez and Midwood, 2015).

Enzymatic activity of CYP450 phase I and phase II metabolism has also been used as an output (Medine et al., 2011, Agarwal et al., 2008, Asplund et al., 2016). It is based on the principle that enzymes in the hepatocytes are inducible upon the presence of substrate that gets metabolised (Walsky and Obach, 2004). A range of substrates are offered for different CYP450 enzymes. Examples are general CYP450 enzymes activity, CYP450 3A4, 3A7, 2D6, 1A2, 2C9 and Alcohol Dehydrogenase activity (Table 24 Appendices). A more thorough in-

vestigation of the metabolic activity requires the use of Liquid Chromatography/Mass spectrometry but it is rarely used due to cost implications (Duan et al., 2010).

Finally, assays are available for a diverse range of hepatocyte functions that confirm a hepatocyte profile (Krishna, 2013). Glycogen synthesis and storage in the hepatocytes occurs naturally as part of the glucose metabolism (Rui, 2014). The periodic acid-Schiff (PAS) stain is used for identifying the presence of glycogen deposition in hepatocytes examples in (Cai et al., 2007, Chen et al., 2012b) and (Table 24 Appendices). The test substance Indocyanine Green (ICG) is exclusively eliminated by hepatocytes (Yamada et al., 2002). Uptake of the visually green ICG substance by metabolically active hepatocytes and successful elimination is used as an assay (Table 24 Appendices). In some occasions, Oil Red O staining is used to identify the presence of fat globules that contain lipids, naturally occurring in hepatocytes (Rui, 2014, Walther and Farese, 2012). Finally, the ability of the hepatocytes to accumulate and uptake Low-Density Lipoprotein is decreasing the risk for development of atherosclerosis and coronary heart disease (Roy, 2014). The presence of the LDL receptor in hepatocytes and anti-LDL antibodies are used to identify active LDL uptake in hepatocytes as a measure of functionality (Table 24 Appendices).

Overall, the diversity of the outputs among studies highlighted the lack of established criteria in HLC characterisation. Frustratingly, even when the same output has been used, variability between laboratories and users lead to limited comparison (Anagnostou et al., 2010, Phetsouvanh et al., 2013).

4.1.2. Need for outputs that specifically measure maturation & current variability in the literature

Differentiation of hPSCs to HLCs leads to the generation of a foetal-like population of hepatocytes rather than mature adult hepatocytes (Baxter et al., 2015) as discussed in Chapter 1. The current literature primarily uses outputs based on characteristics that are

not necessarily mature and not uniquely expressed at the hepatocyte maturation stage.

Timepoint experiments throughout the hepatocyte differentiation in multiple studies, confirm the lack of specificity of the currently used markers towards a mature hepatocyte status. Additionally, comparison studies between HLCs and foetal/adult pHEPs demonstrate similarities or differences in the maturation status. For example, ALB protein and gene expression was present on the hepatoblast stage and the hepatocyte maturation stage and demonstrated in these studies (Asgari et al., 2013, Hay et al., 2007, Si-Tayeb et al., 2010b, Hay et al., 2008b, Medine et al., 2011). Interestingly, in some reports, it was only present during the hepatocyte maturation stage (Agarwal et al., 2008). Compared to foetal and adult pHEPs, its expression, detected by western blot was similar (Hay et al., 2007). Its gene expression was significantly lower in (Chen et al., 2012b) or gradually increasing to reach foetal and adult expression levels (Hay et al., 2008b). Interestingly, when an ALB secretion assay was performed on HLCs, a 10-fold difference (Song et al., 2009a) or a 2-fold difference was identified (Baxter et al., 2015) compared to adult pHEPs.

HNF4a followed a similar protein expression pattern to ALB during hepatoblast and hepatocyte maturation stages (Hay et al., 2007, Si-Tayeb et al., 2010b, Touboul et al., 2010, Agarwal et al., 2008) while gene expression studies showed presence at the initial stage of hepatoblasts (Hay et al., 2008b). As compared to foetal and adult pHEPs, its expression detected by western blot was gradually increasing (Hay et al., 2007) while surprisingly, it was absent from pHEP in (Chen et al., 2012b). Timepoint trial showed that HNF4a mRNA from the hepatoblast stage was detected at a similar intensity as the adult pHEPs (Hay et al., 2008b).

AFP protein expression is mainly detected at the hepatoblast stage (Asgari et al., 2013, Hay et al., 2007, Touboul et al., 2010, Hay et al., 2008b) similar to its gene expression (Agarwal et al., 2008, Medine et al., 2011). However, its presence was also reported only at the initia-

tion of the hepatocyte maturation stage (Si-Tayeb et al., 2010b). Comparing gene expression with pHEPs, AFP was detected at similar levels in HLCs (Chen et al., 2012b) or significantly higher than in adult pHEPs but present in foetal pHEP in (Hay et al., 2008b). Mature hepatocytes completely lack AFP expression (Baxter et al., 2015, Hay et al., 2007) therefore its use as an output is not recommended. A1AT protein expression was detected during the hepatocyte maturation stage but its gene expression was present from the hepatoblast stage (Agarwal et al., 2008). Protein expression and gene expression assays identified the presence of A1AT equally between HLCs generated and pHEP sample (Song et al., 2009a). Additionally, western blot analysis identified similarities between HLCs, foetal and adult pHEPs (Hay et al., 2007).CYP450 3A4 gene and protein expression were identified in HLCs however at a lower rate compared to pHEPs (Song et al., 2009a). Comparison of CYP450 3A4 activity and urea production between HLCs and pHEPs was identified as similar however, the source of pHEPs was not reported (Chen et al., 2012b). Not amongst the most studied markers but it has been reported that CYP450 2A6 expression was significantly higher in the pHEP population compared to HLCs (Baxter et al., 2015). CYP450 1A1 was expressed primarily in HLCs but not in pHEPs while CYP450 1A2 followed the opposite pattern (Asplund et al., 2016). Similarly, CYP450 2C9 was reported as highly expressed in the pHEPs (Asplund et al., 2016) while it is equally expressed in HLC and foetal pHEPs (Hay et al., 2008b). Finally, CYP450 2C19 was reported highly expressed in the pHEPs (Hay et al., 2008b).

Phase II enzymes Transthyretin expression was similar between HLC, foetal pHEPs and adult pHEPs while Tryptophan Dioxygenase was low in HLC, average in foetal and high in adult pHEP (Hay et al., 2007). Overall, the current literature primarily investigates and compares the expression of markers that are expressed throughout the stages of the hepatocyte differentiation and in some cases, also expressed at comparable levels to pHEPs. As a result, a limited number of markers were available for identification of mature hepatocyte charac-

teristics. Therefore, alternative methods were evaluated to identify markers that were specifically expressed at the last stage of the hepatocyte maturation and were highly expressed in pHEPs.

4.2. Results

4.2.1. Screening for a Range of Proteins Across day 17 HLC and Primary Hepatocyte Cells to identify Candidate Proteins differentially expressed.

To investigate the maturation of Hepatocyte Like Cells (HLC), a set of proteins that are highly expressed in primary Hepatocytes (pHEP) cells and low expressed in the HLC were required to form a maturation screening assay. For this reason, the hepatocyte-related antibodies available within the facility were used to compare expression of hepatocyte-related proteins in CP1-derived day 17 HLC and freshly isolated pHEP cells. Isolation and of the pHEP cells from a liver tissue sample was achieved following the liver perfusion protocol, collecting and seeding of the primary hepatocytes into two 96 well plates, kindly prepared by Monika Owen (FRAME Laboratories, School of Medicine, University of Nottingham). The cells were then cultured and fed daily for 2 and 4 days in primary Hepatocyte culture medium and then were fixed.More pHEP cells expressed ALB, CYP450 3A4, HNF4a and CYP450 1A2 than HLCs. In contrast, AFP was not expressed in pHEPs. Both cell types expressed A1AT. While the fluorescent intensity of ALB increased in pHEP between days 2 and 4, there was no change in the other markers (Figures 44-45).

In conclusion, the proteins ALB, CYP450 3A4 and CYP450 1A2 could possibly be used to identify maturation in the HLC since the difference detected was significant and highly expressed in the pHEP cells. Expression of HNF4a and A1AT was similar in HLC and pHEP, therefore they were rejected. Lastly, loss of AFP expression could be associated with a higher maturation profile, although since it could also be a sign of an unsuccessful hepatocyte differentiation, it was rejected.

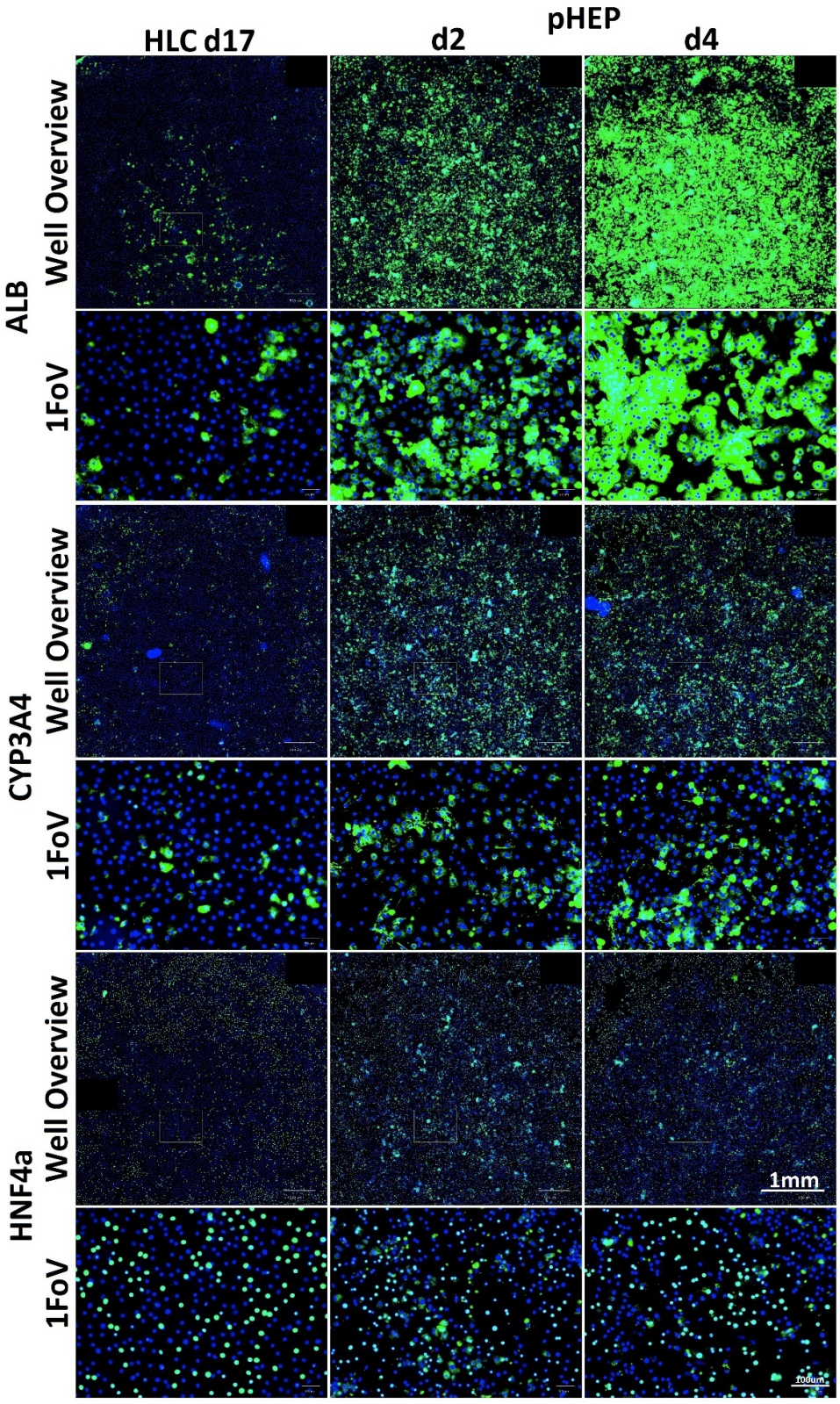

Figure 44 Representative images of ALB, CYP450 3A4 and HNF4a protein expression in HLC generated following the established 17 day Hepatocyte Differentiation protocol compared to fresh pHEP cells seeded and fixed on day 2 and on day 4 upon isolation. Scale bar Overview 1mm, 1FoV 100um.

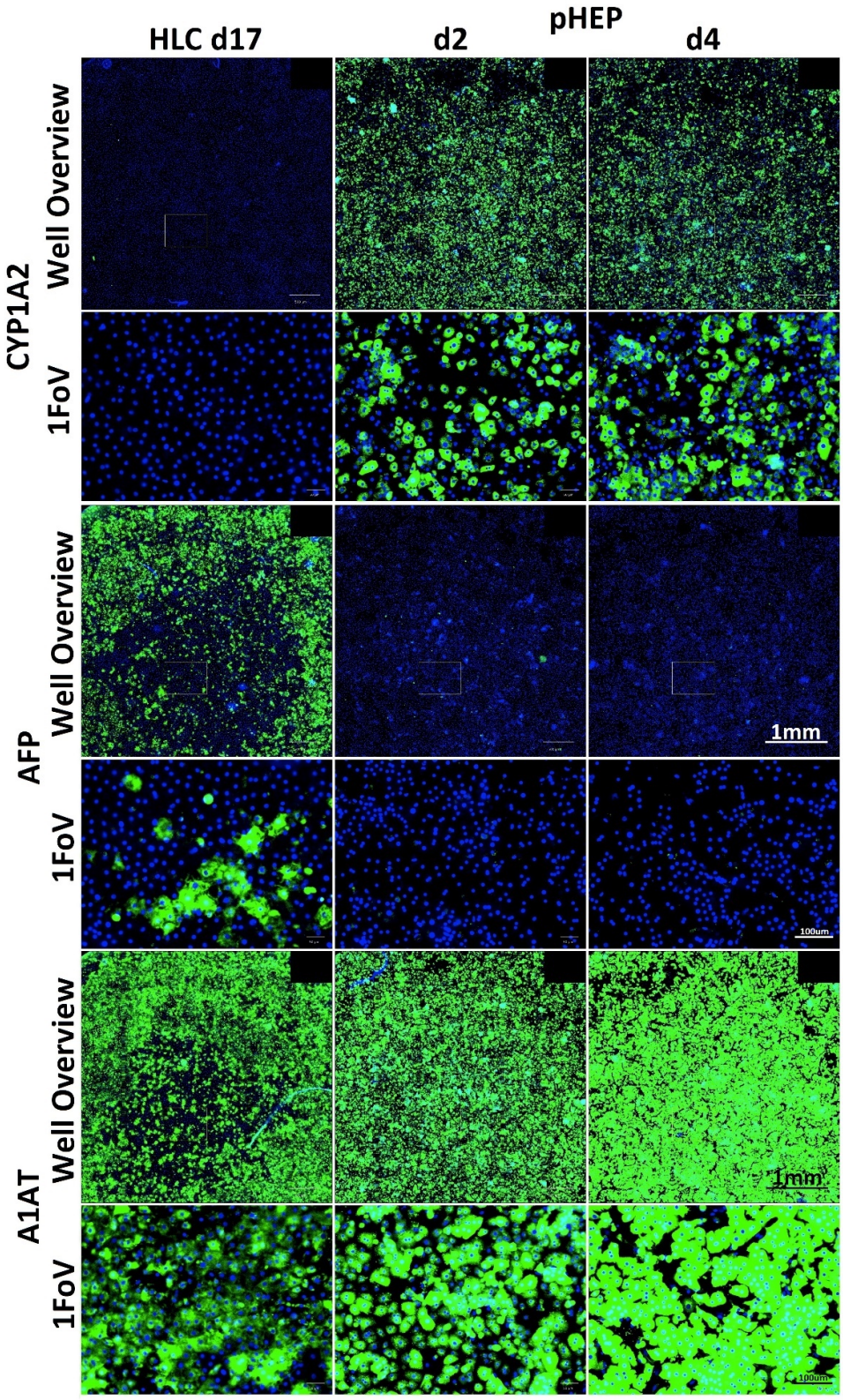

Figure 45 Representative images of CYP450 450 1A2, AFP and A1AT protein expression in HLC generated following the established 17 day Hepatocyte Differentiation protocol compared to fresh pHEP cells seeded and fixed on day 2 and on day 4 upon isolation. Scale bar Overview 1mm, 1FoV 100um.

4.2.2. Differences Between Foetal and Adult Primary Human Hepatocyte Cells were evaluated and differentially expressed proteins were identified

In order to selectively identify proteins that can distinguish foetal stage HLC from adult/mature stage of HLC, a study that has processed and analysed data for the complete human proteome in foetal and adult tissues was used (Kim et al., 2014).

For this reason, the complete protein level expression matrix dataset was downloaded from http://www.humanproteomemap.org. The dataset contained values for 30,058 reference sequences and values for expression across a range of foetal and adult tissue containing foetal and adult liver. Initially, the absolute difference in protein expression between foetal liver and adult liver was calculated. Then, the results were filtered from the highest to the lowest difference and the top 30 genes were selected for further analysis (Figure 46). At the next step, a heatmap of protein expression was generated for the top 30 expressed proteins to aid the analysis and selection of the best candidates.

Initially, it was decided that proteins expressed in both foetal and adult tissue would be less useful as a robust indication of maturation. Instead, Filter 1 selected the proteins that were expressed in the foetal tissue but not expressed in adult tissue and vice versa and restricted the number of potential candidates to 20.

Loss of foetal protein expression is predominantly associated with a mature Hepatocyte profile. However, hepatocyte differentiation, it could also be associated with sub-standard differentiation and/or de-differentiation of cells and general loss of hepatocyte characteristics. Therefore, Filter 2, selected only 16 proteins of these, that are expressed in the adult tissue (Figure 46, Filter 2 column).

Since the expression of candidate proteins was not limited to a liver tissue, but also in tissues derived from all 3 germ layers, Filter 3 was applied to discard the proteins that are expressed in non-liver, Endoderm-derived tissues. Of these, only 11 were selected (Figure 46).

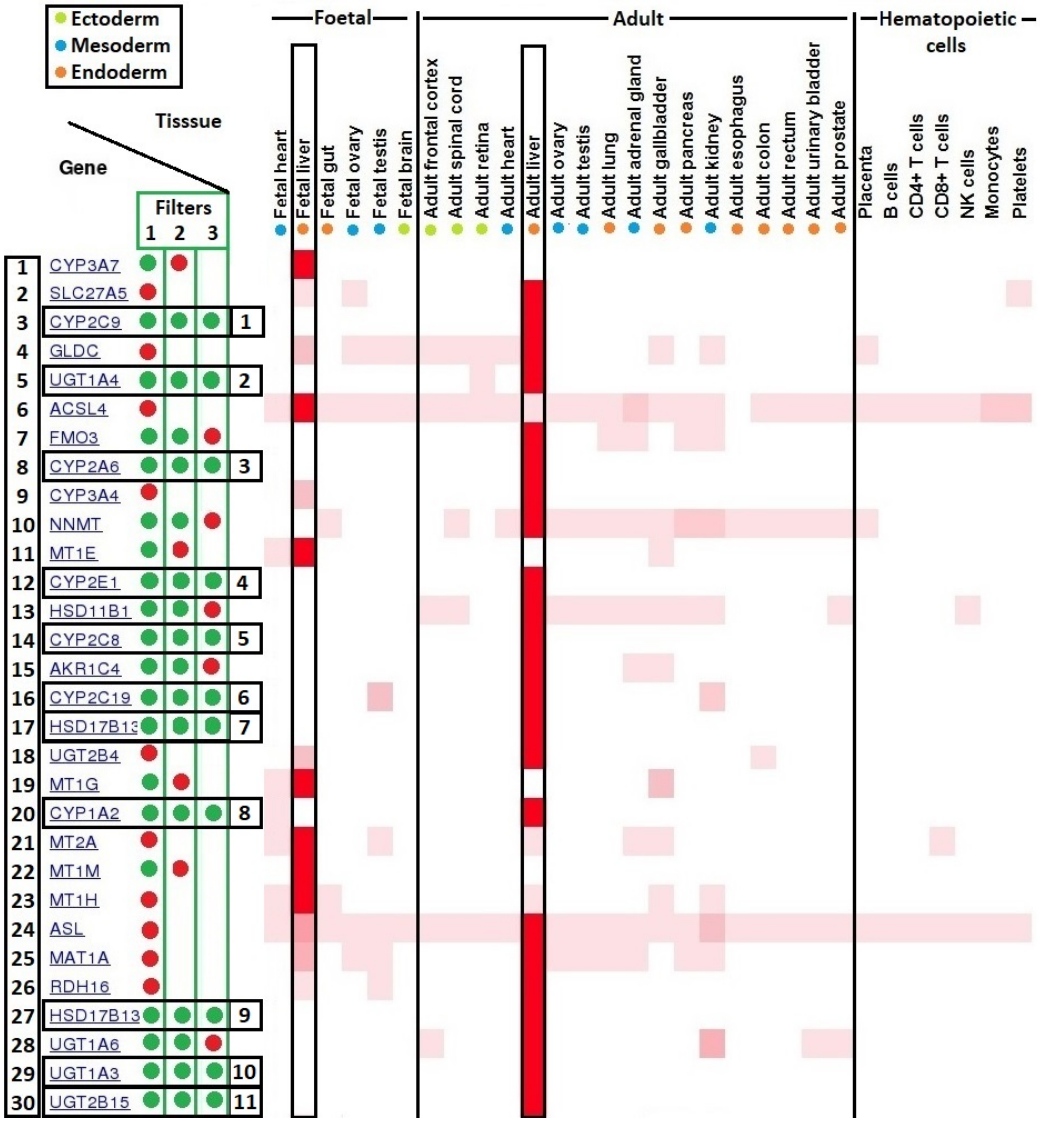

Figure 46 A heatmap of the Top 30 genes selected upon analysis of RefSeq data downloaded from humanproteomemap.org and ranked based on the highest absolute difference in protein expression between foetal liver and adult liver. Expression is depicted by a heat map (red indicates higher expression) in the Human Proteome Map portal.

Application of those 3 filters achieved to restrict the candidate proteins and characterise them as highly expressed by the adult cells, uniquely expressed in the adult liver tissue and absent from any other Endoderm-derived tissue.

CYP450 1A2 was identified as hit number 8 was also shown to be absent in HLC and highly expressed in pHEP cells as seen previously. Other CYP450 family enzymes were represented in the top 8 were CYP450 2C9, 2C8 and 2C19. This data highlights that this enzyme family

was highly expressed in the adult tissue, CYP450 2C9 specifically fulfils the criteria set above and since it was ranked as hit number 1, it was selected for the study. CYP450 2A6 was also selected as a recent study comparing HLC generation upon Hepatocyte Differentiation of hESCs and hiPSCs cell lines including pHEP cells, highlighted the specificity of CYP450 2A6 as an adult liver enzyme that was absent during the foetal stages and highly present during the adult life (Baxter 2015).

In conclusion, the proteins CYP450 1A2, 2C9 and 2A6 were selected based on complete human proteomic expression, previous work within the laboratory and studies comparing HLC cells and pHEP cells as highly specific proteins, selectively expressed in adult Hepatocyte cells. Last but not least, the selection of three maturation related proteins was decided to strengthen the case for differentiation towards the HLCs. A foetal HLC protein that its expression is reduced at the more mature stages was not selected as there is only one final timepoint and not several to compare expression rates.

4.2.3. Evaluation of CYP450 2A6 and 2C9 antibodies for protein expression in HLC and pHEP cells

CYP450 2A6 and 2C9 had not previously been used in our differentiation system. CYP450 2A6 expression was absent from day 17 HLC although in pHEP cells, it was highly expressed on day 2, reducing in intensity by day 4 (Figure 47), confirming the published studies. CYP450 2C9 was expressed in relatively few HLC but expressed in the majority of pHEP cells (Figure 47). This confirmed that the differentiation protocol used for HLC differentiation, could induce expression of CYP450 2C9, although there was opportunity for improvement. In conclusion, CYP450 1A2, 2A6 and 2C9 were appropriate markers for a maturation screening assay.

4.2.4. Development of a Maturation Screening Assay for High-Throughput Study & Proof of Principle Confirmation

Selection of three proteins to indicate maturation of HLCs required combination of them in a format that would involve minimum resources and provide maximum data output from each well. For this reason, a triple stain was desired. Combining primary antibodies usually requires that they are raised in different species. In this case, both CYP450 1A2 and 2A6

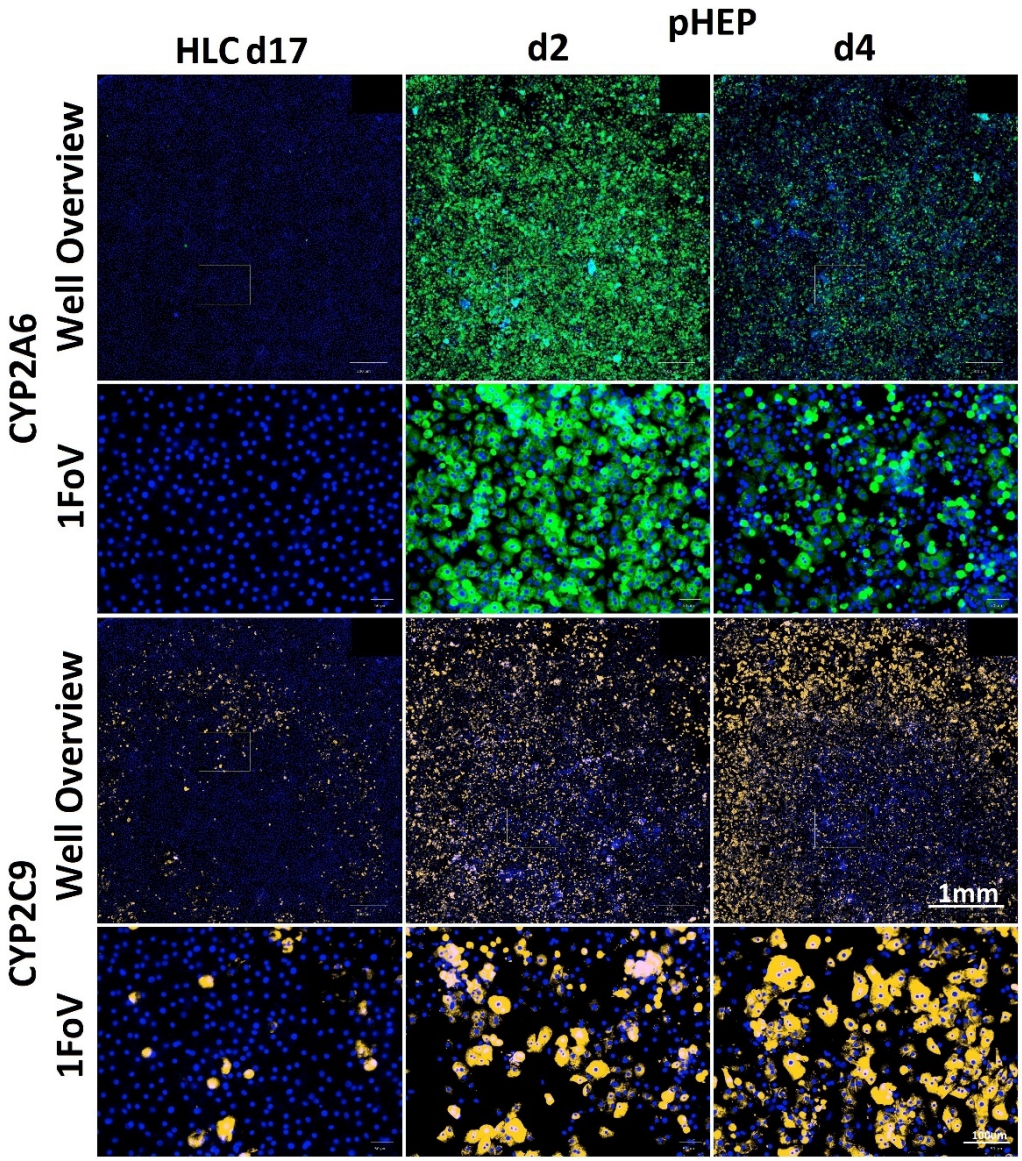

Figure 47 Representative images of CYP450 2A6 and CYP450 2C9 protein expression in HLC generated following the established 17 day Hepatocyte Differentiation protocol compared to fresh pHEP cells seeded and fixed on day 2 and on day 4 upon isolation. Scale bar Overview 1mm, 1FoV 100um.

were raised in Mouse and could be detected by a Goat-anti-Mouse (GaM) pan-IgG AF488 antibody while the CYP450 2C9 was raised in Rabbit and could be identified by a Goat-anti-Rabbit (GaR) pan-IgG AF568 antibody. However, CYP450 1A2 was an IgG1 isotype while CYP450 2A6 was an IgG2a isotype. Therefore, a commercial GaM secondary antibody that had been affinity purified and cross-adsorbed against mouse IgM, mouse IgA, pooled human sera, purified human paraproteins, and mouse isotypes IgG1, IgG2b, and IgG3 prior to conjugation with a different fluorophore (AF647), was selected to specifically identify Mouse IgG2a isotypes.

A triple stain protocol was first evaluated in readily available HepG2 cells. Because in-lab HepG2 cells do not express the CYP450 1A2 protein (variable expression in between laboratories (Guguen-Guillouzo and Guillouzo, 2010)) the CYP450 1A2 antibody was replaced by an AFP also raised in Mouse with IgG1 isotype. Triple staining in one incubation, would lead to detection of both IgG1 and IgG2a mouse primaries by the GaM p-IgG.

Therefore, a two-step approach was developed were Mouse IgG1 and Rabbit IgG1 primaries were incubated at the first step, following by the GaM p-IgG and Rabbit p-IgG1 secondaries and in a second step, the second incubation was with the IgG2a primary and followed by the GaM IgG2a secondary (Figure 48). To confirm that the GaM IgG2a AF647 was specific for IgG2a and did not detect any other IgG isotype, a control treatment was required omitting the CYP450 2A6 primary from the protocol.

To test the triple staining, HepG2 cells plated at 62,500 cells per cm^2 in 96 well plate and incubated with the antibodies as described in Figure 48. As seen in Figure 49A, expression of the proteins AFP, CYP450 2C9 and 2A6 was identified in some HepG2 cells. No GaM IgG2a AF647 signal was detected in the control well that omitted CYP450 2A6, confirming its specificity (Figure 49B). In addition, wells incubated with secondary antibodies, separately or in a step-wise approach, demonstrated absence of signal detection (Figure 49C). In

conclusion, a novel immunocytochemistry maturation screening assay was developed, enabling identification of 3 proteins of interest, at the same time, within the same well.

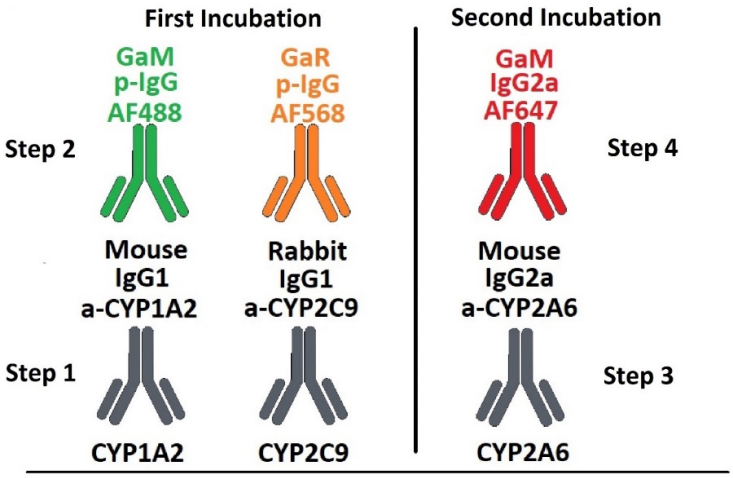

Figure 48 Principle of the triple-staining procedure. Plan for the triple staining incubations with the antibodies.

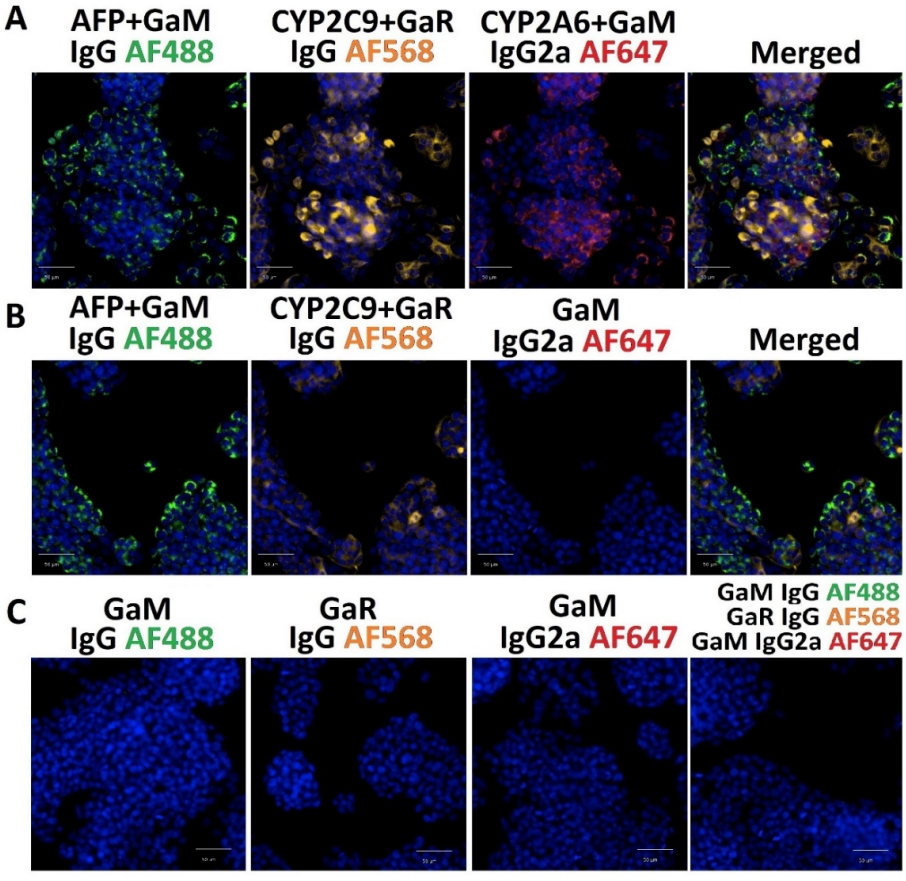

Figure 49 Triple Staining protocol in HepG2 cells A) Positive signal detected in HepG2 cells, C) Specificity of GaM IgG2a, no signal detected when CYP450 2A6 primary was omitted and D) Secondary control for each secondary separately and together.

4.2.5. Evaluation of the Maturation Screening Assay combining CYP450 1A2, 2C9 and 2A6 in HLC and pHEP cells.

To evaluate the triple stain in HLC and pHEP cells, CP1 cells were seeded in a 96 well plate and differentiated to day 17 HLC. Fresh human adult liver tissue from three donors was collected and processed following the liver perfusion protocol within the FRAME laboratories (Prof Andrew Bennett, University of Nottingham). The cells were then seeded, maintained in culture for 2 and 4 days with daily feeds and fixed on day 2 and day 4 as before.

CYP450 1A2, 2C9 and 2A6 expression in HLC was present at a significantly lower proportion of cells (Figure 50) compared to the pHEP population (Figure 51) while no signal was detected in the secondary-only control wells (Figure 50).

Variability in the expression pattern of CYP450 1A2 and 2C9 was identified among the donor isolates. Samples from donor #1, demonstrated a lower expression of CYP450 1A2 and 2C9 compared to the samples from isolations #2 and #3, although expression of CYP450 2A6 was not affected. Samples from isolations #2 and #3 were similar regarding expression of CYP450 1A2 and 2C9 (Figure 51).

In conclusion, the results highlighted the foetal characteristics of the HLC day 17 population compared to pHEP cells and demonstrated that there was potential for the HLC population to increase expression of the selected proteins to a level comparable to pHEP cells. Furthermore, this dataset confirmed the suitability of the triple-staining assay, as a tool to identify maturation characteristics by identifying expression of the mature markers CYP450 1A2, 2C9 and 2A6.

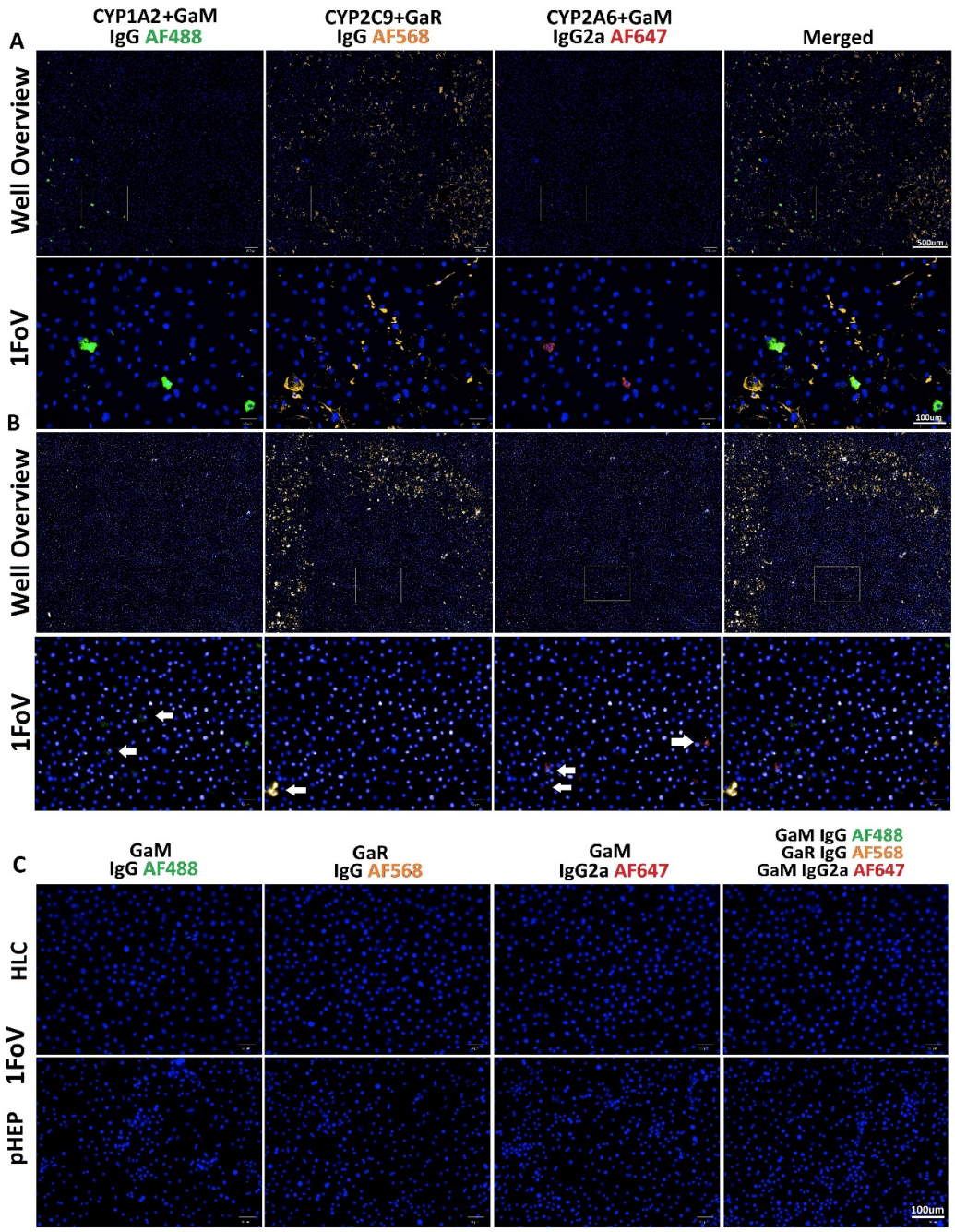

Figure 50 Maturation Screening Assay in HLC day 17 samples. Well overview and 1 Field of View are presented. Two different wells are presented in A) example of expression of CYP450 1A2, 2C9 and 2A6 while in B) early stages of expression for CYP450 1A2, 2C9 and 2A6, highlighted with the arrows. C) Secondary only controls upon triple-staining in HLC and pHEP cells. Absence of signal confirmed the specificity of binding at the positive controls. Scale bar Overview 500um, 1FoV 100um.

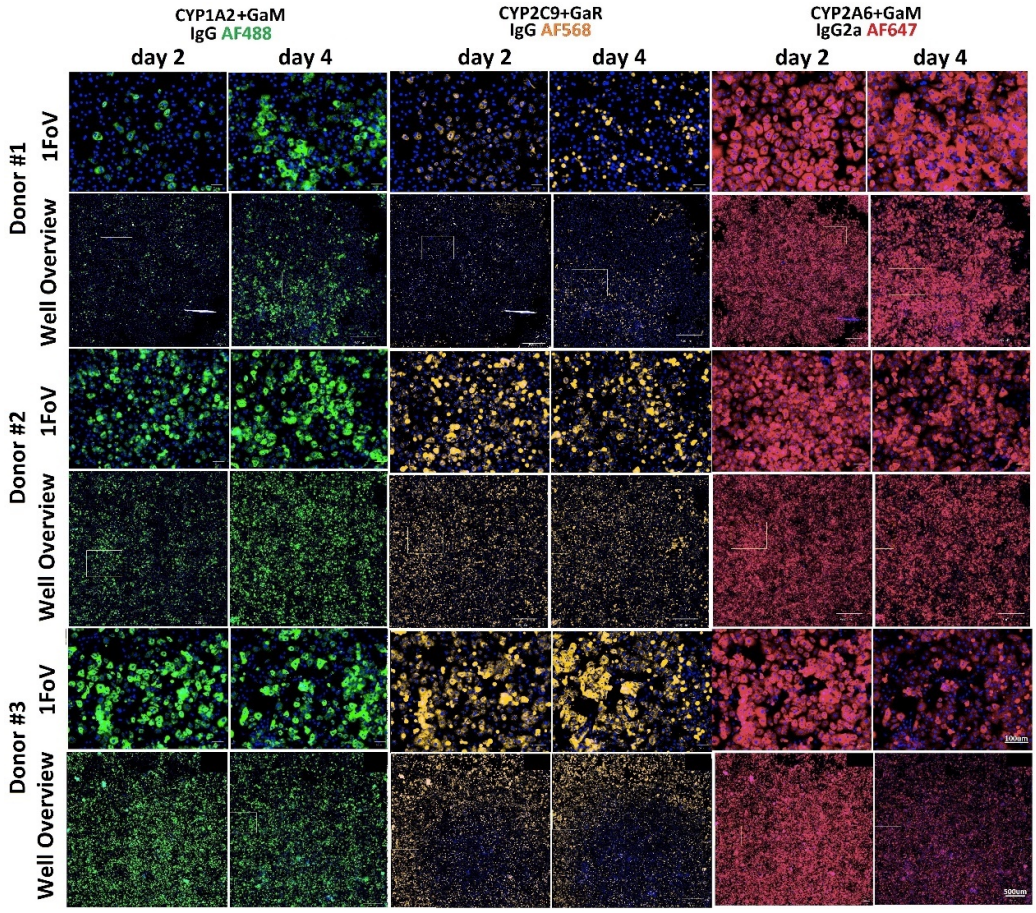

Figure 51 Maturation Screening Assay in 3 Isolations of fresh pHEP cells fixed on day 2 and day 4. Green-AF488 is CYP450 1A2, Yellow-AF568 is CYP2C9 and Red-AF647 is CYP2A6. Well overview and 1 FoV are presented with the expression for CYP450 1A2, 2C9 and 2A6. Scale bar Overview 500um, 1FoV 100um.

4.2.6. Development of Quantifiable Outputs Based on the expression of CYP450 1A2, 2C9 and 2A6

Both percentage positive cells in the populations and any differences in fluorescence intensity within the positive cells were potential distinguishers of maturation-inducing candidates. A quantifiable output that could specify the percentage positive cells was required for the maturation screening assay. For this the Operetta High-Content Imaging System (Perkin Elmer) was used. To develop an analysis method that detects expression of positive cells, two elements were required: a) accurate identification of cells and area of the cell that the protein was localised and b) the threshold of the Fluorescent Intensity (FI) of a cell, that would characterise it as positive for each marker.

4.2.6.1. Development of Signal Recognition Scripts for cytoplasmic CYP450 proteins

The sequence of analysis commands developed to enable accurate identification of a cell and the expected region of CYP450 cytoplasmic localisation is summarised in Figure 52. Initially, DAPI-stained nuclei were recognised as objects. Any objects that fell on the border of two images were then removed to avoid double measurements. Following this, objects smaller than 40um^2 were removed and considered as fragments of nuclei and cell-debris. At this stage, the remaining cell nuclei were characterised as “Accepted Objects”. Because selected CYP450 belong to Phase I drug metabolism enzymes, their expected localisation is in the membrane of the endoplasmic reticulum (Neve and Ingelman-Sundberg, 2010), a ring extending at 60% of the nuclei diameter, around the nuclei was designed (yellow circles, Figure 52Ae) to determine the area of cytoplasm where CYP450 expression would be defined. An example of the finally “Accepted Objects” for each CYP450 is shown in Figure 52B. In conclusion, the quantification script was able to accurately detect protein expression and localisation of each marker.

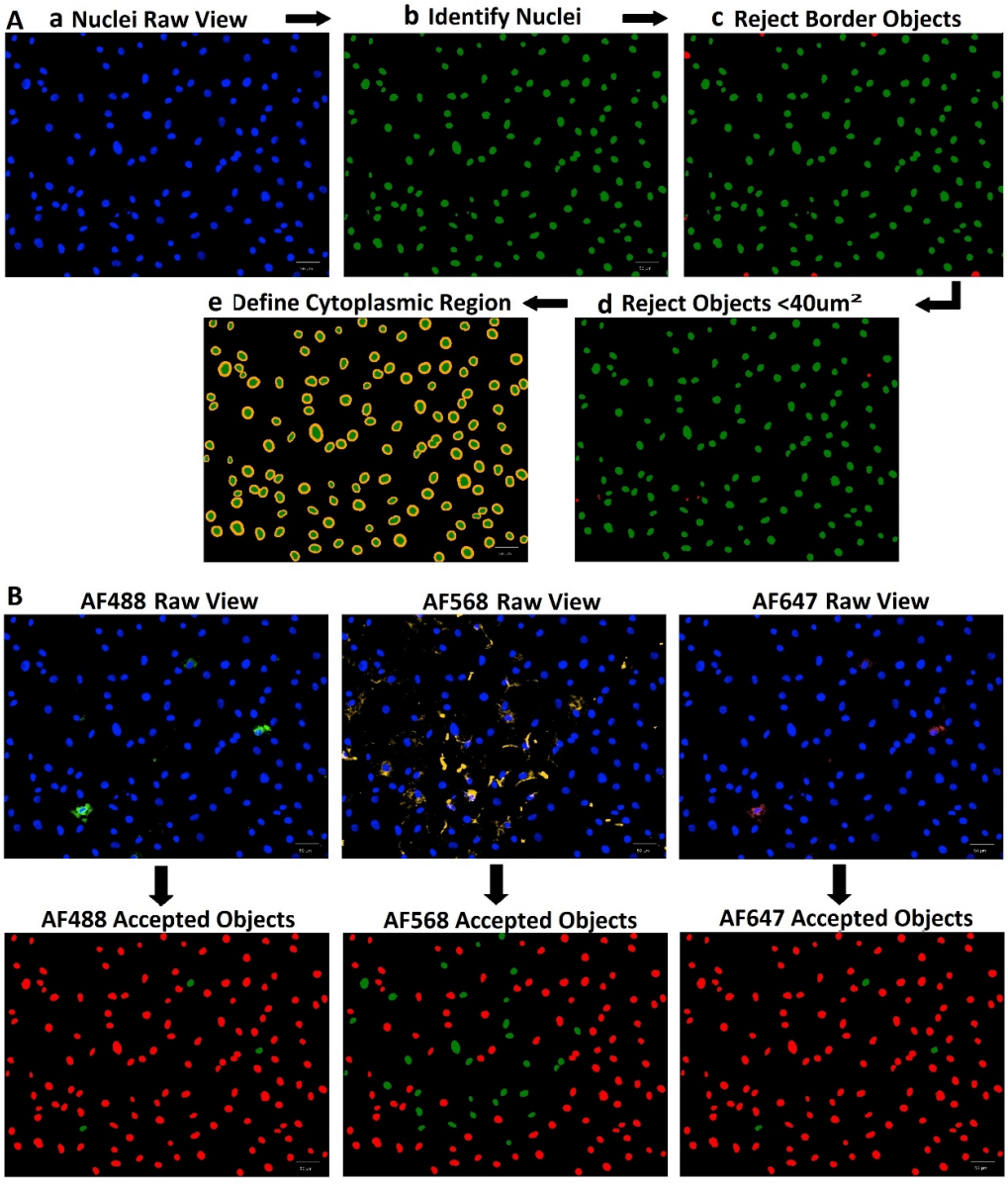

Figure 52 Development of the Quantification script A) Process of defining the Cytoplasmic Region and B) Respective images of "Accepted Objects" for each CYP450.

4.2.6.2. Establishment of Thresholds for Accurate Quantification Measurement of Appropriate CYP450 Expression

Although it is common practice to threshold positive cells against the Fluorescent Intensity of cells stained only with the secondary antibodies, that approach would lead to a population of cells that would not be similar to the pHEPs population where majority of cells express the CYP450 (Figure 50-48). As seen in Figures 47 and 48, few HLCs express CYP450 at a comparable level to pHEPs additionally, their fluorescent intensity is substantially lower than the pHEP population. To identify HLCs that are functionally relevant to the pHEP population, higher thresholds were required.

Figure 53 shows the Fluorescent Intensity for the HLC and pHEP (day 2 and day 4) populations additionally to the secondary only controls, for each CYP450. For CYP450 1A2, the secondary only control for the HLC population was reaching 100 units while for the pHEP population, 150 units. This difference was potentially explained due to the Goat-anti-Mouse (GaM) pan-IgG potentially binding to the rich mix of extracellular matrix proteins excreted by the pHEPs. Therefore, to selectively identify true positive cells in an HLC population that upon maturation could produce a similar set of ECM proteins, the threshold was set at the 150 units.

For CYP450 2C9, the secondary only control for the HLC population was reaching the 70 units and a substantial population of positive HLCs was evident. The Goat-anti-Rabbit (GaR) pan-IgG secondary for the pHEP population was reaching the 150 units, for the same reasons as the GaM pan-IgG. To select a relevant population to the pHEP, the threshold was set at 150 units. For CYP450 2A6, for both populations, the specific secondary GaM IgG2a showed similar values for HLC and pHEP populations. To select HLC population relevant to the pHEP population, the threshold set at 60 units. The percentage positive cells obtained upon use of the

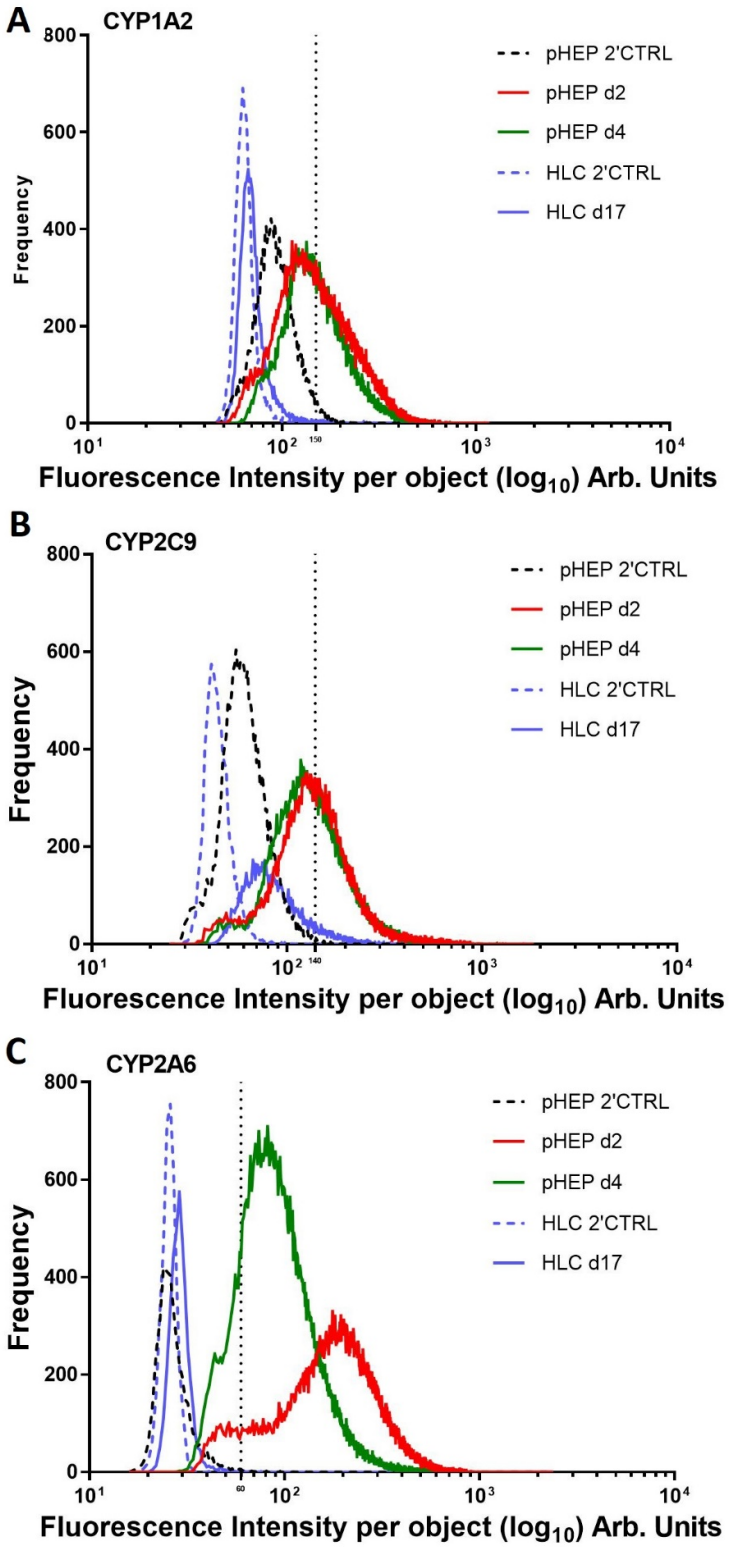

Figure 53 Analysis of the Frequency and the Fluorescence Intensity (FI) per object for Triple-Staining positive and secondary only control (2'CTRL) in HLC and pHEP cells. Increased FI for the pHEP population compared to HLC population. Black vertical dotted line represents the threshold set for each CYP450.

thresholds described above, are shown in Figure 54. As identified, expression of CYP450 1A2 ranged between 10-60%, CYP450 2C9 between 10-68% and 90-98% for CYP450 2A6 in the pHEP population while in the HLCs it was at 1.8±0.7% for CYP450 1A2, 13.1±2.9% for CYP450 2C9 and 0.6±0.3% for CYP450 2A6 (Figure 54).

The difference in expression of CYP450 1A2 and 2A6 between pHEP and HLC populations was characterised as significant upon ANOVA ($p<0.001$). In contrary, expression of CYP450 2C9 in HLC population was not significantly different from Isolation #1 but it was compared to isolations #2 and #3 ($p<0.001$). Regarding variability of protein expression within the pHEP Isolation, it was identified that CYP450 1A2 and 2C9, were significantly lower expressed in Isolation #1 compared to Isolation #2 and #3 ($p<0.001$) but not CYP450 2A6 expression (Figure 54 – red asterisk). In conclusion, it was demonstrated that HLC population was inducing expression of CYP450 1A2, 2C9 and 2A6 at a significantly lower expression rate compared to the pHEP cells.

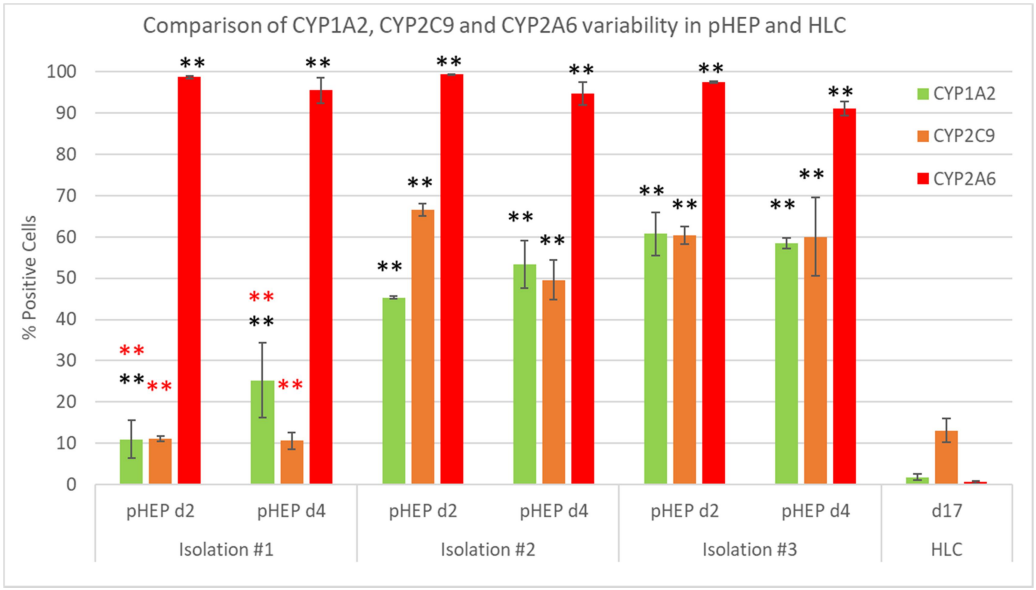

Figure 54 Evaluation of the percentage positive expression of each marker in the 3 Isolations of pHEP cells compared to the HLC generated cells. Significant differences identified between pHEP and HLC (highlighted with ** $p<0.001$). Significant differences identified between Isolation CYP450 1A2 and 2C9 compared to Isolations 2 and 3 (highlighted with ** $p<0.001$).

4.2.7. Percentage of Double Nuclei Cells as an Additional Quantifiable Measure of Maturation

During the study, it was noticed that an increased number of cells with two nuclei was present within the population of the pHEP cells but not in the population of HLC (Figure 55). Since multinucleation is a characteristic of adult primary hepatocytes (Gentric et al., 2012, Davoli and de Lange, 2011), it was decided to evaluate the percentage of Double Nuclei Cells (DNC) in pHEP cells and in HLC cells and identify if that it could be used as an additional quantifiable measure of maturation.

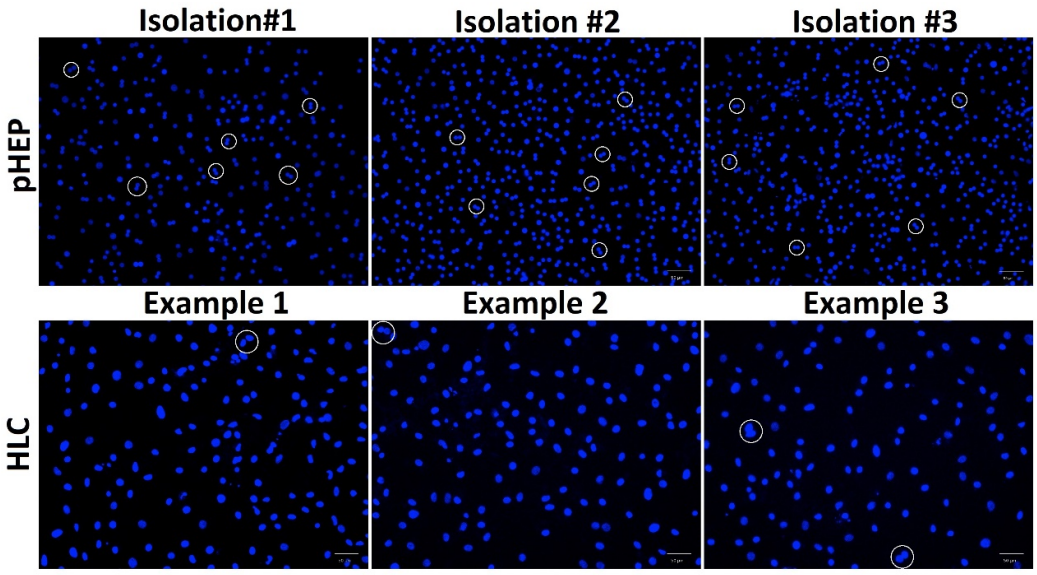

Figure 55 Examples Double Nuclei Cells present in the 3 available pHEP isolations and in the day 17 generated HLC population. Scale bar 50um.

To achieve that, a quantification script was required, to specifically identify and select the DNC population based on morphology properties. Three morphological properties were used to select for the DNC. The first was based on the area of the nucleus. It was identified thresholding area of nucleus at 80um^2 for pHEP and 200um^2 for HLC, it was discarding majority of the single cell population (Figure 56) allowing cells with an increased nucleus area and DNC present for further analysis. Next, was the width to length ratio of the nuclei. In the DNC population, the width of the nucleus was twice the length and vice versa. There-

fore, restricting the ratio to <0.6, it was possible to select specifically the DNC within the population.

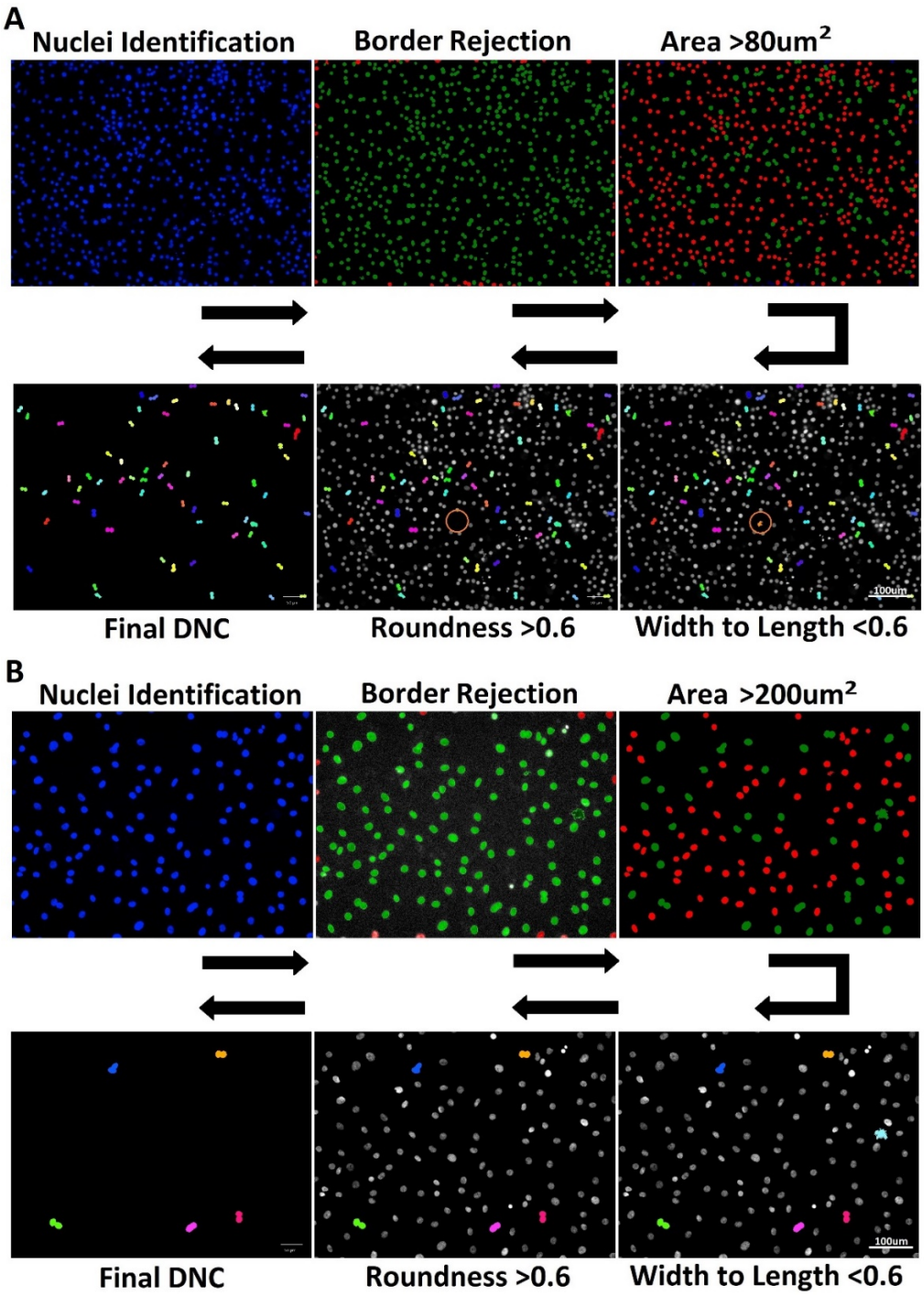

Figure 56 Process of quantification script built with blocks of commands filtering the cells and leading to specific identification of DNC within the population of pHEP (A) or day 17 generated HLC cells (B). Average size of single-nuclei, width to length ratio and roundness ratio were used as filters to exclude the single nuclei cells and specifically select the DNC population. Details in text. Scale bar 100um.

The third property used was the roundness of the nucleus. It was mostly used to discard not-DNC from the pHEP population and didn't make a difference for the HLC population. In the end, the remaining cells were characterised as DNC and their percentage compared to the initial number of nuclei could be calculated (Figure 56).

The DNC quantification script was then run through the raw data of pHEP Isolations #1, #2 and #3 and the HLC population to identify whether the difference was significant. As seen in Figure 57, the average number of DNC within the pHEP isolations ranged between 12-24% while in the HLC population it ranged at 3.6±0.9%. ANOVA analysis demonstrated that the difference was significant between pHEP and HLC populations therefore, the DNC quantification script could be used to specifically identify and quantify the percentage of DNC as an additional measure of maturation for the maturation screening assay.

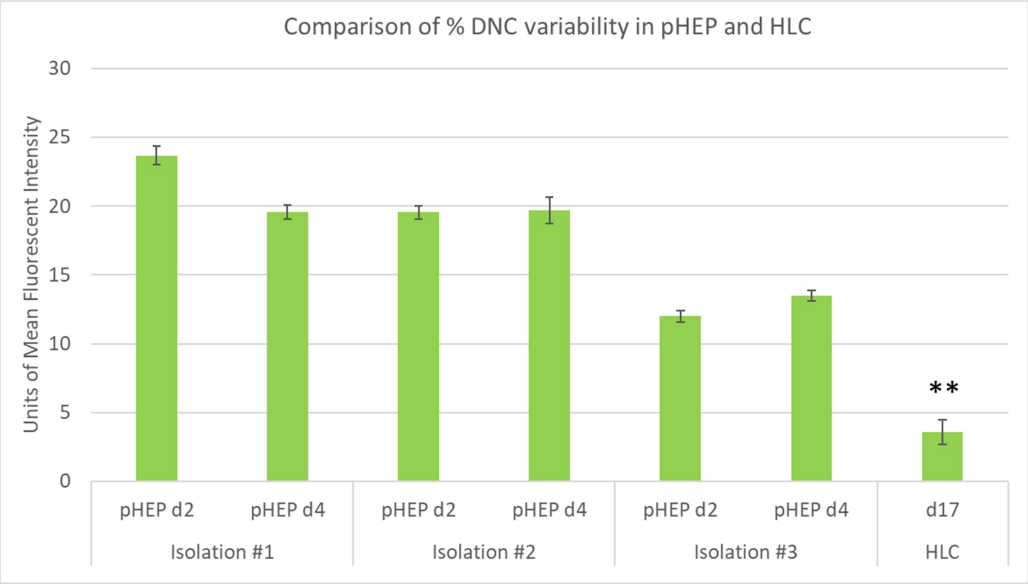

Figure 57 Evaluation of the percentage of DNC in the 3 Isolations of pHEP cells compared to the HLC generated cells. Significant differences identified between pHEP and HLC (highlighted with ** p<0.001).

4.2.8. Distinct Morphological Differences Between HLC and pHEP cells were Used as Qualitative Output

Differences in the morphology of HLC and pHEP cells could be used to identify distinct characteristics that are related to a more mature profile of cells. Comparing HLC and pHEP cells

and reading the literature (Schmelzer et al., 2006, Hannan et al., 2013, Behbahan et al., 2011, Hay et al., 2008b), it was found that some of the characteristics were polygonal cells, visible nuclei, bi-nucleation and distinct cell borders.

For this reason, a grading scale from 1 to 4 was decided as a qualitative guide to rank the morphology of the final day 17 HLCs based on the characteristics above. Those characteristics were set in a scale that grades the morphology of HLC from 1 to 4. Grade 1) was given for absence of HLC morphology and absence of polygonal cells, grade 2) presence of polygonal cells with visible nuclei, grade 3) presence of polygonal cells with visible nuclei & distinct cell borders between hepatocytes and grade 4) pHEP like morphology including presence of polygonal cells with visible nuclei, distinct cell borders between hepatocytes & binucleated cells (Figure 58).

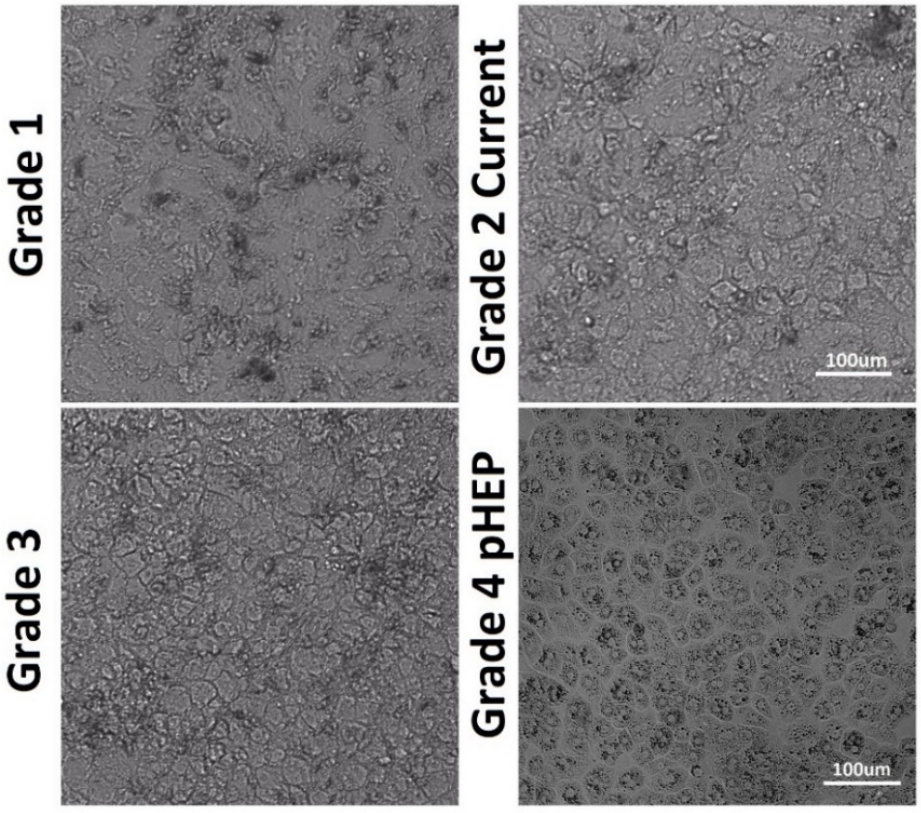

Figure 58 Morphology grading system 1 – 4 for HLC differentiation. Grade 2 is produced following the current 17day Hepatocyte Differentiation Protocol and Grade 4 is pHEP cells. Scale bar 100um

4.3. Discussion

Summary

In this chapter, quantification methods that discriminate adult from foetal characteristics were developed in a high-throughput assay that later is used for the DoE approaches. Initially, investigation of the currently available antibodies for hepatocyte related proteins in HLCs and pHEPs identified candidates and their expression in both cell types. To further investigate the range of proteins expressed, analysis of the complete human proteomic data in foetal and adult pHEPs (Kim et al., 2014) highlighted that CYP450 1A2, 2C9 and 2A6 were specifically and highly expressed in adult pHEPs. These markers were then validated in HLCs and a significantly lower expression was confirmed. Quantification methods were then developed to specifically measure the percentage of marker expressing cells to a comparable efficiency to pHEPs. Additionally, double nuclei cells were identified to be present at a significantly lower number in the HLC and identification of them was then built in the quantification analysis. Finally, morphological criteria were set to evaluate the success of hepatocyte differentiation that could lead to pHEPs morphology.

Immaturity of HLCs compared to pHEPs and limitations of the current methods

The cells generated following the hepatocyte differentiation protocol in this study were identified as immature, as it was expected from the literature (Cai et al., 2007, Hannoun et al., 2016). Several reasons can potentially lead to this phenotype however currently it is poorly understood (Schwartz et al., 2014). Initially, the differentiation protocol generates HLCs from hPSCs within 17 days and most of the differentiation protocols range between 17 and 30 days (Table 6). Developmental processes during human development require approximately 9 months from the stage of the blastocyst to the generation of foetal hepatocytes and adult hepatocytes following strict developmental cues (Zaret, 2002, Zhao and Duncan, 2005). Even though the differentiation protocols can mimic liver development

as close as possible, the time that is required for the changes to take effect is critical. Additionally, limited transcriptional activity of enzymes is also highly correlated with hypermethylation of promoter regions leading to subsequently lower expression levels of downstream associated metabolizing genes (Kim et al., 2016).

Liver development has unravelled the most important signalling cues that take part and lead to the differentiation into foetal HLCs however, important factors that are produced *in vivo* might have been omitted or never identified. Current literature (Chapter 1) has identified a range of factors naturally produced or chemically synthesised that could be the key unlocking signalling pathways for increased expression of mature liver related proteins.

Evidence indicates that the respiratory activity in mitochondria of stem cells is kept low due to the associated induced DNA damage upon generation of reactive oxygen species (Parker et al., 2009). Differentiation into metabolically active HLCs requires increased expression of mitochondrial proteins and biogenesis regulators, within the mitochondria, to support vital roles (Wanet et al., 2014). Changing of mitochondrial functions during the differentiation is essential to support the new hepatocyte functions (Hopkinson et al., 2017) however, the way that this can be achieved at a greater efficiency is still not clear.

Another reason that could limit the potential of HLCs is the expression of foetal proteins. AFP expression in the HLCs generated in this study was highly expressed in between 80% and 90% of the cells. In adult pHEPs, expression of AFP is absent (Baxter et al., 2015, Hay et al., 2008b). Expression of AFP in the HLCs is connected with an inability to switch off gene expression leading to a persistent immature phenotype (Yu et al., 2012b). Repression of AFP postnatally is reported to occur in a species dependent way as the cells are transitioning from the foetal stage to the adult stage (Kuhlmann and Peschke, 2006). Interestingly, in liver disease models and liver cancers, AFP expression is elevated and used as prognostic marker, however its role is still not clear (Sell, 2008, Schiødt et al., 2006).

Expression of CYP450 1A2, 2C9 and 2A6 in relevant cell models

In the results, CYP450 1A2 was identified as absent from the HLCs while it's expression in pHEPs ranged in between 10% and 65% of the cells. In the literature, CYP450 1A2 gene expression in HLCs was identified as low (Baxter et al., 2015) and when it was compared to pHEPs its lower expression in HLCs was demonstrated (Duan et al., 2010). Additionally, gene expression analysis also identified a 200-fold difference in the expression between 25 HLCs and 4 pHEPs lines (Asplund et al., 2016) confirming the results of the above experiment.

In the results, CYP450 2C9 was identified expressed in the HLCs at 13.1±2.9% while it's expression in pHEPs ranged in between 10% and 70% of the cells. In the literature, gene expression of CYP450 2C9 was lower in 4 different HLC lines compared to adult pHEPs (Duan et al., 2010), while surprisingly its gene expression was higher than foetal pHEPs and close to adult pHEPs in (Hay et al., 2008b). The activity of CYP450 2C9 in 25 HLCs was lower compared to adult pHEPs and gene expression analysis indicated at least 25-fold difference in the expression between 25 HLCs and 4 pHEPs lines (Asplund et al., 2016). Activity of CYP450 1A2, 2C9 and other enzymes (CYP450 3A4, 2C19, 2E1 and UGT2B7) assessed by Liquid Chromatography/Mass spectrometry indicated significant differences 15-fold for CYP450 1A2 and 250-fold for CYP450 2C9 metabolic activity, however still reporting presence of enzymes that are responsible for 85% of known oxidative drug metabolism activities in the HLCs (Zhao et al., 2013).

In the results, CYP450 2A6 was identified as absent from the HLCs while it was highly expressed in between 90% and 99% of the pHEPs. In other studies, gene expression was identified as lower in HLC lines compared to the pHEPs (Song et al., 2009b). Gene expression in 4 different HLC lines and adult pHEPs indicated differences, demonstrating higher expression in pHEPs (Duan et al., 2010). Additionally, its enzymatic activity in adult pHEPs was sig-

nificantly higher compared to the HLCs and foetal pHEPs and the results were confirmed by immunocytochemistry (Baxter et al., 2015). CYP450 2A6 was also strongly detected in three out of four adult pHEPs but was not identified in the foetal pHEPs confirming its role as a specialised indicator of hepatocyte differentiation and maturation (Rowe et al., 2013).

Overall, expression of the proteins CYP450 1A2, 2C9 and 2A6 are not investigated to the same extent as other proteins in the literature. However, comparison studies between HLCs and pHEPs lead to the conclusion that their expression is highly specific in the pHEP cells therefore could be used as an indicator for an increased maturation status of the HLCs.

The significance of the binucleated cells

In this study, a significant degree of multinucleation was identified in pHEPs between 12% and 24% while in HLCs it was at 3.6±0.9%. Multinucleation has been described in the literature and in hepatocyte differentiation protocols. Presence of binucleated cells in the differentiation protocol in (Si-Tayeb et al., 2010b) and (Takayama et al., 2014), was considered as a sign of hepatocyte morphology and similar to the pHEPs. Similarly, in (Hannan et al., 2013), it was demonstrated that multinuclear cells appear during the maturation stage of the differentiation. Quantification of the binucleated or multinucleated cells has not been reported in the literature before. An explanation for that could be the use of brightfield microscopes and limited fields of view in the well to get an estimate. The difference in this study was that the nuclei identification was based on a nuclear stain (DAPI) and the images acquired were taken from across the well, generating a well overview and giving the advantage of accurate quantification.

Polyploidisation of hepatocytes is a process that takes place naturally during postnatal growth (Gentric et al., 2012, Davoli and de Lange, 2011) and characterises terminally differentiated cells and aging (Gupta, 2000, Schmucker, 1990) however this can be reversed in the liver cells (Gentric and Desdouets, 2014). The advantages of the multinucleation in the

liver cells are connected with a protective role against oxidative stress and genotoxic damage upon metabolism and elimination of toxic compounds (Storchova and Pellman, 2004). So, in case of developing HLCs where the requirement for elimination of toxic compounds is not as high as in the adult liver, the percentage of multinucleation is not necessarily as high. Last but not least, although polyploidy could be connected with a transcriptionally more active state of cells due to the presence of a second set of chromosomes there are no reports to confirm that. Further investigation is required for the complete understanding of multinucleation in the differentiating HLCs.

Advantages & Limitations of the Assay Developed

Identification of HLC maturation based on an immunocytochemistry assay in this thesis has not been reported before. However, there are approaches for identification of mature HLCs in the literature. Shan et al, screened 12,480 small molecules to identify those that can induce maturation and/or proliferation of the hepatocytes (Shan et al., 2013). The output assay was based on ELISA measurement for ALB secretion that would increase upon the maturation and the number of cells/nuclei that would increase upon proliferation while the study was completed on human pHEPs. However, as seen in the proteomic analysis in this chapter, ALB is not a strong indicator of maturation (Kim et al., 2016) and the logistics for ELISA assays (96 reactions for £375) increase the cost of the experiment. The key advantage in the assay developed in this thesis was the identification of three mature CYP450 enzymes, morphology and number of double nuclei cells compared to ALB secretion assay.

The advantage of using the Operetta confocal plate reader in this thesis was primarily connected with automated scanning of the 96 well plates, with the same settings reproducibly reassuring elimination of manual interference and comparability of captured images between experiments. This is not the case when manual microscopes are involved that require manual adjustments, are labour intensive and not convenient for large scale studies

(Sakurai et al., 2017, Yu et al., 2012b). Immunofluorescence images in studies usually demonstrate a saturated background signal, lack of cells in focus, low resolution of images, sometimes lack of scale bars but predominantly only capturing a specific area in the well, ignoring the overview and overall expression of the protein (Yu et al., 2012b, Peters et al., 2016). Overall, the use and functions of the Operetta plate reader have been recognised and offered great advantages compared to conventional fluorescent microscopes (Stengl et al., 2017, Massey, 2015).

In the current HLC differentiation literature, quantification of immunocytochemistry results rarely happens. Instead, images of a single field of view with positive expressing cells are presented (Song et al., 2009b, Toivonen et al., 2013, Medine et al., 2011). In this study, the quantification is based on an analysis script that follows a step-wise approach to identify the positive expressing cells. In the literature, there are examples where quantification results are presented following a manual counting of positive cells from at least 5 different fields of view (Cameron et al., 2015), or >10 fields of view with >250 cells counted per field of view (Siller et al., 2015), or cell counting/quantitation without further information (Baxter et al., 2015, Cai et al., 2007). In other cases, the ImageJ software with the cell counter plug-in was used (Asplund et al., 2016). However, information regarding thresholding parameters upon which a cell is considered as positive, are not reported. Overall generation of HLCs and expression of markers is usually confirmed with selected images, however the field needs to incorporate quantitative methods to assess the percentage of positive cells.

A limitation of the current assay lies within the qualitative assessment of HLC morphology. Human error could potentially lead to false conclusions. If more time was available for the development of the output assay that would involve the development of machine-learning algorithms that discriminate morphology patterns based on the morphology images of pHEPs, that could be used to quantitatively identify similar patterns in the HLCs. The pro-

cess is called cellular phenotyping and it has been presented in the literature in terms of morphology changes in different populations of cells (Garvey et al., 2016) using the Operetta.

Last but not least, inducers of the CYP450 enzymes lead to a temporary expression of the relevant CYP450 (Gerets et al., 2012, Sa-ngiamsuntorn et al., 2011) Therefore, the need for a wide timeframe of protein expression and activity would need to be addressed upon successful identification of maturation factors.

Variability in the pHEP samples

Variability in the expression of enzymes was identified among the pHEPs in this study. In one of the three samples, the expression of CYP450 1A2 and 2C9 was at significant lower percentage of cells compared to other two. The reasons for this could either be variability in the population or a suboptimal isolation of cells from liver tissue. Variability in the pHEP populations is evident in the literature. Comparison of 12 individual human liver samples, revealed substantial inter-individual differences in CAR receptor expression, correlated with CYP450 2B6 expression and highlighting differences between individuals (Chang et al., 2003). Genome-wide analysis of expression profiles of pHEPs from 6 individuals identified significant variability in the expression of genes related to xenobiotic metabolism, lipid/carbohydrate metabolism and hepatic functions, suggesting that these differences contribute to the huge interindividual variability and susceptibility to drugs and environmental factors (Rogue et al., 2012). More pHEP samples collected from 4 individuals presented variability in the gene expression level and especially for CYP450 2C9 and 1A2 where lower gene expression were identified in some donors (Levy et al., 2015).

The main cause of this variation is explained by the great genetic variation within the human population (Madian et al., 2012). The CYP450 polymorphisms affecting individuals and their response to certain categories of drugs (Preissner et al., 2013) which are mainly

caused by single nucleotide variations (Fujikura et al., 2015). Multiallelic genetic polymorphisms play a major role in the function of CYP450s leading to distinct pharmacogenetic phenotypes named poor, intermediate, extensive and ultrarapid metabolisers (Zanger and Schwab, 2013). Genetic polymorphism of the human CYP450 2C9 with at least 33 variants being identified, all affecting expression and functionality of CYP450 2C9 that should be taken in consideration when new drugs are designed (Wang et al., 2009). Similarly for CYP450 1A2, exhibits a significant degree of interindividual variation affecting xenobiotic metabolism (Sachse et al., 2003). The advantage of hiPSCs can assist towards the identification of those interindividual differences and generate models from patients with single nucleotide polymorphisms that affect the metabolic capacity, essentially generating *in vitro* models that represent the population (Takayama et al., 2014).

In this thesis, the pHEP samples collected were freshly isolated and plated for experiments. However, in the literature the variability expected is not only caused due to interindividual differences but also upon the status of the cells and if they have been cryopreserved. In some studies, the pHEPs used were freshly isolated from adult (Touboul et al., 2010, Baxter et al., 2015, Duan et al., 2010, Magner et al., 2013) or freshly isolated from foetal (Baxter et al., 2015) or cryopreserved adult (Song et al., 2009b, Asplund et al., 2016). Investigating differences between cryopreserved and fresh populations *in vitro* demonstrated that viability, plate attachment efficiency, metabolic enzyme activity and production of ALB were all significantly decreased on thawing after cryopreservation (Terry et al., 2005). Optimising the cryopreservation process was suggested using cytoprotective components such as glucose, fructose (Terry and Hughes, 2009) or trehalose playing cryoprotective roles (Katenz et al., 2007). Despite the developments in cryopreservation, the differences are still evident (Asplund et al., 2016) and the use of fresh hepatocytes highly recommended.

CHAPTER FIVE

SCREENING AND IDENTIFICATION OF FACTORS THAT LEAD TO MATURATION OF HEPATOCYTE-LIKE CELLS USING DESIGN OF EXPERIMENTS

5. Chapter 5

Chapter five aims to:

- Investigate the advantages of Design of Experiment (DoE) approaches and present examples from literature where it has been used to identify critical factors
- Present the types of designs available within the DoE software
- Identify a timepoint of on the 17day HLC differentiation protocol that the DoE treatments can be applied in this study
- Present a literature review for the concentrations of the factors that have been used in relevant cell types and identify a range of concentration
- Apply the DoE principles and evaluate the effect of factors using the output assay developed in Chapter 4

Initially the current advantages and examples from the literature are presented regarding use of DoE followed by an introduction of the main types of DoE designs. A rational for selecting the treatment duration is then explained, followed by a table presenting relevant studies for each of the factors used in the DoE and the concentrations that have been used. Finally, application of DoE principles was employed to investigate the maturation potential of the selected factors.

5.1. Introduction

The increased technological advancements and automation of processes enabled high-throughput studies, statistically designed methodologies that can minimise time and expense required to design, conduct and analyse an experiment. This has helped to

boost research and improve current method development practises. DoE approaches offers tremendous advantages compared to the frequently used “One Factor At a Time” approaches that the majority of today’s literature is based on (Collins et al., 2009).

5.1.1. Applications of DoE

Application of the DoE approach, discussed in Chapter 1, has been described successfully in multiple fields. In the drug discovery field, it offers a revolutionary method for optimisation and screening of experimental parameters within simple experimental designs, that require fewer runs (Tye, 2004). In the pharmaceutical development field, assuring quality of the formulation developed in the final product is a key element where DoE implements modern “Quality By Design” manufacturing methodologies (N Politis et al., 2017). In forensic toxicology where human samples collected on the site are limited in size and extracting more information from the same amount of sample can enable safer conclusions (Costa et al., 2010). Overall, DoE approaches have been used in the development of modern screening methods securing increased productivity, efficiency, reduced cost and time (Buyel and Fischer, 2014, Collins et al., 2009).

Apart from drug development related applications, the contribution of DoE designs enabled optimisation of culture medium for animal cell culture or bacterial culture. Growth of the *S. cerevisiae*, *P. pastoris* species requires a nitrogen source and optimisation of the optimal settings of a cost-effective alternative was achieved (Batista and Fernandes, 2015). Development of a “Chemically Defined Medium” for increased robustness and reproducibility in the culture of the Chinese Hamster Ovaries cell line was achieved upon several rounds of DoE experimentation (Ling et al., 2015) and feeding regime optimisation in a bioreactor improving protein production by three to six-fold (Xiao et al., 2014).

In the field of stem cells, development of serum-free medium for mouse ESC was achieved by balancing the concentration of growth factors and supplements in a way to best maintain survival and proliferation of the cells (Knöspel et al., 2010). Most recently, DoE was applied to increase the yield of hiPSC upon culture in spinner flasks fed with Essential-8 (E8) culture medium. It was reported that the scalable and xeno-free environment could generate larger numbers of hiPSC on demand, to support clinical, drug discovery and/or industrial applications (Badenes et al., 2016).

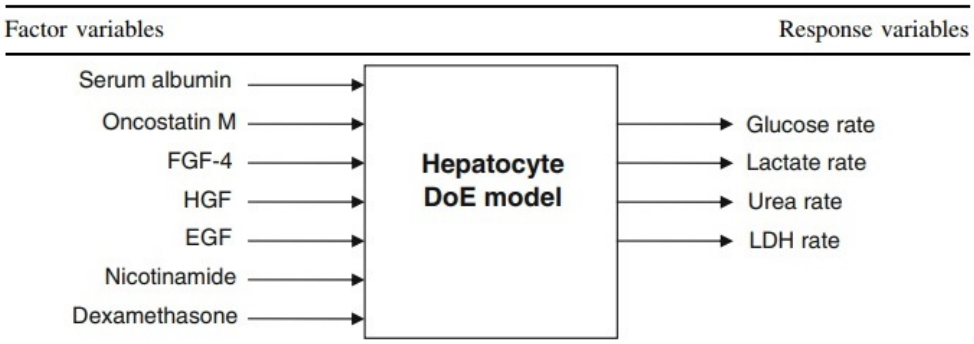

Figure 59 Overview of the DoE approach followed for the optimisation of growth factors and supplements (Factor Variables) in the culture of human hepatoma cell line C3A by measuring the responses (Response Variables) Adapted from (Dong et al., 2008).

In the field of hepatocytes, a single study has been published to date that describes the optimisation of culture media by DoE for the growth of the human hepatoma cell line C3A (Dong et al., 2008). In this study, growth factors and media supplement concentrations were set to a range of interest and the response variables were selected as relevant to the purpose of the design (Figure 59). The analysis highlighted the importance of OSM, HGF and FGF4 as key variables therefore, a second DoE approach was designed and indicated that the best outcomes are 25-30ng/ml HGF and 30-35ng/ml OSM with FGF4 at 20ng/ml (Dong et al., 2008).

5.1.2. Types of Designs in the DoE Software

For application of the DoE approach, specific computer-based software is required. Currently the most popular providers are Design Experts from Statease

(https://www.statease.com/), JMP from SAS Institute (https://www.jmp.com) and MODDE Pro from Umetrics (https://umetrics.com/). Each DoE software offers a range of DoE designs and analytical statistical algorithms to accommodate for specific requirements and limitations of each experimental plan.

The most commonly used design for screening factors is based on a Full Factorial design matrix. For example, in a 3-factor design, each factor can be tested in a low and a high concentration (two-level). This design is presented in a cube, where the axis x, y and z are the factors A, B and C, at their low and high concentrations. Every corner of this design represented in a cube is a condition that Low or High concentration for each factor is used plus the addition of Centre Point used to detect reproducibility and non-linear responses (Figure 60A).

This way, the cube is a representation of the experimental space and is explored with n number of experiments. A compromise between the information taken and a reduced number of experiments is possible with the use of Fractional Factorial Designs by aliasing factors. These designs are more economical because they require fewer experiments, but result in a lower resolution (Tye, 2004).

However, the powerful statistical algorithms embedded within the software can resolve aliasing (estimated effects that are influenced by one or more factors) and determine significant factors affecting the design with similar efficiency to the Full Factorial experiment (Figure 60). The disadvantage of screening designs is that it mainly supports linear responses and a more complex design is necessary to accurately detect non-linear responses and accurately generate a picture of the response surface (a relationship between several variables) (Collins et al., 2009).

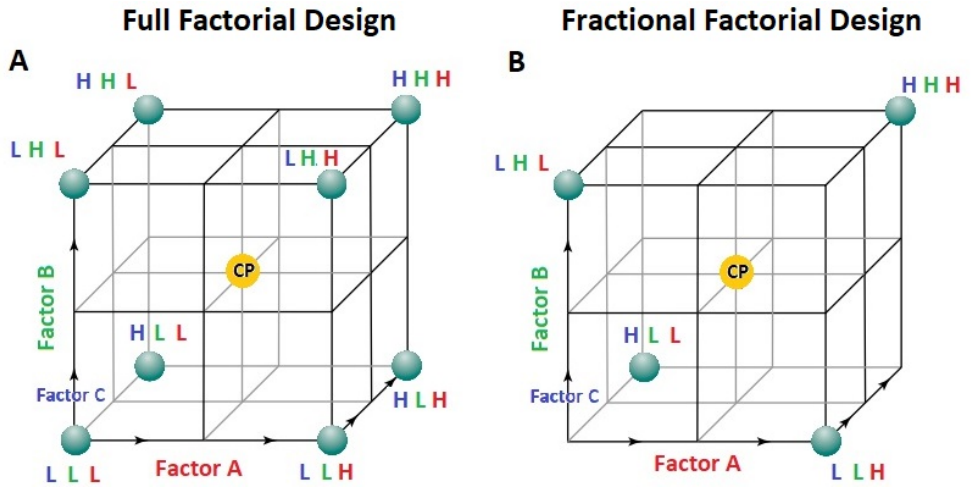

Figure 60 Example of a 3-factor experiment and the run required to explore the experimental space when A) a Full Factorial approach or B) Fractional Factorial approach is followed. Adapted from (Tye, 2004)

A more accurate picture of the response surface can be generated following designs for example Box-Benhken or Central Composite Face that are used mainly for applications of response-surface modelling and optimisation. Generally accepted approach for screening applications is use of a low-resolution fractional factorial experiment to identify the most important factors in one step. While in a second experiment, the key factors have been identified and following a Response Surface Methodology design, the optimum conditions are resolved (Collins et al., 2009, Tye, 2004).

5.1.3. Timing of the DoE experiment

As discussed previously, the hepatocyte differentiation *in vitro* is subdivided into 3 distinct stages and in each of those, the cells develop into a more lineage restricted cell type. Upon generation of hepatoblasts the cells are directed towards hepatocytes with the addition of the basic hepatocyte maturation growth factors. However, in many research groups, the last stage of the differentiation is separated into 2 distinct phases where the hepatoblast cells initially generate Immature Hepatocyte Like cells and then the immature hepatocytes mature into the HLCs (Song et al., 2009a, Agarwal et al., 2008, Hannan et al., 2013, Touboul et al., 2010). A different approach was followed in

each of those studies regarding the factors used to mature the immature hepatocytes however the timing of the mature hepatocyte treatment was similar e.g. halfway through or towards the last stages of the differentiation. Therefore, in this thesis, to ensure that the hepatoblast cells commit to the immature hepatocyte lineage first, the DoE treatments have been applied from day 14 to day 17 (Figure 61).

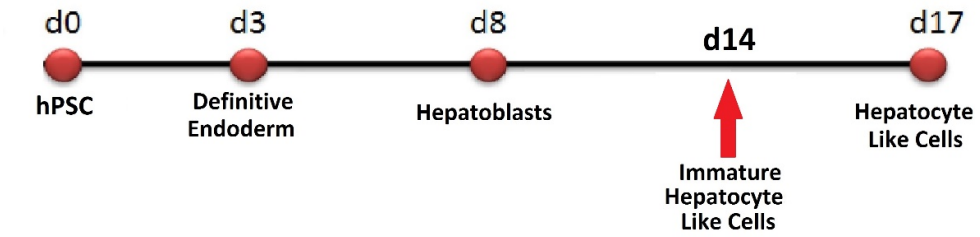

Figure 61 Stages of differentiation from hPSC to HLC stage. Commitment to the hepatocyte lineage is achieved by day 14 and this allows maturation factors to impact of hepatocytes rather than hepatoblasts.

5.1.4. Ranges of Factors Selected

Factors that are related to mature hepatocyte function, mature gene expression and protein expression in the hepatocyte cells were identified in Chapter 1. For the purpose of this thesis, knowledge of a range of these factors is required so the ideal concentration that induces an effect in HLCs cells can be identified. Therefore, a review of the literature for related publications and factor concentration was completed.

Due to the uniqueness of the studies and factors identified in Chapter 1, studies in a similar system were not always available therefore studies in relevant cell types/systems were collected instead, in an attempt to relate information to the hepatocyte differentiation (Table 25 Apprentices).

5.2. Results

5.2.1. Initial DoE Screen for a Limited Range of Factors, to Develop and Test the Compatibility with the Robotic Platform

In the previous sections, experiments were designed and completed using only 2 and 3 treatments within a single 96 well plate. However, when a DoE experiment is employed, more complex automation scripts are required to plate, prepare and dispense the large number of culture medium variants. Therefore, initially a small-scale DoE termed "DoE#1" was conducted to test the effect of 12 factors on the eight outputs developed in Chapter 4 when applied during days 14-17 of hepatocyte differentiation.

5.2.2. Selection of Factors and Diluents

In addition to the HGF, OSM, Hydrocortisone and FBS routinely added to Medium C, a further 8 factors were investigated in the DoE#1 (Table 13). Each factor was tested at a "low" and "high" concentration within the range used in published literature (Table 23).

Name	Low Concentration	High Concentration	Units	Name	Low Concentration	High Concentration	Units
Cyclic AMP	100	1000	uM	Dihexa	10	200	nM
Lithocholic Acid	10	100	uM	Verteporfin	2.5	40	uM
Taurocholate Acid	25	200	uM	HGF	5	50	ng/ml
Vitamin K2	5	100	uM	OSM	5	50	ng/ml
FH1	5	30	uM	FBS	0	8.3	%
T3	10	100	nM	Hydrocortiso	1	10	uM

Table 13 Summary of the factors and the concentration levels that have been used in DoE#1. Blue-shaded are the factors that require water or PBS as diluent, orange-shaded require DMSO and green-shaded require NaOH.

Diluent requirement of the factors had to be taken into consideration since not all were water-soluble. DMSO, as an organic solvent, was the only diluent for Lithocholic Acid, Vitamin K2, FH1, Dihexa and Verteporfin whereas Sodium hydroxide (NaOH) is the diluent for T3. Diluent-only Controls were included to ensure that the results generated were due to factor effects and not DMSO or NaOH-related.

5.2.3. Design of DoE#1

A Fractional Factorial approach was selected for the DoE#1, as an efficient design used to screen many factors to find the few that were significant (Main Effects). Full and fractional designs were available to explore many factors, setting each factor to only two levels (concentrations). In fractional factorial designs compared to full factorial, the experiments performed consist of a carefully selected subset (fraction) of the experimental runs of a full factorial design, saving experimental runs, time and resources (Tye, 2004). Design Expert 9 software offered design resolutions between 16 and 512 single experimental runs for 12 factors (Figure 62). A Yellow resolution design (2_{IV}^{12-7}) was selected for this DoE, that evaluates 12 factors using 32 experimental runs by completing a fraction of the respective full factorial experiment. A full factorial experiment would require 2^{12} = 4096 runs but using this design a 2^{-7} = $1/2^{7}$ = 1/128 fraction of the full factorial experiment was required (4096/128=32).

Resolution IV designs indicate that main effects may be aliased with three-factor interactions and two-factor interactions may be aliased with other two-factor interactions making the design a good choice for a screening design as the main effects will be clear of two-factor interactions. Aliasing refers to some treatment effects that are estimated by the same combination of experimental observations. Resolving aliasing is not described as an issue due to the fact that higher order interactions (effects achieved by 3 or more factors together) are either non-existent or insignificant (Tye, 2004).

The 32 required experimental runs were conducted in triplicates (Figure 63A) to calculate the “Pure Error”. “Pure Error” estimates are derived from replicated runs where replication increases the precision of the response estimate by averaging results. In addition, provides an independent estimate of the experimental variability over the design space calculated within the software adding confidence in the results.

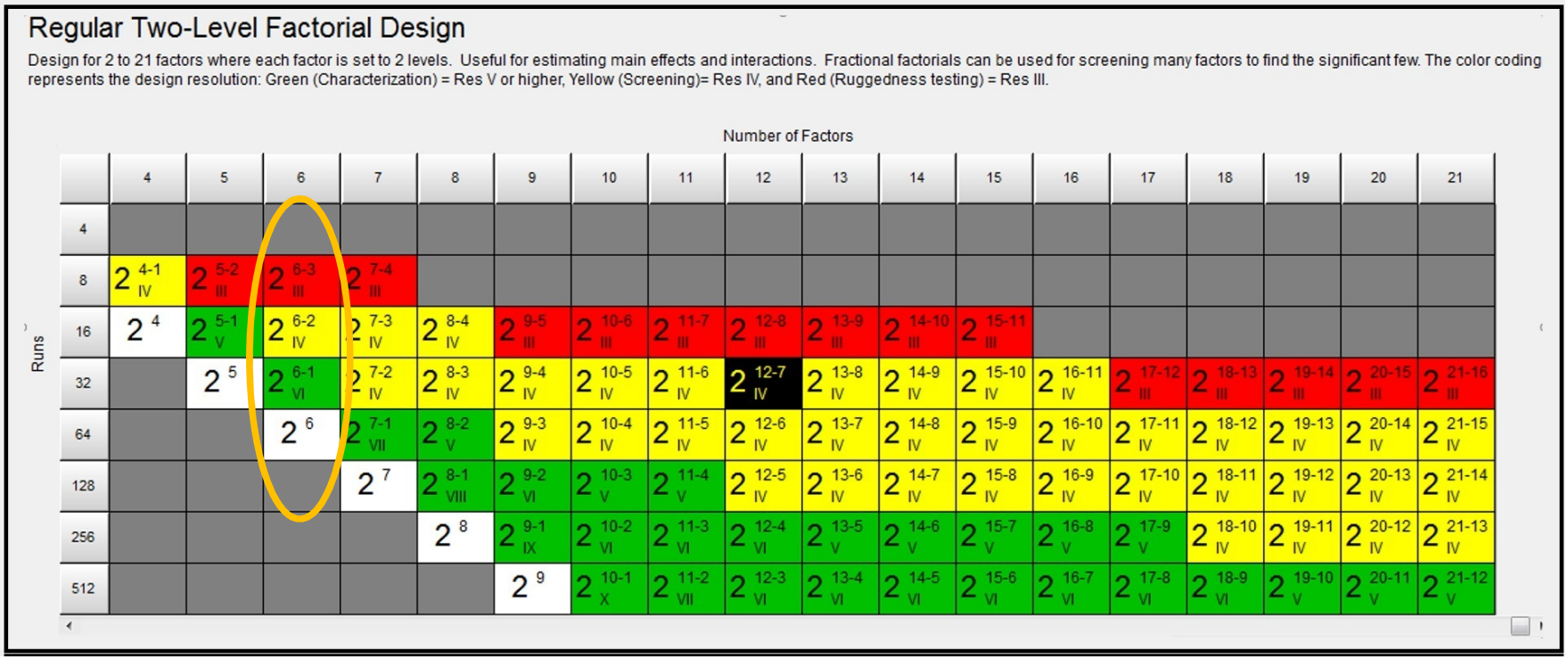

Figure 62 Design Experts 9 software and two-level factorial designs available. The X axis shows maximum capacity of factors that can be screened within a design and the Y axis gives the number of experimental runs required for each selection. Colours represent the resolution of the design. Red for resolution 3, Yellow for resolution 4 and Green for resolution 5 and white for full factorial experiment. The higher the resolution the more confidence for the results. The 2_{IV}^{k-p} represent a specific design and indicate that each factor is tested at 2 levels, a low and a high, IV is the resolution, k= the number of factors tested and p= the fraction of the full factorial design. Designs with Increased number of runs offer increased confidence but require more resources and time compared to designs with smaller number of runs. Example for 6 factors full factorial requires 64 runs, 2_{VI}^{6-1} for 6 factors requires a 2^{-1}=1/2 fraction of the full factorial thus 32 runs, a 2_{IV}^{6-2} requires a 2^{-2}=1/2^2=1/4 fraction thus 16 runs and a 2_{III}^{6-3} requires a 2^{-3}=1/2^3=1/8 thus 8 runs.

The experiment also included six Centre Point runs (Figure 63A). These include all factors at an intermediate concentration level to determine whether the relationship between responses and experimental runs was linear or if curvature was present. Replication of Centre Points was required to provide estimates for "Pure Error". The total number of experimental runs, including 32 experimental runs in triplicates and 6 Centre Points calculated as 102.

For the DoE#1 design, "Signal" values represent the user defined magnitude of response desirable as significant were set at 5x higher than Medium-C for the percentage Positive responses, 2x higher for the Mean Fluorescent Intensity of each CYP450 , 5x for percentage of double nuclei cells and any change in category for the Morphology, would be significant (Figure 63B). "Noise" values were set at those determined previously in Chapter 4.

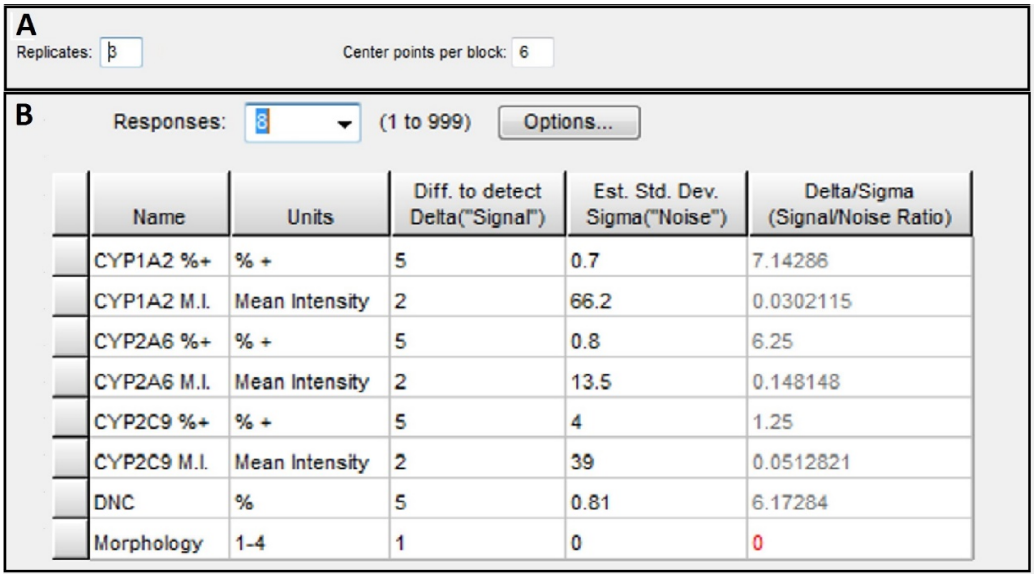

Name	Units	Diff. to detect Delta("Signal")	Est. Std. Dev. Sigma("Noise")	Delta/Sigma (Signal/Noise Ratio)
CYP1A2 %+	% +	5	0.7	7.14286
CYP1A2 M.I.	Mean Intensity	2	66.2	0.0302115
CYP2A6 %+	% +	5	0.8	6.25
CYP2A6 M.I.	Mean Intensity	2	13.5	0.148148
CYP2C9 %+	% +	5	4	1.25
CYP2C9 M.I.	Mean Intensity	2	39	0.0512821
DNC	%	5	0.81	6.17284
Morphology	1-4	1	0	0

Figure 63 Fractional Factorial DoE Design Overview using Design Experts 9 (A) Selection of a number of replicates and number of centre points per block (B) Reponses presented with the values Sigma, Noise and Signal/Noise Ratio.

5.2.4. Preparation of Factors and Diluents for DoE#1

Two 96 well plates were required to accommodate the 102 experimental runs (Table 26 Appendices). Each plate, also included 6 wells allocated to Medium C control runs and 3

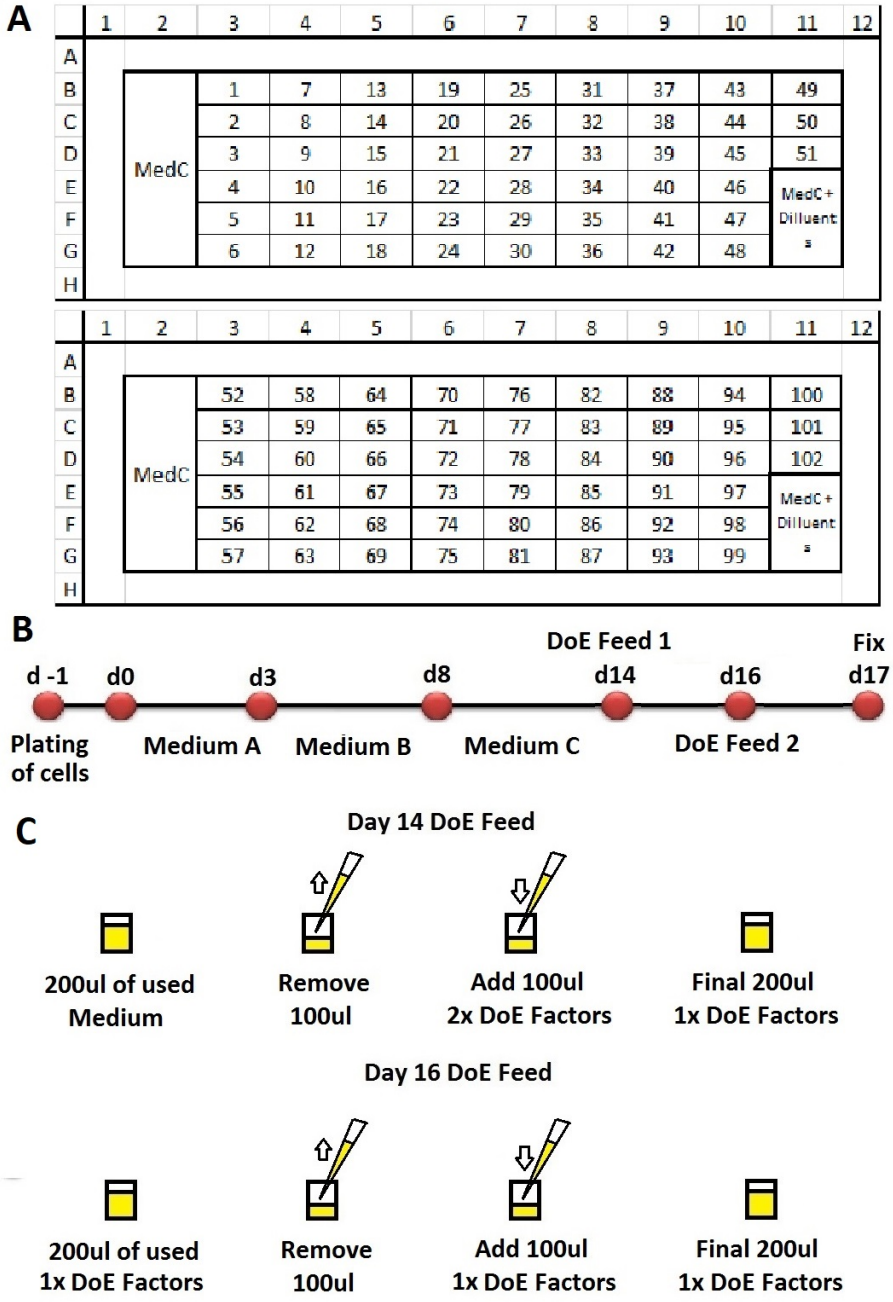

Figure 64 Plate layout for the DoE#1 demonstrating the location of each of the 102 runs, MedC control and MedC + Diluents. A) Timeline for the differentiation protocol, DoE treatments taking place on day 14 and day 16. B) Process for changing medium on day 14 and 16 to maintain appropriate concentration.

wells allocated to the Medium C with diluents control, to investigate if there is an effect induced from their use (Figure 64A). To avoid edge effects, the outside wells of the 96 well-plates were not included in the design. The standard 17-day hepatocyte differentiation protocol in the automated platform was followed, except that DoE specific media replaced medium C on days 14 and 16 (Figure 64B). On days 14 and 16, removal of 100ul Medium C

and replacement with DoE treatments was required. To maintain the factor concentration at the desired levels, 100ul of medium was replaced by a 2x concentrated DoE medium on day 14 and 1x concentrated on day 16 (Figure 64C).

Stock solutions of factors were manually pipetted into a 96-deep well plate (Stock Block) at both high and low concentrations (Figure 65) while a 4-column trough (Stock Trough) was used to hold Medium C.

Since diluents used could be differentiation inducers and potentially interfere with factors evaluated in the study (Pal et al., 2012), an upper limit of 0.5% of DMSO and 0.003% NaOH at the final well, was imposed. DMSO was used to dilute Lithocholic Acid, Vitamin K2, FH1, Dihexa and Verteporfin whereas NaOH was the diluent for T3. Therefore, a vessel in the Stock Trough was used to hold Medium C with 2% DMSO and a vessel in the Stock Block was used to hold the 0.1% NaOH (Figure 65).

To dispense the correct volume from each source well to each destination well, a script was prepared to dispense the appropriate volume of factors/diluents into the feeding blocks. In the feeding blocks 20ul of each high or low concentration factor was added also NaOH to make up a final 0.003%, FBS at the appropriate volume undiluted, MedC 2% DMSO to make up a final 0.5% and MedC to bring the final volume to 600ul.

5.2.5. Preparation of the Worklists-script for DoE#1

To automate generating of the DoE Feeding Blocks, new worklists were required to control the Liquid Handler arm movements and pipetting actions from the source containers to the destination wells. The first worklist had the details for the addition of Medium C, the second for the addition of 2% DMSO in Medium C and the third for the addition of the 12 factors. These worklists were then combined into the new “DoE#1 Feeding Block Script” shown in Table 15.

Stock Block

	1	2	3	4	5	6	7	8	9	10	11	12
A												
B		cAMP	cAMP	DHX	DHX			0.1% NaOH MC		FBS		
C		LCA	LCA	VPF	VPF					FBS		
D		TCA	TCA	HGF	HGF					FBS		
E		VK2	VK2	OSM	OSM							
F		FH1	FH1	H/C	H/C							
G		T3	T3									
H												

Stock Trough

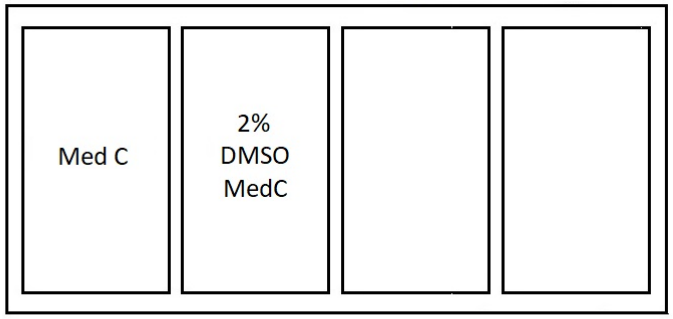

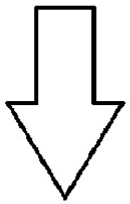

1
20ul x 11 factors at High or Low concentration (10ul for Centre Points)

2
0.1% NaOH added to make up a final 0.003%. 16.2ul for low T3 and 8.1ul for Centre Points

3
FBS added at 49.5ul when High concentration, 24.75ul when Centre Point and 0ul when Low concentration

4
2% DMSO added to make up a final 0.5% in every well. Volume varied between wells

5
Top up to 600ul per well with Med C. Volume varied between wells

Feeding Block 1

	1	2	3	4	5	6	7	8	9	10	11	12
A												
B		MedC	1	7	13	19	25	31	37	43	49	
C			2	8	14	20	26	32	38	44	50	
D			3	9	15	21	27	33	39	45	51	
E			4	10	16	22	28	34	40	46	MedC + Diluents	
F			5	11	17	23	29	35	41	47		
G			6	12	18	24	30	36	42	48		
H												

Feeding Block 2

	1	2	3	4	5	6	7	8	9	10	11	12
A												
B		MedC	52	58	64	70	76	82	88	94	100	
C			53	59	65	71	77	83	89	95	101	
D			54	60	66	72	78	84	90	96	102	
E			55	61	67	73	79	85	91	97	MedC + Diluents	
F			56	62	68	74	80	86	92	98		
G			57	63	69	75	81	87	93	99		
H												

Figure 65 Overview of the Feeding Block preparation. A) Stock for each factor is used to make up 120x concentrated the required high/low concentration and then placed into the Stock Block at the indicated location. B) a volume of 20ul taken from the Stock Block, added into a final volume of 600ul results at a 2x concentrated for feeding of d14 cells. Then a 1:1 dilution makes a final 1x concentrated for feeding the day 16 cells. C) Additives in each well of the Stock Block give a final volume of 600ul. D) Stock Block indicating the position of each factor/component and E) Stock Trough indicating the position of plain MedC and 2% DMSO MedC.

Table 14 Example worklist for the addition of high or low cAMP in the first 10 wells of the Feeding Block 1 in accordance with the 10 first DoE runs shown in table 26.

Step	Source Plate	Source well number	Destination Plate	Destination well number	Volume ul
1	StockBlock	10	Feeding Block 1	18	20
2	StockBlock	10	Feeding Block 1	19	20
3	StockBlock	18	Feeding Block 1	20	20
4	StockBlock	18	Feeding Block 1	21	20
5	StockBlock	18	Feeding Block 1	22	20
6	StockBlock	18	Feeding Block 1	23	10
7	StockBlock	18	Feeding Block 1	26	20
8	StockBlock	10	Feeding Block 1	27	20
9	StockBlock	18	Feeding Block 1	28	20
10	StockBlock	18	Feeding Block 1	29	20

Table 15 Script generated for the preparation of Feeding Blocks containing the required robotic actions. Worklists were embedded and highlighted in red.

Script Editor: Script 1 of Process Lazaros_DoE_RJH

1	Wash Tips	3.0 + 4.0 ml
2	Comment	Add Medium C
3	Worklist Import	C:\Worklists\Lazaros\DoE\MediumC.csv C:\Worklists\Lazaros\DoE\MediumC.gwl
4	Worklist	Load Worklist "C:\Worklists\Lazaros\DoE\MediumC.gwl" Lisa_Medium
5	Worklist	Execute loaded worklist(s)
6	Wash Tips	3.0 + 4.0 ml
7	Comment	Add Medium C + DMSO
8	Worklist Import	C:\Worklists\Lazaros\DoE\MediumC+DMSO.csv C:\Worklists\Lazaros\DoE\MediumC+DMSO.gwl
9	Worklist	Load Worklist "C:\Worklists\Lazaros\DoE\MediumC+DMSO.gwl" Lisa_Medium
10	Worklist	Execute loaded worklist(s)
11	Wash Tips	3.0 + 4.0 ml
12	Comment	Add Compounds
13	Worklist Import	C:\Worklists\Lazaros\DoE\StockBlock1.csv C:\Worklists\Lazaros\DoE\StockBlock1.gwl
14	Worklist	Load Worklist "C:\Worklists\Lazaros\DoE\StockBlock1.gwl" Lisa_Medium
15	Worklist	Execute loaded worklist(s)
16	Wash Tips	3.0 + 4.0 ml

5.2.6. Preparation of the Feeding Blocks DoE#1

Preparation of the feeding blocks was required on day 14 to feed the 102 runs with the DoE#1 treatments. To achieve this, the different components discussed above were positioned at the defined location on the TECAN Evo Freedom deck, as shown in Figure 66. The Stock Block was placed at position 1, the Stock Trough at position 2 and the Feeding Blocks 1 and 2 at positions 3 and 4 respectivelly (Figure 66,64B). The stock block contained the high and low concentration of each factor as shown in Figure 67A and the generated Feeding Blocks 1 and 2 contained 600ul of volume (Figure 67C).

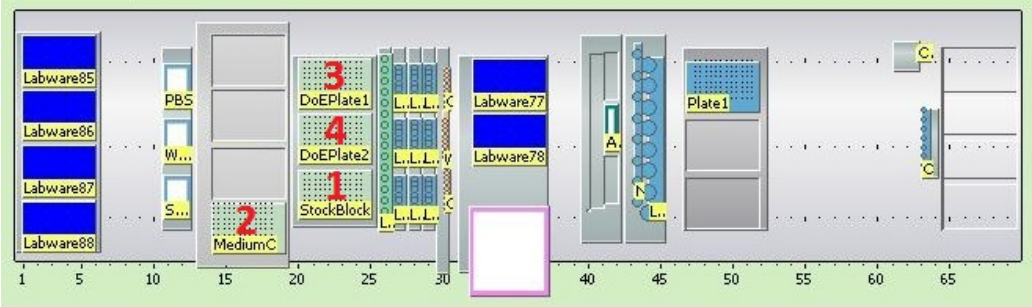

Figure 66 Automated platform overview for the preparation of DoE#1. Labelled as 1) the Stock Block, 2) Stock Trough, 3 and 4) Feeding Blocks 1 and 2 respectively.

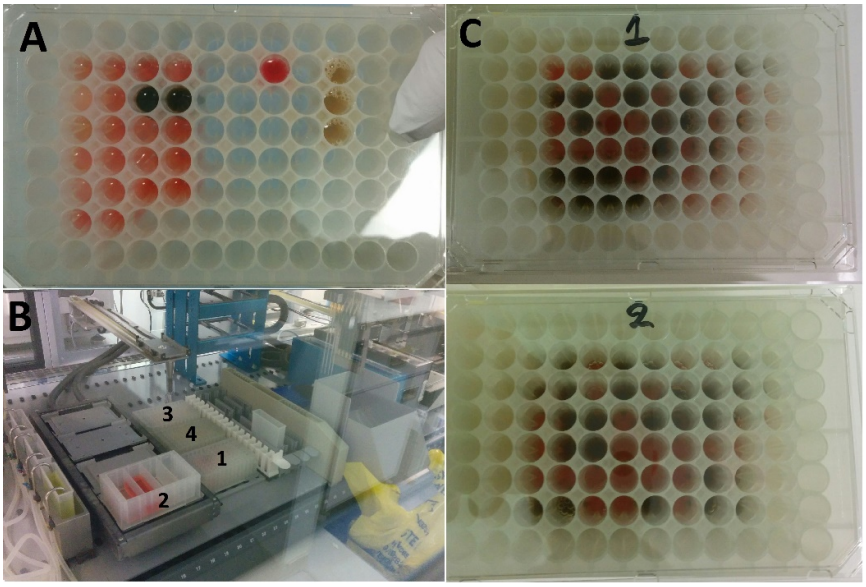

Figure 67 Preparation of the Source Block for the automated production of Feeding Blocks 1 and 2 using the robotic platform and automation. A) Source block, B) Deck set up for the automation process and C) Feeding Blocks 1 and 2 at the end of the automated process with the DoE combinations.

5.2.7. DoE Treatments Lead to Changes in HLC Morphology on day 17

CP1 cells were plated to 40-60% confluency at passage 24 and differentiation initiated and progressed as expected. On day 14 of the differentiation, Feeding Blocks 1 and 2, were generated to feed the cells on day 14 and day 16 of the differentiation protocol.

CellaVista plate reader scans on day 17, indicated that the Medium C control differentiation and Medium C with diluents led to the expected grade 2 morphology of HLC (Figure 68A), together with 15 DoE treatments. 21 Runs generated grade 3 morphology, 19 runs generated grade 4 and the rest 49 runs resulted in grade 1. Figure 68A shows the effect of run treatment and morphology grade and examples of morphologies are shown in Figure 68B.

5.2.8. DoE#1 Treatments Do Not Alter the CYP450 1A2 Expression or Percentage of Double Nuclei Cells but Some Do Increase Expression of CYP450 2C9, 2A6 Compared to Medium C Alone.

Expression of CYP450 1A2 ranged between 0% and 5% in the DoE runs, relative to 2.58% in Medium C (Figure 69). Expression of CYP450 2C9 upon DoE#1 treatments ranged between 1% and 40%, with the most efficient well almost double than the average Medium C response of 21.1% ±6.3 (Figure 70). Interestingly, expression of CYP450 2A6 measured responses ranging between 40% and 100% whereas the Medium C control differentiation generated just 2% of CYP450 2A6 positive cells (Figure 71). No increase in the percentage of double nuclei cells was observed (Figure 72). MedC+0.5%DMSO control present in the study, showed similar results to the MedC control wells not altering expression rates, mean intensities or morphology grade. In terms of Mean Intensity Values, for the selected responses CYP450 2C9 and 2A6, the DoE treatments introduced an increase in the Mean Intensity that as observed in the graphs by more than 2x higher for CYP450 2C9 and 4x higher for CYP450 2A6 (Figure 73).

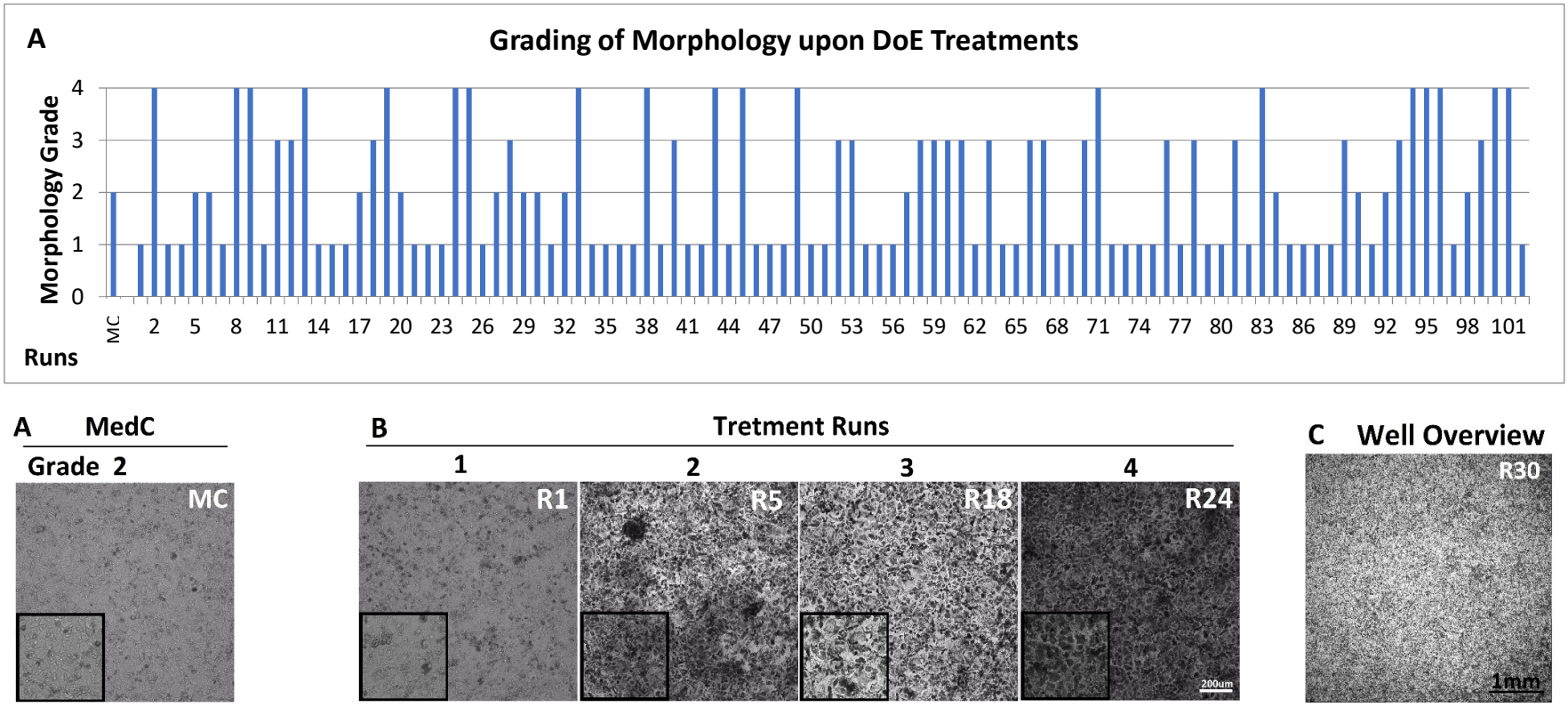

Figure 68 Evaluation of the morphology upon DoE#1 treatments on day 17 of the Hepatocyte Differentiation of H-E8 cultured CP1 hPSC line – Morphology grading 1-4 system for the 102 runs B) Example morphologies generated upon the DoE treatments. Examples from the control Medium C B) Example of a grade 4 well C) Overviews of wells demostrating absence of 3-dimentional structures. Scale bars A) 200um, B,C) 1mm.

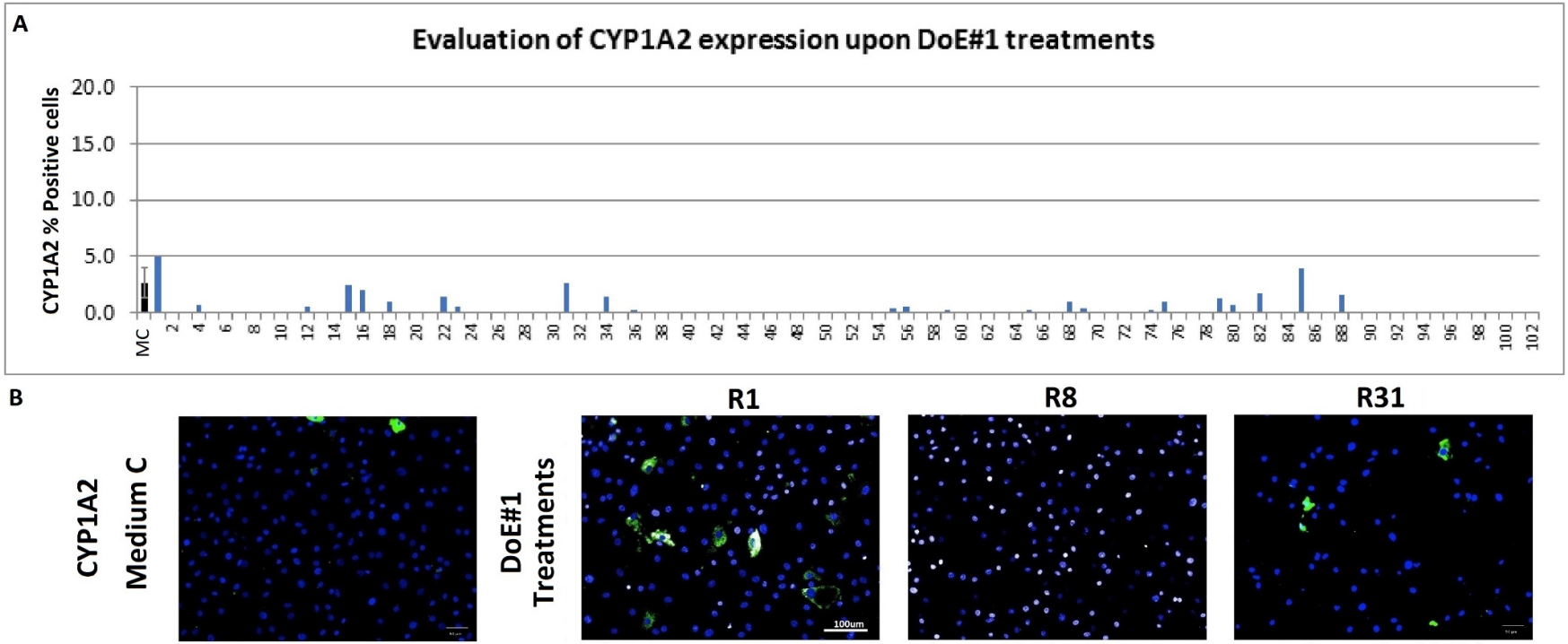

Figure 69 Evaluation of the CYP450 1A2 expression upon DoE#1 treatments on day 17 A) Quantification of CYP450 1A2 percentage positive B) Example images showing pattern of expression of CYP450 1A2. Scale bar 100um

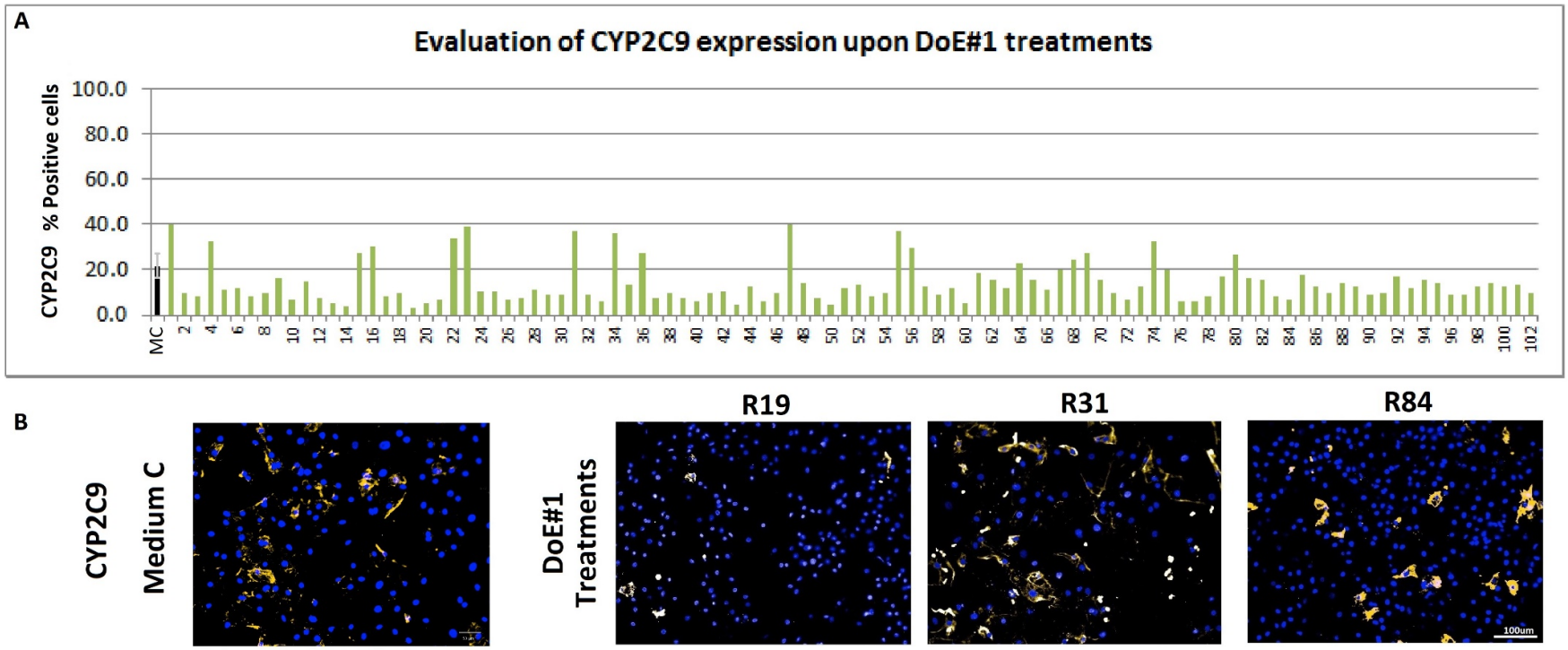

Figure 70 Evaluation of the CYP450 2C9 expression upon DoE#1 treatments on day 17 A) Quantification of CYP450 2C9 percentage positive B) Example images showing pattern of expression of CYP450 2C9. Scale bar 100um

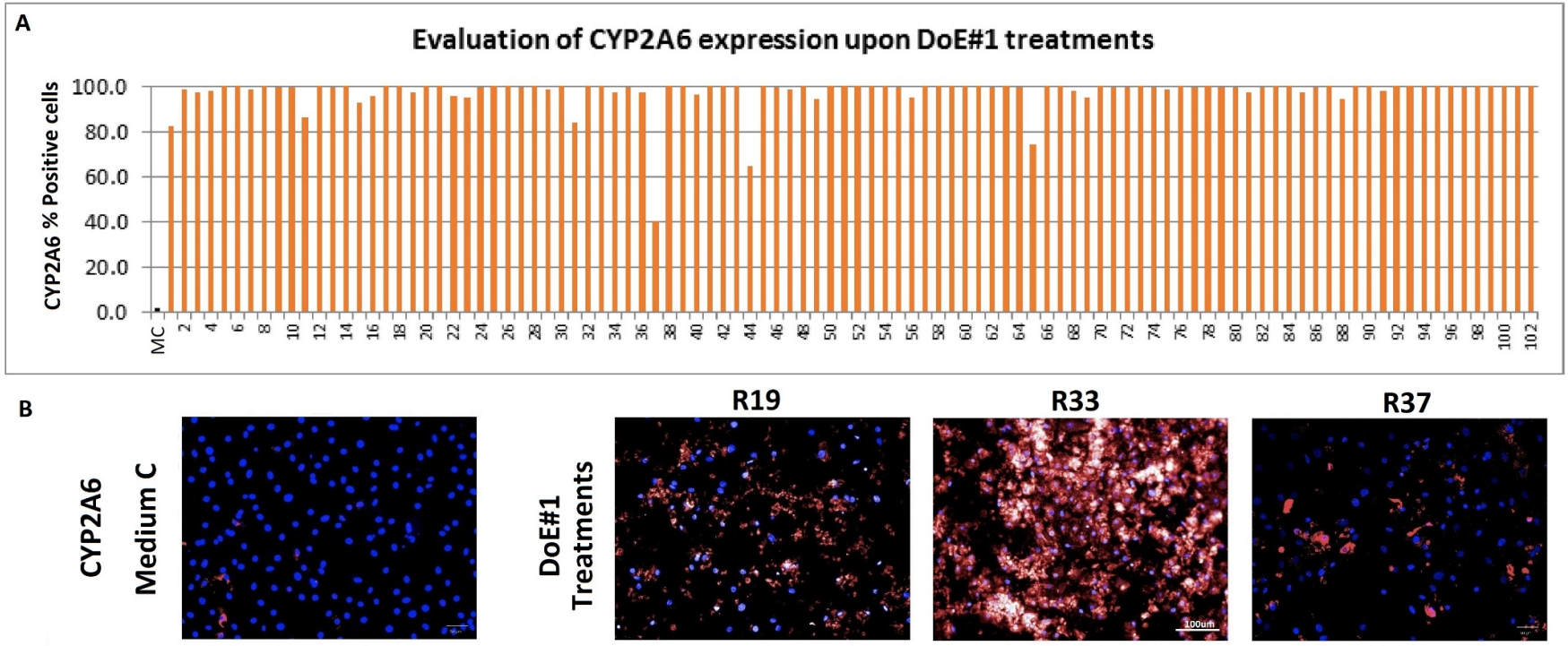

Figure 71 Evaluation of the CYP450 2A6 expression upon DoE#1 treatments on day 17 A) Quantification of CYP450 2A6 percentage positive B) Example images showing pattern of expression of CYP450 2A6. Scale bar 100um

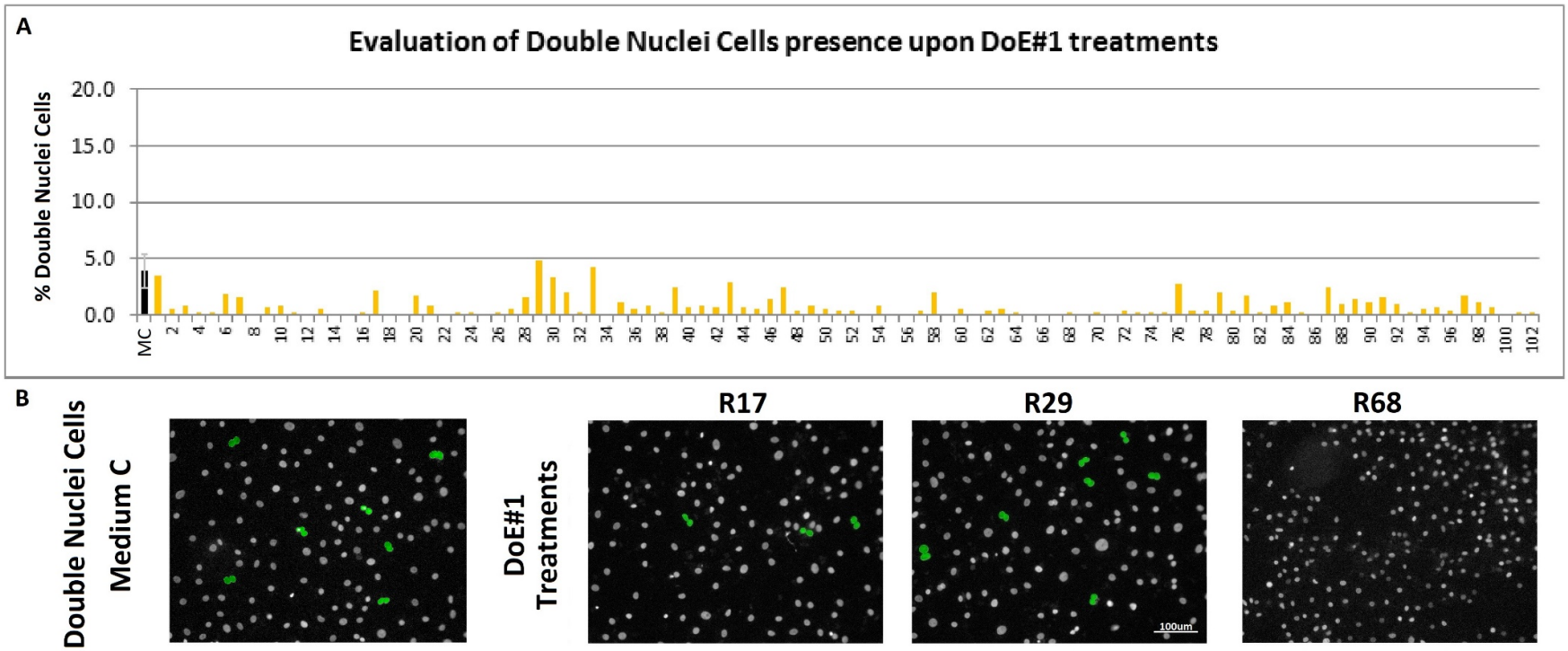

Figure 72 Evaluation of the Double Nuclei Cells percentage upon DoE#1 treatments on day 17 A) Quantification of Double Nuclei Cells presence. B) Example images showing presence of Double Nuclei Cells. Scale bar 100um

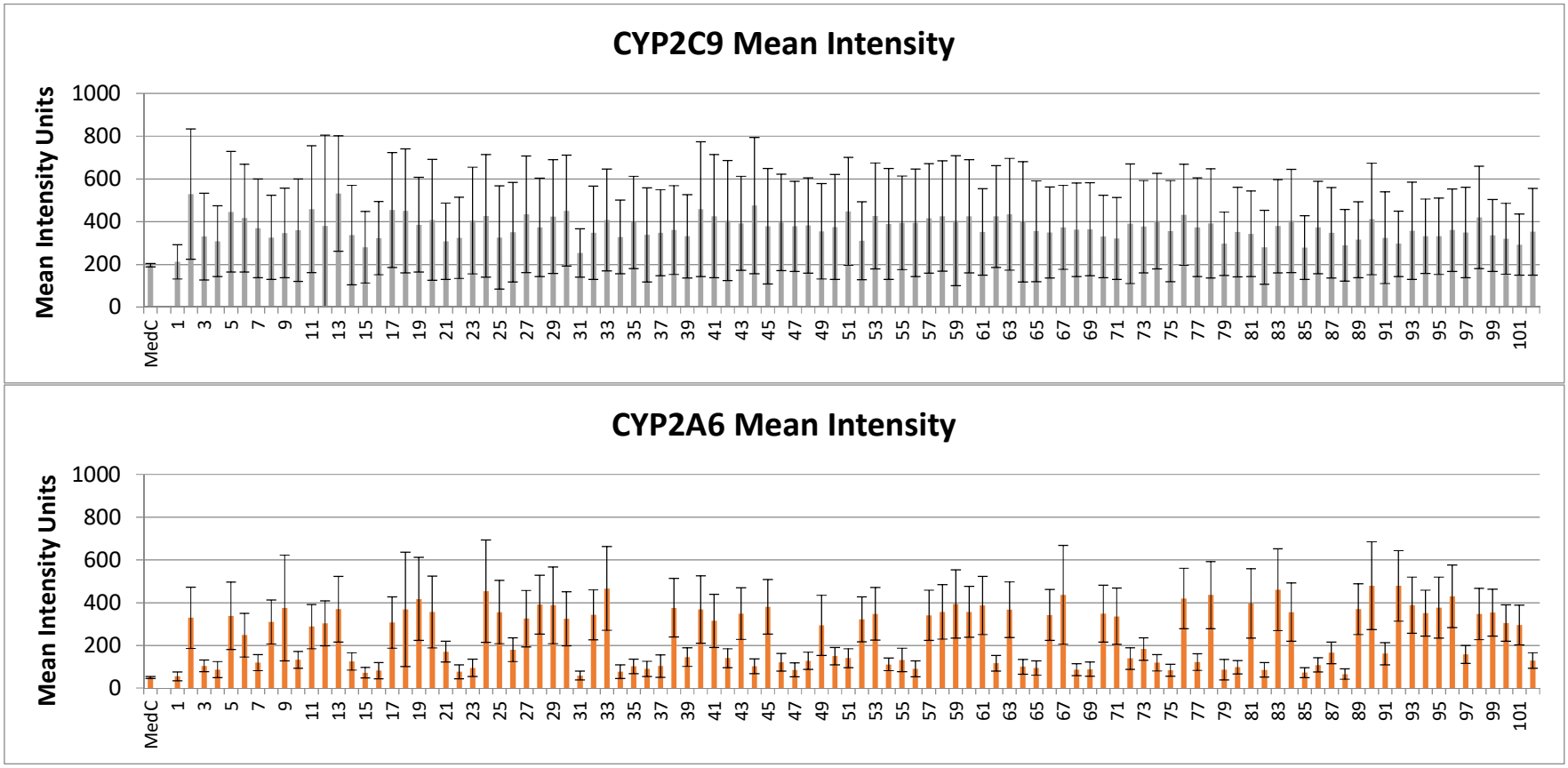

Figure 73 Evaluation of the Mean Intensity of CYP450 2C9 and CYP450 2A6 upon DoE#1 treatments on day 17. Error bars indicate Standard Deviation among the same treatment, on a cell to cell basis.

5.2.9. Identification of Significant Factors and Interactions Improving CYP450 2C9 Percentage Positive & Mean Intensity, CYP450 2A6 Percentage Positive Expression & Mean Intensity and Morphology.

To investigate which factors in the DoE were having significant positive effects, the DX9 software supplied was used to generate a statistical model of the data. Since the use of statistical tests assumes that the analysed dataset is normally distributed, use of non-normalised data is prohibited. If data is not normally distributed, appropriate transformations need to be applied to satisfy the distribution assumption required for statistical tests such as Analysis of Variance (ANOVA) (NIST/SEMATECH, 2012). In DX9, Box-Cox plots were used to provide a measure of data normality and recommend a transformation if needed. To generate the Box-Cox plots, residual values were calculated assuming that the data required no transformation. The residual values represent the difference between the observed from the predicted response. The latter, is generated automatically using the experimental data provided.

In this case, using the DX9 software, significant responses from the previous section were analysed, initially hypothesising that transformation was not required (Figure 74A). At the next step, the data was presented in a Half-Normal Plot, where the significant responses showed a higher “Standardised Effect” (X axis) compared to the majority of non significant responses (Figure 74B). Half-normal plot is the primary selection tool for Fractional Designs where factors that fall below or to the right of the red line have induced a significant effect. Those factors were selected as the most significant to be added in the model (Figure 74C).

An additional graphic used to display the significant effects was the “Pareto Chart” (Figure 74D). Effects were shown as “t-values of Effect” with the most significant factors to the left and the least significant to the right. The Bonferroni limit, red threshold bar, indicated that the t-values above were almost certainly significant and should be added in the model, t-

values above the t-value limit, black threshold bar, were possibly significant and should be added if are likely to be true, based on the literature, while effects below the t-value limit were not likely to be significant.

At the end of the selection and before proceeding to the next analysis step, the list with the factors selected in the model and their aliases was presented (Table 16). For a resolution 4 design, which was selected in this screening approach, aliasing rules indicated that main factors were aliased with 3 factor interactions and 2 factor interactions were aliased with other 2 factor interactions (NIST/SEMATECH, 2012). In this case, the 2-factor effect "BH" (B for Lithocholic Acid and H for Verteporfin) could equally be "AJ", "CG" or "JM" (Table 16), although, the likelihood that it was BH was higher since both B and H factors were involved as significant terms. In the alias list, terms with an "M" were added in the model, terms labelled with an "e" were not and terms with "~" were aliased with other factors. In terms of 3 factor effects, majority were aliased with other factors (Table 16). 3 factor effects were less likely to be identified as significant terms within the Designed experiment.

At the next step, using the DX9 software, an ANOVA analysis was performed on the Model generated so far to identify whether the Model is significant, if there was Curvature and if the "Lack of Fit" of the model was significant (Table 17). As seen in Table 17, the probability (p-value) for the Model to be significant has been calculated at <0.0001 which was significant, similarly for the factor "B-Lithocholic Acid", "H-Verteporfin" and interaction "BH" all were significant. The term "Lack of Fit" used to describe if the model generated has an adequate prediction rate within the design space. If the lack of fit was significant, then the model would be a faulty predictor of the response and should have not been used. In this case, there was an insignificant lack of fit (p=0.8904) therefore the model could be used to predict responses.

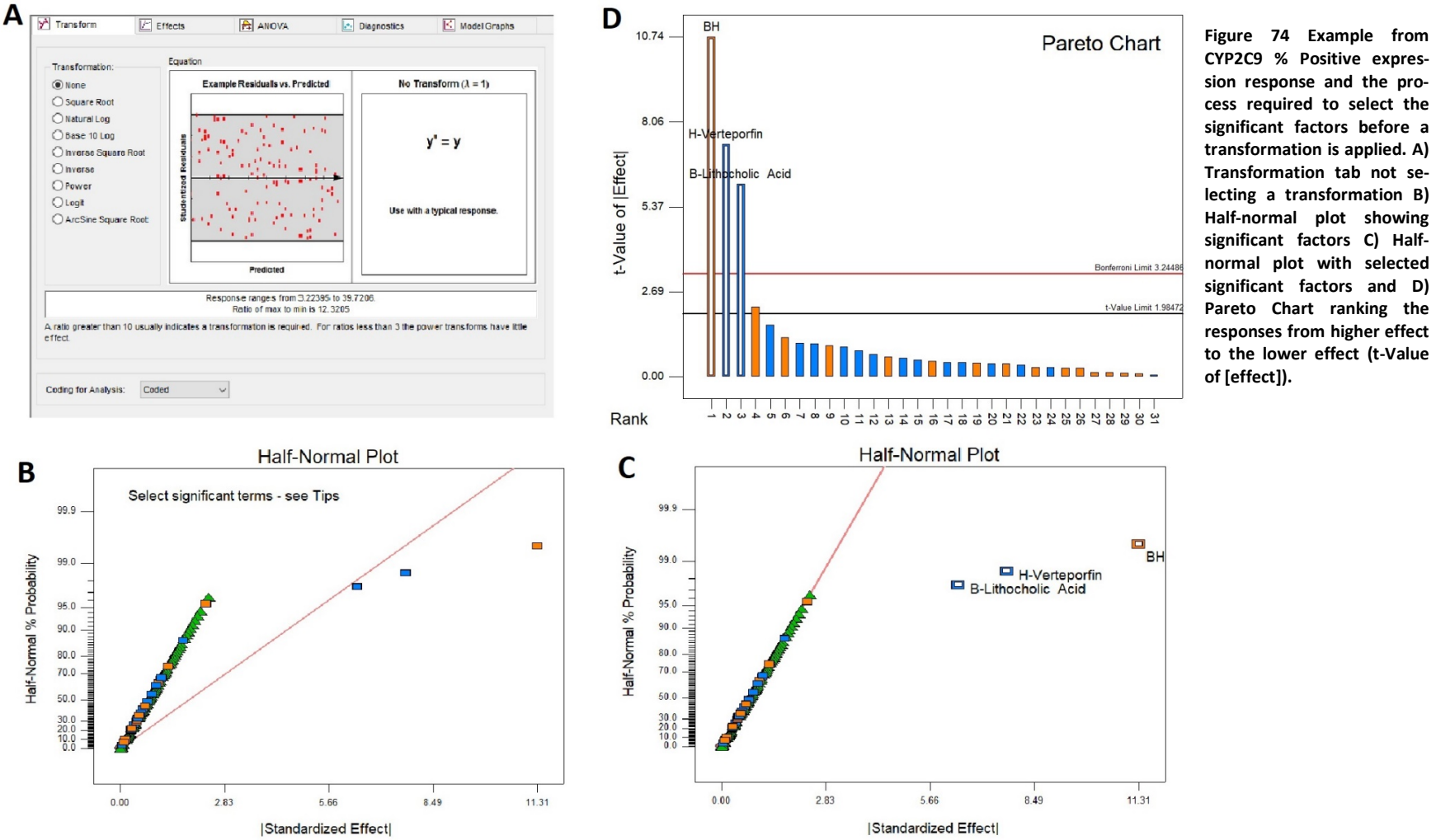

Figure 74 Example from CYP2C9 % Positive expression response and the process required to select the significant factors before a transformation is applied. A) Transformation tab not selecting a transformation B) Half-normal plot showing significant factors C) Half-normal plot with selected significant factors and D) Pareto Chart ranking the responses from higher effect to the lower effect (t-Value of [effect]).

Term	Aliases
1 Factor Effects	
Intercept	
Curvature	
A-Cyclic AMP	BCF BDG BEK BHJ CDH CEL CGJ DEM DFJ FGH FKL GKM HLM
B-Lithocholic Acid	ACF ADG AEK AHJ CDJ CGH CKL DFH DKM EFL EGM FGJ JLM
C-Taurocholate Acid	ABF ADH AEL AGJ BDJ BGH BKL DFG DLM EFK EHM FHJ JKM
D-Vitamin K2	ABG ACH AEM AFJ BCJ BFH BKM CFG CLM EGK EHL GHJ JKL
E-FH1	ABK ACL ADM BFL BGM CFK CHM DGK DHL FJM GJL HJK
F-T3	ABC ADJ AGH AKL BDH BEL BGJ CDG CEK CHJ EJM GLM HKM
G-Dihexa	ABD ACJ AFH AKM BCH BEM BFJ CDF DEK DHJ EJL FLM HKL
H-Verteporfin	ABJ ACD AFG ALM BCG BDF CEM CFJ DEL DGJ EJK FKM GKL
J-HGF	ABH ACG ADF BCD BFG BLM CFH CKM DGH DKL EFM EGL EHK
K-OSM	ABE AFL AGM BCL BDM CEF CJM DEG DJL EHJ FHM GHL
L-H/C	ACE AFK AHM BCK BEF BJM CDM DEH DJK EGJ FGM GHK
M-FBS	ADE AGK AHL BDK BEG BJL CDL CEH CJK EFJ FGL FHK
2 Factor Effects	
AB	CF DG EK HJ
AC	BF DH EL GJ
AD	BG CH EM FJ
AE	BK CL DM
AF	BC DJ GH KL
AG	BD CJ FH KM
AH	BJ CD FG LM
AJ	
AK	BE FL GM
AL	CE FK HM
AM	DE GK HL
BC	
BD	
BE	
BF	
BG	
BH	AJ CG DF
BJ	
BK	
BL	CK EF JM
BM	DK EG JL
CD	
CE	
CF	
CG	
CH	
CJ	
CK	
CL	
CM	DL EH JK
DE	
DF	
DG	
DH	
DJ	
DK	
DL	
DM	
EF	
EG	
EH	
EJ	FM GL HK
EK	
EL	
EM	
FG	
FH	
FJ	
FK	
FL	
FM	
GH	
GJ	
GK	
GL	
GM	
HJ	
HK	
HL	
HM	
JK	
JL	
JM	
KL	
KM	
LM	
3 Factor Effects	
ABC	
ABD	
ABE	
ABF	
ABG	
ABH	
ABJ	
ABK	
ABL	ACK AEF AJM BCE BFK BHM CFL CGM DEJ DFM DGL DHK EGH EKL GJK HJL
ABM	ADK AEG AJL BDE BGK BHL CEJ CFM CGL CHK DFL DGM EFH EKM FJK HJM
ACD	
ACE	
ACF	
ACG	
ACH	
ACJ	
ACK	
ACL	
ACM	ADL AEH AJK BEJ BFM BGL BHK CDE CGK CHL DFK DHM EFG ELM FJL GJM
ADE	

Table 16 Alias list for Fractional Factorial Design selected. 1 Factor Effects are aliased with factor interactions and 2 factor interactions aliased with other 2 factor interactions. 3 factor interactions are aliwased with other 3 factor interactions or main factors, but due to overlap many were already aliased with other factors. Details in text.

Table 17 ANOVA for the CYP450 2C9 percentage positive expression response, without transformation of the data. Significance of the factors is shown as p-value. Model generated was significant, with a non-significant "Lack of Fit".

Transform | Effects | ANOVA | Diagnostics

ANOVA for selected factorial model

Analysis of variance table [Partial sum of squares - Type III]

Source	Sum of Squares	df	Mean Square	F Value	p-value Prob > F	
Model	5501.48	3	1833.83	68.87	< 0.0001	significant
B-Lithocholic	*991.24*	*1*	*991.24*	*37.22*	*< 0.0001*	
H-Verteporfir	*1438.28*	*1*	*1438.28*	*54.01*	*< 0.0001*	
BH	*3071.96*	*1*	*3071.96*	*115.36*	*< 0.0001*	
Curvature	137.43	1	137.43	5.16	0.0253	
Residual	2582.96	97	26.63			
Lack of Fit	*454.74*	*28*	*16.24*	*0.53*	*0.9692*	*not significant*
Pure Error	*2128.22*	*69*	*30.84*			

Lastly, "Pure Error" values describe the experimental error, the normal variation of the response when the experiment is repeated or when replicate points are added. Pure error is used to test the "Lack of Fit" terms for possible significance. If the "Lack of Fit" values were larger than the "Pure Error" values, then a more appropriate model can be used. In this case, sum of squares, degrees of freedom and Mean Square values of Pure Error are larger than "Lack of Fit" values, therefore the model generated was adequate to predict the responses (Table 17).

The next step in the analysis uses the diagnostic tools to evaluate the hypothesis that transformation of the data is not required. In the Box-Cox plot, the y axis represents the Ln (ResidualSS) values, which was the natural log of Residuals Sum of Squares. Residual is the value calculated for each response as the difference between the predicted and the actual response. LN (ResidualSS) were presented in a graph against the lambda (λ) value that represents the transformation required to the data. By default, λ=1 indicates no transformation, λ=-1 for inverse transformation, λ=0 natural log transformation and λ=0.5 square root transformation. In principle, the lower the Ln(ResidualSS) the tighter the model fits to

the data. In this case, λ value was set to 1 (no transformation) but the graph indicates that if λ=0 (natural log) then the model could fit to the data better (Figure 75A). The “Normal Plot of Residuals” indicates whether the residuals follow a normal distribution and this can be identified if the points follow a straight line. A "S-shaped" curve indicated that a transformation of the response may provide a better analysis (Figure 75B). “Residuals vs Predicted” Plot evaluates the assumption of constant variance. If the transformation applied is not ideal then the plot shows an expanding variance (megaphone pattern “<”) but upon the recommended transformation, the plot should be a random scatter (Figure 75C).

“Residuals vs Run” This plot enables to check the responses for lurking variables that may have influenced the response during the experiment. Trends shown on the plot are indicative of a lurking time-related variable, although if not then the plot shows a random scatter. It can be avoided through randomization of the data secures the results against trends (Figure 75D). “Predicted vs Actual” shows in a graph the observed (actual) response values versus the predicted response values calculated based on the model. The data points should be split evenly by the 45-degree line and if they are not, then a transformation would be required (Figure 75E).

As identified with the diagnostic tools, there was a run where the results were outside the allowed space (Figure 75B-E circled). To avoid analyzing the results of a run that doesn’t fit with the data, this run was ignored from the analysis to minimize the variability and error of the model.

The transformation recommended from the Box-Cox plot was then applied to the data and the same process was followed. The significant values were selected in the half normal plot

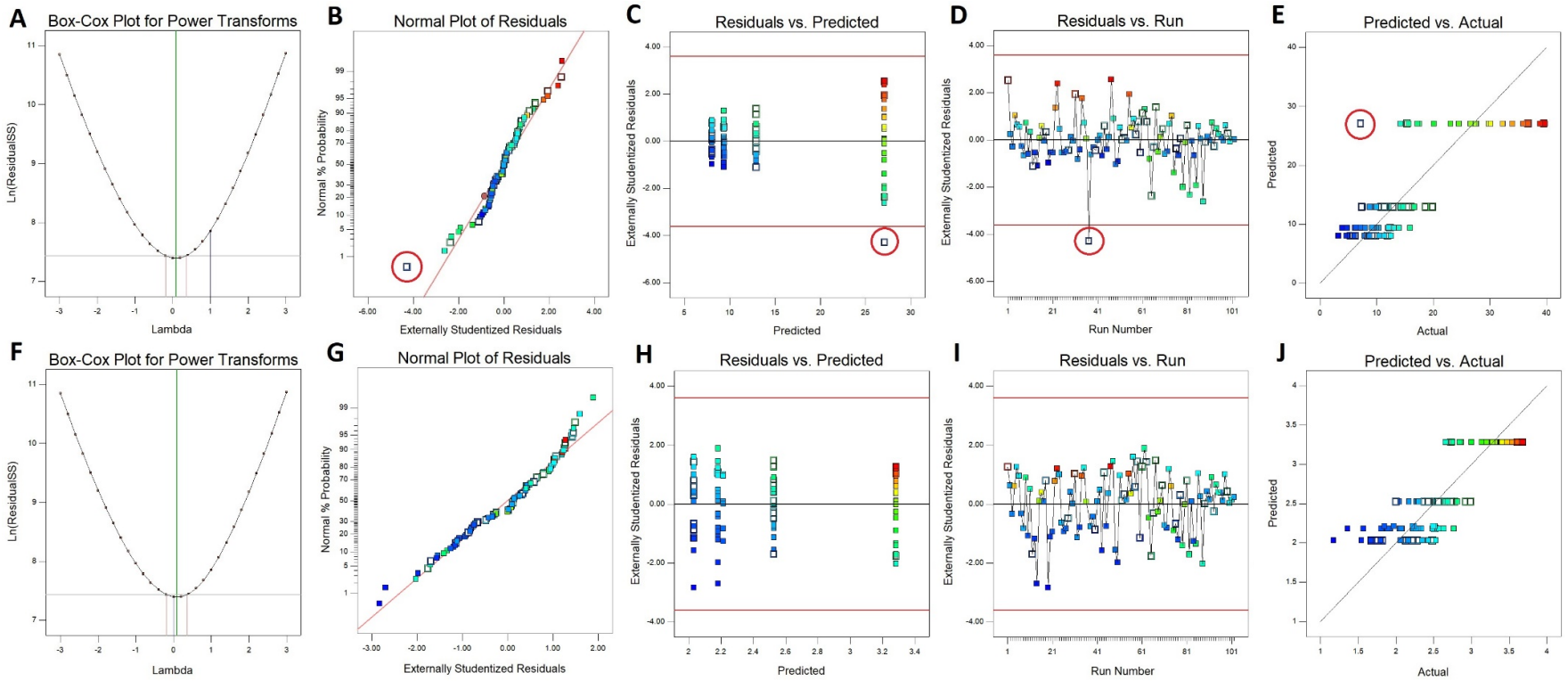

Figure 75 Diagnostic tool overview for CYP450 2C9% positive response analysed without transformation of the data (A-E) and upon transformation of the data (F-J). A,F) Box-Cox plot reccomending a transformation to fit the data. B,G) Normal Plot of residuals, C,H) Residuals vs Predicted, D,I) Residuals vs Run, E,J) Predicted vs Actual. Details in text.

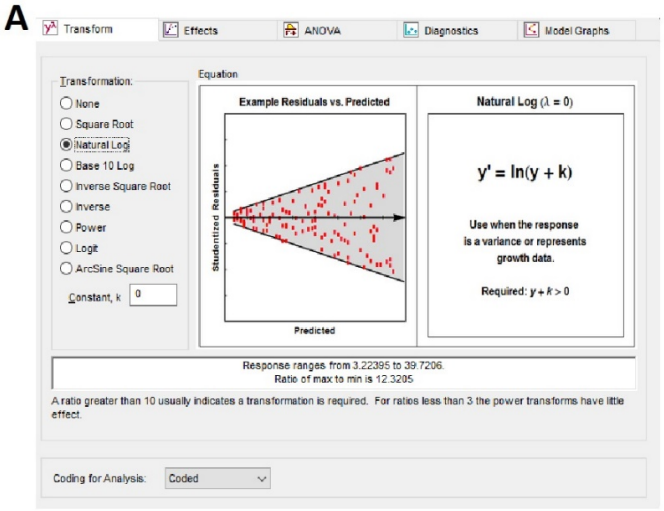

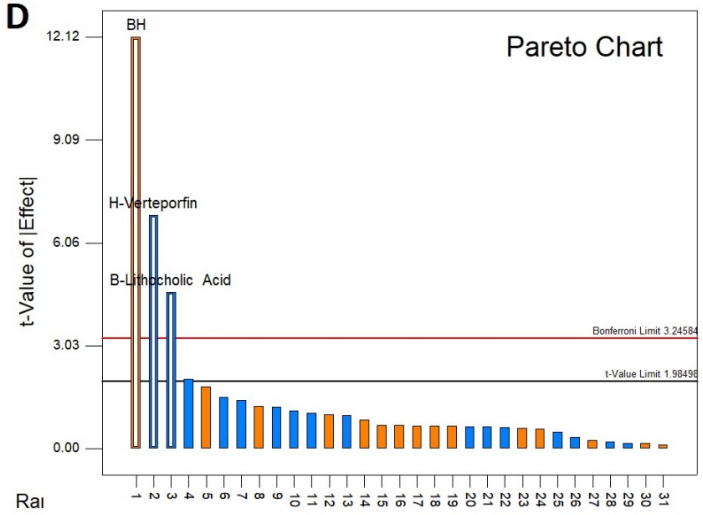

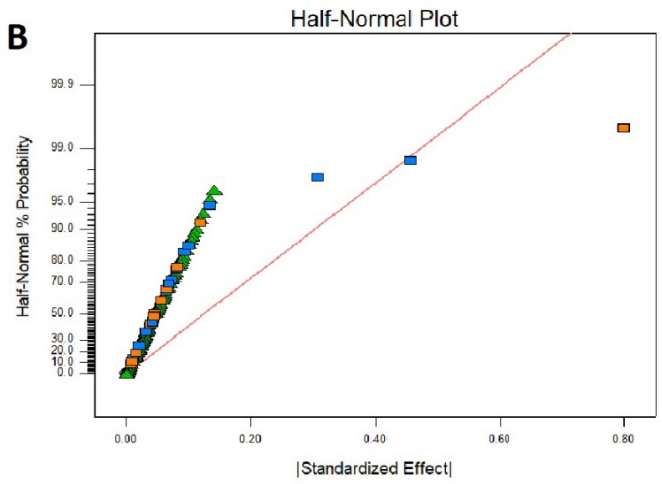

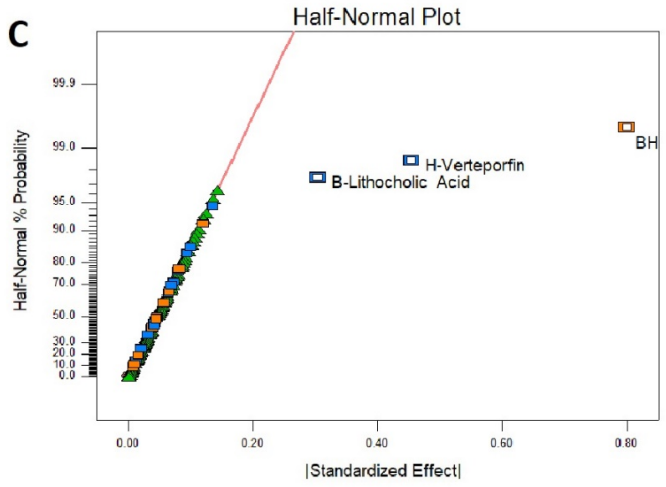

Figure 76 Example from CYP2C9 % Positive expression response and the process required to select the significant factors upon Natural Log transformation of the data. A) Transformation tab selecting the Natural Log option. B) Half-normal plot showing significant factors C) Half-normal plot with selected significant factors and D) Pareto Chart ranking the responses from higher effect to the lower effect (t-Value of [effect]).

Table 18 ANOVA for the CYP450 2C9 percentage positive expression response, upon transformation of the data using the Natural Log transformation. Significance of the factors is shown as p-value. Model generated was significant, with a non-significant "Lack of Fit".

Transform | Effects | ANOVA | Diagnostics

ANOVA for selected factorial model

Analysis of variance table [Partial sum of squares - Type III]

Source	Sum of Squares	df	Mean Square	F Value	p-value Prob > F	
Model	21.80	3	7.27	70.56	< 0.0001	significant
B-Lithocholic	*2.19*	*1*	*2.19*	*21.26*	*< 0.0001*	
H-Verteporfir	*4.88*	*1*	*4.88*	*47.34*	*< 0.0001*	
BH	*15.13*	*1*	*15.13*	*146.94*	*< 0.0001*	
Curvature	0.48	1	0.48	4.67	0.0332	
Residual	9.89	96	0.10			
Lack of Fit	*2.50*	*28*	*0.089*	*0.82*	*0.7101*	*not significant*
Pure Error	*7.38*	*68*	*0.11*			

and shown in the Pareto Chart (Figure 76D). The ANOVA results indicated a significant model with not-significant "Lack of Fit" (Table 18) and lastly, the diagnostic tools evaluated that the transformation was producing the expected type of plots, as explained above, leading to a model that fits to the data tightly (Figure 75F-J) than the previous model without transformation of the data (Figure 75A-E).

In addition to the ANOVA p-values, the results can be viewed in different ways using the DX9 software. The most useful way is the Perturbation Plot that helps to compare the effect of all the factors at a particular point in the design space (Figure 77). Changing one factor over its range, the response was plotted on the graph. When a steep slope was shown, the response was responsive to that factor while if the factor was shown as a relative flat line at the specific concentration settings, the response is not responsive to a change. The perturbation plot could be used to find the factors with the most influence (Figure 77).

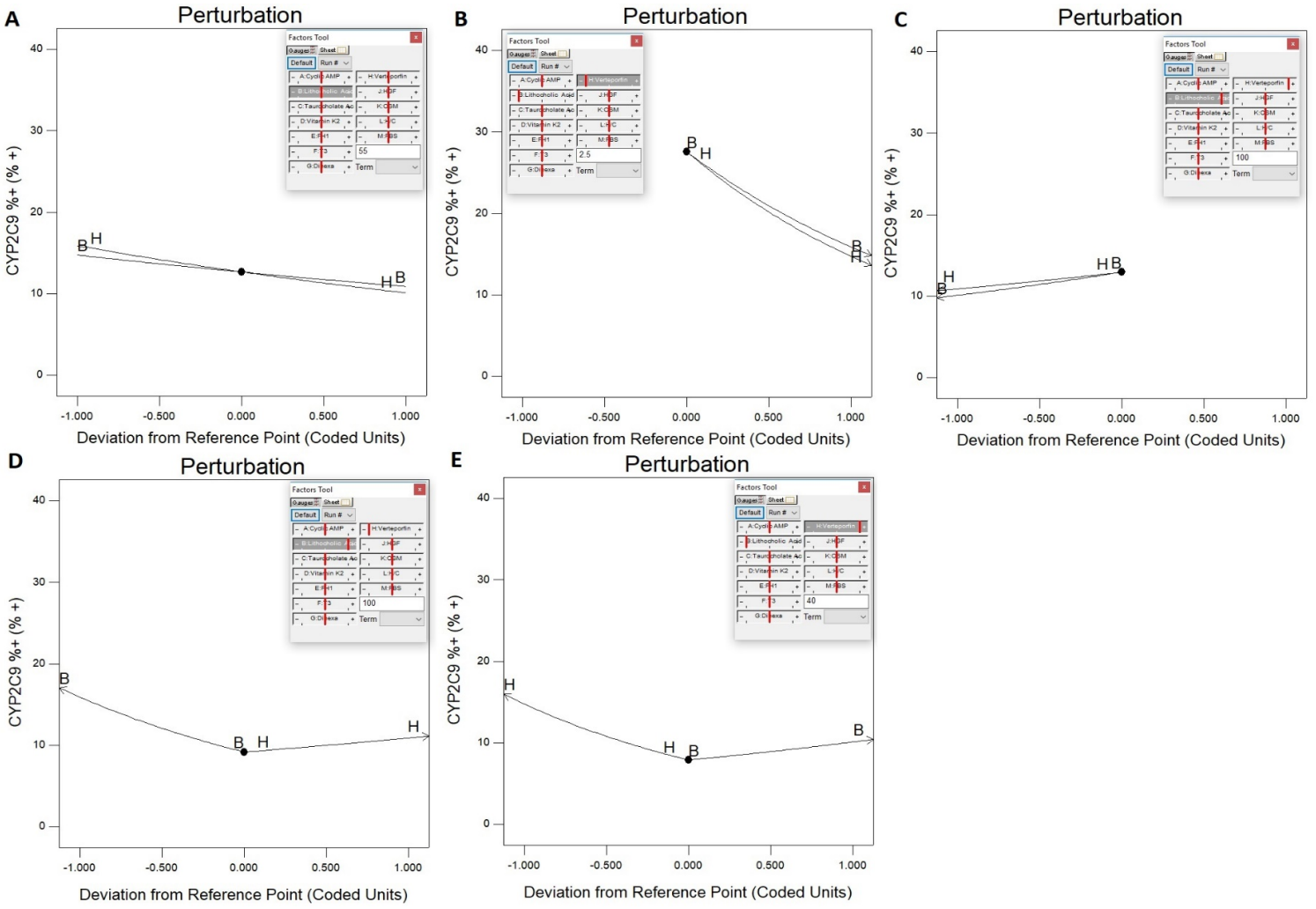

Figure 77 Overview of Perturbation Plots for CYP2C9 % positive Expression. B-Lithocholic Acid and H-Verteporfin added in the model and the expression of CYP2C9 produced (y axis) changes upon different concentration combinations. A) B and H Medium concentration, B) B and L low concentration, C) B and H high concentration, D) B high and H low concentration and E) B low and H high concentration

In this case, the factors added in the model for CYP450 2C9 percentage were the significant factors identified B-Lithocholic Acid and H-Verteporfin. In Figure 77, combinations of High and Low concentrations for B and H are shown. The best settings generating a high CYP450 2C9 percentage expression were identified, when both B and H had the lowest concentration (approximately 30% positive CYP450 2C9). Different settings are shown in Figure 77 but no combination achieved a greater expression of CYP450 2C9 percentage positive cells.

Perturbation Plots were useful to visually understand the effects associated with the factors (Figure 77). However, since the desired outcome of this DoE was to shortlist the factors and identify the important ones, the ANOVA results and the p-values from the significant responses from all the responses with significant changes (CYP450 2C9 percentage positive Expression, CYP450 2C9 Mean Intensity, CYP450 2A6 percentage Positive Expression, CYP450 2A6 Mean Intensity and Morphology) were used to identify the most significant factors and interactions to be used for the next DoE experimentation.

To achieve that, a list of the ANOVA results was made for the responses analysed and the significant factors were identified. For CYP450 2C9 percentage Positive Expression it was Lithocholic Acid and Verteporfin (Table 18). In tables 19 and 20 is shown that for CYP450 2C9 Mean Intensity Lithocholic Acid, Taurocholate Acid, Dihexa, Verteporfin, HGF and H/C were significant factors, Morphology was significantly changed by Verteporfin, CYP450 2A6 percentage Positive by Verteporfin and CYP450 2A6 Mean Intensity by Lithocholic Acid, Verteporfin and FBS. The significant 2 and 3-factor interactions, BC, BG, BH, CH, CL, HL, CHL identified at CYP450 2C9 Mean Intensity and BH, BM identified in CYP450 2A6 Mean Intensity, where combinations of the significant main factors. However, the factors A-Cyclic AMP, D-Vitamin K2, E-FH1, F-T3 and K-OSM were not found to significantly change the responses measured (Tables 19 and 20).

Table 19 ANOVA analysis tables upon transformation for the CYP450 2C9 Mean Intensity response and Morphology response. Significance of the factors is shown as p-value. Models generated were significant, with a non-significant "Lack of Fit".

CYP2C9 Mean Intensity

Transform | Effects | ANOVA | Diagnostics

ANOVA for selected factorial model (Aliased)

Analysis of variance table [Partial sum of squares - Type III]

Source	Sum of Squares	df	Mean Square	F Value	p-value Prob > F	
Model	1.39	12	0.12	13.58	< 0.0001	significant
B-Lithocholic	*0.059*	*1*	*0.059*	*6.89*	*0.0102*	
C-Taurocholi	*0.087*	*1*	*0.087*	*10.15*	*0.0020*	
G-Dihexa	*0.14*	*1*	*0.14*	*16.29*	*0.0001*	
H-Verteporfir	*0.15*	*1*	*0.15*	*17.89*	*< 0.0001*	
J-HGF	*0.095*	*1*	*0.095*	*11.13*	*0.0012*	
L-H/C	*5.478E-004*	*1*	*5.478E-004*	*0.064*	*0.8007*	
BC	*0.050*	*1*	*0.050*	*5.88*	*0.0173*	
BG	*0.071*	*1*	*0.071*	*8.36*	*0.0049*	
BH	*0.64*	*1*	*0.64*	*74.90*	*< 0.0001*	
CH	*0.000*	*0*				
CL	*4.261E-003*	*1*	*4.261E-003*	*0.50*	*0.4820*	
HL	*0.013*	*1*	*0.013*	*1.53*	*0.2194*	
CHL	*0.064*	*1*	*0.064*	*7.44*	*0.0077*	
Curvature	0.13	1	0.13	15.06	0.0002	
Residual	0.74	87	8.546E-003			
Lack of Fit	*0.13*	*19*	*7.101E-003*	*0.79*	*0.7065*	*not significant*
Pure Error	*0.61*	*68*	*8.950E-003*			

Morphology

Transform | Effects | ANOVA | Diagnostics

ANOVA for selected factorial model

Analysis of variance table [Partial sum of squares - Type III]

Source	Sum of Squares	df	Mean Square	F Value	p-value Prob > F	
Model	14.92	1	14.92	2297.56	< 0.0001	significant
H-Verteporfir	*14.92*	*1*	*14.92*	*2298.47*	*< 0.0001*	
Curvature	0.092	1	0.092	14.18	0.0003	
Residual	0.64	98	6.492E-003			
Lack of Fit	*0.14*	*30*	*4.812E-003*	*0.67*	*0.8908*	*not significant*
Pure Error	*0.49*	*68*	*7.233E-003*			

Table 20 ANOVA analysis tables upon transformation for the CYP450 2A6 percentage Positive Expression response and CYP450 2A6 Mean Intensity response. Significance of the factors is shown as p-value. Models generated were significant, with a non-significant "Lack of Fit".

CYP2A6 % Positive

Transform | Effects | ANOVA | Diagnostics

ANOVA for selected factorial model

Analysis of variance table [Partial sum of squares - Type III]

Source	Sum of Squares	df	Mean Square	F Value	p-value Prob > F	
Model	161.80	1	161.80	6.53	0.0121	significant
H-Verteporfir	*162.09*	*1*	*162.09*	*6.54*	*0.0121*	
Curvature	18.74	1	18.74	0.76	0.3866	
Residual	2428.27	98	24.78			
Lack of Fit	*889.64*	*30*	*29.65*	*1.31*	*0.1782*	*not significant*
Pure Error	*1538.63*	*68*	*22.63*			

CYP2A6 Mean Intensity

Transform | Effects | ANOVA | Diagnostics

ANOVA for selected factorial model

Analysis of variance table [Partial sum of squares - Type III]

Source	Sum of Squares	df	Mean Square	F Value	p-value Prob > F	
Model	1915.40	5	383.08	361.02	< 0.0001	significant
B-Lithocholic	*14.27*	*1*	*14.27*	*13.45*	*0.0004*	
H-Verteporfir	*1839.14*	*1*	*1839.14*	*1733.25*	*< 0.0001*	
M-FBS	*2.52*	*1*	*2.52*	*2.37*	*0.1267*	
BH	*60.54*	*1*	*60.54*	*57.05*	*< 0.0001*	
BM	*13.58*	*1*	*13.58*	*12.80*	*0.0006*	
Curvature	51.50	1	51.50	48.53	< 0.0001	
Residual	99.74	94	1.06			
Lack of Fit	*35.71*	*26*	*1.37*	*1.46*	*0.1095*	*not significant*
Pure Error	*64.04*	*68*	*0.94*			

In conclusion, the factors B-Lithocholic Acid, C-Taurocholate Acid, G-Dihexa, H-Verteporfin, J-HGF, K-OSM, L-H/C and M-FBS were included in the next DoE, together with more factors to investigate a greater potential in the maturation of HLC. Although, the significance of Verteporfin was greater than any other factor and its influence was investigated on its own.

5.2.10. Standard curve for Verteporfin Highlighted a false positive signal, directly linked to the concentration of Verteporfin used.

Due to the significant effect of Verteporfin (VPF) in the DoE#1 results, an experiment evaluating the effect of increasing concentrations on the maturation of hepatocyte-like cells was designed. For this purpose, CP1 cells were plated to 40-60% confluency and differentiation initiated. On day 14 and day 16 of the differentiation, concentrations of 0.1uM, 0.25uM, 0.5uM, 1uM, 2.5uM, 5uM and 10uM of VPF applied on the cells. Medium C DMSO control was used to validate whether the effect was based on VPF or a combination between DMSO and VPF. The samples were fixed on day 17 and assessed by immunocytochemistry using the markers described before (Figure 78) and quantification of the positive expression of the markers (Figure 79).

As seen in Figure 78, there wasn't any effect involved on CYP450 1A2 expression in any of the conditions as expression remained as low as 1%-4% (Figure 79). For CYP450 2C9, the protein expression was stable for concentrations between 0.1uM and 5uM although at the higher concentrations of 10uM there was an increase identified (Figure 78) quantified at 20% positive cells (Figure 79). For CYP450 2A6 marker, the expression was identified low for concentrations of up to 0.5uM although, from 1uM onwards, the expression was increased in a concentration-dependent manner. Quantification for CYP450 2A6 showed that increasing the concentration of VPF leads from almost 0% expression to almost 100% expression for the 10uM concentration (Figure 79).

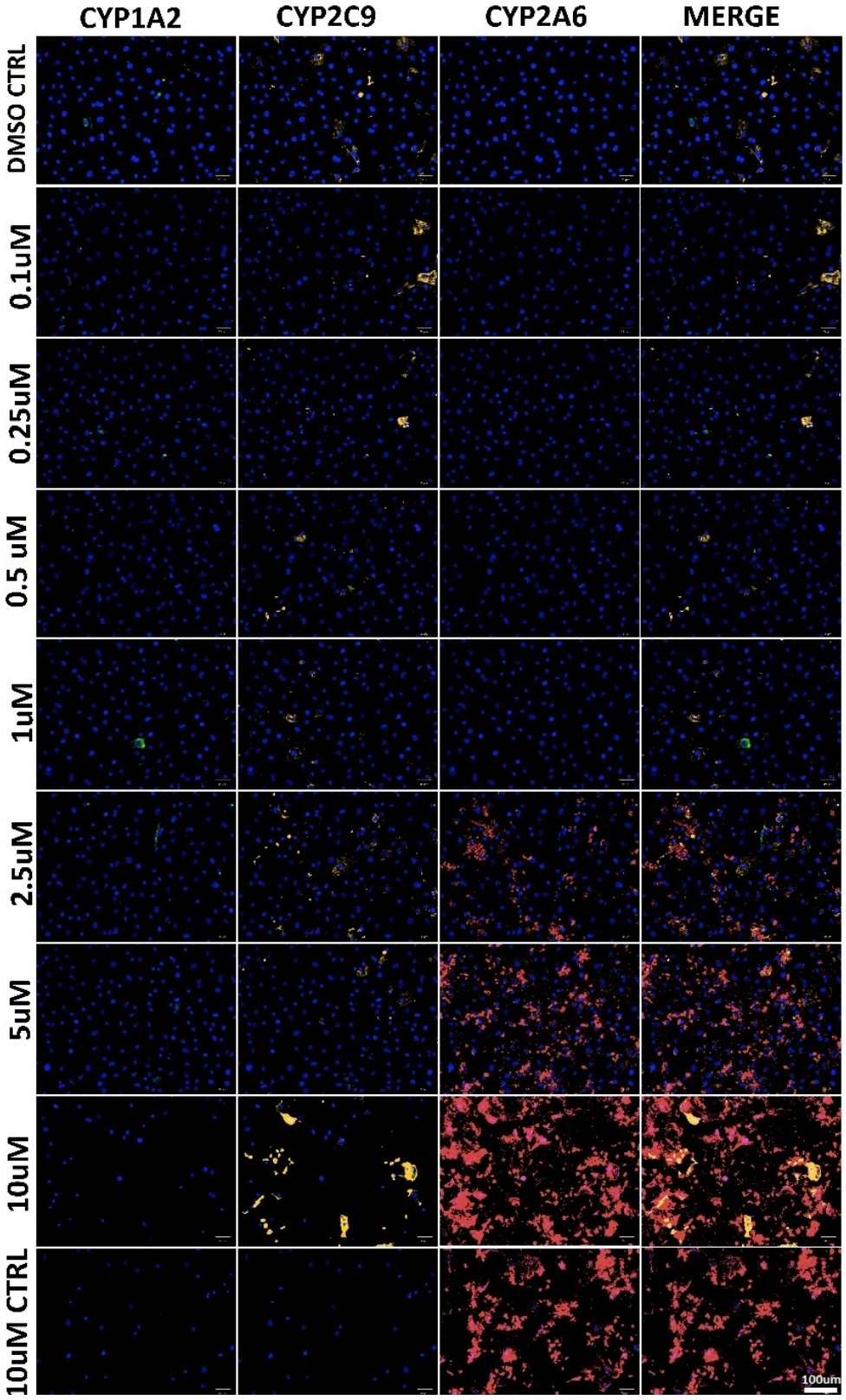

Figure 78 Standard curve for Verteporfin on CP1 cells and immunofluorescence on day 17 for CYP450 1A2, 2C9 and 2A6. Representative images of the 3 markers and a merged image for each condition. Scale Bar at 100um.

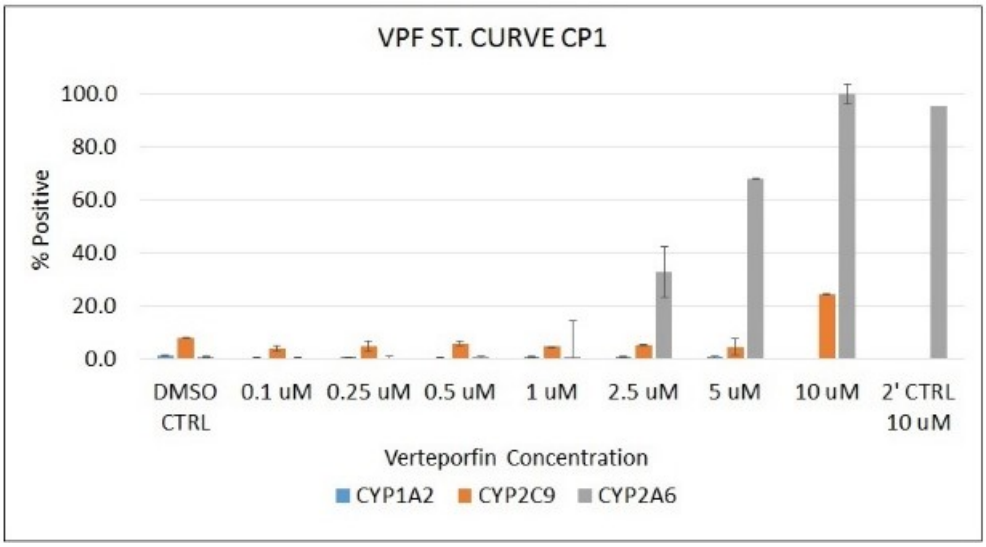

Figure 79 Quantification of the expression of CYP450 1A2, 2C9 and 2A6 upon standard curve treatment for Verteporfin in CP1 cells on say 17. Graph shows the percentage of positive cells. 2'CTRL represents the secondary antibody only control. Error bars represent standard deviation of the mean. N=1 R=3

Furthermore, to exclude the hypothesis that the might be a false-positive signal generated by unspecific binding of the secondary antibody to the VPF compound and not to CYP450 2A6 protein expressed in the cells, secondary antibody-only controls treated with 10uM of VPF were used. The result of the secondary only controls, showed a positive signal for CYP450 2A6 similar to the 10uM treated well (Figure 78). Quantification for the secondary only control and the 10uM treated condition were not different at approximately 100% (Figure 76). Therefore, the hypothesis that the result is independent of the VPF compound cannot be rejected. In conclusion, the effect that VPF showed on the expression of CYP450 2A6 was a false positive outcome and the results regarding CYP450 2A6 were not valid.

Due to the issues identified with Verteporfin, it could not be used in further experiments. Its presence was not only reported to increase the CYP450 2A6 percentage positive and MI, but also CYP450 2C9 percentage positive and MI as well as Morphology of the cells. For this reason, alternatives that could induce activation of the HIPPO Signalling Pathway had to be investigated and evaluated at the next DoE experiment.

Overall, the DoE#1 experiment has shown compounds that have induced a significant effect at the hepatocyte maturation process, upon evaluation through the developed assay. In addition, future experiments, have included control wells treated with all the factors at the highest concentration tested (HCTRL) and used as controls against secondary antibodies only avoiding detection of a false positive signal from the beginning.

5.2.11. Screening of 38 factors using a Central Composite Design for improving the phenotype and the expression of key drug metabolising enzymes in hPSC-derived Hepatocyte Like Cells.

DoE#1 confirmed that the robotic platform could accurately generate the complex run conditions required to screen out a number of ineffective factors and also highlighted the design flaws that needed attention when designing the next set of DoE experiments. In DoE#2, #3, #4 and #5 the extended screen of 33 new factors required a different design to accommodate the increased complexity of the screen at a manageable scale. This phase of the study used the same outputs as DoE#1 and similarly tested factor effects between days 14 and 17 of differentiation.

5.2.12. Design of DoE's #2-#5

The 33 selected factors for this set of DoE's are shown in table 21. The set includes 3 factors that had been successful in DoE#1 Lithocholic Acid, Dihexa and Taurocholate Acid as well as 33 new additions to the current Hepatocyte Differentiation Protocol. Oncostatin M and Hydrocortisone were included to test potential interactions with any of the 33 new factors. Hepatocyte Growth Factor, due to its important role in DoE#1, was added in the base Medium C at the established concentration of 10ng/ml.

DMSO was the diluent for 20 factors while the rest was water soluble (Table 21). Ideally, all 38 factors would have been screened in a single DoE experiment. However, screening of 20 DMSO soluble factors would have resulted in a final concentration of 1.891% of DMSO

when all factors were included at their highest level. Because of the set limit of 0.5% for DMSO concentration discussed previously, the ideal DoE approach of evaluating all the factors in one experiment was not possible. Instead, 4 separate DoE experiments were generated with a maximum of 0.5% DMSO. The water-soluble factors were distributed to generate an even number in each group. Due to the important role of Oncostatin M and Hydrocortisone, these were added as factors in each of the groups making the final number of factors to 11 per group (Table 22). DMSO only controls were included in the design. To check for potential issues caused by factor interference with secondary antibodies as observed with Verteporfin in DoE#1, control wells treated with the high concentration of all factors were included.

Table 21 Factors and their concentration in DoE#2-#5. Light grey-shaded are the factors selected from DoE#1, dark grey-shaded are the main differentiation factors OSM and H/C used in the existing Medium C differentiation protocol.

	Name	Low Concentration	High Concentration	Units		Name	Low Concentration	High Concentration	Units
1	LCA	0.1	100	uM	20	CITCO	50	200	nM
2	DHX	10	400	nM	21	Flavone	20	80	uM
3	TCA	2.5	200	uM	22	SR12813	0.5	5	uM
4	OSM	5	50	ng/ml	23	All trans RA	1	10	uM
5	H/C	0	20	uM	24	SR11237	0.1	5	uM
6	Bexarotene	1	5	uM	25	Epinephrine	0.1	5.0	uM
7	Calcitriol	10	200	nM	26	Glucagon	0.1	2.0	uM
8	Cheno Acid	20	200	uM	27	Cobalt Cl Hex	50.0	200.0	uM
9	ITE	100	2000	nM	28	Sod But	0.5	5000.0	uM
10	Dexamethasone	0.1	5	uM	29	Lipid MIX	1.0	10.0	x
11	Y27632	5	20	uM	30	FGF19	10.0	30.0	ng/ml
12	CHIR99021	3	10	uM	31	KSR	0.0	10.0	%
13	Trichostatin A	1	20	uM	32	AscAcid	0.1	2.0	mM
14	LY294002	5	20	uM	33	Insulin	0.01	2.0	uM
15	Decitabine	1	10	uM	34	D-Glucose	1	10	mM
16	GW7647	0.5	5	uM	35	GlutaMAX	1	5	x
17	Progesterone	0.05	5	uM	36	BSA Solution	0	0.2	%
18	Testosterone	0.05	1	uM	37	MS-1	1	5	x
19	17β Estradiol	0.01	2	uM	38	MS-2	1	5	x

Table 22 DoE's #2, #3, #4 & #5 with the factors included and the DMSO concentration added from each DMSO-soluble factor. Orange-shaded are for DMSO-diluted factors and blue-shaded for water diluted factors.

	DoE#							
	2		3		4		5	
	Factor	DMSO	Factor	DMSO	Factor	DMSO	Factor	DMSO
1	SR11237	0.01	DHX	0.06	ATRA	0.08	Decitabine	0.04
2	Bexarotene	0.01	GW7647	0.01	CITCO	0.001	SR12813	0.05
3	LY 294002	0.08	DEX	0.1	Testosterone	0.002	CHIR99021	0.4
4	Flavone	0.16	LCA	0.2	17β Estradiol	0.004	D-Glucose	
5	Trichostatin A	0.08	Calcitriol	0.04	ITE	0.004	GlutaMAX	
6	Chenodeoxycholic acid	0.16	Glucagon		Y27632	0.4	MS-2 (Transferrin)	
7	Epinephrine		FGF19		MS-1		Progesterone	
8	Cobalt(II) chloride		BSA Solution		Sodium butyrate		TCA	
9	Serum		Insulin		Ascorbic Acid		Lipid Mixture 1	
10	**OSM**		**OSM**		**OSM**		**OSM**	
11	**H/C**		**H/C**		**H/C**		**H/C**	
DMSO		**0.5**		**0.41**		**0.491**		**0.49**

Since many of the factors screened had not previously been tested in HLC differentiation, the high and low levels selected from literature, risked being at an inappropriate dose. For this reason, a DoE approach that would evaluate a larger number of concentration levels, of the factors, would benefit the analysis and exclude extreme highs that might be toxic to the cells. Furthermore, in this round of DoE, evaluation of quadratic effects was a driving force for the design selection. Quadratic effects are a related to the presence of curvature in the model (Figure 80A) and can be assessed when each factor is evaluated at more than 2 concentration levels (NIST/SEMATECH, 2012).

Since the ideal outcomes of the design selected were to estimate interaction of factors and quadratic effects getting an idea of how the experimental space is shaped, RSM designs were evaluated. In order to accommodate for an RSM sub-design that can screen factors at multiple levels, an RSM Central Composite Design (CCD) was selected because it's the only that offers evaluation of multiple concentrations (NIST/SEMATECH, 2012). The CCD design is made up of a two-level factorial design that is augmented with centre and axial (star) points, offering 5 levels of factor screening (Figure 80B&C). Axial points represent concentration of factors outside of the factorial point limits thus evaluating the experimental space at a greater distance from a usual DoE design and generating more information as to how the concentration of the factor affects the response.

According to the values that the axial points are given, the CCD design is sub-divided in two types (Figure 80D). When the axial points are calculated outside of the range, a Circumscribed design (NIST/SEMATECH, 2012). Although, if the range of the concentration is restricted to the low and high, then the axial points become the low and high and the factorial points take values between those two concentrations, called an Inscribed design (Figure 80D). Because the range of some factors in Table 21 is close to 0uM and using the circumscribed design would take it to a negative value which is not possible, the inscribed design was selected (Figure 81A).

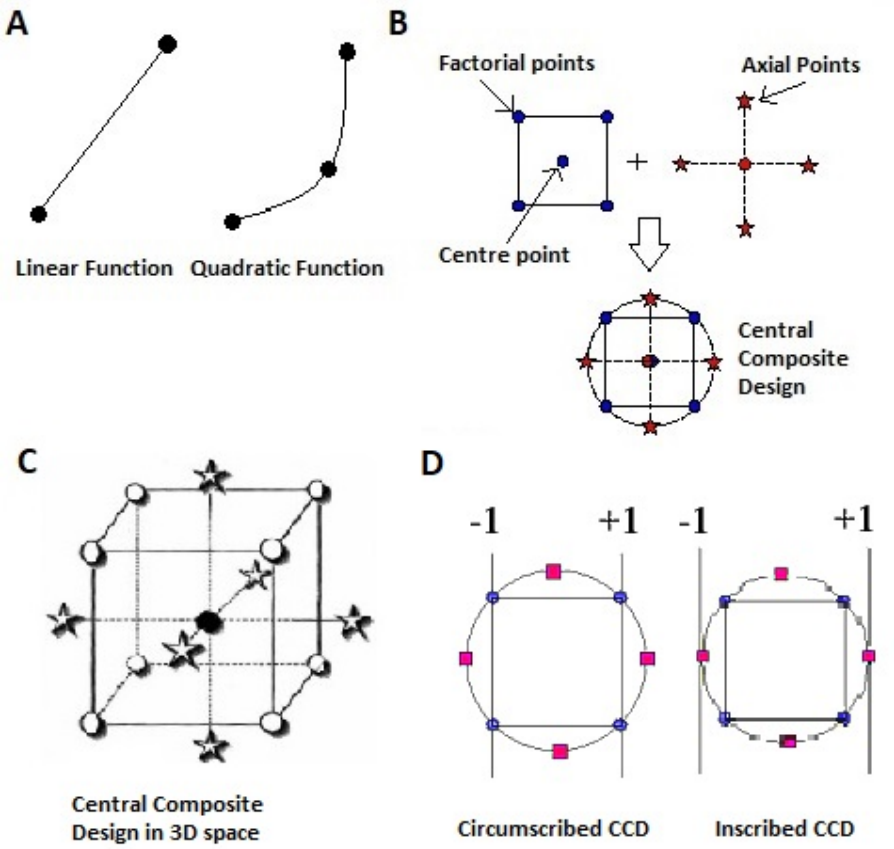

Figure 80 A) Linear and Quadratic function of DoE models B) Generation of Central Composite Design upon a 2-level fractional factorial design augmented by axial points C) Central Composite Design in the 3-dimentional experimental space D) Example of a Circumscribed CCD and Inscribed CCD depending on the range and if it is restricting the use of the outer space Adopted by (NIST/SEMATECH, 2012, Azam, 2014).

Within the CCD, different types of design were available for screening the factors. The options were “¼ Fraction” with 544 runs required, “1/8 fraction” with 288 runs required, “1/16 fraction” with 160 runs required and “Min-Run Res V” with 96 runs required. Since 4 DoE experiments were required for the 4 groups of factors, the “Min-Run Res V” selected as a low-resource requirement (Figure 81B). Within the 96 runs, 6 runs were centre-point runs required to estimate pure error for the “Lack of fit” test (Figure 81C). The factors and concentrations in each run for DoE#2, DoE#3, DoE#4 and DoE#5 are shown in Tables 27 -30.

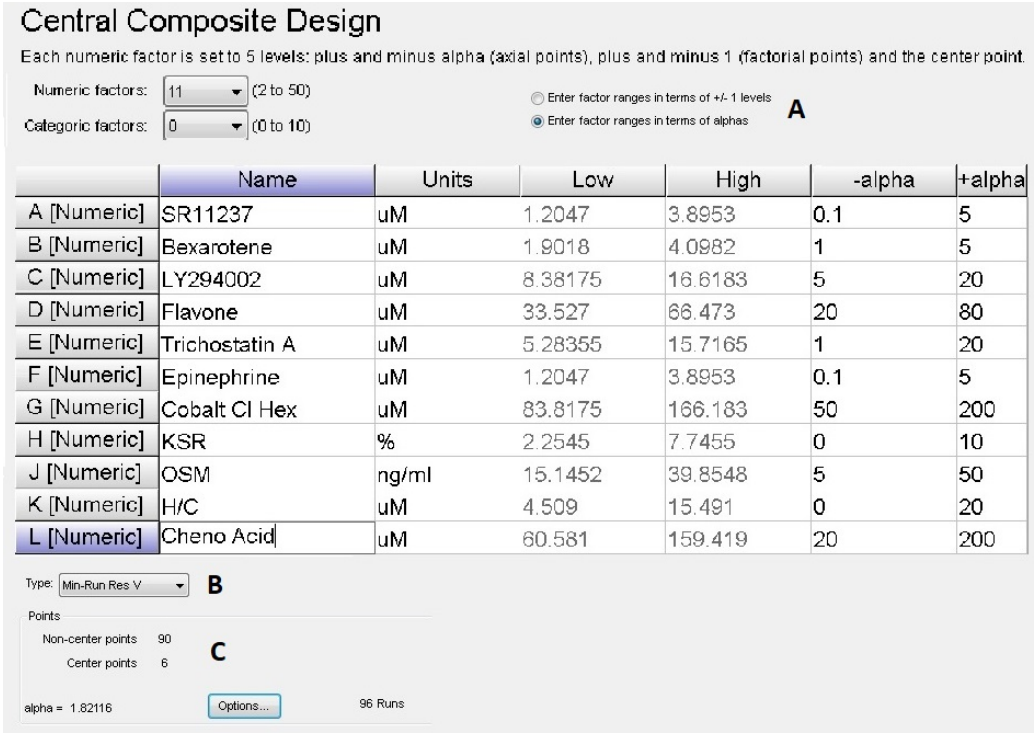

Figure 81 Response Surface Methodology, Central Composite Design Parameters selected in Design Experts 9. Example of factors for DoE#1. Selection of numeric or categoric factors, (A) factor range in terms of alphas, (B) type of the design “Min-Run ResV” and C) number of centre points.

5.2.13. Preparation of Factors and Diluents for DoEs#2, #3, #4 & #5

To avoid edge effects, the 96 experimental runs per DoE were split to two 96 well plates, as shown if Figure 82. Each plate included Medium C, Medium C + 0.5% DMSO and high concentration of all factors for each DoE (All-High), each replicated 4 times (Figure 82).

1-48 Runs Plate 1

	1	2	3	4	5	6	7	8	9	10	11	12
A												
B				1	7	13	19	25	31	37	43	
C				2	8	14	20	26	32	38	44	
D				3	9	15	21	27	33	39	45	
E				4	10	16	22	28	34	40	46	
F				5	11	17	23	29	35	41	47	
G				6	12	18	24	30	36	42	48	
H												

49 - 96 Runs Plate 2

	1	2	3	4	5	6	7	8	9	10	11	12
A												
B				49	55	61	67	73	79	85	91	
C				50	56	62	68	74	80	86	92	
D				51	57	63	69	75	81	87	93	
E				52	58	64	70	76	82	88	94	
F				53	59	65	71	77	83	89	95	
G				54	60	66	72	78	84	90	96	
H												

Medium C
Medium C + 0.5% DMSO
All-High

Figure 82 Plate layout for each DoE. Coloured wells on the left represent Medium C, Medium C + 0.5% DMSO and All-High control with the high concentration for all factors in each DoE.

Similar to DoE#1, the hepatocyte differentiation protocol was followed from day 0 to 17, except that DoE specific media replaced medium C on days 14 and 16 as shown in Figure 67B for DoE#1. On days 14 and 16, removal of 100ul Medium C and replacement with DoE treatments was required. To maintain the factor concentration at the desired levels, 100ul of medium was replaced by a 2x concentrated DoE medium on day 14 and 1x concentrated on day 16 as shown in Figure 67C for DoE#1.

Since the CCD required 5 factor levels instead of 3 used in DoE#1, a medium concentration stock solution was used in the Stock Blocks. The principle of preparing the “Feeding Blocks”

was similar to DoE#1 preparation and as explained in Figure 68. The factors in each DoE, were allocated into Low, Medium and High concentration solution that would make up the 5 different concentrations. Due to some factors requiring use of the larger capacity, fixed tips were used to dispense the desired volume; those were moved to the Stock Trough together with Medium C and 2% DMSO in Medium C (Figure 83).

5.2.14. Preparation of the Worklists-Script for DoE#2-#5

Generation of the DoE blocks was successfully completed in DoE#1 following the "DoE#1 Feeding Block Script". Generation for 4 new Scripts was required for DoE#2, #3, #4 & #5. The new Scripts contained 1 worklist for each solution added from the Stock Trough and 1 worklist for all the factors in the Stock Block. Therefore, DoE#2, #3 & #5 required 4 worklists while DoE#4 only 3 worklists. The worklists for each DoE were combined into the scripts responsible to make up each DoE Feeding Block.

5.2.15. Preparation of the Feeding Blocks DoE#2-#5

In a similar way to the Feeding Blocks preparation on day 14 for the DoE#1, the Feeding Blocks were prepared for DoE#2 ,#3, #4 & #5. The Stock Block, Stock Trough and Feeding Blocks were positioned on the TECAN Evo Freedom deck and upon successful run of the DoE scripts, generated Feeding Blocks 1 and 2, for each DoE that contained the desired final volume.

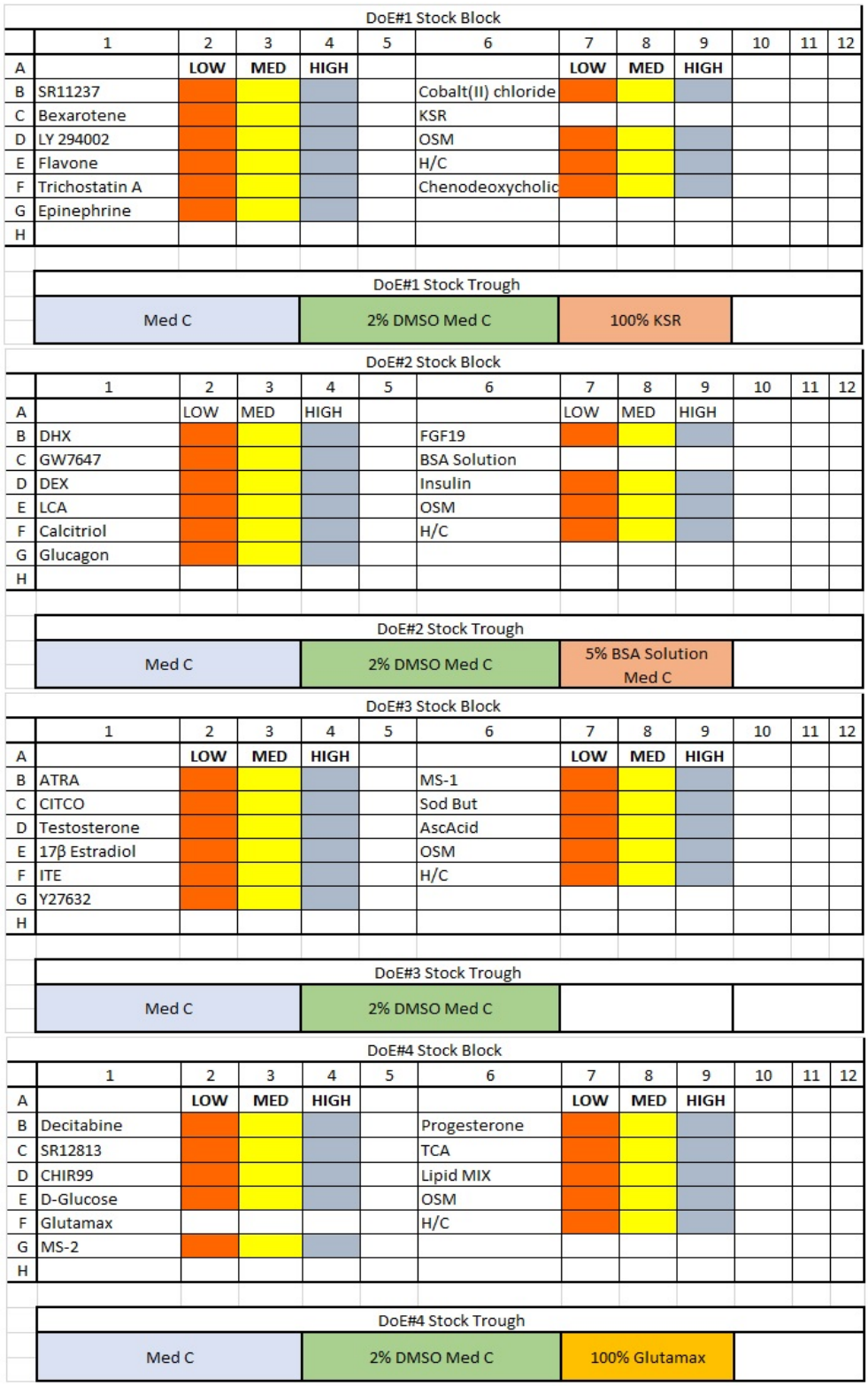

DoE#1 Stock Block

	1	2	3	4	5	6	7	8	9	10	11	12
A		LOW	MED	HIGH			LOW	MED	HIGH			
B	SR11237					Cobalt(II) chloride						
C	Bexarotene					KSR						
D	LY 294002					OSM						
E	Flavone					H/C						
F	Trichostatin A					Chenodeoxycholic						
G	Epinephrine											
H												

DoE#1 Stock Trough

Med C	2% DMSO Med C	100% KSR	

DoE#2 Stock Block

	1	2	3	4	5	6	7	8	9	10	11	12
A		LOW	MED	HIGH			LOW	MED	HIGH			
B	DHX					FGF19						
C	GW7647					BSA Solution						
D	DEX					Insulin						
E	LCA					OSM						
F	Calcitriol					H/C						
G	Glucagon											
H												

DoE#2 Stock Trough

Med C	2% DMSO Med C	5% BSA Solution Med C	

DoE#3 Stock Block

	1	2	3	4	5	6	7	8	9	10	11	12
A		LOW	MED	HIGH			LOW	MED	HIGH			
B	ATRA					MS-1						
C	CITCO					Sod But						
D	Testosterone					AscAcid						
E	17β Estradiol					OSM						
F	ITE					H/C						
G	Y27632											
H												

DoE#3 Stock Trough

Med C	2% DMSO Med C		

DoE#4 Stock Block

	1	2	3	4	5	6	7	8	9	10	11	12
A		LOW	MED	HIGH			LOW	MED	HIGH			
B	Decitabine					Progesterone						
C	SR12813					TCA						
D	CHIR99					Lipid MIX						
E	D-Glucose					OSM						
F	Glutamax					H/C						
G	MS-2											
H												

DoE#4 Stock Trough

Med C	2% DMSO Med C	100% Glutamax	

Figure 83: Stock Blocks and Stock Troughs for each DoE indicating position of the factors within the block and trough. KSR Knock Out Serum Replacement, OSM Oncostatin M, H/C Hydrocortisone, ATRA All Trans Retinoic Acid, DEX Dexamethasone, Sod But Sodium Butyrate, FGF19 Fibroblastic Growth Factor 19, TCA Taurocholate Acid, Asc Acid Ascorbic Acid, MS-1/2 Media Supplement 1/2.

5.2.16. Initiation of Hepatocyte Differentiation for DoE#2-#5 and DoE Treatments on day 14 and day 16

CP1 cells were plated to 40-60% confluency for 4 consecutive passages (28, 29, 30 and 31) to accommodate the plates required for DoE#2, #3, #4 & #5 respectively. In all experiments, hepatocyte differentiation initiated and progressed as expected in terms of culture and morphology.

5.2.17. DoE#2-#5 treatments did not improve HLC morphology on day 17 or Double Nuclei Cell Count

Medium C control differentiation wells lead to expected morphology of HLC (Grade 2) whereas DoE treatments induced either Grade 2 morphologies or showed loss of hepatocyte characteristics Grade 1 (Figure 84). In DoE's #2 and #4, the DoE runs only achieved a Grade 1 morphology with lack of hepatocyte characteristics (Figure 84A and 85A). In DoE#3, 23 runs achieved a Grade 2 morphology and the rest a Grade 1 (Figure 84B). In DoE#5, 69 runs achieved a Grade 2 morphology and the rest a Grade 1 (Figure 85B). In all DoE's, the Med C + 0.5% DMSO (MCDM) control did not affect the morphology and achieved a Grade 2 similar to MC control. However, the secondary-only controls for the High Concentration of all factors treatments (MCAH), in all cases, achieved a Grade 1 morphology (Figures 81, 82). Similarly, no run treatment improved the percentage of DNC when compared to the control wells (results not shown).

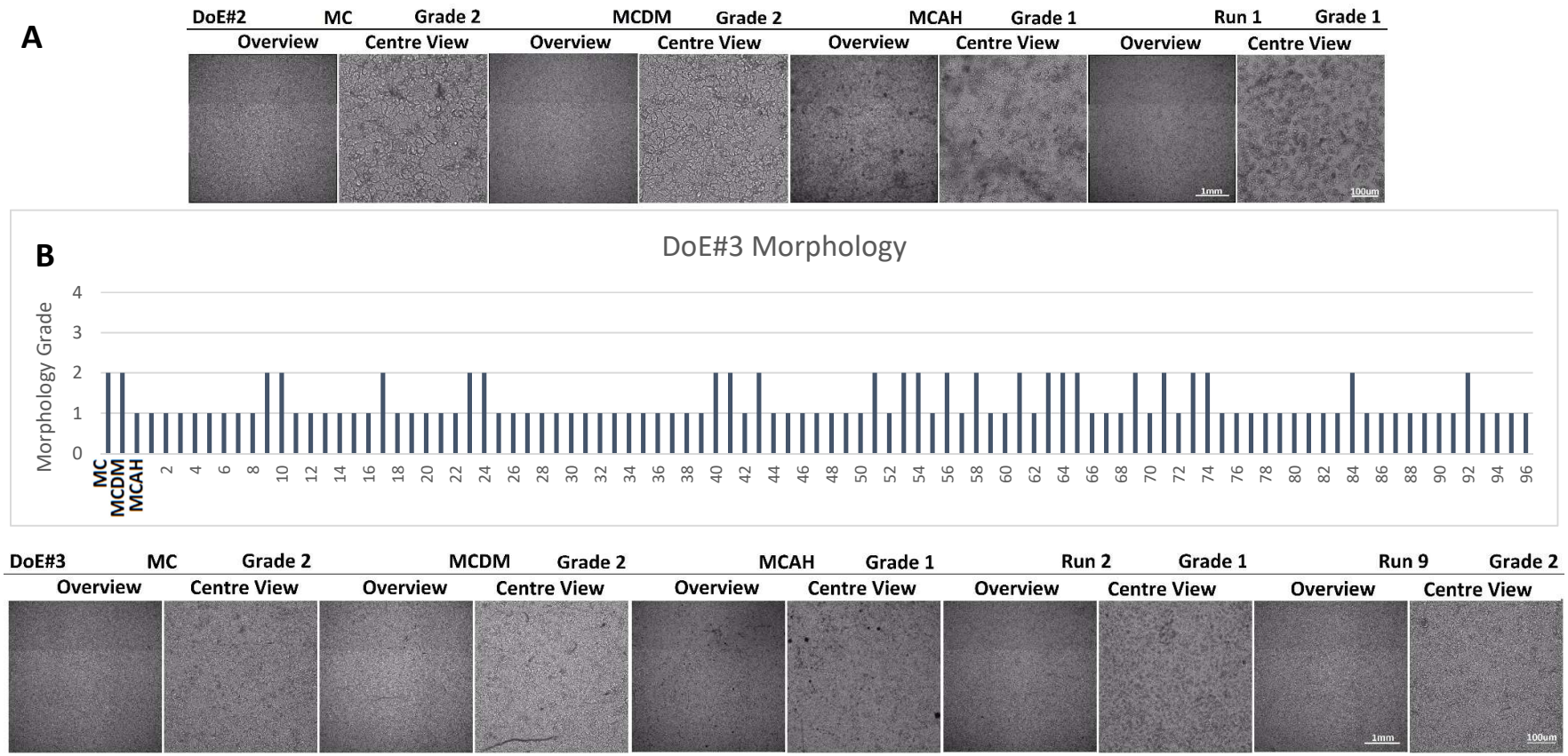

Figure 84 Examples of HLC morphologies identified in DoE#2 (A) and DoE#3(B). Overview of the well and a focused image of the centre view. Medium C control achieved a Grade 2 overall, Medium C with 0.5% DMSO achieved a Grade 2 overall and Medium C with high concentration of all factors achieved a grade 1 overall. A) In DoE#2 a grade 1 morphology was found across the runs. B) In DoE#3, grade 1 and grade 2 morphologies were identified across the runs but none greater than 2.

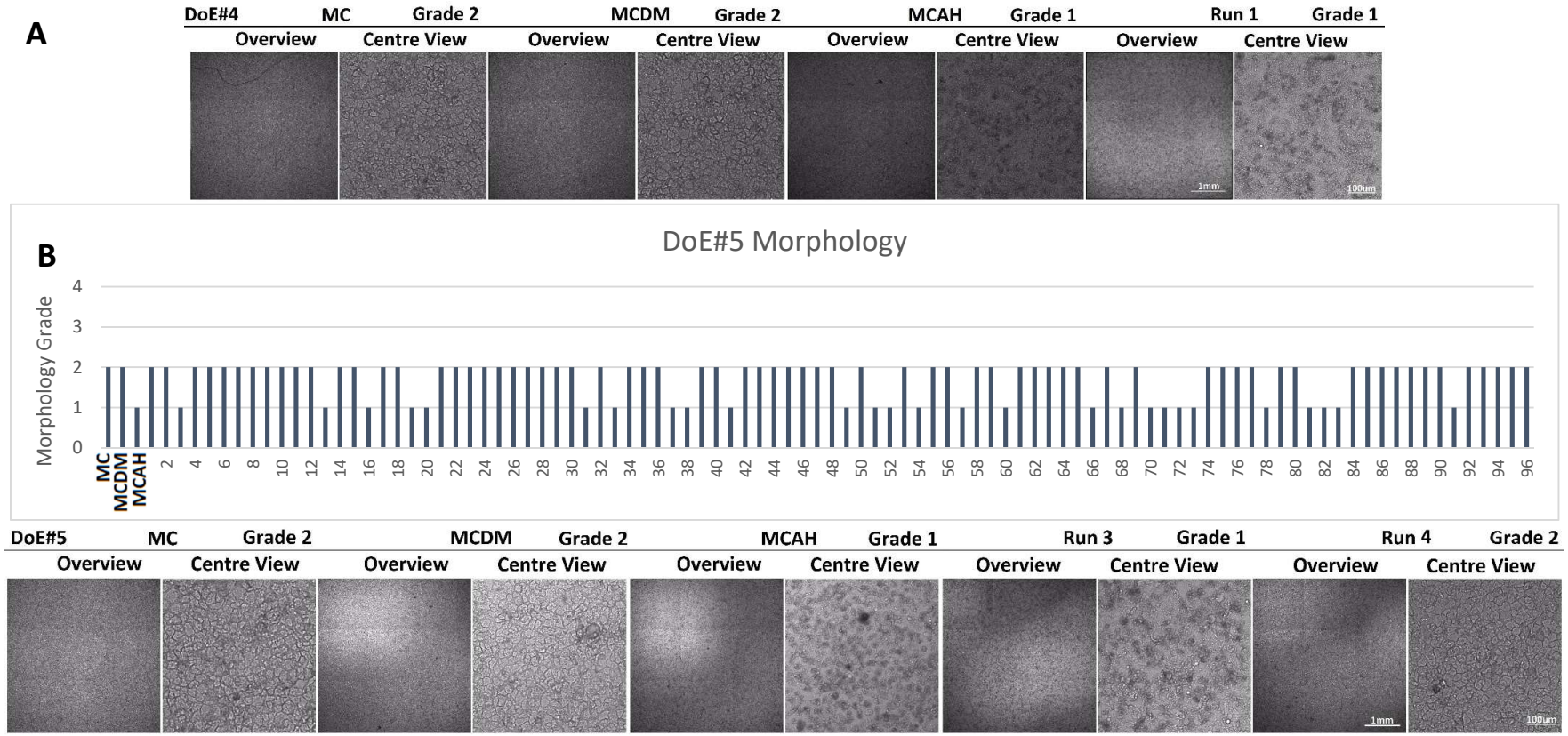

Figure 85 Examples of HLC morphologies identified in DoE#4 (A) and DoE#5(B). Overview of the well and a focused image of the centre view. Medium C control achieved a Grade 2 overall, Medium C with 0.5% DMSO achieved a Grade 2 overall and Medium C with high concentration of all factors achieved a grade 1 overall. A) In DoE#4 a grade 1 morphology was found across the runs. B) In DoE#5, grade 1 and grade 2 morphologies were identified across the runs but none greater than 2.

5.2.18. CYP450 1A2 Expression was Masked by False Positive Signal

In DoE#2, CYP450 1A2 was expressed in between 0% and 0.20% of cells while the Medium C control differentiation (MC) resulted in 0.11%±0.10 (Figure 86A). The best run in DoE#2 did not achieve a higher CYP450 1A2 percentage than the MC, therefore the results were not analysed further. In DoE#3, CYP450 1A2 was expressed in between 0% and 1.88% of cells while the MC resulted in 0.05%±0.03 (Figure 86B). The maximum of 1.88% CYP450 1A2 positive cells detected in the DoE runs was of no interest to this study and therefore was not analysed further.

In DoE#4, CYP450 1A2 was expressed in between 0.01% and 12.32% of cells while the MC resulted in 0.06%±0.01 (Figure 87A). The Medium C + 0.5% DMSO (MCDM) control differentiation achieved a 0.26%±0.20 positive cells, not significantly higher than the MC ($p=0.10$). The secondary only control wells treated with high concentration of all factors (MCAH) resulted in 0.79%±0.21 expression of CYP450 1A2, significantly higher than the MC control ($p=0.004$). Since a significantly higher expression of CYP450 1A2 was detected in the MCAH, the positive DoE runs run the risk of being influenced by a false positive signal. To avoid false conclusions, these results were not analysed further.

In DoE#5, CYP450 1A2 was expressed in between 0.19% and 6.00% while MC resulted in 0.06%±0.06 (Figure 87B). The MCDM achieved a 0.23%±0.15 positive cells, not significantly higher than the MC ($p=0.08$) and the MCAH resulted in 0.12%±0.10 expression of CYP450 1A2 not significantly higher than the MC control ($p=0.34$). The fact that the MC and MCAH controls were expressing CYP450 1A2 at the same levels meant that the DoE runs might have been influenced by false positive signal. To avoid false conclusions, the results were not analysed further. Additionally, an increase up to 12% would be of no relevance to the pHEPs where the range of CYP450 1A2 was identified between 10%-65%.

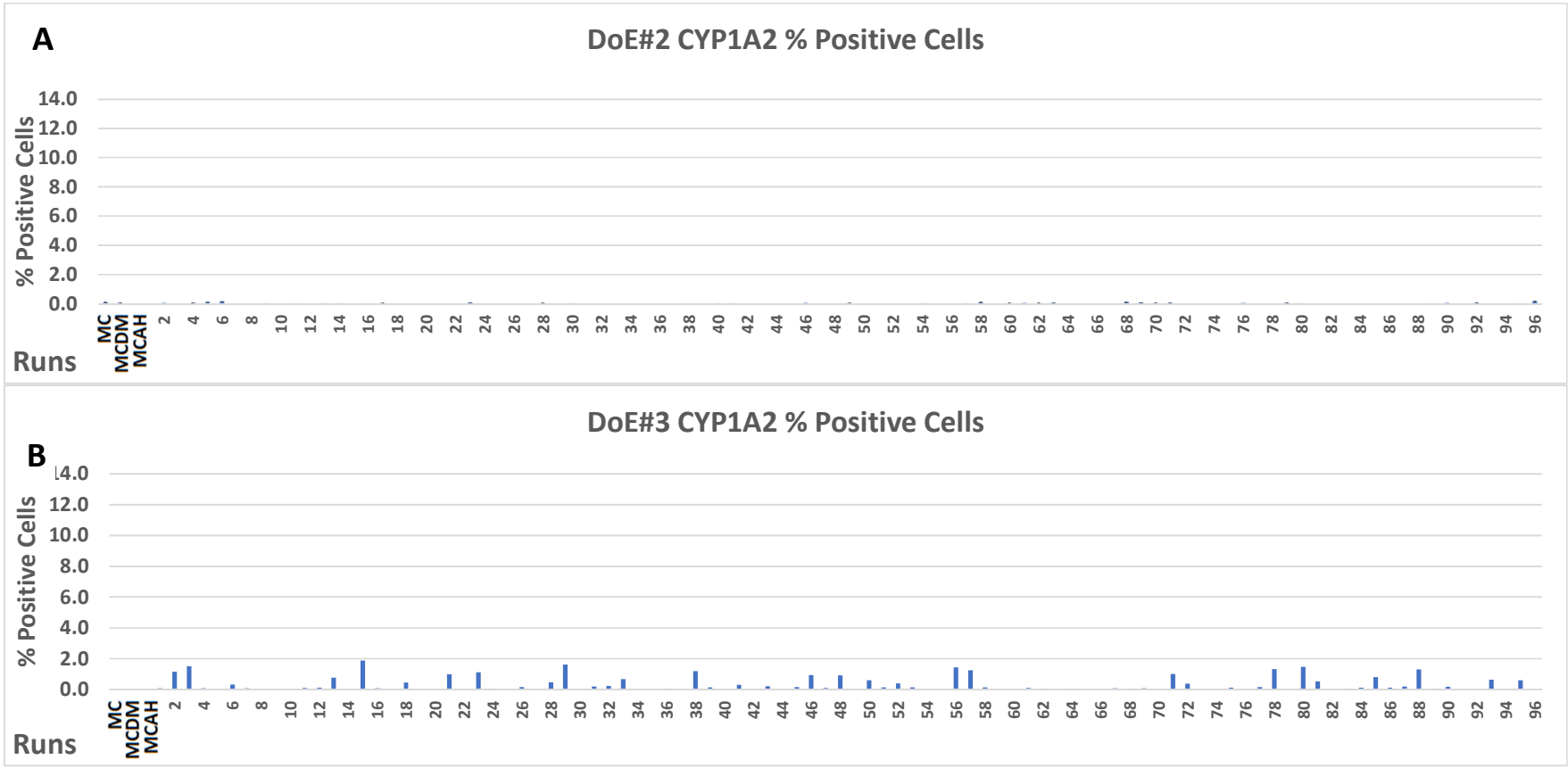

Figure 86 CYP450 1A2 percentage Positive cells in DoE#2 and DoE#3. Medium C (MedC), Medium C + 0.5% DMSO (MCDM) and Medium C with high concentration of factors (MCAH) controls represent Mean ± Standard Deviation of 4 replicates. Numbers correspond to the Runs detailed in tables 27 and 28.

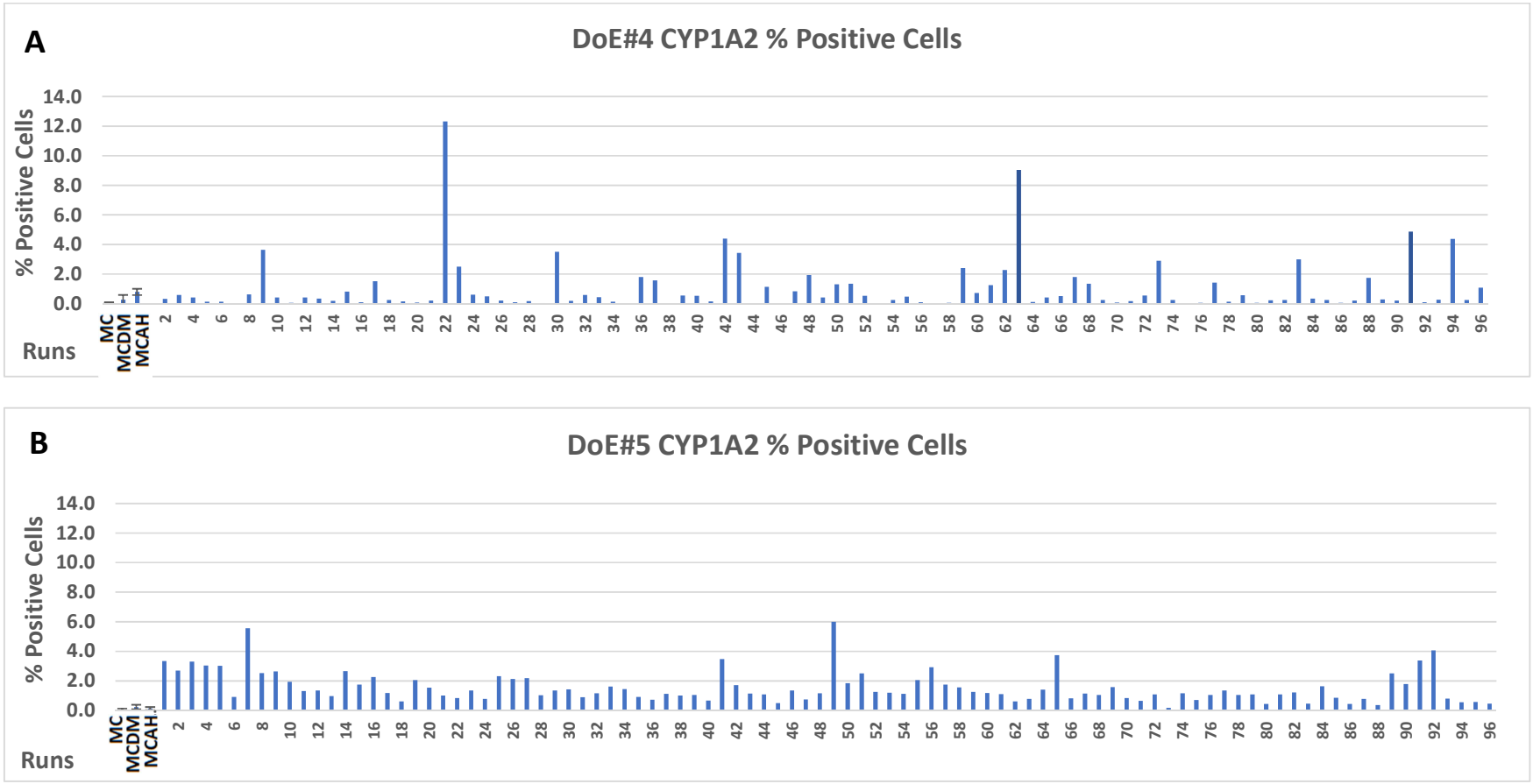

Figure 87 CYP450 1A2 percentage Positive cells in DoE#4 and in DoE#5. Medium C (MedC), Medium C + 0.5% DMSO (MCDM) and Medium C with high concentration of factors (MCAH) controls represent Mean ± Standard Deviation of 4 replicates. Numbers correspond to the Runs detailed in tables 29 and 30.

5.2.19. CYP450 2A6 Expression Was Either Not Improved or Masked by False Positive Signal

In DoE#2, CYP450 2A6 was expressed in between 0% and 1.42% of cells while the MC resulted in 0.37%±0.32 (Figure 88A). The maximum expression identified was at 1.42% of cells and the majority of runs expressed CYP450 2A6 at a similar percentage to the MC control run, DoE#2 CYP450 2A6 results were not analysed further. In DoE#3, CYP450 2A6 was expressed in between 0.01% and 2.10% of cells while the MC resulted in 0.36%±0.29 (Figure 88B). The MCDM expressed CYP450 2A6 at 0.45%±0.24 positive cells, not significantly different than the MC ($p=0.64$) and lower than the best run in DoE#3. The MCAH control resulted in 0.90%±1.44 expression of CYP450 2A6 which wasn't significantly higher than the MC control ($p>0.4$). However, that was equally high to the DoE runs and therefore the likelihood for false positive signal high. The responses were not analysed further.

In DoE#4, CYP450 2A6 was expressed in between 0.27% and 14.70% of cells while the MedC control differentiation resulted in 1.27%±0.33 (Figure 89A). The MCDM control differentiation achieved a 2.57%±1.12 positive cells, not significantly higher than the MC ($p=0.067$) and lower than the best run in DoE#4. The MCAH controls resulted in 3.26%±1.16 expression of CYP450 2A6 which was significantly higher than the MC control ($p=0.016$) but not compared to MCDM control ($p=0.42$). Since the MCAH control achieved a high increase, the chance for false positive signal was high and the results were not taken ahead. Lastly in DoE#5, CYP450 2A6 was expressed in between 0.32% and 8.24% of cells while the MC resulted in 3.93%±0.32 (Figure 89B). The MCDM control differentiation achieved a 5.70%±1.81 positive cells, not significantly different than the MC ($p=0.102$) but similar to the best run in DoE#4. The MCAH controls resulted in 0.33%±0.16 expression of CYP450 2A6 which was significantly lower than the MC and MCDM control ($p<0.001$). Since the best performance runs were not significantly higher to the controls the response was not analysed further.

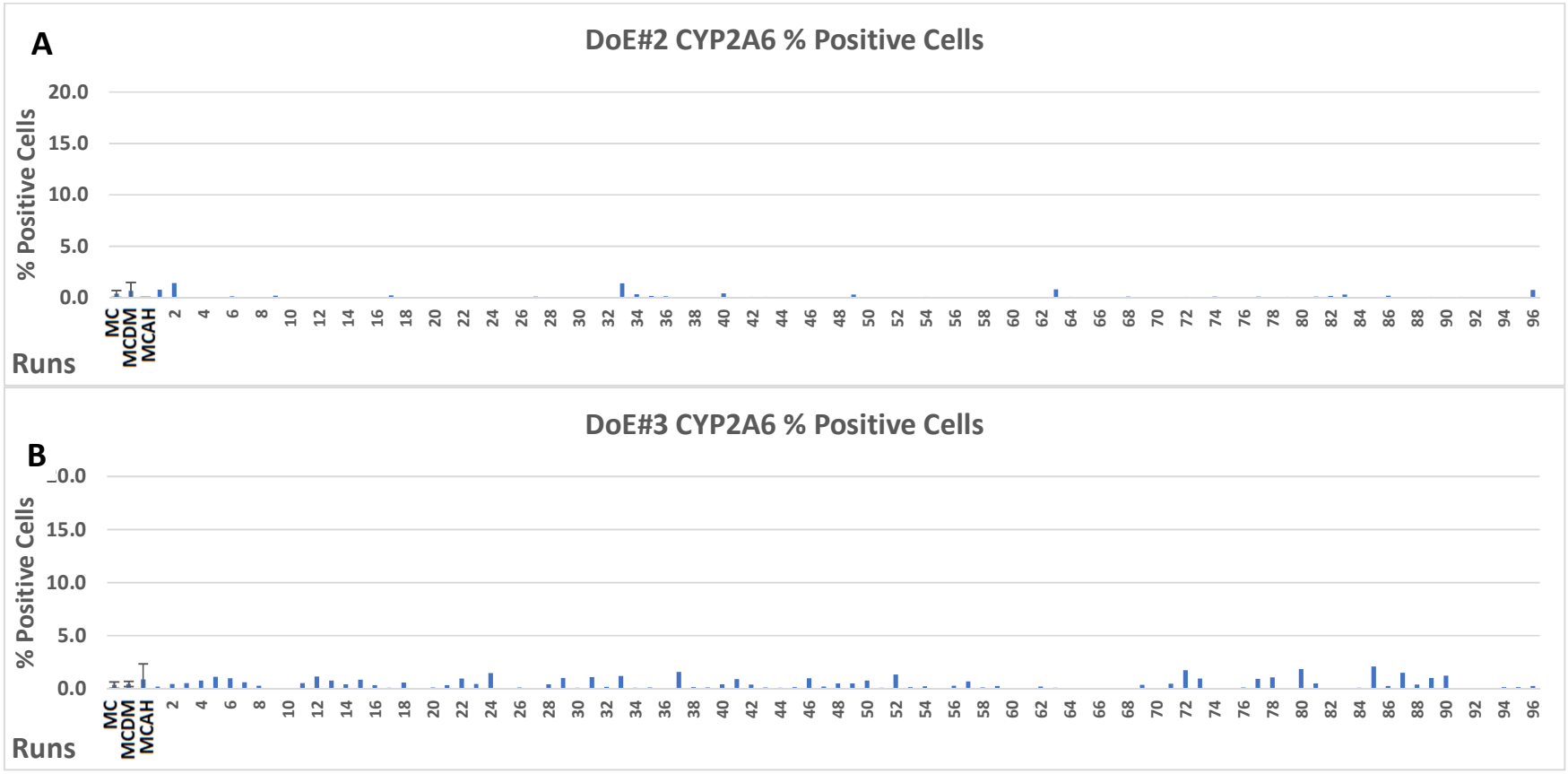

Figure 88 CYP450 2A6 percentage Positive cells in DoE#2 and DoE#3. Medium C (MedC), Medium C + 0.5% DMSO (MCDM) and Medium C with high concentration of factors (MCAH) controls represent Mean ± Standard Deviation of 4 replicates. Numbers correspond to the Runs detailed in tables 27 and 28.

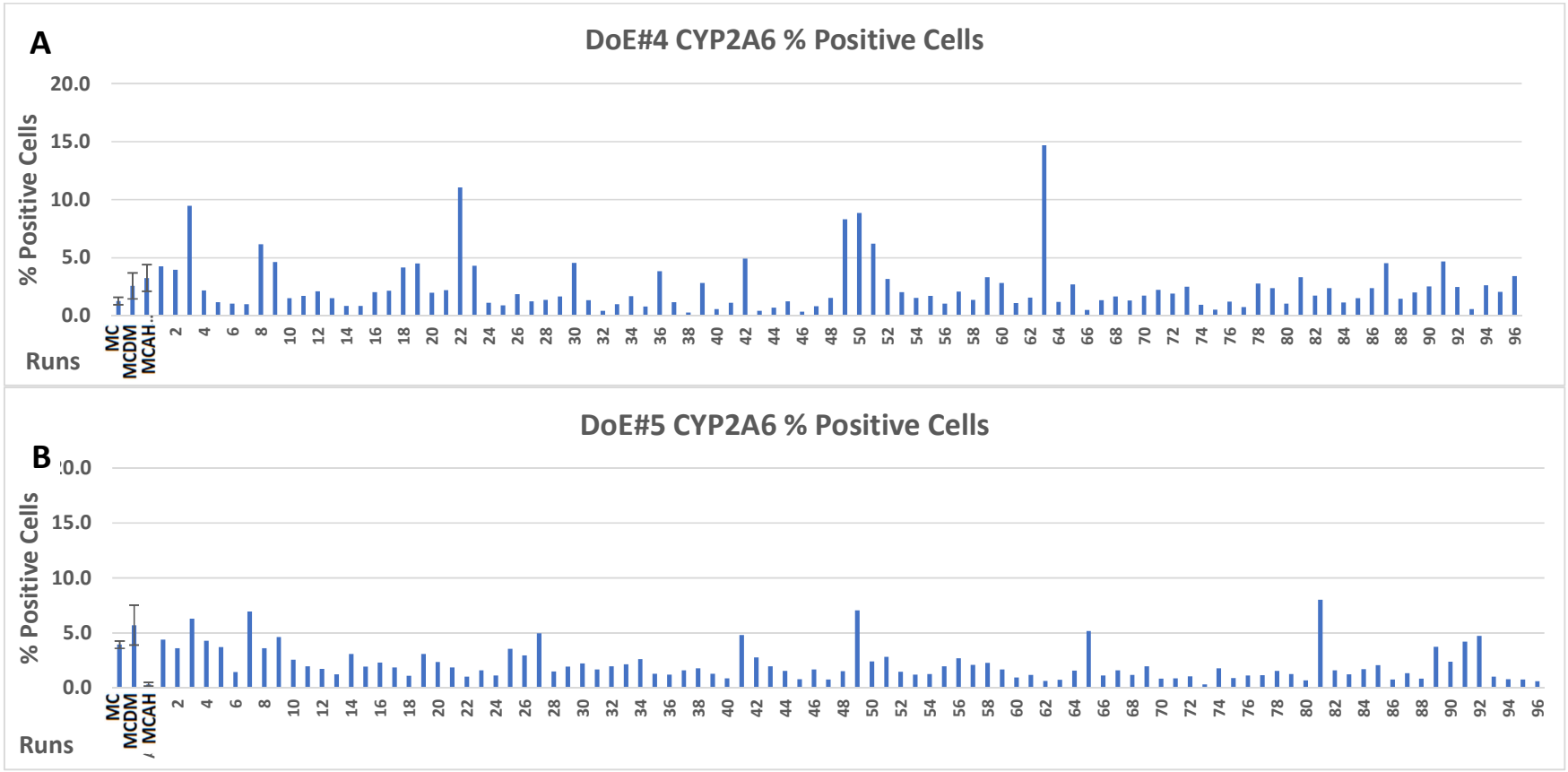

Figure 89 CYP450 2A6 percentage Positive cells in DoE#4 and in DoE#5. Medium C (MedC), Medium C + 0.5% DMSO (MCDM) and Medium C with high concentration of factors (MCAH) controls represent Mean ± Standard Deviation of 4 replicates. Numbers correspond to the Runs detailed in tables 29 and 30.

5.2.20. CYP450 2C9 Responses Were Independent from False Positive or Low Performance Showing Improved percentage of Positive Expression and Mean Intensity compared to the controls

In DoE#2, CYP450 2C9 was expressed in between 0.27% and 11.20% of cells while the MC resulted in 4.16%±0.54 (Figure 90A). The best run in DoE#2 was expressing CYP450 2C9 at higher percentage of cells to the MC control differentiation. The MCDM control differentiation achieved a 5.62%±3.50 positive cells, not significantly different from the MC ($p=0.44$) but at the same range as the DoE#2 runs. Since expression of CYP450 2C9 in the DoE#2 was not greater to the controls, these results were not analysed further. In DoE#3, CYP450 2C9 was expressed in between 0.14% and 9.05% of cells while the MC resulted in 2.99%±0.62 (Figure 90B). The MCDM control differentiation achieved a 3.86%±3.50 positive cells, not significantly different from the MC ($p=0.64$) but at the same range to the DoE#3 runs. The MCAH resulted in 0.15%±0.28 expression of CYP450 2C9 which was significantly lower than the MC ($p<0.0002$). Since expression of CYP450 2C9 was not greater than the controls, the results were not analysed further.

In DoE#4, CYP450 2C9 was expressed in between 0.40% and 18.13% of cells while the Medium C control differentiation resulted in 9.34%±1.83 (Figure 91A). The best run in DoE#3 was expressing CYP450 2C9 at higher percentage of cells to the MC control differentiation. The MCDM control differentiation achieved 8.14%±0.89 of positive cells, not significantly different from the MC ($p=0.28$) and also at a lower range to the DoE#2 runs. The MCAH resulted in 0.22%±0.12 expression of CYP450 2C9 which was significantly lower than the MC and MCDM ($p<0.0001$). This result meant that the positive signal detected in the DoE runs was due to real CYP450 2C9 expression. Additionally, Mean Intensities (MI) were plotted (Figure 91B) to identify any effects in particular treatments that increase the MI. However, the FI were overlapping between the samples failing to indicate towards a particular treatment.

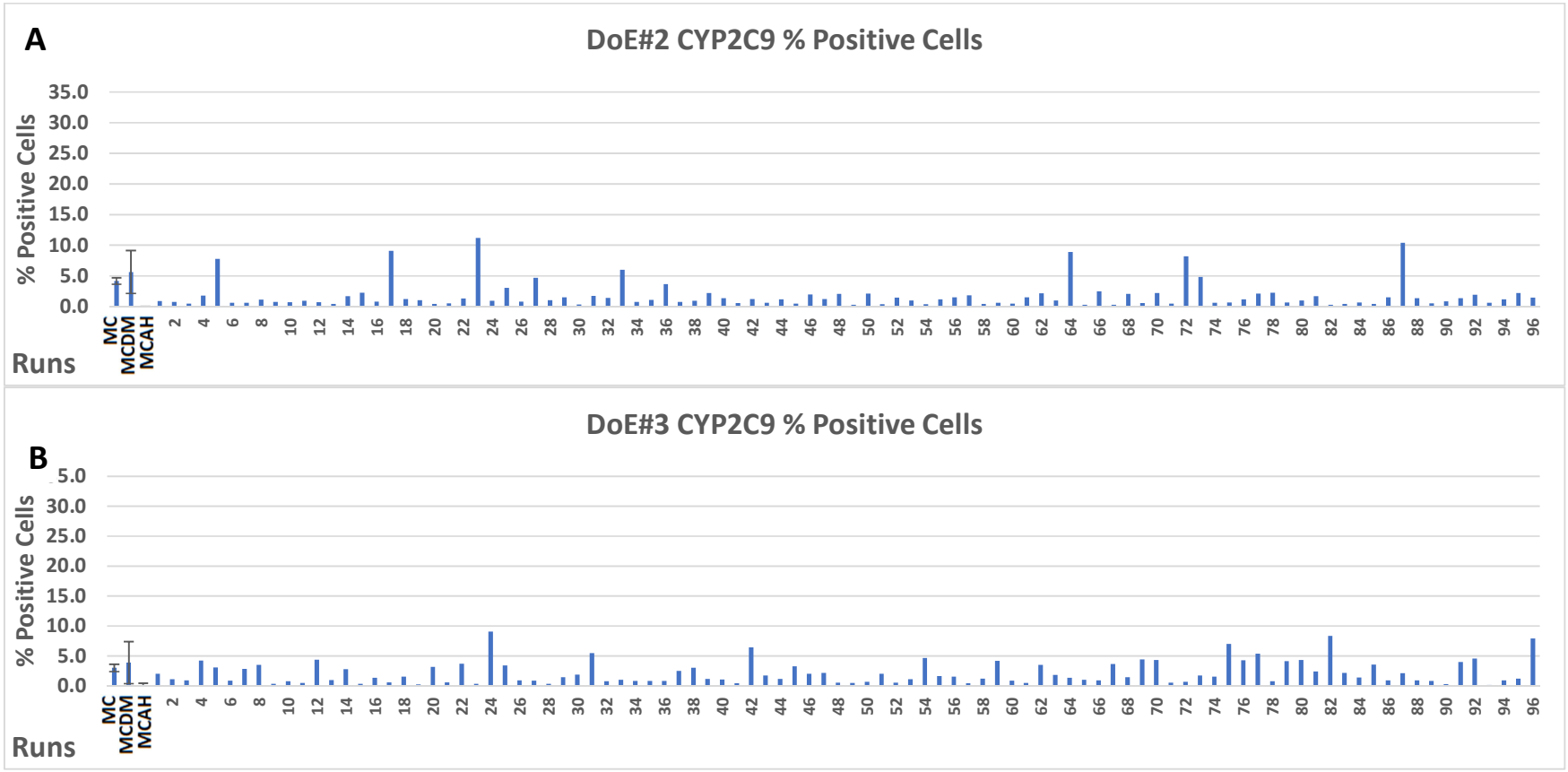

Figure 90 CYP450 2C9 percentage Positive cells in DoE#2 and DoE#3. Medium C (MedC), Medium C + 0.5% DMSO (MCDM) and Medium C with high concentration of factors (MCAH) controls represent Mean ± Standard Deviation of 4 replicates. Numbers correspond to the Runs detailed in tables 27 and 28.

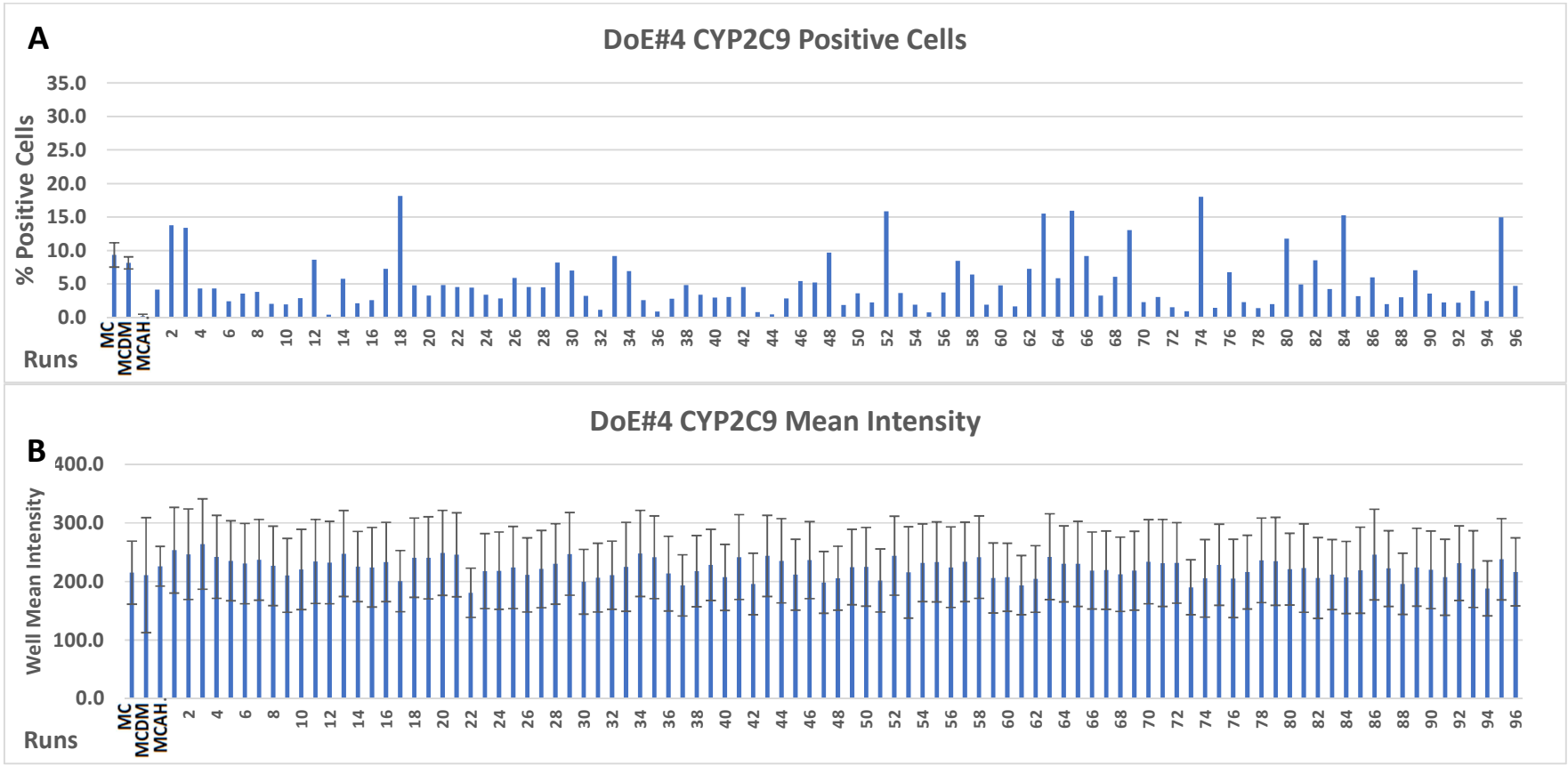

Figure 91 CYP450 2C9 percentage Positive cells and Mean Intensity in DoE#4. Medium C (MedC), Medium C + 0.5% DMSO (MCDM) and Medium C with high concentration of factors (MCAH) controls represent Mean ± Standard Deviation of 4 replicates. Numbers correspond to the Runs detailed in table 29.

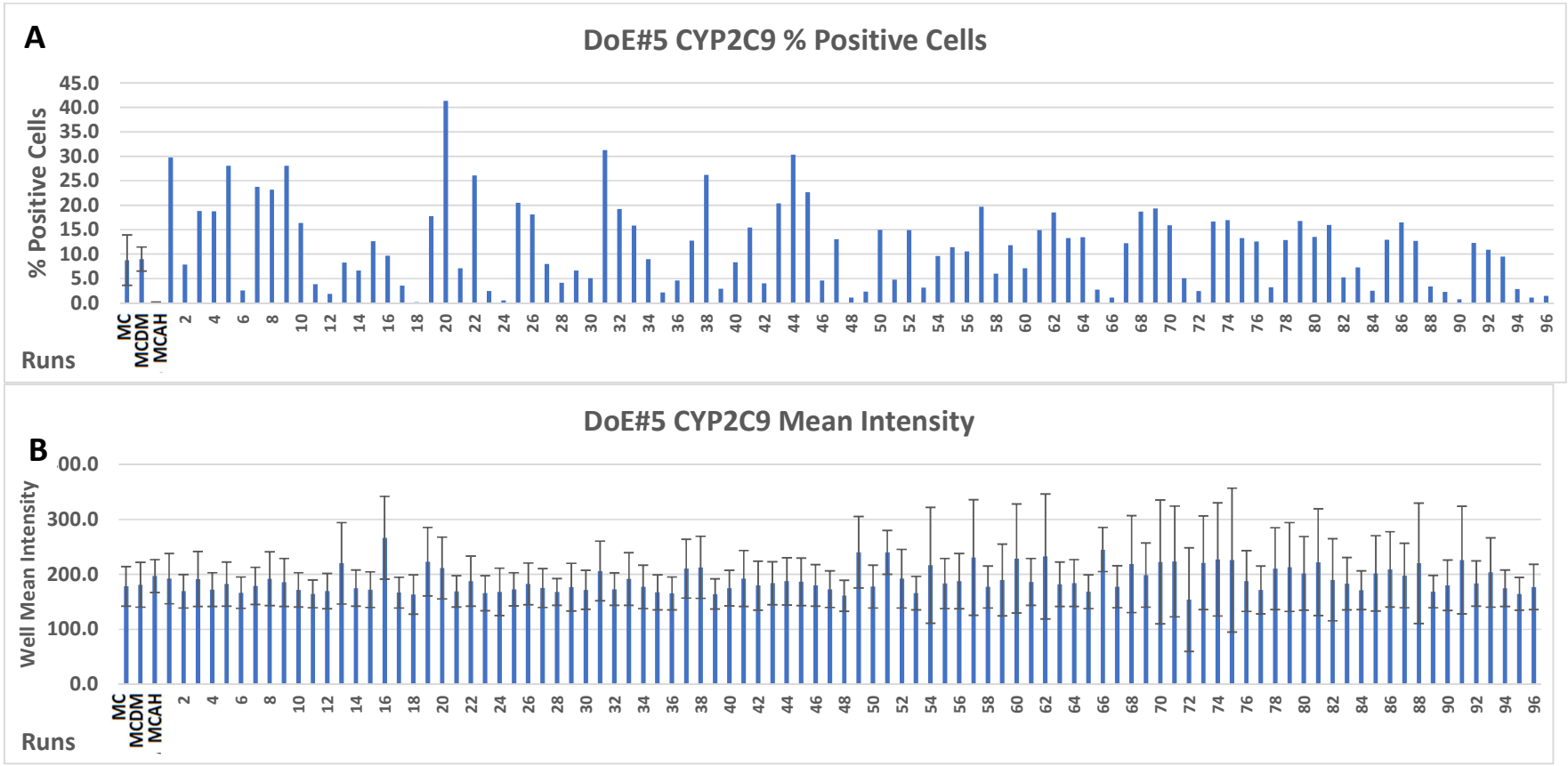

Figure 92 CYP450 2C9 percentage Positive cells and Mean Intensity in DoE#5. Medium C (MedC), Medium C + 0.5% DMSO (MCDM) and Medium C with high concentration of factors (MCAH) controls represent Mean ± Standard Deviation of 4 replicates. Numbers correspond to the Runs detailed in table 30.

In DoE#5, CYP450 2C9 was expressed in between 0.14% and 41.32% of cells while the MC control differentiation resulted in 8.76%±5.13 (Figure 92A) and MCDM achieved 8.99%±2.47 of positive cells, not significantly different from the MC ($p=0.93$). The MCAH resulted in 0.07%±0.09 expression of CYP450 2C9 which was significantly lower than the MC and MCDM ($p<0.02$). These results were indicated for further analysis. To evaluate whether any of the treatments achieved an increased MI, the MI graph was produced however, it was identified that MI were overlapping with no treatments that could induce significantly higher responses (Figure 92B). In conclusion, the CYP450 2C9-related DoE responses succeed to produce runs with a higher proportion of positive cells compared to the MC control differentiations while the MCAH controls were significantly lower than the controls. Overall, the response "CYP450 2C9 percentage Positive Cells" for DoE#4 and DoE#5 continued at the next step of the analysis.

To confirm that the data collected using the analysis script for the expression of CYP450 2C9 was in correlation with the image of the well, image of the whole well are presented in Figures 93 and 94 from the best performing runs in DoE#4 and DoE#5 respectively.

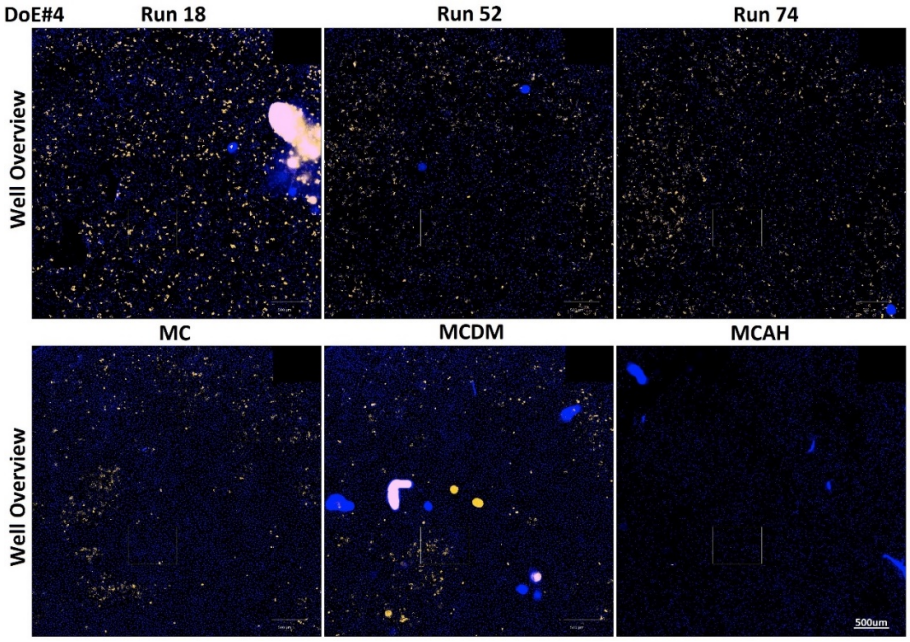

Figure 93 Well overview of selected best Runs in DoE#5 at the top panel and the respective MC, MCDM and MCAH controls at the lower panel. Scale bar 500um

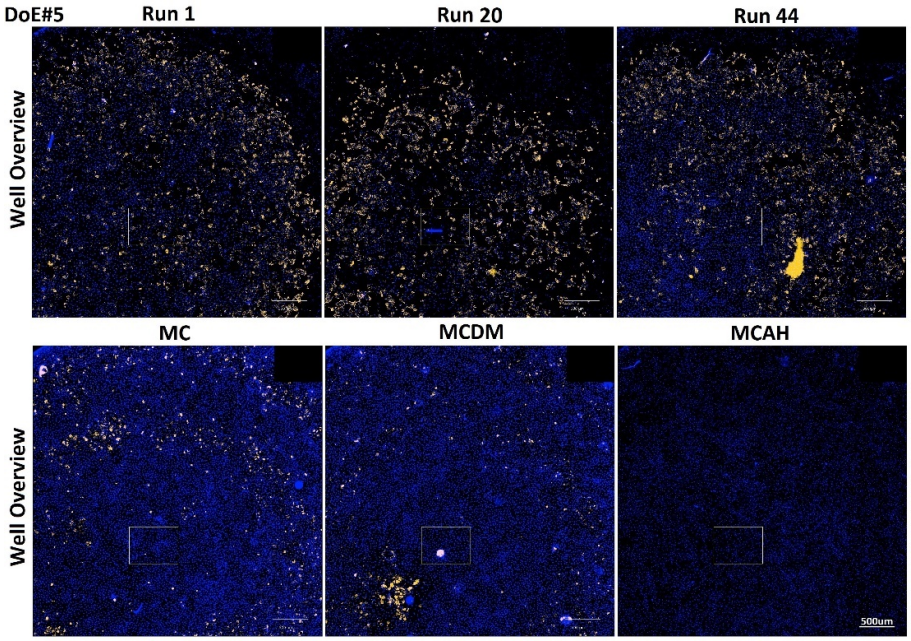

Figure 94 Well overview of selected best Runs in DoE#5 at the top panel and the respective MC, MCDM and MCAH controls at the lower panel. Scale bar 500um.

5.2.21. Analysis for CYP450 2C9 percentage Positive and Mean Intensity Responses Highlighted a High Positive Correlation Between percentage Positive Cells and Mean Intensity, Confirming That the Data Could Be Used to Identify Significant Factors

In order to validate the data collected for the CYP450 2C9 responses from DoE#4 and DoE#5, the DX software was used to draw correlation plots between percentage Positive Cells and Means Intensity. Those plots were based on the hypothesis that an increased percentage Positive Cell value lead to an increased average Mean Intensity. These plots could also be used to highlight and isolate individual runs, outliers, when the results produced are not in correlation with the rest.

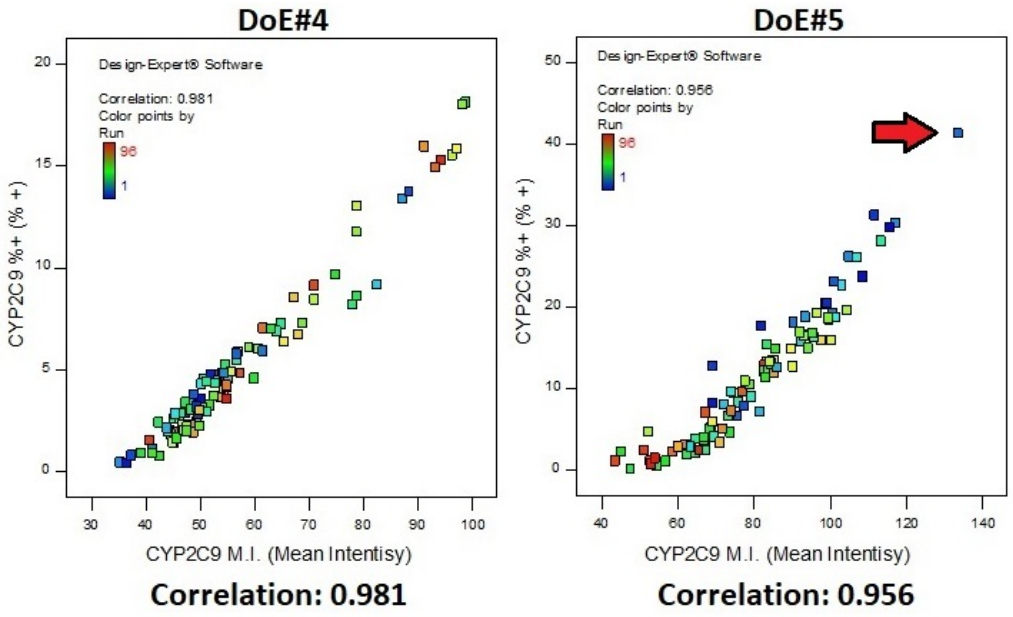

Figure 95 Correlation plots designed using the DX software to demonstrate the Correlation between CYP450 2C9 percentage Positive Cells and Mean Intensity for DoE#3, DoE#4 and DoE#5. Y Axis is the percentage Positive Cells while X axis is the Mean Intensity. Red arrow in DoE#5 highlights a response that potentially could be an outlier and required further investigation.

For DoE#4 a high correlation value of 0.981 was identified and for DoE#5 that value was identified as 0.956 (Figure 95). However, in DoE#5 the value at the top right corner (highlighted with an arrow in Figure 95) was isolated from the group of responses, thus it could potentially be an outlier. To evaluate whether this response was an outlier, the well had to be examined and determine if the higher expression was due to an error or if the expression of CYP450 2C9 was real. Using the software, it was identified as Run 20. In Figure 94, Run 20 was presented as an example of best performing runs. Expression of CYP450 2C9 was characterised as expected in the cytoplasm with absence of unusual events that could affect the analysis. Therefore, this value was included for further analysis. In conclusion, high correlation values in both DoE#4 and DoE#5 confirmed that the data could be used to make conclusions for the significant factors inducing expression of CYP450 2C9.

5.2.22. Identification of Significant Factors and Interactions Improving CYP450 2C9 percentage Positive Cells in DoE#4 and DoE#5

To investigate which factors in DoE's were having significant positive effects, the generated data was analysed using the DX software to generate models of the significant factors (NIST/SEMATECH, 2012). In DoE#1, the need for transformation of the data was explained. Similar to DoE#1, in DoE#5, the CYP450 2C9 percentage Positive Cells were analysed, initially hypothesising that transformation was not required (Figure 96A). At the next step, the Fit Summary data that was calculated by the DX software, it was suggested that a "Linear Model" can fit to the data (p=0.0902) better compared to other Model types, with an insignificant "Lack of Fit" p=0.913 (Figure 96A). Therefore, the Linear process order was selected and the "Automatic Model Selection" tool applied a forward selection using the Akaike Information Corrected Criterion (AICc) (for a given set of data it measures the relative quality of statistical models) (Figure 96B). The AICc selection identified which of the main factors, initially added in the Model, had a significant p-value to remain within the Model and highlighted them with an **M** (Figure 96C). At the ANOVA tab, evaluation of the Model generated based on the Response Surface Reduced Linear Model, suggested that it was significant with a p-value <0.0001 and the factors B-SR12813 and H-TCA were significantly influencing the Model with p-values <0.05 and an insignificant "Lack of Fit" p=0.92 confirming that the model fits to the data (Figure 97).

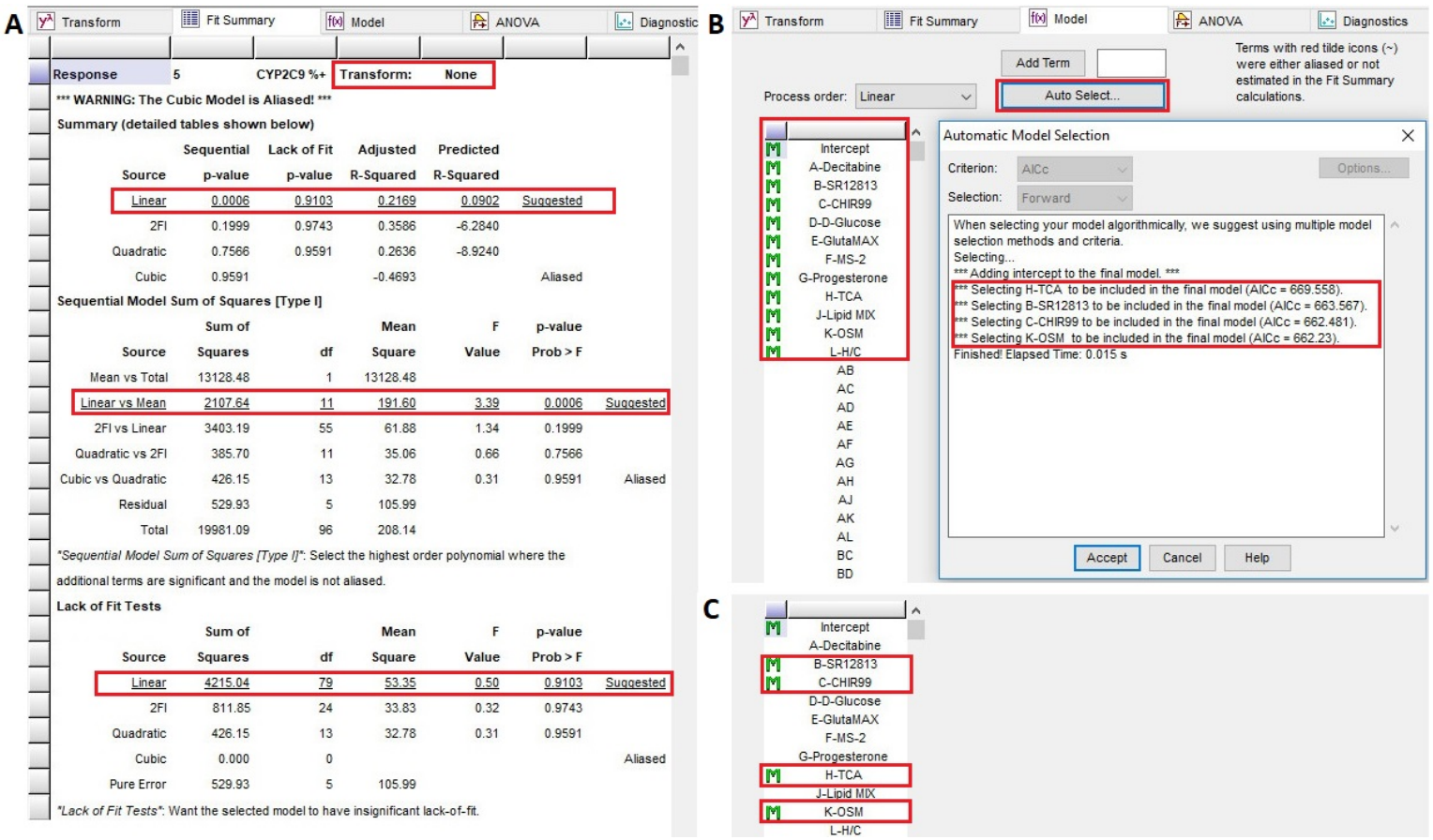

Figure 96 Analysis of the DoE#5 percentage CYP450 2C9 Positive cell data. Fit Summary and Model selection tabs are presented upon no transformation. A) Fit Summary suggested the Linear Model to be applied, additionally the Sum of Squares analysis suggested the Linear vs Mean was significant and an overal incignificant Lack of Fit for the Linear Model. B) Linear Model selected the main factors in the Model and Automatic Model Selection included the most significant factors (C) to keep in the Model.

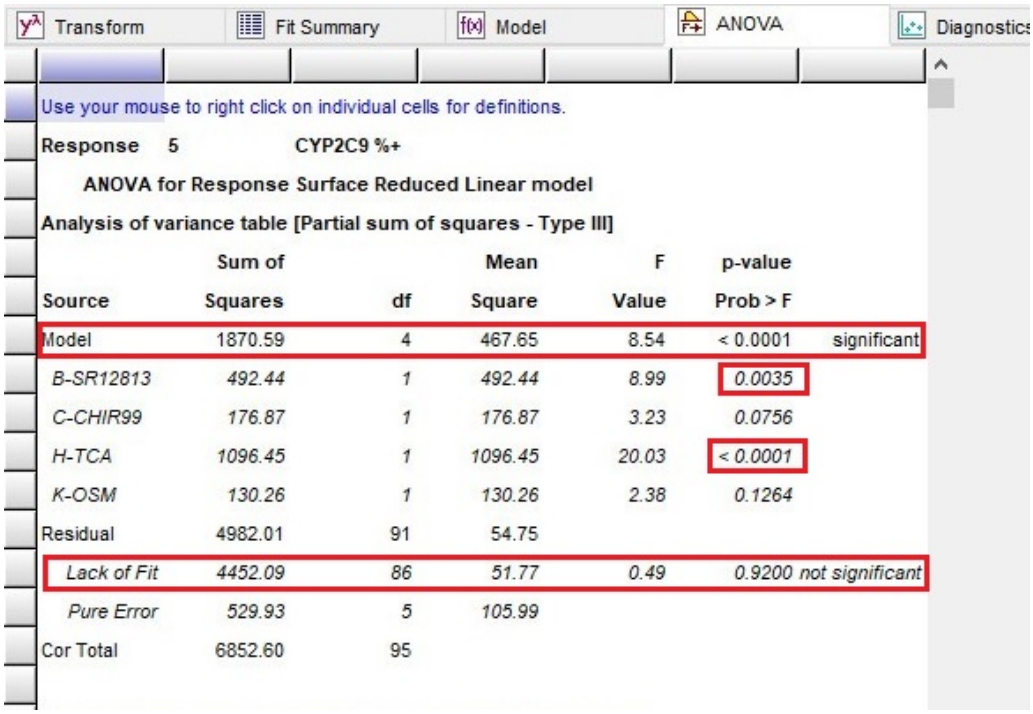

Figure 97 ANOVA analysis results upon no transformation and Linear Relationship Model selection using the DoE#5 percentage CYP450 2C9 Positive cell data. Model was identified as significant with an insignificant "Lack of Fit". Factors affecting the Model were identified with a significant p-value.

Using the Diagnostics tools and the Box-Cox plot, it was identified that a λ=0.5 (Square Root transformation) would fit the Ln(Residuals) better than the current λ=1 (No transformation) (Figure 98A). The Diagnostic plots demonstrated a spread of the data within the allowed design space although, since a transformation was required, a better fit for the data was available (Figure 98A).

Upon selection of the suggested Square Root transformation, the Fit Summary results suggested that the Linear Model was significant, against other available models, with a p-value=0.0496, a significant Linear vs Mean and an insignificant "Lack of Fit" p=0.9021 (Figure 99A). The selected Linear process order automatically identified the factors that had a significant p-value to remain within the Model and highlighted with an **M** (Figure 99B-C). The ANOVA analysis identified that the Model was significant with a p-value <0.0001 and factors B-SR12813 and H-TCA remained significant with p-values <0.05 and an insignificant "Lack of Fit" p=0.919 (Figure 100).

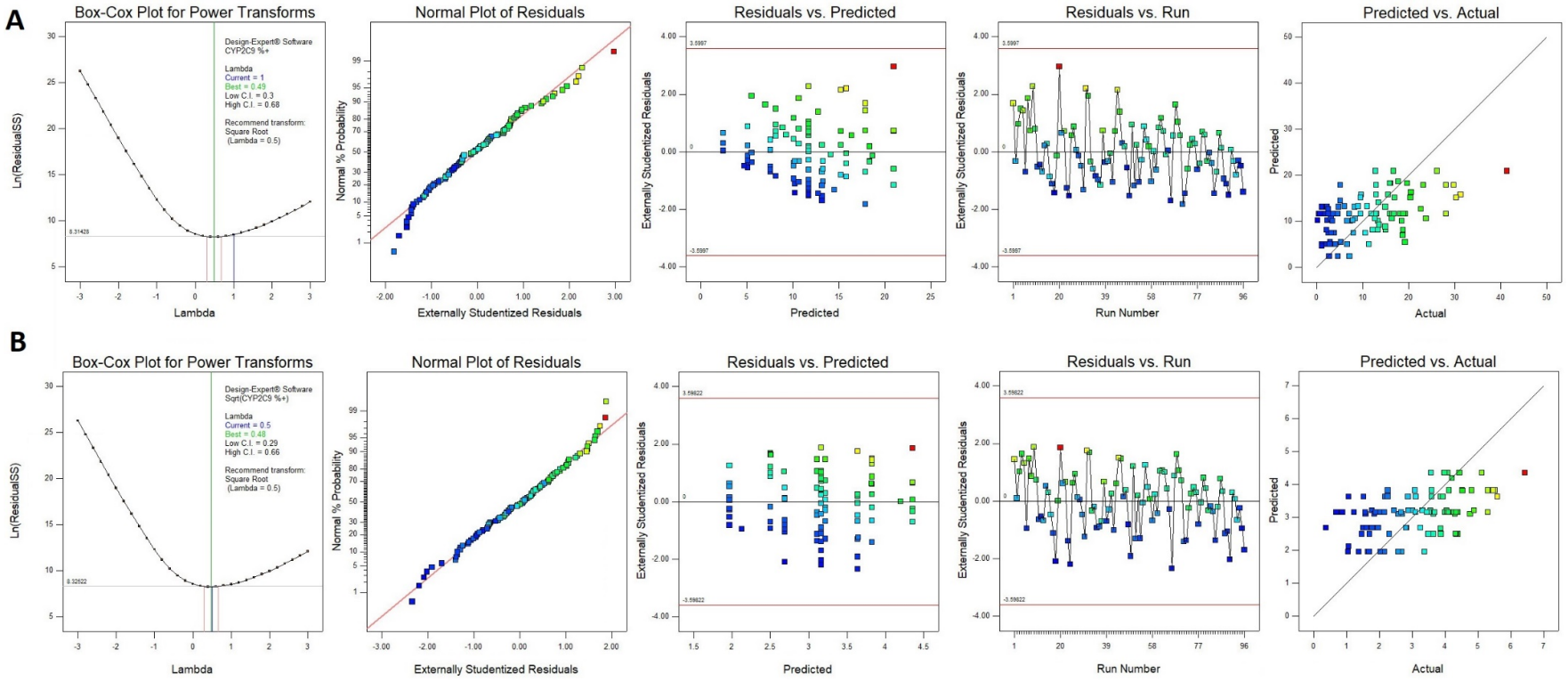

Figure 98 Diagnostic tool overview for percentage CYP450 2C9 Positive cells in DoE#5 analysed with no transformation of the data (A) and upon Square Root transformation of the data (B). Box-Cox plot reccomending a transformation to fit the data, Normal Plot of residuals, Residuals vs Predicted, Residuals vs Run, Predicted vs Actual, details in text

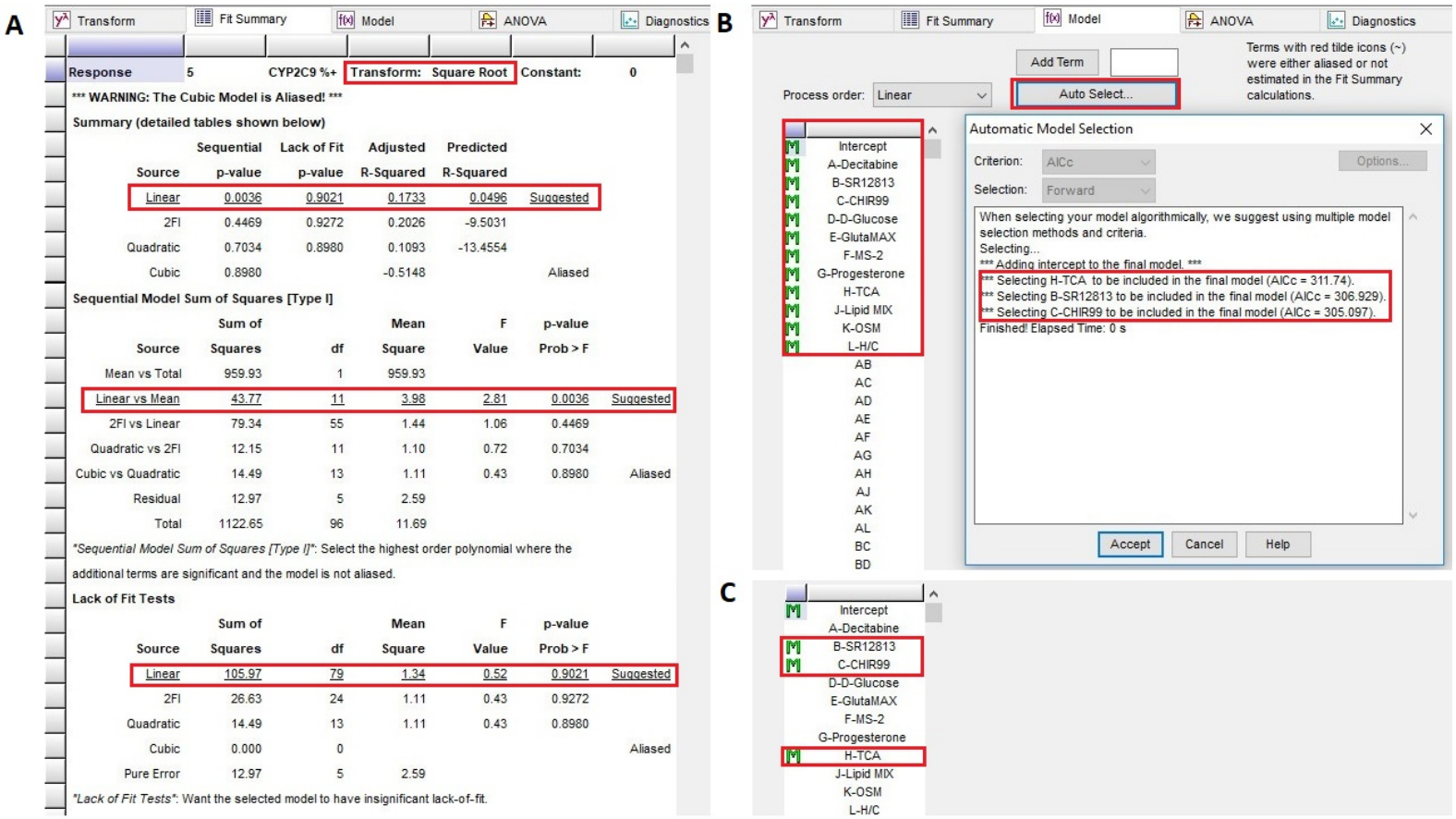

Figure 99 Analysis of the DoE#5 percentage CYP450 2C9 Positive cell data. Fit Summary and Model selection tabs are presented upon Square Root transformation. A) Fit Summary suggested the Linear Model to be applied, additionally the Sum of Squares analysis suggested the Linear vs Mean was significant and an overal incignificant Lack of Fit for the Linear Model. B) Linear Model selected the main factors in the Model and Automatic Model Selection included the most significant factors (C) to keep in the Model.

Transform | Fit Summary | Model | ANOVA | Diagnostics

Use your mouse to right click on individual cells for definitions.

Response 5 CYP2C9 %+

Transform: Square Root Constant: 0

ANOVA for Response Surface Reduced Linear model

Analysis of variance table [Partial sum of squares - Type III]

Source	Sum of Squares	df	Mean Square	F Value	p-value Prob > F	
Model	39.17	3	13.06	9.72	< 0.0001	significant
B-SR12813	*9.66*	*1*	*9.66*	*7.19*	*0.0087*	
C-CHIR99	*5.27*	*1*	*5.27*	*3.93*	*0.0506*	
H-TCA	*24.24*	*1*	*24.24*	*18.05*	*< 0.0001*	
Residual	123.55	92	1.34			
Lack of Fit	*110.58*	*87*	*1.27*	*0.49*	*0.9194*	*not significant*
Pure Error	*12.97*	*5*	*2.59*			
Cor Total	162.72	95				

Figure 100 ANOVA analysis results upon Square Root transformation and Linear Relationship Model selection using the DoE#5 percentage CYP450 2C9 Positive cell data. Model was identified as significant with an insignificant "Lack of Fit". Factors affecting the Model were identified with a significant p-value.

The Diagnostic tools confirmed that the Square Root transformation was still the best fit for the data and that the Ln(Residual) plots were improved with a better spread of the data and random scatter (Figure 98B).

As identified at the ANOVA table, following the Square Root transformation, the factors SR12813 and TCA were significantly involved in achieving a greater degree of percentage CYP450 2C9 expression cells, CHIR99 approached significance (Figure 100). To visualise the relationship among the factors, the Perturbation Plots and 3D surface-graph were used. Using the gauges in the Factors Tool-Box, the concentration was altered to achieve the highest possible percentage CYP450 2C9 Positive cell expression (Figure 101A). The Model generated, could predict that a high concentration of TCA and CHIR99 in combination with a low concentration of SB12813 could achieve an approximately 20% CYP450 2C9 expression (Figure 101B). Even though the original data derived from DoE#5 succeed a high expression of CYP450 2C9, the DX software analysing the data and fitting the Model, could only safely predict an approximate 20% CYP450 2C9 upon use of the significant factors.

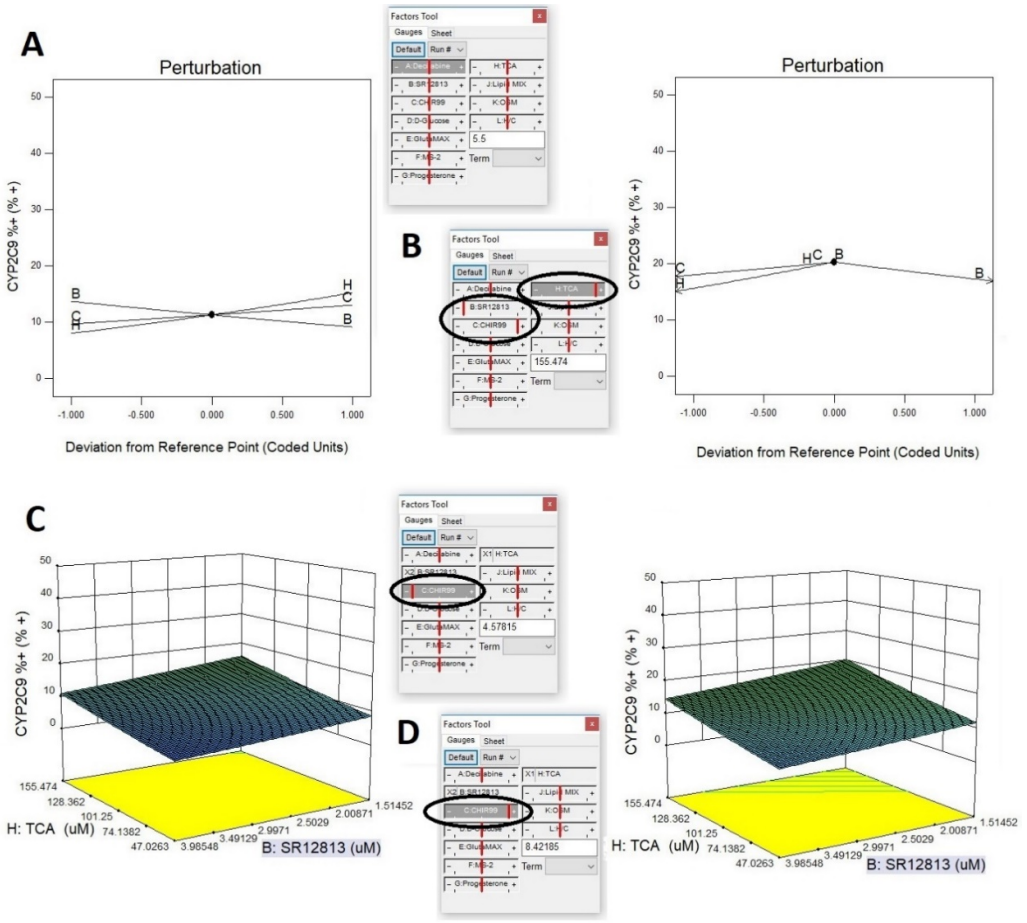

Figure 101 Perturbation Plots and 3D Surface graph designed using percentage CYP450 2C9 Positive Cell data from DoE#5 runs. A) Perturbation Plot at the centre concentration for each factor, significant factors are shown in the plot B) Changed significant factor concentration to achieve the highest percentage CYP450 2C9. C) 3D graph demonstrating the linear relationship between the factors and the effect when low CHIR99 was used compared to D) when high CHIR99 was used.

Using the 3D Surface graphs, it was predicted that the factor CHIR99, at the lowest concentration could achieve a 17% CYP450 2C9 Positive expression (Figure 101C) while the high concentration could achieve a maximum of 20% CYP450 2C9 expression (Figure 101D). Overall, the DoE#5 results demonstrated that the factors SR12813 at 1.5uM, TCA at 155uM and CHIR99 at 8.5uM had a significant effect on the percentage CYP450 2C9 Positive cells.

In DoE#4, the analysis initiated without a transformation on the data and following the principles from DoE#5, the Box-Co Plots suggested that a Natural Log transformation would be a better fit for the Ln(Residuals). The transformation was applied and the Linear Model was selected as the most significant to fit the data. The ANOVA results upon analysis of the

Model, suggested that the Model was significant with a p-value<0.0001 and an insignificant "Lack of Fit" with a p-value=0.3368 (Figure 102). The factors identified as significant in DoE were A-ATRA and J-Ascorbic Acid with p-value<0.0008 (Figure 102).

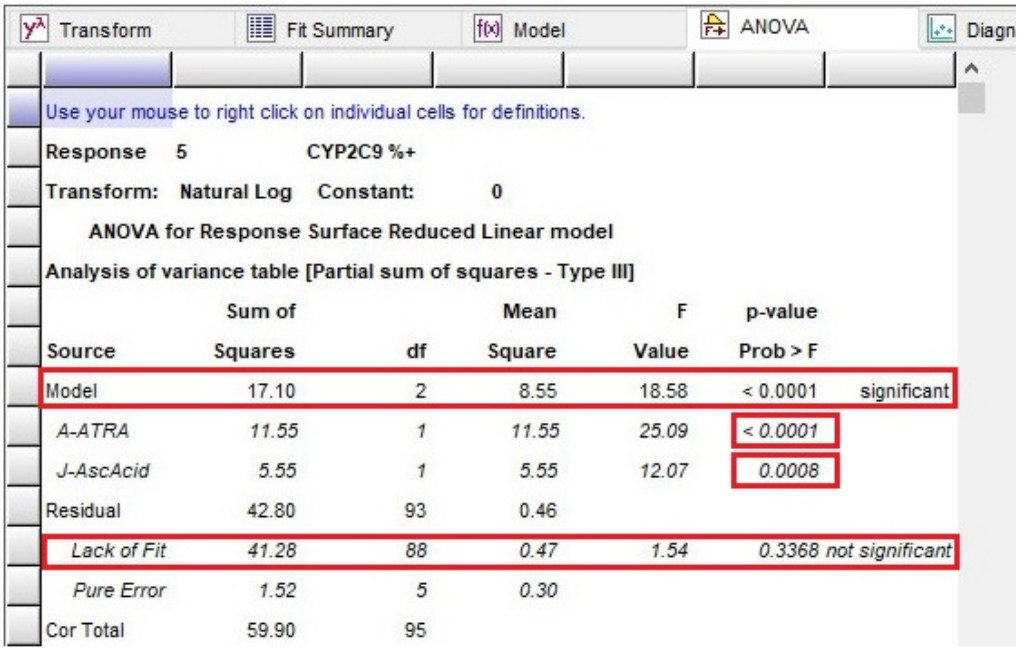

Transform | Fit Summary | Model | ANOVA | Diagn

Use your mouse to right click on individual cells for definitions.

Response 5 CYP2C9 %+

Transform: Natural Log Constant: 0

ANOVA for Response Surface Reduced Linear model

Analysis of variance table [Partial sum of squares - Type III]

Source	Sum of Squares	df	Mean Square	F Value	p-value Prob > F	
Model	17.10	2	8.55	18.58	< 0.0001	significant
A-ATRA	*11.55*	*1*	*11.55*	*25.09*	*< 0.0001*	
J-AscAcid	*5.55*	*1*	*5.55*	*12.07*	*0.0008*	
Residual	42.80	93	0.46			
Lack of Fit	*41.28*	*88*	*0.47*	*1.54*	*0.3368*	*not significant*
Pure Error	*1.52*	*5*	*0.30*			
Cor Total	59.90	95				

Figure 102 ANOVA analysis results upon Natural Log transformation and Linear Relationship Model selection using the DoE#4 percentage CYP450 2C9 Positive cell data. Model was identified as significant with an insignificant "Lack of Fit". Factors affecting the Model were identified with a significant p-value.

Using the Perturbation Plots, it was demonstrated that at the default medium concentration of A-ATRA and J-AscAcid, a 5% CYP450 2C9 Positive cells were achieved (Figure 103A). Although, when low concentration of A-ATRA and high concentration of J-AscAcid were combined, a final 9% CYP450 2C9 Positive cells was generated (Figure 103B). In addition, the 3D Surface demonstrated the linear relationship between those 2 factors and confirmed the percentage reported from the Perturbation Plots (Figure 103C). Similar to DoE#5, the DX software could safely explain a maximum of 9%.

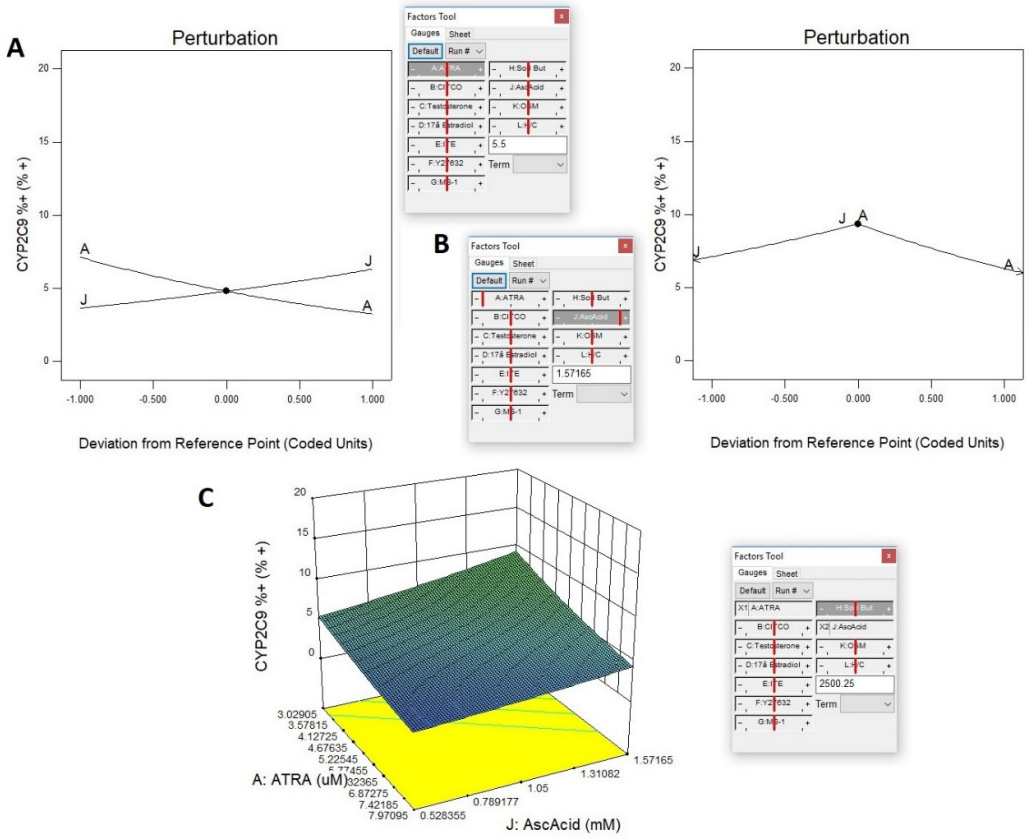

Figure 103 Perturbation Plots and 3D Surface graph designed using percentage CYP450 2C9 Positive Cell data from DoE#4 runs. A) Perturbation Plot at the centre concentration for each factor, significant factors are shown in the plot B) Change significant factor concentration to achieve the highest percentage CYP450 2C9. C) 3D graph demonstrating the linear relationship between ATRA and AscAcid.

Overall, in DoE#4 it was demonstrated that the factors ATRA at 3uM and AscAcid at 1.5mM were important to achieve a significantly greater expression of percentage CYP450 2C9 Positive cells while in DoE#5 the factors SR12813 at 1.5uM, TCA at 155uM and CHIR99 at 8.5uM had a significant effect on the percentage CYP450 2C9 Positive cells.

5.3. Discussion

Summary

The objective of this chapter was to combine and treat differentiating HLCs with factors at a range of effective concentrations aiming to identify and uncover a) combinations of factors and b) critical factors that can improve the overall performance of the cells. The overall performance of cells is measured as expression of a) a set of mature markers, b) the multinucleation or c) the morphology of the differentiating HLCs. Overall, the 1st DoE screen indicated a number of factors as critical with significant influence that have been incorporated in the design of the 2nd DoE for further investigation. Finally, from the 2nd DoE, the factors ATRA, AscAcid, SR12813, TCA and CHIR99 demonstrated significant maturation differences to the HLCs. However, their full potential requires resolving through a more specific future DoE approach.

Study and DoE Design

The current chapter aimed to investigate factors identified from the literature to enhance the maturation of hepatocyte-like cells using DoE approach. It has been said that the coupling of DoE with modern high-throughput automation systems could potentially maximise the capabilities for producing data relevant for drug discovery applications (Tye, 2004). DoE approaches have been used, although not widely, to overcome expensive and low-throughput OFAT designs (N Politis et al., 2017). The majority of DoE studies have been completed in the industry (pharmaceutical & engineering) but not many in academia (Pramod et al., 2016), primarily due to the high cost involved in high-throughput development (Collins et al., 2009). To our knowledge, the scale of the screening approach used in this thesis is unique in the field.

DMSO Considerations and Limitations

Ideally, all factors identified in this thesis would have been screened in a single DoE experi-

ment. However, a key limitation was the DMSO concentration. Populations of hESCs are very responsive to DMSO which can change gene expression, protein content and functionality of differentiated cells (Pal et al., 2012) and induce differentiation in multiple systems (Morley and Whitfield, 1993). For example during the differentiation of Definitive Endoderm cells to Hepatoblasts, DMSO is used in multiple labs as main differentiation inducer (Duan et al., 2010, Chen et al., 2012b) although the underlying mechanism is unknown (Duan et al., 2010). Additionally, DMSO has been reported to induce differentiation of HUES6 cells into DE cells when used at 2% (Chetty et al., 2013). The maximum concentration of 0.5% in this thesis was set due to reports of impaired cell survival above 1% and critical changes and cell death above 5% (Yuan et al., 2014) and of induction of inhibitory or stimulatory effects in a range of cell types at greater than 0.5% (Timm et al., 2013). Lack of discernible alterations in the proteins of interest and hepatocyte morphology in the DMSO only control used in the current work was consistent with the appropriate use of the 0.5% concentration.

Indirect Versus Direct Immunofluorescence

The advantages of the output methods have been discussed before however, the challenges of staining the cells in a direct or indirect way haven't. The advantage of the protocol developed with separate primary and secondary antibodies was based on reported stronger detection of signal compared to direct staining (Lamvik et al., 2001). However, in the current study, this led to the detection of a false positive signal. The demand for a control condition where the cells were treated with the highest of the concentration of all compounds together, became apparent at the end of the first DoE. Expression of CYP450 2A6 in the DoE#1, was masked due to binding of the secondary antibody on recognition sites of Verteporfin generating the impression of a positive signal. In the literature, Verteporfin has been used to limit YAP1 interaction with TEAD2 and YAP1 has been detected, however a false positive signal was not reported before in a similar case.

Generally, the addition of secondary antibodies that can bind to mouse/rabbit epitopes means that they are selective, but the presence of unknown factors/drugs and chemicals in the same wells could lead to recognition of a pattern leading to interferences in immunoassays as reported in studies (Tate and Ward, 2004). That could have been avoided by the use of primary antibodies directly conjugated to the fluorophore, which would also decrease the number of steps required (Pástor, 2010).

Therefore, when the second set of DoE's was designed, the appropriate secondary only control where the cells are treated with a combined high concentration of all the compounds was included. This was useful because as seen in Chapter 5, a compound, or a combination of them, in Group 3 led to a 3.3% of positive cells in the secondary control differentiation. Future studies based on the same triple-staining protocol should consider developing a robust direct immunostaining approach that will eliminate detection of the unspecific signal from the samples.

Robotics & Automation

Use of the Freedom Evo 200 automated platform enabled and automated parts of the process that manually would require a large number of high accuracy pipetting actions to generate the factor dilutions. Manual preparation would have an increased risk or human error, pipetting error and time required for the same process (Kami et al., 2013). Previously, liquid handling robots have been used for quantitative-pcr assays, gene sequencing and protein crystallisation (Kong et al., 2012, Gaisford, 2012). However, the complexity of the system used in this thesis offered the unique flexibility to accommodate processes of cell maintenance, differentiation and production of the worklists for complex DoE studies.

Factors Identified to Increase CYP450 2C9 Expression

In this study, it was identified that ATRA, SR12813, TCA and CHIR99 do play a role inducing expression of CYP450 2C9 in day 17 HLCs. All Trans Retinoic Acid (ATRA) is described as a

powerful regulator of gene transcription primarily for lipid homeostasis, binding and activating the nuclear RARα receptors that crosstalk with PXR and FXR (He et al., 2013). ATRA is metabolised by certain CYP450s in the liver (Ross and Zolfaghari, 2011, McSorley and Daly, 2000). These include CYP450 2C9 and members of the CYP450 2C family (Nadin and Murray, 1999, Qian et al., 2010), which contain a RA response element in the promoter that is bound by RAR and RXR establishing a transcriptional activity between ATRA and CYP450 2C9. A recent study reported the use of RA in the differentiation of Wharton's Jelly mesenchymal stem cells to HLC, although the medium used was the same for 28 days straight resembling maturation medium and the study only reported functional assays for ALB production, PAS staining, glycogen analysis, q-pcr data for HNF1a and AFP but not staining of mature markers or other CYP450 enzymes (Mortezaee et al., 2015). Overall, ATRA is not commonly used on the hepatocyte maturation stage, however indications for a positive role in CYP450 2C9 were identified.

SR12813 is a synthetic, well characterised PXR agonist (Delfosse et al., 2015) used as a reference compound for PXR activation (Watkins et al., 2001). In this study SR12813 achieved an increased CYP450 2C9 expression in the day 17 HLC. Even though the connection between PXR and CYP450 2C9 activation is known (Pascussi et al., 2003, Kohalmy et al., 2007) a direct link between SR12813 and CYP450 2C9 has not been reported before. This could be due to the use of CYP450 3A4 and CYP450 2B6 expression as primary output measurements when SR12813 is used in studies and not an assay that demonstrates alterations to the CYP450 2C9 (Duniec-Dmuchowski et al., 2007).

Taurocholate Acid was previously reported to induce the development of a branched canaliculi network in rat hepatocytes, trigger the hepatocyte polarisation program (Fu et al., 2011) and to increase intracellular cAMP (Thomas et al., 2008). This thesis, provides the first link between expression of CYP450 2C9 and TCA. Transcriptional activation of the

CYP450 2C9 upon cAMP is mediated by the expression of PGC1a which collaborates with HNF4a to induce expression of liver enzymes (Dankel et al., 2010).

Ascorbic Acid is used in the culture medium as an antioxidant to reduce the effect of reactive oxygen species on inducing cellular injury and oxidative stress (Cichoż-Lach and Michalak, 2014, Miler et al., 2008). In the current literature, a connection between Ascorbic Acid and the expression of CYP450 2C9 is not reported, however investigation of the effect of ascorbic acid on CYP450 2C9 kinetics has been evaluated. In the study by Hagen et al, human recombinant CYP450 2C9, 2D6 and 3A4 were co-expressed in *E.coli* and K(m) and V(max) properties were compared to human liver microsomes (Hagen et al., 2002). Presence of 5mM ascorbic acid increased the V(max) of CYP450 2C9 by 75%, which meant that the catalytic activity was increased upon. This study highlights the need for antioxidants to enhance CYP450 activity which can also be connected with a feedback loop that induces expression of CYP450 2C9.

CHIR 99021 activates the WNT/β-catenin pathway by inhibiting GSK3 kinase and allowing β-catenin in the nucleus (Naujok et al., 2014). In hepatocyte differentiation from hPSCs, the WNT pathway is primarily targeted during the differentiation into DE cells (Hay et al., 2008a, Chen et al., 2012b). For DE formation, CHIR 99021 has been used to replace the expensive WNT3a recombinant protein in a small-molecule driven hepatocyte differentiation protocol, efficiently producing hepatocytes compared to the growth-factor driven protocol (Siller et al., 2015). Its role in liver development is also connected with the later stages of the process and involvement in liver zonation and adhesion of cells (Nejak-Bowen and Monga, 2008). Studies for WNT pathway in the later stages confirmed that inhibition of β-catenin in embryonic liver cultures reported an essential role in hepatocyte maturation, regulating proliferation and apoptosis (Monga et al., 2003). In hPSC differentiation to HLC protocols, the stage specific regulation of WNT pathway reported to allow generation of

proliferative hepatoblasts (Touboul et al., 2016). Generation of hepatoblasts using also CHIR 99021, achieved to then generated functional hepatocytes as assessed by the expression of CYP450 3A7, 3A4 and 1A1 but expression of CYP450 2C9 was not investigated.

Transcription Factors and activation of CYP450s

In the literature, it is shown that binding of the complex HNF4a-PGC1a on CYP450 2C9 promoter sequences, activates CYP450 2C9's transcriptional upregulation (Martínez-Jiménez et al., 2006). In other studies, the complex HNF4a-PGC1a reported to not only upregulate CYP450 2C9 expression but generally liver Phase I, Phase II enzyme expression, enzymes related to glucose metabolism (Rhee et al., 2003, Finck and Kelly, 2006). A higher degree of HLC maturation has been described in correlation with increasing expression of PXR, CAR and HNF4a confirming the involvement in various responses HLC-related (Sa-ngiamsuntorn et al., 2011). In the grand scheme of things, data from mouse studies during pregnancy, showed that in the mouse liver and ovary, expression of PXR was increased approximately 50-fold (Masuyama et al., 2001) and that was due to pregnancy hormones. That proved an essential role for PXR, protecting the foetus and/or mother from xenobiotics and high levels of endogenous steroids (Kliewer et al., 2002).

Indirect activation of the WNT3a pathway has been reported upon binding of HGF on its receptor Met (Monga et al., 2002). Activation of the receptor leads to Met-directed phosphorylation of the b-catenin that leads to translocation to the nucleus and act as transcription factor. The effect is primarily induced by increased proliferation of hepatocytes, as studies in hepatocellular carcinoma confirmed (Purcell et al., 2011) but also as explained above in the hepatocyte maturation (Nejak-Bowen and Monga, 2008, Monga et al., 2003). Overall, transcriptional regulation of CYP450s is a complex process involving activation of intermediate transcriptional factors and signalling pathways that still need to be investigated in depth to gain a good understanding and induce a mature HLCs phenotype.

Future work

Even though increased CYP450 2C9 was identified in the outputs, factors that lead to increased CYP450 1A2 and 2A6 were not identified. Increased CYP450 1A2 and 2A6 were both identified as responses in DoE's #2-5 however since the MCAH control values were higher than the MC controls, those results were not processed. This was essential due to the high chance of detecting a factor that only induces a false positive signal, as happened with the Verteporfin in DoE#1. In a similar case in the future, evaluation of the effect of each different factor in immunostained 96 well plates should take place prior to the DoE experiment and ways to bypass detection of a false signal should be developed.

Even though a combination that leads to a higher expression of CYP450 2C9 was detected, further experiments to validate that the combination of these factors can indeed increase it didn't take place due to time restrictions. However, if the validation takes place in the future, time-points should be considered and evaluation of the CYP450 2C9 expression after the 17 days of the differentiation. This will give an insight and distinguish a real increase in expression or a temporary increase from molecules acting as inducers. Ideally, mass spectrometry experiment should take place and identification of CYP450 2C9 metabolites.

Due to the DMSO limitations as explained above, in this study the factors had to be grouped according to a maximum of 0.5%. This has resulted in ignoring interactions between factors that belong in different groups. A solution to this problem would be the development of a custom-made DoE Design that combines all factors in one experiment and each run/treatment is limited to a 0.5% of DMSO. The custom-made approach is not commercially available through the DoE software and has to be designed by experienced statisticians and could offer advantages that separation of the factors has ignored. Last but not least, these approaches are better suited.

CHAPTER SIX

GENERAL DISCUSSION

6. General Discussion

The aim of this thesis was to identify factors that can activate expression of key mature metabolising enzymes and subsequently lead to a more mature functional profile in hPSC-derived HLCs. This target was divided into three chapters. Initially, a stepwise approach was followed for the establishment and maintenance of hPSC cultures in a chemically defined culture medium that reduced potential variability induced by unknown MEF-CM originating factors and led to increased expression of hepatocyte related proteins in the final population of day 17 HLCs. Evaluation of hPSC maintenance and differentiation into HLCs was successful using the automated platform TECAN Freedom Evo while confirming that use of a Home-Made chemically defined medium recipe could reduce the cost and generate HLCs. Then an automated quantification script was developed that could identify the expression of mature hepatocyte proteins based on a human proteomics study. Finally, the use of statistically powerful tools described under DoE approach were utilised to attempt and identify key maturation factors. Each part of this thesis was incorporated into the final chapter that succeeds to identify factors achieving an increased CYP450 2C9 metabolising enzyme expression. Overall, this thesis has contributed to the field with the development of a quantifiable assay for the detection of maturation in HLCs and with innovative, for the HLC field, DoE approaches that screened multiple factors at different concentration levels to identify potential key maturation factors.

Implications of Findings for the HLC field

Ideally, evaluation of the identified factors using an RSM DoE approach to confirm and identify the effect of the factors presented to increase CYP450 2C9 expression should be considered. If successful, then HLCs with higher CYP450 2C9 expression could serve as a

cellular model for the study of categories of compounds specifically metabolised by the CYP450 2C9 enzyme (Van Booven et al., 2010). CYP450 2C9 is one of the major enzymes estimated to clear up to 15-20% of drugs currently requiring metabolism through Phase I enzymes. Common categories of CYP450 2C9 metabolised drugs include antiepileptic drugs (Veronese et al., 1991), anti-estrogen (Coller et al., 2002), Nonsteroidal anti-inflammatory drugs (Ali et al., 2009) and Sulfonylurea based antidiabetic compounds (Niemi et al., 2002). Therefore, successful expression of CYP450 2C9 enzyme in the HLCs at a comparable intensity to the pHEP cells could potentially open new avenues for drug testing and toxicity screening for CYP450 2C9 metabolised compounds. However, production of HLCs for the above purpose would require initially elimination of undefined and xenogeneic factors from the hepatocyte differentiation protocol as discussed before and also, potential use of clinical grade cell lines that have been derived under Good Manufacturing Procedures (Ye et al., 2017). Increased expression of metabolising enzymes is not always related to the maintenance of the expression for long-term. Therefore, potential future studies have to evaluate the length of the increased metabolic profile of HLCs and not only a single increased measurement.

Limitations of the DoE Screen

A major limitation of this study was the required separation of factors into groups due to the DMSO considerations. Currently, when DoE approaches are employed, the factors participating in the study are investigated under the same experiment (Dong et al., 2008). Separating factors can lead to missing interactions between two factors that may be more significant than single factor effect (NIST/SEMATECH, 2012). In this thesis, this could be the reason for only detecting few significant factors that only increased 1 of the 5 parameters measured in the output assay. Future experiments should consider employment of custom-made designs that can combine the same number of factors and apply limitations such as maximum DMSO concentration per treatment.

However, DoE approaches were employed and experience will be important to assist potential application in the future. Future use of knowledge developed in this thesis could assist screening of libraries of small molecule compounds (Dandapani et al., 2012, Wawer et al., 2014). Those factors and their unknown functions can be screened on developing HLCs at a range of concentrations using methods developed in this thesis to identify any maturation potential.

Approaches to generate HLCs treated with Chinese medicinal herbs and significantly improving the hepatocyte function by increasing gene expression for CYP450 2C9 and 1A2 between 2-4 times among other genes (Chen et al., 2016). However, the variability collecting the herbs and preparing for treatment would increase batch to batch variation. Since the results were reported as promising, investigation of the active compounds included in those herbs should be considered using methods such as Liquid Chromatography/Mass Spectrometry (Zhang and Kang, 2013).

Even if the identification of key factors that lead to the generation of mature HLCs is achieved, the problem that would then arise is the duration of their functional capacity. In pHEPs, the window of opportunity for drug screening and toxicity testing lasts a short time and then significant deterioration of metabolic functions occur (Zeilinger et al., 2016). Therefore ways to identify the correct signalling pathway combination that maintains the adult liver functions long-term need to be considered.

Cost Considerations for HLCs Production

HLCs production cost and batch-to-batch variability of required recombinant growth factors is a major bottleneck for the bulk generation of HLCs. These issues can be solved upon alternative hepatocyte differentiation protocols that involve chemically synthesised small molecules that replace the need for expensive growth factors. Currently there are reports of small molecule based differentiation protocols (Tasnim et al., 2015, Siller et al., 2015)

demonstrating efficiencies similar to the growth-factor derived counterparts but with a significant 67% cost reduction or 81% when these HLCs are compared with the pHEPs however, is still expensive as use of Activin is required (Tasnim et al., 2015).

The DoE experiments in this thesis have investigated the effect of small molecules and chemically synthesised factors. In future DoE designs, identification of small molecules that can induce a mature phenotype can have a major impact on cost reduction and lead to an inexpensive bulk generation of functional HLCs. Combination of robotic platforms with a cost effective HLC differentiation protocol could also overcome the above limitations, reduce user variability and enable scalability (Kami et al., 2013).

Automation and Large Scale HLCs Production

Generation of HLCs in a robotic platform has not been reported in the literature before. The TECAN Freedom Evo 200 platform presented here had unique elements of automation, engineering, a modular set up combining multiple functions and also liquid handling capabilities enabling automation of the complete protocol. Most of the automated platforms currently used in research laboratories can support liquid handling (Jiang et al., 2012, Gaisford, 2012) and bulk generation of HLCs could be possible. Generated HLCs in an automated manner would increase reproducibility, reduce labour, user variability and potential for human error (Veraitch et al., 2008). In non-modular systems where passaging of cells is not possible, semi-automated protocols can be employed by only using the liquid handling facilities for seeding of cells and media changes. Overall, automation could enable large scale production of HLCs to support further applications (Schwartz et al., 2014).

Uses of Foetal-like HLCs

The current need in the pharmaceutical field is the generation of adult-like HLCs that can be used for drug screening and toxicity testing to replace human pHEP cells. However, the foetal liver cells and subsequently foetal-like HLCs can still be used in a range of applications.

Foetal liver cells can be a good model for infection with hepatitis B virus, to replicate infection via maternal-foetal transmission, the major pathway for infection in young children (Sakurai et al., 2017). Foetal liver cells can also be an alternative option for patients with end-stage liver disease that requires hepatic cell transplantation (Yovchev and Oertel, 2017). Studies have demonstrated that when transplanted, are morphologically and functionally fully integrated and remain viable long-term (Oertel, 2011, Gridelli et al., 2012, Haridass et al., 2009). Similarly, generated HLCs have been transplanted into mouse liver and functional integration was demonstrated (Asgari et al., 2013). In the future, clinical grade generated HLCs could be transplanted in patients with liver disease. And upon the development of hiPSC, the HLCs generated could also be patient specific offering autologous therapies (Angelos and Kaufman, 2015).

Use of Technology Developed from the HLC and Wider hPSC Field

The quantifiable maturation assay could readily be used in studies investigating maturation effects in HLCs. The markers CYP450 1A2, 2C9 and 2A6 have been selected upon analysis of human proteomics data (Kim et al., 2014) for their expression in adult pHEP cells compared to foetal pHEP cells. The number of binucleated cells can also identify maturation of the HLC population as seen in the literature (Gentric et al., 2012, Davoli and de Lange, 2011). Examples could involve studies that have been described above such as treatment with cAMP (Ogawa et al., 2013) or attempt combination of Lithocholic Acid and Vitamin K2 (Avior et al., 2015) or evaluation of female/male sex hormones and how these affect the expression of CYP450s (Koh et al., 2012).

Another advantage of the developed assay could be its use as an evaluation tool in high-throughput screening studies for the identification of compounds for maturation studies in HLCs. In that study, 12.480 small molecules were screened and the output assay was based on ELISA measurements for ALB secretion (Shan et al., 2013). The cost and labour associat-

ed with the replicate samples for the ALB secretion assay could be significantly minimised upon the use of this assay. Additionally, the relevance of the outcome using the developed assay would closer fit the profile of pHEP cells since ALB was not identified as a mature marker (Kim et al., 2014). On the same note, studies using selected Phase I, II or III enzymes expressed in the liver or the commonly used markers of hepatocyte related proteins CYP450 3A4, HNF4a, A1AT or others, can assess them to identify whether are representative of the adult/mature state or not.

In the biology and stem cell field, commercial assays that compare cell characteristics to a common reference set can enable cross-comparison between laboratories. Examples include the "TaqMan hPSC Scorecard assay" that is using RT-PCR assays and data analysis software to determine the tri-lineage differentiation potential of hPSC lines (Bock et al., 2011). In a similar area, a screening assay that evaluates the potential of hPSCs to generate endoderm based on the DE morphology has helped to avoid costs and labour related to the derivation of endodermal lineages (Siller et al., 2016).

Successful solutions to the issues generated upon indirect immunostaining and false positive signal and additional development of cellular phenotyping algorithms (Massey, 2015, Garvey et al., 2016) could also establish this assay into a commercially available option for assessing HLC quality compared to reference values derived from pHEPs. However, development of this would also require the use of software algorithms and analysis tools that combine the data collected from every single measurement to calculate a single value or "score" (Huang et al., 2012). The advantage of this functional assay is that HLC generation could be compared across different laboratories and differentiation protocols, something that currently is impossible as discussed in Chapter 4.

The proteomics study has not only investigated foetal and adult liver tissue, but also it has screened tissue from foetal brain, heart, gut, testis, ovary, placenta and their adult coun-

terparts. This can open new opportunities in the investigation of mature markers for each of those pairs of foetal and adult tissues. Currently, the hPSC-derived cardiomyocytes are presenting immature morphology and foetal-like electrophysiological properties that limit further applications (Vuorenpää et al., 2017, Kolanowski et al., 2017). Similarly, differentiated hPSCs into neurons present functional deficits limiting the potential applications and further research (Kemp et al., 2016). Therefore, a study that identifies the most differentially expressed proteins in foetal and adult cells can lead to the identification of markers that can accurately identify the two states.

A unique advantage of the TECAN Freedom Evo robotic platform and the liquid handling options offered within, could be used to automate the complete immunostaining protocol. Robotic platforms have been used to accommodate techniques such as gene sequencing, antibody testing and quantitative PCR (Gaisford, 2012, Kong et al., 2012). In the TECAN Freedom EVO 200 platform, availability of large/small liquid handling functions, arms for handling a range of plate/vessel and transportation of those within the platform can create an environment that can facilitate the development of an automated immunostaining protocol. Similar scenarios have been used for dual immunostaining using a TECAN Freedom Evo 150 platform (Rumballe et al., 2008) and nuclei propidium iodide staining on the NCGC robotic platform (Michael et al., 2008). Automating the immunostaining part for HLCs in the TECAN Freedom Evo or in a similar platform would have an impact on time and labour required, cost of assay by enabling the use of low volumes, eliminate user variability (Veraitch et al., 2008) and subsequently increasing the reproducibility of the assay.

The disadvantage of the assay is that the results rely on the use of an automated plate reader, in this study the Operetta (Perkin Elmer), for High Content measurements and analysis using the developed quantification script. However, automated plate readers and high content screening is readily available in similar platforms (Singh et al., 2014, Zock, 2009)

that include analysis software but open source software is also currently available for these purposes (Stockwell and Mittnacht, 2014).

Final Remarks

Human PSC-derived HLCs could potentially replace the need for primary hepatocytes in drug testing and toxicity screening applications. However, the disadvantage currently limiting further applications is the immature phenotype and low expression of mature CYP450 enzyme expression. This thesis has demonstrated that the HLCs, under the correct signalling modulation, can differentiate into more mature counterparts. The results were achieved upon the employment of a statistically powerful approach "Design of Experiments" and screened factors identified to potentially increase maturation of hepatic cells. Initially, the development of the hepatocyte differentiation protocol succeeded to generate HLCs with increased expression of hepatocyte related markers. Then, the need for a quantifiable assay to identify mature outputs was discussed, developed and evaluated in HLCs and pHEPs populations. Finally, DoE designs were employed to screen groups of factors and identify maturation characteristics evaluating responses using the quantification assay developed. The current study demonstrated limitations, however yielded a set of factors that could potentially induce a more mature phenotype when differentiating to HLCs. Methods and technologies developed during the study can readily be used in the HLC field or adapted to accommodate studies in the wider stem cell field. Future work has to take into consideration screening of a wider number of factors in a way that is combined and not separated into groups, and potentially lead to identify missing interactions and unravel a set of factors that could induce a mature, pHEP comparable, HLC population. Last but not least the difference between the temporary induction of expression and mature phenotype has to be taken into account and identify ways to maintain an increased long-term metabolising profile.

7. Appendices

Table 23 Evidences supporting the selection of the activators and their relation to the appropriate signalling pathway and reponses that have been recorded in the literature.

Pathway/ Molecule	Evidences & Reports	Activators
Constitutive Androstane Receptor (CAR)	Regulating dispositional fate of drugs, chemical carcinogens, endogenous substances such as steroids, heme and bilirubin, thyroid hormone, cholesterol and bile acids as discussed in (Chen et al., 2013)	Dexamethasone has a proven role to enhance CAR expression in human hepatocytes (Pascussi et al., 2000, (Yang and Wang, 2014)
	Drug clearance and detoxification (Chang and Waxman, 2006). Regulating lipid and energy metabolism in the liver (Wada et al., 2009)	
	Lentiviral transduction of CAR in hESCs, accelerated the maturation of hepatic-like cells and demonstrated that CAR over-expressing cells exhibited a 2.5-fold increase in ALB, levels of mRNA expression of biotransformation enzymes, hepatic transcription factors, plasma proteins and metabolic enzymes were significantly enhanced (Chen et al., 2013)	CITCO has been reported as a novel human CAR agonist that shows increased potency, selectivity for hCAR and ability to induce the prototypical CAR target gene CYP450 2B6 in primary human hepatocytes (Maglich et al., 2003)
	Highly enriched expression in the liver and in tissues with capacity for drug metabolism such as kidney and small intestine (Timsit and Negishi, 2007, Swales and Negishi, 2004)	Flavone demonstrated nuclear translocation of hCAR however, the percentage of nuclear translocation was lower that CITCO (Lynch et al., 2015)
	Use of a CAR deactivator, fully confirmed the relation of CAR to the expression of the detoxification enzymes (Funakoshi et al., 2011)	Use of the LY29004 compound, a PI3K inhibitor, could potentially block insulin's response and allow CAR/PXR to activate the response (Kodama et al., 2004)
	Insulin is reported to inhibit the role of CAR and PXR in the induction of drug-metabolising enzymes (Kodama et al., 2004). Insulin's signal is mediated through Phosphoinositide 3-kinase – Protein Kinase B (PI3K-AKT) pathway (Kodama et al., 2004).	

Pregnane X Receptor	Important regulator for xenobiotic-induced regulation of CYP450 isotypes (Sinz et al., 2008).	SR12813 reported as a full PXR agonist due to its chemistry and binding patterns on hPXR (Watkins et al., 2001) It is used as reference compound for hPXR activation in multiple studies (Delfosse et al., 2015, Shukla et al., 2011, Sui et al., 2012).
	Proven that multiple compounds such as steroids, antibiotics, antimycotics, bile acids, hormones, toxins, organophosphate pesticides, glucocorticoids, prescription drugs and environmental chemicals can activate PXR and trigger activation of a detoxification process (Kliewer et al., 2002).	
Retinoid acid-related orphan receptors (RORs)	RORs are expressed in the brain, central nervous system but also in the liver, having an active role in the xenobiotic and endobiotic regulatory network (Xiao et al., 2010). Melatonin is a pineal gland produced hormone regulating mainly sleep timing patterns and body temperature (Cajochen et al., 2003, Brown, 1994)	In human breast cancer cell lines, treatment with Melatonin activates nuclear receptors including Estrogen Receptor α and Retinoic Acid Receptor α, mediating maintenance and metabolic cellular activities (Carbajo-Pescador et al., 2011, He et al., 2016, Eck-Enriquez et al., 2000, Lai et al., 2008)
Retinoic Acid Receptors (RAR)	Retinoic Acid (RA) treatment could lead to the production of unsaturated fatty acids, induce triglyceride breakdown, lipolysis, bile acid secretion and retinoids elimination, all of which are characteristics of mature liver cells (He et al., 2013).	The all-trans-retinoic acid (ATRA) can induce an effect regulating cell responses upon binding on nuclear receptors (RAR-a/β/γ) (di Masi et al., 2015)
Retinoic X Receptors (RXR)	RXRs are differentially expressed in tissues while the RXRα is mainly expressed in the liver, kidney, spleen, placenta, epidermis, visceral tissues (Szanto et al., 2004)	The isomer 9-cis-retinoic acid (9CRA) binds on the retinoic-X-receptors (RXR-a/β/γ) (di Masi et al., 2015)
		RXR receptor is also activated by the synthetic Pan-RXR agonist SR11237 (Dawson and Xia, 2012)
		A synthetic compound known as bexarotene, initially approved to treat cutaneous T-cell lymphoma, showed that it is acting as retinoid X receptor (RXR)-specific agonists (Wagner et al., 2009)

Vitamin D	The effect of vitamin D is mediated by Vitamin D Receptor (VDR) and binding patterns of VDR response elements (VDRE) have been identified on their promoters (Zúñiga et al., 2011)	Confirmed Vitamin D's role to lead detoxifying activities in human primary cultured hepatocytes measured by increased expression of CYP450 enzymes such as CYP450 3A4, 2B6 and 2C9 (Drocourt et al., 2002).
		Expression of CYP450 7A1 was increased by Calcitriol, which is the hormonally active vitamin D metabolite, treatment in human primary cultured hepatocytes (Han and Chiang, 2009)
Vitamin K	Vitamin K has an essential role in the synthesis of GLA-protein family members that are blood coagulation factors and are exclusively formed in the liver. Administration of Vitamin K to new-borns is a common practise to avoid bleeding events (Vermeer, 2012)	In presence of Vitamin K, synthesis of blood coagulation factors occurs in the liver inducing an adult liver characteristic and leading to a more mature liver cells phenotype (Conly and Stein, 1992, Walther et al., 2013)
Farnesoid X receptor (FXR)	FXR is highly expressed in tissues that are exposed to bile acids such as liver, intestine, kidney and adrenal gland (Zhang et al., 2003) (Zhang et al., 2003)	In human hepatocytes, activation of FXR with GW4064 is possible leading to enhanced promoter activity of CYP450 2B6 however, represses CYP450 3A4 mRNA expression (Zhang et al., 2015)
	FXR is activated by endogenous bile acids regulating genes involved in bile acid, lipid and glucose homeostasis (Modica et al., 2010)	Cholesterol metabolism is regulated through FXR and directly activated by a primary bile acid, Chenodeoxycholic acid that regulates expression of cholesterol 7 alpha-hydroxylase (CYP450 7A1) limiting or allowing bile acid biosynthesis (Tu et al., 2000)
Fibroblast Growth Factor 19	Fibroblast growth factor 19 (FGF19), an enterokine, been reported to have an essential role governing bile acid synthesis, glucose homeostasis and nutrient metabolism in the human liver (Kir et al., 2011b, Beenken and Mohammadi, 2009)	FGF19 regulates hepatic protein synthesis, improve metabolic rate lowering serum glucose, triglyceride and cholesterol levels (Kir et al., 2011a, Wu et al., 2011)

Bile Acids - Lithocholic Acid (LCA)	LCA is a secondary bile acid that is produced by intestinal bacteria and induces PXR receptor activity to protect against liver toxicity (Staudinger et al., 2001)	Confirmed that LCA also induces expression of PXR that results in 70% nuclear localisation and increase in CYP450 induction response (Avior et al., 2015)
Bile Acids - Taurocholate Acid (TCA)	In isolated primary hepatocytes cultured with TCA, the development of a branched canaliculi network and polarisation of cells was demonstrated (Fu et al., 2011)	The mechanism of TCA action is mediated by increasing the cellular Cyclic Adenosine Monophosphate (cAMP) and kinases responsible to trigger the hepatocyte polarisation gene programme (Fu et al., 2011)
Cyclic Adenosine Monophosphate (cAMP)	cAMP-mediated expression of PPARγ co-activator 1a (PGC1a) which functions together with HNF4a to regulate expression of liver specific genes (Dankel et al., 2010, Parviz et al., 2003, Finck and Kelly, 2006)	Use of 8-Br-cAMP in the maturation stage of HLCs, induces gene expression of Glutathione 6 phosphatase (G6P) and Tyrosine Amino-Transferase (TAT) while AFP protein expression reported low compared to the control. Additionally, CYP450 enzymes 1A2 and 3A4 showed an increased expression reporting inductive ability of cells to metabolise drugs (Ogawa et al., 2013)
Aryl Hydrocarbon Receptor	AHR can sense a range of exogenous ligands such as benzo[a]pyrene, 2,3,7,8-tetrachlorodibenzodioxin and 3-methylcholanthrene (Hu et al., 2013, Kim et al., 2016) and functions by binding to Xenobiotic Response Elements leading to the transcription of metabolising genes such as CYP450 1A1, 1A2 and 1B1 (Noakes, 2015, Stockinger et al., 2014)	hPSC derived HLCs activation of AhR by "2-(1H-Indol-3-ylcarbonyl)-4-thiazolecarboxylic acid methyl ester" (ITE) led to prominent induction and robust expression of genes including CYP450 1A1 and 1B1 but not 1A2 suggesting that AhR is transcriptionally active in hPSC-HLC types (Kim et al., 2016)
HIPPO Signalling pathway	When the HIPPO pathway is inactive, the transcriptional coactivator "Yes-associated pro-tein 1" (YAP1) is allowed to promote expression of genes associated with embryonic enhancer regions, influencing an embryonic state of the cells (Alder et al., 2014, Yimlamai et al.,	Y27632, a Rho kinase inhibitor, reported to cause nuclear export of YAP (Johnson and Halder, 2014, Alder et al., 2014, Dupont et al., 2011)

	2014). During maturation of liver, the HIPPO pathway is activated and YAP1 is inhibited from binding on the embryonic enhancer regions thus allowing a maturate gene expression programme to take place (Yimlamai et al., 2014). Activation of the HIPPO Signalling Pathway can be achieved by using Verteporfin. Has also been found to bind and inhibit YAP1 leading to hepatocyte maturation events (Liu-Chittenden et al., 2012)	Epinephrine inhibits YAP1 through G-protein Coupled Receptor (GPCR) activation and by activating kinases that phosphorylate YAP1 at key residues leading to inhibition of its role (Ghanouni et al., 2001, Kobilka, 2007, Yu et al., 2012a). Through GPCR activation, YAP1 is inhibited by Glucagon. Glucagon receptor is expressed in hepatocytes and leads to phosphorylation of YAP1 (Yu et al., 2012a).
Peroxisome Proliferator Activated Receptors (PPAR)	PPARα is highly expressed in liver and skeletal muscle, PPARβ is expressed in most cell types and PPARγ preferentially expressed in adipose tissues but also in the liver (Smith, 2002). Activation of the receptors occur upon binding of endogenous fatty acids, environmental chemicals, and drugs that induce a multi-enzyme metabolic response that affects lipid and fatty acid processing (McMullen et al., 2014, Finck and Kelly, 2006).	The potent and highly selective PPARα activator GW7647 has shown to increase several key transcription factors, including HNF4α, and lead to expression of enzymes for organic acid metabolism, cell lipid metabolism and lipid transport (McMullen et al., 2014)
Hypoxia	A low 4% oxygen concentration for the hepatoblast and immature hepatocyte stage and a 20% concentration at the final stage of differentiation mimic oxygen concentration in the human uterus and decreased the expression of AFP, increased ALB expression, indocyanine green uptake and urea metabolism (Si-Tayeb et al., 2010b).	Investigation of a high oxygen concentration was not possible hence induction of hypoxia and identification of decrease in enzyme expression was tested evaluated. Cobalt(II) chloride hexahydrate was described to provide a stable 5% oxygen level in various cell lines and used to reduce the oxygen concentration (Xia et al., 2009, Wu and Yotnda, 2011)
Epigenetic Factors	Chromatin structure can be modified upon histone modifications and DNA methylation essentially regulating gene expression affecting accessibility of target sites to transcriptional regulators	5'-Azadeoxycytidine induces global de-methylation, enhances open chromatin formation and increases gene expression.

	(Meshorer and Misteli, 2006). Histone modifications induced by Histone Deacetylases lead to hypoacetylated histones that are usually associated with transcriptionally inactive chromatin structure (Wu and Sun, 2006). Overall, studies suggest that stem cell differentiation protocols can be affected by DNA demethylation, which could lead to studies evaluating the use of DNA epigenetic modification agents (Zhou and Hu, 2015)	Trichostatin A (TSA) is an HDAC inhibitor, commonly used in the stem cell differentiation field, enhancing differentiation of human induced pluripotent stem cells to cardiomyocytes that could be used for cardiac tissue engineering (Lim et al., 2013) Sodium Butyrate carries a function inhibiting Histone Deacetylation, essentially allowing more genes to be expressed (Berni Canani et al., 2012)
Hormones 17β Estradiol/Progesterone & Testosterone	In primary hepatocytes, 17β Estradiol upregulates the expression of the CYP450 2B6 and in HepG2 cells it activates the CAR receptor and enhances promoter activity of CYP450 2B6 (Koh et al., 2012). Progesterone, is also significantly increased during pregnancy (Kumar and Magon, 2012). Their role was evaluated using human primary hepatocytes and significant changes in CYP450 enzyme expression were identified (Choi et al., 2013)	Estradiol is associated with enhanced CYP450 2A6, 2B6 and 3A4 gene expression while Progesterone enhanced CYP450 2A6, 2B6, 2C8, 3A4, and 3A5 gene expression (Choi et al., 2013). Testosterone is the major male hormone metabolised in the liver by CYP450 2B6, 3A4/5 and/or by 2C9 and 1A1 (Zanger and Schwab, 2013). Multiple roles in male hormonal regulation (Hines et al., 2015, Bain, 2007).
Thyroid Hormones	Thyroid hormones L-thyroxine (T4) and 3,5,3'-L-tri-iodothyronine (T3) are produced and secreted by the thyroid gland (Malik and Hodgson, 2002). Their role is known since the 1980's in liver cell proliferation (Short and Ove, 1983), liver regeneration (Leffert and Alexander, 1976) and more recently differentiation of rat liver progenitor cells into hepatocytes (László et al., 2008). Thyroid hormones affect hepatic gene expression though a diverse range of cellular pathways and functions (Feng et al., 2000, Miler et al., 2008)	T3 is reported upon increased expression of (Low Density Lipoproteins) LDL receptors on the hepatocytes and decreased LDL cholesterol levels (Ness et al., 1998, Malik and Hodgson, 2002). Administration of T3 leads to increased activity of enzymes responsible for lipid-lowering resulting in the reduction of low density lipoprotein levels from serum, characteristic of mature human hepatocytes (Ness and Lopez, 1995)

Lipids and Fatty Acids	The liver is a key site for lipid metabolism and hub for fatty acid synthesis (Nguyen et al., 2008). For neonates, a main energy source is fatty acids from breastfeeding (Lucendo-Villarin et al., 2016, Borum, 1992)	A chemically defined lipid mixture supplement contains the non-animal derived fatty acids arachidonic, linoleic, linolenic, myristic, oleic, palmitic and stearic acids, cholesterol and tocopherol acetate solubilized in cell culture medium. Presence of lipids and fatty acids in developing HLC could replicate processes in the human liver (Jump et al., 2005, Nguyen et al., 2008)
Antioxidants	During detoxification processes in the liver, an excessive number of toxic and reactive oxygen species (ROS) are produced as by-products, resulting in oxidative damage to the hepatocytes and compromising its functions (Chojnacki et al., 2014). Oxidative stress induces damage to proteins, lipids and DNA within the liver cells leading to structural and functional liver abnormalities (Cichoż-Lach and Michalak, 2014)	Ascorbic Acid is used as a reducing agent in hepatocytes mediating the oxidation process (Buettner and Jurkiewicz, 1996, Miler et al., 2008). Melatonin, regulates ROR binding and detoxification enzyme expression, also plays an important role in the liver as an antioxidant (Chojnacki et al., 2014, Reiter et al., 2003)
FH1 and FPH1	A small-molecule screening approach targeting to identify factors that can induce proliferation but also maturation of human HLCs (Shan et al., 2013) highlighted that FH1 (Functional Hit 1) and FPH1 (Functional & Proliferative Hit 1) doubled ALB secretion. Morphology of the cells was improved with pronounced hepatocyte morphology including polygonal cells, visible nuclei and identifiable bile canaliculi regions between hepatocytes (Shan et al., 2013)	Increased expression of the characteristic mature bile salt export pump and reduced expression of the foetal GSTp1 expression. Immunocytochemistry for protein expression showed increased ALB, CYP450 3A4 and low. Functional activity of CYP450 3A4 was found multiple times higher while presence of OSM induced additive positive effects in regards to CYP450 3A4 and 2A6 activity (Shan et al., 2013)
Dihexa	The “N-hexanoic-Tyr, Ile-(6) amino hexanoic amide”, commercially known as Dihexa, was originally developed as therapeutic intervention for dementia (McCoy et al., 2013). It was also identified as a highly potent HGF receptor activator (Siller et al., 2015). Dihexa acts similarly to HGF and when combined with Dexamethasone can substitute a maturation effect (Siller et al., 2015, Sullivan et al., 2010).	Advantages of the chemically synthesised Dihexa are its potency at very low concentrations such as 100nM equals to 10ng/ml of HGF, as well as stable under cell culture conditions.

Essential factors for Culture of Primary Human Hepatocytes	The basic culture medium for the primary human hepatocyte cells contains a) Bovine Serum Albumin, b) D-Glucose and c) Media Supplements 1 (MS1), 2 (MS2) and 3 (MS3). MS1 contains trace elements for basic cell viability copper sulphate, zinc sulphate, sodium selenite, niacinamide and dexamethasone, MS2 contains transferrin essential for delivery of iron (Kasvosve and Delanghe, 2002) and MS3 contains Insulin discussed above.	BSA is an isolated and less variable fraction of the total Fetal Bovine Serum (FBS). FBS use been reported to cause loss of hepatocyte polarity and significant lower expression of CYP450 1A enzymes (Kidambi et al., 2009)
		Use of D-Glucose in mammalian cell cultures provides a stable fuel source to support basic metabolic activity (Zhao et al., 2008). However, another stable energy source in cell culture is the GlutaMAX supplement consisting of the dipeptide l-alanyl-l-glutamine that is more efficiently taken up by cells.

Table 24 Comparison of outputs for the Hepatocyte Differentiation protocols in the current literature

Reference	Morphology Images	Immunostaining	Gene Expression	Flow Cytometry	Western Blot	Albumin Secretion	AFP Secretion	A1AT Secretion	Urea Synthesis	Fibrinogen Synthesis	P450 Activity	CYP450 3A4	CYP450 3A7	CYP450 2D6	CYP450 1A2	CYP450 2C9	Alcohol Dehydrogenase	Liquid Chromatography / Mass Spectrometry	PAS Staining	ICG Staining	Oil Red Staining	LDL Uptake
(Toivonen et al., 2013)		ALB, AFP	ALB, AFP																			
(Medine et al., 2011)		ALB, AFP, ECAD										Y										
(Cai et al., 2007)	Y	AAT, AFP, ALB, CK18	ALB, A1AT, HNF4a, PEPCK, TDO2, TAT, CYP450 7A1, CYP450 2B6, CYP450 3A4			Y													Y	Y		
(Hay et al., 2008a)			ALB, AFP, HNF4a, TAT, TO, APOF, CYP450 3A4, CYP450 7A1			Y	Y		Y	Y	Y											
(Si-Tayeb et al., 2010)	Y	ALB, AFP, HNF4a		ALB		Y													Y	Y	Y	Y
(Song et al., 2009)	Y		AFP, ALB, CK8, CK18, CK19, A1AT, TDO2, CYP450 2A6, CYP450 3A4, IF A1AT, CYP450 3A4			Y			Y		Y								Y			
(Hay et al., 2008b)	Y	ALB, CK18, CK19, CYP450 3A4, c-MET	HNF4a, AFP, ALB, A1AT, c-MET, E-CAD, CYP450 3A4, CYP450 3A7, CYP450 2C9, CYP450 2C19, PXR		HNF4a, AFP, ALB, TAT, TTR, TO, CAR, APOF	Y						Y			Y								

Reference	Morphology Images	Immunostaining	Gene Expression	Flow Cytometry	Western Blot	Albumin Secretion	AFP Secretion	A1AT Secretion	Urea Synthesis	Fibrinogen Synthesis	P450 Activity	CYP450 3A4	CYP450 3A7	CYP450 2D6	CYP450 1A2	CYP450 2C9	Alcohol Dehydrogenase	Liquid Chromatography / Mass Spectrometry	PAS Staining	ICG Staining	Oil Red Staining	LDL Uptake
(Agarwal et al., 2008)	Y	GATA4, HNF4a, AFP, ALB, A1AT	AFP, ALB, CYP450 3A4, CYP450 7A1			Y													Y	Y		
(Asgari et al., 2013)	Y	AFP, CK18, ALB, A1AT, CYP450 1A1				Y	Y		Y		Y								Y	Y	Y	Y
(Chen et al., 2012)	Y		AFP, HNF4a, ALB, CK18, G6P, TDO2, TAT, CYP450 3A4, CYP450 7A1						Y			Y							Y			Y
(Touboul et al., 2010)	Y	CK18, A1AT, ALB, AFP, CK19	HNF4a, HNF6, CEBPa, AFP, ALB, A1AT, TO, TAT, CYP450 3A7, CYP450 7A1	ASGPR1, cMET, LDLR									Y							Y		Y
(Hannan et al., 2013)	Y	ALB, A1AT, CK18		AFP, ALB, A1AT							Y								Y			Y
(Duan et al., 2010)		MRP1, OATP2	ALB, A1AT, CYP450 1A1, 1A2, 1B1, 2A6, 2A7, 2B6, 3A4, 2C8, 2C9, 2C19, 2E1, 7A1, UGT1A1, UGT1A3, UGT1A6, UGT1A8, UGT1A10, UGT2B7, GST P1-1, GST A1-1	A1AT, ASGPR1 and ALB		Y											Y			Y		

Reference	Morphology Images	Immunostaining	Gene Expression	Flow Cytometry	Western Blot	Albumin Secretion	AFP Secretion	A1AT Secretion	Urea Synthesis	Fibrinogen Synthesis	P450 Activity	CYP450 3A4	CYP450 3A7	CYP450 2D6	CYP450 1A2	CYP450 2C9	Alcohol Dehydrogenase	Liquid Chromatography / Mass Spectrometry	PAS Staining	ICG Staining	Oil Red Staining	LDL Uptake
(Magner et al., 2013)		ALB	ALB, ASGPR1, A1AT, AFP, CYP450 3A4																			
(Siller et al., 2015)	Y	ALB, AFP, HNF4a, A1AT	A1AT, AFP, ALB, APOA2, AS-GPR1, CYP450 3A4, HNF4a, TDO2, TTR			Y		Y		Y		Y			Y				Y	Y		
(Baxter et al., 2015)	Y	ALB, A1AT, CYP450 2A6, AFP, GSTp, HSP47	CYP450 1A1, 1A2, 1B1, 27A1, 2A13, 2B6, 2C18, 2C19, 2C8, 2C9, 2D6, 2E1, 2F1, 3A4, 3A5, 3A7, 4A11, 4F11, 4F2, 4F3, 7A1, 7B1, 8B1, ALDH Family, FMO Family	CYP450 2A6, AFP, GSTp, HSP47	CYP450 2A6, GSTp, HSP47	Y						Y		Y			Y					
(Takayama et al., 2014)	Y	A1AT		ASGPR1, ALB		Y			Y													
(Asplund et al., 2016)	Y	HNF4a, CK18, A1AT, ALB	A1AT, ALB, CYP450 1A1, 1A2, 2C9, 3A4, 3A7, 3A5, GSTA1-1, UGT2B7, NTCP, OATP1B1								Y			Y	Y	Y						
Total	13	15	13	6	2	10	2	1	5	2	5	4	1	2	2	1	1	1	7	7	2	5

Table 25 Literature review for the factor concentrations used in the literature to decide the range of concentration tested in the DoE approaches.

Signalling Pathway Factor **Final Range**	Concentration range in studies	Cell type – Experimental Plan	Reference
Cyclic Adenosine Monophosphate 8-Br-cAMP **100uM – 1000uM**	2mM	Investigation of BCRP/ABCG2 transporters transcription upon EGF or 8-Br-cAMP treatment in human ovarian carcinoma cells	(Xie et al., 2015)
	1mM	Hepatocyte like cells treatment with 8-Br-cAMP leads to expression of mature hepatocyte proteins G6P and TAT	(Ogawa et al., 2013)
	100uM	Increase survival and protect Pancreatic cancer cells from serum withdrawal cell death	(Zimmerman et al., 2015)
	125uM	Examine the long-term effects of cAMP on Neuromuscular junction maturation. Elevation of cAMP essential for maturation	(Song and Jin, 2015)
	50uM	Increased cAMP leads to Dendritic cells activation and regulate immunity and allergic asthma	(Lee et al., 2015)
Pregnane X Receptor Lithocholic Acid **10uM – 100uM**	75uM – 200uM	Used to selectively kill Neuroblastoma cells at 150uM protecting primary cultures of human neurons	(Goldberg et al., 2011)
	10uM – 50uM	HLC treatment in combination with Vitamin K2 increased CYP450 enzyme expression. Mild toxicity at 50uM	(Avior et al., 2015)
	1uM – 1mM	Lithocholic Acid decreases osteoblast viability by downregulating vitamin D related effects	(Ruiz-Gaspà et al., 2010)
	0uM – 50uM	Increased expression of the urokinase-type plasminogen activator receptor and enhanced cell invasiveness in colon cancer cells	(Baek et al., 2010)
	10uM – 30uM	Treatment of Caco-2 cells showed that lithocholic acid activates FXR that may play an essential role in lithocholic acid homeostasis	(Lu et al., 2005)
Cyclic Adenosine Monophosphate Taurocholate Acid **25uM – 200uM**	0uM – 100uM	High concentration of Taurocholate acid induces apoptosis in human placenta-trophoblast epithelial cells	(Zhang et al., 2014)
	0uM – 200uM	Human cholangiocarcinoma cells treated with Taurocholate increased their invasion rates	(Liu et al., 2015)
	25uM – 200uM	Rat pHEPs 100uM Maximal effect to induce polarisation of cells and	(Fu et al., 2011)

		development of branched canaliculi network	
	1uM	Human and rat hepatocytes treated with Taurocholate to investigate their transporter activity and IC50 values of compounds	(Jemnitz et al., 2012)
	0.2uM and 2uM	In human ovarian tumour cells, treatment led to expression of OATP 1A2 transporter and highlighted potential role of FXR in activation	(Yang et al., 2014)
Vitamin K Receptor Vitamin K2 **5uM – 100uM**	5uM	In Human leukemia cells, treatment with Vitamin K induces growth arrest supressing c-MYC expression	(Maniwa et al., 2015)
	1uM and 5uM	Growth inhibition effects were detected by testing Vitamin K2 treatment in Hepatocellular carcinoma cells	(Zhang et al., 2012)
	100uM – 150uM	Evaluation as an effective anticancer drug in breast cancer cells showed decrease in adhesion and viability of cells	(Kiely et al., 2015)
	100uM	Protective role against osteoporosis, atherosclerosis and carcinogenesis suppressing NFkB expression in Hepatocellular carcinoma cells	(Xia et al., 2012)
	10uM	HLC treatment in combination with LCA increased CYP450 enzyme expression.	(Avior et al., 2015)
Small Molecules FH1 **5uM – 30uM**	15uM	Unique study identified the role of FH1 and FPH1 factors increasing mature gene expression and mature morphological characteristics in Hepatocyte Like Cells	(Shan et al., 2013)
Thyroid Hormones T3 **10nM – 100nM**	7.5nM – 750nM	In astrocytes, treatment with thyroid hormone T3 lead to upregulation of apolipoprotein E gene expression through activation of RXRα	(Roman et al., 2015)
	0.1nM – 1000nM	In Piglet Sertoli cells, T3 inhibits the proliferation via modulating the PI3K/Akt signalling pathway	(Sun et al., 2015)
	10nM	Role in cancer progression upon T3 treatment in HepG2 cells through upregulation of BSSP4, a protease participating in ECM remodelling	(Chen et al., 2014a)
	100nM	In hepatic cells, miRNA-181d is regulated by T3 negatively regulates CDX2 and SOAT2 mRNA expression levels	(Yap et al., 2013)
	0nM – 10nM	Treatment of HepG2-TRa1 cells with T3 leads to enhanced tumour metastasis profile by repressing miR-17 expression	(Lin et al., 2013)

HGF Receptor Dihexa **10nM – 200nM**	1uM	Evaluation of Dihexa as a potential hair cell protectant in Zebrafish lateral line hair cells through HGF-mediated mechanism	(Uribe et al., 2015)
	100nM	Differentiation of Hepatocyte like cells demonstrating expression of markers, key hepatic functions and cytochrome CYP450 activity	(Siller et al., 2015)
HIPPO Signalling Pathway Verteporfin **3uM – 40uM**	0uM – 5uM	Using Trebecular meshwork cells, it was shown that verteporfin inhibits the expression of YAP	(Chen et al., 2015b)
	0uM – 35uM	Investigating new therapies for ocular cells used Verteporfin to pre-treat the cells before laser therapy	(Ammar and Kahook, 2013)
	0.56uM	Therapeutic potential of Photodynamic therapy in Endothelial and Tumour cells in response to verteporfin treatment	(Fateye et al., 2015)
	250nM	Treatment of Pancreatic cancer using Photodynamic therapy and pretreating with Verteporfin	(Celli et al., 2011)
	0.6uM – 6uM	Treatment of HepG2 cells with verteporfin and photoinduced treatment led to lethal apoprotic process	(Chiou et al., 2010)
HGF Receptor HGF **5ng/ml – 50ng/ml**	50ng/ml	Differentiation of hPSC into HLC demonstrating liver functions by immunocytochemistry and/or functional assays	(Touboul et al., 2010)
	20ng/ml		(Si-Tayeb et al., 2010b)
	10ng/ml		(Hay et al., 2008b)
	0ng/ml		(Song et al., 2009b)
Oncostatin M OSM **5ng/ml – 50ng/ml**	50ng/ml	Differentiation of hPSC into HLC demonstrating liver functions by immunocytochemistry and/or functional assays	(Magner et al., 2013)
	30ng/ml		(Hannan et al., 2013)
	20ng/ml		(Toivonen et al., 2013)
	10ng/ml		(Asgari et al., 2013)
	0ng/ml		(Touboul et al., 2010)
Glucocorticoid Receptor Hydrocortisone **1uM – 10uM**	10uM	Differentiation of hPSC into HLC demonstrating liver functions by immunocytochemistry and/or functional assays	(Toivonen et al., 2013)
	10uM		(Hay et al., 2008b)
Constitutive Androstane	100nM	Induction of CYP450 2B6 and CYP450 3A4 expression in human hepato-	(Yang et al., 2010)

Receptor CITCO **50nM – 200nM**		cytes Freshly isolated human hepatocytes CITCO treatment	
	100nM	Identification of a novel human constitutive androstane receptor (CAR) agonist and its use in the identification of CAR target genes. CITCO in Primary Human Hepatocytes	(Maglich et al., 2003)
	1nM – 1uM	Regulation of cytochrome CYP450 2C9 expression in primary cultures of human hepatocytes	(Sahi et al., 2009)
	100nM	Xeno-sensing activity of the aryl hydrocarbon receptor in human pluripotent stem cell-derived hepatocyte-like cells. Activation of CAR – PXR and AhR	(Kim et al., 2016)
	100nM	Primary human hepatocytes, CITCO treatment improves long term culture and expansion	(Levy et al., 2015)
Constitutive Androstane Receptor Dexamethasone **0.1uM – 5uM**	100nM	Hepatocyte culture treatment for CYP450 studies	(Kostrubsky et al., 1999)
	5uM	Protected role of Dex on Hepatocytes against apoptosis	(Oh et al., 2006)
	0-10uM	Effect of Dex on CYP450 1A activity primary human hepatocytes	(Monostory et al., 2005)
	0-10uM	PXR activation on PXR-transfected T293 cells	(Song et al., 2004)
	1nM to 1uM	Dexamethasone Induces CAR Expression in Human Hepatocytes	(Pascussi et al., 2000)
Constitutive Androstane Receptor Flavone **20uM – 80uM**	60uM	Identification study for CAR activators	(Lynch et al., 2015)
	40uM	Treating cancer cell lines Caco2 and Paco with Flavone isomers	(LeJeune et al., 2015)
Protein Supplementation Serum or Knock-out Serum **0% - 10%**	8.3% FBS	8.3% of FBS in the final Medium for primary hepatocyte culture	QMC Isolation and culture of pHEPs
	10% FBS	FBS in the medium C stage of differentiating hepatocytes	(Medine et al., 2011)
	8.3% FBS	Differentiation of stem cells into hepatocyte like cells	(Toivonen et al., 2013)
	10% KSR	Differentiation of hiPSC into hepatocyte like cells	(Asgari et al., 2013)
	5% FBS	Differentiation and characterization of metabolically functioning hepatocytes from human embryonic stem cells	(Duan et al., 2010)
Pregnane X Receptor SR12813	10nM – 30uM	Regulation of CYP450 3A4 and 2B6 Expression by Liver X Receptor Agonists	(Duniec-Dmuchowski et al., 2007)

0.5uM – 5uM	3uM	Identification of PXR activators from pharmaceutical and environmental compounds	(Delfosse et al., 2015)
	0 - 38uM	Identification of Clinically Used Drugs That Activate Pregnane X Receptors – HepG2 cells	(Shukla et al., 2011)
	0.3uM	Effect of PXR expression on drug resistance in breast cancer cells	(Qiao and Yang, 2014)
	200nM	Xeno-sensing activity of the aryl hydrocarbon receptor in human pluripotent stem cell-derived hepatocyte-like cells. Comparing activation of PXR – CAR and AhR)	(Kim et al., 2016)
Retinoic Acid-related Orphan Receptors (ROR) Melatonin **0.01mM – 1mM**	5mM	Treatment of differentiating or proliferating hepatocytes. As a control for steatosis causing agents.	(Levy et al., 2015)
	50uM – 2mM	Melatonin treatment induces apoptosis in HepG2 cells, but not in primary human hepatocytes.	(Carbajo-Pescador et al., 2013)
	20uM – 2mM	Treatment of 293S cells with melatonin to investigate effect on cell growth, metabolic activity and cell cycle distribution	(Natarajan et al., 2001)
	10uM	Melatonin promotes hepatic differentiation of human dental pulp stem cells	(Cho et al., 2015)
	10uM	Melatonin suppresses activation of hepatic stellate cells through RORα-mediated inhibition of 5-lipoxygenase	(Shajari et al., 2015)
Retinoic Acid Receptor All Trans Retinoic Acid **1uM – 10uM**	0.1uM – 1uM	Activation of RXR-RAR homodimers in keratinocytes	(Xiao et al., 1995)
	1uM	Regulation of vitamin D receptor expression by retinoic acid receptor alpha in acute myeloid leukemia cells	(Marchwicka et al., 2016)
	10uM	Effect of ATRA on the expression of HOXA5 gene in K562 cells and its relationship with cell cycle and apoptosis	(Liu et al., 2016)
	5uM	Differential regulation of drug transporter expression by all-trans retinoic acid in hepatoma HepaRG cells and human hepatocytes	(Le Vee et al., 2013)
	1uM	ATRA modulates mechanical activation of TGF-β by pancreatic stellate cells	(Sarper et al., 2016)
Retinoid X Receptor SR11237	1uM	RXR receptor function using agonists and antagonists on PLB 985 and NB4 leukemia cell lines	(Nahoum et al., 2007)

0.1uM – 5uM	11nM	Activation of RXR-RAR homodimers in keratinocytes	(Rodin et al., 2014)
	1uM or 10uM	Activation of PXR to investigate another PXR activator, docosahexanoic acid. In 293T cells.	(de Urquiza et al., 2000)
	100nM	RXR agonists inhibit high glucose-induced upregulation of inflammation by suppressing activation of the NADPH oxidase-nuclear factor-κB pathway in human endothelial cells	(Ning et al., 2013)
	1uM	Regulation of retinoic acid receptor beta expression by peroxisome proliferator-activated receptor gamma ligands in breast cancer and lung cancer cells.	(James et al., 2003)
Retinoid X Receptor Bexarotene **1uM – 5uM**	1uM	Investigation on the RXR activation upon cytotoxic agent treatment on breast cancer cell model	(Yen and Lamph, 2005)
	1uM	Effect of Bexarotene on angiogenesis and metastasis in solid tumours (Lung cancer cells and breast cancer cells)	(Yen et al., 2006)
	1uM	Role of RXR activation using bexarotene to prevent and overcome paclitaxel resistance in Human Non–Small Cell Lung Cancer Calu3 cell model	(Yen et al., 2004)
	0.5 – 5uM	Driving neuronal differentiation and dentritic complexity in mouse ES cell model	(Mounier et al., 2015)
	5uM	Guggulsterone and bexarotene induce secretion of exosome-associated breast cancer resistance protein and reduce doxorubicin resistance in MDA-MB-231 cells	(Kong et al., 2015)
Vitamin D Receptor Calcitriol (Vitamin D3 active metabolite) **10nM – 200nM**	10nM	Regulation of vitamin D receptor expression by retinoic acid receptor alpha in acute myeloid leukemia cells	(Marchwicka et al., 2016)
	10-100nM	Vitamin D3 modulated gene expression patterns in human primary normal and cancer prostate cells	(Guzey et al., 2004)
	1nM	Expression of CYP450 3A4, 2B6, and 2C9 Is Regulated by the Vitamin D Receptor Pathway in Primary Human Hepatocytes	(Drocourt et al., 2002)
	100nM	The Impact of 1,25(OH)2D3 and its Structural Analogs on Gene Expression in Breast Cancer Cells, colon cancer cells and leukemia cells - A Microarray Approach	(Kriebitzsch et al., 2009)

	1-100nM	Effects of 1α,25-(OH)2D3 on the formation and activity of osteoclasts in RAW264.7 cells	(Gu et al., 2015)
Farnesoid X Receptor Chenodeoxycholic acid **20uM – 200uM**	0-200uM & 100uMBest	Chenodeoxycholic acid stimulates the progression of human esophageal cancer cells, role in VEGF expression.	(Soma et al., 2006)
	50/100/200uM	Direct Effect of Chenodeoxycholic Acid on Differentiation of Mouse Embryonic Stem Cells Cultured under Feeder-Free Culture Conditions	(Park et al., 2013)
	20/40uM	Chenodeoxycholic acid, an endogenous FXR ligand alters adipokines and reverses insulin resistance in 3T3-L1 preadipocytes	(Shihabudeen et al., 2015)
	50uM	Significant impact on the expression of miRNAs and genes involved in lipid, bile acid and drug metabolism in human hepatocytes	(Krattinger et al., 2016)
Aryl Hydrocarbon Receptor ITE "2-(1H-Indol-3-ylcarbonyl)-4-thiazolecarboxylic acid methyl ester" **0.1uM – 2uM**	1uM	The Aryl Hydrocarbon Receptor Ligand ITE Inhibits TGFβ1-Induced Human Myofibroblast Differentiation	(Lehmann et al., 2011)
	100nM	Activation of the aryl hydrocarbon receptor affects activation and function of human monocyte-derived dendritic cells	(Wang et al., 2014)
	500nM	Xeno-sensing activity of the aryl hydrocarbon receptor in human pluripotent stem cell-derived hepatocyte-like cells	(Kim et al., 2016)
	0.001 – 1uM with1uM best	Effects of AhR ligands on the production of immunoglobulins in purified mouse B cells	(Yoshida et al., 2012)
	10nM 50nM & 100nM with 100nM best	An aryl hydrocarbon receptor ligand acts on dendritic cells and T cells to suppress the Th17 response in allergic rhinitis patients. Reduction of pre-inflammatory cytokine release	(Wei et al., 2014)
HIPPO Signalling Pathway Y27632 **5uM – 20uM**	10uM	Culture of pluripotent stem cell upon single cell dissociation	C.Denning Lab SOP
	10uM	Single cell culture of small intestinal crypt cells	(Yin et al., 2014)
	20uM	HIPPO pathway regulation by cell morphology and stress fibers	(Wada et al., 2011)
	50uM	Role of YAP/TAZ in mechanotransduction. Use of Y27632 reduces significantly nuclear YAP/TAZ translocation	(Dupont et al., 2011)
	3uM, 10uM and 30uM	Down-regulation of RhoA is involved in the cytotoxic action of lipophilic statins in HepG2 cells	(Maeda et al., 2010)
HIPPO Signalling Path-	1-50uM	Induction of an inflammatory response in human hepatocytes by cate-	(Aninat et al., 2008)

way Epinephrine **0.05uM – 5uM**		cholamines (epinephrine)	
	30nM	B2 adrenergic receptor is a key regular of hepatic autophagy and epinephrine stimulates autophagic flux in hepatoma cells, primary hepatocytes and *in vivo*.	(Farah et al., 2014)
	2.72uM	Epinephrine Activation of the β2-Adrenoceptor Is Required for IL-13-Induced Mucin Production in Human Bronchial Epithelial Cells	(Al-Sawalha et al., 2015)
	1nM and 1uM	Differential β2-adrenergic receptor expression defines the phenotype of non-tumorigenic and malignant human breast cell lines. Study the effect of the 2 concentrations on cell adhesion and migration of breast cancer cell line.	(Gargiulo et al., 2014)
	50nM to 1uM with 50nM best	Crosstalk Between Adrenergic and Toll-Like Receptors in Human Mesenchymal Stem Cells and Keratinocytes. EPI induces TLR2, MyD88, and IL-6 expression in BM-MSCs	(Dasu et al., 2014)
HIPPO Signalling Pathway Glucagon **0.1uM – 2uM**	1uM	Periportal hepatocytes culture and treatment. PGC-1α Promotes Ureagenesis in Mouse Periportal Hepatocytes through SIRT3 and SIRT5 in Response to Glucagon	(Li et al., 2016)
	100nM	Glucagon inhibits glucose-induced glucokinase translocation and glucose phosphorylation in rat hepatocytes	(Cullen et al., 2014)
	25nM	Rat hepatocytes incubated with glucagon to assess FGF21 secretion via a mechanism not involving changes in FGF21 mRNA abundance	(Cyphert et al., 2014)
	100nM	The effect of glucagon stimulation upon venlafaxine and atenolol treatment in glucose production in rainbow trout hepatocytes	(Ings et al., 2012)
	1uM	Glucagon treated hepatocytes had increased expression of aquaporin in the cellular membrane, increased water transport during cryopreservation, and increased post-thaw viability in rat primary hepatocytes	(Kumar et al., 2015)
Peroxisome proliferator-activated receptors (PPAR) GW7647 **0.5uM – 5uM**	1-10uM	A map of the PPARα transcription regulatory network for primary human hepatocytes. Activation of PPARa in human hepatocytes	(McMullen et al., 2014)
	1uM	PPARα-mediated SREBP1c activation through an LXRE binding site. Human SREBP1c Expression in Liver Is Directly Regulated by Peroxisome Proliferator-activated Receptor α (PPARα)	(Fernández-Alvarez et al., 2011)

	0.01, 0.1 and 1uM with 1uM best	Long-Term Stability of Primary Rat Hepatocytes in Micropatterned Co-cultures	(Ukairo et al., 2013)
	0.1, 0.25 & 0.5 uM with 0.5 as best	Roles of a-linolenic acid on IGF-I secretion and GH/IGF system gene expression in porcine primary hepatocytes. GW7647 (0.1, 0.25 and 0.5 uM) IGF-I secretion in a dose-dependent manner.	(Fang et al., 2012b)
	1uM	Morphological and Functional Characterization and Assessment of iPSC-Derived Hepatocytes for *In vitro* Toxicity Testing. Evaluation of nuclear receptor-mediated CYP450 induction of target genes in primary human hepatocytes.	(Lu et al., 2015)
Canonical WNT pathway CHIR99021 **3uM – 10uM**	5uM	Previous work with CHI99021 showed increased CYP450 1A2 expression	In-lab trial experiments
	3uM	GSK3 inhibitors CHIR99021 and 6-bromoindirubin-3'-oxime inhibit microRNA maturation in mouse embryonic stem cells	(Wu et al., 2015)
	3uM	Effect of Gsk3 inhibitor CHIR99021 on aneuploidy levels in rat embryonic stem cells	(Bock et al., 2014)
	3uM	CHIR99021 and valproic acid, synergistically maintain self-renewal of mouse Lgr5+ intestinal stem cells, resulting in nearly homogeneous cultures	(Yin et al., 2014)
	3uM to 50uM	Demonstrated that in primary human hepatocytes wnt3a activations acts as a major regulator of the zonal organization	(Briolotti et al., 2015)
Hypoxia Signalling Cobalt(II) chloride hexahydrate **50uM – 200uM**	100uM	Study evaluating the effect inducing cobalt chloride hexahydrate in cancer cell lines to correspond a 5% Oxygen level in the final culture	(Wu and Yotnda, 2011)
	42uM – 420uM	Effect of cobalt(II) chloride hexahydrate on some human cancer cell lines. Induces more cell death in cancerous cells as compared to normal non-cancerous cells	(Mahey et al., 2016)
Epigenetics and Methylation 5-Aza-2'-deoxycytidine **1uM – 10uM**	10uM	Efficient Programming of Human Mesenchymal Stem Cell Derived Hepatocytes by Epigenetic Regulations. Beneficial impact to apply HDACi and DNMTi as potent modulators for hMSCs to liver differentiation – During differentiation stage 2	(Tsai et al., 2016)
	1-500uM with 1-	Synergetic effects of DNA demethylation and histone deacetylase inhi-	(Fraczek et al., 2012)

	10uM best	bition in primary rat hepatocytes. The combination of lower concentrations of DAC promoted the maintenance of the differentiated phenotype of the cells as a function of culture time	
	5uM	5-Aza-2'-deoxycytidine (5-Aza-dC) and AhR receptor activation by PCB 126, increases Expression of CYP450 1A1 mRNA in HeLa Cells	(Vorrink et al., 2014)
	20uM	Effect of Chromatin-Remodelling Agents in Hepatic Differentiation of Rat Bone Marrow-Derived Mesenchymal Stem Cells *In vitro* and *In vivo* – Pre-treatment before differentiation	(Ye et al., 2016)
Epigenetics and Histone Deacetylation Inhibitor Trichostatin A **1uM – 20uM**	25uM	Effects of Trichostatin A on drug uptake transporters in primary rat hepatocyte cultures. TSA does not seem to exert a positive effect on the expression and activity of the investigated uptake transporters in primary rat hepatocyte cultures	(Ramboer et al., 2015a)
	1uM	Efficient Programming of Human Mesenchymal Stem Cell Derived Hepatocytes by Epigenetic Regulations. Beneficial impact to apply HDACi and DNMTi as potent modulators for hMSCs to liver differentiation	(Tsai et al., 2016)
	1uM	Trichostatin A induces differential cell cycle arrests but does not induce apoptosis in primary cultures of mitogen-stimulated rat hepatocytes	(Papeleu et al., 2003)
	25uM, 50uM	A metabolic screening study of trichostatin A (TSA) and TSA-like histone deacetylase inhibitors in rat and human primary hepatocyte cultures	(Elaut et al., 2007)
	250nM and 500nM	Histone deacetylase inhibitor trichostatin A induces cell-cycle arrest/apoptosis and hepatocyte differentiation in human hepatoma cells.	(Yamashita et al., 2003)
Epigenetic and Histone Deacetylase Inhibitor Sodium butyrate	1mM	Efficient differentiation of hepatocytes from human embryonic stem cells exhibiting markers recapitulating liver development *in vivo*. NaB treatment during endoderm specification	(Hay et al., 2008b)
	1mM or 2.5mM	Efficient derivation of functional hepatocytes from mouse induced pluripotent stem cells by a combination of cytokines and sodium butyrate	(Zhang et al., 2011c)

0.5uM – 5000uM		during stage 2	
	1mM – 5mM	Sodium butyrate preserves aspects of the differentiated phenotype of normal adult rat hepatocytes in culture	(Staecker et al., 1988)
	2.5mM	Differentiation of mouse embryonic stem cells into hepatocytes induced by a combination of cytokines and sodium butyrate	(Zhou et al., 2010)
	250nM	Cost-effective differentiation of hepatocyte-like cells from human pluripotent stem cells using small molecules and sodium butyrate during the second stage of differentiation	(Tasnim et al., 2015)
Hormones Progesterone **0.05uM – 5uM**	10, 25 and 50nM	Effect of sex hormones on n-3 polyunsaturated fatty acid biosynthesis in HepG2 cells and in human primary hepatocytes	(Sibbons et al., 2014)
	1uM or 10uM	Elimination of estradiol and progesterone in culture of human hepatocytes. Rapidly metabolised.	(Choi et al., 2013)
	540nM and 5.4uM	Induction of Hepatic CYP450 3A Enzymes by Pregnancy-Related Hormones: Studies in Human Hepatocytes and Hepatic Cell Lines	(Papageorgiou et al., 2013)
	1uM	Treatment of HepG2 cells with estradiol and Progesterone investigating role of progesterone and estradiol in insulin resistance through constitutive androstane receptor	(Masuyama and Hiramatsu, 2011)
Hormones Testosterone **0.05uM – 1uM**	100nM	Upregulation of androgen receptor in human skeletal muscle and cultured muscle satellite cells upon testosterone treatment	(Sinha-Hikim et al., 2004)
	100uM	Study of CYP450 related enzymes upon testosterone treatment. Testosterone 6β-hydroxylase activity	(Kostrubsky et al., 1999)
	1-500nM	Treatment of HepG2 cells to investigate connection to androgen/estrogen treatment	(Chen et al., 2012a)
	10, 25 and 50nM	Effect of sex hormones on n-3 polyunsaturated fatty acid biosynthesis in HepG2 cells and in human primary hepatocytes	(Sibbons et al., 2014)
	10nM	Role for testosterone in vascular calcification in mouse vascular smooth muscle cell	(Zhu et al., 2016)
Hormones 17β Estradiol	10uM	Study of steroid metabolism and role of 3β-Hydroxysteroid Dehydrogenase in isolated pig hepatocytes	(Chen et al., 2015a)
	1-100nM	Detection of MDM2 oncogene alterations, in cultured human hepato-	(Schlott et al., 2002)

0.01uM – 2uM		cytes treated with 17beta-estradiol or 17alpha-ethinylestradiol	
	70nM	Effects of 17-Beta-estradiol related to transformation and tumorigenesis in human breast epithelial cells	(Russo et al., 2006)
	1uM	Elimination of estradiol and progesterone in culture of human hepatocytes. Rapidly metabolised	(Choi et al., 2013)
	1-100nM	Studying the role of 17Beta-estradiol at endothelin-1 expression and release in human endothelial cells	(Bilsel et al., 2000)
	10nM	Treatment of HepG2 cells to investigate connection to androgen/estrogen treatment	(Chen et al., 2012a)
Antioxidants Ascorbic Acid **0.1mM – 2mM**	0.245uM	Hepatocyte Differentiation protocol in Nottingham	
	0.1mM	Coexposure of HepG2 cells to physiological concentrations of some micronutrients, like β-carotene (10 μM) or ascorbic acid (0.1 mM), along with Pb (1 mg/L) for 24 h significantly reduced the levels of ROS production and recovered AhR mRNA expression into the normal levels	(Darwish et al., 2016)
	0.1mM and 1mM	Ascorbic acid partly antagonizes resveratrol mediated heme oxygenase-1 but not paraoxonase-1 induction in cultured hepatocytes - role of the redox-regulated transcription factor Nrf2	(Wagner et al., 2011)
	100uM	Isolation of hADMSC and culture. Properties of Hepatocyte-like Cell clusters from Human Adipose Tissue-Derived Mesenchymal Stem Cells	(Okura et al., 2010)
	1mM	Long-Term Culture and Coculture of Primary Rat and Human Hepatocytes	(Shulman and Nahmias, 2013)
Lipid Mixture 1 **1x – 10x**	100x Use as 1x	Directions from Sigma website	
Insulin **0.01uM – 2uM**	100nM	Culture of primary human HEPs for study of CYP450 enzyme expression	(Kostrubsky et al., 1999)
	10nM	Culture of primary rat hepatocytes	(Cullen et al., 2014)
	1uM	Differentiation of hepatocytes from human embryonic stem cells exhibiting markers recapitulating liver development *in vivo*	(Hay et al., 2008b)
	1uM	Specification of human definitive endoderm cells into hepatocytes	(Toivonen et al., 2013)
	10nM	Pathogenesis of Selective Insulin Resistance in Isolated mouse primary	(Cook et al., 2015)

		Hepatocytes	
PI3K Pathway Inhibition LY294002 **5uM – 20uM**	10uM	Inhibition of PI3K in hepatocytes and study on inducible nitric oxide synthase expression	(Zhang et al., 2011a)
	10uM	Studying the role of SLIT-ROBO signalling in proliferative diabetic retinopathy and retinal pigment epithelial cells	(Zhou et al., 2011)
	10uM	Study the effect of PI3K inhibition on calcium signalling in airway smooth muscle cells	(Tolloczko et al., 2004)
	50uM	Mouse hepatoma, rat hepatoma and primary mouse hepatocytes treated to study hepatic gluconeogenesis	(He et al., 2009)
Energy source D-Glucose **1mM – 10mM**	3.9 – 7.2mM	Liver maintenance of blood glucose levels	(Davidson et al., 2016)
	4mM for lipid studies, 11mM for maintenance	Human pHEP culture in QMC	
	5mM Glucose	Mouse ES cells for neural differentiation studies	(Yang et al., 2016)
	1mM, 5mM and 25mM with 5mM as ideal	Bone marrow stem cells maintained in hydrogel for viability studies and production of key matrix proteins	(Naqvi and Buckley, 2015)
Energy source GlutaMAX **1x – 5x**	100x and use at 1x		
Bile Acid Homeostasis FGF19 **10ng/ml – 30ng/ml**	40ng/ml for 10,30 and 60min	FGF19 in human hepatocytes activation through bile acids	(Song et al., 2009a)
	0.01 – 10ng/ml	Increased proliferation of HCC cells upon treatment with FGF19. Highest when FGF19 was 1ng/ml	(Miura et al., 2012)
Protein Supplementation BSA Solution **0% - 0.2%**	0.1%	Human pHEP culture in QMC	
	0.2%	Isolation and Culture of Animal and Human Hepatocytes	(Guguen-Guillouzo and Guillouzo, 2010)
	0.075%	Culture of human primary hepatocyte cells	(Levy et al., 2015)
Human Primary Hepato-	Used at 1x to sup-	Zinc Sulphate, Copper sulphate, Sodium Selenite, Nicotinamide	

cyte Culture MS-1 (Elements) **1x – 5x**	plement basic pHEPs Medium		
Human Primary Hepato-	15ug/ml	Human pHEP culture in QMC	
cyte Culture MS-2 (Transferrin) **5ug/ml – 25ug/ml**	40ug/ml	Human cells cultured in bovine or human diferric transferrin at 40ug/ml.	(Young and Garner, 1990)

Table 26 Fractional Factorial experiment for DoE#1. Factor combinations and concentrations within each DoE#1 run. Red/Green-shaded represent the low/high concentration respectively while yellow-shaded are the centre points. All combinations added to Medium C utilising the automated Liquid Handling Arm.

Run	cAMP	LCA	TCA	VK2	FH1	T3	DHX	VPF	HGF	OSM	H/C	FBS
1	100	10	25	5	5	10	10	2.5	5	5	1	0
2	100	10	25	100	5	10	200	40	50	5	1	8.3
3	1000	100	25	100	30	10	200	2.5	5	50	1	8.3
4	1000	10	25	100	5	100	10	2.5	50	50	10	0
5	1000	10	200	100	5	10	10	40	5	50	1	0
6	550	55	112.5	52.5	17.5	55	105	21.25	27.5	27.5	5.5	4.15
7	1000	100	25	100	30	10	200	2.5	5	50	1	8.3
8	100	100	200	5	5	10	200	40	5	50	10	0
9	1000	100	25	5	5	10	10	40	50	5	10	8.3
10	1000	100	25	100	5	10	200	2.5	5	5	10	0
11	1000	100	200	100	30	100	200	40	50	50	10	8.3
12	1000	100	200	100	30	100	200	40	50	50	10	8.3
13	100	10	200	5	30	100	10	40	50	50	1	8.3
14	1000	100	200	5	5	100	10	2.5	5	5	1	8.3
15	1000	10	25	100	30	100	10	2.5	50	5	1	8.3
16	100	10	25	5	30	10	10	2.5	5	50	10	8.3
17	1000	10	25	5	30	100	200	40	5	5	1	0
18	100	10	200	5	5	100	10	40	50	5	10	0
19	100	10	200	5	30	100	10	40	50	50	1	8.3
20	1000	10	25	5	30	100	200	40	5	5	1	0
21	1000	100	200	5	30	100	10	2.5	5	50	10	0
22	100	10	25	5	30	10	10	2.5	5	50	10	8.3
23	1000	10	200	5	5	10	200	2.5	50	50	1	8.3
24	1000	10	200	100	30	10	10	40	5	5	10	8.3
25	100	100	200	5	5	10	200	40	5	50	10	0
26	1000	100	200	5	30	100	10	2.5	5	50	10	0
27	550	55	112.5	52.5	17.5	55	105	21.25	27.5	27.5	5.5	4.15
28	100	100	25	100	5	100	10	40	5	50	1	8.3
29	100	10	200	5	5	100	10	40	50	5	10	0
30	550	55	112.5	52.5	17.5	55	105	21.25	27.5	27.5	5.5	4.15
31	100	10	25	5	5	10	10	2.5	5	5	1	0
32	100	100	25	100	30	100	10	40	5	5	10	0
33	1000	10	25	5	5	100	200	40	5	50	10	8.3
34	100	10	200	100	5	100	200	2.5	5	5	10	8.3
35	100	100	25	5	30	100	200	2.5	50	5	10	8.3
36	100	10	200	100	30	100	200	2.5	5	50	1	0
37	1000	10	200	5	30	10	200	2.5	50	5	10	0
38	1000	100	200	100	5	100	200	40	50	5	1	0
39	1000	100	200	5	30	100	10	2.5	5	50	10	0
40	100	10	25	100	30	10	200	40	50	50	10	0
41	550	55	112.5	52.5	17.5	55	105	21.25	27.5	27.5	5.5	4.15
42	1000	100	25	100	5	10	200	2.5	5	5	10	0
43	1000	10	200	100	5	10	10	40	5	50	1	0
44	1000	100	200	5	5	100	10	2.5	5	5	1	8.3
45	1000	10	200	100	30	10	10	40	5	5	10	8.3
46	100	100	200	100	5	10	10	2.5	50	50	10	8.3
47	100	10	200	100	30	100	200	2.5	5	50	1	0
48	100	100	200	100	30	10	10	2.5	50	5	1	0
49	100	100	25	100	5	100	10	40	5	50	1	8.3
50	100	100	25	5	5	100	200	2.5	50	50	1	0
51	100	100	200	100	30	10	10	2.5	50	5	1	0
52	100	100	25	100	30	100	10	40	5	5	10	0
53	1000	10	25	5	30	100	200	40	5	5	1	0
54	1000	100	25	100	30	10	200	2.5	5	50	1	8.3
55	1000	10	200	5	30	10	200	2.5	50	5	10	0
56	100	10	200	100	5	100	200	2.5	5	5	10	8.3
57	1000	10	200	100	30	10	10	40	5	5	10	8.3
58	100	10	25	100	30	10	200	40	50	50	10	0
59	100	10	200	5	5	100	10	40	50	5	10	0
60	1000	10	200	100	5	10	10	40	5	50	1	0
61	1000	100	25	5	30	10	10	40	50	50	1	0
62	100	100	25	5	30	100	200	2.5	50	5	10	8.3
63	1000	10	25	5	5	100	200	40	5	50	10	8.3
64	1000	10	200	5	5	10	200	2.5	50	50	1	8.3
65	1000	10	200	5	5	10	200	2.5	50	50	1	8.3
66	1000	100	200	100	5	100	200	40	50	5	1	0
67	100	100	200	5	30	10	200	40	5	5	1	8.3
68	1000	10	25	100	30	100	10	2.5	50	5	1	8.3
69	100	10	200	100	5	100	200	2.5	5	5	10	8.3
70	1000	100	25	5	30	10	10	40	50	50	1	0

Run	cAMP	LCA	TCA	VK2	FH1	T3	DHX	VPF	HGF	OSM	H/C	FBS
71	100	100	200	5	30	10	200	40	5	5	1	8.3
72	100	100	25	5	30	100	200	2.5	50	5	10	8.3
73	100	100	25	5	5	100	200	2.5	50	50	1	0
74	1000	10	200	5	30	10	200	2.5	50	5	10	0
75	1000	10	25	100	5	100	10	2.5	50	50	10	0
76	100	10	25	100	5	10	200	40	50	5	1	8.3
77	100	100	200	100	5	10	10	2.5	50	50	10	8.3
78	100	10	25	100	5	10	200	40	50	5	1	8.3
79	1000	10	25	100	5	100	10	2.5	50	50	10	0
80	100	10	200	100	30	100	200	2.5	5	50	1	0
81	1000	100	25	5	30	10	10	40	50	50	1	0
82	1000	10	25	100	30	100	10	2.5	50	5	1	8.3
83	1000	10	25	5	5	100	200	40	5	50	10	8.3
84	550	55	112.5	52.5	17.5	55	105	21.25	27.5	27.5	5.5	4.15
85	100	10	25	5	5	10	10	2.5	5	5	1	0
86	100	100	200	100	5	10	10	2.5	50	50	10	8.3
87	100	100	200	100	30	10	10	2.5	50	5	1	0
88	100	10	25	5	30	10	10	2.5	5	50	10	8.3
89	1000	100	200	100	5	100	200	40	50	5	1	0
90	100	10	25	100	30	10	200	40	50	50	10	0
91	1000	100	25	100	5	10	200	2.5	5	5	10	0
92	100	100	25	100	30	100	10	40	5	5	10	0
93	1000	100	25	5	5	10	10	40	50	5	10	8.3
94	100	100	25	100	5	100	10	40	5	50	1	8.3
95	1000	100	200	100	30	100	200	40	50	50	10	8.3
96	100	10	200	5	30	100	10	40	50	50	1	8.3
97	100	100	25	5	5	100	200	2.5	50	50	1	0
98	550	55	112.5	52.5	17.5	55	105	21.25	27.5	27.5	5.5	4.15
99	100	100	200	5	5	10	200	40	5	50	10	0
100	100	100	200	5	30	10	200	40	5	5	1	8.3
101	1000	100	25	5	5	10	10	40	50	5	10	8.3
102	1000	100	200	5	5	100	10	2.5	5	5	1	8.3

Run	SR11237	Bexarotene	LY294002	Flavone	Trichostatin A	Epinephrine	Cobalt Cl Hex	KSR	OSM	H/C	Cheno Acid
1	1.20	4.10	16.62	66.47	5.28	1.20	83.82	2.25	39.85	15.49	60.58
2	2.55	3.00	12.50	50.00	20.00	2.55	125.00	5.00	27.50	10.00	110.00
3	1.20	4.10	8.38	66.47	5.28	3.90	83.82	7.75	15.15	15.49	60.58
4	2.55	3.00	12.50	50.00	10.50	2.55	125.00	5.00	27.50	10.00	110.00
5	3.90	1.90	8.38	66.47	5.28	3.90	83.82	7.75	15.15	4.51	159.42
6	3.90	1.90	16.62	66.47	5.28	1.20	166.18	2.25	39.85	15.49	159.42
7	1.20	1.90	16.62	66.47	5.28	3.90	83.82	2.25	15.15	15.49	159.42
8	3.90	4.10	8.38	66.47	15.72	1.20	83.82	2.25	15.15	15.49	60.58
9	5.00	3.00	12.50	50.00	10.50	2.55	125.00	5.00	27.50	10.00	110.00
10	2.55	1.00	12.50	50.00	10.50	2.55	125.00	5.00	27.50	10.00	110.00
11	2.55	3.00	12.50	20.00	10.50	2.55	125.00	5.00	27.50	10.00	110.00
12	1.20	4.10	16.62	66.47	5.28	3.90	83.82	7.75	39.85	4.51	159.42
13	2.55	3.00	12.50	50.00	10.50	2.55	125.00	5.00	27.50	10.00	200.00
14	3.90	4.10	16.62	66.47	15.72	1.20	166.18	7.75	39.85	4.51	60.58
15	3.90	4.10	8.38	66.47	15.72	3.90	166.18	7.75	15.15	15.49	159.42
16	3.90	1.90	8.38	33.53	5.28	1.20	166.18	7.75	39.85	4.51	159.42
17	2.55	3.00	12.50	50.00	10.50	2.55	125.00	5.00	27.50	10.00	20.00
18	3.90	4.10	8.38	66.47	5.28	1.20	166.18	2.25	39.85	15.49	60.58
19	1.20	1.90	16.62	33.53	5.28	1.20	83.82	7.75	39.85	15.49	159.42
20	2.55	3.00	12.50	50.00	10.50	2.55	125.00	5.00	27.50	20.00	110.00
21	2.55	3.00	12.50	50.00	10.50	2.55	125.00	0.00	27.50	10.00	110.00
22	3.90	1.90	8.38	66.47	15.72	3.90	166.18	7.75	39.85	4.51	60.58
23	3.90	4.10	16.62	33.53	5.28	3.90	83.82	7.75	15.15	15.49	60.58
24	1.20	1.90	8.38	66.47	15.72	3.90	83.82	2.25	39.85	4.51	159.42
25	1.20	1.90	8.38	33.53	5.28	3.90	166.18	7.75	15.15	4.51	60.58
26	1.20	1.90	16.62	33.53	15.72	1.20	166.18	7.75	39.85	4.51	60.58
27	2.55	3.00	12.50	50.00	10.50	2.55	125.00	5.00	27.50	10.00	110.00
28	2.55	3.00	12.50	80.00	10.50	2.55	125.00	5.00	27.50	10.00	110.00
29	3.90	1.90	16.62	66.47	15.72	3.90	166.18	2.25	15.15	15.49	60.58
30	1.20	4.10	16.62	66.47	15.72	1.20	166.18	2.25	39.85	15.49	159.42
31	1.20	4.10	8.38	33.53	5.28	1.20	166.18	2.25	39.85	4.51	60.58
32	1.20	4.10	8.38	33.53	15.72	1.20	83.82	2.25	39.85	4.51	60.58
33	1.20	1.90	16.62	66.47	15.72	3.90	166.18	7.75	15.15	4.51	159.42
34	3.90	4.10	8.38	33.53	15.72	3.90	83.82	2.25	39.85	15.49	159.42
35	2.55	3.00	12.50	50.00	10.50	2.55	50.00	5.00	27.50	10.00	110.00
36	2.55	3.00	12.50	50.00	10.50	0.10	125.00	5.00	27.50	10.00	110.00
37	3.90	4.10	16.62	66.47	5.28	1.20	166.18	2.25	15.15	4.51	60.58
38	3.90	4.10	16.62	33.53	15.72	1.20	166.18	7.75	39.85	15.49	159.42
39	1.20	4.10	8.38	33.53	5.28	1.20	166.18	7.75	15.15	15.49	159.42
40	3.90	1.90	8.38	33.53	15.72	3.90	83.82	2.25	15.15	15.49	60.58
41	2.55	3.00	5.00	50.00	10.50	2.55	125.00	5.00	27.50	10.00	110.00
42	1.20	1.90	8.38	33.53	5.28	1.20	83.82	2.25	39.85	15.49	159.42
43	1.20	4.10	8.38	33.53	15.72	3.90	166.18	7.75	39.85	15.49	60.58
44	3.90	4.10	16.62	66.47	15.72	3.90	83.82	2.25	15.15	4.51	159.42
45	3.90	1.90	16.62	33.53	15.72	3.90	166.18	7.75	39.85	15.49	159.42
46	2.55	3.00	12.50	50.00	10.50	5.00	125.00	5.00	27.50	10.00	110.00
47	1.20	1.90	8.38	66.47	15.72	3.90	166.18	2.25	15.15	15.49	159.42
48	2.55	3.00	12.50	50.00	10.50	2.55	125.00	5.00	27.50	10.00	110.00
49	3.90	1.90	16.62	33.53	15.72	1.20	83.82	2.25	15.15	15.49	159.42
50	1.20	4.10	16.62	33.53	15.72	3.90	83.82	7.75	15.15	15.49	159.42
51	3.90	1.90	8.38	33.53	5.28	3.90	166.18	2.25	15.15	15.49	159.42
52	3.90	1.90	8.38	66.47	5.28	1.20	166.18	7.75	15.15	15.49	60.58
53	3.90	1.90	16.62	33.53	15.72	3.90	83.82	7.75	15.15	4.51	60.58
54	1.20	4.10	8.38	66.47	15.72	1.20	83.82	7.75	15.15	4.51	159.42
55	3.90	4.10	16.62	66.47	5.28	1.20	83.82	7.75	15.15	15.49	159.42
56	3.90	1.90	8.38	33.53	15.72	1.20	166.18	2.25	39.85	15.49	60.58
57	3.90	4.10	8.38	33.53	15.72	1.20	83.82	7.75	15.15	4.51	60.58
58	1.20	1.90	16.62	66.47	15.72	1.20	83.82	2.25	15.15	4.51	60.58
59	3.90	1.90	8.38	66.47	15.72	1.20	166.18	2.25	15.15	4.51	159.42
60	1.20	4.10	8.38	33.53	15.72	3.90	166.18	7.75	39.85	4.51	159.42
61	2.55	3.00	12.50	50.00	10.50	2.55	125.00	5.00	27.50	10.00	110.00
62	1.20	1.90	16.62	33.53	5.28	1.20	166.18	2.25	15.15	4.51	159.42
63	1.20	1.90	16.62	33.53	15.72	3.90	83.82	2.25	39.85	15.49	60.58
64	3.90	4.10	16.62	33.53	15.72	3.90	166.18	2.25	39.85	4.51	60.58
65	3.90	1.90	8.38	33.53	5.28	1.20	83.82	2.25	15.15	4.51	60.58
66	3.90	4.10	16.62	33.53	5.28	3.90	166.18	7.75	15.15	4.51	159.42
67	1.20	4.10	8.38	33.53	5.28	3.90	83.82	2.25	15.15	4.51	159.42
68	2.55	3.00	12.50	50.00	10.50	2.55	125.00	5.00	50.00	10.00	110.00
69	1.20	1.90	16.62	33.53	5.28	1.20	166.18	2.25	15.15	15.49	60.58
70	3.90	1.90	16.62	66.47	5.28	3.90	166.18	7.75	39.85	4.51	60.58
71	2.55	3.00	20.00	50.00	10.50	2.55	125.00	5.00	27.50	10.00	110.00
72	3.90	4.10	8.38	66.47	5.28	1.20	83.82	2.25	39.85	4.51	159.42
73	2.55	3.00	12.50	50.00	10.50	2.55	125.00	5.00	27.50	0.00	110.00
74	2.55	5.00	12.50	50.00	10.50	2.55	125.00	5.00	27.50	10.00	110.00
75	0.10	3.00	12.50	50.00	10.50	2.55	125.00	5.00	27.50	10.00	110.00
76	2.55	3.00	12.50	50.00	1.00	2.55	125.00	5.00	27.50	10.00	110.00
77	2.55	3.00	12.50	50.00	10.50	2.55	125.00	5.00	27.50	10.00	110.00
78	1.20	4.10	8.38	66.47	5.28	3.90	166.18	2.25	15.15	4.51	159.42
79	2.55	3.00	12.50	50.00	10.50	2.55	200.00	5.00	27.50	10.00	110.00
80	1.20	4.10	16.62	66.47	5.28	1.20	166.18	7.75	15.15	15.49	60.58
81	1.20	4.10	16.62	33.53	5.28	3.90	166.18	2.25	39.85	15.49	159.42
82	1.20	1.90	8.38	33.53	15.72	1.20	83.82	7.75	15.15	15.49	60.58
83	3.90	1.90	16.62	66.47	15.72	1.20	83.82	7.75	39.85	4.51	159.42
84	1.20	1.90	8.38	66.47	5.28	3.90	166.18	7.75	39.85	15.49	159.42
85	3.90	4.10	8.38	66.47	5.28	3.90	83.82	2.25	39.85	4.51	60.58
86	1.20	4.10	16.62	33.53	15.72	1.20	166.18	2.25	15.15	4.51	60.58
87	3.90	4.10	8.38	66.47	15.72	1.20	83.82	7.75	39.85	15.49	159.42
88	2.55	3.00	12.50	50.00	10.50	2.55	125.00	5.00	5.00	10.00	110.00
89	3.90	1.90	8.38	33.53	5.28	3.90	83.82	7.75	39.85	15.49	60.58
90	2.55	3.00	12.50	50.00	10.50	2.55	125.00	10.00	27.50	10.00	110.00
91	1.20	1.90	16.62	66.47	15.72	3.90	83.82	7.75	39.85	15.49	60.58
92	1.20	4.10	16.62	33.53	5.28	1.20	83.82	7.75	15.15	4.51	60.58
93	1.20	1.90	8.38	66.47	5.28	1.20	83.82	7.75	39.85	4.51	60.58
94	3.90	1.90	16.62	33.53	5.28	3.90	83.82	2.25	39.85	4.51	159.42
95	2.55	3.00	12.50	50.00	10.50	2.55	125.00	5.00	27.50	10.00	110.00
96	1.20	4.10	16.62	66.47	15.72	3.90	166.18	2.25	39.85	4.51	60.58

Table 27: Central Composite Design for DoE#2. Table of combinations of the 12 factors to induce maturation of hepatocytes upon hepatocyte differentiation on day 17 following a DoE approach. All combinations were added to Medium C+HGF.

Run	DHX	GW7647	DEX	LCA	Calcitriol	Glucagon	FGF19	BSA Solution	Insulin	OSM	H/C
1	312.07	1.51	3.90	77.48	52.84	1.57	25.49	0.15	1.55	15.15	4.51
2	312.07	3.99	3.90	22.62	157.16	1.57	25.49	0.05	1.55	15.15	4.51
3	97.93	3.99	3.90	22.62	157.16	0.53	25.49	0.05	0.46	15.15	4.51
4	205.00	2.75	2.55	50.05	105.00	1.05	20.00	0.10	1.01	27.50	10.00
5	97.93	3.99	3.90	77.48	52.84	0.53	25.49	0.15	0.46	39.85	4.51
6	205.00	2.75	2.55	50.05	105.00	1.05	20.00	0.10	1.01	27.50	10.00
7	312.07	3.99	1.20	77.48	157.16	0.53	14.51	0.15	1.55	39.85	15.49
8	312.07	1.51	1.20	22.62	157.16	0.53	25.49	0.05	1.55	39.85	4.51
9	97.93	3.99	3.90	22.62	52.84	0.53	14.51	0.15	0.46	15.15	4.51
10	97.93	1.51	3.90	22.62	157.16	0.53	25.49	0.15	1.55	15.15	4.51
11	205.00	2.75	2.55	50.05	105.00	2.00	20.00	0.10	1.01	27.50	10.00
12	205.00	2.75	2.55	100.00	105.00	1.05	20.00	0.10	1.01	27.50	10.00
13	97.93	1.51	1.20	77.48	52.84	0.53	14.51	0.15	1.55	15.15	4.51
14	97.93	3.99	3.90	22.62	52.84	1.57	25.49	0.05	1.55	39.85	15.49
15	97.93	1.51	1.20	22.62	52.84	0.53	14.51	0.05	1.55	39.85	15.49
16	205.00	2.75	2.55	50.05	105.00	1.05	10.00	0.10	1.01	27.50	10.00
17	97.93	1.51	3.90	22.62	52.84	0.53	14.51	0.15	1.55	39.85	15.49
18	97.93	1.51	3.90	22.62	157.16	1.57	14.51	0.05	1.55	39.85	4.51
19	97.93	3.99	3.90	77.48	52.84	0.53	14.51	0.05	1.55	39.85	4.51
20	97.93	1.51	3.90	77.48	157.16	0.53	14.51	0.05	0.46	15.15	4.51
21	205.00	2.75	2.55	50.05	105.00	1.05	20.00	0.10	1.01	27.50	0.00
22	205.00	2.75	0.10	50.05	105.00	1.05	20.00	0.10	1.01	27.50	10.00
23	97.93	3.99	3.90	22.62	157.16	1.57	14.51	0.15	0.46	39.85	15.49
24	97.93	3.99	1.20	22.62	157.16	1.57	25.49	0.15	1.55	39.85	4.51
25	312.07	1.51	1.20	77.48	157.16	0.53	25.49	0.05	0.46	15.15	15.49
26	205.00	2.75	2.55	50.05	105.00	1.05	20.00	0.10	1.01	27.50	10.00
27	205.00	0.50	2.55	50.05	105.00	1.05	20.00	0.10	1.01	27.50	10.00
28	205.00	2.75	2.55	50.05	105.00	1.05	20.00	0.10	1.01	27.50	10.00
29	205.00	2.75	2.55	50.05	105.00	1.05	20.00	0.10	1.01	27.50	10.00
30	312.07	3.99	1.20	77.48	52.84	0.53	14.51	0.05	1.55	15.15	15.49
31	97.93	3.99	1.20	22.62	157.16	0.53	14.51	0.05	1.55	15.15	4.51
32	312.07	3.99	1.20	77.48	52.84	0.53	25.49	0.05	1.55	39.85	4.51
33	97.93	3.99	3.90	77.48	157.16	0.53	25.49	0.05	1.55	39.85	15.49
34	312.07	1.51	3.90	22.62	52.84	1.57	14.51	0.05	1.55	15.15	15.49
35	312.07	1.51	3.90	77.48	157.16	0.53	14.51	0.15	1.55	15.15	15.49
36	97.93	1.51	3.90	77.48	157.16	1.57	25.49	0.15	0.46	15.15	15.49
37	205.00	2.75	2.55	50.05	105.00	1.05	20.00	0.00	1.01	27.50	10.00
38	205.00	2.75	2.55	50.05	105.00	1.05	20.00	0.10	1.01	27.50	20.00
39	205.00	2.75	2.55	50.05	105.00	0.10	20.00	0.10	1.01	27.50	10.00
40	312.07	3.99	3.90	77.48	52.84	0.53	25.49	0.05	0.46	15.15	4.51
41	205.00	2.75	2.55	0.10	105.00	1.05	20.00	0.10	1.01	27.50	10.00
42	97.93	1.51	1.20	77.48	52.84	1.57	25.49	0.15	1.55	39.85	15.49
43	312.07	1.51	3.90	77.48	52.84	0.53	25.49	0.05	1.55	39.85	15.49
44	97.93	3.99	1.20	22.62	52.84	0.53	25.49	0.15	0.46	39.85	15.49
45	97.93	1.51	1.20	77.48	157.16	1.57	14.51	0.05	1.55	15.15	15.49
46	312.07	1.51	1.20	22.62	52.84	1.57	25.49	0.05	0.46	39.85	15.49
47	97.93	1.51	3.90	22.62	52.84	0.53	25.49	0.05	0.46	39.85	4.51
48	205.00	2.75	2.55	50.05	105.00	1.05	20.00	0.10	1.01	27.50	10.00
49	97.93	3.99	1.20	22.62	52.84	0.53	25.49	0.05	1.55	15.15	4.51
50	205.00	2.75	2.55	50.05	105.00	1.05	30.00	0.10	1.01	27.50	10.00
51	312.07	3.99	3.90	22.62	52.84	1.57	14.51	0.15	0.46	39.85	4.51
52	400.00	2.75	2.55	50.05	105.00	1.05	20.00	0.10	1.01	27.50	10.00
53	312.07	1.51	3.90	22.62	157.16	1.57	14.51	0.15	0.46	15.15	4.51
54	312.07	1.51	3.90	22.62	157.16	1.57	25.49	0.15	1.55	39.85	15.49
55	205.00	2.75	2.55	50.05	200.00	1.05	20.00	0.10	1.01	27.50	10.00
56	312.07	3.99	3.90	22.62	52.84	1.57	25.49	0.15	0.46	15.15	15.49
57	312.07	3.99	3.90	77.48	52.84	0.53	14.51	0.15	0.46	39.85	15.49
58	312.07	1.51	1.20	22.62	52.84	0.53	25.49	0.15	1.55	15.15	15.49
59	312.07	3.99	3.90	77.48	157.16	0.53	25.49	0.15	1.55	15.15	4.51
60	312.07	1.51	1.20	22.62	157.16	1.57	14.51	0.05	0.46	39.85	4.51
61	312.07	3.99	1.20	22.62	157.16	0.53	14.51	0.15	0.46	15.15	4.51
62	97.93	3.99	3.90	77.48	157.16	1.57	25.49	0.05	1.55	15.15	4.51
63	97.93	1.51	3.90	77.48	157.16	1.57	14.51	0.15	1.55	39.85	4.51
64	312.07	1.51	3.90	22.62	157.16	0.53	14.51	0.05	0.46	39.85	15.49
65	312.07	3.99	1.20	22.62	157.16	1.57	14.51	0.05	1.55	39.85	15.49
66	97.93	1.51	1.20	77.48	157.16	1.57	25.49	0.05	0.46	39.85	15.49
67	205.00	2.75	2.55	50.05	105.00	1.05	20.00	0.10	2.00	27.50	10.00
68	312.07	1.51	1.20	22.62	52.84	0.53	14.51	0.05	0.46	15.15	4.51
69	97.93	3.99	1.20	22.62	157.16	1.57	25.49	0.15	1.55	15.15	15.49
70	312.07	3.99	3.90	77.48	157.16	1.57	14.51	0.05	0.46	15.15	15.49
71	205.00	2.75	2.55	50.05	105.00	1.05	20.00	0.20	1.01	27.50	10.00
72	205.00	2.75	2.55	50.05	105.00	1.05	20.00	0.10	1.01	50.00	10.00
73	97.93	1.51	1.20	22.62	52.84	1.57	25.49	0.15	0.46	15.15	4.51
74	97.93	1.51	1.20	22.62	157.16	0.53	14.51	0.15	0.46	39.85	4.51
75	312.07	3.99	1.20	77.48	52.84	1.57	14.51	0.05	1.55	15.15	4.51
76	312.07	1.51	3.90	77.48	157.16	1.57	25.49	0.05	0.46	39.85	4.51
77	10.00	2.75	2.55	50.05	105.00	1.05	20.00	0.10	1.01	27.50	10.00
78	97.93	3.99	1.20	77.48	52.84	1.57	14.51	0.15	0.46	39.85	4.51
79	97.93	3.99	1.20	77.48	52.84	1.57	25.49	0.05	0.46	15.15	15.49
80	312.07	3.99	1.20	77.48	157.16	0.53	14.51	0.05	0.46	39.85	4.51
81	312.07	1.51	1.20	77.48	52.84	1.57	14.51	0.15	0.46	15.15	15.49
82	205.00	5.00	2.55	50.05	105.00	1.05	20.00	0.10	1.01	27.50	10.00
83	205.00	2.75	5.00	50.05	105.00	1.05	20.00	0.10	1.01	27.50	10.00
84	312.07	3.99	3.90	22.62	157.16	0.53	25.49	0.15	1.55	39.85	15.49
85	312.07	1.51	1.20	77.48	157.16	1.57	25.49	0.15	1.55	15.15	4.51
86	97.93	3.99	1.20	22.62	52.84	1.57	14.51	0.05	0.46	15.15	15.49
87	205.00	2.75	2.55	50.05	10.00	1.05	20.00	0.10	1.01	27.50	10.00
88	205.00	2.75	2.55	50.05	105.00	1.05	20.00	0.10	1.01	5.00	10.00
89	97.93	3.99	3.90	77.48	52.84	1.57	14.51	0.15	1.55	15.15	15.49
90	97.93	3.99	1.20	77.48	157.16	0.53	14.51	0.15	0.46	15.15	15.49
91	312.07	3.99	1.20	77.48	157.16	1.57	25.49	0.15	0.46	39.85	15.49
92	312.07	1.51	1.20	22.62	52.84	1.57	14.51	0.15	1.55	39.85	4.51
93	97.93	1.51	3.90	22.62	52.84	0.53	25.49	0.05	0.46	15.15	15.49
94	205.00	2.75	2.55	50.05	105.00	1.05	20.00	0.10	0.01	27.50	10.00
95	312.07	1.51	1.20	77.48	52.84	0.53	25.49	0.15	0.46	39.85	4.51
96	97.93	1.51	3.90	77.48	52.84	1.57	14.51	0.05	0.46	39.85	15.49

Table 28: Central Composite Design for DoE#3. Table of combinations of the 12 factors to induce maturation of hepatocytes upon hepatocyte differentiation on day 17 following a DoE approach. All combinations were added to Medium C+HGF.

Run	ATRA	CITCO	Testosterone	17β Estradiol	ITE	Y27632	MS-1	Sod But	Asc Acid	OSM	H/C
1	3.03	83.82	0.79	1.55	1571.65	16.62	4.10	3872.86	0.53	15.15	15.49
2	3.03	166.18	0.79	1.55	528.35	8.38	1.90	1127.64	1.57	39.85	4.51
3	3.03	83.82	0.79	0.46	528.35	8.38	1.90	3872.86	1.57	39.85	15.49
4	3.03	166.18	0.26	1.55	1571.65	8.38	1.90	3872.86	0.53	15.15	15.49
5	3.03	83.82	0.26	1.55	1571.65	16.62	4.10	1127.64	0.53	39.85	15.49
6	5.50	125.00	0.53	1.01	1050.00	12.50	3.00	2500.25	1.05	50.00	10.00
7	5.50	125.00	0.53	1.01	2000.00	12.50	3.00	2500.25	1.05	27.50	10.00
8	3.03	166.18	0.79	0.46	1571.65	16.62	1.90	3872.86	0.53	39.85	15.49
9	5.50	125.00	0.53	1.01	1050.00	20.00	3.00	2500.25	1.05	27.50	10.00
10	7.97	83.82	0.26	0.46	528.35	8.38	1.90	1127.64	0.53	15.15	4.51
11	5.50	125.00	0.53	1.01	1050.00	12.50	3.00	2500.25	1.05	27.50	10.00
12	3.03	166.18	0.26	0.46	1571.65	8.38	1.90	1127.64	1.57	15.15	4.51
13	7.97	166.18	0.26	1.55	1571.65	8.38	1.90	1127.64	0.53	39.85	4.51
14	3.03	166.18	0.79	1.55	528.35	8.38	4.10	3872.86	0.53	39.85	4.51
15	5.50	125.00	0.53	1.01	1050.00	12.50	3.00	2500.25	1.05	27.50	20.00
16	3.03	166.18	0.26	0.46	528.35	8.38	4.10	3872.86	0.53	39.85	15.49
17	7.97	83.82	0.26	1.55	1571.65	16.62	4.10	3872.86	1.57	15.15	4.51
18	7.97	166.18	0.79	0.46	1571.65	16.62	4.10	1127.64	1.57	15.15	4.51
19	5.50	125.00	0.53	1.01	1050.00	12.50	3.00	2500.25	1.05	27.50	10.00
20	7.97	166.18	0.26	0.46	1571.65	8.38	1.90	3872.86	0.53	15.15	4.51
21	7.97	83.82	0.79	1.55	528.35	16.62	4.10	3872.86	1.57	15.15	4.51
22	7.97	83.82	0.79	0.46	1571.65	16.62	1.90	3872.86	0.53	15.15	4.51
23	7.97	83.82	0.26	0.46	528.35	16.62	1.90	3872.86	1.57	39.85	4.51
24	5.50	125.00	0.53	1.01	1050.00	12.50	3.00	2500.25	0.10	27.50	10.00
25	3.03	83.82	0.26	0.46	528.35	16.62	4.10	3872.86	0.53	15.15	4.51
26	7.97	83.82	0.79	0.46	1571.65	16.62	4.10	3872.86	1.57	39.85	15.49
27	7.97	83.82	0.79	1.55	528.35	8.38	4.10	1127.64	1.57	39.85	15.49
28	7.97	166.18	0.79	0.46	528.35	16.62	4.10	3872.86	0.53	15.15	15.49
29	3.03	83.82	0.26	1.55	528.35	8.38	1.90	3872.86	1.57	15.15	4.51
30	3.03	166.18	0.26	0.46	528.35	16.62	1.90	1127.64	0.53	15.15	15.49
31	3.03	166.18	0.79	0.46	528.35	16.62	4.10	1127.64	1.57	39.85	15.49
32	5.50	125.00	0.05	1.01	1050.00	12.50	3.00	2500.25	1.05	27.50	10.00
33	5.50	125.00	0.53	1.01	1050.00	12.50	3.00	0.50	1.05	27.50	10.00
34	7.97	166.18	0.26	0.46	1571.65	16.62	1.90	1127.64	1.57	39.85	15.49
35	7.97	83.82	0.26	0.46	528.35	16.62	4.10	1127.64	0.53	39.85	15.49
36	5.50	125.00	0.53	1.01	1050.00	12.50	3.00	2500.25	1.05	27.50	10.00
37	7.97	166.18	0.79	1.55	1571.65	8.38	4.10	3872.86	1.57	15.15	4.51
38	3.03	83.82	0.79	1.55	528.35	16.62	1.90	1127.64	0.53	39.85	15.49
39	7.97	166.18	0.26	1.55	528.35	8.38	1.90	1127.64	1.57	15.15	15.49
40	3.03	83.82	0.79	0.46	1571.65	8.38	4.10	3872.86	1.57	15.15	4.51
41	5.50	125.00	0.53	1.01	1050.00	12.50	3.00	2500.25	2.00	27.50	10.00
42	3.03	166.18	0.26	0.46	528.35	8.38	4.10	1127.64	1.57	15.15	4.51
43	7.97	83.82	0.79	1.55	1571.65	8.38	1.90	3872.86	1.57	15.15	15.49
44	7.97	166.18	0.79	1.55	1571.65	16.62	1.90	1127.64	0.53	15.15	15.49
45	5.50	125.00	0.53	1.01	1050.00	12.50	1.00	2500.25	1.05	27.50	10.00
46	3.03	83.82	0.79	1.55	1571.65	8.38	1.90	1127.64	0.53	15.15	4.51
47	3.03	166.18	0.79	0.46	1571.65	8.38	4.10	1127.64	0.53	15.15	4.51
48	3.03	83.82	0.26	1.55	1571.65	16.62	1.90	1127.64	1.57	15.15	15.49
49	7.97	166.18	0.79	0.46	528.35	16.62	1.90	3872.86	0.53	39.85	4.51
50	7.97	166.18	0.79	1.55	528.35	8.38	4.10	1127.64	0.53	15.15	4.51
51	5.50	200.00	0.53	1.01	1050.00	12.50	3.00	2500.25	1.05	27.50	10.00
52	3.03	83.82	0.79	1.55	1571.65	16.62	1.90	3872.86	1.57	39.85	4.51
53	5.50	125.00	0.53	1.01	1050.00	12.50	3.00	2500.25	1.05	27.50	0.00
54	5.50	125.00	0.53	1.01	1050.00	12.50	3.00	2500.25	1.05	27.50	10.00
55	7.97	83.82	0.26	0.46	1571.65	16.62	1.90	1127.64	0.53	39.85	4.51
56	7.97	83.82	0.26	1.55	528.35	8.38	4.10	3872.86	0.53	39.85	4.51
57	3.03	83.82	0.79	0.46	528.35	8.38	4.10	1127.64	0.53	39.85	4.51
58	3.03	166.18	0.26	0.46	1571.65	16.62	4.10	3872.86	1.57	39.85	4.51
59	5.50	125.00	0.53	1.01	1050.00	12.50	3.00	2500.25	1.05	27.50	10.00
60	3.03	83.82	0.26	1.55	528.35	16.62	4.10	3872.86	1.57	39.85	15.49
61	7.97	83.82	0.79	0.46	1571.65	8.38	1.90	1127.64	0.53	39.85	15.49
62	3.03	166.18	0.79	1.55	1571.65	16.62	4.10	1127.64	1.57	15.15	4.51
63	3.03	166.18	0.26	1.55	528.35	16.62	4.10	1127.64	0.53	15.15	15.49
64	5.50	125.00	0.53	1.01	1050.00	12.50	5.00	2500.25	1.05	27.50	10.00
65	3.03	83.82	0.79	0.46	528.35	8.38	4.10	1127.64	0.53	15.15	15.49
66	7.97	166.18	0.26	1.55	528.35	16.62	1.90	1127.64	1.57	15.15	4.51
67	7.97	83.82	0.26	0.46	1571.65	8.38	4.10	1127.64	1.57	39.85	4.51
68	3.03	166.18	0.79	1.55	1571.65	8.38	4.10	1127.64	1.57	39.85	15.49
69	3.03	83.82	0.26	0.46	1571.65	8.38	1.90	3872.86	0.53	39.85	4.51
70	5.50	125.00	0.53	1.01	100.00	12.50	3.00	2500.25	1.05	27.50	10.00
71	5.50	125.00	0.53	0.01	1050.00	12.50	3.00	2500.25	1.05	27.50	10.00
72	7.97	83.82	0.26	1.55	528.35	16.62	1.90	3872.86	0.53	15.15	15.49
73	7.97	166.18	0.79	1.55	528.35	8.38	1.90	3872.86	0.53	39.85	15.49
74	3.03	166.18	0.79	1.55	528.35	16.62	1.90	3872.86	1.57	15.15	15.49
75	5.50	125.00	1.00	1.01	1050.00	12.50	3.00	2500.25	1.05	27.50	10.00
76	1.00	125.00	0.53	1.01	1050.00	12.50	3.00	2500.25	1.05	27.50	10.00
77	5.50	50.00	0.53	1.01	1050.00	12.50	3.00	2500.25	1.05	27.50	10.00
78	5.50	125.00	0.53	1.01	1050.00	12.50	3.00	2500.25	1.05	5.00	10.00
79	5.50	125.00	0.53	1.01	1050.00	12.50	3.00	2500.25	1.05	27.50	10.00
80	3.03	166.18	0.79	0.46	528.35	8.38	1.90	3872.86	0.53	15.15	4.51
81	7.97	166.18	0.26	1.55	1571.65	16.62	4.10	3872.86	0.53	39.85	15.49
82	7.97	83.82	0.26	0.46	528.35	8.38	4.10	3872.86	1.57	15.15	15.49
83	7.97	83.82	0.79	1.55	1571.65	16.62	4.10	1127.64	0.53	39.85	4.51
84	3.03	83.82	0.79	0.46	1571.65	16.62	1.90	1127.64	1.57	39.85	4.51
85	3.03	166.18	0.26	1.55	528.35	16.62	1.90	3872.86	0.53	39.85	4.51
86	7.97	83.82	0.79	0.46	528.35	16.62	1.90	1127.64	1.57	15.15	15.49
87	5.50	125.00	0.53	2.00	1050.00	12.50	3.00	2500.25	1.05	27.50	10.00
88	5.50	125.00	0.53	1.01	1050.00	12.50	3.00	5000.00	1.05	27.50	10.00
89	3.03	166.18	0.26	0.46	1571.65	16.62	4.10	3872.86	1.57	15.15	15.49
90	7.97	166.18	0.79	0.46	1571.65	8.38	4.10	3872.86	1.57	39.85	15.49
91	10.00	125.00	0.53	1.01	1050.00	12.50	3.00	2500.25	1.05	27.50	10.00
92	5.50	125.00	0.53	1.01	1050.00	5.00	3.00	2500.25	1.05	27.50	10.00
93	7.97	166.18	0.26	1.55	528.35	8.38	4.10	1127.64	1.57	39.85	4.51
94	7.97	83.82	0.26	1.55	1571.65	8.38	4.10	1127.64	0.53	15.15	15.49
95	3.03	83.82	0.26	0.46	528.35	8.38	1.90	1127.64	1.57	39.85	15.49
96	7.97	166.18	0.26	1.55	1571.65	8.38	1.90	3872.86	1.57	39.85	15.49

Table 29: Central Composite Design for DoE#4. Table of combinations of the 12 factors to induce maturation of hepatocytes upon hepatocyte differentiation on day 17 following a DoE approach. All combinations were added to Medium C+HGF.

Run	Decitabine	SR12813	CHIR99	D-Glucose	GlutaMAX	MS-2	Progesterone	TCA	Lipid MIX	OSM	H/C
1	7.97	1.51	4.58	7.97	4.10	4.10	3.88	155.47	7.97	15.15	4.51
2	7.97	1.51	4.58	3.03	1.90	1.90	1.17	47.03	3.03	15.15	4.51
3	5.50	2.75	6.50	5.50	3.00	3.00	2.53	101.25	5.50	27.50	10.00
4	7.97	3.99	8.42	3.03	4.10	4.10	3.88	47.03	7.97	15.15	4.51
5	3.03	1.51	4.58	3.03	1.90	4.10	3.88	155.47	3.03	15.15	4.51
6	3.03	1.51	4.58	7.97	4.10	4.10	3.88	47.03	3.03	39.85	15.49
7	7.97	1.51	8.42	3.03	4.10	1.90	1.17	47.03	3.03	39.85	15.49
8	7.97	1.51	4.58	7.97	1.90	4.10	1.17	155.47	3.03	15.15	15.49
9	5.50	2.75	6.50	5.50	3.00	3.00	2.53	101.25	5.50	27.50	10.00
10	7.97	1.51	8.42	7.97	4.10	4.10	3.88	47.03	3.03	39.85	4.51
11	7.97	1.51	4.58	3.03	4.10	1.90	3.88	47.03	7.97	39.85	4.51
12	3.03	3.99	4.58	7.97	1.90	4.10	3.88	47.03	3.03	15.15	15.49
13	3.03	3.99	8.42	3.03	4.10	4.10	1.17	155.47	3.03	39.85	15.49
14	7.97	3.99	4.58	7.97	1.90	1.90	1.17	47.03	7.97	15.15	15.49
15	7.97	1.51	8.42	7.97	1.90	1.90	3.88	47.03	7.97	39.85	15.49
16	7.97	3.99	8.42	3.03	1.90	4.10	3.88	155.47	3.03	15.15	15.49
17	5.50	2.75	6.50	5.50	3.00	3.00	2.53	101.25	5.50	27.50	10.00
18	7.97	1.51	4.58	7.97	4.10	1.90	3.88	47.03	3.03	15.15	15.49
19	5.50	2.75	6.50	5.50	3.00	3.00	2.53	200.00	5.50	27.50	10.00
20	7.97	1.51	8.42	3.03	4.10	4.10	1.17	155.47	3.03	15.15	4.51
21	7.97	3.99	4.58	3.03	4.10	4.10	1.17	47.03	7.97	39.85	15.49
22	3.03	1.51	8.42	7.97	4.10	4.10	3.88	155.47	3.03	15.15	15.49
23	5.50	2.75	6.50	5.50	3.00	3.00	2.53	101.25	5.50	27.50	20.00
24	5.50	2.75	6.50	5.50	5.00	3.00	2.53	101.25	5.50	27.50	10.00
25	5.50	0.50	6.50	5.50	3.00	3.00	2.53	101.25	5.50	27.50	10.00
26	5.50	2.75	6.50	5.50	3.00	1.00	2.53	101.25	5.50	27.50	10.00
27	3.03	1.51	4.58	3.03	1.90	1.90	1.17	47.03	7.97	39.85	15.49
28	3.03	3.99	4.58	3.03	4.10	1.90	1.17	47.03	7.97	15.15	4.51
29	3.03	3.99	4.58	7.97	1.90	4.10	1.17	155.47	3.03	39.85	4.51
30	5.50	2.75	10.00	5.50	3.00	3.00	2.53	101.25	5.50	27.50	10.00
31	3.03	3.99	8.42	3.03	1.90	1.90	1.17	155.47	3.03	15.15	4.51
32	3.03	3.99	8.42	7.97	4.10	1.90	3.88	47.03	7.97	39.85	15.49
33	7.97	1.51	8.42	3.03	4.10	4.10	3.88	155.47	7.97	39.85	15.49
34	3.03	1.51	8.42	3.03	1.90	1.90	3.88	47.03	3.03	15.15	15.49
35	7.97	3.99	8.42	7.97	4.10	4.10	1.17	47.03	3.03	15.15	15.49
36	5.50	2.75	6.50	5.50	3.00	3.00	2.53	101.25	5.50	27.50	0.00
37	3.03	1.51	8.42	3.03	4.10	1.90	3.88	155.47	7.97	15.15	4.51
38	7.97	1.51	8.42	7.97	4.10	1.90	1.17	155.47	7.97	15.15	15.49
39	3.03	3.99	8.42	7.97	1.90	1.90	1.17	47.03	7.97	39.85	4.51
40	3.03	1.51	8.42	3.03	4.10	4.10	1.17	47.03	7.97	39.85	4.51
41	7.97	3.99	8.42	7.97	4.10	1.90	3.88	155.47	7.97	15.15	4.51
42	5.50	2.75	6.50	10.00	3.00	3.00	2.53	101.25	5.50	27.50	10.00
43	7.97	1.51	4.58	3.03	1.90	4.10	1.17	155.47	7.97	39.85	4.51
44	7.97	1.51	4.58	7.97	1.90	1.90	3.88	155.47	3.03	39.85	4.51
45	3.03	3.99	4.58	7.97	4.10	1.90	1.17	155.47	3.03	15.15	15.49
46	7.97	3.99	4.58	7.97	1.90	1.90	3.88	47.03	7.97	39.85	4.51
47	1.00	2.75	6.50	5.50	3.00	3.00	2.53	101.25	5.50	27.50	10.00
48	3.03	3.99	4.58	3.03	1.90	1.90	3.88	47.03	7.97	15.15	4.51
49	7.97	3.99	8.42	3.03	1.90	4.10	1.17	155.47	3.03	39.85	4.51
50	3.03	3.99	8.42	3.03	4.10	1.90	3.88	47.03	3.03	15.15	4.51
51	7.97	3.99	8.42	7.97	1.90	1.90	1.17	155.47	3.03	39.85	15.49
52	7.97	3.99	8.42	3.03	4.10	1.90	3.88	155.47	7.97	39.85	15.49
53	3.03	1.51	8.42	3.03	1.90	1.90	3.88	47.03	3.03	39.85	4.51
54	5.50	2.75	6.50	5.50	3.00	3.00	2.53	101.25	5.50	27.50	10.00
55	3.03	3.99	4.58	3.03	1.90	4.10	1.17	47.03	3.03	15.15	15.49
56	7.97	1.51	4.58	3.03	4.10	4.10	1.17	47.03	3.03	39.85	4.51
57	3.03	1.51	8.42	3.03	1.90	1.90	1.17	155.47	7.97	39.85	15.49
58	7.97	1.51	8.42	3.03	1.90	4.10	1.17	47.03	7.97	15.15	15.49
59	5.50	2.75	6.50	5.50	3.00	3.00	5.00	101.25	5.50	27.50	10.00
60	5.50	2.75	6.50	5.50	3.00	3.00	2.53	101.25	5.50	27.50	10.00
61	5.50	2.75	3.00	5.50	3.00	3.00	2.53	101.25	5.50	27.50	10.00
62	7.97	3.99	4.58	7.97	4.10	1.90	1.17	155.47	7.97	39.85	15.49
63	3.03	3.99	8.42	7.97	4.10	4.10	3.88	47.03	7.97	15.15	4.51
64	5.50	2.75	6.50	5.50	3.00	3.00	2.53	101.25	5.50	5.00	10.00
65	7.97	3.99	4.58	7.97	4.10	1.90	1.17	47.03	3.03	39.85	4.51
66	3.03	3.99	8.42	7.97	1.90	1.90	3.88	155.47	3.03	39.85	4.51
67	7.97	3.99	8.42	7.97	1.90	1.90	3.88	47.03	3.03	15.15	4.51
68	5.50	5.00	6.50	5.50	3.00	3.00	2.53	101.25	5.50	27.50	10.00
69	5.50	2.75	6.50	5.50	3.00	3.00	2.53	101.25	1.00	27.50	10.00
70	10.00	2.75	6.50	5.50	3.00	3.00	2.53	101.25	5.50	27.50	10.00
71	7.97	1.51	4.58	3.03	1.90	1.90	3.88	155.47	7.97	15.15	15.49
72	3.03	3.99	4.58	3.03	4.10	4.10	3.88	155.47	7.97	15.15	15.49
73	7.97	1.51	8.42	7.97	1.90	4.10	3.88	155.47	7.97	15.15	4.51
74	3.03	1.51	4.58	3.03	4.10	1.90	1.17	155.47	3.03	39.85	4.51
75	7.97	3.99	4.58	7.97	4.10	4.10	3.88	155.47	3.03	39.85	15.49
76	3.03	1.51	8.42	7.97	1.90	4.10	1.17	47.03	3.03	39.85	15.49
77	7.97	1.51	4.58	3.03	1.90	4.10	3.88	47.03	3.03	39.85	15.49
78	3.03	3.99	8.42	7.97	1.90	4.10	1.17	155.47	7.97	15.15	15.49
79	5.50	2.75	6.50	5.50	3.00	3.00	0.05	101.25	5.50	27.50	10.00
80	5.50	2.75	6.50	5.50	3.00	3.00	2.53	101.25	5.50	50.00	10.00
81	3.03	1.51	8.42	7.97	4.10	4.10	1.17	155.47	7.97	39.85	4.51
82	3.03	3.99	8.42	3.03	1.90	4.10	3.88	47.03	7.97	39.85	15.49
83	3.03	3.99	4.58	3.03	1.90	1.90	3.88	155.47	3.03	39.85	15.49
84	7.97	3.99	4.58	3.03	4.10	1.90	1.17	155.47	3.03	15.15	4.51
85	3.03	1.51	4.58	7.97	1.90	1.90	1.17	155.47	7.97	15.15	4.51
86	5.50	2.75	6.50	5.50	1.00	3.00	2.53	101.25	5.50	27.50	10.00
87	5.50	2.75	6.50	5.50	3.00	5.00	2.53	101.25	5.50	27.50	10.00
88	3.03	3.99	4.58	3.03	4.10	4.10	3.88	155.47	7.97	39.85	4.51
89	3.03	1.51	4.58	7.97	4.10	4.10	1.17	47.03	7.97	15.15	15.49
90	5.50	2.75	6.50	5.50	3.00	3.00	2.53	101.25	5.50	27.50	10.00
91	5.50	2.75	6.50	1.00	3.00	3.00	2.53	101.25	5.50	27.50	10.00
92	3.03	1.51	8.42	7.97	4.10	1.90	1.17	47.03	3.03	15.15	4.51
93	3.03	1.51	4.58	7.97	1.90	4.10	3.88	155.47	7.97	39.85	15.49
94	7.97	3.99	4.58	7.97	1.90	4.10	1.17	47.03	7.97	15.15	4.51
95	5.50	2.75	6.50	5.50	3.00	3.00	2.53	2.50	5.50	27.50	10.00
96	5.50	2.75	6.50	5.50	3.00	3.00	2.53	101.25	10.00	27.50	10.00

Table 30: Central Composite Design for DoE#5. Table of combinations of the 12 factors to induce maturation of hepatocytes upon hepatocyte differentiation on day 17 following a DoE approach. All combinations were added to Medium C+HGF.

8. References

AGARWAL, S., HOLTON, K. L. & LANZA, R. 2008. Efficient differentiation of functional hepatocytes from human embryonic stem cells. *Stem Cells,* 26**,** 1117-27.

AKHTAR, A. 2013. The need to include animal protection in public health policies. *J Public Health Policy,* 34**,** 549-59.

AKHTAR, A. 2015. The flaws and human harms of animal experimentation. *Camb Q Healthc Ethics,* 24**,** 407-19.

AL-SAWALHA, N., POKKUNURI, I., OMOLUABI, O., KIM, H., THANAWALA, V. J., HERNANDEZ, A., BOND, R. A. & KNOLL, B. J. 2015. Epinephrine Activation of the β2-Adrenoceptor Is Required for IL-13-Induced Mucin Production in Human Bronchial Epithelial Cells. *PLoS One,* 10**,** e0132559.

ALDER, O., CULLUM, R., LEE, S., KAN, A. C., WEI, W., YI, Y., GARSIDE, V. C., BILENKY, M., GRIFFITH, M., MORRISSY, A. S., ROBERTSON, G. A., THIESSEN, N., ZHAO, Y., CHEN, Q., PAN, D., JONES, S. J., MARRA, M. A. & HOODLESS, P. A. 2014. Hippo signaling influences HNF4A and FOXA2 enhancer switching during hepatocyte differentiation. *Cell Rep,* 9**,** 261-71.

ALI, Z. K., KIM, R. J. & YSLA, F. M. 2009. CYP2C9 polymorphisms: considerations in NSAID therapy. *Curr Opin Drug Discov Devel,* 12**,** 108-14.

ALLEGRUCCI, C. & YOUNG, L. E. 2007. Differences between human embryonic stem cell lines. *Hum Reprod Update,* 13**,** 103-20.

ALMAZROO, O. A., MIAH, M. K. & VENKATARAMANAN, R. 2017. Drug Metabolism in the Liver. *Clin Liver Dis,* 21**,** 1-20.

AMIT, M., MARGULETS, V., SEGEV, H., SHARIKI, K., LAEVSKY, I., COLEMAN, R. & ITSKOVITZ-ELDOR, J. 2003. Human feeder layers for human embryonic stem cells. *Biol Reprod,* 68**,** 2150-6.

AMIT, M., SHARIKI, C., MARGULETS, V. & ITSKOVITZ-ELDOR, J. 2004. Feeder layer-and serum-free culture of human embryonic stem cells. *Biol Reprod,* 70**,** 837-45.

AMMAR, D. A. & KAHOOK, M. Y. 2013. In vitro effects of verteporfin on ocular cells. *Mol Vis,* 19**,** 424-9.

ANAGNOSTOU, V. K., WELSH, A. W., GILTNANE, J. M., SIDDIQUI, S., LICEAGA, C., GUSTAVSON, M., SYRIGOS, K. N., REITER, J. L. & RIMM, D. L. 2010. Analytic variability in immunohistochemistry biomarker studies. *Cancer Epidemiol Biomarkers Prev,* 19**,** 982-91.

ANDERSON, M. 2010. Design of Experiments. *In:* J, W. P. (ed.). Kirk-Othmer Encyclopedia of Chemical Technology.

ANGELOS, M. G. & KAUFMAN, D. S. 2015. Pluripotent stem cell applications for regenerative medicine. *Curr Opin Organ Transplant,* 20**,** 663-70.

ANINAT, C., SEGUIN, P., DESCHEEMAEKER, P. N., MOREL, F., MALLEDANT, Y. & GUILLOUZO, A. 2008. Catecholamines induce an inflammatory response in human hepatocytes. *Crit Care Med,* 36**,** 848-54.

ARCHER, R. & WILLIAMS, D. J. 2005. Why tissue engineering needs process engineering. *Nat Biotechnol,* 23**,** 1353-5.

ARNOLD, S. J. & ROBERTSON, E. J. 2009. Making a commitment: cell lineage allocation and axis patterning in the early mouse embryo. *Nat Rev Mol Cell*

Biol, 10**,** 91-103.

ASGARI, S., MOSLEM, M., BAGHERI-LANKARANI, K., POURNASR, B., MIRYOUNESI, M. & BAHARVAND, H. 2013. Differentiation and transplantation of human induced pluripotent stem cell-derived hepatocyte-like cells. *Stem Cell Rev,* 9**,** 493-504.

ASPLUND, A., PRADIP, A., VAN GIEZEN, M., ASPEGREN, A., CHOUKAIR, H., REHNSTRÖM, M., JACOBSSON, S., GHOSHEH, N., EL HAJJAM, D., HOLMGREN, S., LARSSON, S., BENECKE, J., BUTRON, M., WIGANDER, A., NOAKSSON, K., SARTIPY, P., BJÖRQUIST, P., EDSBAGGE, J. & KÜPPERS-MUNTHER, B. 2016. One Standardized Differentiation Procedure Robustly Generates Homogenous Hepatocyte Cultures Displaying Metabolic Diversity from a Large Panel of Human Pluripotent Stem Cells. *Stem Cell Rev,* 12**,** 90-104.

AVIOR, Y., LEVY, G., ZIMERMAN, M., KITSBERG, D., SCHWARTZ, R., SADEH, R., MOUSSAIEFF, A., COHEN, M., ITSKOVITZ-ELDOR, J. & NAHMIAS, Y. 2015. Microbial-derived lithocholic acid and vitamin K2 drive the metabolic maturation of pluripotent stem cells-derived and fetal hepatocytes. *Hepatology,* 62**,** 265-78.

AVIOR, Y., SAGI, I. & BENVENISTY, N. 2016. Pluripotent stem cells in disease modelling and drug discovery. *Nat Rev Mol Cell Biol,* 17**,** 170-82.

AVORN, J. 2015. The $2.6 billion pill--methodologic and policy considerations. *N Engl J Med,* 372**,** 1877-9.

AZAM, M. 2014. Surface roughness modeling using RSM for HSLA steel by coated carbide tools.

BADENES, S. M., FERNANDES, T. G., CORDEIRO, C. S., BOUCHER, S., KUNINGER, D., VEMURI, M. C., DIOGO, M. M. & CABRAL, J. M. 2016. Defined Essential 8™ Medium and Vitronectin Efficiently Support Scalable Xeno-Free Expansion of Human Induced Pluripotent Stem Cells in Stirred Microcarrier Culture Systems. *PLoS One,* 11**,** e0151264.

BAEK, M. K., PARK, J. S., PARK, J. H., KIM, M. H., KIM, H. D., BAE, W. K., CHUNG, I. J., SHIN, B. A. & JUNG, Y. D. 2010. Lithocholic acid upregulates uPAR and cell invasiveness via MAPK and AP-1 signaling in colon cancer cells. *Cancer Lett,* 290**,** 123-8.

BAILLIE, T. A. & RETTIE, A. E. 2011. Role of biotransformation in drug-induced toxicity: influence of intra- and inter-species differences in drug metabolism. *Drug Metab Pharmacokinet,* 26**,** 15-29.

BAIN, J. 2007. The many faces of testosterone. *Clin Interv Aging,* 2**,** 567-76.

BALE, S. S., GOLBERG, I., JINDAL, R., MCCARTY, W. J., LUITJE, M., HEGDE, M., BHUSHAN, A., USTA, O. B. & YARMUSH, M. L. 2015. Long-term coculture strategies for primary hepatocytes and liver sinusoidal endothelial cells. *Tissue Eng Part C Methods,* 21**,** 413-22.

BATISTA, K. A. & FERNANDES, K. F. 2015. Development and optimization of a new culture media using extruded bean as nitrogen source. *MethodsX,* 2**,** 154-8.

BATTLE, M. A., KONOPKA, G., PARVIZ, F., GAGGL, A. L., YANG, C., SLADEK, F. M. & DUNCAN, S. A. 2006. Hepatocyte nuclear factor 4alpha orchestrates expression of cell adhesion proteins during the epithelial transformation of the developing liver. *Proc Natl Acad Sci U S A,* 103**,** 8419-24.

BAXTER, M., WITHEY, S., HARRISON, S., SEGERITZ, C. P., ZHANG, F., ATKINSON-DELL,

R., ROWE, C., GERRARD, D. T., SISON-YOUNG, R., JENKINS, R., HENRY, J., BERRY, A. A., MOHAMET, L., BEST, M., FENWICK, S. W., MALIK, H., KITTERINGHAM, N. R., GOLDRING, C. E., PIPER HANLEY, K., VALLIER, L. & HANLEY, N. A. 2015. Phenotypic and functional analyses show stem cell-derived hepatocyte-like cells better mimic fetal rather than adult hepatocytes. *J Hepatol,* 62**,** 581-9.

BEENKEN, A. & MOHAMMADI, M. 2009. The FGF family: biology, pathophysiology and therapy. *Nat Rev Drug Discov,* 8**,** 235-53.

BEERS, J., GULBRANSON, D. R., GEORGE, N., SINISCALCHI, L. I., JONES, J., THOMSON, J. A. & CHEN, G. 2012. Passaging and colony expansion of human pluripotent stem cells by enzyme-free dissociation in chemically defined culture conditions. *Nat Protoc,* 7**,** 2029-40.

BEHBAHAN, I. S., DUAN, Y., LAM, A., KHOOBYARI, S., MA, X., AHUJA, T. P. & ZERN, M. A. 2011. New approaches in the differentiation of human embryonic stem cells and induced pluripotent stem cells toward hepatocytes. *Stem Cell Rev,* 7**,** 748-59.

BELL, C. C., HENDRIKS, D. F., MORO, S. M., ELLIS, E., WALSH, J., RENBLOM, A., FREDRIKSSON PUIGVERT, L., DANKERS, A. C., JACOBS, F., SNOEYS, J., SISON-YOUNG, R. L., JENKINS, R. E., NORDLING, Å., MKRTCHIAN, S., PARK, B. K., KITTERINGHAM, N. R., GOLDRING, C. E., LAUSCHKE, V. M. & INGELMAN-SUNDBERG, M. 2016. Characterization of primary human hepatocyte spheroids as a model system for drug-induced liver injury, liver function and disease. *Sci Rep,* 6**,** 25187.

BENEDETTI, M. S., WHOMSLEY, R., POGGESI, I., CAWELLO, W., MATHY, F. X., DELPORTE, M. L., PAPELEU, P. & WATELET, J. B. 2009. Drug metabolism and pharmacokinetics. *Drug Metab Rev,* 41**,** 344-90.

BENET, M., LAHOZ, A., GUZMÁN, C., CASTELL, J. V. & JOVER, R. 2010. CCAAT/enhancer-binding protein alpha (C/EBPalpha) and hepatocyte nuclear factor 4alpha (HNF4alpha) synergistically cooperate with constitutive androstane receptor to transactivate the human cytochrome P450 2B6 (CYP2B6) gene: application to the development of a metabolically competent human hepatic cell model. *J Biol Chem,* 285**,** 28457-71.

BERNI CANANI, R., DI COSTANZO, M. & LEONE, L. 2012. The epigenetic effects of butyrate: potential therapeutic implications for clinical practice. *Clin Epigenetics,* 4**,** 4.

BILSEL, A. S., MOINI, H., TETIK, E., AKSUNGAR, F., KAYNAK, B. & OZER, A. 2000. 17Beta-estradiol modulates endothelin-1 expression and release in human endothelial cells. *Cardiovasc Res,* 46**,** 579-84.

BISWAS, D. & JIANG, P. 2016. Chemically Induced Reprogramming of Somatic Cells to Pluripotent Stem Cells and Neural Cells. *Int J Mol Sci,* 17**,** 226.

BJÖRNSSON, E. S. 2016. Hepatotoxicity by Drugs: The Most Common Implicated Agents. *Int J Mol Sci,* 17**,** 224.

BLADT, F., RIETHMACHER, D., ISENMANN, S., AGUZZI, A. & BIRCHMEIER, C. 1995. Essential role for the c-met receptor in the migration of myogenic precursor cells into the limb bud. *Nature,* 376**,** 768-71.

BOCK, A. S., LEIGH, N. D. & BRYDA, E. C. 2014. Effect of Gsk3 inhibitor CHIR99021 on aneuploidy levels in rat embryonic stem cells. *In Vitro Cell Dev Biol Anim,* 50**,**

572-9.
BOCK, C., KISKINIS, E., VERSTAPPEN, G., GU, H., BOULTING, G., SMITH, Z. D., ZILLER, M., CROFT, G. F., AMOROSO, M. W., OAKLEY, D. H., GNIRKE, A., EGGAN, K. & MEISSNER, A. 2011. Reference Maps of human ES and iPS cell variation enable high-throughput characterization of pluripotent cell lines. *Cell,* 144**,** 439-52.
BOLLEYN, J., ROGIERS, V. & VANHAECKE, T. 2015. Functionality Testing of Primary Hepatocytes in Culture by Measuring Urea Synthesis. *Methods Mol Biol,* 1250**,** 317-21.
BORT, R., SIGNORE, M., TREMBLAY, K., MARTINEZ BARBERA, J. P. & ZARET, K. S. 2006. Hex homeobox gene controls the transition of the endoderm to a pseudostratified, cell emergent epithelium for liver bud development. *Dev Biol,* 290**,** 44-56.
BORUM, P. R. 1992. Medium-chain triglycerides in formula for preterm neonates: implications for hepatic and extrahepatic metabolism. *J Pediatr,* 120**,** S139-45.
BOTTING, J. 2002. The History of Thalidomide. *Drug News Perspect,* 15**,** 604-611.
BRAAM, S. R., ZEINSTRA, L., LITJENS, S., WARD-VAN OOSTWAARD, D., VAN DEN BRINK, S., VAN LAAKE, L., LEBRIN, F., KATS, P., HOCHSTENBACH, R., PASSIER, R., SONNENBERG, A. & MUMMERY, C. L. 2008. Recombinant vitronectin is a functionally defined substrate that supports human embryonic stem cell self-renewal via alphavbeta5 integrin. *Stem Cells,* 26**,** 2257-65.
BREHM, M. A., SHULTZ, L. D., LUBAN, J. & GREINER, D. L. 2013. Overcoming current limitations in humanized mouse research. *J Infect Dis,* 208 Suppl 2**,** S125-30.
BRIOLOTTI, P., CHALOIN, L., BALAGUER, P., DA SILVA, F., TOMÁNKOVÁ, V., PASCUSSI, J. M., DURET, C., FABRE, J. M., RAMOS, J., KLIEBER, S., MAUREL, P., DAUJAT-CHAVANIEU, M. & GERBAL-CHALOIN, S. 2015. Analysis of Glycogen Synthase Kinase Inhibitors That Regulate Cytochrome P450 Expression in Primary Human Hepatocytes by Activation of β-Catenin, Aryl Hydrocarbon Receptor and Pregnane X Receptor Signaling. *Toxicol Sci,* 148**,** 261-75.
BROLÉN, G., SIVERTSSON, L., BJÖRQUIST, P., ERIKSSON, G., EK, M., SEMB, H., JOHANSSON, I., ANDERSSON, T. B., INGELMAN-SUNDBERG, M. & HEINS, N. 2010. Hepatocyte-like cells derived from human embryonic stem cells specifically via definitive endoderm and a progenitor stage. *J Biotechnol,* 145**,** 284-94.
BROWN, G. M. 1994. Light, melatonin and the sleep-wake cycle. *J Psychiatry Neurosci,* 19**,** 345-53.
BROWN, S., TEO, A., PAUKLIN, S., HANNAN, N., CHO, C. H., LIM, B., VARDY, L., DUNN, N. R., TROTTER, M., PEDERSEN, R. & VALLIER, L. 2011. Activin/Nodal signaling controls divergent transcriptional networks in human embryonic stem cells and in endoderm progenitors. *Stem Cells,* 29**,** 1176-85.
BUETTNER, G. R. & JURKIEWICZ, B. A. 1996. Catalytic metals, ascorbate and free radicals: combinations to avoid. *Radiat Res,* 145**,** 532-41.
BURKE, Z. & OLIVER, G. 2002. Prox1 is an early specific marker for the developing liver and pancreas in the mammalian foregut endoderm. *Mech Dev,* 118**,** 147-55.

BURRIDGE, P. W., HOLMSTRÖM, A. & WU, J. C. 2015. Chemically Defined Culture and Cardiomyocyte Differentiation of Human Pluripotent Stem Cells. *Curr Protoc Hum Genet,* 87**,** 21.3.1-15.

BURRIDGE, P. W., MATSA, E., SHUKLA, P., LIN, Z. C., CHURKO, J. M., EBERT, A. D., LAN, F., DIECKE, S., HUBER, B., MORDWINKIN, N. M., PLEWS, J. R., ABILEZ, O. J., CUI, B., GOLD, J. D. & WU, J. C. 2014. Chemically defined generation of human cardiomyocytes. *Nat Methods,* 11**,** 855-60.

BUYEL, J. F. & FISCHER, R. 2014. Characterization of complex systems using the design of experiments approach: transient protein expression in tobacco as a case study. *J Vis Exp***,** e51216.

BUYL, K., DE KOCK, J., BOLLEYN, J., ROGIERS, V. & VANHAECKE, T. 2015. Measurement of Albumin Secretion as Functionality Test in Primary Hepatocyte Cultures. *Methods Mol Biol,* 1250**,** 303-8.

CAHAN, P. & DALEY, G. Q. 2013. Origins and implications of pluripotent stem cell variability and heterogeneity. *Nat Rev Mol Cell Biol,* 14**,** 357-68.

CAI, J., ZHAO, Y., LIU, Y., YE, F., SONG, Z., QIN, H., MENG, S., CHEN, Y., ZHOU, R., SONG, X., GUO, Y., DING, M. & DENG, H. 2007. Directed differentiation of human embryonic stem cells into functional hepatic cells. *Hepatology,* 45**,** 1229-39.

CAJOCHEN, C., KRÄUCHI, K. & WIRZ-JUSTICE, A. 2003. Role of melatonin in the regulation of human circadian rhythms and sleep. *J Neuroendocrinol,* 15**,** 432-7.

CALMONT, A., WANDZIOCH, E., TREMBLAY, K. D., MINOWADA, G., KAESTNER, K. H., MARTIN, G. R. & ZARET, K. S. 2006. An FGF response pathway that mediates hepatic gene induction in embryonic endoderm cells. *Dev Cell,* 11**,** 339-48.

CAMERON, K., TAN, R., SCHMIDT-HECK, W., CAMPOS, G., LYALL, M. J., WANG, Y., LUCENDO-VILLARIN, B., SZKOLNICKA, D., BATES, N., KIMBER, S. J., HENGSTLER, J. G., GODOY, P., FORBES, S. J. & HAY, D. C. 2015. Recombinant Laminins Drive the Differentiation and Self-Organization of hESC-Derived Hepatocytes. *Stem Cell Reports,* 5**,** 1250-62.

CARBAJO-PESCADOR, S., GARCÍA-PALOMO, A., MARTÍN-RENEDO, J., PIVA, M., GONZÁLEZ-GALLEGO, J. & MAURIZ, J. L. 2011. Melatonin modulation of intracellular signaling pathways in hepatocarcinoma HepG2 cell line: role of the MT1 receptor. *J Pineal Res,* 51**,** 463-71.

CARBAJO-PESCADOR, S., STEINMETZ, C., KASHYAP, A., LORENZ, S., MAURIZ, J. L., HEISE, M., GALLE, P. R., GONZÁLEZ-GALLEGO, J. & STRAND, S. 2013. Melatonin induces transcriptional regulation of Bim by FoxO3a in HepG2 cells. *Br J Cancer,* 108**,** 442-9.

CELLI, J. P., SOLBAN, N., LIANG, A., PEREIRA, S. P. & HASAN, T. 2011. Verteporfin-based photodynamic therapy overcomes gemcitabine insensitivity in a panel of pancreatic cancer cell lines. *Lasers Surg Med,* 43**,** 565-74.

CHALASANI, N. & BJÖRNSSON, E. 2010. Risk factors for idiosyncratic drug-induced liver injury. *Gastroenterology,* 138**,** 2246-59.

CHAMBERLAIN, S. J. 2016. Disease modelling using human iPSCs. *Hum Mol Genet,* 25**,** R173-R181.

CHANG, T. K., BANDIERA, S. M. & CHEN, J. 2003. Constitutive androstane receptor and pregnane X receptor gene expression in human liver: interindividual

variability and correlation with CYP2B6 mRNA levels. *Drug Metab Dispos,* 31**,** 7-10.

CHANG, T. K. & WAXMAN, D. J. 2006. Synthetic drugs and natural products as modulators of constitutive androstane receptor (CAR) and pregnane X receptor (PXR). *Drug Metab Rev,* 38**,** 51-73.

CHEN, C. Y., CHUNG, I. H., TSAI, M. M., TSENG, Y. H., CHI, H. C., TSAI, C. Y., LIN, Y. H., WANG, Y. C., CHEN, C. P., WU, T. I., YEH, C. T., TAI, D. I. & LIN, K. H. 2014a. Thyroid hormone enhanced human hepatoma cell motility involves brain-specific serine protease 4 activation via ERK signaling. *Mol Cancer,* 13**,** 162.

CHEN, F., ZAMULE, S. M., COSLO, D. M., CHEN, T. & OMIECINSKI, C. J. 2013. The human constitutive androstane receptor promotes the differentiation and maturation of hepatic-like cells. *Dev Biol,* 384**,** 155-65.

CHEN, G., BAI, Y., REN, L., ZHU, D., LI, Y., FANG, M., AL-KATEB, H. & DORAN, O. 2015a. Metabolism of androstenone, 17β-estradiol and dihydrotestosterone in primary cultured pig hepatocytes and the role of 3β-hydroxysteroid dehydrogenase in this process. *PLoS One,* 10**,** e113194.

CHEN, G., GULBRANSON, D. R., HOU, Z., BOLIN, J. M., RUOTTI, V., PROBASCO, M. D., SMUGA-OTTO, K., HOWDEN, S. E., DIOL, N. R., PROPSON, N. E., WAGNER, R., LEE, G. O., ANTOSIEWICZ-BOURGET, J., TENG, J. M. & THOMSON, J. A. 2011. Chemically defined conditions for human iPSC derivation and culture. *Nat Methods,* 8**,** 424-9.

CHEN, G., LI, S., DONG, X., BAI, Y., CHEN, A., YANG, S., FANG, M., ZAMARATSKAIA, G. & DORAN, O. 2012a. Investigation of testosterone, androstenone, and estradiol metabolism in HepG2 cells and primary culture pig hepatocytes and their effects on 17βHSD7 gene expression. *PLoS One,* 7**,** e52255.

CHEN, J., GAO, W., ZHOU, P., MA, X., TSCHUDY-SENEY, B., LIU, C., ZERN, M. A., LIU, P. & DUAN, Y. 2016. Enhancement of hepatocyte differentiation from human embryonic stem cells by Chinese medicine Fuzhenghuayu. *Sci Rep,* 6**,** 18841.

CHEN, K. G., MALLON, B. S., MCKAY, R. D. & ROBEY, P. G. 2014b. Human pluripotent stem cell culture: considerations for maintenance, expansion, and therapeutics. *Cell Stem Cell,* 14**,** 13-26.

CHEN, T. S. & CHEN, P. S. 1994. The myth of Prometheus and the liver. *J R Soc Med,* 87**,** 754-5.

CHEN, W. S., CAO, Z., KRISHNAN, C. & PANJWANI, N. 2015b. Verteporfin without light stimulation inhibits YAP activation in trabecular meshwork cells: Implications for glaucoma treatment. *Biochem Biophys Res Commun,* 466**,** 221-5.

CHEN, Y. F., TSENG, C. Y., WANG, H. W., KUO, H. C., YANG, V. W. & LEE, O. K. 2012b. Rapid generation of mature hepatocyte-like cells from human induced pluripotent stem cells by an efficient three-step protocol. *Hepatology,* 55**,** 1193-203.

CHETTY, S., PAGLIUCA, F. W., HONORE, C., KWEUDJEU, A., REZANIA, A. & MELTON, D. A. 2013. A simple tool to improve pluripotent stem cell differentiation. *Nat Methods,* 10**,** 553-6.

CHIOU, J. F., WANG, Y. H., JOU, M. J., LIU, T. Z. & SHIAU, C. Y. 2010. Verteporfin-photoinduced apoptosis in HepG2 cells mediated by reactive oxygen and nitrogen species intermediates. *Free Radic Res,* 44**,** 155-70.

CHO, Y. A., NOH, K., JUE, S. S., LEE, S. Y. & KIM, E. C. 2015. Melatonin promotes hepatic differentiation of human dental pulp stem cells: clinical implications for the prevention of liver fibrosis. *J Pineal Res,* 58**,** 127-35.

CHOI, H. J., HUBER, A. H. & WEIS, W. I. 2006. Thermodynamics of beta-catenin-ligand interactions: the roles of the N- and C-terminal tails in modulating binding affinity. *J Biol Chem,* 281**,** 1027-38.

CHOI, S. Y., KOH, K. H. & JEONG, H. 2013. Isoform-specific regulation of cytochromes P450 expression by estradiol and progesterone. *Drug Metab Dispos,* 41**,** 263-9.

CHOJNACKI, C., WALECKA-KAPICA, E., ROMANOWSKI, M., CHOJNACKI, J. & KLUPINSKA, G. 2014. Protective role of melatonin in liver damage. *Curr Pharm Des,* 20**,** 4828-33.

CICHOŻ-LACH, H. & MICHALAK, A. 2014. Oxidative stress as a crucial factor in liver diseases. *World J Gastroenterol,* 20**,** 8082-91.

CLEVERS, H. 2006. Wnt/beta-catenin signaling in development and disease. *Cell,* 127**,** 469-80.

CLOTMAN, F., JACQUEMIN, P., PLUMB-RUDEWIEZ, N., PIERREUX, C. E., VAN DER SMISSEN, P., DIETZ, H. C., COURTOY, P. J., ROUSSEAU, G. G. & LEMAIGRE, F. P. 2005. Control of liver cell fate decision by a gradient of TGF beta signaling modulated by Onecut transcription factors. *Genes Dev,* 19**,** 1849-54.

COLLER, J. K., KREBSFAENGER, N., KLEIN, K., ENDRIZZI, K., WOLBOLD, R., LANG, T., NÜSSLER, A., NEUHAUS, P., ZANGER, U. M., EICHELBAUM, M. & MÜRDTER, T. E. 2002. The influence of CYP2B6, CYP2C9 and CYP2D6 genotypes on the formation of the potent antioestrogen Z-4-hydroxy-tamoxifen in human liver. *Br J Clin Pharmacol,* 54**,** 157-67.

COLLINS, L. M., DZIAK, J. J. & LI, R. 2009. Design of experiments with multiple independent variables: a resource management perspective on complete and reduced factorial designs. *Psychol Methods,* 14**,** 202-24.

CONLY, J. M. & STEIN, K. 1992. The production of menaquinones (vitamin K2) by intestinal bacteria and their role in maintaining coagulation homeostasis. *Prog Food Nutr Sci,* 16**,** 307-43.

COOK, J. R., LANGLET, F., KIDO, Y. & ACCILI, D. 2015. Pathogenesis of selective insulin resistance in isolated hepatocytes. *J Biol Chem,* 290**,** 13972-80.

CORLESS, J. K. & MIDDLETON, H. M. 1983. Normal liver function. A basis for understanding hepatic disease. *Arch Intern Med,* 143**,** 2291-4.

COSTA, S., BARROSO, M., CASTAÑERA, A. & DIAS, M. 2010. Design of experiments, a powerful tool for method development in forensic toxicology: application to the optimization of urinary morphine 3-glucuronide acid hydrolysis. *Anal Bioanal Chem,* 396**,** 2533-42.

COSTELLO, I., PIMEISL, I. M., DRÄGER, S., BIKOFF, E. K., ROBERTSON, E. J. & ARNOLD, S. J. 2011. The T-box transcription factor Eomesodermin acts upstream of Mesp1 to specify cardiac mesoderm during mouse gastrulation. *Nat Cell Biol,* 13**,** 1084-91.

COWAN, C. A., KLIMANSKAYA, I., MCMAHON, J., ATIENZA, J., WITMYER, J., ZUCKER, J. P., WANG, S., MORTON, C. C., MCMAHON, A. P., POWERS, D. & MELTON, D. A. 2004. Derivation of embryonic stem-cell lines from human blastocysts. *N Engl J Med,* 350**,** 1353-6.

CRETTOL, S., PETROVIC, N. & MURRAY, M. 2010. Pharmacogenetics of phase I and phase II drug metabolism. *Curr Pharm Des,* 16**,** 204-19.

CROMBIE, D. E., DANISZEWSKI, M., LIANG, H. H., KULKARNI, T., LI, F., LIDGERWOOD, G. E., CONQUEST, A., HERNÁNDEZ, D., HUNG, S. S., GILL, K. P., DE SMIT, E., KEARNS, L. S., CLARKE, L., SLUCH, V. M., CHAMLING, X., ZACK, D. J., WONG, R. C. B., HEWITT, A. W. & PÉBAY, A. 2017. Development of a Modular Automated System for Maintenance and Differentiation of Adherent Human Pluripotent Stem Cells. *SLAS Discov,* 22**,** 1016-1025.

CSÖBÖNYEIOVÁ, M., POLÁK, Š. & DANIŠOVIČ, L. 2016. Toxicity testing and drug screening using iPSC-derived hepatocytes, cardiomyocytes, and neural cells. *Can J Physiol Pharmacol***,** 1-8.

CULLEN, K. S., AL-OANZI, Z. H., O'HARTE, F. P., AGIUS, L. & ARDEN, C. 2014. Glucagon induces translocation of glucokinase from the cytoplasm to the nucleus of hepatocytes by transfer between 6-phosphofructo 2-kinase/fructose 2,6-bisphosphatase-2 and the glucokinase regulatory protein. *Biochim Biophys Acta,* 1843**,** 1123-34.

CURTIS, C. G., CHIEN, B., BAR-OR, D. & RAMU, K. 2002. Organ perfusion and mass spectrometry: a timely merger for drug development. *Curr Top Med Chem,* 2**,** 77-86.

CYPHERT, H. A., ALONGE, K. M., IPPAGUNTA, S. M. & HILLGARTNER, F. B. 2014. Glucagon stimulates hepatic FGF21 secretion through a PKA- and EPAC-dependent posttranscriptional mechanism. *PLoS One,* 9**,** e94996.

D'AMOUR, K. A., AGULNICK, A. D., ELIAZER, S., KELLY, O. G., KROON, E. & BAETGE, E. E. 2005. Efficient differentiation of human embryonic stem cells to definitive endoderm. *Nat Biotechnol,* 23**,** 1534-41.

DANDAPANI, S., ROSSE, G., SOUTHALL, N., SALVINO, J. M. & THOMAS, C. J. 2012. Selecting, Acquiring, and Using Small Molecule Libraries for High-Throughput Screening. *Curr Protoc Chem Biol,* 4**,** 177-191.

DANISZEWSKI, M., CROMBIE, D. E., HENDERSON, R., LIANG, H. H., WONG, R. C. B., HEWITT, A. W. & PÉBAY, A. 2017. Automated Cell Culture Systems and Their Applications to Human Pluripotent Stem Cell Studies. *SLAS Technol***,** 2472630317712220.

DANKEL, S. N., HOANG, T., FLÅGENG, M. H., SAGEN, J. V. & MELLGREN, G. 2010. cAMP-mediated regulation of HNF-4alpha depends on the level of coactivator PGC-1alpha. *Biochim Biophys Acta,* 1803**,** 1013-9.

DARWISH, W. S., IKENAKA, Y., NAKAYAMA, S. M., MIZUKAWA, H. & ISHIZUKA, M. 2016. Constitutive Effects of Lead on Aryl Hydrocarbon Receptor Gene Battery and Protection by β-carotene and Ascorbic Acid in Human HepG2 Cells. *J Food Sci,* 81**,** T275-81.

DASU, M. R., RAMIREZ, S. R., LA, T. D., GOROUHI, F., NGUYEN, C., LIN, B. R., MASHBURN, C., STEWART, H., PEAVY, T. R., NOLTA, J. A. & ISSEROFF, R. R. 2014. Crosstalk between adrenergic and toll-like receptors in human mesenchymal stem cells and keratinocytes: a recipe for impaired wound healing. *Stem Cells Transl Med,* 3**,** 745-59.

DAVIDSON, M. D., BALLINGER, K. R. & KHETANI, S. R. 2016. Long-term exposure to abnormal glucose levels alters drug metabolism pathways and insulin sensitivity in primary human hepatocytes. *Sci Rep,* 6**,** 28178.

DAVIDSON, M. D., WARE, B. R. & KHETANI, S. R. 2015. Stem cell-derived liver cells for drug testing and disease modeling. *Discov Med,* 19**,** 349-58.

DAVOLI, T. & DE LANGE, T. 2011. The causes and consequences of polyploidy in normal development and cancer. *Annu Rev Cell Dev Biol,* 27**,** 585-610.

DAWSON, M. I. & XIA, Z. 2012. The retinoid X receptors and their ligands. *Biochim Biophys Acta,* 1821**,** 21-56.

DE KANTER, R., OLINGA, P., DE JAGER, M. H., MEREMA, M. T., MEIJER, D. K. & GROOTHIUS, G. M. 1999. Organ slices as an in vitro test system for drug metabolism in human liver, lung and kidney. *Toxicol In Vitro,* 13**,** 737-44.

DE SERRES, F. & BLANCO, I. 2014. Role of alpha-1 antitrypsin in human health and disease. *J Intern Med,* 276**,** 311-35.

DE URQUIZA, A. M., LIU, S., SJÖBERG, M., ZETTERSTRÖM, R. H., GRIFFITHS, W., SJÖVALL, J. & PERLMANN, T. 2000. Docosahexaenoic acid, a ligand for the retinoid X receptor in mouse brain. *Science,* 290**,** 2140-4.

DELFOSSE, V., DENDELE, B., HUET, T., GRIMALDI, M., BOULAHTOUF, A., GERBAL-CHALOIN, S., BEUCHER, B., ROECKLIN, D., MULLER, C., RAHMANI, R., CAVAILLÈS, V., DAUJAT-CHAVANIEU, M., VIVAT, V., PASCUSSI, J. M., BALAGUER, P. & BOURGUET, W. 2015. Synergistic activation of human pregnane X receptor by binary cocktails of pharmaceutical and environmental compounds. *Nat Commun,* 6**,** 8089.

DELRASO, N. J. 1993. In vitro methodologies for enhanced toxicity testing. *Toxicol Lett,* 68**,** 91-9.

DENAYER, T. 2014. Animal models in translational medicine: Validation and prediction. *In:* TINNEKE DENAYER, T. S., MAARTEN VAN ROY (ed.). New Horizons in Translational Medicine: Elsevier.

DENHAM, M. & DOTTORI, M. 2011. Neural differentiation of induced pluripotent stem cells. *Methods Mol Biol,* 793**,** 99-110.

DENNING, C., ALLEGRUCCI, C., PRIDDLE, H., BARBADILLO-MUÑOZ, M. D., ANDERSON, D., SELF, T., SMITH, N. M., PARKIN, C. T. & YOUNG, L. E. 2006. Common culture conditions for maintenance and cardiomyocyte differentiation of the human embryonic stem cell lines, BG01 and HUES-7. *Int J Dev Biol,* 50**,** 27-37.

DHAR, D. & HSI-EN HO, J. 2009. Stem cell research policies around the world. *Yale J Biol Med,* 82**,** 113-5.

DI GIORGIO, F. P., BOULTING, G. L., BOBROWICZ, S. & EGGAN, K. C. 2008. Human embryonic stem cell-derived motor neurons are sensitive to the toxic effect of glial cells carrying an ALS-causing mutation. *Cell Stem Cell,* 3**,** 637-48.

DI MASI, A., LEBOFFE, L., DE MARINIS, E., PAGANO, F., CICCONI, L., ROCHETTE-EGLY, C., LO-COCO, F., ASCENZI, P. & NERVI, C. 2015. Retinoic acid receptors: from molecular mechanisms to cancer therapy. *Mol Aspects Med,* 41**,** 1-115.

DING, L. & MORRISON, S. J. 2013. Haematopoietic stem cells and early lymphoid progenitors occupy distinct bone marrow niches. *Nature,* 495**,** 231-5.

DONG, J., MANDENIUS, C. F., LÜBBERSTEDT, M., URBANIAK, T., NÜSSLER, A. K., KNOBELOCH, D., GERLACH, J. C. & ZEILINGER, K. 2008. Evaluation and optimization of hepatocyte culture media factors by design of experiments (DoE) methodology. *Cytotechnology,* 57**,** 251-61.

DOOGUE, M. P. & POLASEK, T. M. 2013. The ABCD of clinical pharmacokinetics. *Ther*

Adv Drug Saf, 4**,** 5-7.

DROCOURT, L., OURLIN, J. C., PASCUSSI, J. M., MAUREL, P. & VILAREM, M. J. 2002. Expression of CYP3A4, CYP2B6, and CYP2C9 is regulated by the vitamin D receptor pathway in primary human hepatocytes. *J Biol Chem,* 277**,** 25125-32.

DU, Y., LI, N., YANG, H., LUO, C., GONG, Y., TONG, C., GAO, Y., LÜ, S. & LONG, M. 2017. Mimicking liver sinusoidal structures and functions using a 3D-configured microfluidic chip. *Lab Chip,* 17**,** 782-794.

DUAN, Y., MA, X., ZOU, W., WANG, C., BAHBAHAN, I. S., AHUJA, T. P., TOLSTIKOV, V. & ZERN, M. A. 2010. Differentiation and characterization of metabolically functioning hepatocytes from human embryonic stem cells. *Stem Cells,* 28**,** 674-86.

DUNIEC-DMUCHOWSKI, Z., ELLIS, E., STROM, S. C. & KOCAREK, T. A. 2007. Regulation of CYP3A4 and CYP2B6 expression by liver X receptor agonists. *Biochem Pharmacol,* 74**,** 1535-40.

DUPONT, S., MORSUT, L., ARAGONA, M., ENZO, E., GIULITTI, S., CORDENONSI, M., ZANCONATO, F., LE DIGABEL, J., FORCATO, M., BICCIATO, S., ELVASSORE, N. & PICCOLO, S. 2011. Role of YAP/TAZ in mechanotransduction. *Nature,* 474**,** 179-83.

DYE, B. R., DEDHIA, P. H., MILLER, A. J., NAGY, M. S., WHITE, E. S., SHEA, L. D. & SPENCE, J. R. 2016. A bioengineered niche promotes in vivo engraftment and maturation of pluripotent stem cell derived human lung organoids. *Elife,* 5.

EBRAHIMKHANI, M. R., NEIMAN, J. A., RAREDON, M. S., HUGHES, D. J. & GRIFFITH, L. G. 2014. Bioreactor technologies to support liver function in vitro. *Adv Drug Deliv Rev,* 69-70**,** 132-57.

ECK-ENRIQUEZ, K., KIEFER, T. L., SPRIGGS, L. L. & HILL, S. M. 2000. Pathways through which a regimen of melatonin and retinoic acid induces apoptosis in MCF-7 human breast cancer cells. *Breast Cancer Res Treat,* 61**,** 229-39.

ELAUT, G., HENKENS, T., PAPELEU, P., SNYKERS, S., VINKEN, M., VANHAECKE, T. & ROGIERS, V. 2006. Molecular mechanisms underlying the dedifferentiation process of isolated hepatocytes and their cultures. *Curr Drug Metab,* 7**,** 629-60.

ELAUT, G., LAUS, G., ALEXANDRE, E., RICHERT, L., BACHELLIER, P., TOURWÉ, D., ROGIERS, V. & VANHAECKE, T. 2007. A metabolic screening study of trichostatin A (TSA) and TSA-like histone deacetylase inhibitors in rat and human primary hepatocyte cultures. *J Pharmacol Exp Ther,* 321**,** 400-8.

ELLERSTRÖM, C., STREHL, R., NOAKSSON, K., HYLLNER, J. & SEMB, H. 2007. Facilitated expansion of human embryonic stem cells by single-cell enzymatic dissociation. *Stem Cells,* 25**,** 1690-6.

EVANS, W. E. & RELLING, M. V. 1999. Pharmacogenomics: translating functional genomics into rational therapeutics. *Science,* 286**,** 487-91.

FANG, B., MANE-PADROS, D., BOLOTIN, E., JIANG, T. & SLADEK, F. M. 2012a. Identification of a binding motif specific to HNF4 by comparative analysis of multiple nuclear receptors. *Nucleic Acids Res,* 40**,** 5343-56.

FANG, X. L., SHU, G., ZHANG, Z. Q., WANG, S. B., ZHU, X. T., GAO, P., XI, Q. Y., ZHANG, Y. L. & JIANG, Q. Y. 2012b. Roles of α-linolenic acid on IGF-I secretion and GH/IGF system gene expression in porcine primary

hepatocytes. *Mol Biol Rep,* 39**,** 10987-96.
FARAH, B. L., SINHA, R. A., WU, Y., SINGH, B. K., ZHOU, J., BAY, B. H. & YEN, P. M. 2014. β-Adrenergic agonist and antagonist regulation of autophagy in HepG2 cells, primary mouse hepatocytes, and mouse liver. *PLoS One,* 9**,** e98155.
FATEYE, B., WAN, A., YANG, X., MYERS, K. & CHEN, B. 2015. Comparison between endothelial and tumor cells in the response to verteporfin-photodynamic therapy and a PI3K pathway inhibitor. *Photodiagnosis Photodyn Ther,* 12**,** 19-26.
FENG, X., JIANG, Y., MELTZER, P. & YEN, P. M. 2000. Thyroid hormone regulation of hepatic genes in vivo detected by complementary DNA microarray. *Mol Endocrinol,* 14**,** 947-55.
FERNÁNDEZ-ALVAREZ, A., ALVAREZ, M. S., GONZALEZ, R., CUCARELLA, C., MUNTANÉ, J. & CASADO, M. 2011. Human SREBP1c expression in liver is directly regulated by peroxisome proliferator-activated receptor alpha (PPARalpha). *J Biol Chem,* 286**,** 21466-77.
FESTING, S. & WILKINSON, R. 2007. The ethics of animal research. Talking Point on the use of animals in scientific research. *EMBO Rep,* 8**,** 526-30.
FINCK, B. N. & KELLY, D. P. 2006. PGC-1 coactivators: inducible regulators of energy metabolism in health and disease. *J Clin Invest,* 116**,** 615-22.
FLECKNELL, P. 2002. Replacement, reduction and refinement. *ALTEX,* 19**,** 73-8.
FRACZEK, J. E., VINKEN, M., TOURWÉ, D., VANHAECKE, T. & ROGIERS, V. 2012. Synergetic effects of DNA demethylation and histone deacetylase inhibition in primary rat hepatocytes. *Invest New Drugs,* 30**,** 1715-24.
FREEDMAN, D. A., KASHIMA, Y. & ZARET, K. S. 2007. Endothelial cell promotion of early liver and pancreas development. *Novartis Found Symp,* 283**,** 207-16; discussion 216-9, 238-41.
FU, D., WAKABAYASHI, Y., LIPPINCOTT-SCHWARTZ, J. & ARIAS, I. M. 2011. Bile acid stimulates hepatocyte polarization through a cAMP-Epac-MEK-LKB1-AMPK pathway. *Proc Natl Acad Sci U S A,* 108**,** 1403-8.
FUJIKURA, K., INGELMAN-SUNDBERG, M. & LAUSCHKE, V. M. 2015. Genetic variation in the human cytochrome P450 supergene family. *Pharmacogenet Genomics,* 25**,** 584-94.
FUNAKOSHI, N., DURET, C., PASCUSSI, J. M., BLANC, P., MAUREL, P., DAUJAT-CHAVANIEU, M. & GERBAL-CHALOIN, S. 2011. Comparison of hepatic-like cell production from human embryonic stem cells and adult liver progenitor cells: CAR transduction activates a battery of detoxification genes. *Stem Cell Rev,* 7**,** 518-31.
FUSAKI, N., BAN, H., NISHIYAMA, A., SAEKI, K. & HASEGAWA, M. 2009. Efficient induction of transgene-free human pluripotent stem cells using a vector based on Sendai virus, an RNA virus that does not integrate into the host genome. *Proc Jpn Acad Ser B Phys Biol Sci,* 85**,** 348-62.
GAGE, B. K., WEBBER, T. D. & KIEFFER, T. J. 2013. Initial cell seeding density influences pancreatic endocrine development during in vitro differentiation of human embryonic stem cells. *PLoS One,* 8**,** e82076.
GAISFORD, W. 2012. Robotic liquid handling and automation in epigenetics. *J Lab Autom,* 17**,** 327-9.
GAJOWIAK, A., STYŚ, A., STARZYŃSKI, R. R., BEDNARZ, A., LENARTOWICZ, M.,

STAROŃ, R. & LIPIŃSKI, P. 2015. Mice Overexpressing Both Non-Mutated Human SOD1 and Mutated SOD1(G93A) Genes: A Competent Experimental Model for Studying Iron Metabolism in Amyotrophic Lateral Sclerosis. *Front Mol Neurosci,* 8**,** 82.

GARCIA, M. C., THANGAVEL, C. & SHAPIRO, B. H. 2001. Epidermal growth factor regulation of female-dependent CYP2A1 and CYP2C12 in primary rat hepatocyte culture. *Drug Metab Dispos,* 29**,** 111-20.

GARGIULO, L., COPSEL, S., RIVERO, E. M., GALÉS, C., SÉNARD, J. M., LÜTHY, I. A., DAVIO, C. & BRUZZONE, A. 2014. Differential β_2-adrenergic receptor expression defines the phenotype of non-tumorigenic and malignant human breast cell lines. *Oncotarget,* 5**,** 10058-69.

GARVEY, C. M., SPILLER, E., LINDSAY, D., CHIANG, C. T., CHOI, N. C., AGUS, D. B., MALLICK, P., FOO, J. & MUMENTHALER, S. M. 2016. A high-content image-based method for quantitatively studying context-dependent cell population dynamics. *Sci Rep,* 6**,** 29752.

GENBACEV, O., KRTOLICA, A., ZDRAVKOVIC, T., BRUNETTE, E., POWELL, S., NATH, A., CACERES, E., MCMASTER, M., MCDONAGH, S., LI, Y., MANDALAM, R., LEBKOWSKI, J. & FISHER, S. J. 2005. Serum-free derivation of human embryonic stem cell lines on human placental fibroblast feeders. *Fertil Steril,* 83**,** 1517-29.

GENTRIC, G. & DESDOUETS, C. 2014. Polyploidization in liver tissue. *Am J Pathol,* 184**,** 322-31.

GENTRIC, G., DESDOUETS, C. & CELTON-MORIZUR, S. 2012. Hepatocytes polyploidization and cell cycle control in liver physiopathology. *Int J Hepatol,* 2012**,** 282430.

GERETS, H. H., TILMANT, K., GERIN, B., CHANTEUX, H., DEPELCHIN, B. O., DHALLUIN, S. & ATIENZAR, F. A. 2012. Characterization of primary human hepatocytes, HepG2 cells, and HepaRG cells at the mRNA level and CYP activity in response to inducers and their predictivity for the detection of human hepatotoxins. *Cell Biol Toxicol,* 28**,** 69-87.

GHANOUNI, P., GRYCZYNSKI, Z., STEENHUIS, J. J., LEE, T. W., FARRENS, D. L., LAKOWICZ, J. R. & KOBILKA, B. K. 2001. Functionally different agonists induce distinct conformations in the G protein coupling domain of the beta 2 adrenergic receptor. *J Biol Chem,* 276**,** 24433-6.

GOLDBERG, A. A., BEACH, A., DAVIES, G. F., HARKNESS, T. A., LEBLANC, A. & TITORENKO, V. I. 2011. Lithocholic bile acid selectively kills neuroblastoma cells, while sparing normal neuronal cells. *Oncotarget,* 2**,** 761-82.

GRAFFMANN, N., RING, S., KAWALA, M. A., WRUCK, W., NCUBE, A., TROMPETER, H. I. & ADJAYE, J. 2016. Modeling Nonalcoholic Fatty Liver Disease with Human Pluripotent Stem Cell-Derived Immature Hepatocyte-Like Cells Reveals Activation of PLIN2 and Confirms Regulatory Functions of Peroxisome Proliferator-Activated Receptor Alpha. *Stem Cells Dev,* 25**,** 1119-33.

GRAHAM, M. J. & LAKE, B. G. 2008. Induction of drug metabolism: species differences and toxicological relevance. *Toxicology,* 254**,** 184-91.

GRIDELLI, B., VIZZINI, G., PIETROSI, G., LUCA, A., SPADA, M., GRUTTADAURIA, S., CINTORINO, D., AMICO, G., CHINNICI, C., MIKI, T., SCHMELZER, E., CONALDI, P. G., TRIOLO, F. & GERLACH, J. C. 2012. Efficient human fetal liver cell

isolation protocol based on vascular perfusion for liver cell-based therapy and case report on cell transplantation. *Liver Transpl,* 18**,** 226-37.

GRIPON, P., RUMIN, S., URBAN, S., LE SEYEC, J., GLAISE, D., CANNIE, I., GUYOMARD, C., LUCAS, J., TREPO, C. & GUGUEN-GUILLOUZO, C. 2002. Infection of a human hepatoma cell line by hepatitis B virus. *Proc Natl Acad Sci U S A,* 99**,** 15655-60.

GU, J., TONG, X. S., CHEN, G. H., WANG, D., CHEN, Y., YUAN, Y., LIU, X. Z., BIAN, J. C. & LIU, Z. P. 2015. Effects of 1α,25-(OH)2D3 on the formation and activity of osteoclasts in RAW264.7 cells. *J Steroid Biochem Mol Biol,* 152**,** 25-33.

GUGUEN-GUILLOUZO, C. & GUILLOUZO, A. 2010. General review on in vitro hepatocyte models and their applications. *Methods Mol Biol,* 640**,** 1-40.

GUILLOUZO, A., CORLU, A., ANINAT, C., GLAISE, D., MOREL, F. & GUGUEN-GUILLOUZO, C. 2007. The human hepatoma HepaRG cells: a highly differentiated model for studies of liver metabolism and toxicity of xenobiotics. *Chem Biol Interact,* 168**,** 66-73.

GUO, L., DIAL, S., SHI, L., BRANHAM, W., LIU, J., FANG, J. L., GREEN, B., DENG, H., KAPUT, J. & NING, B. 2011. Similarities and differences in the expression of drug-metabolizing enzymes between human hepatic cell lines and primary human hepatocytes. *Drug Metab Dispos,* 39**,** 528-38.

GUO, R., XU, X., LU, Y. & XIE, X. 2017. Physiological oxygen tension reduces hepatocyte dedifferentiation in in vitro culture. *Sci Rep,* 7**,** 5923.

GUPTA, S. 2000. Hepatic polyploidy and liver growth control. *Semin Cancer Biol,* 10**,** 161-71.

GUZEY, M., LUO, J. & GETZENBERG, R. H. 2004. Vitamin D3 modulated gene expression patterns in human primary normal and cancer prostate cells. *J Cell Biochem,* 93**,** 271-85.

HACKAM, D. G. 2007. Translating animal research into clinical benefit. *BMJ,* 334**,** 163-4.

HAGEN, N., OLSEN, A. K., ANDERSEN, J. V., TJØRNELUND, J. & HANSEN, S. H. 2002. Characterization of mixtures of recombinant human cytochrome p450s as a screening model for metabolic stability in drug discovery. *Xenobiotica,* 32**,** 749-59.

HAMAZAKI, T., IIBOSHI, Y., OKA, M., PAPST, P. J., MEACHAM, A. M., ZON, L. I. & TERADA, N. 2001. Hepatic maturation in differentiating embryonic stem cells in vitro. *FEBS Lett,* 497**,** 15-9.

HAN, S. & CHIANG, J. Y. 2009. Mechanism of vitamin D receptor inhibition of cholesterol 7alpha-hydroxylase gene transcription in human hepatocytes. *Drug Metab Dispos,* 37**,** 469-78.

HAND, D. J. 2015. From evidence to understanding: a commentary on Fisher (1922) 'On the mathematical foundations of theoretical statistics'. *Philos Trans A Math Phys Eng Sci,* 373.

HANNAN, N. R., SEGERITZ, C. P., TOUBOUL, T. & VALLIER, L. 2013. Production of hepatocyte-like cells from human pluripotent stem cells. *Nat Protoc,* 8**,** 430-7.

HANNOUN, Z., STEICHEN, C., DIANAT, N., WEBER, A. & DUBART-KUPPERSCHMITT, A. 2016. The Potential of Induced Pluripotent Stem Cell derived Hepatocytes. *J Hepatol*.

HARIDASS, D., YUAN, Q., BECKER, P. D., CANTZ, T., IKEN, M., ROTHE, M., NARAIN, N., BOCK, M., NÖRDER, M., LEGRAND, N., WEDEMEYER, H., WEIJER, K., SPITS, H., MANNS, M. P., CAI, J., DENG, H., DI SANTO, J. P., GUZMAN, C. A. & OTT, M. 2009. Repopulation efficiencies of adult hepatocytes, fetal liver progenitor cells, and embryonic stem cell-derived hepatic cells in albumin-promoter-enhancer urokinase-type plasminogen activator mice. *Am J Pathol,* 175**,** 1483-92.

HAY, D. C., FLETCHER, J., PAYNE, C., TERRACE, J. D., GALLAGHER, R. C., SNOEYS, J., BLACK, J. R., WOJTACHA, D., SAMUEL, K., HANNOUN, Z., PRYDE, A., FILIPPI, C., CURRIE, I. S., FORBES, S. J., ROSS, J. A., NEWSOME, P. N. & IREDALE, J. P. 2008a. Highly efficient differentiation of hESCs to functional hepatic endoderm requires ActivinA and Wnt3a signaling. *Proc Natl Acad Sci U S A,* 105**,** 12301-6.

HAY, D. C., ZHAO, D., FLETCHER, J., HEWITT, Z. A., MCLEAN, D., URRUTICOECHEA-URIGUEN, A., BLACK, J. R., ELCOMBE, C., ROSS, J. A., WOLF, R. & CUI, W. 2008b. Efficient differentiation of hepatocytes from human embryonic stem cells exhibiting markers recapitulating liver development in vivo. *Stem Cells,* 26**,** 894-902.

HAY, D. C., ZHAO, D., ROSS, A., MANDALAM, R., LEBKOWSKI, J. & CUI, W. 2007. Direct differentiation of human embryonic stem cells to hepatocyte-like cells exhibiting functional activities. *Cloning Stem Cells,* 9**,** 51-62.

HE, B., ZHAO, Y., XU, L., GAO, L., SU, Y., LIN, N. & PU, J. 2016. The nuclear melatonin receptor RORα is a novel endogenous defender against myocardial ischemia/reperfusion injury. *J Pineal Res,* 60**,** 313-26.

HE, L., SABET, A., DJEDJOS, S., MILLER, R., SUN, X., HUSSAIN, M. A., RADOVICK, S. & WONDISFORD, F. E. 2009. Metformin and insulin suppress hepatic gluconeogenesis through phosphorylation of CREB binding protein. *Cell,* 137**,** 635-46.

HE, Y., GONG, L., FANG, Y., ZHAN, Q., LIU, H. X., LU, Y., GUO, G. L., LEHMAN-MCKEEMAN, L., FANG, J. & WAN, Y. J. 2013. The role of retinoic acid in hepatic lipid homeostasis defined by genomic binding and transcriptome profiling. *BMC Genomics,* 14**,** 575.

HELSEN, N., DEBING, Y., PAESHUYSE, J., DALLMEIER, K., BOON, R., COLL, M., SANCHO-BRU, P., CLAES, C., NEYTS, J. & VERFAILLIE, C. M. 2016. Stem cell-derived hepatocytes: A novel model for hepatitis E virus replication. *J Hepatol,* 64**,** 565-73.

HENG, B. C., LIU, H. & CAO, T. 2004. Feeder cell density--a key parameter in human embryonic stem cell culture. *In Vitro Cell Dev Biol Anim,* 40**,** 255-7.

HENG, B. C., LIU, H., GE, Z. & CAO, T. 2007. Mechanical dissociation of human embryonic stem cell colonies by manual scraping after collagenase treatment is much more detrimental to cellular viability than is trypsinization with gentle pipetting. *Biotechnol Appl Biochem,* 47**,** 33-7.

HEUBERGER, J. & BIRCHMEIER, W. 2010. Interplay of cadherin-mediated cell adhesion and canonical Wnt signaling. *Cold Spring Harb Perspect Biol,* 2**,** a002915.

HINES, M., CONSTANTINESCU, M. & SPENCER, D. 2015. Early androgen exposure and human gender development. *Biol Sex Differ,* 6**,** 3.

HOLMQVIST, S., LEHTONEN, Š., CHUMARINA, M., PUTTONEN, K. A., AZEVEDO, C., LEBEDEVA, O., RUPONEN, M., OKSANEN, M., DJELLOUL, M., COLLIN, A., GOLDWURM, S., MEYER, M., LAGARKOVA, M., KISELEV, S., KOISTINAHO, J. & ROYBON, L. 2016. Creation of a library of induced pluripotent stem cells from Parkinsonian patients. *NPJ Parkinsons Dis,* 2**,** 16009.

HOPKINSON, B. M., DESLER, C., KALISZ, M., VESTENTOFT, P. S., JUEL RASMUSSEN, L. & BISGAARD, H. C. 2017. Bioenergetic Changes during Differentiation of Human Embryonic Stem Cells along the Hepatic Lineage. *Oxid Med Cell Longev,* 2017**,** 5080128.

HU, W., ZHAO, J. & PEI, G. 2013. Activation of aryl hydrocarbon receptor (ahr) by tranilast, an anti-allergy drug, promotes miR-302 expression and cell reprogramming. *J Biol Chem,* 288**,** 22972-84.

HUANG, Y., ZHAO, Z., XU, H., SHYR, Y. & ZHANG, B. 2012. Advances in systems biology: computational algorithms and applications. *BMC Syst Biol,* 6 Suppl 3**,** S1.

HUBER, A. H., STEWART, D. B., LAURENTS, D. V., NELSON, W. J. & WEIS, W. I. 2001. The cadherin cytoplasmic domain is unstructured in the absence of beta-catenin. A possible mechanism for regulating cadherin turnover. *J Biol Chem,* 276**,** 12301-9.

HUGHES, C. S., POSTOVIT, L. M. & LAJOIE, G. A. 2010. Matrigel: a complex protein mixture required for optimal growth of cell culture. *Proteomics,* 10**,** 1886-90.

HUGHES, J. P., REES, S., KALINDJIAN, S. B. & PHILPOTT, K. L. 2011. Principles of early drug discovery. *Br J Pharmacol,* 162**,** 1239-49.

HUNTER, M. P., WILSON, C. M., JIANG, X., CONG, R., VASAVADA, H., KAESTNER, K. H. & BOGUE, C. W. 2007. The homeobox gene Hhex is essential for proper hepatoblast differentiation and bile duct morphogenesis. *Dev Biol,* 308**,** 355-67.

HWANG, T. J., CARPENTER, D., LAUFFENBURGER, J. C., WANG, B., FRANKLIN, J. M. & KESSELHEIM, A. S. 2016. Failure of Investigational Drugs in Late-Stage Clinical Development and Publication of Trial Results. *JAMA Intern Med,* 176**,** 1826-1833.

ILIC, D. & OGILVIE, C. 2017. Concise Review: Human Embryonic Stem Cells-What Have We Done? What Are We Doing? Where Are We Going? *Stem Cells,* 35**,** 17-25.

INGS, J. S., GEORGE, N., PETER, M. C., SERVOS, M. R. & VIJAYAN, M. M. 2012. Venlafaxine and atenolol disrupt epinephrine-stimulated glucose production in rainbow trout hepatocytes. *Aquat Toxicol,* 106-107**,** 48-55.

ISHIKAWA, T., FACTOR, V. M., MARQUARDT, J. U., RAGGI, C., SEO, D., KITADE, M., CONNER, E. A. & THORGEIRSSON, S. S. 2012. Hepatocyte growth factor/c-met signaling is required for stem-cell-mediated liver regeneration in mice. *Hepatology,* 55**,** 1215-26.

IYANAGI, T. 2007. Molecular mechanism of phase I and phase II drug-metabolizing enzymes: implications for detoxification. *Int Rev Cytol,* 260**,** 35-112.

JAGANNATHAN-BOGDAN, M. & ZON, L. I. 2013. Hematopoiesis. *Development,* 140**,** 2463-7.

JAMES, S. Y., LIN, F., KOLLURI, S. K., DAWSON, M. I. & ZHANG, X. K. 2003. Regulation of retinoic acid receptor beta expression by peroxisome proliferator-

activated receptor gamma ligands in cancer cells. *Cancer Res,* 63**,** 3531-8.
JANCOVA, P., ANZENBACHER, P. & ANZENBACHEROVA, E. 2010. Phase II drug metabolizing enzymes. *Biomed Pap Med Fac Univ Palacky Olomouc Czech Repub,* 154**,** 103-16.
JEMNITZ, K., VERES, Z., SZABO, M., BARANYAI, Z., JAKAB, F. & VERECZKEY, L. 2012. Differential inhibitory effect of cyclosporin A and bosentan on taurocholate uptake in human and rat hepatocytes as a function of culturing time. *Toxicol In Vitro,* 26**,** 174-81.
JENSEN, J., HYLLNER, J. & BJÖRQUIST, P. 2009. Human embryonic stem cell technologies and drug discovery. *J Cell Physiol,* 219**,** 513-9.
JIA, F., WILSON, K. D., SUN, N., GUPTA, D. M., HUANG, M., LI, Z., PANETTA, N. J., CHEN, Z. Y., ROBBINS, R. C., KAY, M. A., LONGAKER, M. T. & WU, J. C. 2010. A nonviral minicircle vector for deriving human iPS cells. *Nat Methods,* 7**,** 197-9.
JIANG, H., OUYANG, Z., ZENG, J., YUAN, L., ZHENG, N., JEMAL, M. & ARNOLD, M. E. 2012. A user-friendly robotic sample preparation program for fully automated biological sample pipetting and dilution to benefit the regulated bioanalysis. *J Lab Autom,* 17**,** 211-21.
JIANG, X. L., GONZALEZ, F. J. & YU, A. M. 2011. Drug-metabolizing enzyme, transporter, and nuclear receptor genetically modified mouse models. *Drug Metab Rev,* 43**,** 27-40.
JOANNIDES, A., FIORE-HÉRICHÉ, C., WESTMORE, K., CALDWELL, M., COMPSTON, A., ALLEN, N. & CHANDRAN, S. 2006. Automated mechanical passaging: a novel and efficient method for human embryonic stem cell expansion. *Stem Cells,* 24**,** 230-5.
JOHNSON, R. & HALDER, G. 2014. The two faces of Hippo: targeting the Hippo pathway for regenerative medicine and cancer treatment. *Nat Rev Drug Discov,* 13**,** 63-79.
JUMP, D. B., BOTOLIN, D., WANG, Y., XU, J., CHRISTIAN, B. & DEMEURE, O. 2005. Fatty acid regulation of hepatic gene transcription. *J Nutr,* 135**,** 2503-6.
KALISTA, T., FREEMAN, H. A., BEHR, B., PERA, R. R. & SCOTT, C. T. 2011. Donation of embryos for human development and stem cell research. *Cell Stem Cell,* 8**,** 360-2.
KALLURI, R. & WEINBERG, R. A. 2009. The basics of epithelial-mesenchymal transition. *J Clin Invest,* 119**,** 1420-8.
KAMI, D., WATAKABE, K., YAMAZAKI-INOUE, M., MINAMI, K., KITANI, T., ITAKURA, Y., TOYODA, M., SAKURAI, T., UMEZAWA, A. & GOJO, S. 2013. Large-scale cell production of stem cells for clinical application using the automated cell processing machine. *BMC Biotechnol,* 13**,** 102.
KAMIMURA, H., NAKADA, N., SUZUKI, K., MERA, A., SOUDA, K., MURAKAMI, Y., TANAKA, K., IWATSUBO, T., KAWAMURA, A. & USUI, T. 2010. Assessment of chimeric mice with humanized liver as a tool for predicting circulating human metabolites. *Drug Metab Pharmacokinet,* 25**,** 223-35.
KAMIYA, A., KINOSHITA, T., ITO, Y., MATSUI, T., MORIKAWA, Y., SENBA, E., NAKASHIMA, K., TAGA, T., YOSHIDA, K., KISHIMOTO, T. & MIYAJIMA, A. 1999. Fetal liver development requires a paracrine action of oncostatin M through the gp130 signal transducer. *EMBO J,* 18**,** 2127-36.

KAMIYA, A., KINOSHITA, T. & MIYAJIMA, A. 2001. Oncostatin M and hepatocyte growth factor induce hepatic maturation via distinct signaling pathways. *FEBS Lett,* 492**,** 90-4.

KASVOSVE, I. & DELANGHE, J. 2002. Total iron binding capacity and transferrin concentration in the assessment of iron status. *Clin Chem Lab Med,* 40**,** 1014-8.

KATENZ, E., VONDRAN, F. W., SCHWARTLANDER, R., PLESS, G., GONG, X., CHENG, X., NEUHAUS, P. & SAUER, I. M. 2007. Cryopreservation of primary human hepatocytes: the benefit of trehalose as an additional cryoprotective agent. *Liver Transpl,* 13**,** 38-45.

KATO, R., IEJIMA, D., AGATA, H., ASAHINA, I., OKADA, K., UEDA, M., HONDA, H. & KAGAMI, H. 2010. A compact, automated cell culture system for clinical scale cell expansion from primary tissues. *Tissue Eng Part C Methods,* 16**,** 947-56.

KATO, T. & TAKADA, S. 2017. In vivo and in vitro disease modeling with CRISPR/Cas9. *Brief Funct Genomics,* 16**,** 13-24.

KATOH, M. & YOKOI, T. 2007. Application of chimeric mice with humanized liver for predictive ADME. *Drug Metab Rev,* 39**,** 145-57.

KEEMINK, J., OORTS, M. & ANNAERT, P. 2015. Primary Hepatocytes in Sandwich Culture. *Methods Mol Biol,* 1250**,** 175-88.

KEMP, P. J., RUSHTON, D. J., YAROVA, P. L., SCHNELL, C., GEATER, C., HANCOCK, J. M., WIELAND, A., HUGHES, A., BADDER, L., COPE, E., RICCARDI, D., RANDALL, A. D., BROWN, J. T., ALLEN, N. D. & TELEZHKIN, V. 2016. Improving and accelerating the differentiation and functional maturation of human stem cell-derived neurons: role of extracellular calcium and GABA. *J Physiol,* 594**,** 6583-6594.

KER, D. F., WEISS, L. E., JUNKERS, S. N., CHEN, M., YIN, Z., SANDBOTHE, M. F., HUH, S. I., EOM, S., BISE, R., OSUNA-HIGHLEY, E., KANADE, T. & CAMPBELL, P. G. 2011. An engineered approach to stem cell culture: automating the decision process for real-time adaptive subculture of stem cells. *PLoS One,* 6**,** e27672.

KHODABUKUS, A. & BAAR, K. 2014. The effect of serum origin on tissue engineered skeletal muscle function. *J Cell Biochem,* 115**,** 2198-207.

KIA, R., SISON, R. L., HESLOP, J., KITTERINGHAM, N. R., HANLEY, N., MILLS, J. S., PARK, B. K. & GOLDRING, C. E. 2013. Stem cell-derived hepatocytes as a predictive model for drug-induced liver injury: are we there yet? *Br J Clin Pharmacol,* 75**,** 885-96.

KIDAMBI, S., YARMUSH, R. S., NOVIK, E., CHAO, P., YARMUSH, M. L. & NAHMIAS, Y. 2009. Oxygen-mediated enhancement of primary hepatocyte metabolism, functional polarization, gene expression, and drug clearance. *Proc Natl Acad Sci U S A,* 106**,** 15714-9.

KIELY, M., HODGINS, S. J., MERRIGAN, B. A., TORMEY, S., KIELY, P. A. & O'CONNOR, E. M. 2015. Real-time cell analysis of the inhibitory effect of vitamin K2 on adhesion and proliferation of breast cancer cells. *Nutr Res,* 35**,** 736-43.

KILPINEN, H., GONCALVES, A., LEHA, A., AFZAL, V., ALASOO, K., ASHFORD, S., BALA, S., BENSADDEK, D., CASALE, F. P., CULLEY, O. J., DANECEK, P., FAULCONBRIDGE, A., HARRISON, P. W., KATHURIA, A., MCCARTHY, D., MCCARTHY, S. A., MELECKYTE, R., MEMARI, Y., MOENS, N., SOARES, F., MANN, A., STREETER, I., AGU, C. A., ALDERTON, A., NELSON, R., HARPER, S.,

PATEL, M., WHITE, A., PATEL, S. R., CLARKE, L., HALAI, R., KIRTON, C. M., KOLB-KOKOCINSKI, A., BEALES, P., BIRNEY, E., DANOVI, D., LAMOND, A. I., OUWEHAND, W. H., VALLIER, L., WATT, F. M., DURBIN, R., STEGLE, O. & GAFFNEY, D. J. 2017. Common genetic variation drives molecular heterogeneity in human iPSCs. *Nature,* 546**,** 370-375.

KIM, D., KIM, C. H., MOON, J. I., CHUNG, Y. G., CHANG, M. Y., HAN, B. S., KO, S., YANG, E., CHA, K. Y., LANZA, R. & KIM, K. S. 2009. Generation of human induced pluripotent stem cells by direct delivery of reprogramming proteins. *Cell Stem Cell,* 4**,** 472-6.

KIM, H. M., KIM, J. W., CHOI, Y., CHUN, H. S., IM, I., HAN, Y. M., SONG, C. W., YOON, S. & PARK, H. J. 2016. Xeno-sensing activity of the aryl hydrocarbon receptor in human pluripotent stem cell-derived hepatocyte-like cells. *Sci Rep,* 6**,** 21684.

KIM, M. S., PINTO, S. M., GETNET, D., NIRUJOGI, R. S., MANDA, S. S., CHAERKADY, R., MADUGUNDU, A. K., KELKAR, D. S., ISSERLIN, R., JAIN, S., THOMAS, J. K., MUTHUSAMY, B., LEAL-ROJAS, P., KUMAR, P., SAHASRABUDDHE, N. A., BALAKRISHNAN, L., ADVANI, J., GEORGE, B., RENUSE, S., SELVAN, L. D., PATIL, A. H., NANJAPPA, V., RADHAKRISHNAN, A., PRASAD, S., SUBBANNAYYA, T., RAJU, R., KUMAR, M., SREENIVASAMURTHY, S. K., MARIMUTHU, A., SATHE, G. J., CHAVAN, S., DATTA, K. K., SUBBANNAYYA, Y., SAHU, A., YELAMANCHI, S. D., JAYARAM, S., RAJAGOPALAN, P., SHARMA, J., MURTHY, K. R., SYED, N., GOEL, R., KHAN, A. A., AHMAD, S., DEY, G., MUDGAL, K., CHATTERJEE, A., HUANG, T. C., ZHONG, J., WU, X., SHAW, P. G., FREED, D., ZAHARI, M. S., MUKHERJEE, K. K., SHANKAR, S., MAHADEVAN, A., LAM, H., MITCHELL, C. J., SHANKAR, S. K., SATISHCHANDRA, P., SCHROEDER, J. T., SIRDESHMUKH, R., MAITRA, A., LEACH, S. D., DRAKE, C. G., HALUSHKA, M. K., PRASAD, T. S., HRUBAN, R. H., KERR, C. L., BADER, G. D., IACOBUZIO-DONAHUE, C. A., GOWDA, H. & PANDEY, A. 2014. A draft map of the human proteome. *Nature,* 509**,** 575-81.

KIM, Y. E., PARK, J. A., HA, Y. W., PARK, S. K., KIM, H. S., OH, S. K. & LEE, Y. 2012. Chromosomal Modification in Human Embryonic Stem Cells Cultured in a Feeder-Free Condition after Single Cell Dissociation using Accutase. *Dev Reprod,* 16**,** 353-61.

KIR, S., BEDDOW, S. A., SAMUEL, V. T., MILLER, P., PREVIS, S. F., SUINO-POWELL, K., XU, H. E., SHULMAN, G. I., KLIEWER, S. A. & MANGELSDORF, D. J. 2011a. FGF19 as a postprandial, insulin-independent activator of hepatic protein and glycogen synthesis. *Science,* 331**,** 1621-4.

KIR, S., KLIEWER, S. A. & MANGELSDORF, D. J. 2011b. Roles of FGF19 in liver metabolism. *Cold Spring Harb Symp Quant Biol,* 76**,** 139-44.

KIRCHMAIR, J., GÖLLER, A. H., LANG, D., KUNZE, J., TESTA, B., WILSON, I. D., GLEN, R. C. & SCHNEIDER, G. 2015. Predicting drug metabolism: experiment and/or computation? *Nat Rev Drug Discov,* 14**,** 387-404.

KLIEWER, S. A., GOODWIN, B. & WILLSON, T. M. 2002. The nuclear pregnane X receptor: a key regulator of xenobiotic metabolism. *Endocr Rev,* 23**,** 687-702.

KNÖSPEL, F., SCHINDLER, R. K., LÜBBERSTEDT, M., PETZOLT, S., GERLACH, J. C. & ZEILINGER, K. 2010. Optimization of a serum-free culture medium for mouse embryonic stem cells using design of experiments (DoE) methodology.

Cytotechnology, 62**,** 557-71.

KOBILKA, B. K. 2007. G protein coupled receptor structure and activation. *Biochim Biophys Acta,* 1768**,** 794-807.

KODAMA, S., KOIKE, C., NEGISHI, M. & YAMAMOTO, Y. 2004. Nuclear receptors CAR and PXR cross talk with FOXO1 to regulate genes that encode drug-metabolizing and gluconeogenic enzymes. *Mol Cell Biol,* 24**,** 7931-40.

KOH, K. H., JURKOVIC, S., YANG, K., CHOI, S. Y., JUNG, J. W., KIM, K. P., ZHANG, W. & JEONG, H. 2012. Estradiol induces cytochrome P450 2B6 expression at high concentrations: implication in estrogen-mediated gene regulation in pregnancy. *Biochem Pharmacol,* 84**,** 93-103.

KOHALMY, K., TAMÁSI, V., KÓBORI, L., SÁRVÁRY, E., PASCUSSI, J. M., PORROGI, P., ROZMAN, D., PROUGH, R. A., MEYER, U. A. & MONOSTORY, K. 2007. Dehydroepiandrosterone induces human CYP2B6 through the constitutive androstane receptor. *Drug Metab Dispos,* 35**,** 1495-501.

KOIVISTO, H., HYVÄRINEN, M., STRÖMBERG, A. M., INZUNZA, J., MATILAINEN, E., MIKKOLA, M., HOVATTA, O. & TEERIJOKI, H. 2004. Cultures of human embryonic stem cells: serum replacement medium or serum-containing media and the effect of basic fibroblast growth factor. *Reprod Biomed Online,* 9**,** 330-7.

KOLANOWSKI, T. J., ANTOS, C. L. & GUAN, K. 2017. Making human cardiomyocytes up to date: Derivation, maturation state and perspectives. *Int J Cardiol,* 241**,** 379-386.

KONAGAYA, S., ANDO, T., YAMAUCHI, T., SUEMORI, H. & IWATA, H. 2015. Long-term maintenance of human induced pluripotent stem cells by automated cell culture system. *Sci Rep,* 5**,** 16647.

KONG, F., YUAN, L., ZHENG, Y. F. & CHEN, W. 2012. Automatic liquid handling for life science: a critical review of the current state of the art. *J Lab Autom,* 17**,** 169-85.

KONG, J. N., HE, Q., WANG, G., DASGUPTA, S., DINKINS, M. B., ZHU, G., KIM, A., SPASSIEVA, S. & BIEBERICH, E. 2015. Guggulsterone and bexarotene induce secretion of exosome-associated breast cancer resistance protein and reduce doxorubicin resistance in MDA-MB-231 cells. *Int J Cancer,* 137**,** 1610-20.

KOPPER, O. & BENVENISTY, N. 2012. Stepwise differentiation of human embryonic stem cells into early endoderm derivatives and their molecular characterization. *Stem Cell Res,* 8**,** 335-45.

KOSTRUBSKY, V. E., RAMACHANDRAN, V., VENKATARAMANAN, R., DORKO, K., ESPLEN, J. E., ZHANG, S., SINCLAIR, J. F., WRIGHTON, S. A. & STROM, S. C. 1999. The use of human hepatocyte cultures to study the induction of cytochrome P-450. *Drug Metab Dispos,* 27**,** 887-94.

KRATTINGER, R., BOSTRÖM, A., LEE, S. M., THASLER, W. E., SCHIÖTH, H. B., KULLAK-UBLICK, G. A. & MWINYI, J. 2016. Chenodeoxycholic acid significantly impacts the expression of miRNAs and genes involved in lipid, bile acid and drug metabolism in human hepatocytes. *Life Sci,* 156**,** 47-56.

KRIEBITZSCH, C., VERLINDEN, L., EELEN, G., TAN, B. K., VAN CAMP, M., BOUILLON, R. & VERSTUYF, A. 2009. The impact of 1,25(OH)2D3 and its structural analogs on gene expression in cancer cells--a microarray approach. *Anticancer Res,*

29**,** 3471-83.
KRISHNA, D. R. & KLOTZ, U. 1994. Extrahepatic metabolism of drugs in humans. *Clin Pharmacokinet,* 26**,** 144-60.
KRISHNA, M. 2013. Role of special stains in diagnostic liver pathology. *Clinical Liver Disease,* 2.
KRUEGER, W. H., TANASIJEVIC, B., BARBER, V., FLAMIER, A., GU, X., MANAUTOU, J. & RASMUSSEN, T. P. 2013. Cholesterol-secreting and statin-responsive hepatocytes from human ES and iPS cells to model hepatic involvement in cardiovascular health. *PLoS One,* 8**,** e67296.
KUHLMANN, W. D. & PESCHKE, P. 2006. Hepatic progenitor cells, stem cells, and AFP expression in models of liver injury. *Int J Exp Pathol,* 87**,** 343-59.
KUMAR, B. K., COGER, R. N., SCHRUM, L. W. & LEE, C. Y. 2015. The effects of over expressing aquaporins on the cryopreservation of hepatocytes. *Cryobiology,* 71**,** 273-8.
KUMAR, P. & MAGON, N. 2012. Hormones in pregnancy. *Niger Med J,* 53**,** 179-83.
LAI, L., YUAN, L., CHEN, Q., DONG, C., MAO, L., ROWAN, B., FRASCH, T. & HILL, S. M. 2008. The Galphai and Galphaq proteins mediate the effects of melatonin on steroid/thyroid hormone receptor transcriptional activity and breast cancer cell proliferation. *J Pineal Res,* 45**,** 476-88.
LAM, R. S., TÖPFER, F. M., WOOD, P. G., BUSSKAMP, V. & BAMBERG, E. 2017. Functional Maturation of Human Stem Cell-Derived Neurons in Long-Term Cultures. *PLoS One,* 12**,** e0169506.
LAMVIK, J., HELLA, H., LIABAKK, N. B. & HALAAS, Ø. 2001. Nonlabeled secondary antibodies augment/maintain the binding of primary, specific antibodies to cell membrane antigens. *Cytometry,* 45**,** 187-93.
LARSEN, M., TREMBLAY, M. L. & YAMADA, K. M. 2003. Phosphatases in cell-matrix adhesion and migration. *Nat Rev Mol Cell Biol,* 4**,** 700-11.
LE BRAS, G. F., TAUBENSLAG, K. J. & ANDL, C. D. 2012. The regulation of cell-cell adhesion during epithelial-mesenchymal transition, motility and tumor progression. *Cell Adh Migr,* 6**,** 365-73.
LE LAY, J. & KAESTNER, K. H. 2010. The Fox genes in the liver: from organogenesis to functional integration. *Physiol Rev,* 90**,** 1-22.
LE VEE, M., JOUAN, E., STIEGER, B. & FARDEL, O. 2013. Differential regulation of drug transporter expression by all-trans retinoic acid in hepatoma HepaRG cells and human hepatocytes. *Eur J Pharm Sci,* 48**,** 767-74.
LEACH, L. L., BUCHHOLZ, D. E., NADAR, V. P., LOWENSTEIN, S. E. & CLEGG, D. O. 2015. Canonical/β-catenin Wnt pathway activation improves retinal pigmented epithelium derivation from human embryonic stem cells. *Invest Ophthalmol Vis Sci,* 56**,** 1002-13.
LECLUYSE, E. L. 2001. Human hepatocyte culture systems for the in vitro evaluation of cytochrome P450 expression and regulation. *Eur J Pharm Sci,* 13**,** 343-68.
LECLUYSE, E. L. & ALEXANDRE, E. 2010. Isolation and culture of primary hepatocytes from resected human liver tissue. *Methods Mol Biol,* 640**,** 57-82.
LECLUYSE, E. L., ALEXANDRE, E., HAMILTON, G. A., VIOLLON-ABADIE, C., COON, D. J., JOLLEY, S. & RICHERT, L. 2005. Isolation and culture of primary human hepatocytes. *Methods Mol Biol,* 290**,** 207-29.
LEE, J., KIM, T. H., MURRAY, F., LI, X., CHOI, S. S., BROIDE, D. H., CORR, M., WEBSTER,

N. J., INSEL, P. A. & RAZ, E. 2015. Cyclic AMP concentrations in dendritic cells induce and regulate Th2 immunity and allergic asthma. *Proc Natl Acad Sci U S A,* 112**,** 1529-34.

LEE, J. B., LEE, J. E., PARK, J. H., KIM, S. J., KIM, M. K., ROH, S. I. & YOON, H. S. 2005. Establishment and maintenance of human embryonic stem cell lines on human feeder cells derived from uterine endometrium under serum-free condition. *Biol Reprod,* 72**,** 42-9.

LEE, K. L., LIM, S. K., ORLOV, Y. L., YIT, L. Y., YANG, H., ANG, L. T., POELLINGER, L. & LIM, B. 2011. Graded Nodal/Activin signaling titrates conversion of quantitative phospho-Smad2 levels into qualitative embryonic stem cell fate decisions. *PLoS Genet,* 7**,** e1002130.

LEE, S. M., SCHELCHER, C., DEMMEL, M., HAUNER, M. & THASLER, W. E. 2013. Isolation of human hepatocytes by a two-step collagenase perfusion procedure. *J Vis Exp*.

LEFFERT, H. L. & ALEXANDER, N. M. 1976. Thyroid hormone metabolism during liver regeneration in rats. *Endocrinology,* 98**,** 1241-7.

LEHMANN, G. M., XI, X., KULKARNI, A. A., OLSEN, K. C., POLLOCK, S. J., BAGLOLE, C. J., GUPTA, S., CASEY, A. E., HUXLIN, K. R., SIME, P. J., FELDON, S. E. & PHIPPS, R. P. 2011. The aryl hydrocarbon receptor ligand ITE inhibits TGFβ1-induced human myofibroblast differentiation. *Am J Pathol,* 178**,** 1556-67.

LEI, T., JACOB, S., AJIL-ZARAA, I., DUBUISSON, J. B., IRION, O., JACONI, M. & FEKI, A. 2007. Xeno-free derivation and culture of human embryonic stem cells: current status, problems and challenges. *Cell Res,* 17**,** 682-8.

LEJEUNE, T. M., TSUI, H. Y., PARSONS, L. B., MILLER, G. E., WHITTED, C., LYNCH, K. E., RAMSAUER, R. E., PATEL, J. U., WYATT, J. E., STREET, D. S., ADAMS, C. B., MCPHERSON, B., TSUI, H. M., EVANS, J. A., LIVESAY, C., TORRENEGRA, R. D. & PALAU, V. E. 2015. Mechanism of Action of Two Flavone Isomers Targeting Cancer Cells with Varying Cell Differentiation Status. *PLoS One,* 10**,** e0142928.

LEVITT, D. G. & LEVITT, M. D. 2016. Human serum albumin homeostasis: a new look at the roles of synthesis, catabolism, renal and gastrointestinal excretion, and the clinical value of serum albumin measurements. *Int J Gen Med,* 9**,** 229-55.

LEVY, G., BOMZE, D., HEINZ, S., RAMACHANDRAN, S. D., NOERENBERG, A., COHEN, M., SHIBOLET, O., SKLAN, E., BRASPENNING, J. & NAHMIAS, Y. 2015. Long-term culture and expansion of primary human hepatocytes. *Nat Biotechnol,* 33**,** 1264-1271.

LI, L., ZHANG, P., BAO, Z., WANG, T., LIU, S. & HUANG, F. 2016. PGC-1α Promotes Ureagenesis in Mouse Periportal Hepatocytes through SIRT3 and SIRT5 in Response to Glucagon. *Sci Rep,* 6**,** 24156.

LI, V. S., NG, S. S., BOERSEMA, P. J., LOW, T. Y., KARTHAUS, W. R., GERLACH, J. P., MOHAMMED, S., HECK, A. J., MAURICE, M. M., MAHMOUDI, T. & CLEVERS, H. 2012. Wnt signaling through inhibition of β-catenin degradation in an intact Axin1 complex. *Cell,* 149**,** 1245-56.

LIANG, G. & ZHANG, Y. 2013. Genetic and epigenetic variations in iPSCs: potential causes and implications for application. *Cell Stem Cell,* 13**,** 149-59.

LIANG, P., LAN, F., LEE, A. S., GONG, T., SANCHEZ-FREIRE, V., WANG, Y., DIECKE, S.,

SALLAM, K., KNOWLES, J. W., WANG, P. J., NGUYEN, P. K., BERS, D. M., ROBBINS, R. C. & WU, J. C. 2013. Drug screening using a library of human induced pluripotent stem cell-derived cardiomyocytes reveals disease-specific patterns of cardiotoxicity. *Circulation,* 127**,** 1677-91.

LIEU, P. T., FONTES, A., VEMURI, M. C. & MACARTHUR, C. C. 2013. Generation of induced pluripotent stem cells with CytoTune, a non-integrating Sendai virus. *Methods Mol Biol,* 997**,** 45-56.

LIM, S. M., PEREIRA, L., WONG, M. S., HIRST, C. E., VAN VRANKEN, B. E., PICK, M., TROUNSON, A., ELEFANTY, A. G. & STANLEY, E. G. 2009. Enforced expression of Mixl1 during mouse ES cell differentiation suppresses hematopoietic mesoderm and promotes endoderm formation. *Stem Cells,* 27**,** 363-74.

LIM, S. Y., SIVAKUMARAN, P., CROMBIE, D. E., DUSTING, G. J., PÉBAY, A. & DILLEY, R. J. 2013. Trichostatin A enhances differentiation of human induced pluripotent stem cells to cardiogenic cells for cardiac tissue engineering. *Stem Cells Transl Med,* 2**,** 715-25.

LIM, S. Y., SIVAKUMARAN, P., CROMBIE, D. E., DUSTING, G. J., PÉBAY, A. & DILLEY, R. J. 2016. Enhancing Human Cardiomyocyte Differentiation from Induced Pluripotent Stem Cells with Trichostatin A. *Methods Mol Biol,* 1357**,** 415-21.

LIN, Y. H., LIAO, C. J., HUANG, Y. H., WU, M. H., CHI, H. C., WU, S. M., CHEN, C. Y., TSENG, Y. H., TSAI, C. Y., CHUNG, I. H., WU, T. I., TSAI, M. M., LIN, C. D. & LIN, K. H. 2013. Thyroid hormone receptor represses miR-17 expression to enhance tumor metastasis in human hepatoma cells. *Oncogene,* 32**,** 4509-18.

LING, W. L., BAI, Y., CHENG, C., PADAWER, I. & WU, C. 2015. Development and manufacturability assessment of chemically-defined medium for the production of protein therapeutics in CHO cells. *Biotechnol Prog,* 31**,** 1163-71.

LIPPMANN, E. S., ESTEVEZ-SILVA, M. C. & ASHTON, R. S. 2014. Defined human pluripotent stem cell culture enables highly efficient neuroepithelium derivation without small molecule inhibitors. *Stem Cells,* 32**,** 1032-42.

LIU, R., LI, X., QIANG, X., LUO, L., HYLEMON, P. B., JIANG, Z., ZHANG, L. & ZHOU, H. 2015. Taurocholate Induces Cyclooxygenase-2 Expression via the Sphingosine 1-phosphate Receptor 2 in a Human Cholangiocarcinoma Cell Line. *J Biol Chem,* 290**,** 30988-1002.

LIU, W. J., ZHANG, T., GUO, Q. L., LIU, C. Y. & BAI, Y. Q. 2016. Effect of ATRA on the expression of HOXA5 gene in K562 cells and its relationship with cell cycle and apoptosis. *Mol Med Rep,* 13**,** 4221-8.

LIU, Y., HOURD, P., CHANDRA, A. & WILLIAMS, D. J. 2010. Human cell culture process capability: a comparison of manual and automated production. *J Tissue Eng Regen Med,* 4**,** 45-54.

LIU, Y., LI, H., YAN, S., WEI, J. & LI, X. 2014. Hepatocyte cocultures with endothelial cells and fibroblasts on micropatterned fibrous mats to promote liver-specific functions and capillary formation capabilities. *Biomacromolecules,* 15**,** 1044-54.

LIU-CHITTENDEN, Y., HUANG, B., SHIM, J. S., CHEN, Q., LEE, S. J., ANDERS, R. A., LIU, J. O. & PAN, D. 2012. Genetic and pharmacological disruption of the TEAD-YAP complex suppresses the oncogenic activity of YAP. *Genes Dev,* 26**,** 1300-

5.
LU, J., EINHORN, S., VENKATARANGAN, L., MILLER, M., MANN, D. A., WATKINS, P. B. & LECLUYSE, E. 2015. Morphological and Functional Characterization and Assessment of iPSC-Derived Hepatocytes for In Vitro Toxicity Testing. *Toxicol Sci,* 147**,** 39-54.
LU, Y., HEYDEL, J. M., LI, X., BRATTON, S., LINDBLOM, T. & RADOMINSKA-PANDYA, A. 2005. Lithocholic acid decreases expression of UGT2B7 in Caco-2 cells: a potential role for a negative farnesoid X receptor response element. *Drug Metab Dispos,* 33**,** 937-46.
LUCENDO-VILLARIN, B., RASHIDI, H., CAMERON, K. & HAY, D. C. 2016. Pluripotent stem cell derived hepatocytes: using materials to define cellular differentiation and tissue engineering. *J Mater Chem B Mater Biol Med,* 4**,** 3433-3442.
LUND, R. J., NÄRVÄ, E. & LAHESMAA, R. 2012. Genetic and epigenetic stability of human pluripotent stem cells. *Nat Rev Genet,* 13**,** 732-44.
LYNCH, C., ZHAO, J., HUANG, R., XIAO, J., LI, L., HEYWARD, S., XIA, M. & WANG, H. 2015. Quantitative high-throughput identification of drugs as modulators of human constitutive androstane receptor. *Sci Rep,* 5**,** 10405.
LÁSZLÓ, V., DEZSO, K., BAGHY, K., PAPP, V., KOVALSZKY, I., SÁFRÁNY, G., THORGEIRSSON, S. S., NAGY, P. & PAKU, S. 2008. Triiodothyronine accelerates differentiation of rat liver progenitor cells into hepatocytes. *Histochem Cell Biol,* 130**,** 1005-14.
MADIAN, A. G., WHEELER, H. E., JONES, R. B. & DOLAN, M. E. 2012. Relating human genetic variation to variation in drug responses. *Trends Genet,* 28**,** 487-95.
MAEDA, A., YANO, T., ITOH, Y., KAKUMORI, M., KUBOTA, T., EGASHIRA, N. & OISHI, R. 2010. Down-regulation of RhoA is involved in the cytotoxic action of lipophilic statins in HepG2 cells. *Atherosclerosis,* 208**,** 112-8.
MAGLICH, J. M., PARKS, D. J., MOORE, L. B., COLLINS, J. L., GOODWIN, B., BILLIN, A. N., STOLTZ, C. A., KLIEWER, S. A., LAMBERT, M. H., WILLSON, T. M. & MOORE, J. T. 2003. Identification of a novel human constitutive androstane receptor (CAR) agonist and its use in the identification of CAR target genes. *J Biol Chem,* 278**,** 17277-83.
MAGNER, N. L., JUNG, Y., WU, J., NOLTA, J. A., ZERN, M. A. & ZHOU, P. 2013. Insulin and IGFs enhance hepatocyte differentiation from human embryonic stem cells via the PI3K/AKT pathway. *Stem Cells,* 31**,** 2095-103.
MAHEY, S., KUMAR, R., ARORA, R., MAHAJAN, J., ARORA, S., BHARDWAJ, R. & THUKRAL, A. K. 2016. Effect of cobalt(II) chloride hexahydrate on some human cancer cell lines. *Springerplus,* 5**,** 930.
MAITRA, A., ARKING, D. E., SHIVAPURKAR, N., IKEDA, M., STASTNY, V., KASSAUEI, K., SUI, G., CUTLER, D. J., LIU, Y., BRIMBLE, S. N., NOAKSSON, K., HYLLNER, J., SCHULZ, T. C., ZENG, X., FREED, W. J., CROOK, J., ABRAHAM, S., COLMAN, A., SARTIPY, P., MATSUI, S., CARPENTER, M., GAZDAR, A. F., RAO, M. & CHAKRAVARTI, A. 2005. Genomic alterations in cultured human embryonic stem cells. *Nat Genet,* 37**,** 1099-103.
MAK, I. W., EVANIEW, N. & GHERT, M. 2014. Lost in translation: animal models and clinical trials in cancer treatment. *Am J Transl Res,* 6**,** 114-8.
MALIK, R. & HODGSON, H. 2002. The relationship between the thyroid gland and

the liver. *QJM,* 95**,** 559-69.
MANIWA, Y., KASUKABE, T. & KUMAKURA, S. 2015. Vitamin K2 and cotylenin A synergistically induce monocytic differentiation and growth arrest along with the suppression of c-MYC expression and induction of cyclin G2 expression in human leukemia HL-60 cells. *Int J Oncol,* 47**,** 473-80.
MARCHWICKA, A., CEBRAT, M., ŁASZKIEWICZ, A., ŚNIEŻEWSKI, Ł., BROWN, G. & MARCINKOWSKA, E. 2016. Regulation of vitamin D receptor expression by retinoic acid receptor alpha in acute myeloid leukemia cells. *J Steroid Biochem Mol Biol,* 159**,** 121-30.
MARGAGLIOTTI, S., CLOTMAN, F., PIERREUX, C. E., BEAUDRY, J. B., JACQUEMIN, P., ROUSSEAU, G. G. & LEMAIGRE, F. P. 2007. The Onecut transcription factors HNF-6/OC-1 and OC-2 regulate early liver expansion by controlling hepatoblast migration. *Dev Biol,* 311**,** 579-89.
MARTIGNONI, M., GROOTHUIS, G. M. & DE KANTER, R. 2006. Species differences between mouse, rat, dog, monkey and human CYP-mediated drug metabolism, inhibition and induction. *Expert Opin Drug Metab Toxicol,* 2**,** 875-94.
MARTÍNEZ-JIMÉNEZ, C. P., CASTELL, J. V., GÓMEZ-LECHÓN, M. J. & JOVER, R. 2006. Transcriptional activation of CYP2C9, CYP1A1, and CYP1A2 by hepatocyte nuclear factor 4alpha requires coactivators peroxisomal proliferator activated receptor-gamma coactivator 1alpha and steroid receptor coactivator 1. *Mol Pharmacol,* 70**,** 1681-92.
MASSEY, A. J. 2015. Multiparametric Cell Cycle Analysis Using the Operetta High-Content Imager and Harmony Software with PhenoLOGIC. *PLoS One,* 10**,** e0134306.
MASUYAMA, H. & HIRAMATSU, Y. 2011. Potential role of estradiol and progesterone in insulin resistance through constitutive androstane receptor. *J Mol Endocrinol,* 47**,** 229-39.
MASUYAMA, H., HIRAMATSU, Y., MIZUTANI, Y., INOSHITA, H. & KUDO, T. 2001. The expression of pregnane X receptor and its target gene, cytochrome P450 3A1, in perinatal mouse. *Mol Cell Endocrinol,* 172**,** 47-56.
MATOUŠKOVÁ, P., VOKŘÁL, I., LAMKA, J. & SKÁLOVÁ, L. 2016. The Role of Xenobiotic-Metabolizing Enzymes in Anthelmintic Deactivation and Resistance in Helminths. *Trends Parasitol,* 32**,** 481-491.
MATSUMOTO, K., MIKI, R., NAKAYAMA, M., TATSUMI, N. & YOKOUCHI, Y. 2008. Wnt9a secreted from the walls of hepatic sinusoids is essential for morphogenesis, proliferation, and glycogen accumulation of chick hepatic epithelium. *Dev Biol,* 319**,** 234-47.
MCCOY, A. T., BENOIST, C. C., WRIGHT, J. W., KAWAS, L. H., BULE-GHOGARE, J. M., ZHU, M., APPLEYARD, S. M., WAYMAN, G. A. & HARDING, J. W. 2013. Evaluation of metabolically stabilized angiotensin IV analogs as procognitive/antidementia agents. *J Pharmacol Exp Ther,* 344**,** 141-54.
MCLEAN, A. B., D'AMOUR, K. A., JONES, K. L., KRISHNAMOORTHY, M., KULIK, M. J., REYNOLDS, D. M., SHEPPARD, A. M., LIU, H., XU, Y., BAETGE, E. E. & DALTON, S. 2007. Activin a efficiently specifies definitive endoderm from human embryonic stem cells only when phosphatidylinositol 3-kinase signaling is suppressed. *Stem Cells,* 25**,** 29-38.

MCLIN, V. A., RANKIN, S. A. & ZORN, A. M. 2007. Repression of Wnt/beta-catenin signaling in the anterior endoderm is essential for liver and pancreas development. *Development,* 134**,** 2207-17.

MCMULLEN, P. D., BHATTACHARYA, S., WOODS, C. G., SUN, B., YARBOROUGH, K., ROSS, S. M., MILLER, M. E., MCBRIDE, M. T., LECLUYSE, E. L., CLEWELL, R. A. & ANDERSEN, M. E. 2014. A map of the PPARα transcription regulatory network for primary human hepatocytes. *Chem Biol Interact,* 209**,** 14-24.

MCSORLEY, L. C. & DALY, A. K. 2000. Identification of human cytochrome P450 isoforms that contribute to all-trans-retinoic acid 4-hydroxylation. *Biochem Pharmacol,* 60**,** 517-26.

MEDINE, C. N., LUCENDO-VILLARIN, B., ZHOU, W., WEST, C. C. & HAY, D. C. 2011. Robust generation of hepatocyte-like cells from human embryonic stem cell populations. *J Vis Exp***,** e2969.

MESHORER, E. & MISTELI, T. 2006. Chromatin in pluripotent embryonic stem cells and differentiation. *Nat Rev Mol Cell Biol,* 7**,** 540-6.

MICHAEL, S., AULD, D., KLUMPP, C., JADHAV, A., ZHENG, W., THORNE, N., AUSTIN, C. P., INGLESE, J. & SIMEONOV, A. 2008. A robotic platform for quantitative high-throughput screening. *Assay Drug Dev Technol,* 6**,** 637-57.

MICHALOPOULOS, G. K., BOWEN, W. C., MULÈ, K. & LUO, J. 2003. HGF-, EGF-, and dexamethasone-induced gene expression patterns during formation of tissue in hepatic organoid cultures. *Gene Expr,* 11**,** 55-75.

MILER, E. A., RÍOS DE MOLINA, M. E. C., DOMÍNGUEZ, G. & GUERRA, L. N. 2008. Thyroid hormone effect in human hepatocytes. *Redox Rep,* 13**,** 185-91.

MIURA, S., MITSUHASHI, N., SHIMIZU, H., KIMURA, F., YOSHIDOME, H., OTSUKA, M., KATO, A., SHIDA, T., OKAMURA, D. & MIYAZAKI, M. 2012. Fibroblast growth factor 19 expression correlates with tumor progression and poorer prognosis of hepatocellular carcinoma. *BMC Cancer,* 12**,** 56.

MIYOSHI, N., ISHII, H., NAGANO, H., HARAGUCHI, N., DEWI, D. L., KANO, Y., NISHIKAWA, S., TANEMURA, M., MIMORI, K., TANAKA, F., SAITO, T., NISHIMURA, J., TAKEMASA, I., MIZUSHIMA, T., IKEDA, M., YAMAMOTO, H., SEKIMOTO, M., DOKI, Y. & MORI, M. 2011. Reprogramming of mouse and human cells to pluripotency using mature microRNAs. *Cell Stem Cell,* 8**,** 633-8.

MIZEJEWSKI, G. J. 2004. Biological roles of alpha-fetoprotein during pregnancy and perinatal development. *Exp Biol Med (Maywood),* 229**,** 439-63.

MODICA, S., GADALETA, R. M. & MOSCHETTA, A. 2010. Deciphering the nuclear bile acid receptor FXR paradigm. *Nucl Recept Signal,* 8**,** e005.

MOLINARI, E., SRIVASTAVA, S., SAYER, J. A. & RAMSBOTTOM, S. A. 2017. From disease modelling to personalised therapy in patients with CEP290 mutations. *F1000Res,* 6**,** 669.

MONGA, S. P., MARS, W. M., PEDIADITAKIS, P., BELL, A., MULÉ, K., BOWEN, W. C., WANG, X., ZARNEGAR, R. & MICHALOPOULOS, G. K. 2002. Hepatocyte growth factor induces Wnt-independent nuclear translocation of beta-catenin after Met-beta-catenin dissociation in hepatocytes. *Cancer Res,* 62**,** 2064-71.

MONGA, S. P., MONGA, H. K., TAN, X., MULÉ, K., PEDIADITAKIS, P. & MICHALOPOULOS, G. K. 2003. Beta-catenin antisense studies in embryonic

liver cultures: role in proliferation, apoptosis, and lineage specification. *Gastroenterology,* 124**,** 202-16.

MONOSTORY, K., KOHALMY, K., PROUGH, R. A., KÓBORI, L. & VERECZKEY, L. 2005. The effect of synthetic glucocorticoid, dexamethasone on CYP1A1 inducibility in adult rat and human hepatocytes. *FEBS Lett,* 579**,** 229-35.

MOORE-SCOTT, B. A., OPOKA, R., LIN, S. C., KORDICH, J. J. & WELLS, J. M. 2007. Identification of molecular markers that are expressed in discrete anterior-posterior domains of the endoderm from the gastrula stage to mid-gestation. *Dev Dyn,* 236**,** 1997-2003.

MORLEY, P. & WHITFIELD, J. F. 1993. The differentiation inducer, dimethyl sulfoxide, transiently increases the intracellular calcium ion concentration in various cell types. *J Cell Physiol,* 156**,** 219-25.

MORTEZAEE, K., MINAII, B., SABBAGHZIARANI, F., RAGERDI KASHANI, I., HASSANZADEH, G., PASBAKHSH, P., BARBARESTANI, M. & LATIFPOUR, M. 2015. Retinoic Acid as the Stimulating Factor for Differentiation of Wharton's Jelly-Mesenchymal Stem Cells into Hepatocyte-like Cells. *Avicenna J Med Biotechnol,* 7**,** 106-12.

MOUNIER, A., GEORGIEV, D., NAM, K. N., FITZ, N. F., CASTRANIO, E. L., WOLFE, C. M., CRONICAN, A. A., SCHUG, J., LEFTEROV, I. & KOLDAMOVA, R. 2015. Bexarotene-Activated Retinoid X Receptors Regulate Neuronal Differentiation and Dendritic Complexity. *J Neurosci,* 35**,** 11862-76.

MULLIS, K. B. 1990. The unusual origin of the polymerase chain reaction. *Sci Am,* 262**,** 56-61, 64-5.

MURRY, C. E. & KELLER, G. 2008. Differentiation of embryonic stem cells to clinically relevant populations: lessons from embryonic development. *Cell,* 132**,** 661-80.

N POLITIS, S., COLOMBO, P., COLOMBO, G. & M REKKAS, D. 2017. Design of experiments (DoE) in pharmaceutical development. *Drug Dev Ind Pharm,* 43**,** 889-901.

NADIN, L. & MURRAY, M. 1999. Participation of CYP2C8 in retinoic acid 4-hydroxylation in human hepatic microsomes. *Biochem Pharmacol,* 58**,** 1201-8.

NAHOUM, V., PÉREZ, E., GERMAIN, P., RODRÍGUEZ-BARRIOS, F., MANZO, F., KAMMERER, S., LEMAIRE, G., HIRSCH, O., ROYER, C. A., GRONEMEYER, H., DE LERA, A. R. & BOURGUET, W. 2007. Modulators of the structural dynamics of the retinoid X receptor to reveal receptor function. *Proc Natl Acad Sci U S A,* 104**,** 17323-8.

NAKAMURA, T. & MIZUNO, S. 2010. The discovery of hepatocyte growth factor (HGF) and its significance for cell biology, life sciences and clinical medicine. *Proc Jpn Acad Ser B Phys Biol Sci,* 86**,** 588-610.

NAQVI, S. M. & BUCKLEY, C. T. 2015. Extracellular matrix production by nucleus pulposus and bone marrow stem cells in response to altered oxygen and glucose microenvironments. *J Anat,* 227**,** 757-66.

NATARAJAN, M., REITER, R. J., MELTZ, M. L. & HERMAN, T. S. 2001. Effect of melatonin on cell growth, metabolic activity, and cell cycle distribution. *J Pineal Res,* 31**,** 228-33.

NAUJOK, O., LENTES, J., DIEKMANN, U., DAVENPORT, C. & LENZEN, S. 2014.

Cytotoxicity and activation of the Wnt/beta-catenin pathway in mouse embryonic stem cells treated with four GSK3 inhibitors. *BMC Res Notes,* 7**,** 273.

NEJAK-BOWEN, K. & MONGA, S. P. 2008. Wnt/beta-catenin signaling in hepatic organogenesis. *Organogenesis,* 4**,** 92-9.

NESS, G. C. & LOPEZ, D. 1995. Transcriptional regulation of rat hepatic low-density lipoprotein receptor and cholesterol 7 alpha hydroxylase by thyroid hormone. *Arch Biochem Biophys,* 323**,** 404-8.

NESS, G. C., LOPEZ, D., CHAMBERS, C. M., NEWSOME, W. P., CORNELIUS, P., LONG, C. A. & HARWOOD, H. J. 1998. Effects of L-triiodothyronine and the thyromimetic L-94901 on serum lipoprotein levels and hepatic low-density lipoprotein receptor, 3-hydroxy-3-methylglutaryl coenzyme A reductase, and apo A-I gene expression. *Biochem Pharmacol,* 56**,** 121-9.

NEVE, E. P. & INGELMAN-SUNDBERG, M. 2010. Cytochrome P450 proteins: retention and distribution from the endoplasmic reticulum. *Curr Opin Drug Discov Devel,* 13**,** 78-85.

NGUYEN, P., LERAY, V., DIEZ, M., SERISIER, S., LE BLOC'H, J., SILIART, B. & DUMON, H. 2008. Liver lipid metabolism. *J Anim Physiol Anim Nutr (Berl),* 92**,** 272-83.

NIEMI, M., CASCORBI, I., TIMM, R., KROEMER, H. K., NEUVONEN, P. J. & KIVISTÖ, K. T. 2002. Glyburide and glimepiride pharmacokinetics in subjects with different CYP2C9 genotypes. *Clin Pharmacol Ther,* 72**,** 326-32.

NING, R. B., ZHU, J., CHAI, D. J., XU, C. S., XIE, H., LIN, X. Y., ZENG, J. Z. & LIN, J. X. 2013. RXR agonists inhibit high glucose-induced upregulation of inflammation by suppressing activation of the NADPH oxidase-nuclear factor-κB pathway in human endothelial cells. *Genet Mol Res,* 12**,** 6692-707.

NISHIMURA, T., HU, Y., WU, M., PHAM, E., SUEMIZU, H., ELAZAR, M., LIU, M., IDILMAN, R., YURDAYDIN, C., ANGUS, P., STEDMAN, C., MURPHY, B., GLENN, J., NAKAMURA, M., NOMURA, T., CHEN, Y., ZHENG, M., FITCH, W. L. & PELTZ, G. 2013. Using chimeric mice with humanized livers to predict human drug metabolism and a drug-drug interaction. *J Pharmacol Exp Ther,* 344**,** 388-96.

NIST/SEMATECH 2012. e-Handbook of Statistical Methods http://www.itl.nist.gov/div898/handbook/.

NOAKES, R. 2015. The aryl hydrocarbon receptor: a review of its role in the physiology and pathology of the integument and its relationship to the tryptophan metabolism. *Int J Tryptophan Res,* 8**,** 7-18.

NOTE, T. A. 2010. Automation improves development of stem cell cultures - Advantages of automation in stem cell culturing.

O'REILLY, L. P., PERLMUTTER, D. H., SILVERMAN, G. A. & PAK, S. C. 2014. α1-antitrypsin deficiency and the hepatocytes - an elegans solution to drug discovery. *Int J Biochem Cell Biol,* 47**,** 109-12.

OBACH, R. S. 2013. Pharmacologically active drug metabolites: impact on drug discovery and pharmacotherapy. *Pharmacol Rev,* 65**,** 578-640.

ODOM, D. T., ZIZLSPERGER, N., GORDON, D. B., BELL, G. W., RINALDI, N. J., MURRAY, H. L., VOLKERT, T. L., SCHREIBER, J., ROLFE, P. A., GIFFORD, D. K., FRAENKEL, E., BELL, G. I. & YOUNG, R. A. 2004. Control of pancreas and liver gene expression by HNF transcription factors. *Science,* 303**,** 1378-81.

OERTEL, M. 2011. Fetal liver cell transplantation as a potential alternative to whole

liver transplantation? *J Gastroenterol,* 46**,** 953-65.

OGAWA, S., SURAPISITCHAT, J., VIRTANEN, C., OGAWA, M., NIAPOUR, M., SUGAMORI, K. S., WANG, S., TAMBLYN, L., GUILLEMETTE, C., HOFFMANN, E., ZHAO, B., STROM, S., LAPOSA, R. R., TYNDALE, R. F., GRANT, D. M. & KELLER, G. 2013. Three-dimensional culture and cAMP signaling promote the maturation of human pluripotent stem cell-derived hepatocytes. *Development,* 140**,** 3285-96.

OH, H. Y., NAMKOONG, S., LEE, S. J., POR, E., KIM, C. K., BILLIAR, T. R., HAN, J. A., HA, K. S., CHUNG, H. T., KWON, Y. G., LEE, H. & KIM, Y. M. 2006. Dexamethasone protects primary cultured hepatocytes from death receptor-mediated apoptosis by upregulation of cFLIP. *Cell Death Differ,* 13**,** 512-23.

OHNUMA, K., FUJIKI, A., YANAGIHARA, K., TACHIKAWA, S., HAYASHI, Y., ITO, Y., ONUMA, Y., CHAN, T., MICHIUE, T., FURUE, M. K. & ASASHIMA, M. 2014. Enzyme-free passage of human pluripotent stem cells by controlling divalent cations. *Sci Rep,* 4**,** 4646.

OKITA, K., ICHISAKA, T. & YAMANAKA, S. 2007. Generation of germline-competent induced pluripotent stem cells. *Nature,* 448**,** 313-7.

OKURA, H., KOMODA, H., SAGA, A., KAKUTA-YAMAMOTO, A., HAMADA, Y., FUMIMOTO, Y., LEE, C. M., ICHINOSE, A., SAWA, Y. & MATSUYAMA, A. 2010. Properties of hepatocyte-like cell clusters from human adipose tissue-derived mesenchymal stem cells. *Tissue Eng Part C Methods,* 16**,** 761-70.

ONITSUKA, I., TANAKA, M. & MIYAJIMA, A. 2010. Characterization and functional analyses of hepatic mesothelial cells in mouse liver development. *Gastroenterology,* 138**,** 1525-35, 1535.e1-6.

ORTMANN, D. & VALLIER, L. 2017. Variability of human pluripotent stem cell lines. *Curr Opin Genet Dev,* 46**,** 179-185.

OSAFUNE, K., CARON, L., BOROWIAK, M., MARTINEZ, R. J., FITZ-GERALD, C. S., SATO, Y., COWAN, C. A., CHIEN, K. R. & MELTON, D. A. 2008. Marked differences in differentiation propensity among human embryonic stem cell lines. *Nat Biotechnol,* 26**,** 313-5.

OWENS, P. K., RADDAD, E., MILLER, J. W., STILLE, J. R., OLOVICH, K. G., SMITH, N. V., JONES, R. S. & SCHERER, J. C. 2015. A decade of innovation in pharmaceutical R&D: the Chorus model. *Nat Rev Drug Discov,* 14**,** 17-28.

PAL, R., MAMIDI, M. K., DAS, A. K. & BHONDE, R. 2012. Diverse effects of dimethyl sulfoxide (DMSO) on the differentiation potential of human embryonic stem cells. *Arch Toxicol,* 86**,** 651-61.

PAPAGEORGIOU, I., GREPPER, S. & UNADKAT, J. D. 2013. Induction of hepatic CYP3A enzymes by pregnancy-related hormones: studies in human hepatocytes and hepatic cell lines. *Drug Metab Dispos,* 41**,** 281-90.

PAPELEU, P., LOYER, P., VANHAECKE, T., ELAUT, G., GEERTS, A., GUGUEN-GUILLOUZO, C. & ROGIERS, V. 2003. Trichostatin A induces differential cell cycle arrests but does not induce apoptosis in primary cultures of mitogen-stimulated rat hepatocytes. *J Hepatol,* 39**,** 374-82.

PARK, S., GIANOTTI-SOMMER, A., MOLINA-ESTEVEZ, F. J., VANUYTSEL, K., SKVIR, N., LEUNG, A., ROZELLE, S. S., SHAIKHO, E. M., WEIR, I., JIANG, Z., LUO, H. Y., CHUI, D. H. K., FIGUEIREDO, M. S., ALSULTAN, A., AL-ALI, A., SEBASTIANI, P., STEINBERG, M. H., MOSTOSLAVSKY, G. & MURPHY, G. J. 2017. A

Comprehensive, Ethnically Diverse Library of Sickle Cell Disease-Specific Induced Pluripotent Stem Cells. *Stem Cell Reports,* 8**,** 1076-1085.

PARK, S. J., LEE, S. B., LEE, D. S., RYU, Y. J., LEE, G. & CHO, J. 2013. Direct effect of chenodeoxycholic acid on differentiation of mouse embryonic stem cells cultured under feeder-free culture conditions. *Biomed Res Int,* 2013**,** 375076.

PARKER, G. C., ACSADI, G. & BRENNER, C. A. 2009. Mitochondria: determinants of stem cell fate? *Stem Cells Dev,* 18**,** 803-6.

PARVIZ, F., MATULLO, C., GARRISON, W. D., SAVATSKI, L., ADAMSON, J. W., NING, G., KAESTNER, K. H., ROSSI, J. M., ZARET, K. S. & DUNCAN, S. A. 2003. Hepatocyte nuclear factor 4alpha controls the development of a hepatic epithelium and liver morphogenesis. *Nat Genet,* 34**,** 292-6.

PASCUSSI, J. M., GERBAL-CHALOIN, S., DROCOURT, L., MAUREL, P. & VILAREM, M. J. 2003. The expression of CYP2B6, CYP2C9 and CYP3A4 genes: a tangle of networks of nuclear and steroid receptors. *Biochim Biophys Acta,* 1619**,** 243-53.

PASCUSSI, J. M., GERBAL-CHALOIN, S., FABRE, J. M., MAUREL, P. & VILAREM, M. J. 2000. Dexamethasone enhances constitutive androstane receptor expression in human hepatocytes: consequences on cytochrome P450 gene regulation. *Mol Pharmacol,* 58**,** 1441-50.

PAULL, D., SEVILLA, A., ZHOU, H., HAHN, A. K., KIM, H., NAPOLITANO, C., TSANKOV, A., SHANG, L., KRUMHOLZ, K., JAGADEESAN, P., WOODARD, C. M., SUN, B., VILBOUX, T., ZIMMER, M., FORERO, E., MOROZIEWICZ, D. N., MARTINEZ, H., MALICDAN, M. C., WEISS, K. A., VENSAND, L. B., DUSENBERRY, C. R., POLUS, H., SY, K. T., KAHLER, D. J., GAHL, W. A., SOLOMON, S. L., CHANG, S., MEISSNER, A., EGGAN, K. & NOGGLE, S. A. 2015. Automated, high-throughput derivation, characterization and differentiation of induced pluripotent stem cells. *Nat Methods,* 12**,** 885-92.

PEREIRA, L. A., WONG, M. S., LIM, S. M., SIDES, A., STANLEY, E. G. & ELEFANTY, A. G. 2011. Brachyury and related Tbx proteins interact with the Mixl1 homeodomain protein and negatively regulate Mixl1 transcriptional activity. *PLoS One,* 6**,** e28394.

PETERS, D. T., HENDERSON, C. A., WARREN, C. R., FRIESEN, M., XIA, F., BECKER, C. E., MUSUNURU, K. & COWAN, C. A. 2016. Asialoglycoprotein receptor 1 is a specific cell-surface marker for isolating hepatocytes derived from human pluripotent stem cells. *Development,* 143**,** 1475-81.

PHETSOUVANH, R., THOJAIKONG, T., PHOUMIN, P., SIBOUNHEUANG, B., PHOMMASONE, K., CHANSAMOUTH, V., LEE, S. J., NEWTON, P. N. & BLACKSELL, S. D. 2013. Inter- and intra-operator variability in the reading of indirect immunofluorescence assays for the serological diagnosis of scrub typhus and murine typhus. *Am J Trop Med Hyg,* 88**,** 932-6.

PINKSE, G. G., VOORHOEVE, M. P., NOTEBORN, M., TERPSTRA, O. T., BRUIJN, J. A. & DE HEER, E. 2004. Hepatocyte survival depends on beta1-integrin-mediated attachment of hepatocytes to hepatic extracellular matrix. *Liver Int,* 24**,** 218-26.

POUND, P., EBRAHIM, S., SANDERCOCK, P., BRACKEN, M. B., ROBERTS, I. & GROUP, R. A. T. S. R. 2004. Where is the evidence that animal research benefits

humans? *BMJ,* 328**,** 514-7.
POWER, C. & RASKO, J. E. 2008. Whither prometheus' liver? Greek myth and the science of regeneration. *Ann Intern Med,* 149**,** 421-6.
PRAMOD, K., TAHIR, M. A., CHAROO, N. A., ANSARI, S. H. & ALI, J. 2016. Pharmaceutical product development: A quality by design approach. *Int J Pharm Investig,* 6**,** 129-38.
PREISSNER, S., KROLL, K., DUNKEL, M., SENGER, C., GOLDSOBEL, G., KUZMAN, D., GUENTHER, S., WINNENBURG, R., SCHROEDER, M. & PREISSNER, R. 2010. SuperCYP: a comprehensive database on Cytochrome P450 enzymes including a tool for analysis of CYP-drug interactions. *Nucleic Acids Res,* 38**,** D237-43.
PREISSNER, S. C., HOFFMANN, M. F., PREISSNER, R., DUNKEL, M., GEWIESS, A. & PREISSNER, S. 2013. Polymorphic cytochrome P450 enzymes (CYPs) and their role in personalized therapy. *PLoS One,* 8**,** e82562.
PRODANOV, L., JINDAL, R., BALE, S. S., HEGDE, M., MCCARTY, W. J., GOLBERG, I., BHUSHAN, A., YARMUSH, M. L. & USTA, O. B. 2016. Long-term maintenance of a microfluidic 3D human liver sinusoid. *Biotechnol Bioeng,* 113**,** 241-6.
PURCELL, R., CHILDS, M., MAIBACH, R., MILES, C., TURNER, C., ZIMMERMANN, A. & SULLIVAN, M. 2011. HGF/c-Met related activation of β-catenin in hepatoblastoma. *J Exp Clin Cancer Res,* 30**,** 96.
PÁSTOR, M. V. 2010. Direct immunofluorescent labeling of cells. *Methods Mol Biol,* 588**,** 135-42.
QIAN, L., ZOLFAGHARI, R. & ROSS, A. C. 2010. Liver-specific cytochrome P450 CYP2C22 is a direct target of retinoic acid and a retinoic acid-metabolizing enzyme in rat liver. *J Lipid Res,* 51**,** 1781-92.
QIAO, E. Q. & YANG, H. J. 2014. Effect of pregnane X receptor expression on drug resistance in breast cancer. *Oncol Lett,* 7**,** 1191-1196.
RAJAMANI, K., LI, Y. S., HSIEH, D. K., LIN, S. Z., HARN, H. J. & CHIOU, T. W. 2014. Genetic and epigenetic instability of stem cells. *Cell Transplant,* 23**,** 417-33.
RAMADORI, G., MORICONI, F., MALIK, I. & DUDAS, J. 2008. Physiology and pathophysiology of liver inflammation, damage and repair. *J Physiol Pharmacol,* 59 Suppl 1**,** 107-17.
RAMBHATLA, L., CHIU, C. P., KUNDU, P., PENG, Y. & CARPENTER, M. K. 2003. Generation of hepatocyte-like cells from human embryonic stem cells. *Cell Transplant,* 12**,** 1-11.
RAMBOER, E., ROGIERS, V., VANHAECKE, T. & VINKEN, M. 2015a. Effects of Trichostatin A on drug uptake transporters in primary rat hepatocyte cultures. *EXCLI J,* 14**,** 567-76.
RAMBOER, E., VANHAECKE, T., ROGIERS, V. & VINKEN, M. 2015b. Immortalized Human Hepatic Cell Lines for In Vitro Testing and Research Purposes. *Methods Mol Biol,* 1250**,** 53-76.
RASHID, S. T., CORBINEAU, S., HANNAN, N., MARCINIAK, S. J., MIRANDA, E., ALEXANDER, G., HUANG-DORAN, I., GRIFFIN, J., AHRLUND-RICHTER, L., SKEPPER, J., SEMPLE, R., WEBER, A., LOMAS, D. A. & VALLIER, L. 2010. Modeling inherited metabolic disorders of the liver using human induced pluripotent stem cells. *J Clin Invest,* 120**,** 3127-36.
RASHID, T., TAKEBE, T. & NAKAUCHI, H. 2015. Novel strategies for liver therapy

using stem cells. *Gut,* 64**,** 1-4.
REBUZZINI, P., ZUCCOTTI, M., REDI, C. A. & GARAGNA, S. 2015. Chromosomal Abnormalities in Embryonic and Somatic Stem Cells. *Cytogenet Genome Res,* 147**,** 1-9.
REHMAN, W., ARFONS, L. M. & LAZARUS, H. M. 2011. The rise, fall and subsequent triumph of thalidomide: lessons learned in drug development. *Ther Adv Hematol,* 2**,** 291-308.
REITER, R. J., TAN, D. X., MAYO, J. C., SAINZ, R. M., LEON, J. & CZARNOCKI, Z. 2003. Melatonin as an antioxidant: biochemical mechanisms and pathophysiological implications in humans. *Acta Biochim Pol,* 50**,** 1129-46.
RHEE, J., INOUE, Y., YOON, J. C., PUIGSERVER, P., FAN, M., GONZALEZ, F. J. & SPIEGELMAN, B. M. 2003. Regulation of hepatic fasting response by PPARgamma coactivator-1alpha (PGC-1): requirement for hepatocyte nuclear factor 4alpha in gluconeogenesis. *Proc Natl Acad Sci U S A,* 100**,** 4012-7.
RICHARDS, C. D. 2013. The Enigmatic Cytokine Oncostatin M and Roles in Disease. *ISRN Inflamm,* 2013**,** 512103.
RICHARDSON, S. J., BAI, A., KULKARNI, A. A. & MOGHADDAM, M. F. 2016. Efficiency in Drug Discovery: Liver S9 Fraction Assay As a Screen for Metabolic Stability. *Drug Metab Lett,* 10**,** 83-90.
RODIN, S., ANTONSSON, L., NIAUDET, C., SIMONSON, O. E., SALMELA, E., HANSSON, E. M., DOMOGATSKAYA, A., XIAO, Z., DAMDIMOPOULOU, P., SHEIKHI, M., INZUNZA, J., NILSSON, A. S., BAKER, D., KUIPER, R., SUN, Y., BLENNOW, E., NORDENSKJÖLD, M., GRINNEMO, K. H., KERE, J., BETSHOLTZ, C., HOVATTA, O. & TRYGGVASON, K. 2014. Clonal culturing of human embryonic stem cells on laminin-521/E-cadherin matrix in defined and xeno-free environment. *Nat Commun,* 5**,** 3195.
RODIN, S., DOMOGATSKAYA, A., STRÖM, S., HANSSON, E. M., CHIEN, K. R., INZUNZA, J., HOVATTA, O. & TRYGGVASON, K. 2010. Long-term self-renewal of human pluripotent stem cells on human recombinant laminin-511. *Nat Biotechnol,* 28**,** 611-5.
ROGUE, A., LAMBERT, C., SPIRE, C., CLAUDE, N. & GUILLOUZO, A. 2012. Interindividual variability in gene expression profiles in human hepatocytes and comparison with HepaRG cells. *Drug Metab Dispos,* 40**,** 151-8.
ROMAN, C., FUIOR, E. V., TRUSCA, V. G., KARDASSIS, D., SIMIONESCU, M. & GAFENCU, A. V. 2015. Thyroid hormones upregulate apolipoprotein E gene expression in astrocytes. *Biochem Biophys Res Commun,* 468**,** 190-5.
ROSS, A. C. & ZOLFAGHARI, R. 2011. Cytochrome P450s in the regulation of cellular retinoic acid metabolism. *Annu Rev Nutr,* 31**,** 65-87.
ROSSI, J. M., DUNN, N. R., HOGAN, B. L. & ZARET, K. S. 2001. Distinct mesodermal signals, including BMPs from the septum transversum mesenchyme, are required in combination for hepatogenesis from the endoderm. *Genes Dev,* 15**,** 1998-2009.
ROWE, C., GERRARD, D. T., JENKINS, R., BERRY, A., DURKIN, K., SUNDSTROM, L., GOLDRING, C. E., PARK, B. K., KITTERINGHAM, N. R., HANLEY, K. P. & HANLEY, N. A. 2013. Proteome-wide analyses of human hepatocytes during differentiation and dedifferentiation. *Hepatology,* 58**,** 799-809.

ROY, S. 2014. Atherosclerotic Cardiovascular Disease Risk and Evidence-based Management of Cholesterol. *N Am J Med Sci,* 6**,** 191-8.

RUI, L. 2014. Energy metabolism in the liver. *Compr Physiol,* 4**,** 177-97.

RUIZ-GASPÀ, S., GUAÑABENS, N., ENJUANES, A., PERIS, P., MARTINEZ-FERRER, A., DE OSABA, M. J., GONZALEZ, B., ALVAREZ, L., MONEGAL, A., COMBALIA, A. & PARÉS, A. 2010. Lithocholic acid downregulates vitamin D effects in human osteoblasts. *Eur J Clin Invest,* 40**,** 25-34.

RUMBALLE, B., GEORGAS, K. & LITTLE, M. H. 2008. High-throughput paraffin section in situ hybridization and dual immunohistochemistry on mouse tissues. *CSH Protoc,* 2008**,** pdb.prot5030.

RUSSO, J., FERNANDEZ, S. V., RUSSO, P. A., FERNBAUGH, R., SHERIFF, F. S., LAREEF, H. M., GARBER, J. & RUSSO, I. H. 2006. 17-Beta-estradiol induces transformation and tumorigenesis in human breast epithelial cells. *FASEB J,* 20**,** 1622-34.

SA-NGIAMSUNTORN, K., WONGKAJORNSILP, A., KASETSINSOMBAT, K., DUANGSA-ARD, S., NUNTAKARN, L., BORWORNPINYO, S., AKARASEREENONT, P., LIMSRICHAMRERN, S. & HONGENG, S. 2011. Upregulation of CYP 450s expression of immortalized hepatocyte-like cells derived from mesenchymal stem cells by enzyme inducers. *BMC Biotechnol,* 11**,** 89.

SACHSE, C., BHAMBRA, U., SMITH, G., LIGHTFOOT, T. J., BARRETT, J. H., SCOLLAY, J., GARNER, R. C., BOOBIS, A. R., WOLF, C. R., GOODERHAM, N. J. & GROUP, C. C. S. 2003. Polymorphisms in the cytochrome P450 CYP1A2 gene (CYP1A2) in colorectal cancer patients and controls: allele frequencies, linkage disequilibrium and influence on caffeine metabolism. *Br J Clin Pharmacol,* 55**,** 68-76.

SAHI, J., GREPPER, S. & SMITH, C. 2010. Hepatocytes as a tool in drug metabolism, transport and safety evaluations in drug discovery. *Curr Drug Discov Technol,* 7**,** 188-98.

SAHI, J., SHORD, S. S., LINDLEY, C., FERGUSON, S. & LECLUYSE, E. L. 2009. Regulation of cytochrome P450 2C9 expression in primary cultures of human hepatocytes. *J Biochem Mol Toxicol,* 23**,** 43-58.

SAKURAI, F., MITANI, S., YAMAMOTO, T., TAKAYAMA, K., TACHIBANA, M., WATASHI, K., WAKITA, T., IIJIMA, S., TANAKA, Y. & MIZUGUCHI, H. 2017. Human induced-pluripotent stem cell-derived hepatocyte-like cells as an in vitro model of human hepatitis B virus infection. *Sci Rep,* 7**,** 45698.

SARKAR, P., RANDALL, S. M., MUDDIMAN, D. C. & RAO, B. M. 2012. Targeted proteomics of the secretory pathway reveals the secretome of mouse embryonic fibroblasts and human embryonic stem cells. *Mol Cell Proteomics,* 11**,** 1829-39.

SARPER, M., CORTES, E., LIEBERTHAL, T. J. & DEL RÍO HERNÁNDEZ, A. 2016. ATRA modulates mechanical activation of TGF-β by pancreatic stellate cells. *Sci Rep,* 6**,** 27639.

SATOHISA, S., CHIBA, H., OSANAI, M., OHNO, S., KOJIMA, T., SAITO, T. & SAWADA, N. 2005. Behavior of tight-junction, adherens-junction and cell polarity proteins during HNF-4alpha-induced epithelial polarization. *Exp Cell Res,* 310**,** 66-78.

SCHADT, E. E., MOLONY, C., CHUDIN, E., HAO, K., YANG, X., LUM, P. Y., KASARSKIS,

A., ZHANG, B., WANG, S., SUVER, C., ZHU, J., MILLSTEIN, J., SIEBERTS, S., LAMB, J., GUHATHAKURTA, D., DERRY, J., STOREY, J. D., AVILA-CAMPILLO, I., KRUGER, M. J., JOHNSON, J. M., ROHL, C. A., VAN NAS, A., MEHRABIAN, M., DRAKE, T. A., LUSIS, A. J., SMITH, R. C., GUENGERICH, F. P., STROM, S. C., SCHUETZ, E., RUSHMORE, T. H. & ULRICH, R. 2008. Mapping the genetic architecture of gene expression in human liver. *PLoS Biol,* 6**,** e107.

SCHIØDT, F. V., OSTAPOWICZ, G., MURRAY, N., SATYANARANA, R., ZAMAN, A., MUNOZ, S. & LEE, W. M. 2006. Alpha-fetoprotein and prognosis in acute liver failure. *Liver Transpl,* 12**,** 1776-81.

SCHLOTT, T., THASLER, W., GORZEL, C., PAHERNIK, S., BRINCK, U., EIFFERT, H. & DROESE, M. 2002. Detection of MDM2 alterations in cultured human hepatocytes treated with 17beta-estradiol or 17alpha-ethinylestradiol. *Anticancer Res,* 22**,** 1545-51.

SCHMELZER, E., WAUTHIER, E. & REID, L. M. 2006. The phenotypes of pluripotent human hepatic progenitors. *Stem Cells,* 24**,** 1852-8.

SCHMUCKER, D. L. 1990. Hepatocyte fine structure during maturation and senescence. *J Electron Microsc Tech,* 14**,** 106-25.

SCHULZ, T. C., PALMARINI, G. M., NOGGLE, S. A., WEILER, D. A., MITALIPOVA, M. M. & CONDIE, B. G. 2003. Directed neuronal differentiation of human embryonic stem cells. *BMC Neurosci,* 4**,** 27.

SCHWARTZ, R. E., BRAM, Y. & FRANKEL, A. 2016. Pluripotent Stem Cell-Derived Hepatocyte-like Cells: A Tool to Study Infectious Disease. *Curr Pathobiol Rep,* 4**,** 147-156.

SCHWARTZ, R. E., FLEMING, H. E., KHETANI, S. R. & BHATIA, S. N. 2014. Pluripotent stem cell-derived hepatocyte-like cells. *Biotechnol Adv,* 32**,** 504-13.

SCUDERI, G. J. & BUTCHER, J. 2017. Naturally Engineered Maturation of Cardiomyocytes. *Front Cell Dev Biol,* 5**,** 50.

SCULLY, J. L., HAIMES, E., MITZKAT, A., PORZ, R. & REHMANN-SUTTER, C. 2012. Donating embryos to stem cell research. *J Bioeth Inq,* 9**,** 19-28.

SEKI, T. & FUKUDA, K. 2015. Methods of induced pluripotent stem cells for clinical application. *World J Stem Cells,* 7**,** 116-25.

SELL, S. 2008. Alpha-fetoprotein, stem cells and cancer: how study of the production of alpha-fetoprotein during chemical hepatocarcinogenesis led to reaffirmation of the stem cell theory of cancer. *Tumour Biol,* 29**,** 161-80.

SERLS, A. E., DOHERTY, S., PARVATIYAR, P., WELLS, J. M. & DEUTSCH, G. H. 2005. Different thresholds of fibroblast growth factors pattern the ventral foregut into liver and lung. *Development,* 132**,** 35-47.

SHAJARI, S., LALIENA, A., HEEGSMA, J., TUÑÓN, M. J., MOSHAGE, H. & FABER, K. N. 2015. Melatonin suppresses activation of hepatic stellate cells through RORα-mediated inhibition of 5-lipoxygenase. *J Pineal Res,* 59**,** 391-401.

SHAN, J., SCHWARTZ, R. E., ROSS, N. T., LOGAN, D. J., THOMAS, D., DUNCAN, S. A., NORTH, T. E., GOESSLING, W., CARPENTER, A. E. & BHATIA, S. N. 2013. Identification of small molecules for human hepatocyte expansion and iPS differentiation. *Nat Chem Biol,* 9**,** 514-20.

SHANKS, N., GREEK, R. & GREEK, J. 2009. Are animal models predictive for humans? *Philos Ethics Humanit Med,* 4**,** 2.

SHEN, M. M. 2007. Nodal signaling: developmental roles and regulation.

Development, 134**,** 1023-34.
SHI, Y., INOUE, H., WU, J. C. & YAMANAKA, S. 2017. Induced pluripotent stem cell technology: a decade of progress. *Nat Rev Drug Discov,* 16**,** 115-130.
SHIHABUDEEN, M. S., ROY, D., JAMES, J. & THIRUMURUGAN, K. 2015. Chenodeoxycholic acid, an endogenous FXR ligand alters adipokines and reverses insulin resistance. *Mol Cell Endocrinol,* 414**,** 19-28.
SHIN, D. & MONGA, S. P. 2013. Cellular and molecular basis of liver development. *Compr Physiol,* 3**,** 799-815.
SHIRAHASHI, H., WU, J., YAMAMOTO, N., CATANA, A., WEGE, H., WAGER, B., OKITA, K. & ZERN, M. A. 2004. Differentiation of human and mouse embryonic stem cells along a hepatocyte lineage. *Cell Transplant,* 13**,** 197-211.
SHORT, J. & OVE, P. 1983. Synthesis of an hypothesis advocating a prominent role for the thyroid hormones in mammalian liver cell proliferation in vivo. *Cytobios,* 38**,** 39-49.
SHUKLA, S. J., SAKAMURU, S., HUANG, R., MOELLER, T. A., SHINN, P., VANLEER, D., AULD, D. S., AUSTIN, C. P. & XIA, M. 2011. Identification of clinically used drugs that activate pregnane X receptors. *Drug Metab Dispos,* 39**,** 151-9.
SHULMAN, M. & NAHMIAS, Y. 2013. Long-term culture and coculture of primary rat and human hepatocytes. *Methods Mol Biol,* 945**,** 287-302.
SI-TAYEB, K., DUCLOS-VALLÉE, J. C. & PETIT, M. A. 2012. Hepatocyte-like cells differentiated from human induced pluripotent stem cells (iHLCs) are permissive to hepatitis C virus (HCV) infection: HCV study gets personal. *J Hepatol,* 57**,** 689-91.
SI-TAYEB, K., LEMAIGRE, F. P. & DUNCAN, S. A. 2010a. Organogenesis and development of the liver. *Dev Cell,* 18**,** 175-89.
SI-TAYEB, K., NOTO, F. K., NAGAOKA, M., LI, J., BATTLE, M. A., DURIS, C., NORTH, P. E., DALTON, S. & DUNCAN, S. A. 2010b. Highly efficient generation of human hepatocyte-like cells from induced pluripotent stem cells. *Hepatology,* 51**,** 297-305.
SIBBONS, C. M., BRENNA, J. T., LAWRENCE, P., HOILE, S. P., CLARKE-HARRIS, R., LILLYCROP, K. A. & BURDGE, G. C. 2014. Effect of sex hormones on n-3 polyunsaturated fatty acid biosynthesis in HepG2 cells and in human primary hepatocytes. *Prostaglandins Leukot Essent Fatty Acids,* 90**,** 47-54.
SILLER, R., GREENHOUGH, S., NAUMOVSKA, E. & SULLIVAN, G. J. 2015. Small-molecule-driven hepatocyte differentiation of human pluripotent stem cells. *Stem Cell Reports,* 4**,** 939-52.
SILLER, R., NAUMOVSKA, E., MATHAPATI, S., LYCKE, M., GREENHOUGH, S. & SULLIVAN, G. J. 2016. Development of a rapid screen for the endodermal differentiation potential of human pluripotent stem cell lines. *Sci Rep,* 6**,** 37178.
SILLS, E. S., TAKEUCHI, T., TANAKA, N., NERI, Q. V. & PALERMO, G. D. 2005. Identification and isolation of embryonic stem cells in reproductive endocrinology: theoretical protocols for conservation of human embryos derived from in vitro fertilization. *Theor Biol Med Model,* 2**,** 25.
SINGH, A. M., REYNOLDS, D., CLIFF, T., OHTSUKA, S., MATTHEYSES, A. L., SUN, Y., MENENDEZ, L., KULIK, M. & DALTON, S. 2012. Signaling network crosstalk in human pluripotent cells: a Smad2/3-regulated switch that controls the

balance between self-renewal and differentiation. *Cell Stem Cell,* 10**,** 312-26.
SINGH, S., CARPENTER, A. E. & GENOVESIO, A. 2014. Increasing the Content of High-Content Screening: An Overview. *J Biomol Screen,* 19**,** 640-50.
SINHA-HIKIM, I., TAYLOR, W. E., GONZALEZ-CADAVID, N. F., ZHENG, W. & BHASIN, S. 2004. Androgen receptor in human skeletal muscle and cultured muscle satellite cells: up-regulation by androgen treatment. *J Clin Endocrinol Metab,* 89**,** 5245-55.
SINZ, M., WALLACE, G. & SAHI, J. 2008. Current industrial practices in assessing CYP450 enzyme induction: preclinical and clinical. *AAPS J,* 10**,** 391-400.
SINZ, M. A. 2012. *In Vitro* and *In Vivo* Models of Drug Metabolism. Encyclopedia of Drug Metabolism and Interactions. I:1–31.
SISON-YOUNG, R. L., MITSA, D., JENKINS, R. E., MOTTRAM, D., ALEXANDRE, E., RICHERT, L., AERTS, H., WEAVER, R. J., JONES, R. P., JOHANN, E., HEWITT, P. G., INGELMAN-SUNDBERG, M., GOLDRING, C. E., KITTERINGHAM, N. R. & PARK, B. K. 2015. Comparative Proteomic Characterization of 4 Human Liver-Derived Single Cell Culture Models Reveals Significant Variation in the Capacity for Drug Disposition, Bioactivation, and Detoxication. *Toxicol Sci,* 147**,** 412-24.
SKOTTMAN, H. & HOVATTA, O. 2006. Culture conditions for human embryonic stem cells. *Reproduction,* 132**,** 691-8.
SMITH, J. R., VALLIER, L., LUPO, G., ALEXANDER, M., HARRIS, W. A. & PEDERSEN, R. A. 2008. Inhibition of Activin/Nodal signaling promotes specification of human embryonic stem cells into neuroectoderm. *Dev Biol,* 313**,** 107-17.
SMITH, S. A. 2002. Peroxisome proliferator-activated receptors and the regulation of mammalian lipid metabolism. *Biochem Soc Trans,* 30**,** 1086-90.
SOARES, F. A., CHANDRA, A., THOMAS, R. J., PEDERSEN, R. A., VALLIER, L. & WILLIAMS, D. J. 2014. Investigating the feasibility of scale up and automation of human induced pluripotent stem cells cultured in aggregates in feeder free conditions. *J Biotechnol,* 173**,** 53-8.
SOLDATOW, V. Y., LECLUYSE, E. L., GRIFFITH, L. G. & RUSYN, I. 2013. In vitro models for liver toxicity testing. *Toxicol Res (Camb),* 2**,** 23-39.
SOMA, T., KAGANOI, J., KAWABE, A., KONDO, K., TSUNODA, S., IMAMURA, M. & SHIMADA, Y. 2006. Chenodeoxycholic acid stimulates the progression of human esophageal cancer cells: A possible mechanism of angiogenesis in patients with esophageal cancer. *Int J Cancer,* 119**,** 771-82.
SONG, K. H., LI, T., OWSLEY, E., STROM, S. & CHIANG, J. Y. 2009a. Bile acids activate fibroblast growth factor 19 signaling in human hepatocytes to inhibit cholesterol 7alpha-hydroxylase gene expression. *Hepatology,* 49**,** 297-305.
SONG, W. & JIN, X. A. 2015. Cyclic AMP inhibits neuromuscular junction maturation mediated by intracellular Ca2+. *Neurosci Lett,* 589**,** 104-9.
SONG, X., XIE, M., ZHANG, H., LI, Y., SACHDEVA, K. & YAN, B. 2004. The pregnane X receptor binds to response elements in a genomic context-dependent manner, and PXR activator rifampicin selectively alters the binding among target genes. *Drug Metab Dispos,* 32**,** 35-42.
SONG, Z., CAI, J., LIU, Y., ZHAO, D., YONG, J., DUO, S., SONG, X., GUO, Y., ZHAO, Y., QIN, H., YIN, X., WU, C., CHE, J., LU, S., DING, M. & DENG, H. 2009b. Efficient generation of hepatocyte-like cells from human induced pluripotent stem

cells. *Cell Res,* 19**,** 1233-42.
STACEY, G. N. 2011. Cell culture contamination. *Methods Mol Biol,* 731**,** 79-91.
STADTFELD, M., NAGAYA, M., UTIKAL, J., WEIR, G. & HOCHEDLINGER, K. 2008. Induced pluripotent stem cells generated without viral integration. *Science,* 322**,** 945-9.
STAECKER, J. L., SATTLER, C. A. & PITOT, H. C. 1988. Sodium butyrate preserves aspects of the differentiated phenotype of normal adult rat hepatocytes in culture. *J Cell Physiol,* 135**,** 367-76.
STARZL, T. E. & LAKKIS, F. G. 2006. The unfinished legacy of liver transplantation: emphasis on immunology. *Hepatology,* 43**,** S151-63.
STAUDINGER, J. L., GOODWIN, B., JONES, S. A., HAWKINS-BROWN, D., MACKENZIE, K. I., LATOUR, A., LIU, Y., KLAASSEN, C. D., BROWN, K. K., REINHARD, J., WILLSON, T. M., KOLLER, B. H. & KLIEWER, S. A. 2001. The nuclear receptor PXR is a lithocholic acid sensor that protects against liver toxicity. *Proc Natl Acad Sci U S A,* 98**,** 3369-74.
STENGL, A., HÖRL, D., LEONHARDT, H. & HELMA, J. 2017. A Simple and Sensitive High-Content Assay for the Characterization of Antiproliferative Therapeutic Antibodies. *SLAS Discov,* 22**,** 309-315.
STINE, J. G. & CHALASANI, N. 2015. Chronic liver injury induced by drugs: a systematic review. *Liver Int,* 35**,** 2343-53.
STOCKINGER, B., DI MEGLIO, P., GIALITAKIS, M. & DUARTE, J. H. 2014. The aryl hydrocarbon receptor: multitasking in the immune system. *Annu Rev Immunol,* 32**,** 403-32.
STOCKWELL, S. R. & MITTNACHT, S. 2014. Workflow for high-content, individual cell quantification of fluorescent markers from universal microscope data, supported by open source software. *J Vis Exp*.
STORCHOVA, Z. & PELLMAN, D. 2004. From polyploidy to aneuploidy, genome instability and cancer. *Nat Rev Mol Cell Biol,* 5**,** 45-54.
STORM, M. P., SORRELL, I., SHIPLEY, R., REGAN, S., LUETCHFORD, K. A., SATHISH, J., WEBB, S. & ELLIS, M. J. 2016. Hollow Fiber Bioreactors for In Vivo-like Mammalian Tissue Culture. *J Vis Exp*.
STROM, S. C., DAVILA, J. & GROMPE, M. 2010. Chimeric mice with humanized liver: tools for the study of drug metabolism, excretion, and toxicity. *Methods Mol Biol,* 640**,** 491-509.
STÉPHENNE, X., NAJIMI, M. & SOKAL, E. M. 2010. Hepatocyte cryopreservation: is it time to change the strategy? *World J Gastroenterol,* 16**,** 1-14.
SU, T. & WAXMAN, D. J. 2004. Impact of dimethyl sulfoxide on expression of nuclear receptors and drug-inducible cytochromes P450 in primary rat hepatocytes. *Arch Biochem Biophys,* 424**,** 226-34.
SUI, L., BOUWENS, L. & MFOPOU, J. K. 2013. Signaling pathways during maintenance and definitive endoderm differentiation of embryonic stem cells. *Int J Dev Biol,* 57**,** 1-12.
SULLIVAN, G. J., HAY, D. C., PARK, I. H., FLETCHER, J., HANNOUN, Z., PAYNE, C. M., DALGETTY, D., BLACK, J. R., ROSS, J. A., SAMUEL, K., WANG, G., DALEY, G. Q., LEE, J. H., CHURCH, G. M., FORBES, S. J., IREDALE, J. P. & WILMUT, I. 2010. Generation of functional human hepatic endoderm from human induced pluripotent stem cells. *Hepatology,* 51**,** 329-35.

SULZBACHER, S., SCHROEDER, I. S., TRUONG, T. T. & WOBUS, A. M. 2009. Activin A-induced differentiation of embryonic stem cells into endoderm and pancreatic progenitors-the influence of differentiation factors and culture conditions. *Stem Cell Rev,* 5**,** 159-73.

SUN, Y., YANG, W., LUO, H., WANG, X., CHEN, Z., ZHANG, J., WANG, Y. & LI, X. 2015. Thyroid hormone inhibits the proliferation of piglet Sertoli cell via PI3K signaling pathway. *Theriogenology,* 83**,** 86-94.

SUNMAN, J. A., HAWKE, R. L., LECLUYSE, E. L. & KASHUBA, A. D. 2004. Kupffer cell-mediated IL-2 suppression of CYP3A activity in human hepatocytes. *Drug Metab Dispos,* 32**,** 359-63.

SUZUKI, A., IWAMA, A., MIYASHITA, H., NAKAUCHI, H. & TANIGUCHI, H. 2003. Role for growth factors and extracellular matrix in controlling differentiation of prospectively isolated hepatic stem cells. *Development,* 130**,** 2513-24.

SWALES, K. & NEGISHI, M. 2004. CAR, driving into the future. *Mol Endocrinol,* 18**,** 1589-98.

SZANTO, A., NARKAR, V., SHEN, Q., URAY, I. P., DAVIES, P. J. & NAGY, L. 2004. Retinoid X receptors: X-ploring their (patho)physiological functions. *Cell Death Differ,* 11 Suppl 2**,** S126-43.

SZKOLNICKA, D., FARNWORTH, S. L., LUCENDO-VILLARIN, B., STORCK, C., ZHOU, W., IREDALE, J. P., FLINT, O. & HAY, D. C. 2013. Accurate Prediction of Drug-Induced Liver Injury Using Stem Cell-Derived Populations. *Stem Cells Transl Med*.

SZKOLNICKA, D. & HAY, D. C. 2016. Concise Review: Advances in Generating Hepatocytes from Pluripotent Stem Cells for Translational Medicine. *Stem Cells,* 34**,** 1421-6.

TAKAHASHI, K., TANABE, K., OHNUKI, M., NARITA, M., ICHISAKA, T., TOMODA, K. & YAMANAKA, S. 2007. Induction of pluripotent stem cells from adult human fibroblasts by defined factors. *Cell,* 131**,** 861-72.

TAKAHASHI, K. & YAMANAKA, S. 2006. Induction of pluripotent stem cells from mouse embryonic and adult fibroblast cultures by defined factors. *Cell,* 126**,** 663-76.

TAKAYAMA, K., MORISAKI, Y., KUNO, S., NAGAMOTO, Y., HARADA, K., FURUKAWA, N., OHTAKA, M., NISHIMURA, K., IMAGAWA, K., SAKURAI, F., TACHIBANA, M., SUMAZAKI, R., NOGUCHI, E., NAKANISHI, M., HIRATA, K., KAWABATA, K. & MIZUGUCHI, H. 2014. Prediction of interindividual differences in hepatic functions and drug sensitivity by using human iPS-derived hepatocytes. *Proc Natl Acad Sci U S A,* 111**,** 16772-7.

TAKAYAMA, K., NAGAMOTO, Y., MIMURA, N., TASHIRO, K., SAKURAI, F., TACHIBANA, M., HAYAKAWA, T., KAWABATA, K. & MIZUGUCHI, H. 2013. Long-Term Self-Renewal of Human ES/iPS-Derived Hepatoblast-like Cells on Human Laminin 111-Coated Dishes. *Stem Cell Reports,* 1**,** 322-35.

TAM, P. P. & LOEBEL, D. A. 2007. Gene function in mouse embryogenesis: get set for gastrulation. *Nat Rev Genet,* 8**,** 368-81.

TANG, W. W., KOBAYASHI, T., IRIE, N., DIETMANN, S. & SURANI, M. A. 2016. Specification and epigenetic programming of the human germ line. *Nat Rev Genet,* 17**,** 585-600.

TANIMIZU, N. & MIYAJIMA, A. 2004. Notch signaling controls hepatoblast

differentiation by altering the expression of liver-enriched transcription factors. *J Cell Sci,* 117**,** 3165-74.

TASNIM, F., PHAN, D., TOH, Y. C. & YU, H. 2015. Cost-effective differentiation of hepatocyte-like cells from human pluripotent stem cells using small molecules. *Biomaterials,* 70**,** 115-25.

TATE, J. & WARD, G. 2004. Interferences in immunoassay. *Clin Biochem Rev,* 25**,** 105-20.

TATSUMI, N., MIKI, R., KATSU, K. & YOKOUCHI, Y. 2007. Neurturin-GFRalpha2 signaling controls liver bud migration along the ductus venosus in the chick embryo. *Dev Biol,* 307**,** 14-28.

TCHORZ, J. S., KINTER, J., MÜLLER, M., TORNILLO, L., HEIM, M. H. & BETTLER, B. 2009. Notch2 signaling promotes biliary epithelial cell fate specification and tubulogenesis during bile duct development in mice. *Hepatology,* 50**,** 871-9.

TEO, A. K., ALI, Y., WONG, K. Y., CHIPPERFIELD, H., SADASIVAM, A., POOBALAN, Y., TAN, E. K., WANG, S. T., ABRAHAM, S., TSUNEYOSHI, N., STANTON, L. W. & DUNN, N. R. 2012. Activin and BMP4 synergistically promote formation of definitive endoderm in human embryonic stem cells. *Stem Cells,* 30**,** 631-42.

TERRY, C. & HUGHES, R. D. 2009. An optimised method for cryopreservation of human hepatocytes. *Methods Mol Biol,* 481**,** 25-34.

TERRY, C., MITRY, R. R., LEHEC, S. C., MUIESAN, P., RELA, M., HEATON, N. D., HUGHES, R. D. & DHAWAN, A. 2005. The effects of cryopreservation on human hepatocytes obtained from different sources of liver tissue. *Cell Transplant,* 14**,** 585-94.

TESCHKE, R. & DANAN, G. 2016. Diagnosis and Management of Drug-Induced Liver Injury (DILI) in Patients with Pre-Existing Liver Disease. *Drug Saf,* 39**,** 729-44.

THOMAS, C., PELLICCIARI, R., PRUZANSKI, M., AUWERX, J. & SCHOONJANS, K. 2008. Targeting bile-acid signalling for metabolic diseases. *Nat Rev Drug Discov,* 7**,** 678-93.

THOMAS, R. J., ANDERSON, D., CHANDRA, A., SMITH, N. M., YOUNG, L. E., WILLIAMS, D. & DENNING, C. 2009. Automated, scalable culture of human embryonic stem cells in feeder-free conditions. *Biotechnol Bioeng,* 102**,** 1636-44.

THOMSON, J. A., ITSKOVITZ-ELDOR, J., SHAPIRO, S. S., WAKNITZ, M. A., SWIERGIEL, J. J., MARSHALL, V. S. & JONES, J. M. 1998. Embryonic stem cell lines derived from human blastocysts. *Science,* 282**,** 1145-7.

TIMM, M., SAABY, L., MOESBY, L. & HANSEN, E. W. 2013. Considerations regarding use of solvents in in vitro cell based assays. *Cytotechnology,* 65**,** 887-94.

TIMSIT, Y. E. & NEGISHI, M. 2007. CAR and PXR: the xenobiotic-sensing receptors. *Steroids,* 72**,** 231-46.

TOIVONEN, S., LUNDIN, K., BALBOA, D., USTINOV, J., TAMMINEN, K., PALGI, J., TROKOVIC, R., TUURI, T. & OTONKOSKI, T. 2013. Activin A and Wnt-dependent specification of human definitive endoderm cells. *Exp Cell Res,* 319**,** 2535-44.

TOLLOCZKO, B., TURKEWITSCH, P., AL-CHALABI, M. & MARTIN, J. G. 2004. LY-294002 [2-(4-morpholinyl)-8-phenyl-4H-1-benzopyran-4-one] affects calcium signaling in airway smooth muscle cells independently of phosphoinositide 3-kinase inhibition. *J Pharmacol Exp Ther,* 311**,** 787-93.

TOSCA, L., FERAUD, O., MAGNIEZ, A., BAS, C., GRISCELLI, F., BENNACEUR-GRISCELLI, A. & TACHDJIAN, G. 2015. Genomic instability of human embryonic stem cell lines using different passaging culture methods. *Mol Cytogenet,* 8**,** 30.

TOUBOUL, T., CHEN, S., TO, C. C., MORA-CASTILLA, S., SABATINI, K., TUKEY, R. H. & LAURENT, L. C. 2016. Stage-specific regulation of the WNT/β-catenin pathway results in improved differentiation of hESCs to functional hepatocytes. *J Hepatol*.

TOUBOUL, T., HANNAN, N. R., CORBINEAU, S., MARTINEZ, A., MARTINET, C., BRANCHEREAU, S., MAINOT, S., STRICK-MARCHAND, H., PEDERSEN, R., DI SANTO, J., WEBER, A. & VALLIER, L. 2010. Generation of functional hepatocytes from human embryonic stem cells under chemically defined conditions that recapitulate liver development. *Hepatology,* 51**,** 1754-65.

TREMBLAY, K. D. & ZARET, K. S. 2005. Distinct populations of endoderm cells converge to generate the embryonic liver bud and ventral foregut tissues. *Dev Biol,* 280**,** 87-99.

TREYER, A. & MÜSCH, A. 2013. Hepatocyte polarity. *Compr Physiol,* 3**,** 243-87.

TSAI, W. L., YEH, P. H., TSAI, C. Y., TING, C. T., CHIU, Y. H., TAO, M. H., LI, W. C. & HUNG, S. C. 2016. Efficient Programming of Human Mesenchymal Stem Cell Derived Hepatocytes by Epigenetic Regulations. *J Gastroenterol Hepatol*.

TU, H., OKAMOTO, A. Y. & SHAN, B. 2000. FXR, a bile acid receptor and biological sensor. *Trends Cardiovasc Med,* 10**,** 30-5.

TURNER, R., LOZOYA, O., WANG, Y., CARDINALE, V., GAUDIO, E., ALPINI, G., MENDEL, G., WAUTHIER, E., BARBIER, C., ALVARO, D. & REID, L. M. 2011. Human hepatic stem cell and maturational liver lineage biology. *Hepatology,* 53**,** 1035-45.

TYE, H. 2004. Application of statistical 'design of experiments' methods in drug discovery. *Drug Discov Today,* 9**,** 485-91.

UKAIRO, O., KANCHAGAR, C., MOORE, A., SHI, J., GAFFNEY, J., AOYAMA, S., ROSE, K., KRZYZEWSKI, S., MCGEEHAN, J., ANDERSEN, M. E., KHETANI, S. R. & LECLUYSE, E. L. 2013. Long-term stability of primary rat hepatocytes in micropatterned cocultures. *J Biochem Mol Toxicol,* 27**,** 204-12.

URIBE, P. M., KAWAS, L. H., HARDING, J. W. & COFFIN, A. B. 2015. Hepatocyte growth factor mimetic protects lateral line hair cells from aminoglycoside exposure. *Front Cell Neurosci,* 9**,** 3.

VAN BOOVEN, D., MARSH, S., MCLEOD, H., CARRILLO, M. W., SANGKUHL, K., KLEIN, T. E. & ALTMAN, R. B. 2010. Cytochrome P450 2C9-CYP2C9. *Pharmacogenet Genomics,* 20**,** 277-81.

VAN DER MEULEN, T. & HUISING, M. O. 2014. Maturation of stem cell-derived beta-cells guided by the expression of urocortin 3. *Rev Diabet Stud,* 11**,** 115-32.

VAN ROY, F. & BERX, G. 2008. The cell-cell adhesion molecule E-cadherin. *Cell Mol Life Sci,* 65**,** 3756-88.

VERAITCH, F. S., SCOTT, R., WONG, J. W., LYE, G. J. & MASON, C. 2008. The impact of manual processing on the expansion and directed differentiation of embryonic stem cells. *Biotechnol Bioeng,* 99**,** 1216-29.

VERMEER, C. 2012. Vitamin K: the effect on health beyond coagulation - an overview. *Food Nutr Res,* 56.

VERONESE, M. E., MACKENZIE, P. I., DOECKE, C. J., MCMANUS, M. E., MINERS, J. O.

& BIRKETT, D. J. 1991. Tolbutamide and phenytoin hydroxylations by cDNA-expressed human liver cytochrome P4502C9. *Biochem Biophys Res Commun,* 175**,** 1112-8.

VICKERS, A. E. & FISHER, R. L. 2004. Organ slices for the evaluation of human drug toxicity. *Chem Biol Interact,* 150**,** 87-96.

VILLA-DIAZ, L. G., PACUT, C., SLAWNY, N. A., DING, J., O'SHEA, K. S. & SMITH, G. D. 2009. Analysis of the factors that limit the ability of feeder cells to maintain the undifferentiated state of human embryonic stem cells. *Stem Cells Dev,* 18**,** 641-51.

VINCENT, S. D., DUNN, N. R., HAYASHI, S., NORRIS, D. P. & ROBERTSON, E. J. 2003. Cell fate decisions within the mouse organizer are governed by graded Nodal signals. *Genes Dev,* 17**,** 1646-62.

VORRINK, S. U., HUDACHEK, D. R. & DOMANN, F. E. 2014. Epigenetic determinants of CYP1A1 induction by the aryl hydrocarbon receptor agonist 3,3',4,4',5-pentachlorobiphenyl (PCB 126). *Int J Mol Sci,* 15**,** 13916-31.

VUORENPÄÄ, H., PENTTINEN, K., HEINONEN, T., PEKKANEN-MATTILA, M., SARKANEN, J. R., YLIKOMI, T. & AALTO-SETÄLÄ, K. 2017. Maturation of human pluripotent stem cell derived cardiomyocytes is improved in cardiovascular construct. *Cytotechnology*.

WADA, K., ITOGA, K., OKANO, T., YONEMURA, S. & SASAKI, H. 2011. Hippo pathway regulation by cell morphology and stress fibers. *Development,* 138**,** 3907-14.

WADA, T., GAO, J. & XIE, W. 2009. PXR and CAR in energy metabolism. *Trends Endocrinol Metab,* 20**,** 273-9.

WAGNER, A. E., BOESCH-SAADATMANDI, C., BRECKWOLDT, D., SCHRADER, C., SCHMELZER, C., DÖRING, F., HASHIDA, K., HORI, O., MATSUGO, S. & RIMBACH, G. 2011. Ascorbic acid partly antagonizes resveratrol mediated heme oxygenase-1 but not paraoxonase-1 induction in cultured hepatocytes - role of the redox-regulated transcription factor Nrf2. *BMC Complement Altern Med,* 11**,** 1.

WAGNER, C. E., JURUTKA, P. W., MARSHALL, P. A., GROY, T. L., VAN DER VAART, A., ZILLER, J. W., FURMICK, J. K., GRAEBER, M. E., MATRO, E., MIGUEL, B. V., TRAN, I. T., KWON, J., TEDESCHI, J. N., MOOSAVI, S., DANISHYAR, A., PHILP, J. S., KHAMEES, R. O., JACKSON, J. N., GRUPE, D. K., BADSHAH, S. L. & HART, J. W. 2009. Modeling, synthesis and biological evaluation of potential retinoid X receptor (RXR) selective agonists: novel analogues of 4-[1-(3,5,5,8,8-pentamethyl-5,6,7,8-tetrahydro-2-naphthyl)ethynyl]benzoic acid (bexarotene). *J Med Chem,* 52**,** 5950-66.

WALSKY, R. L. & OBACH, R. S. 2004. Validated assays for human cytochrome P450 activities. *Drug Metab Dispos,* 32**,** 647-60.

WALTHER, B., KARL, J. P., BOOTH, S. L. & BOYAVAL, P. 2013. Menaquinones, bacteria, and the food supply: the relevance of dairy and fermented food products to vitamin K requirements. *Adv Nutr,* 4**,** 463-73.

WALTHER, T. C. & FARESE, R. V. 2012. Lipid droplets and cellular lipid metabolism. *Annu Rev Biochem,* 81**,** 687-714.

WANET, A., REMACLE, N., NAJAR, M., SOKAL, E., ARNOULD, T., NAJIMI, M. & RENARD, P. 2014. Mitochondrial remodeling in hepatic differentiation and dedifferentiation. *Int J Biochem Cell Biol,* 54**,** 174-85.

WANG, B., WANG, J., HUANG, S. Q., SU, H. H. & ZHOU, S. F. 2009. Genetic polymorphism of the human cytochrome P450 2C9 gene and its clinical significance. *Curr Drug Metab,* 10**,** 781-834.

WANG, C., YE, Z., KIJLSTRA, A., ZHOU, Y. & YANG, P. 2014. Activation of the aryl hydrocarbon receptor affects activation and function of human monocyte-derived dendritic cells. *Clin Exp Immunol,* 177**,** 521-30.

WANG, Y., CHOU, B. K., DOWEY, S., HE, C., GERECHT, S. & CHENG, L. 2013. Scalable expansion of human induced pluripotent stem cells in the defined xeno-free E8 medium under adherent and suspension culture conditions. *Stem Cell Res,* 11**,** 1103-16.

WARE, B. R. & KHETANI, S. R. 2016. Engineered Liver Platforms for Different Phases of Drug Development. *Trends Biotechnol*.

WARREN, L., MANOS, P. D., AHFELDT, T., LOH, Y. H., LI, H., LAU, F., EBINA, W., MANDAL, P. K., SMITH, Z. D., MEISSNER, A., DALEY, G. Q., BRACK, A. S., COLLINS, J. J., COWAN, C., SCHLAEGER, T. M. & ROSSI, D. J. 2010. Highly efficient reprogramming to pluripotency and directed differentiation of human cells with synthetic modified mRNA. *Cell Stem Cell,* 7**,** 618-30.

WATANABE, H., TAKAYAMA, K., INAMURA, M., TACHIBANA, M., MIMURA, N., KATAYAMA, K., TASHIRO, K., NAGAMOTO, Y., SAKURAI, F., KAWABATA, K., FURUE, M. K. & MIZUGUCHI, H. 2014. HHEX Promotes Hepatic-Lineage Specification through the Negative Regulation of Eomesodermin. *PLoS One,* 9**,** e90791.

WATKINS, R. E., WISELY, G. B., MOORE, L. B., COLLINS, J. L., LAMBERT, M. H., WILLIAMS, S. P., WILLSON, T. M., KLIEWER, S. A. & REDINBO, M. R. 2001. The human nuclear xenobiotic receptor PXR: structural determinants of directed promiscuity. *Science,* 292**,** 2329-33.

WATT, F. M. & DRISKELL, R. R. 2010. The therapeutic potential of stem cells. *Philos Trans R Soc Lond B Biol Sci,* 365**,** 155-63.

WAWER, M. J., LI, K., GUSTAFSDOTTIR, S. M., LJOSA, V., BODYCOMBE, N. E., MARTON, M. A., SOKOLNICKI, K. L., BRAY, M. A., KEMP, M. M., WINCHESTER, E., TAYLOR, B., GRANT, G. B., HON, C. S., DUVALL, J. R., WILSON, J. A., BITTKER, J. A., DANČÍK, V., NARAYAN, R., SUBRAMANIAN, A., WINCKLER, W., GOLUB, T. R., CARPENTER, A. E., SHAMJI, A. F., SCHREIBER, S. L. & CLEMONS, P. A. 2014. Toward performance-diverse small-molecule libraries for cell-based phenotypic screening using multiplexed high-dimensional profiling. *Proc Natl Acad Sci U S A,* 111**,** 10911-6.

WAX, P. M. 1995. Elixirs, diluents, and the passage of the 1938 Federal Food, Drug and Cosmetic Act. *Ann Intern Med,* 122**,** 456-61.

WEEKS, C. A., NEWMAN, K., TURNER, P. A., RODYSILL, B., HICKEY, R. D., NYBERG, S. L. & JANORKAR, A. V. 2013. Suspension culture of hepatocyte-derived reporter cells in presence of albumin to form stable three-dimensional spheroids. *Biotechnol Bioeng,* 110**,** 2548-55.

WEI, P., HU, G. H., KANG, H. Y., YAO, H. B., KOU, W., LIU, H., ZHANG, C. & HONG, S. L. 2014. An aryl hydrocarbon receptor ligand acts on dendritic cells and T cells to suppress the Th17 response in allergic rhinitis patients. *Lab Invest,* 94**,** 528-35.

WESTRA, I. M., MUTSAERS, H. A., LUANGMONKONG, T., HADI, M., OOSTERHUIS, D.,

DE JONG, K. P., GROOTHUIS, G. M. & OLINGA, P. 2016. Human precision-cut liver slices as a model to test antifibrotic drugs in the early onset of liver fibrosis. *Toxicol In Vitro,* 35**,** 77-85.

WOLTJEN, K., MICHAEL, I. P., MOHSENI, P., DESAI, R., MILEIKOVSKY, M., HÄMÄLÄINEN, R., COWLING, R., WANG, W., LIU, P., GERTSENSTEIN, M., KAJI, K., SUNG, H. K. & NAGY, A. 2009. piggyBac transposition reprograms fibroblasts to induced pluripotent stem cells. *Nature,* 458**,** 766-70.

WU, A. L., COULTER, S., LIDDLE, C., WONG, A., EASTHAM-ANDERSON, J., FRENCH, D. M., PETERSON, A. S. & SONODA, J. 2011. FGF19 regulates cell proliferation, glucose and bile acid metabolism via FGFR4-dependent and independent pathways. *PLoS One,* 6**,** e17868.

WU, D. & YOTNDA, P. 2011. Induction and testing of hypoxia in cell culture. *J Vis Exp*.

WU, H. & SUN, Y. E. 2006. Epigenetic regulation of stem cell differentiation. *Pediatr Res,* 59**,** 21R-5R.

WU, M. Y. & HILL, C. S. 2009. Tgf-beta superfamily signaling in embryonic development and homeostasis. *Dev Cell,* 16**,** 329-43.

WU, X., ROBOTHAM, J. M., LEE, E., DALTON, S., KNETEMAN, N. M., GILBERT, D. M. & TANG, H. 2012. Productive hepatitis C virus infection of stem cell-derived hepatocytes reveals a critical transition to viral permissiveness during differentiation. *PLoS Pathog,* 8**,** e1002617.

WU, Y., LIU, F., LIU, Y., LIU, X., AI, Z., GUO, Z. & ZHANG, Y. 2015. GSK3 inhibitors CHIR99021 and 6-bromoindirubin-3'-oxime inhibit microRNA maturation in mouse embryonic stem cells. *Sci Rep,* 5**,** 8666.

XIA, J., MATSUHASHI, S., HAMAJIMA, H., IWANE, S., TAKAHASHI, H., EGUCHI, Y., MIZUTA, T., FUJIMOTO, K., KURODA, S. & OZAKI, I. 2012. The role of PKC isoforms in the inhibition of NF-κB activation by vitamin K2 in human hepatocellular carcinoma cells. *J Nutr Biochem,* 23**,** 1668-75.

XIA, M., HUANG, R., SUN, Y., SEMENZA, G. L., ALDRED, S. F., WITT, K. L., INGLESE, J., TICE, R. R. & AUSTIN, C. P. 2009. Identification of chemical compounds that induce HIF-1alpha activity. *Toxicol Sci,* 112**,** 153-63.

XIAO, J. H., DURAND, B., CHAMBON, P. & VOORHEES, J. J. 1995. Endogenous retinoic acid receptor (RAR)-retinoid X receptor (RXR) heterodimers are the major functional forms regulating retinoid-responsive elements in adult human keratinocytes. Binding of ligands to RAR only is sufficient for RAR-RXR heterodimers to confer ligand-dependent activation of hRAR beta 2/RARE (DR5). *J Biol Chem,* 270**,** 3001-11.

XIAO, L., XIE, X. & ZHAI, Y. 2010. Functional crosstalk of CAR-LXR and ROR-LXR in drug metabolism and lipid metabolism. *Adv Drug Deliv Rev,* 62**,** 1316-21.

XIAO, Z., SABOURIN, M., PIRAS, G. & GORFIEN, S. F. 2014. Screening and optimization of chemically defined media and feeds with integrated and statistical approaches. *Methods Mol Biol,* 1104**,** 117-35.

XIE, Y., NAKANISHI, T., NATARAJAN, K., SAFREN, L., HAMBURGER, A. W., HUSSAIN, A. & ROSS, D. D. 2015. Functional cyclic AMP response element in the breast cancer resistance protein (BCRP/ABCG2) promoter modulates epidermal growth factor receptor pathway- or androgen withdrawal-mediated BCRP/ABCG2 transcription in human cancer cells. *Biochim Biophys Acta,*

1849**,** 317-27.
XU, C., INOKUMA, M. S., DENHAM, J., GOLDS, K., KUNDU, P., GOLD, J. D. & CARPENTER, M. K. 2001. Feeder-free growth of undifferentiated human embryonic stem cells. *Nat Biotechnol,* 19**,** 971-4.
XU, C., LI, C. Y. & KONG, A. N. 2005. Induction of phase I, II and III drug metabolism/transport by xenobiotics. *Arch Pharm Res,* 28**,** 249-68.
YAMADA, T., YOSHIKAWA, M., KANDA, S., KATO, Y., NAKAJIMA, Y., ISHIZAKA, S. & TSUNODA, Y. 2002. In vitro differentiation of embryonic stem cells into hepatocyte-like cells identified by cellular uptake of indocyanine green. *Stem Cells,* 20**,** 146-54.
YAMASAKI, H., SADA, A., IWATA, T., NIWA, T., TOMIZAWA, M., XANTHOPOULOS, K. G., KOIKE, T. & SHIOJIRI, N. 2006. Suppression of C/EBPalpha expression in periportal hepatoblasts may stimulate biliary cell differentiation through increased Hnf6 and Hnf1b expression. *Development,* 133**,** 4233-43.
YAMASHITA, Y., SHIMADA, M., HARIMOTO, N., RIKIMARU, T., SHIRABE, K., TANAKA, S. & SUGIMACHI, K. 2003. Histone deacetylase inhibitor trichostatin A induces cell-cycle arrest/apoptosis and hepatocyte differentiation in human hepatoma cells. *Int J Cancer,* 103**,** 572-6.
YANAGIDA, A., ITO, K., CHIKADA, H., NAKAUCHI, H. & KAMIYA, A. 2013. An in vitro expansion system for generation of human iPS cell-derived hepatic progenitor-like cells exhibiting a bipotent differentiation potential. *PLoS One,* 8**,** e67541.
YANG, H. & WANG, H. 2014. Signaling control of the constitutive androstane receptor (CAR). *Protein Cell,* 5**,** 113-23.
YANG, K., KOH, K. H. & JEONG, H. 2010. Induction of CYP2B6 and CYP3A4 expression by 1-aminobenzotriazole (ABT) in human hepatocytes. *Drug Metab Lett,* 4**,** 129-33.
YANG, P., SHEN, W. B., REECE, E. A. & CHEN, X. 2016. High glucose suppresses embryonic stem cell differentiation into neural lineage cells. *Biochem Biophys Res Commun,* 472**,** 306-12.
YANG, X. H., LIU, S. Y. & XING, A. Y. 2014. Molecular regulation of organic anion transporting polypeptide 1A2 (OATP1A2)by taurocholic acid in Bewo Cells. *Cell Mol Biol (Noisy-le-grand),* 60**,** 22-6.
YAO & TATSUMA 2017. Animal-cell culture media: History, characteristics, and

current issues. *In:* ASAYAMA, Y. (ed.). Reproductive

Medicine and Biology: John

Wiley & Sons, Ltd.
YAP, C. S., SINHA, R. A., OTA, S., KATSUKI, M. & YEN, P. M. 2013. Thyroid hormone negatively regulates CDX2 and SOAT2 mRNA expression via induction of miRNA-181d in hepatic cells. *Biochem Biophys Res Commun,* 440**,** 635-9.
YE, D., LI, T., HERAUD, P. & PARNPAI, R. 2016. Effect of Chromatin-Remodeling Agents in Hepatic Differentiation of Rat Bone Marrow-Derived Mesenchymal Stem Cells In Vitro and In Vivo. *Stem Cells Int,* 2016**,** 3038764.
YE, J., BATES, N., SOTERIOU, D., GRADY, L., EDMOND, C., ROSS, A., KERBY, A., LEWIS, P. A., ADENIYI, T., WRIGHT, R., POULTON, K. V., LOWE, M., KIMBER, S. J. & BRISON, D. R. 2017. High quality clinical grade human embryonic stem cell

lines derived from fresh discarded embryos. *Stem Cell Res Ther,* 8**,** 128.

YEN, W. C., CORPUZ, M. R., PRUDENTE, R. Y., COOKE, T. A., BISSONNETTE, R. P., NEGRO-VILAR, A. & LAMPH, W. W. 2004. A selective retinoid X receptor agonist bexarotene (Targretin) prevents and overcomes acquired paclitaxel (Taxol) resistance in human non-small cell lung cancer. *Clin Cancer Res,* 10**,** 8656-64.

YEN, W. C. & LAMPH, W. W. 2005. The selective retinoid X receptor agonist bexarotene (LGD1069, Targretin) prevents and overcomes multidrug resistance in advanced breast carcinoma. *Mol Cancer Ther,* 4**,** 824-34.

YEN, W. C., PRUDENTE, R. Y., CORPUZ, M. R., NEGRO-VILAR, A. & LAMPH, W. W. 2006. A selective retinoid X receptor agonist bexarotene (LGD1069, targretin) inhibits angiogenesis and metastasis in solid tumours. *Br J Cancer,* 94**,** 654-60.

YIMLAMAI, D., CHRISTODOULOU, C., GALLI, G. G., YANGER, K., PEPE-MOONEY, B., GURUNG, B., SHRESTHA, K., CAHAN, P., STANGER, B. Z. & CAMARGO, F. D. 2014. Hippo pathway activity influences liver cell fate. *Cell,* 157**,** 1324-38.

YIN, X., FARIN, H. F., VAN ES, J. H., CLEVERS, H., LANGER, R. & KARP, J. M. 2014. Niche-independent high-purity cultures of Lgr5+ intestinal stem cells and their progeny. *Nat Methods,* 11**,** 106-12.

YOSHIDA, T., KATSUYA, K., OKA, T., KOIZUMI, S., WAKITA, D., KITAMURA, H. & NISHIMURA, T. 2012. Effects of AhR ligands on the production of immunoglobulins in purified mouse B cells. *Biomed Res,* 33**,** 67-74.

YOUNG, S. P. & GARNER, C. 1990. Delivery of iron to human cells by bovine transferrin. Implications for the growth of human cells in vitro. *Biochem J,* 265**,** 587-91.

YOVCHEV, M. I. & OERTEL, M. 2017. Fetal Liver Stem/Progenitor Cell Transplantation: A Model to Study Tissue Mass Replacement and Cell-Based Therapies. *Methods Mol Biol,* 1506**,** 101-115.

YU, F. X., ZHAO, B., PANUPINTHU, N., JEWELL, J. L., LIAN, I., WANG, L. H., ZHAO, J., YUAN, H., TUMANENG, K., LI, H., FU, X. D., MILLS, G. B. & GUAN, K. L. 2012a. Regulation of the Hippo-YAP pathway by G-protein-coupled receptor signaling. *Cell,* 150**,** 780-91.

YU, J., HU, K., SMUGA-OTTO, K., TIAN, S., STEWART, R., SLUKVIN, I. I. & THOMSON, J. A. 2009. Human induced pluripotent stem cells free of vector and transgene sequences. *Science,* 324**,** 797-801.

YU, Y., LIU, H., IKEDA, Y., AMIOT, B. P., RINALDO, P., DUNCAN, S. A. & NYBERG, S. L. 2012b. Hepatocyte-like cells differentiated from human induced pluripotent stem cells: relevance to cellular therapies. *Stem Cell Res,* 9**,** 196-207.

YUAN, C., GAO, J., GUO, J., BAI, L., MARSHALL, C., CAI, Z., WANG, L. & XIAO, M. 2014. Dimethyl sulfoxide damages mitochondrial integrity and membrane potential in cultured astrocytes. *PLoS One,* 9**,** e107447.

YUSA, K., RASHID, S. T., STRICK-MARCHAND, H., VARELA, I., LIU, P. Q., PASCHON, D. E., MIRANDA, E., ORDÓÑEZ, A., HANNAN, N. R., ROUHANI, F. J., DARCHE, S., ALEXANDER, G., MARCINIAK, S. J., FUSAKI, N., HASEGAWA, M., HOLMES, M. C., DI SANTO, J. P., LOMAS, D. A., BRADLEY, A. & VALLIER, L. 2011. Targeted gene correction of α1-antitrypsin deficiency in induced pluripotent stem cells. *Nature,* 478**,** 391-4.

ZANGER, U. M. & SCHWAB, M. 2013. Cytochrome P450 enzymes in drug metabolism: regulation of gene expression, enzyme activities, and impact of genetic variation. *Pharmacol Ther,* 138**,** 103-41.

ZARET, K. S. 2002. Regulatory phases of early liver development: paradigms of organogenesis. *Nat Rev Genet,* 3**,** 499-512.

ZARET, K. S. 2008. Genetic programming of liver and pancreas progenitors: lessons for stem-cell differentiation. *Nat Rev Genet,* 9**,** 329-40.

ZEILINGER, K., FREYER, N., DAMM, G., SEEHOFER, D. & KNÖSPEL, F. 2016. Cell sources for in vitro human liver cell culture models. *Exp Biol Med (Maywood),* 241**,** 1684-98.

ZHANG, B., LI, S. & HARBRECHT, B. G. 2011a. Akt-mediated signaling is induced by cytokines and cyclic adenosine monophosphate and suppresses hepatocyte inducible nitric oxide synthase expression independent of MAPK P44/42. *Biochim Biophys Acta,* 1813**,** 73-9.

ZHANG, M., TENG, H., SHI, J. & ZHANG, Y. 2011b. Disruption of β-arrestins blocks glucocorticoid receptor and severely retards lung and liver development in mice. *Mech Dev,* 128**,** 368-75.

ZHANG, Q., YANG, Y., ZHANG, J., WANG, G. Y., LIU, W., QIU, D. B., HEI, Z. Q., YING, Q. L. & CHEN, G. H. 2011c. Efficient derivation of functional hepatocytes from mouse induced pluripotent stem cells by a combination of cytokines and sodium butyrate. *Chin Med J (Engl),* 124**,** 3786-93.

ZHANG, S., PAN, X. & JEONG, H. 2015. GW4064, an agonist of farnesoid X receptor, represses CYP3A4 expression in human hepatocytes by inducing small heterodimer partner expression. *Drug Metab Dispos,* 43**,** 743-8.

ZHANG, T., ZHAO, C., LUO, L., XIANG, J., CHENG, J., WANG, T. & CHEN, D. 2014. High concentraction of taurocholic acid induced apoptosis in HTR-8/SVneo cells via overexpression of ERp29 and activation of p38. *Placenta,* 35**,** 496-500.

ZHANG, Y. & KANG, J. 2013. [Screening of the active ingredients in natural products by capillary electrophoresis and high performance liquid chromatography-mass spectrometry]. *Se Pu,* 31**,** 640-5.

ZHANG, Y., KAST-WOELBERN, H. R. & EDWARDS, P. A. 2003. Natural structural variants of the nuclear receptor farnesoid X receptor affect transcriptional activation. *J Biol Chem,* 278**,** 104-10.

ZHANG, Y., ZHANG, B., ZHANG, A., ZHAO, Y., ZHAO, J., LIU, J., GAO, J., FANG, D. & RAO, Z. 2012. Synergistic growth inhibition by sorafenib and vitamin K2 in human hepatocellular carcinoma cells. *Clinics (Sao Paulo),* 67**,** 1093-9.

ZHANG, Z., RANKIN, S. A. & ZORN, A. M. 2013. Different thresholds of Wnt-Frizzled 7 signaling coordinate proliferation, morphogenesis and fate of endoderm progenitor cells. *Dev Biol,* 378**,** 1-12.

ZHAO, D., CHEN, S., DUO, S., XIANG, C., JIA, J., GUO, M., LAI, W., LU, S. & DENG, H. 2013. Promotion of the efficient metabolic maturation of human pluripotent stem cell-derived hepatocytes by correcting specification defects. *Cell Res,* 23**,** 157-61.

ZHAO, R. & DUNCAN, S. A. 2005. Embryonic development of the liver. *Hepatology,* 41**,** 956-67.

ZHAO, Y., WIEMAN, H. L., JACOBS, S. R. & RATHMELL, J. C. 2008. Mechanisms and methods in glucose metabolism and cell death. *Methods Enzymol,* 442**,** 439-

57.
ZHENG, Y. L. 2016. Some Ethical Concerns About Human Induced Pluripotent Stem Cells. *Sci Eng Ethics,* 22**,** 1277-1284.
ZHOU, M., LI, P., TAN, L., QU, S., YING, Q. L. & SONG, H. 2010. Differentiation of mouse embryonic stem cells into hepatocytes induced by a combination of cytokines and sodium butyrate. *J Cell Biochem,* 109**,** 606-14.
ZHOU, W., YU, W., XIE, W., HUANG, L., XU, Y. & LI, X. 2011. The role of SLIT-ROBO signaling in proliferative diabetic retinopathy and retinal pigment epithelial cells. *Mol Vis,* 17**,** 1526-36.
ZHOU, Y. & HU, Z. 2015. Genome-wide demethylation by 5-aza-2'-deoxycytidine alters the cell fate of stem/progenitor cells. *Stem Cell Rev,* 11**,** 87-95.
ZHU, D., HADOKE, P. W., WU, J., VESEY, A. T., LERMAN, D. A., DWECK, M. R., NEWBY, D. E., SMITH, L. B. & MACRAE, V. E. 2016. Ablation of the androgen receptor from vascular smooth muscle cells demonstrates a role for testosterone in vascular calcification. *Sci Rep,* 6**,** 24807.
ZIMMERMAN, N. P., ROY, I., HAUSER, A. D., WILSON, J. M., WILLIAMS, C. L. & DWINELL, M. B. 2015. Cyclic AMP regulates the migration and invasion potential of human pancreatic cancer cells. *Mol Carcinog,* 54**,** 203-15.
ZOCK, J. M. 2009. Applications of high content screening in life science research. *Comb Chem High Throughput Screen,* 12**,** 870-76.
ZORN, A. M. 2008. Liver Development. In: StemBook [Internet]. Cambridge (MA): Harvard Stem Cell Institute; 2008-. Available from: http://www.ncbi.nlm.nih.gov/books/NBK27068/.
ZORN, A. M. & WELLS, J. M. 2007. Molecular basis of vertebrate endoderm development. *Int Rev Cytol,* 259**,** 49-111.
ZORN, A. M. & WELLS, J. M. 2009. Vertebrate endoderm development and organ formation. *Annu Rev Cell Dev Biol,* 25**,** 221-51.
ZULIANI-ALVAREZ, L. & MIDWOOD, K. S. 2015. Fibrinogen-Related Proteins in Tissue Repair: How a Unique Domain with a Common Structure Controls Diverse Aspects of Wound Healing. *Adv Wound Care (New Rochelle),* 4**,** 273-285.
ZWEIGERDT, R., BURG, M., WILLBOLD, E., ABTS, H. & RUEDIGER, M. 2003. Generation of confluent cardiomyocyte monolayers derived from embryonic stem cells in suspension: a cell source for new therapies and screening strategies. *Cytotherapy,* 5**,** 399-413.
ZÚÑIGA, S., FIRRINCIELI, D., HOUSSET, C. & CHIGNARD, N. 2011. Vitamin D and the vitamin D receptor in liver pathophysiology. *Clin Res Hepatol Gastroenterol,* 35**,** 295-302.